STATE OF CALIFORNIA • DEPARTMENT OF TRANSPORTATION

TECHNICAL REPORT DOCUMENTATION PAGE

TR0003 (REV 10/98)

ADA Notice

For individuals with sensory disabilities, this document is available in alternate formats. For information call (916) 654-6410 or TDD (916) 654-3880 or write Records and Forms Management, 1120 N Street, MS-89, Sacramento, CA 95814.

1. REPORT NUMBER	2. GOVERNMENT ASSOCIATION NUMBER	3. RECIPIENT'S CATALOG NUMBER
CA16-2419		

4. TITLE AND SUBTITLE

Parametric Study of Ordinary Standard Bridges using OpenSees and CSiBridge

5. REPORT DATE

July 2015

6. PERFORMING ORGANIZATION CODE

7. AUTHOR

Jinchi Lu, Ahmed Elgamal, and Kevin R. Mackie

8. PERFORMING ORGANIZATION REPORT NO.

UCSD / SSRP-14/03

9. PERFORMING ORGANIZATION NAME AND ADDRESS

Department of Structural Engineering
School of Engineering
10. Work Unit No. (TRAIS)
University of California, San Diego
La Jolla, California 92093-0085

10. WORK UNIT NUMBER

11. CONTRACT OR GRANT NUMBER

65A0445

12. SPONSORING AGENCY AND ADDRESS

California Department of Transportation
Division of Engineering Services
1801 30th St., MS-9-2/5i
Sacramento, California 95816

13. TYPE OF REPORT AND PERIOD COVERED

Final Report

14. SPONSORING AGENCY CODE

15. SUPPLEMENTARY NOTES

Prepared in cooperation with the State of California Department of Transportation.

16. ABSTRACT

Parametric studies of representative Ordinary Standard Bridges (OSB) were performed comparing the results of OpenSees nonlinear time history analysis with those from CSiBridge simulations. Four OSB Study Bridges (OSB1, OSB2, OSB3 and OSB4) are addressed. The analysis procedures and results were presented in this report. Results of the Equivalent Static Analysis (ESA) procedure are presented as well.

To facilitate the conducted analyses in OpenSees, a recently developed user interface MSBridge was employed. MSBridge is a PC-based graphical pre- and post-processor (userinterface) for conducting nonlinear Finite Element (FE) studies for multi-span bridge systems. Finite element computations in MSBridge are conducted using OpenSees.

17. KEY WORDS

Finite Element, Time History Analysis, Ordinary Standard Bridge, Parametric Study

18. DISTRIBUTION STATEMENT

No restrictions. This document is available to the public through the National Technical Information Service, Springfield, VA 22161

19. SECURITY CLASSIFICATION *(of this report)*	20. NUMBER OF PAGES	21. COST OF REPORT CHARGED
Unclassified	362	

STRUCTURAL SYSTEMS

RESEARCH PROJECT

Report No.
SSRP–14/03

PARAMETRIC STUDY OF ORDINARY STANDARD BRIDGES USING OPENSEES AND CSIBRIDGE

by

JINCHI LU

AHMED ELGAMAL

KEVIN R. MACKIE

Final Report Submitted to the California Department of Transportation (Caltrans) under Contract No. 65A0445.

July 2015

Department of Structural Engineering
University of California, San Diego
La Jolla, California 92093-0085

University of California, San Diego
Department of Structural Engineering
Structural Systems Research Project

Report No. SSRP-14/03

Parametric Study of Ordinary Standard Bridges using OpenSees and CSiBridge

by

Jinchi Lu
Associate Project Scientist, UC San Diego

Ahmed Elgamal
Professor of Geotechnical Engineering, UC San Diego

and

Kevin R. Mackie
Associate Professor of Structural Engineering, Univ. of Central Florida

Final Report Submitted to the California Department of Transportation under Contract No. 65A0445

Department of Structural Engineering
University of California, San Diego
La Jolla, California 92093-0085

July 2015

DISCLAIMER STATEMENT

This document is disseminated in the interest of information exchange. The contents of this report reflect the views of the authors who are responsible for the facts and accuracy of the data presented herein. The contents do not necessarily reflect the official views or policies of the State of California or the Federal Highway Administration. This publication does not constitute a standard, specification or regulation. This report does not constitute an endorsement by the Department of any product described herein.

For individuals with sensory disabilities, this document is available in alternate formats. For information, call (916) 654-8899, TTY 711, or write to California Department of Transportation, Division of Research, Innovation and System Information, MS-83, P.O. Box 942873, Sacramento, CA 94273-0001.

ACKNOWLEDGMENTS

The research described in this report was supported by the California Department of Transportation (Caltrans) under Contract No. 65A0445 with Dr. Charles Sikorsky as the project manager. This support is most appreciated. In addition, we are grateful for the valuable technical suggestions, comments and contributions provided by Caltrans engineers, particularly Dr. Toorak Zokaie, Mr. Yeo (Tony) Yoon, Dr. Mark Mahan, Dr. Anoosh Shamsabadi, and Mr. Steve Mitchell. In this study, employed ground shaking motions, and the Caltrans OSB CSiBridge input files were prepared and provided by Caltrans. The authors would also like to thank Computers & Structures, Inc for providing a complimentary copy of CSiBridge.

ABSTRACT

Parametric studies of representative Ordinary Standard Bridges (OSB) were performed comparing the results of OpenSees nonlinear time history analysis with those from CSiBridge simulations. Four OSB Study Bridges (OSB1, OSB2, OSB3 and OSB4) are addressed. The analysis procedures and results were presented in this report. Results of the Equivalent Static Analysis (ESA) procedure are presented as well.

To facilitate the conducted analyses in OpenSees, a recently developed user interface MSBridge was employed. MSBridge is a PC-based graphical pre- and post-processor (user-interface) for conducting nonlinear Finite Element (FE) studies for multi-span bridge systems. Finite element computations in MSBridge are conducted using OpenSees.

TABLE OF CONTENTS

LIST OF FIGURES

LIST OF TABLES

1 INTRODUCTION

1.1 Background

According to Caltrans (2013), Ordinary Standard Bridge (OSB) is a term used by Caltrans to identify bridges designed using the direct and basic approach outlined in the Seismic Design Criteria SDC-2013 (Caltrans 2013). For a bridge to be considered as an OSB, SDC-2013 sets forth the following basic requirements: (1) each span length should be less than 300 feet (.i.e., 91 m); (2) the bridge should have single superstructures on either a horizontally curved, vertically curved, or straight alignment; (3) the bridge should be constructed with a precast or cast-in-place concrete girder, concrete slab superstructure on pile extensions, column or pier walls; (4) foundations must be supported on spread footings, pile caps with piles or pile shafts, and (5) the soil is not susceptible to liquefaction or scour.

In this report, four Caltrans OSB Study Bridges were addressed (these bridges are used by Caltrans for the purpose of design related investigations). The analyses were conducted using OpenSees (ver. 2.4.0) and CSiBridge (ver. 2015). OpenSees is an open source software framework for simulating the seismic response of structural and geotechnical systems (McKenna et al. 2010, Mazzoni et al. 2009). OpenSees has been developed by the Pacific Earthquake Engineering Research (PEER) Center since 1998. CSiBridge is an integrated software program for modeling, analysis, and design of bridge structures (CSI 2015a).

To facilitate the conducted analyses in OpenSees, a recently developed user interface MSBridge was employed. MSBridge is a PC-based graphical pre- and post-processor (user-interface) for conducting nonlinear Finite Element (FE) studies for multi-span bridge systems. Finite element computations in MSBridge are conducted using OpenSees. The analysis options available in MSBridge include i) Pushover Analysis; ii) Mode Shape Analysis; iii) Single 3D Input Acceleration Analysis; iv) Multiple 3D Input Acceleration Analysis; and v) Equivalent Static Analysis (ESA). For more information about MSBridge, please see Appendix A.

1.2 Report Scope and Layout

This report is composed of six chapters. Chapters 2-5 present the analysis procedures and results for OSB Study Bridges 2 (OSB2), 1 (OSB1), 4 (OSB4) and 3 (OSB3), respectively. Finally, an assessment of outcomes and conclusions is presented in Chapter 6.

A set of 50 input ground motions (provided by Caltrans) was employed in the Nonlinear THA (Time History Analysis) of the four OSB Study Bridges. Further details regarding these motions are provided in Appendix B.

For OSB1 & OSB2 in the conducted OpenSees analysis, three types of abutment models (Roller, EPP-Gap and EPP-Gap with Bearings) were addressed. The forceBeamColumn (BeamWithHinges) element in OpenSees was employed to model the column while the deck was considered linearly elastic and the bentcap was assumed rigid. Detailed modeling techniques for

OSB2 and OSB1 are presented in Appendices C and D, respectively. As suggested by Caltrans, only the EPP-Gap model was simulated in the CSiBridge nonlinear THA.

For OSB3 & OSB4 in the conducted OpenSees analysis, two types of abutment models (Roller with Isolation Bearings, and EPP-Gap with Isolation Bearings) were addressed. The forceBeamColumn (with the distributed plasticity integration method) element in OpenSees was employed to model the column while the deck was considered linearly elastic and the bentcap was assumed rigid. Detailed modeling techniques for OSB4 and OSB3 are presented in Appendices E and F, respectively. As suggested by Caltrans, only the EPP-Gap with Isolation Bearings model was simulated in the CSiBridge nonlinear THA.

In Appendix G, a comparison study of OpenSees and CSibridge bridge column response was first explored, before the nonlinear THA of the 50 input motions was conducted for the four OSB bridges. For the column Fiber section model, it was found that the column stiffness and strenght responses appear to be different between CSiBridge and OpenSees (e.g., the CSiBridge model appears to reduce the initial stiffness much more than expected).

To address the above-mentioned initial column stiffness/strength issues for the Fiber section in CSiBridge, a special column modeling approach was proposed by Caltrans (please see Appendix H). The procedure in this approach involves (Appendix H): i) Discretize the column into at least two elements (one for the hinge length centered at the hinge position and the other(s) for the remainder of the column); ii) Place the hinge at the center of the hinge length element; iii) Add a stiff section modifier to the hinge length element (increase the element Moment of Inertia) to avoid double counting the elastic deformation over the hinge length; iv) As usual, assign cracked section modifiers to all elements in the column except the hinge region. On this basis, it was found that a section modifier of 3 for the hinge length element gave reasonable overall initial column stiffness/strength response (Appendix H). Therefore, the section modifier of 3 was used in all the CSiBridge analyses for OSB1 (Chapter 3) and OSB2 (Chapter 2).

Finally, Appendix I is concerned with an additional issue that might result in significant differences when comparing the OpenSees and CSiBridge seismic response. In the conducted OpenSees simulations, no viscous damping is associated with any prescribed abutment force-displacement relationship (e.g., Elastic Spring, EPP-Gap). However, the corresponding CSiBridge simulations imply that there is an associated viscous damping force associated with the stiffness of the selected abutment model. As such, when viscous damping is included: i) both programs give the same results when an abutment Roller model is specified (i.e., there is no stiffness force associated with the abutment model), and ii) conversely, the Elastic spring and the EPP-Gap abutment model OpenSees and CSiBridge results are different. Without viscous damping, all cases result in agreement between OpenSees and CSiBridge (when an elastic column response is specified as discussed above).

2 OSB STUDY BRIDGE 2

2.1 Bridge Description

OSB Study Bridge 2 (herein referred to as OSB2) is a single bent reinforced concrete box-girder bridge with two spans of 150 feet in length (OSB2 is presented first herein, with a simpler geometric configuration compared to that of OSB1). This single-bent bridge is supported on one circular reinforced concrete column (Figure 2.1).

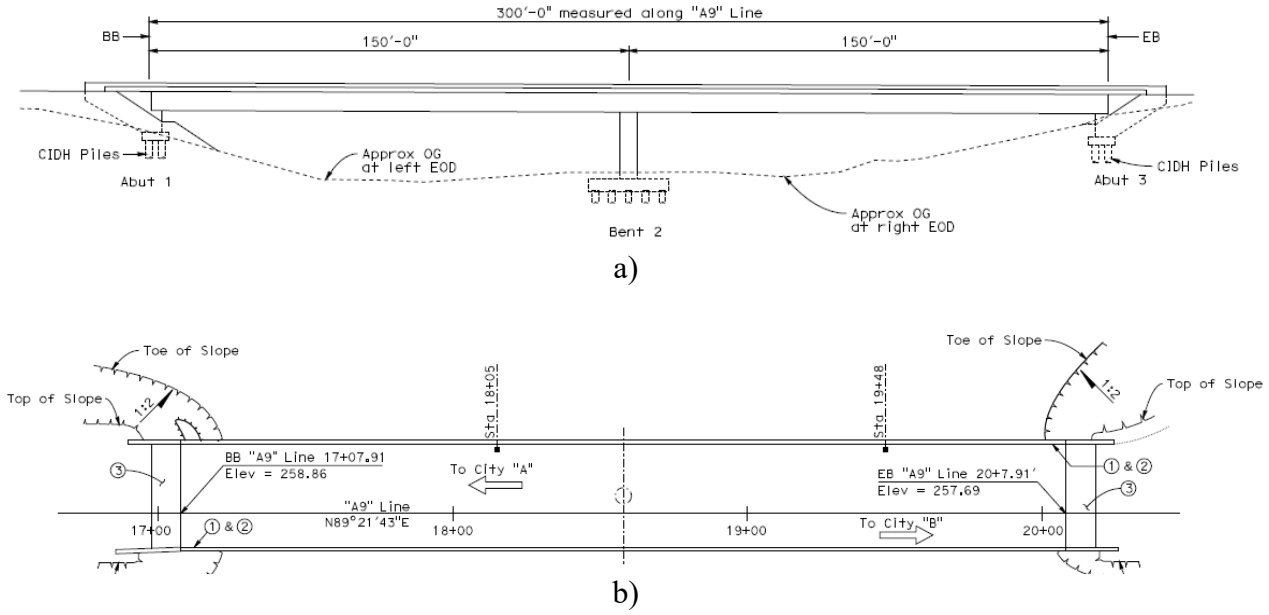

Figure 2.1 Schematic of OSB2 (drawings provided by Caltrans): (a) Elevation view; (b) Plan view

2.2 Geometric Configuration

Figure 2.2 shows a sectional view of OSB2 along with the column reinforcement details. The three-cell box girder is 37.5 feet wide by 6 feet deep; and the deck and soffit slabs are 8.375 inches and 7 inches thick, respectively.

The column is 20 feet high with a diameter of 66 inches. The column is considered as fixed at the top and at the base. The offset (3 ft) between column top and the deck was not represented in this study.

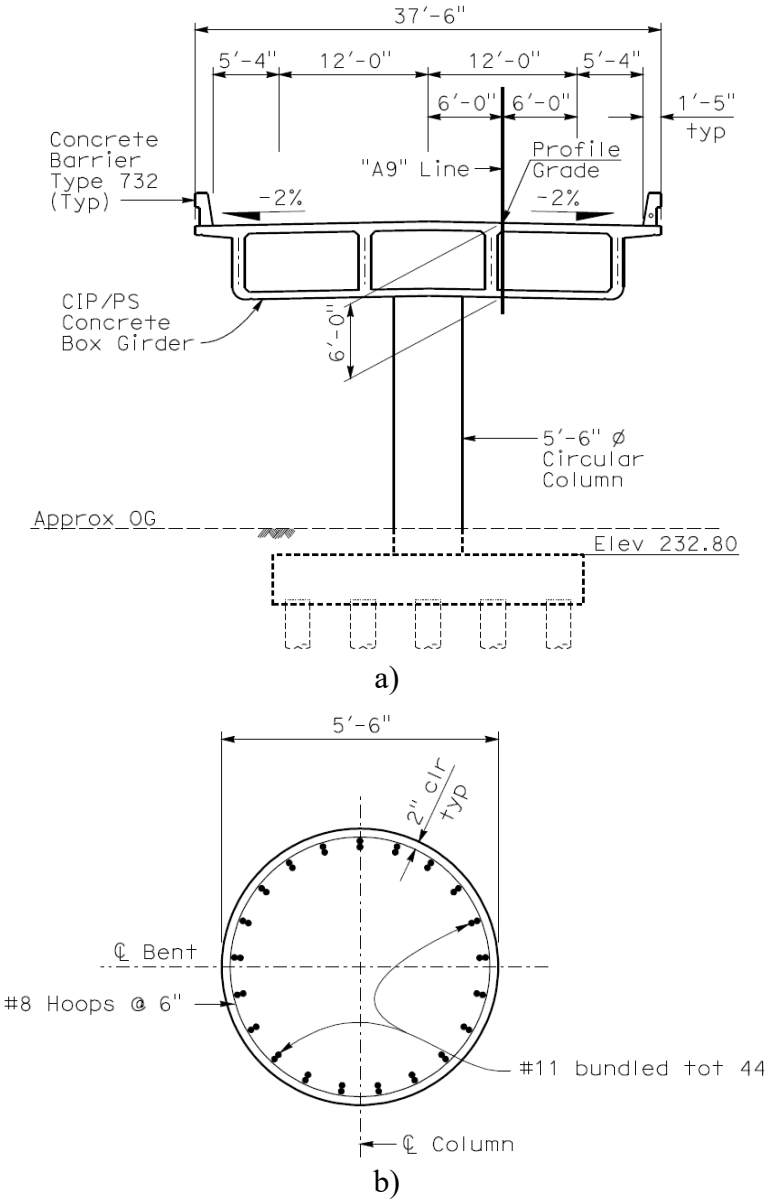

Figure 2.2 Sectional details of OSB2: (a) deck; (b) circular column cross section (Caltrans 2012)

2.3 OSB2 OpenSees Modeling and Response

2.3.1 Finite Element Model

The employed modeling techniques and associated model properties are presented in Appendix C. To facilitate the conducted analyses, a recently developed user interface MSBridge was employed (please see Appendix A for more information about MSBridge). Figure 2.3 shows the OSB2 model created in MSBridge and CSiBridge.

The forceBeamColumn (BeamWithHinges) element in OpenSees was used to model the column. A plastic hinge length of 2.8 ft, obtained based on Eq. 7.6.2.1-1 of SDC (2013), was employed (see Appendix C for the calculation of the plastic hinge length). The deck was considered linearly elastic (see Appendix C for the deck geometric and material properties).

As shown in Figure 2.3a, two equal-length elements were used for the column (the column height is 20 ft). Both column top and base are fixed. The offset between the column top and the deck was not considered (due to limitations in the current version of MSBridge). No rotation around the bridge longitudinal direction is allowed for the deck (at the abutments).

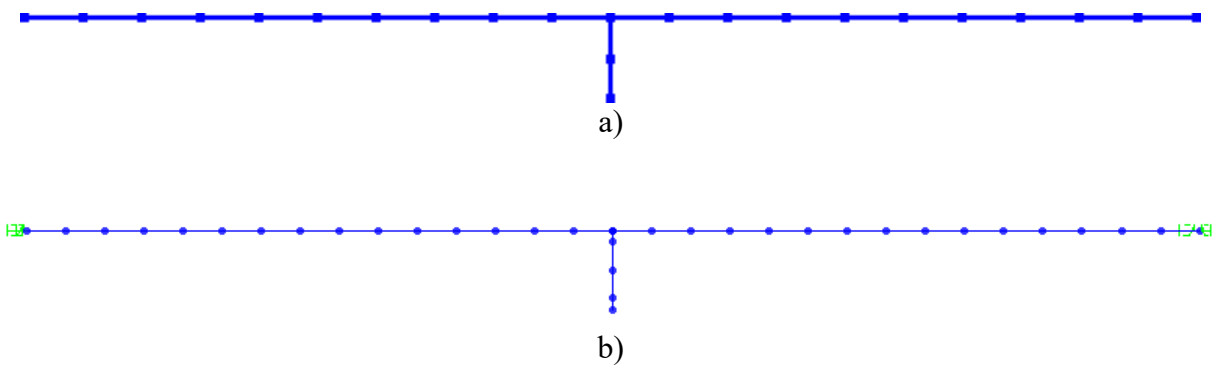

Figure 2.3 OSB2 model (side view) created in: a) MSBridge; b) CSiBridge

Three types of abutment models were employed in OpenSees analysis:

i) Roller abutment model,
ii) EPP-Gap abutment model (bearing pads were not considered), and
iii) EPP-Gap with Bearings abutment model (4 bearing pads were included).

The resulting OSB2 bridge models will be hereinafter referred to as "Roller model", "EPP-Gap model" and EPP-Gap with Bearings model", respectively. The first natural periods for OSB2 with the above 3 models are 0.69, 0.69, and 0.68 second, respectively. The Gaps were 2 in (longitudinal) and 1 in (transverse). For detailed information about the above 3 abutment models, please see Appendix C. As suggested by Caltrans, only the EPP-Gap model (the one without abutment bearing pads) was simulated in the CSiBridge nonlinear THA.

2.3.2 Column Response

Pushover analysis was conducted to document the corresponding column response. The Roller model was employed in this case. For CSiBridge, the approach presented in Appendix H was employed to model the column. Figure 2.4 shows the column force-displacement response due to pushover loading (Figure 2.5 shows the column force versus drift ratio response for the same pushover loading case).

The column force-displacement response shows significant yielding to start at about a 0.6% drift ratio (OpenSees result in Figure 2.5a) or 1.4 in of displacement (OpenSees result in Figure 2.4a) in the case of longitudinal pushover. A shear force of 1,250 kip was reached when this yielding occurs. In the case of transverse pushover, similar yielding is observed at a 1% drift ratio (OpenSees result in Figure 2.5b) or 2.4 in of displacement (OpenSees result in Figure 2.4b). Both cases show the column strength to dramatically degrade at a 4.8% drift ratio or 11.5 in of displacement (OpenSees result in Figure 2.4 and Figure 2.5). For more discussions about the OSB2 column response (linear and nonlinear), please see Appendix E.

2.4 Equivalent Static Analysis (ESA)

ESA was conducted for OSB2 in the bridge longitudinal and transverse directions. For the procedure to conduct ESA in MSBridge, please refer to the MSBridge user manual (Elgamal et al. 2014).

2.4.1 ESA in the Longitudinal Direction

The entire bridge system was employed in the longitudinal ESA. A load of 5% of the total bridge weight was used for the longitudinal pushover analysis. The pushover load was applied at the bridge center (i.e., the column top in this case) along the bridge deck (longitudinal) direction. For the acceleration response spectrum (ARS) employed in the ESA, please see Appendix C.

Table 2.1 shows the ESA result for OSB2. The final elastic displacement demand is 2.6 in (for Roller and EPP-Gap models) or 2.5 in (for EPP-Gap with Bearings model). Table 2.2 lists the parameters related to this longitudinal ESA.

2.4.2 ESA in the Transverse Direction

A load of 5% of the tributary weight of the bent was used for the (transverse) pushover analysis. A fixed-fixed boundary condition was considered for the column in this case. The same acceleration response spectrum (ARS) was used in the transverse ESA.

The elastic displacement demand was found to be 1.1 inch (Table 2.1) in the transverse ESA. Table 2.3 lists the parameters related to this transverse ESA. The stiffness in the transverse direction (i.e., 2,782.47 kip/in as shown in Table 2.3) is much higher than the stiffness in the longitudinal direction (e.g., 1,943 kip/in for the EPP-Gap with Bearings model as shown in Table 2.2), due to the fixed-fixed boundary conditions employed in the transverse ESA.

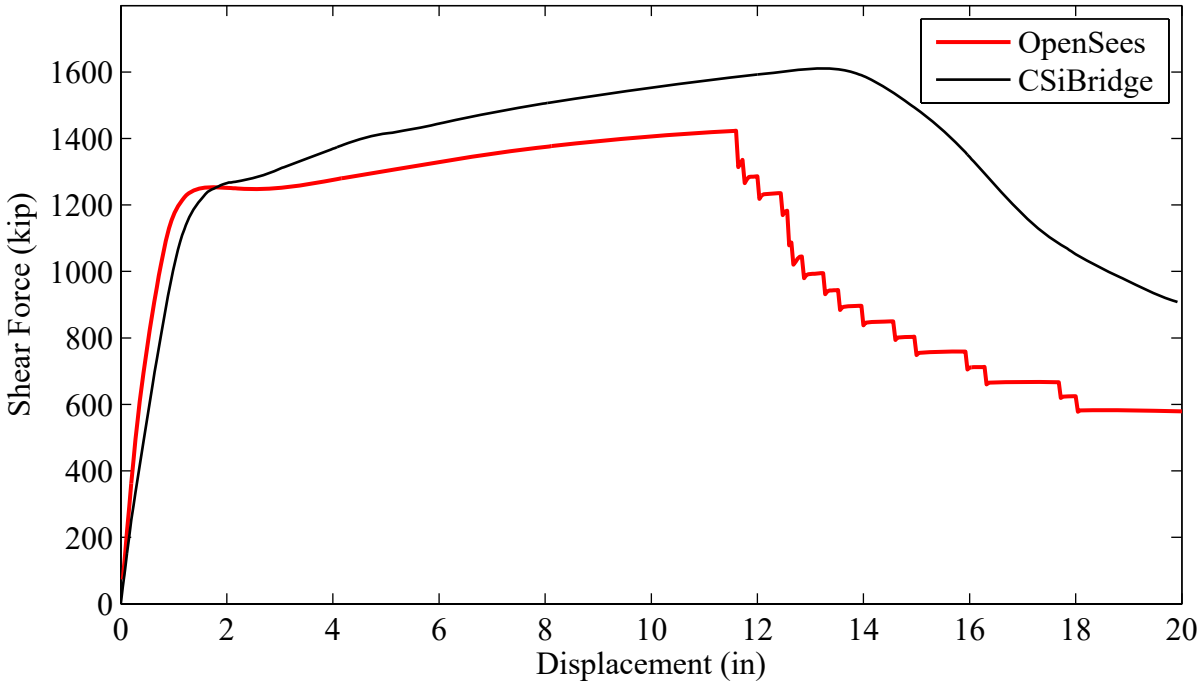

a)

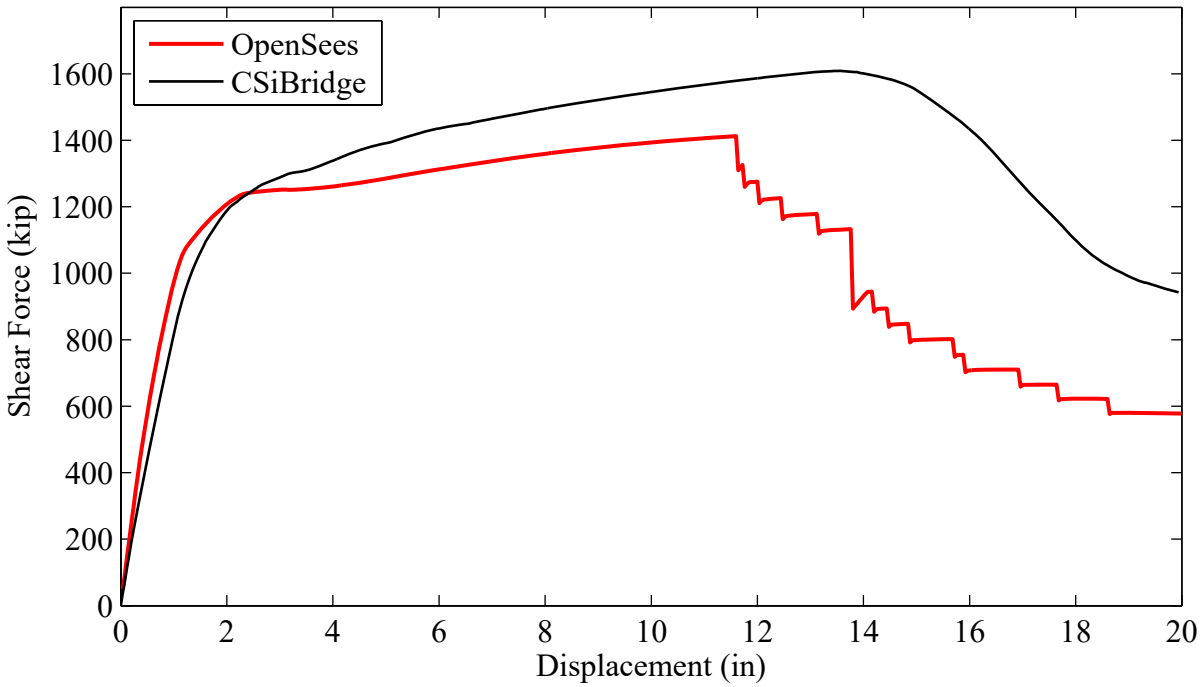

b)

Figure 2.4 OSB2 column force-displacement response: a) longitudinal direction; b) transverse direction

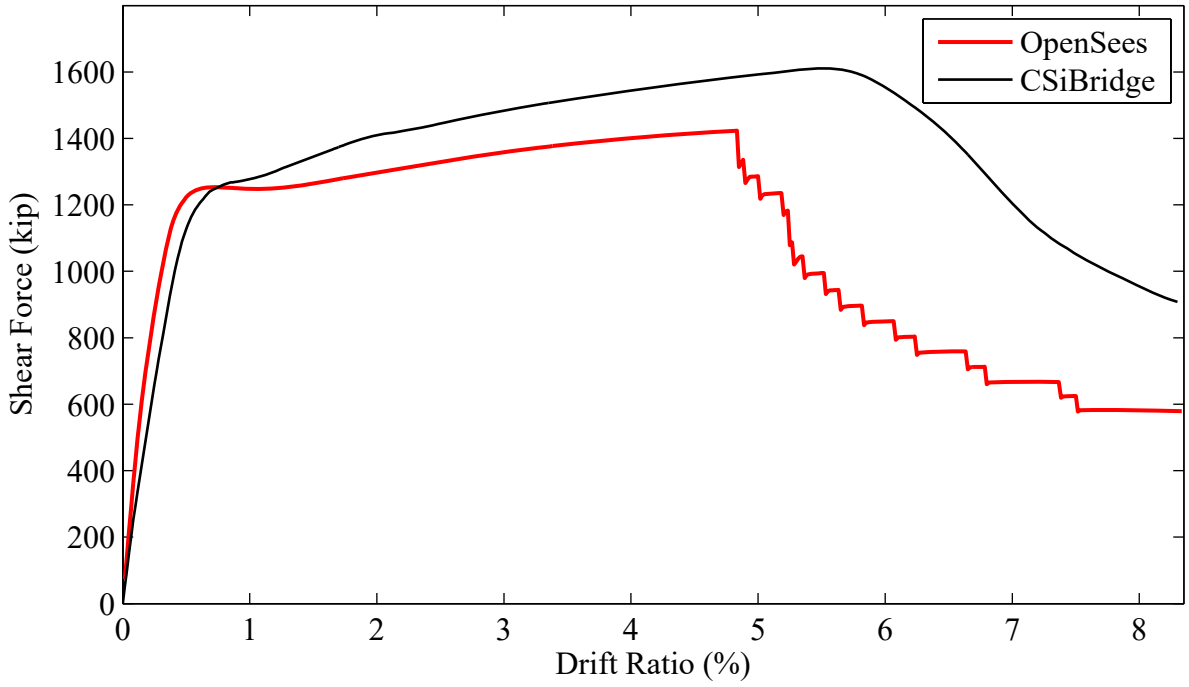

a)

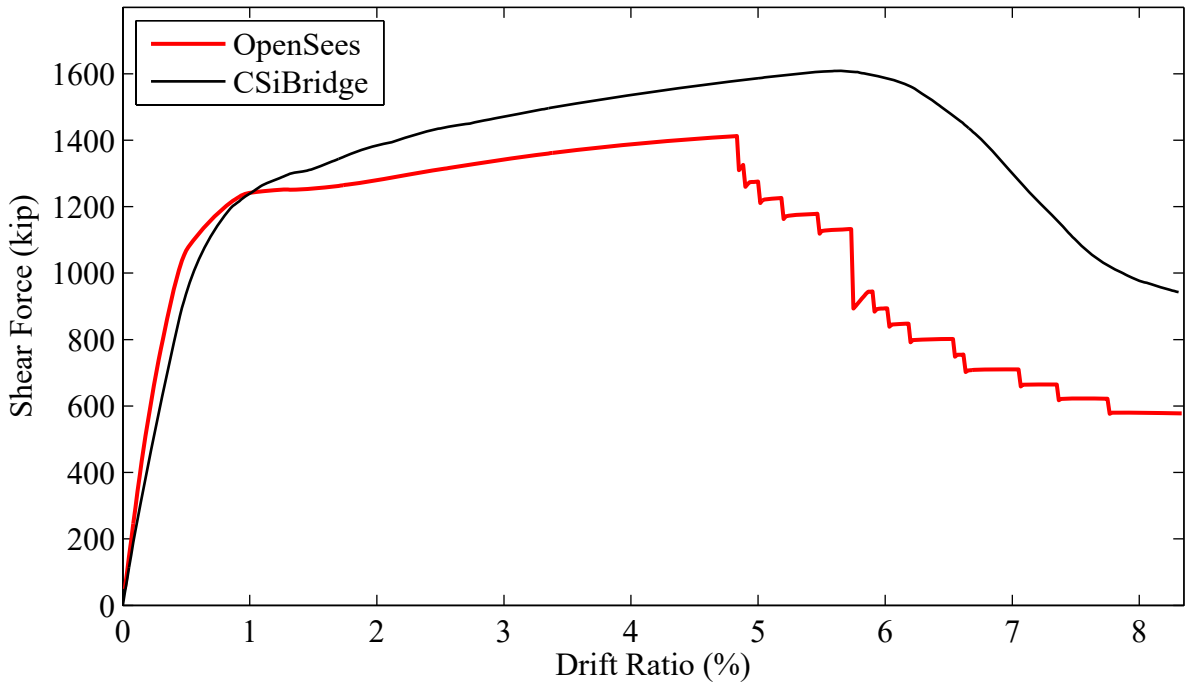

b)

Figure 2.5 OSB2 column force versus drift ratio response: a) longitudinal direction; b) transverse direction

Table 2.1. ESA Result for OSB2

Parameter	Longitudinal Direction	Transverse Direction
Displacement Demand (in)	2.6 (for Roller and EPP-Gap models) or 2.5 (for EPP-Gap with Bearings model)	1.1

Table 2.2. Longitudinal ESA Parameters for OSB2

Parameter	Roller and EPP-Gap models	EPP-Gap with Bearings model
Total weight calculated (kip)	3,221	Same
Total mass calculated (kip-sec^2/in)	8.34	Same
Pushover load specified (kip)	161.1	Same
Displacement due to pushover (in)	0.088	0.081
Calculated stiffness (kip/in)	1,830	1,943
Calculated period (sec)	0.42	0.41

Table 2.3. Transverse ESA Parameters for OSB2

Parameter	Value
Tributary weight calculated (kip)	1,628
Tributary mass calculated (kip-sec^2/in)	4.21
Pushover load specified (kip)	81.43
Displacement due to pushover (in)	0.029
Calculated stiffness (kip/in)	2,782.47
Calculated period (sec)	0.25

2.5 Nonlinear Time History Analysis

Nonlinear THA was conducted for the 50 input motions provided by Caltrans (see Appendix B for the characteristics of the 50 motions). The input motions were applied directly at the column base as well as at both abutments.

Rayleigh damping was used with a 5% damping ratio (defined at periods of 0.889 and 0.692 second) in the nonlinear THA. For the time integration scheme, the Newmark's average acceleration method ($\gamma = 0.5$ and $\beta = 0.25$) was employed.

In OpenSees, the variable time-stepping scheme was used in the analysis. The starting value for each step was 0.005 second (same as the time step of the input motions) and the minimum time step was 5×10^{-5} second (upon splitting of time step when needed).

2.5.1 Maximum Displacement and Acceleration

Table 2.4 lists OSB2 column top maximum displacement for the 50 motions from the nonlinear THA in OpenSees. Results for the 3 models (Roller, EPP-Gap, and EPP-Gap with Bearings) are shown for comparison (Table 2.4).

Among the motions with longitudinal component only (Motions 1-21), Motion 4 (ROCKS1N3) gave the least maximum displacement (1.4 in for the 3 types of abutment models) while Motion 15 (SANDS1N1) gave the largest maximum displacement (5.4 in, 4.0 in and 3.3 in for the Roller, EPP-Gap, and EPP-Gap with Bearings models, respectively).

Note that the Roller and EPP-Gap models gave the same maximum longitudinal displacement when the displacement is around 2 in or less (Table 2.4). This is because the specified longitudinal gap is 2 in in the EPP-Gap model. As such, both OSB2 models (Roller and EPP-Gap) essentially behave in the same way under longitudinal loading, when the gap is not closed during seismic response.

The OSB2 column generally deformed more in the transverse direction, compared to the longitudinal direction, when subjected to the same input excitation (Table 2.4). This might be due to the more flexible transverse column response, compared to that in the longitudinal direction (Figures 2.4 and 2.5).

As mentioned earlier, the case with the EPP-Gap model was simulated in CSiBridge. Table 2.5 lists the column top maximum displacement from the OpenSees and CSiBridge analyses. The maximum displacement comparison of Table 2.5 is also presented in Bar Chart graphical form in Figures 2.6-2.9. As mentioned earlier in Chapter 1, viscous damping abutment forces are only present in the CSiBridge simulation. This difference in the abutment exerted forces accounts partially for the discrepancy (Table 2.5) in the CSiBridge and OpenSees maximum displacement estimates. Appendix J lists additional CSiBridge results (column top shear force-displacement hysteresis and bending moment time history for each input motion).

Table 2.6 displays OSB2 deck maximum acceleration (for the 3 bridge models). Among the 3 bridge models, the Roller model resulted in the least deck maximum acceleration (Table 2.6).

For the EPP-Gap model, Table 2.7 lists the column top maximum acceleration from the OpenSees and CSiBridge analyses. The maximum acceleration comparison of Table 2.7 is also presented in Bar Chart graphical form in Figures 2.10-2.13.

For the OpenSees model, the maximum displacements of Table 2.4 are also presented in graphical form against Peak Ground Acceleration (PGA) in Figures 2.14-2.19. The maximum acceleration is also shown graphically against PGA in Figure 2.20-Figure 2.25.

Table 2.4. OSB2 Column Top Maximum Displacement (OpenSees)

(The ESA longitudinal displacement demands are 2.6 in, 2.6 in and 2.5 in for Roller, EPP-Gap, EPP-Gap with Bearings models, respectively. The ESA transverse displacement demands are 1.1 in for all cases)

Motion	Longitudinal Input	Transverse Input	Longitudinal Displacement (in)			Transverse Displacement (in)		
			Roller	EPP-Gap	EPP-Gap with Bearings	Roller	EPP-Gap	EPP-Gap with Bearings
1	ROCKS1N1 (0.7g)	-	2.0	2.0	1.8	-	-	-
2	ROCKS1N2 (0.38g)	-	1.9	1.9	1.6	-	-	-
3	ROCKS1N3 (0.32g)	-	1.7	1.7	1.5	-	-	-
4	ROCKS1N4 (0.34g)	-	1.4	1.4	1.4	-	-	-
5	ROCKS1N5 (0.53g)	-	2.1	2.1	2.1	-	-	-
6	ROCKS1N6 (0.42g)	-	2.1	2.1	1.8	-	-	-
7	ROCKS1N7 (0.36g)	-	1.6	1.6	1.5	-	-	-
8	ROCKS1P1 (0.71g)	-	2.1	2.1	1.9	-	-	-
9	ROCKS1P2 (0.44g)	-	2.2	2.2	1.8	-	-	-
10	ROCKS1P3 (0.48g)	-	1.8	1.8	1.9	-	-	-
11	ROCKS1P4 (0.32g)	-	1.4	1.4	1.4	-	-	-
12	ROCKS1P5 (0.67g)	-	1.9	1.9	1.9	-	-	-
13	ROCKS1P6 (0.41g)	-	2.0	2.0	1.8	-	-	-
14	ROCKS1P7 (0.4g)	-	1.9	1.9	1.5	-	-	-
15	SANDS1N1 (0.61g)	-	5.4	4.0	3.3	-	-	-
16	SANDS1N2 (0.51g)	-	4.2	3.2	2.9	-	-	-
17	SANDS1N3 (0.57g)	-	3.1	2.6	2.3	-	-	-
18	SANDS1N4 (0.96g)	-	4.4	3.6	3.0	-	-	-
19	SANDS1N5 (0.79g)	-	4.2	3.3	3.2	-	-	-
20	SANDS1N6 (0.67g)	-	4.1	3.4	3.0	-	-	-
21	SANDS1N7 (0.58g)	-	4.2	3.4	2.6	-	-	-
22	ROCKN1N1N (0.4g)	ROCKN1N1P (0.58g)	1.7	1.7	1.5	4.1	3.3	2.7
23	ROCKN1P1N (1.42g)	ROCKN1P1P (1.42g)	1.7	1.8	1.6	2.6	2.6	2.2
24	SANDN1N1N (0.78g)	SANDN1N1P (0.81g)	4.3	3.6	2.9	3.6	3.6	3.7
25	CLAYN1N1N (0.79g)	CLAYN1N1P (0.71g)	4.7	3.7	3.1	5.8	5.5	4.2
26	-	ROCKS1N1 (0.7g)	-	-	-	2.8	2.6	2.3
27	-	ROCKS1N2 (0.38g)	-	-	-	3.2	2.8	2.4
28	-	ROCKS1N3 (0.32g)	-	-	-	3.2	2.9	2.5
29	-	ROCKS1N4 (0.34g)	-	-	-	2.5	2.3	2.1
30	-	ROCKS1N5 (0.53g)	-	-	-	3.1	2.7	2.3
31	-	ROCKS1N6 (0.42g)	-	-	-	2.9	2.5	2.4
32	-	ROCKS1N7 (0.36g)	-	-	-	3.1	2.9	2.5
33	-	ROCKS1P1 (0.71g)	-	-	-	2.7	2.5	2.3
34	-	ROCKS1P2 (0.44g)	-	-	-	3.8	3.2	2.2
35	-	ROCKS1P3 (0.48g)	-	-	-	2.7	2.7	2.4
36	-	ROCKS1P4 (0.32g)	-	-	-	2.4	2.3	2.0
37	-	ROCKS1P5 (0.67g)	-	-	-	2.8	2.6	2.4
38	-	ROCKS1P6 (0.41g)	-	-	-	2.9	2.5	2.4
39	-	ROCKS1P7 (0.4g)	-	-	-	3.6	3.2	2.4
40	-	SANDS1N1 (0.61g)	-	-	-	7.0	6.0	3.8
41	-	SANDS1N2 (0.51g)	-	-	-	5.4	4.8	3.6
42	-	SANDS1N3 (0.57g)	-	-	-	4.4	3.5	3.4
43	-	SANDS1N4 (0.96g)	-	-	-	5.9	5.1	3.4
44	-	SANDS1N5 (0.79g)	-	-	-	5.3	4.5	3.9
45	-	SANDS1N6 (0.67g)	-	-	-	4.9	4.3	3.4
46	-	SANDS1N7 (0.58g)	-	-	-	5.7	4.9	3.1
47	ROCKN1N1P (0.58g)	ROCKN1N1N (0.4g)	1.9	1.9	1.6	2.5	2.3	2.4
48	ROCKN1P1P (1.42g)	ROCKN1P1N (1.42g)	1.7	1.8	1.6	2.6	2.6	2.2
49	SANDN1N1P (0.81g)	SANDN1N1N (0.78g)	2.4	2.3	2.4	5.9	5.5	4.3
50	CLAYN1N1P (0.71g)	CLAYN1N1N (0.79g)	4.5	3.8	3.6	5.9	5.2	4.3

Table 2.5. OSB2 Column Top Maximum Displacement for EPP-Gap Model (Comparison of OpenSees and CSiBridge)

(The ESA longitudinal displacement demand is 2.6 in and the ESA transverse displacement demand is 1.1 in; Difference is relative to OpenSees result)

Motion	Longitudinal Input	Transverse Input	Longitudinal Displacement (in)			Transverse Displacement (in)		
			OpenSees	CSiBridge	Difference	OpenSees	CSiBridge	Difference
1	ROCKS1N1 (0.7g)	-	2.0	1.8	-9%	-	-	-
2	ROCKS1N2 (0.38g)	-	1.9	1.9	1%	-	-	-
3	ROCKS1N3 (0.32g)	-	1.7	1.5	-10%	-	-	-
4	ROCKS1N4 (0.34g)	-	1.4	1.3	-4%	-	-	-
5	ROCKS1N5 (0.53g)	-	2.1	1.9	-11%	-	-	-
6	ROCKS1N6 (0.42g)	-	2.1	1.7	-20%	-	-	-
7	ROCKS1N7 (0.36g)	-	1.6	1.4	-10%	-	-	-
8	ROCKS1P1 (0.71g)	-	2.1	1.9	-12%	-	-	-
9	ROCKS1P2 (0.44g)	-	2.2	2.1	-5%	-	-	-
10	ROCKS1P3 (0.48g)	-	1.8	1.6	-9%	-	-	-
11	ROCKS1P4 (0.32g)	-	1.4	1.3	-10%	-	-	-
12	ROCKS1P5 (0.67g)	-	1.9	1.9	0%	-	-	-
13	ROCKS1P6 (0.41g)	-	2.0	1.7	-17%	-	-	-
14	ROCKS1P7 (0.4g)	-	1.9	1.7	-8%	-	-	-
15	SANDS1N1 (0.61g)	-	4.0	3.0	-24%	-	-	-
16	SANDS1N2 (0.51g)	-	3.2	2.6	-19%	-	-	-
17	SANDS1N3 (0.57g)	-	2.6	2.1	-17%	-	-	-
18	SANDS1N4 (0.96g)	-	3.6	2.5	-29%	-	-	-
19	SANDS1N5 (0.79g)	-	3.3	2.6	-20%	-	-	-
20	SANDS1N6 (0.67g)	-	3.4	2.7	-22%	-	-	-
21	SANDS1N7 (0.58g)	-	3.4	2.2	-36%	-	-	-
22	ROCKN1N1N (0.4g)	ROCKN1N1P (0.58g)	1.7	1.3	-21%	3.3	2.5	-23%
23	ROCKN1P1N (1.42g)	ROCKN1P1P (1.42g)	1.8	1.5	-15%	2.6	2.0	-23%
24	SANDN1N1N (0.78g)	SANDN1N1P (0.81g)	3.6	2.6	-27%	3.6	3.3	-7%
25	CLAYN1N1N (0.79g)	CLAYN1N1P (0.71g)	3.7	2.5	-31%	5.5	3.6	-35%
26	-	ROCKS1N1 (0.7g)	-	-	-	2.6	2.2	-15%
27	-	ROCKS1N2 (0.38g)	-	-	-	2.8	2.3	-18%
28	-	ROCKS1N3 (0.32g)	-	-	-	2.9	2.3	-21%
29	-	ROCKS1N4 (0.34g)	-	-	-	2.3	1.8	-22%
30	-	ROCKS1N5 (0.53g)	-	-	-	2.7	1.9	-30%
31	-	ROCKS1N6 (0.42g)	-	-	-	2.5	2.0	-20%
32	-	ROCKS1N7 (0.36g)	-	-	-	2.9	2.2	-24%
33	-	ROCKS1P1 (0.71g)	-	-	-	2.5	2.1	-16%
34	-	ROCKS1P2 (0.44g)	-	-	-	3.2	2.6	-19%
35	-	ROCKS1P3 (0.48g)	-	-	-	2.7	2.2	-19%
36	-	ROCKS1P4 (0.32g)	-	-	-	2.3	1.9	-17%
37	-	ROCKS1P5 (0.67g)	-	-	-	2.6	2.1	-19%
38	-	ROCKS1P6 (0.41g)	-	-	-	2.5	2.0	-20%
39	-	ROCKS1P7 (0.4g)	-	-	-	3.2	2.1	-34%
40	-	SANDS1N1 (0.61g)	-	-	-	6.0	3.0	-50%
41	-	SANDS1N2 (0.51g)	-	-	-	4.8	3.0	-38%
42	-	SANDS1N3 (0.57g)	-	-	-	3.5	3.1	-11%
43	-	SANDS1N4 (0.96g)	-	-	-	5.1	3.0	-41%
44	-	SANDS1N5 (0.79g)	-	-	-	4.5	3.2	-29%
45	-	SANDS1N6 (0.67g)	-	-	-	4.3	3.1	-28%
46	-	SANDS1N7 (0.58g)	-	-	-	4.9	2.9	-41%
47	ROCKN1N1P (0.58g)	ROCKN1N1N (0.4g)	1.9	1.7	-11%	2.3	2.2	-4%
48	ROCKN1P1P (1.42g)	ROCKN1P1N (1.42g)	1.8	1.5	-17%	2.6	2.0	-23%
49	SANDN1N1P (0.81g)	SANDN1N1N (0.78g)	2.3	2.1	-9%	5.5	3.6	-35%
50	CLAYN1N1P (0.71g)	CLAYN1N1N (0.79g)	3.8	3.1	-18%	5.2	3.7	-29%

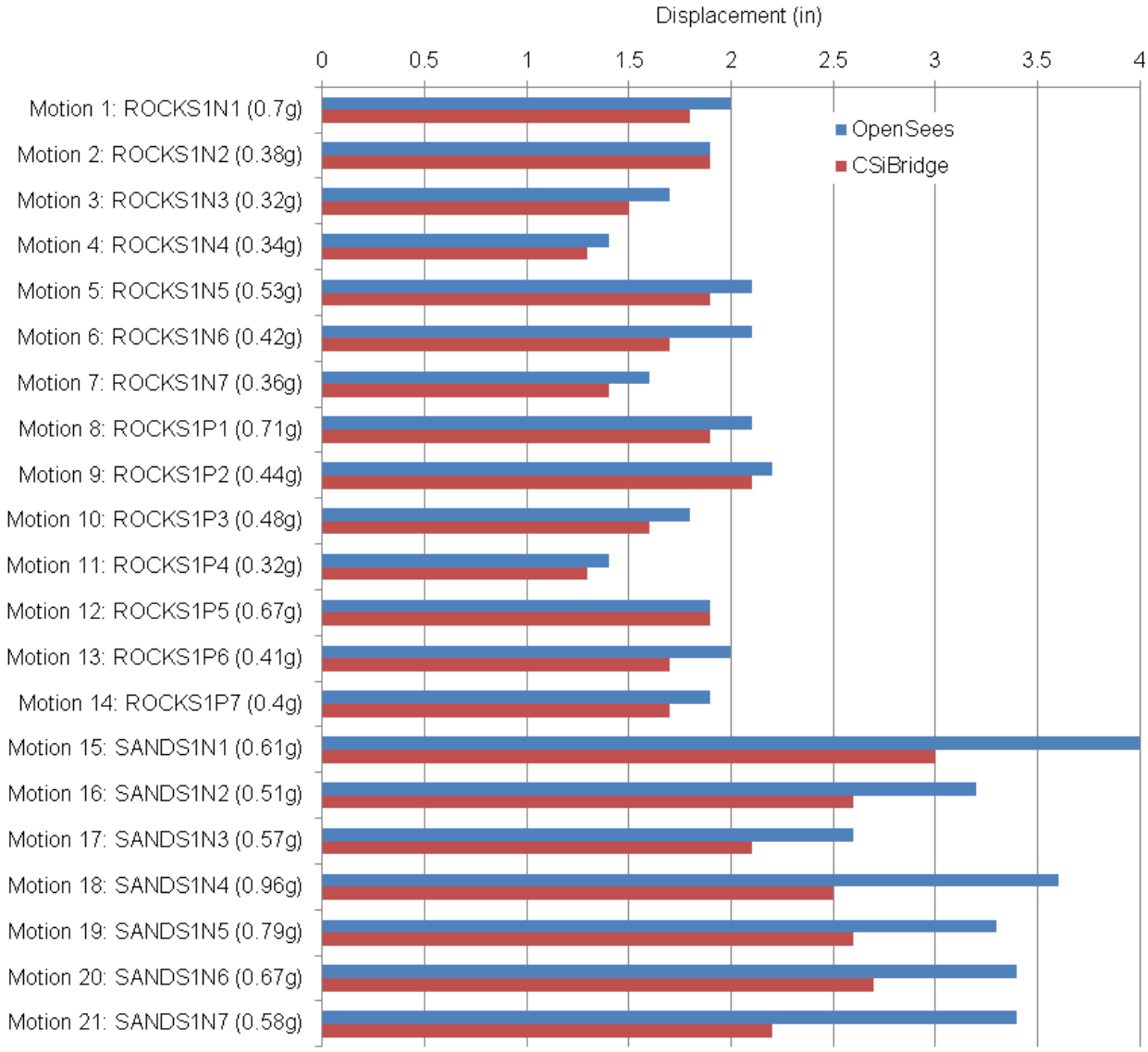

Figure 2.6 OSB2 column top maximum lonitudinal displacement for Motions 1-21 (EPP-Gap model)

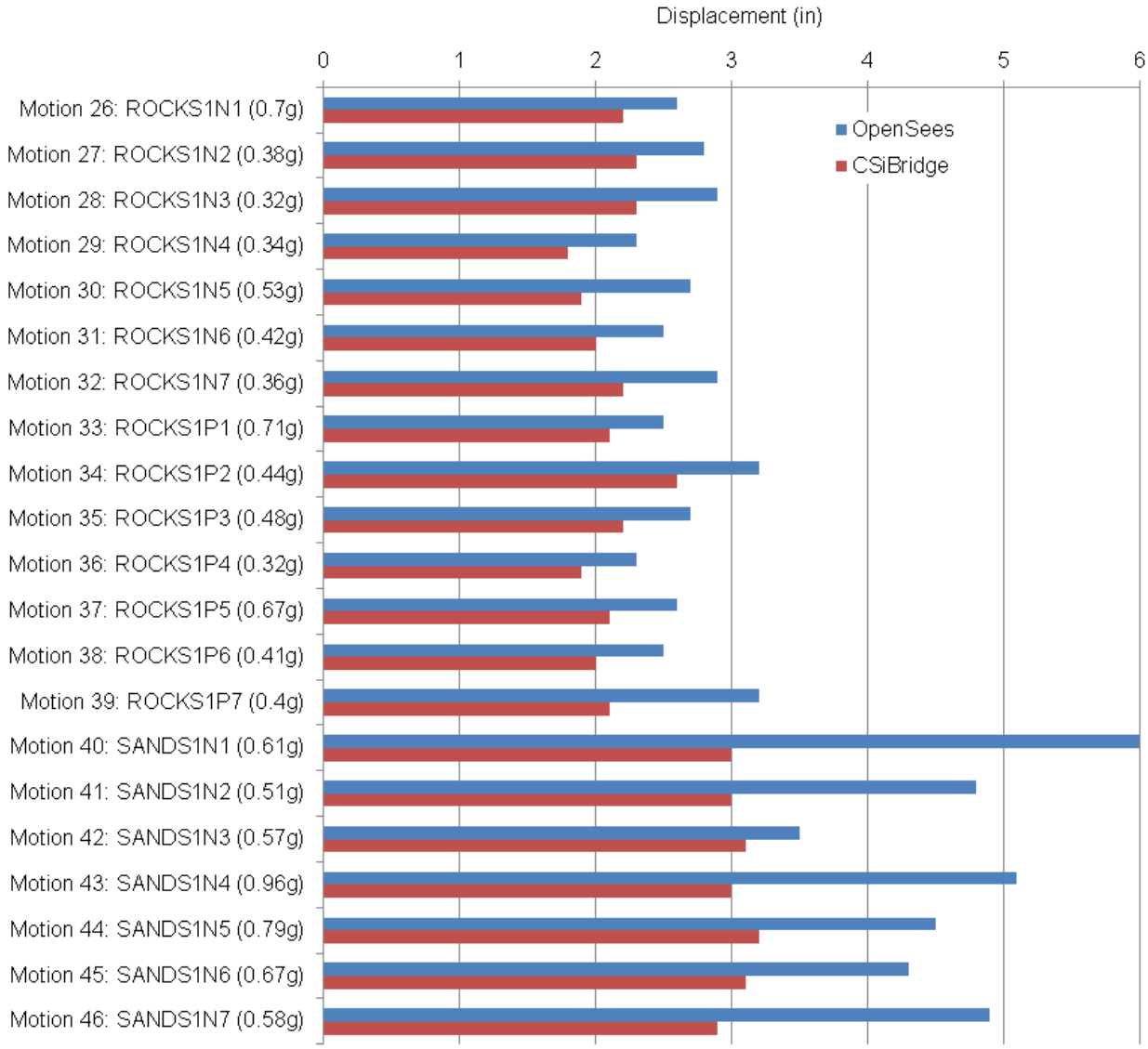

Figure 2.7 OSB2 column top maximum transverse displacement for Motions 26-46 (EPP-Gap model)

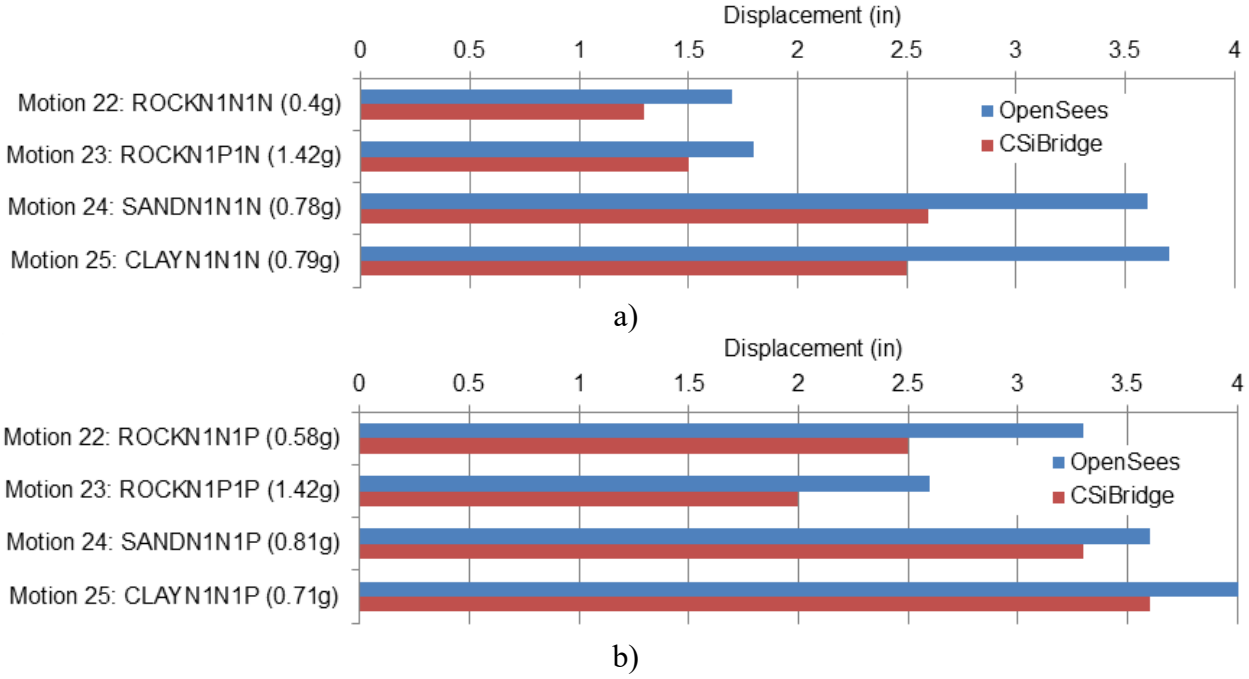

Figure 2.8 OSB2 column top maximum displacement for Motions 22-25 (EPP-Gap model): a) Lonitudinal direction; b) Transverse direction

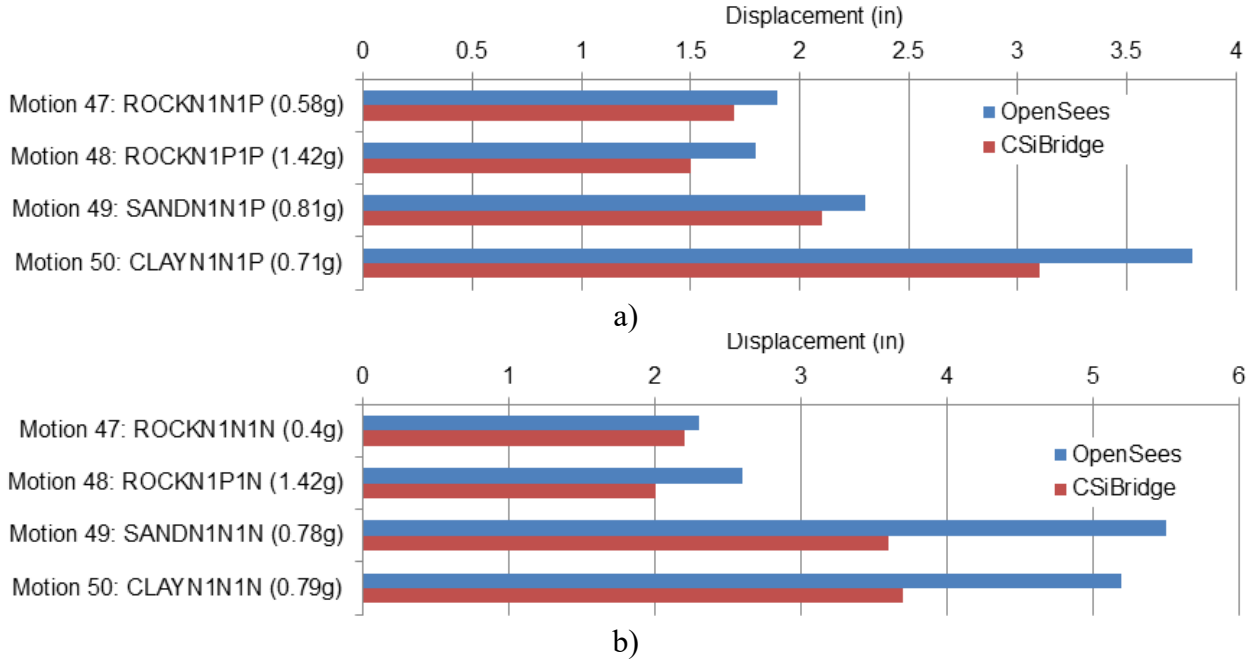

Figure 2.9 OSB2 column top maximum displacement for Motions 47-50 (EPP-Gap model): a) Lonitudinal direction; b) Transverse direction

Table 2.6. OSB2 Deck Maximum Acceleration (OpenSees)

Motion	Longitudinal Input	Transverse Input	Longitudinal Acceleration (g)			Transverse Acceleration (g)		
			Roller	EPP-Gap	EPP-Gap with Bearings	Roller	EPP-Gap	EPP-Gap with Bearings
1	ROCKS1N1 (0.7g)	-	0.57	0.70	0.67	-	-	-
2	ROCKS1N2 (0.38g)	-	0.51	0.38	0.56	-	-	-
3	ROCKS1N3 (0.32g)	-	0.49	0.32	0.53	-	-	-
4	ROCKS1N4 (0.34g)	-	0.49	0.34	0.55	-	-	-
5	ROCKS1N5 (0.53g)	-	0.57	0.53	0.66	-	-	-
6	ROCKS1N6 (0.42g)	-	0.52	0.42	0.57	-	-	-
7	ROCKS1N7 (0.36g)	-	0.49	0.36	0.56	-	-	-
8	ROCKS1P1 (0.71g)	-	0.56	0.71	0.66	-	-	-
9	ROCKS1P2 (0.44g)	-	0.53	0.44	0.58	-	-	-
10	ROCKS1P3 (0.48g)	-	0.54	0.48	0.63	-	-	-
11	ROCKS1P4 (0.32g)	-	0.49	0.32	0.56	-	-	-
12	ROCKS1P5 (0.67g)	-	0.55	0.67	0.62	-	-	-
13	ROCKS1P6 (0.41g)	-	0.53	0.41	0.59	-	-	-
14	ROCKS1P7 (0.4g)	-	0.51	0.40	0.53	-	-	-
15	SANDS1N1 (0.61g)	-	0.67	0.61	1.09	-	-	-
16	SANDS1N2 (0.51g)	-	0.61	0.51	0.95	-	-	-
17	SANDS1N3 (0.57g)	-	0.53	0.57	0.68	-	-	-
18	SANDS1N4 (0.96g)	-	0.69	0.96	1.11	-	-	-
19	SANDS1N5 (0.79g)	-	0.60	0.79	1.08	-	-	-
20	SANDS1N6 (0.67g)	-	0.67	0.67	1.06	-	-	-
21	SANDS1N7 (0.58g)	-	0.65	0.58	0.89	-	-	-
22	ROCKN1N1N (0.4g)	ROCKN1N1P (0.58g)	0.39	0.39	0.45	0.62	0.69	0.74
23	ROCKN1P1N (1.42g)	ROCKN1P1P (1.42g)	0.50	0.51	0.56	0.58	0.64	0.62
24	SANDN1N1N (0.78g)	SANDN1N1P (0.81g)	0.58	1.01	0.97	0.72	0.91	1.09
25	CLAYN1N1N (0.79g)	CLAYN1N1P (0.71g)	0.56	0.99	0.97	0.74	0.80	1.05
26	-	ROCKS1N1 (0.7g)	-	-	-	0.72	0.75	0.85
27	-	ROCKS1N2 (0.38g)	-	-	-	0.68	0.71	0.78
28	-	ROCKS1N3 (0.32g)	-	-	-	0.62	0.68	0.73
29	-	ROCKS1N4 (0.34g)	-	-	-	0.51	0.57	0.63
30	-	ROCKS1N5 (0.53g)	-	-	-	0.63	0.66	0.68
31	-	ROCKS1N6 (0.42g)	-	-	-	0.56	0.59	0.84
32	-	ROCKS1N7 (0.36g)	-	-	-	0.56	0.64	0.73
33	-	ROCKS1P1 (0.71g)	-	-	-	0.70	0.75	0.83
34	-	ROCKS1P2 (0.44g)	-	-	-	0.68	0.72	0.70
35	-	ROCKS1P3 (0.48g)	-	-	-	0.57	0.60	0.72
36	-	ROCKS1P4 (0.32g)	-	-	-	0.55	0.56	0.66
37	-	ROCKS1P5 (0.67g)	-	-	-	0.61	0.76	0.75
38	-	ROCKS1P6 (0.41g)	-	-	-	0.55	0.59	0.83
39	-	ROCKS1P7 (0.4g)	-	-	-	0.61	0.67	0.69
40	-	SANDS1N1 (0.61g)	-	-	-	0.82	0.83	0.87
41	-	SANDS1N2 (0.51g)	-	-	-	0.78	0.81	0.90
42	-	SANDS1N3 (0.57g)	-	-	-	0.59	0.68	0.91
43	-	SANDS1N4 (0.96g)	-	-	-	0.81	0.81	0.90
44	-	SANDS1N5 (0.79g)	-	-	-	0.74	0.79	0.98
45	-	SANDS1N6 (0.67g)	-	-	-	0.74	0.75	0.88
46	-	SANDS1N7 (0.58g)	-	-	-	0.70	0.77	0.82
47	ROCKN1N1P (0.58g)	ROCKN1N1N (0.4g)	0.40	0.40	0.43	0.47	0.55	0.71
48	ROCKN1P1P (1.42g)	ROCKN1P1N (1.42g)	0.50	0.51	0.56	0.58	0.64	0.62
49	SANDN1N1P (0.81g)	SANDN1N1N (0.78g)	0.63	0.66	0.84	0.72	0.75	0.89
50	CLAYN1N1P (0.71g)	CLAYN1N1N (0.79g)	0.61	1.04	1.12	0.63	0.72	0.87

Table 2.7. OSB2 Deck Maximum Acceleration for EPP-Gap Model (Comparison of OpenSees and CSiBridge)

(Difference is relative to OpenSees result)

Motion	Longitudinal Input	Transverse Input	Longitudinal Acceleration (g)			Transverse Acceleration (g)		
			OpenSees	CSiBridge	Difference	OpenSees	CSiBridge	Difference
1	ROCKS1N1 (0.7g)	-	0.70	0.69	-1%	-	-	-
2	ROCKS1N2 (0.38g)	-	0.38	0.55	45%	-	-	-
3	ROCKS1N3 (0.32g)	-	0.32	0.50	56%	-	-	-
4	ROCKS1N4 (0.34g)	-	0.34	0.49	44%	-	-	-
5	ROCKS1N5 (0.53g)	-	0.53	0.59	11%	-	-	-
6	ROCKS1N6 (0.42g)	-	0.42	0.58	37%	-	-	-
7	ROCKS1N7 (0.36g)	-	0.36	0.51	41%	-	-	-
8	ROCKS1P1 (0.71g)	-	0.71	0.69	-3%	-	-	-
9	ROCKS1P2 (0.44g)	-	0.44	0.60	36%	-	-	-
10	ROCKS1P3 (0.48g)	-	0.48	0.54	12%	-	-	-
11	ROCKS1P4 (0.32g)	-	0.32	0.47	46%	-	-	-
12	ROCKS1P5 (0.67g)	-	0.67	0.62	7%	-	-	-
13	ROCKS1P6 (0.41g)	-	0.41	0.56	37%	-	-	-
14	ROCKS1P7 (0.4g)	-	0.40	0.55	38%	-	-	-
15	SANDS1N1 (0.61g)	-	0.61	1.12	84%	-	-	-
16	SANDS1N2 (0.51g)	-	0.51	0.90	76%	-	-	-
17	SANDS1N3 (0.57g)	-	0.57	0.67	18%	-	-	-
18	SANDS1N4 (0.96g)	-	0.96	1.06	11%	-	-	-
19	SANDS1N5 (0.79g)	-	0.79	0.97	23%	-	-	-
20	SANDS1N6 (0.67g)	-	0.67	1.05	57%	-	-	-
21	SANDS1N7 (0.58g)	-	0.58	0.77	33%	-	-	-
22	ROCKN1N1N (0.4g)	ROCKN1N1P (0.58g)	0.39	0.45	16%	0.69	0.65	-6%
23	ROCKN1P1N (1.42g)	ROCKN1P1P (1.42g)	0.51	0.52	1%	0.64	0.51	-20%
24	SANDN1N1N (0.78g)	SANDN1N1P (0.81g)	1.01	0.93	-8%	0.91	0.78	-14%
25	CLAYN1N1N (0.79g)	CLAYN1N1P (0.71g)	0.99	0.81	-18%	0.80	0.84	6%
26	-	ROCKS1N1 (0.7g)	-			0.75	0.60	-20%
27	-	ROCKS1N2 (0.38g)	-			0.71	0.62	-13%
28	-	ROCKS1N3 (0.32g)	-			0.68	0.60	-12%
29	-	ROCKS1N4 (0.34g)	-			0.57	0.51	-11%
30	-	ROCKS1N5 (0.53g)	-			0.66	0.52	-21%
31	-	ROCKS1N6 (0.42g)	-			0.59	0.55	-7%
32	-	ROCKS1N7 (0.36g)	-			0.64	0.60	-6%
33	-	ROCKS1P1 (0.71g)	-			0.75	0.58	-23%
34	-	ROCKS1P2 (0.44g)	-			0.72	0.66	-8%
35	-	ROCKS1P3 (0.48g)	-			0.60	0.57	-5%
36	-	ROCKS1P4 (0.32g)	-			0.56	0.51	-9%
37	-	ROCKS1P5 (0.67g)	-			0.76	0.55	-28%
38	-	ROCKS1P6 (0.41g)	-			0.59	0.55	-7%
39	-	ROCKS1P7 (0.4g)	-			0.67	0.55	-18%
40	-	SANDS1N1 (0.61g)	-			0.83	0.73	-12%
41	-	SANDS1N2 (0.51g)	-			0.81	0.77	-5%
42	-	SANDS1N3 (0.57g)	-			0.68	0.83	22%
43	-	SANDS1N4 (0.96g)	-			0.81	0.76	-6%
44	-	SANDS1N5 (0.79g)	-			0.79	0.80	1%
45	-	SANDS1N6 (0.67g)	-			0.75	0.80	7%
46	-	SANDS1N7 (0.58g)	-			0.77	0.72	-6%
47	ROCKN1N1P (0.58g)	ROCKN1N1N (0.4g)	0.40	0.41	2%	0.55	0.58	5%
48	ROCKN1P1P (1.42g)	ROCKN1P1N (1.42g)	0.51	0.52	2%	0.64	0.51	-20%
49	SANDN1N1P (0.81g)	SANDN1N1N (0.78g)	0.66	0.77	17%	0.75	0.81	8%
50	CLAYN1N1P (0.71g)	CLAYN1N1N (0.79g)	1.04	1.03	-1%	0.72	0.79	10%

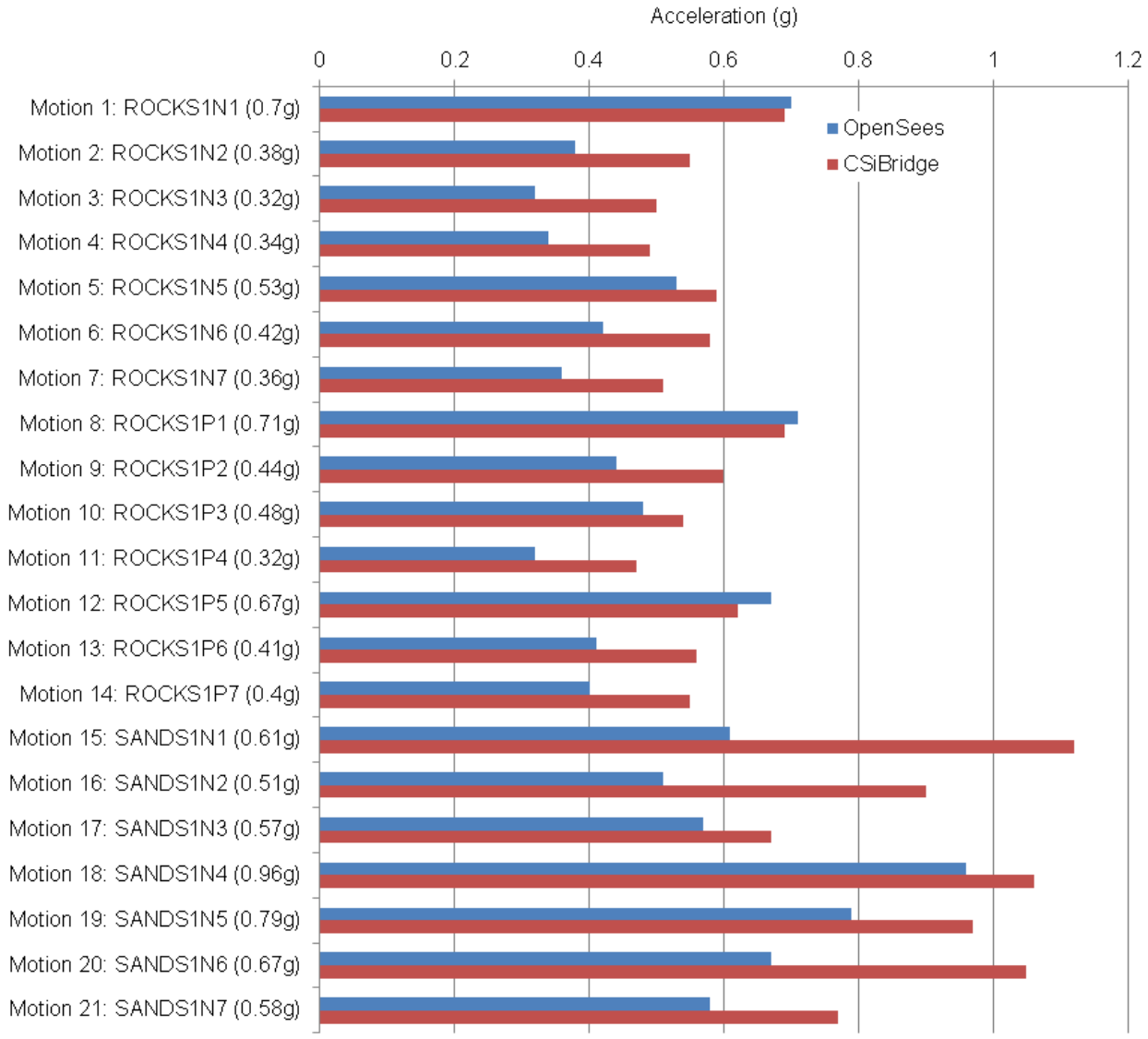

Figure 2.10 OSB2 deck maximum longituindal acceleration for Motions 1-21 (EPP-Gap model)

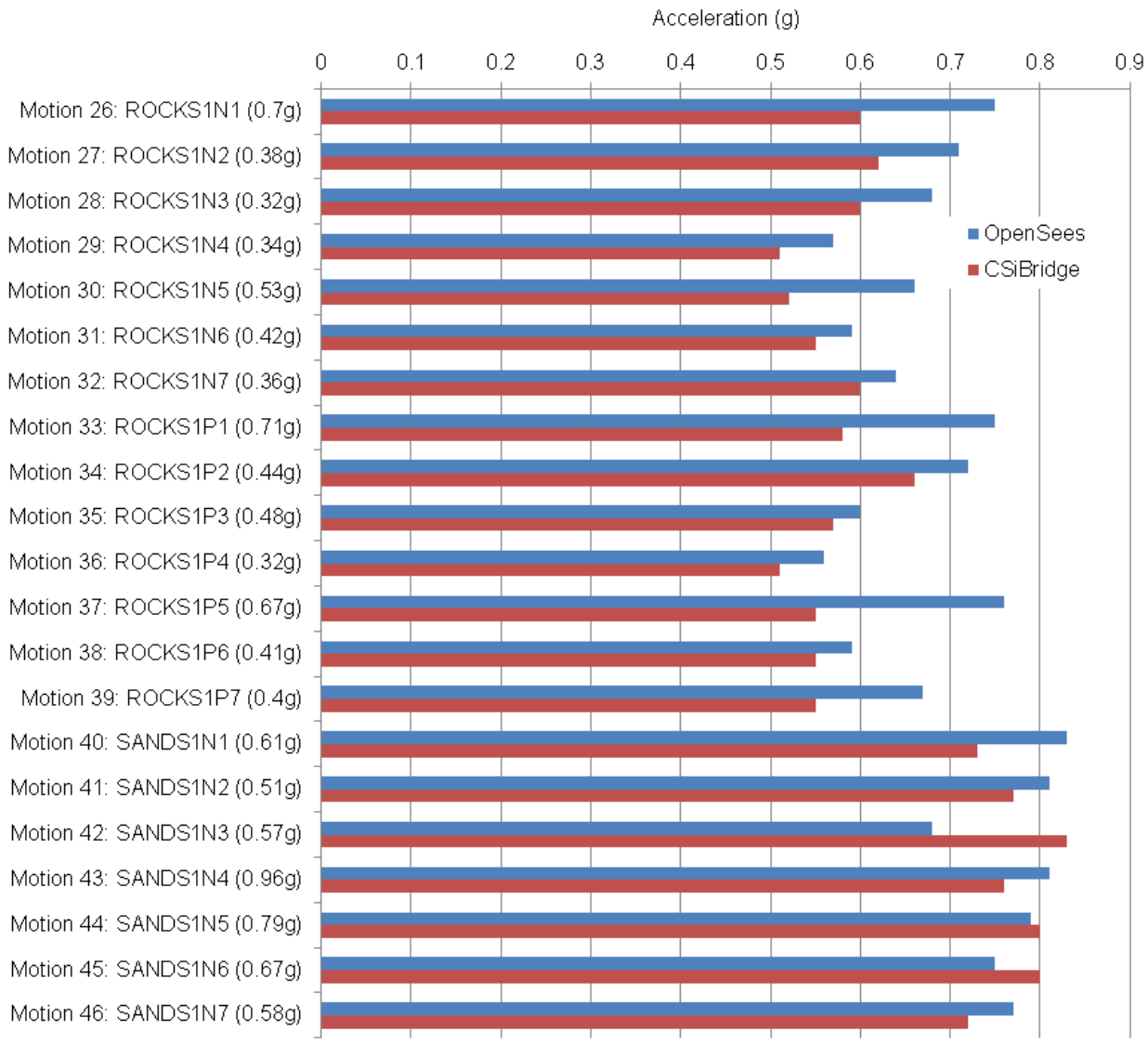

Figure 2.11 OSB2 deck maximum transverse acceleration for Motions 26-46 (EPP-Gap model)

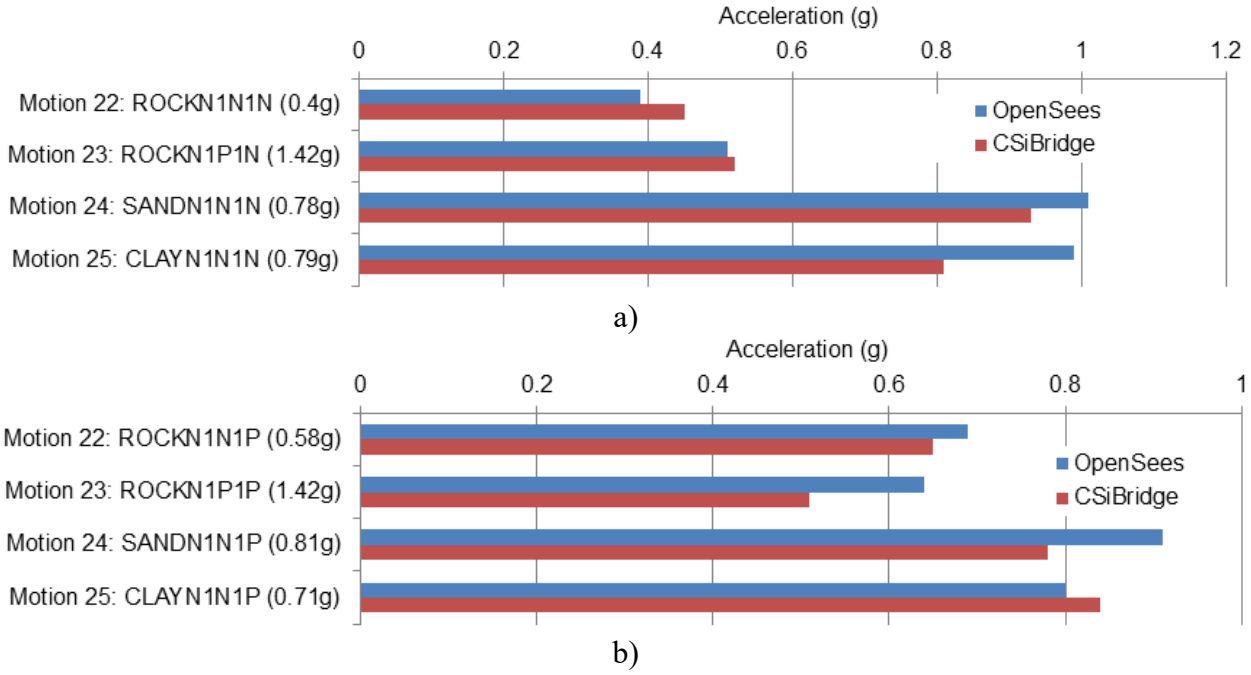

Figure 2.12 OSB2 deck maximum acceleration for Motions 22-25 (EPP-Gap model): a) Lonitudinal direction; b) Transverse direction

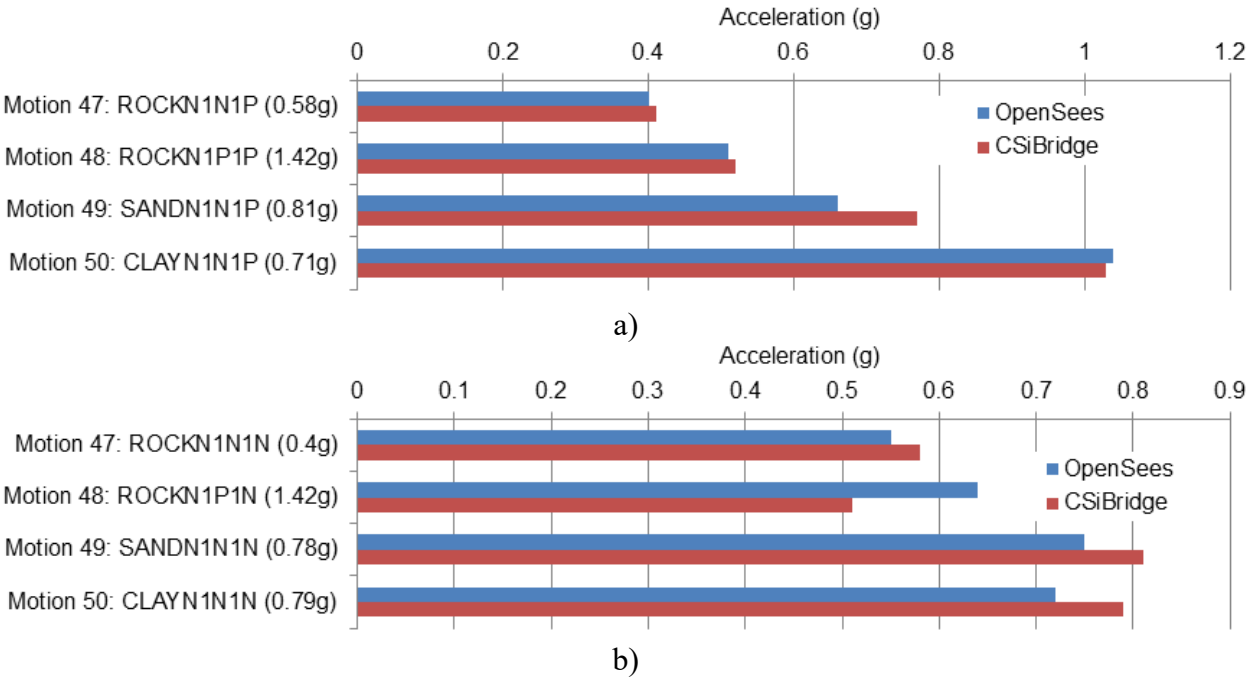

Figure 2.13 OSB2 deck maximum acceleration for Motions 47-50 (EPP-Gap model): a) Lonitudinal direction; b) Transverse direction

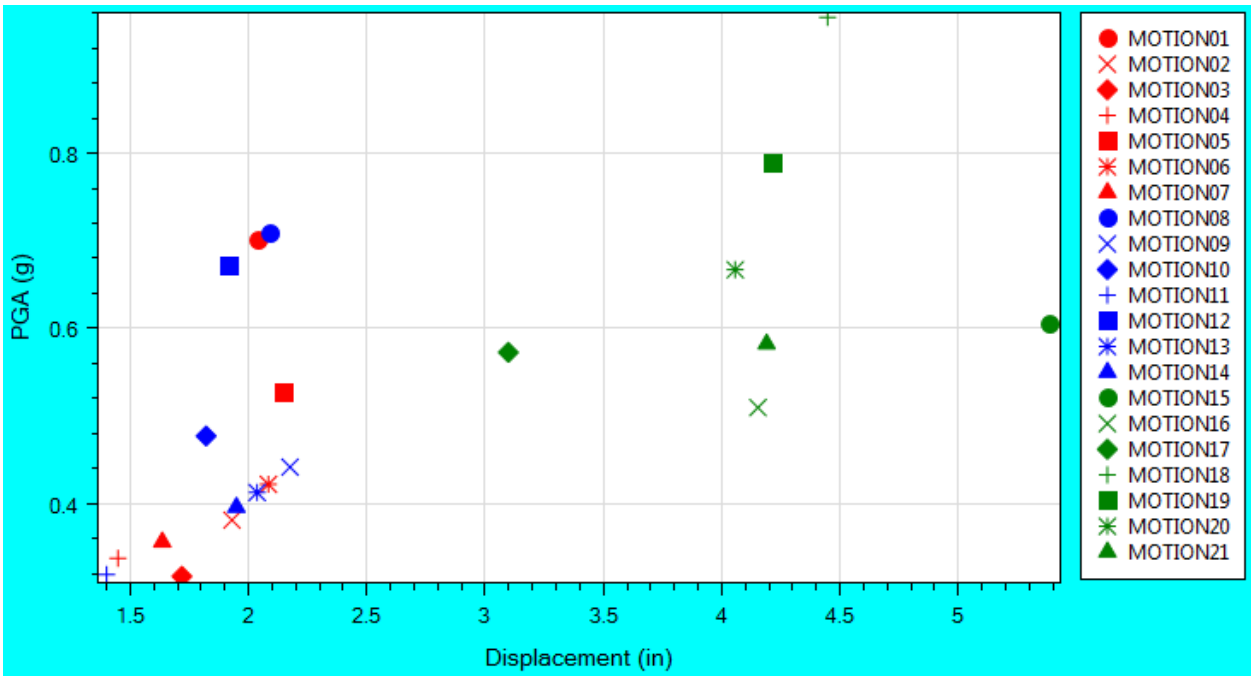

Figure 2.14 OSB2 column top maximum longitudinal displacement in OpenSees (Motions 1-21; Roller model)

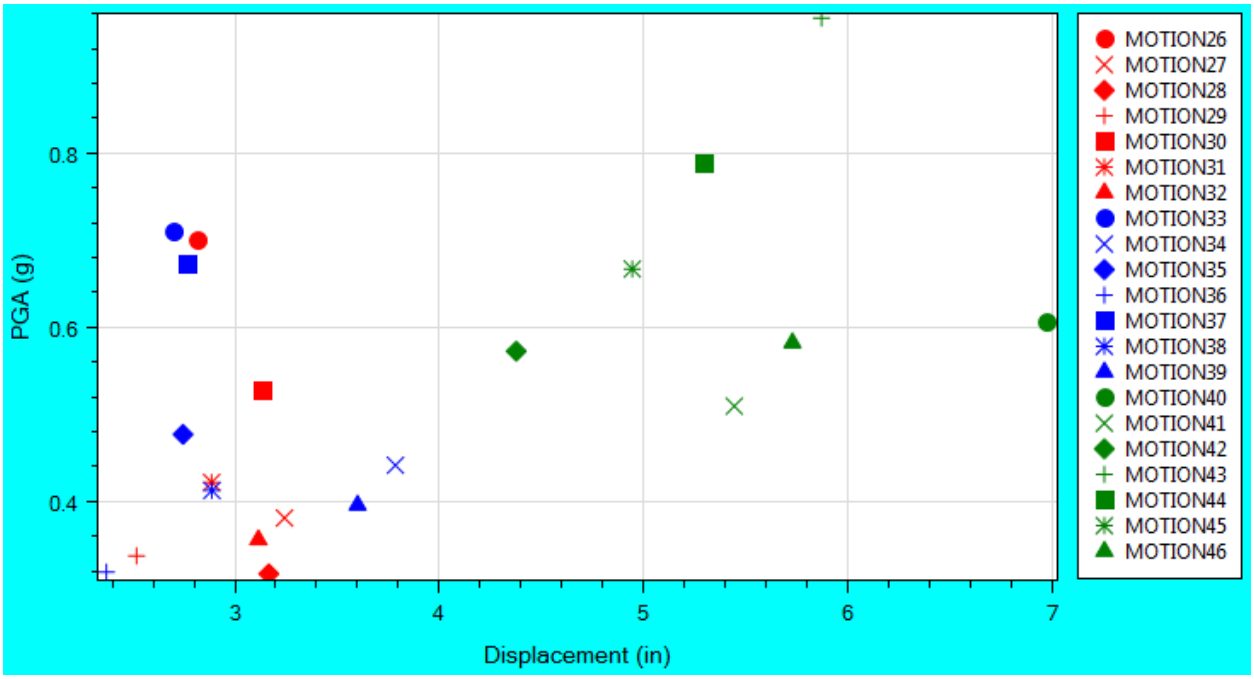

Figure 2.15 OSB2 column top maximum transverse displacement in OpenSees (Motions 26-46; Roller model)

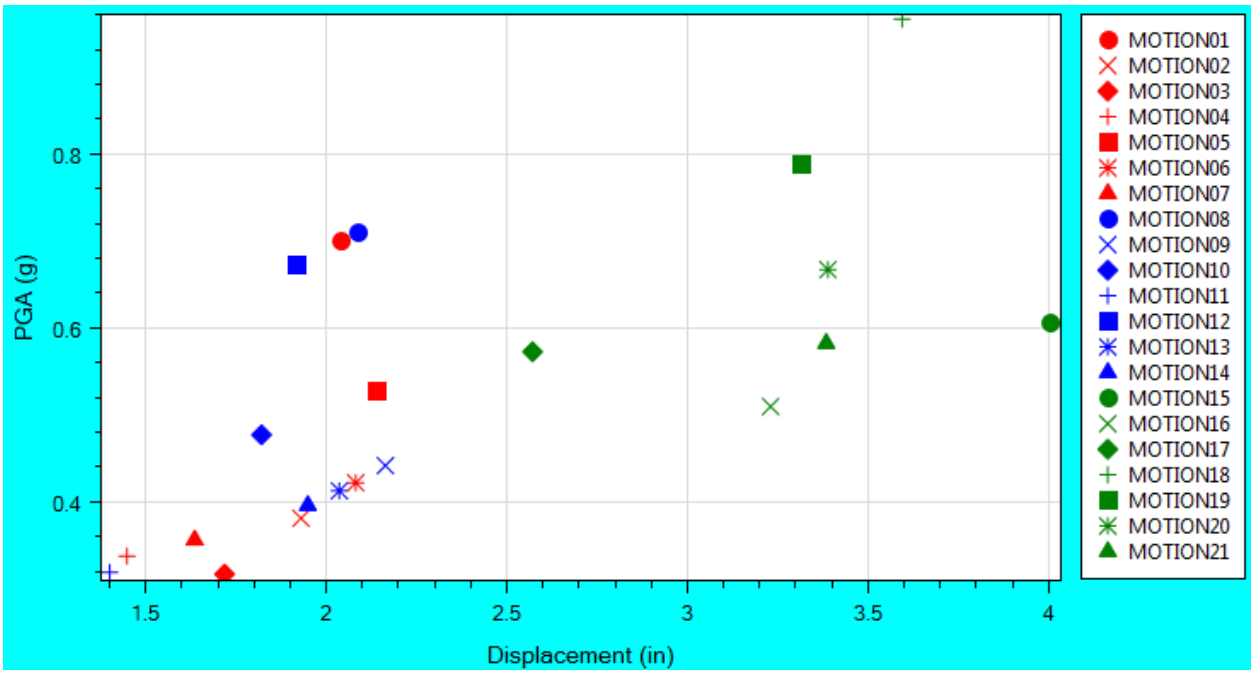

Figure 2.16 OSB2 column top maximum longitudinal displacement in OpenSees (Motions 1-21; EPP-Gap model)

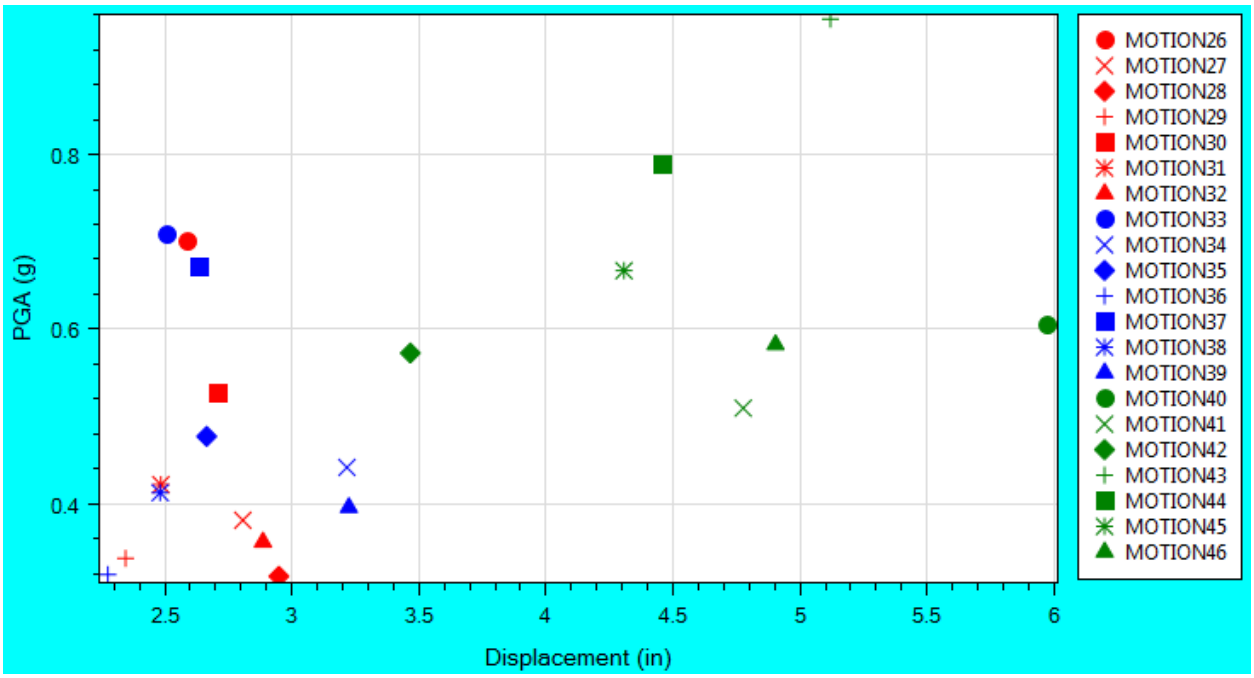

Figure 2.17 OSB2 column top maximum transverse displacement in OpenSees (Motions 26-46; EPP-Gap model)

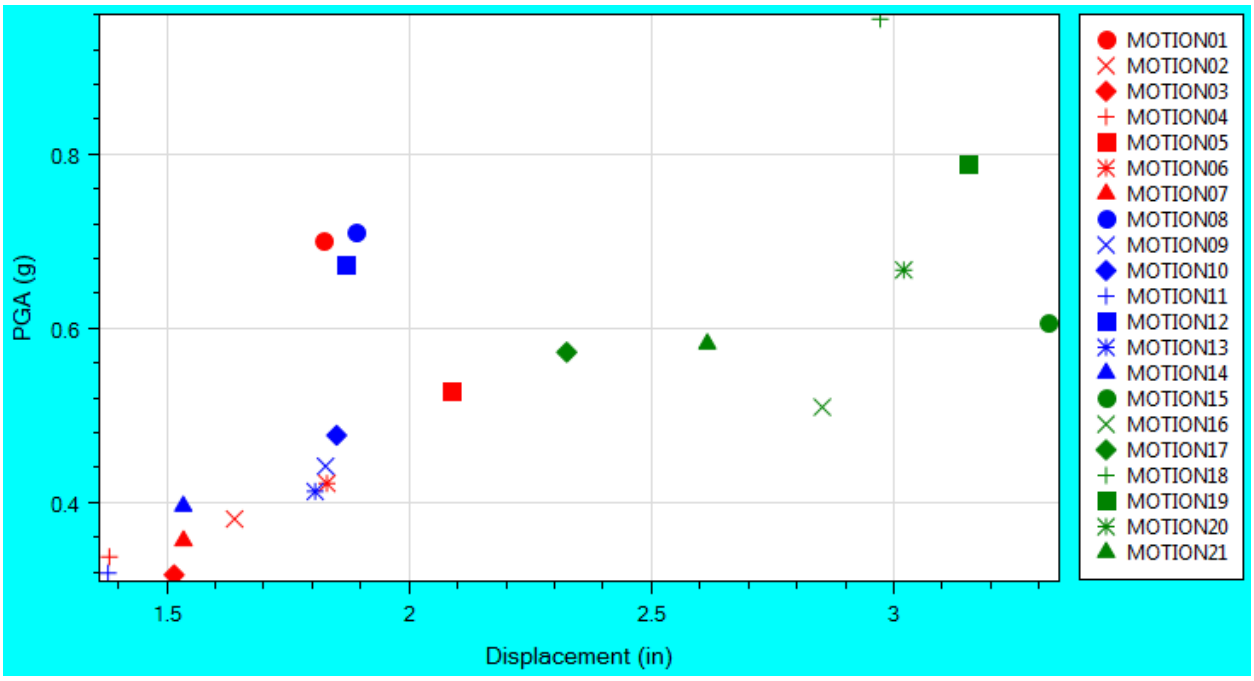

Figure 2.18 OSB2 column top maximum longitudinal displacement in OpenSees (Motions 1-21; EPP-Gap with Bearings model)

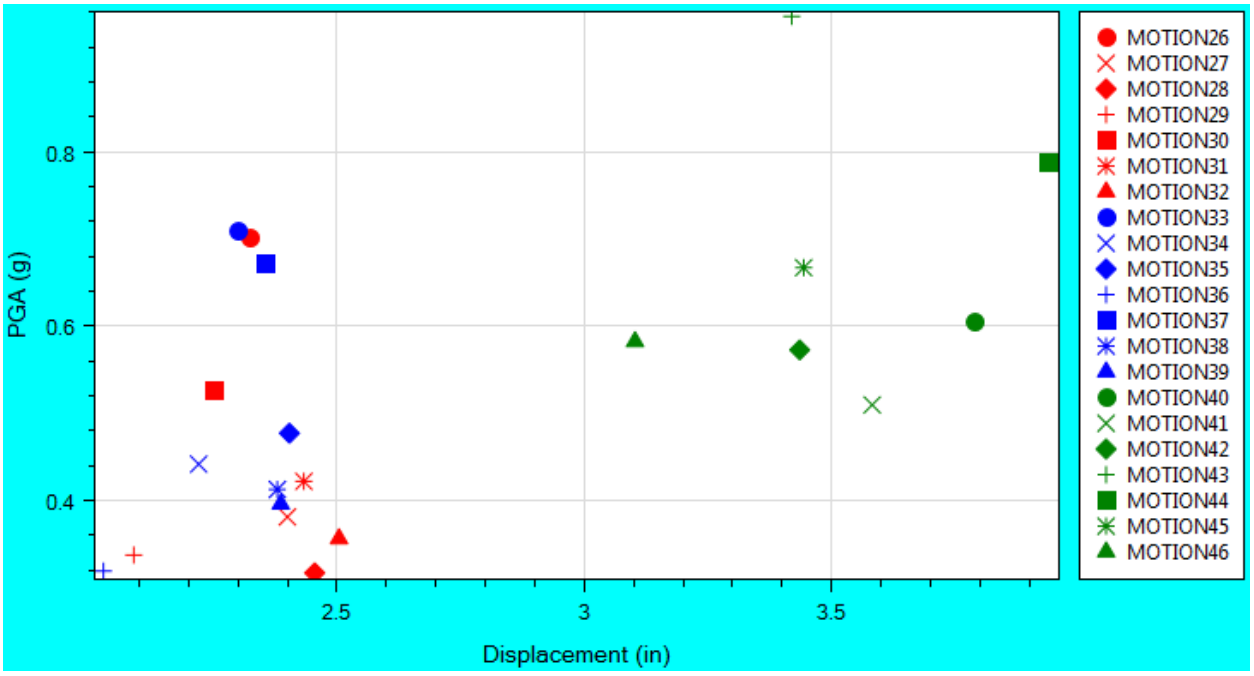

Figure 2.19 OSB2 column top maximum transverse displacement in OpenSees (Motions 26-46; EPP-Gap with Bearings model)

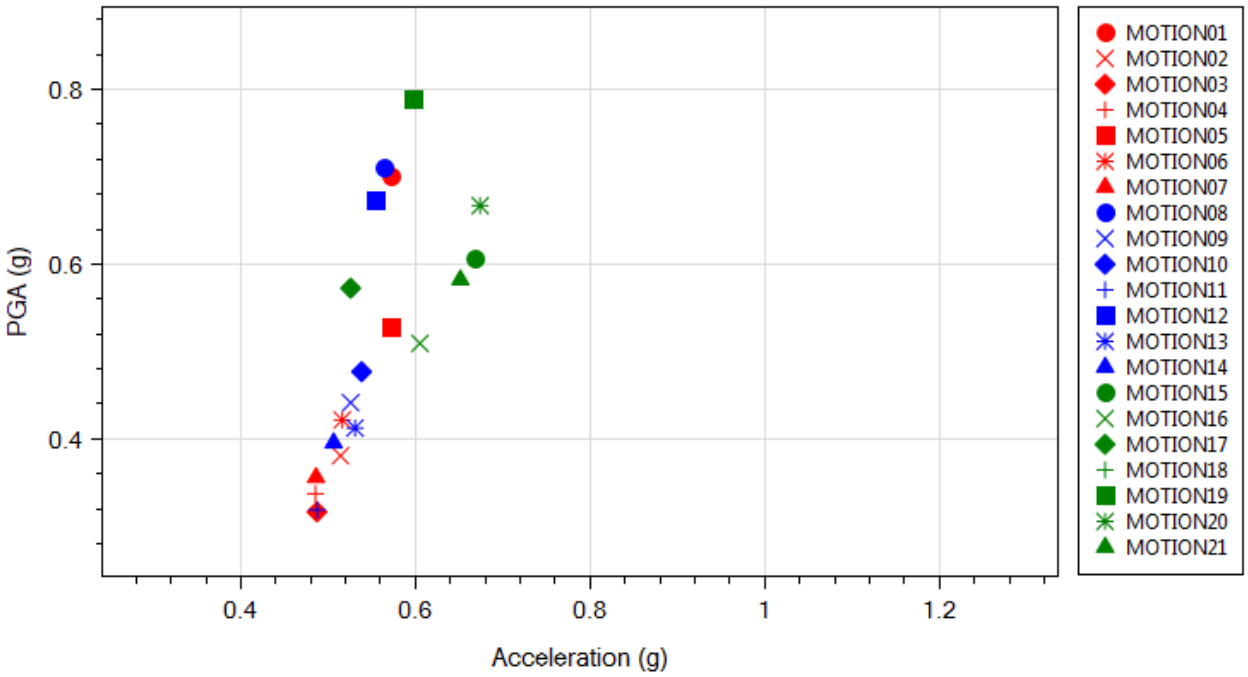

Figure 2.20 OSB2 deck maximum longitudinal acceleration in OpenSees (Motions 1-21; Roller model)

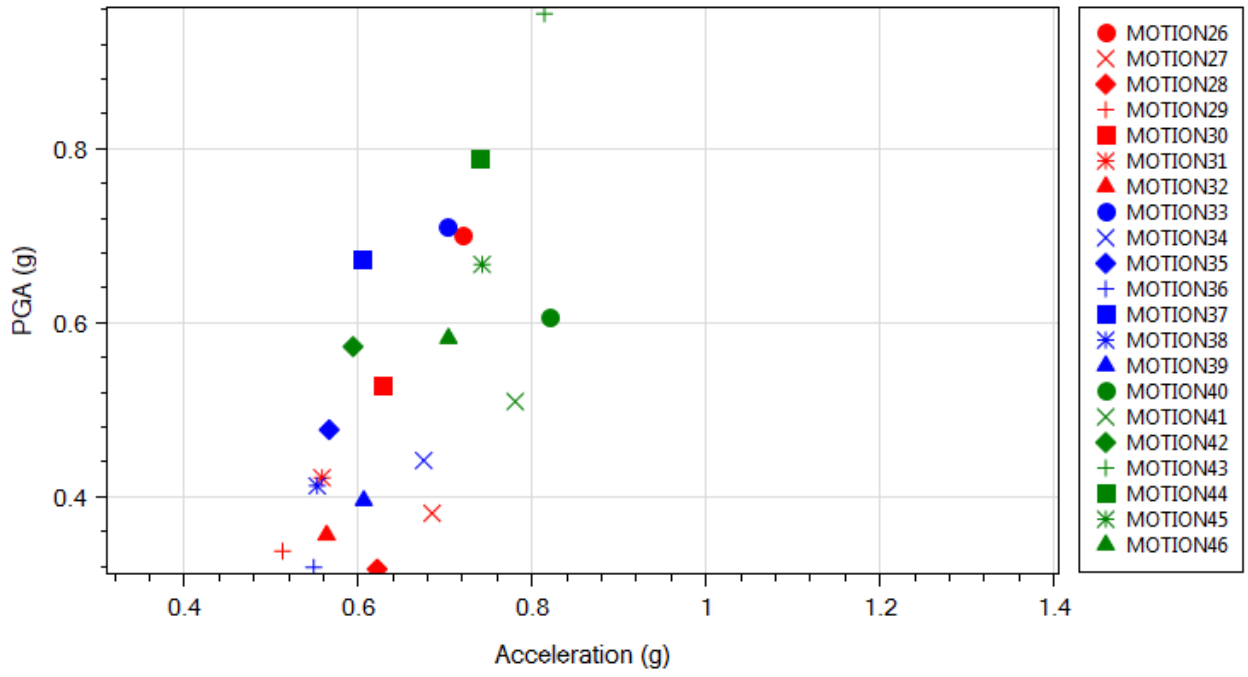

Figure 2.21 OSB2 deck maximum transverse acceleration in OpenSees (Motions 26-46; Roller model)

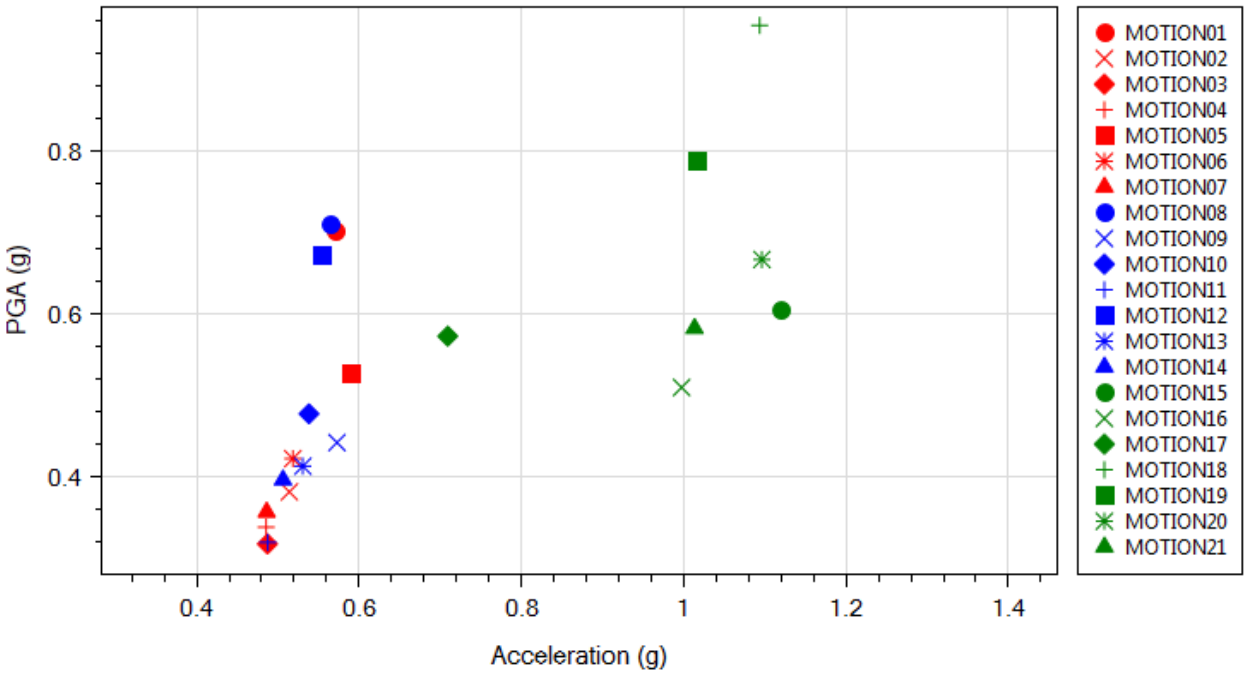

Figure 2.22 OSB2 deck maximum longitudinal acceleration in OpenSees (Motions 1-21; EPP-Gap model)

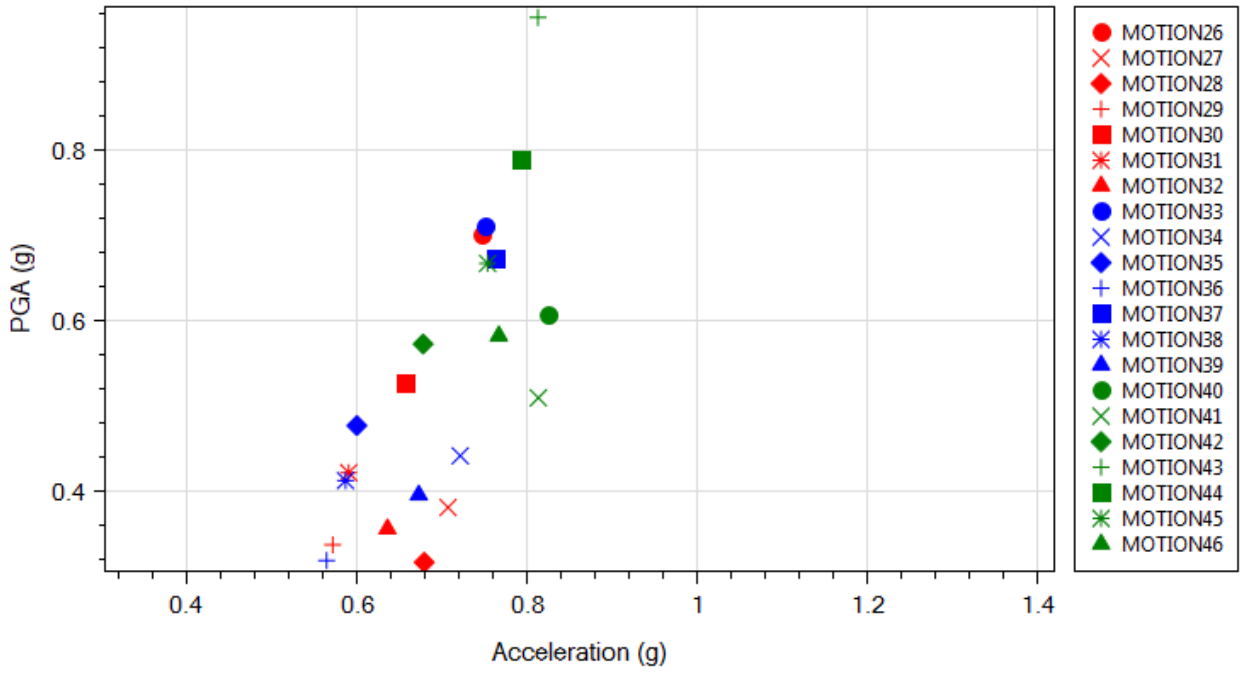

Figure 2.23 OSB2 deck maximum transverse acceleration in OpenSees (Motions 26-46; EPP-Gap model)

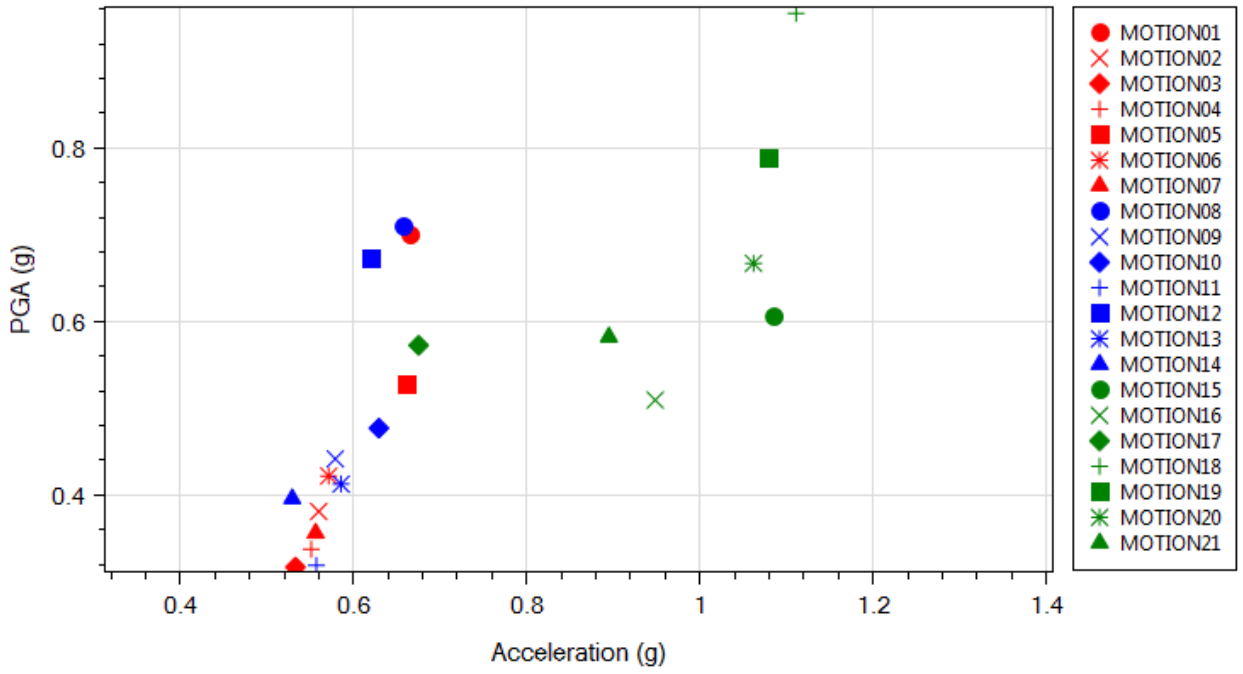

Figure 2.24 OSB2 deck maximum longitudinal acceleration in OpenSees (Motions 1-21; EPP-Gap with Bearings model)

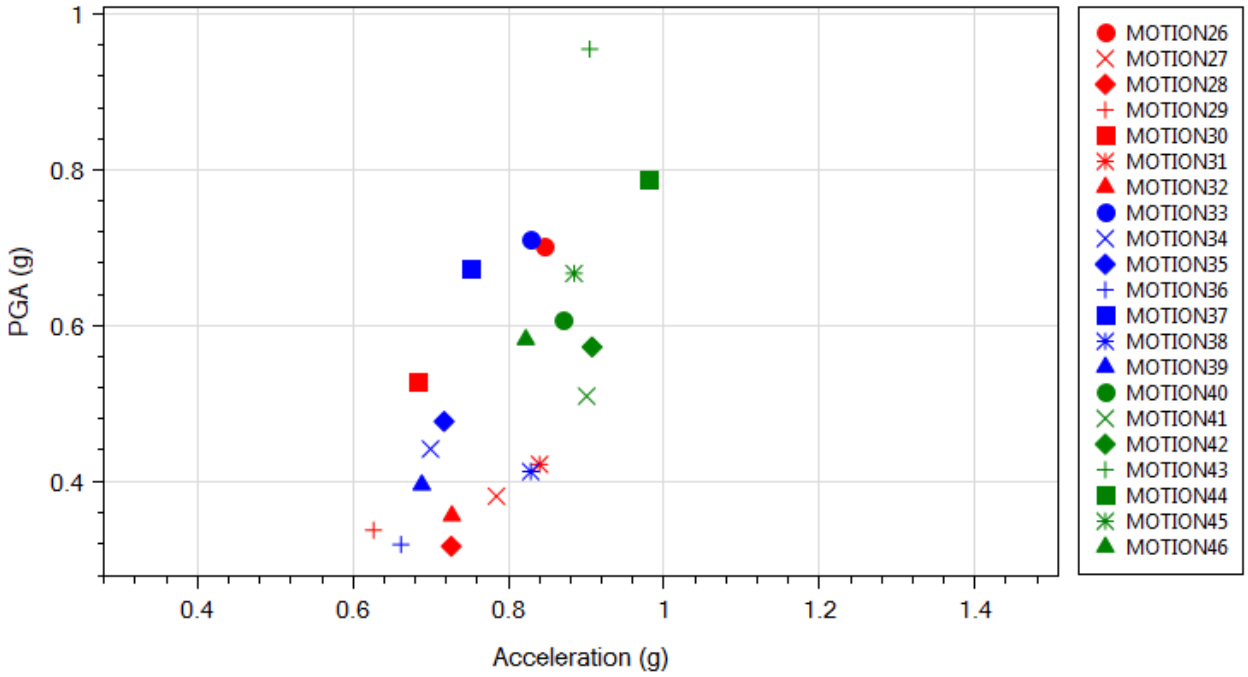

Figure 2.25 OSB2 deck maximum transverse acceleration in OpenSees (Motions 26-46; EPP-Gap with Bearings model)

2.5.2 Response Time History (OpenSees)

In this section, OpenSees response time histories for 2 representative input motions (Motions 1 and 15) for the EPP-Gap with Bearings model are presented (Longitudinal seismic excitation). Note that the CSiBridge analysis for OSB2 (see Table 2.5 and Table 2.7) was conducted for a different bridge model (the EPP-Gap model, without abutment bearing pads). As such, no CSiBridge output is available to compare with the OpenSees result presented in this section.

1) Motion 1 ROCKS1N1

For Motion 1, the column top maximum displacement is 1.8 in (Table 2.4) at which the abutment gap is close to closing (the specified longitudinal gap is 2 in). Figure 2.26 displays OSB2 column response time history for Motion 1 (ROCKS1N1). The input motion ROCKS1N1 is shown in Figure 2.26d for reference.

The column and abutment force-displacement response is displayed in Figure 2.27. The abutment force-displacement response is a straight line which indicates that the embankment is not activated yet and only the bearings are in effect in the longitudinal direction (Figure 2.27c and d). The slope of the straight line is the overall initial elastic stiffness of all 4 bearing pads.

Figure 2.28 displays the moment-curvature response at the column top. A maximum curvature of 0.00019 was reached at the maximum bending moment of about 13,000 kip-ft (Figure 2.28). A level of yielding may be seen in the column response (Figure 2.28).

2) Motion 15 SANDS1N1

Motion 15 gave the largest maximum displacement among the motions with longitudinal components only (Motions 1-21). Figure 2.29 shows OSB2 column response time history for the EPP-Gap with Bearings model.

The column and abutment force-displacement response is displayed in Figure 2.30. The abutment force-displacement response shows that the embankment at the left abutment was activated and also yielded (the yield force -1031 kip was reached) during the shaking. Figure 2.31 displays the moment-curvature response at the column top. A maximum curvature of 0.00023 was reached at the maximum bending moment of about 13,000 kip-ft (Figure 2.31). A higher level of yielding in the column may be noted compared to the Motion 1 ROCKS1N1 case.

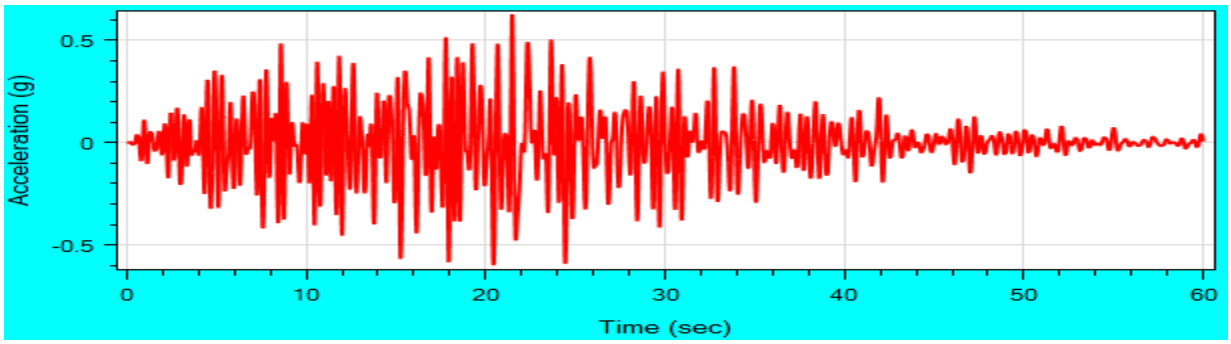

a)

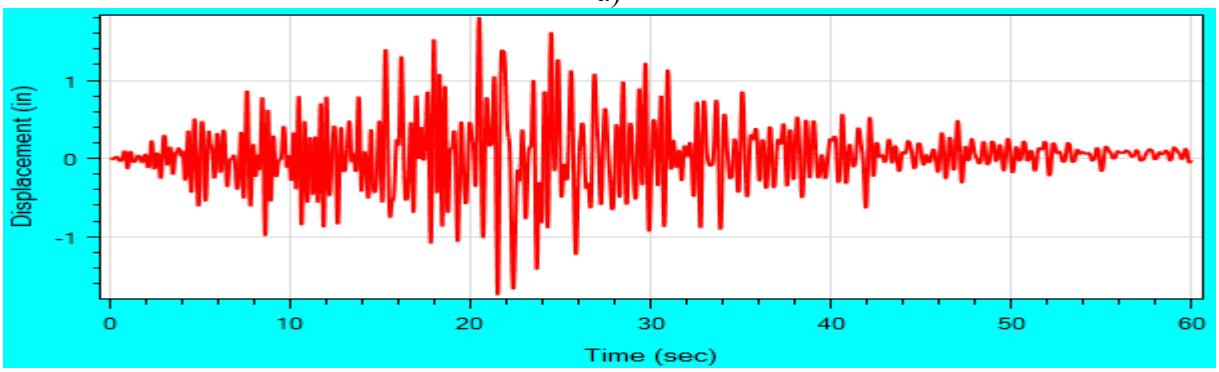

b)

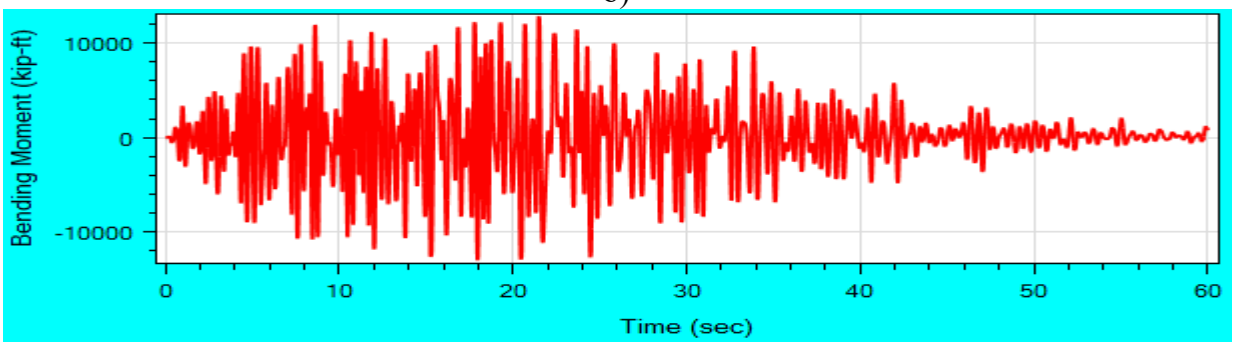

c)

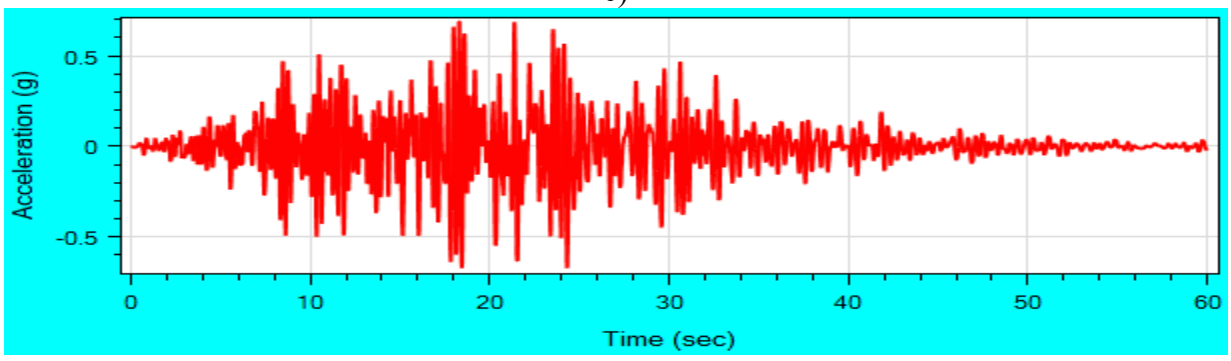

d)

Figure 2.26 OSB2 column top longitudinal response time histories for Motion 1 ROCKS1N1 (EPP-Gap with Bearings model): a) acceleration; b) displacement; c) bending moment; d) base excitation ROCKS1N1

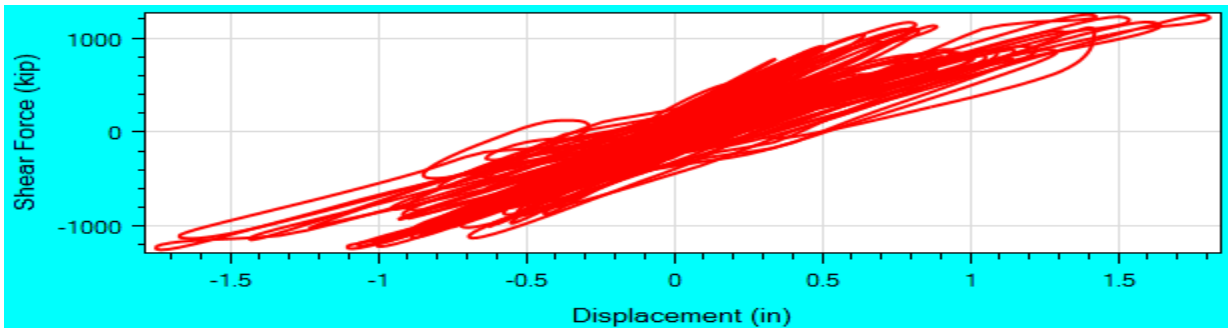

a)

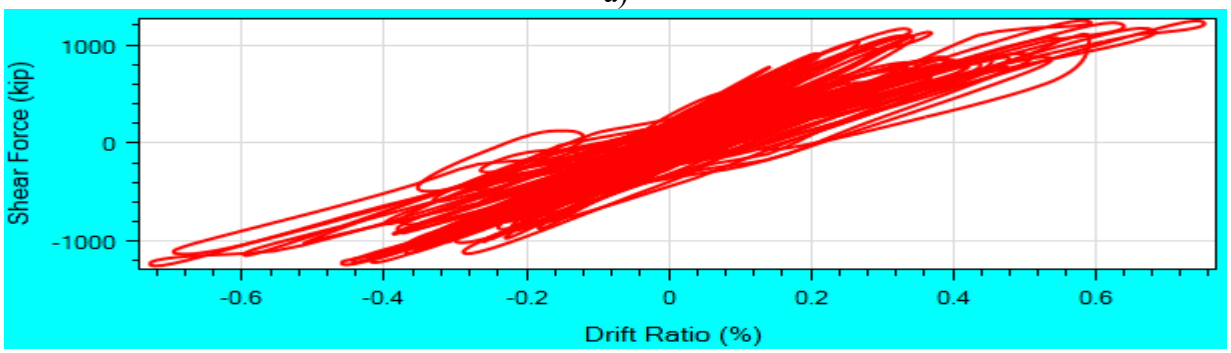

b)

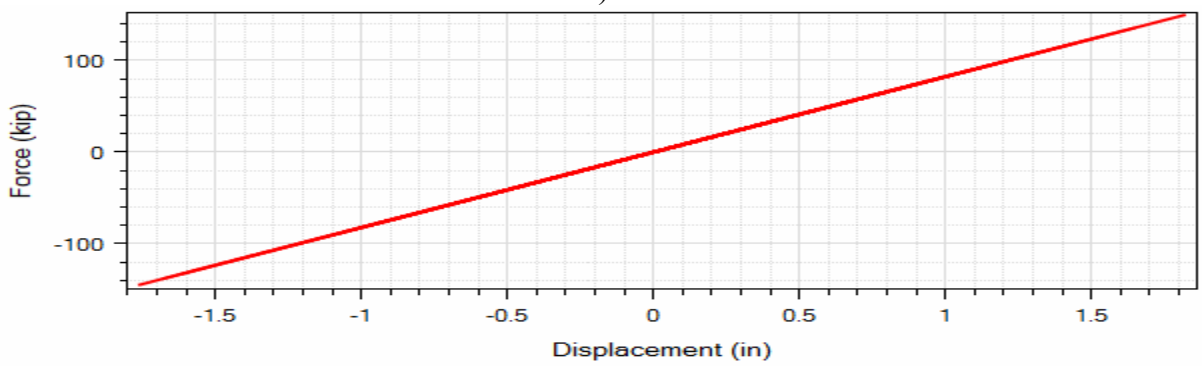

c)

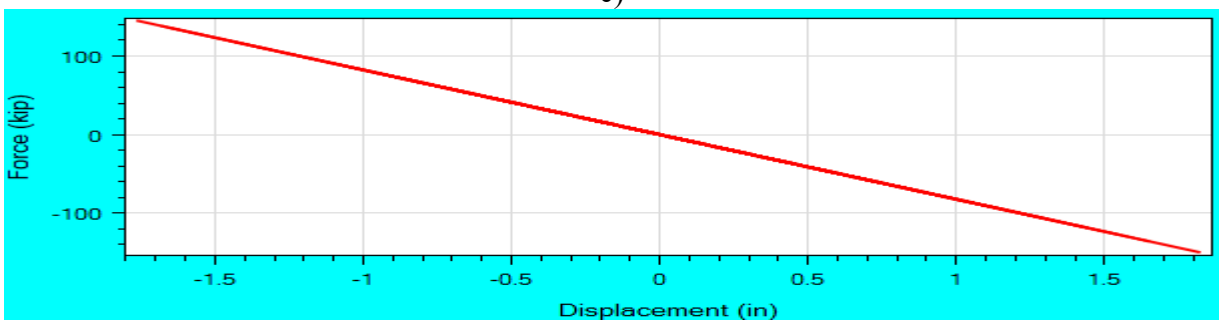

d)

Figure 2.27 OSB2 longitudinal force-displacement response for Motion 1 ROCKS1N1 (EPP-Gap with Bearings model): a) column top force-displacement; b) column top force-drift ratio; c) left abutment force-displacement response; d) right abutment force-displacement response

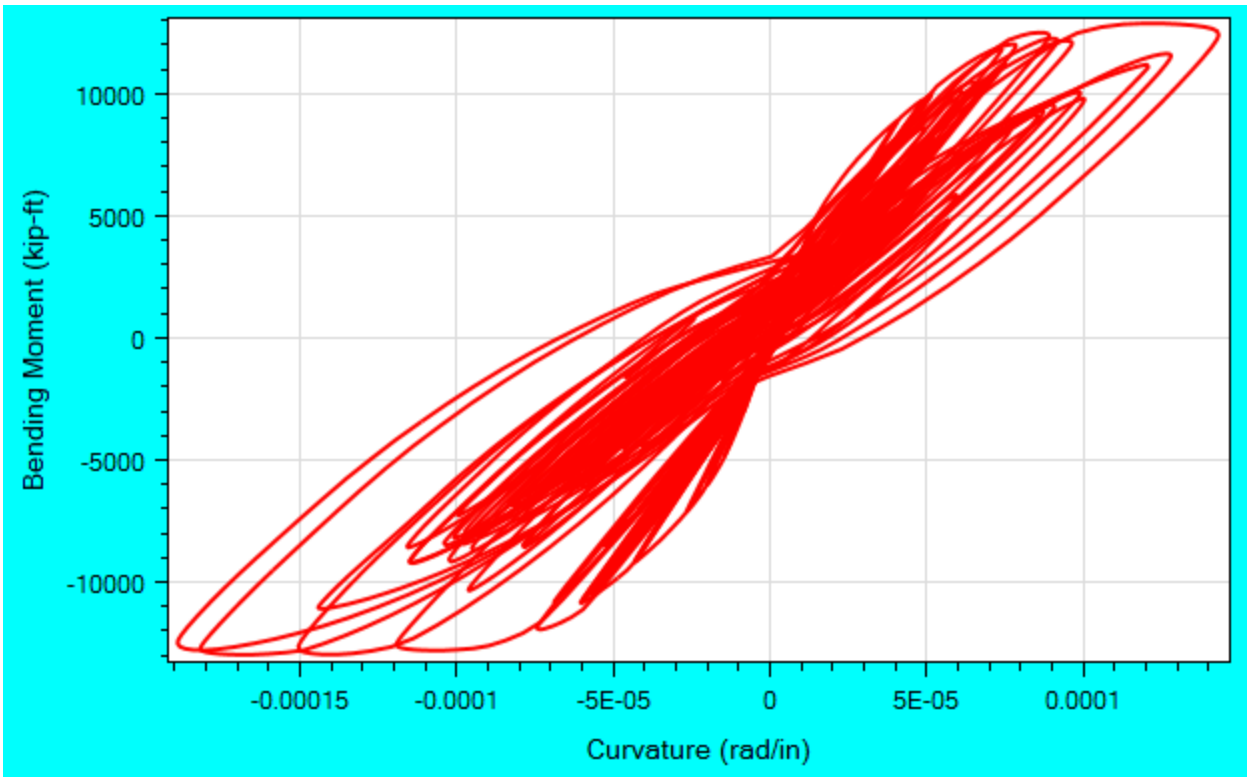

Figure 2.28 OSB2 column top longitudinal moment-curvature response for Motion 1 ROCKS1N1 (EPP-Gap with Bearings model)

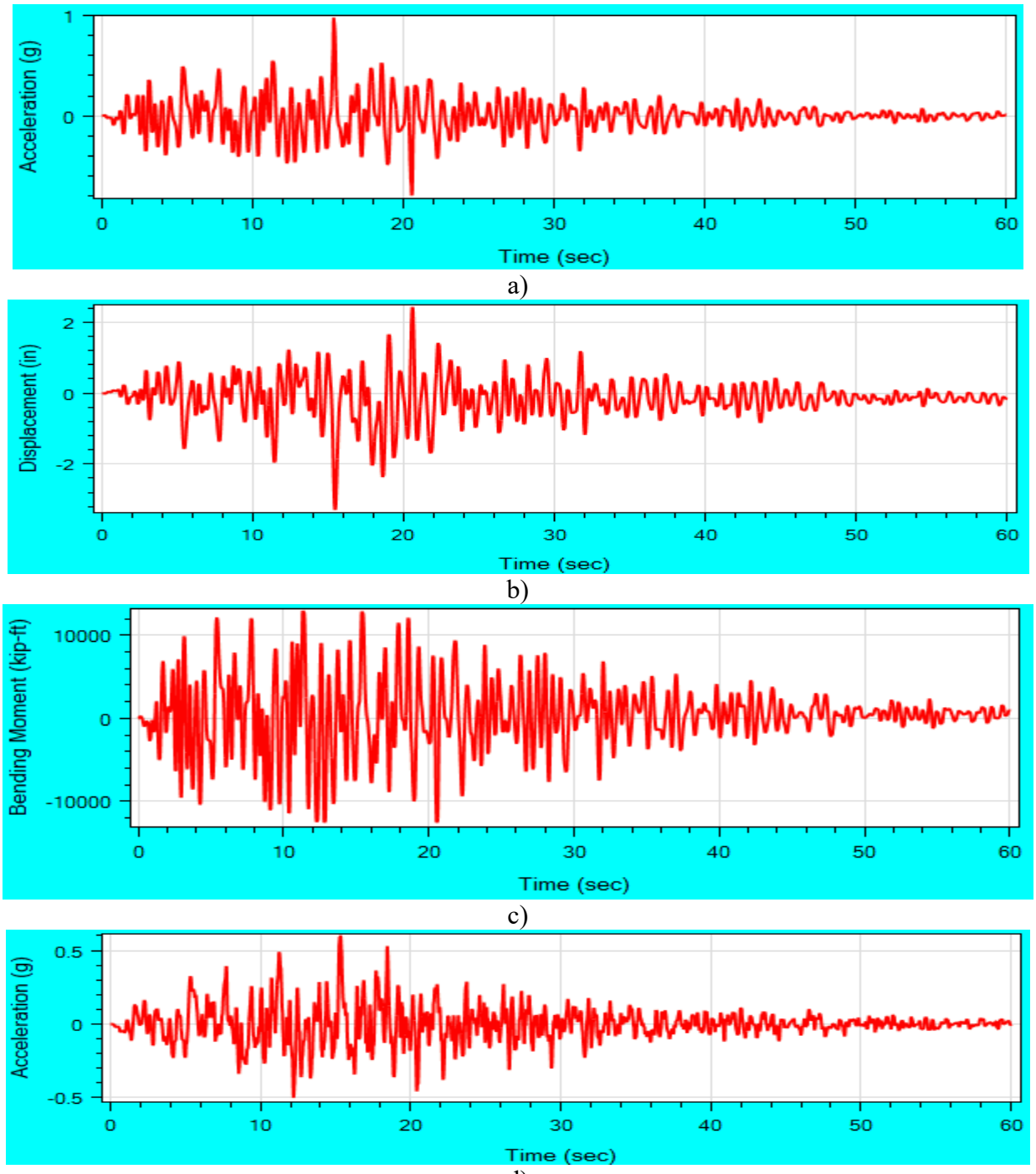

Figure 2.29 OSB2 column top longitudinal response time histories for Motion 15 SANDS1N1 (EPP-Gap with Bearings model): a) acceleration; b) displacement; c) bending moment; d) base excitation SANDS1N1

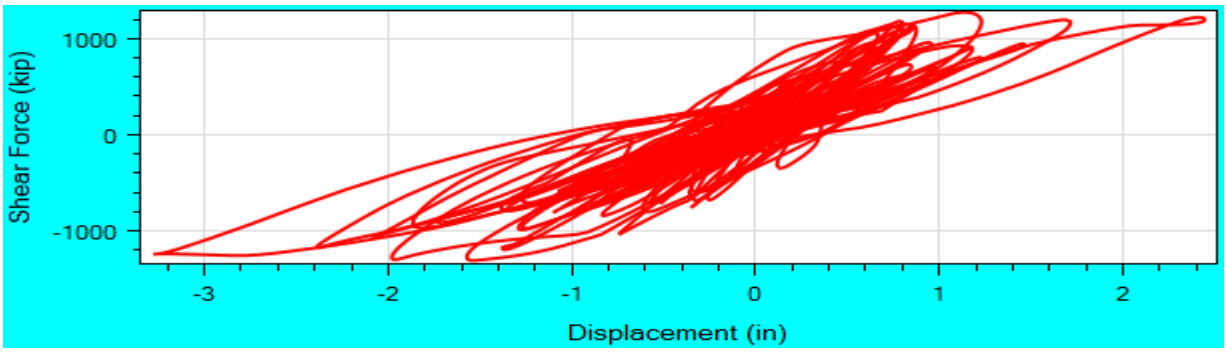

a)

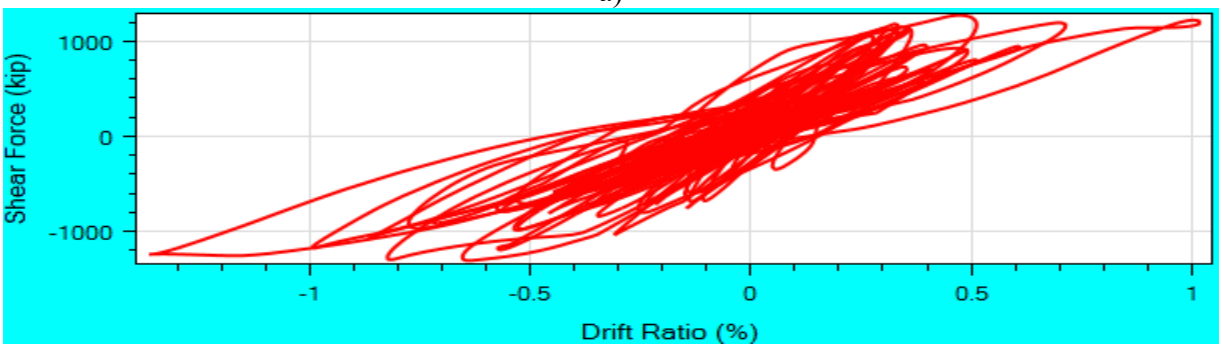

b)

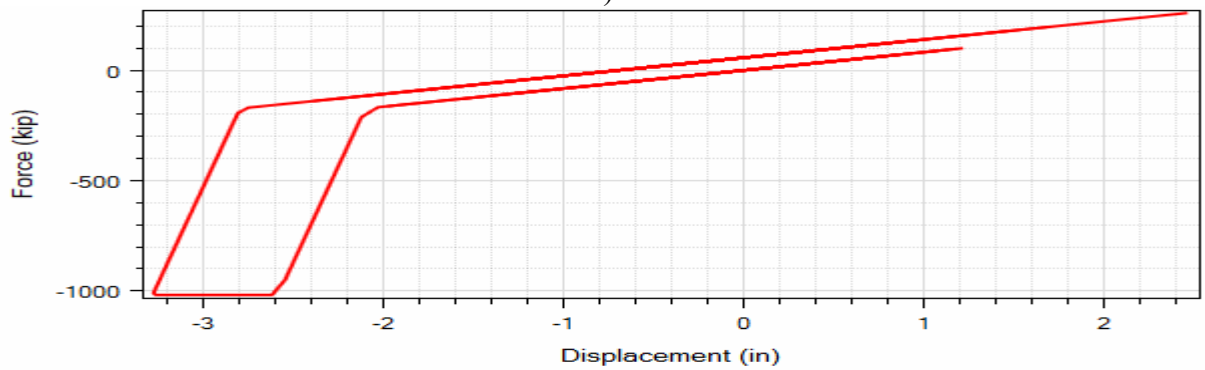

c)

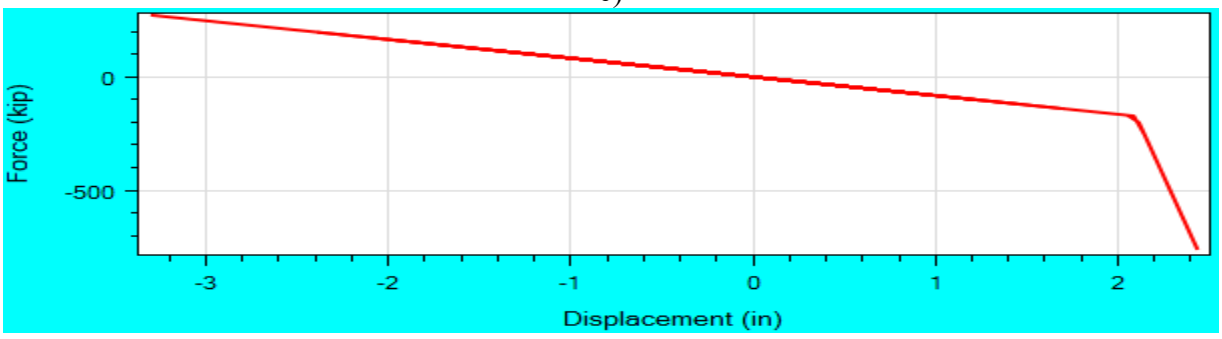

d)

Figure 2.30 OSB2 longitudinal force-displacement response for Motion 15 SANDS1N1 (EPP-Gap with Bearings model): a) column top force-displacement; b) column top force-drift ratio; c) left abutment force-displacement response; d) right abutment force-displacement response

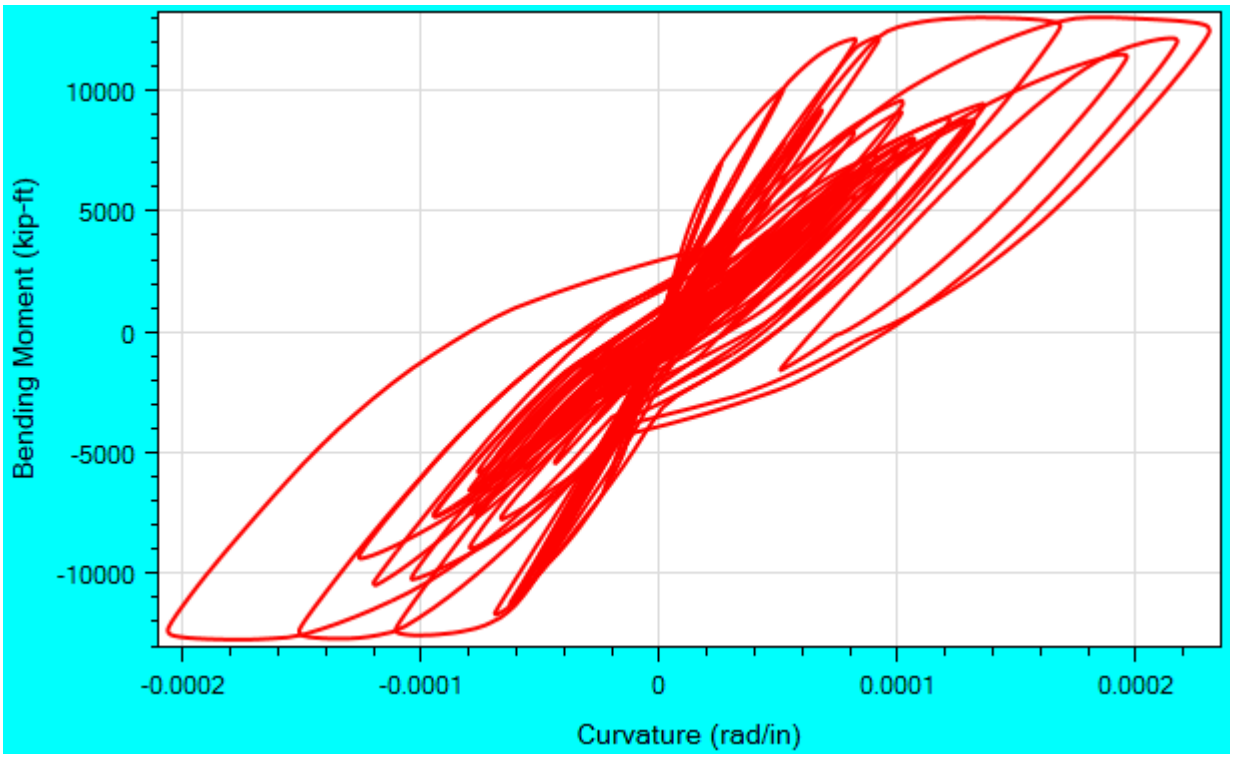

Figure 2.31 OSB2 column top longitudinal moment-curvature response for Motion 15 SANDS1N1 (EPP-Gap with Bearings model)

2.6 Summary

OSB2 was modeled in OpenSees and CSiBridge. A recently developed user interface MSBridge was employed for pre- and post-processing in the conducted OpenSees analysis.

Nonlinear THA was conducted for the 50 motions provided by Caltrans. Three types of abutment models (Roller, EPP-Gap, and EPP-Gap with Bearings) were addressed in OpenSees. For the EPP-Gap with Bearings model, the maximum displacement was 1.4-3.6 inches in the bridge longitudinal direction and 2.0-4.3 inches in the transverse direction. As suggested by Caltrans, only the EPP-Gap model was simulated in CSiBridge.

ESA was also conducted for OSB2 using MSBridge. The longitudinal ESA shows the displacement demand to be 2.5 inches for the case of the EPP-Gap with Bearings model. The displacement demand was 1.1 inches from the transverse ESA (all abutment cases).

2.7 Conclusions

1. For the employed ESA spectrum, column drift ratio demand was about 1 % in the longitudinal and about 0.5% in the transverse directions.

2. For the investigated set of ground motions in the OpenSees analysis (EPP-Gap with Bearings model):

2.1. In the longitudinal direction, about 20 % of the shaking events resulted in column drift demand that exceeded that of the ESA. This demand reached a maximum of 40 % in excess of that from the corresponding ESA (peak column drift ratio of about 1.5 %). With the 2 in gap, the abutment reduced the peak maximum displacement from 5.4 in (for the Roller model) to 3.6 in (for the EPP-Gap with Bearings model).

2.2 In the transverse direction, all of the shaking events resulted in column drift demand that exceeded that of the ESA (1.1 in). With the 1 in gap, the abutment reduced the peak maximum displacement from 7.0 in (for the Roller model) to 4.3 in (for the EPP-Gap with Bearings model).

3. For the OpenSees model, the ground input motions of the SANDS1 group (Figure B.4, Figure B.8 and Table 2.4) appear to result consistently in a larger longitudinal and transverse displacement demand (Figures 2.14-2.19).

4. For the EPP-Gap model (without abutment bearing pads), nearly all shaking events resulted in lower maximum displacement as predicted by CSiBridge, compared to the OpenSees result (Table 2.5). The maximum displacement difference between the OpenSees and CSibridge results is relatively large for the input motions of the SANDS1 group, compared to the ROCKS1N and ROCKS1P groups. In the longitudinal direction, the difference (between OpenSees and CSiBridge) is within 20% for the input motions of the ROCKS1N and ROCKS1P groups and 17%-36% for the SANDS1 group (Table 2.5 and Figure 2.6). In the transverse direction, the difference is 15%-34% for the input motions of the ROCKS1N and ROCKS1P groups and 11%-50% for the SANDS1 group (Table 2.5 and Figure 2.7).

3 OSB STUDY BRIDGE 1

3.1 Bridge Description

OSB Study Bridge 1 (herein referred to as "OSB1") is a single bent reinforced concrete box-girder bridge with two spans of 150 feet in length (Figure 3.1). The single-bent is composed of two circular reinforced concrete columns. Figure 3.1 shows the general configuration of OSB1.

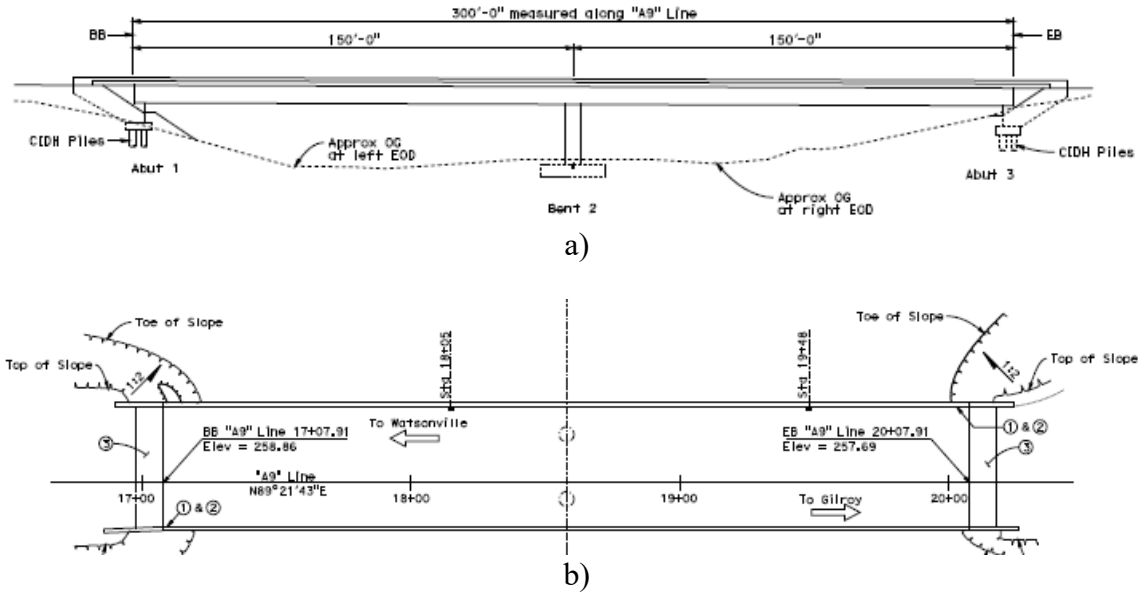

Figure 3.1 Schematic of OSB1 (drawings provided by Caltrans): (a) Elevation view; (b) Plan view

3.2 Geometric Configuration

Figure 3.2 shows a sectional view of OSB1 along with the column reinforcement details. The five-cell box girder is 47.5 feet wide by 6 feet deep. Deck and soffit slabs are 7.75 inches and 6.375 inches thick, respectively. The bentcap is assumed to be rigid.

Similar to OSB2, each of the OSB1 columns is 20 feet high with a diameter of 66 inches. The column is fixed at top and assumed pinned at base.

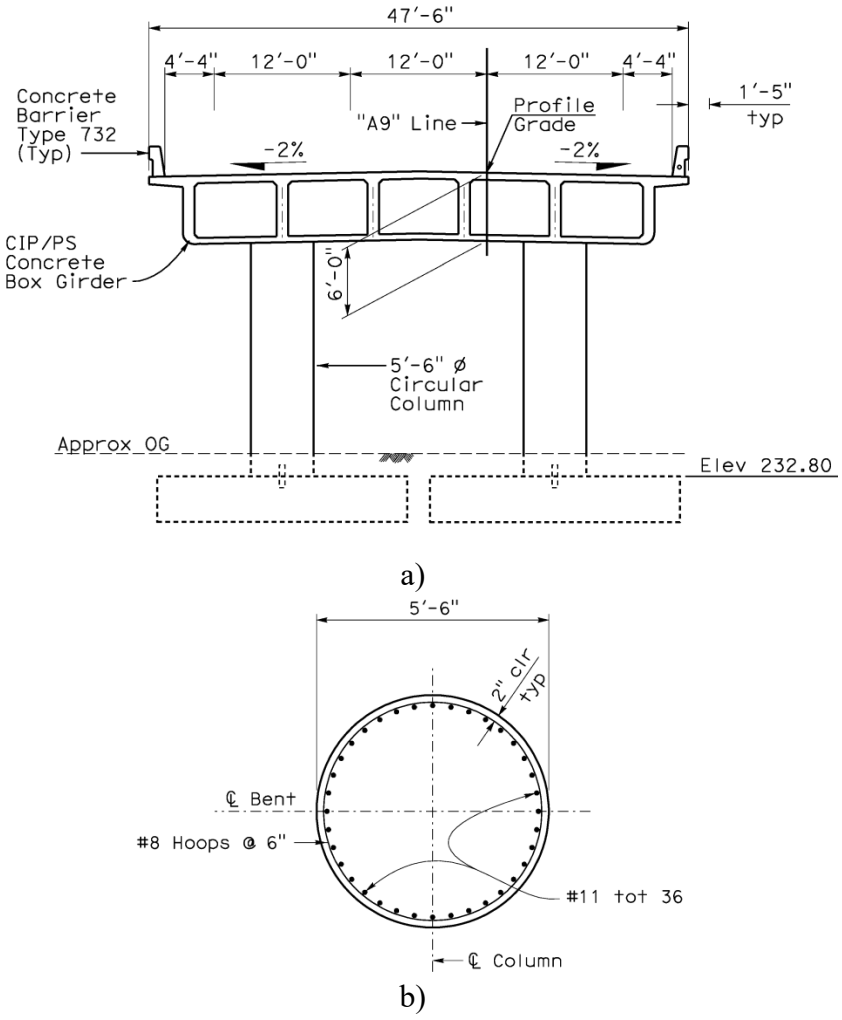

Figure 3.2 Sectional details of OSB1: (a) deck; (b) circular column cross section (Caltrans 2012)

3.3 OSB1 OpenSees Modeling and Response

3.3.1 Finite Element Model

OSB1 was modeled using OpenSees and CSiBridge. The employed modeling techniques in OpenSees and associated model properties are presented in Appendix D. Figure 3.3 shows the OSB1 model created in MSBridge and CSiBridgeo. The offset (3 ft) between column top and the deck was not represented in this study.

The forceBeamColumn (BeamWithHinges) element in OpenSees was used to model the OSB1 columns. A plastic hinge length of 2.8 ft was employed (see Appendix C for the calculation of the plastic hinge length). The deck was considered to be linearly elastic and the bentcap was considered to be essentially rigid.

As shown in Figure 3.3, two equal-length elements were used for the column (the column height is 20 ft and the column spacing is 24 ft). No rotation around the bridge longitudinal direction is allowed for the deck (at the abutments).

Similar to the OSB2 study, three types of abutment models were addressed:

i) Roller abutment model,
ii) EPP-Gap abutment model (bearing pads were not considered), and
iii) EPP-Gap with Bearings abutment model (6 bearing pads were included).

Also similarly, the resulting OSB1 bridge models will be hereinafter referred to as "Roller model", "EPP-Gap model" and "EPP-Gap with Bearings model", respectively. The first natural periods for OSB1 with the above 3 bridge models are 1.0, 1.0, and 0.82 second, respectively. The Gap was 0.14 in (longitudinal), and elastic response is assumed in the transverse direction. For detailed information about the above abutment models, please see Appendix D. As suggested by Caltrans, only the EPP-Gap model (without abutment bearing pads) was simulated in the CSiBridge nonlinear THA.

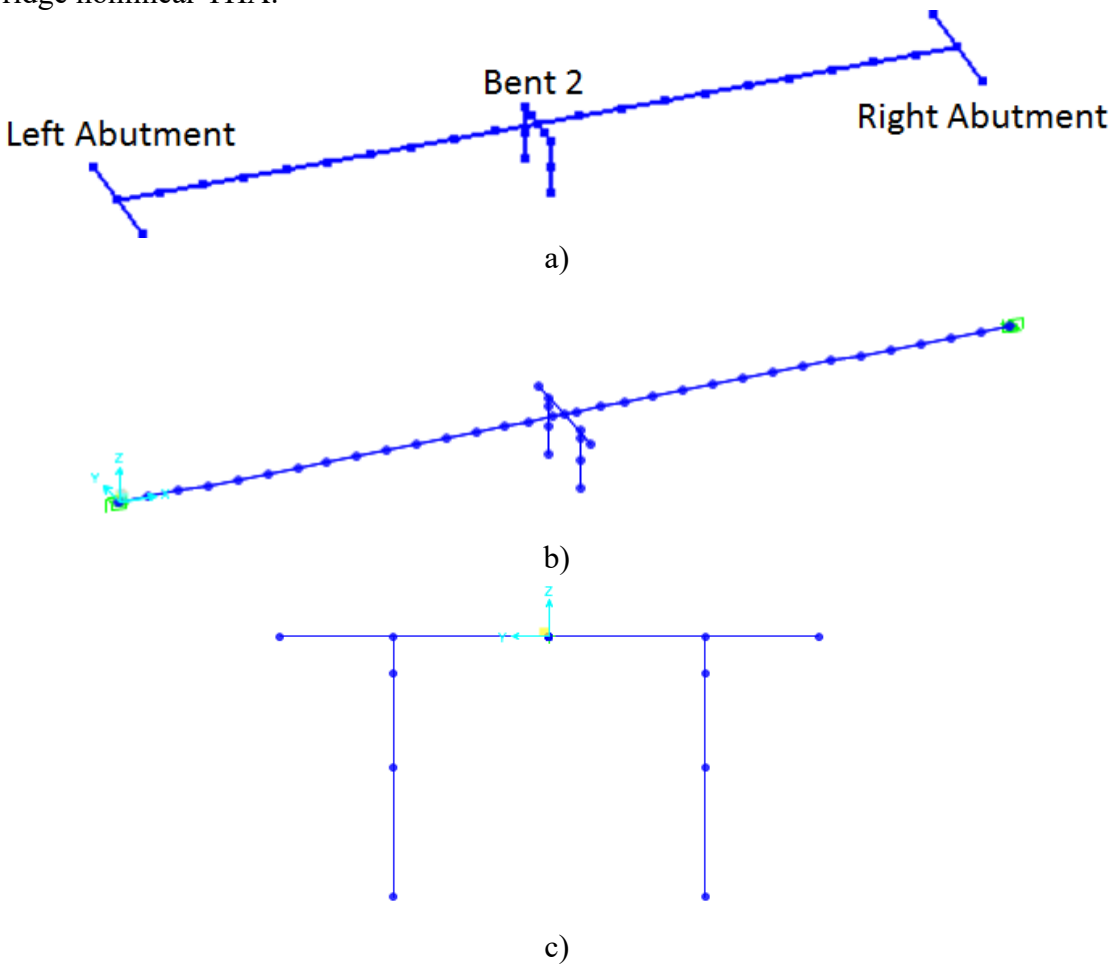

a)

b)

c)

Figure 3.3 OSB1 model created in: a) MSBridge; b) CSiBridge (3D view); c) CSiBridge

3.3.2 Column Response

Pushover analysis was conducted to document the column response in the longitudinal and transverse directions. The Roller model was employed in this case. In CSiBridge, the approach presented in Appendix H was employed to model the columns. Figure 3.4 shows the column force-displacement response due to pushover loading (Figure 3.5 shows the column force versus drift ratio response).

The column force-displacement response shows the beginning of significant yielding to occur at a 1% drift ratio approximately (OpenSees result in Figure 3.5a) or 2.4 inches of displacement (OpenSees result in Figure 3.4a) in the case of longitudinal pushover. A shear force of 450 kip was reached when this yielding occurs (OpenSees result in Figure 3.4a and Figure 3.5a). In the case of transverse pushover, similar yielding is observed to occur at a 0.8% drift ratio approximately (OpenSees result in Figure 3.5b) or 1.9 inches of displacement (OpenSees result in Figure 3.4b).

In the longitudinal pushover case, the column lost more than 20% of its strength at a 5.5% drift ratio or 13 inches of displacement (OpenSees result in Figure 3.4a and Figure 3.5a). For the transverse pushover case, the column also lost more than 20% of its strength at a 5% drift ratio or 12 inches of displacement (OpenSees result in Figure 3.4b and Figure 3.5b). For detailed discussion about the OSB1 column response (linear and nonlinear), please see Appendix E.

3.4 Equivalent Static Analysis (ESA) in OpenSees

ESA was conducted in OpenSees for OSB1 in the longitudinal and transverse directions. Details and results are presented below.

3.4.1 ESA in the Longitudinal Direction

A load of 5% of the total bridge weight was used for pushover in the longitudinal ESA. The pushover load was applied at the bridge center (i.e., the deck center at the bent) along the bridge deck (longitudinal) direction. The ARS employed earlier for OSB2 was also used for OSB1.

Table 3.1 shows the ESA result for OSB1. The final elastic displacement demand is 6.5 in (Roller model), 5.8 in (EPP-Gap model) or 4.2 in (EPP-Gap with Bearings model). Table 3.2 lists the parameters related to this longitudinal ESA.

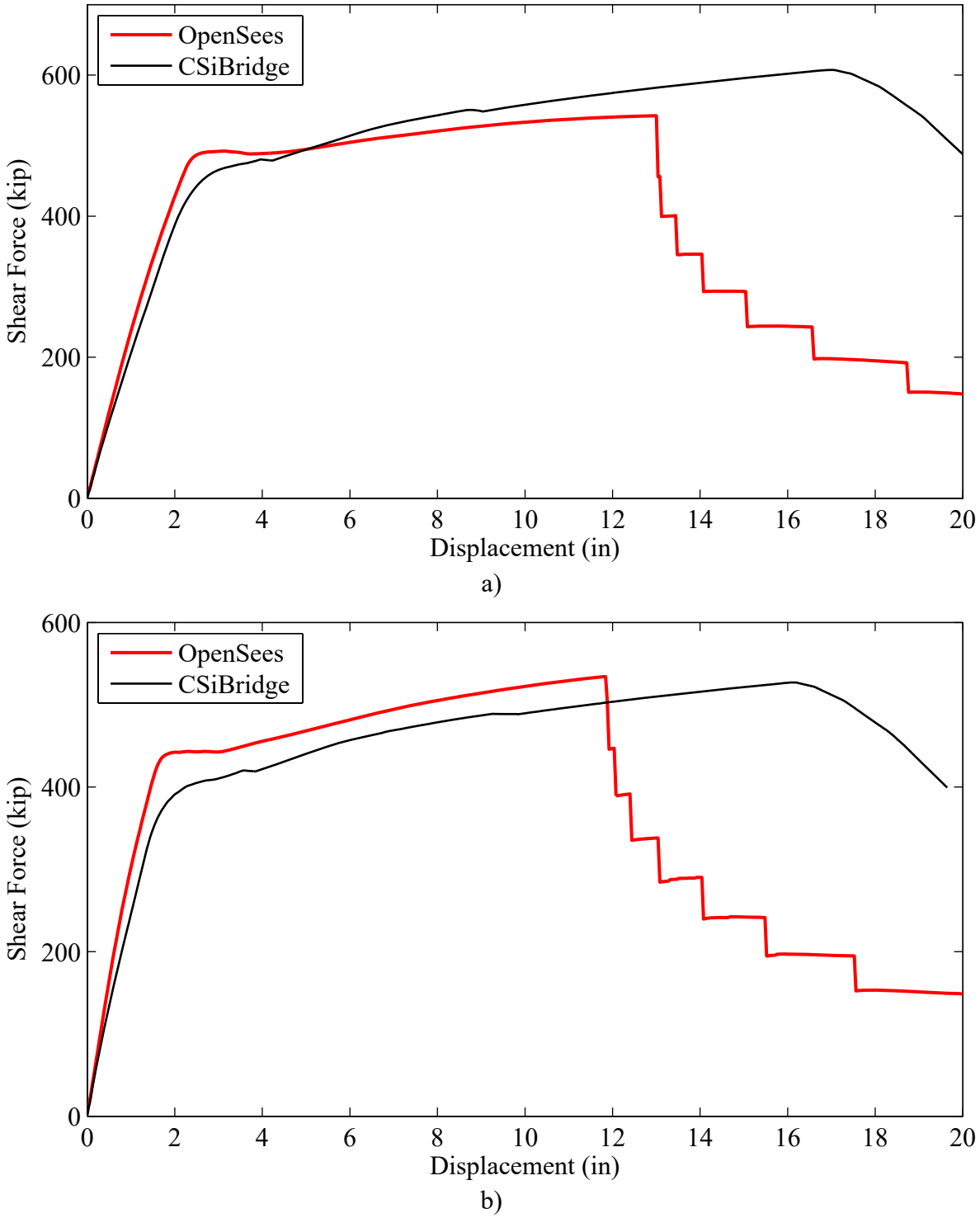

Figure 3.4 Force-displacement response for each OSB1 column: a) longitudinal direction; b) transverse direction

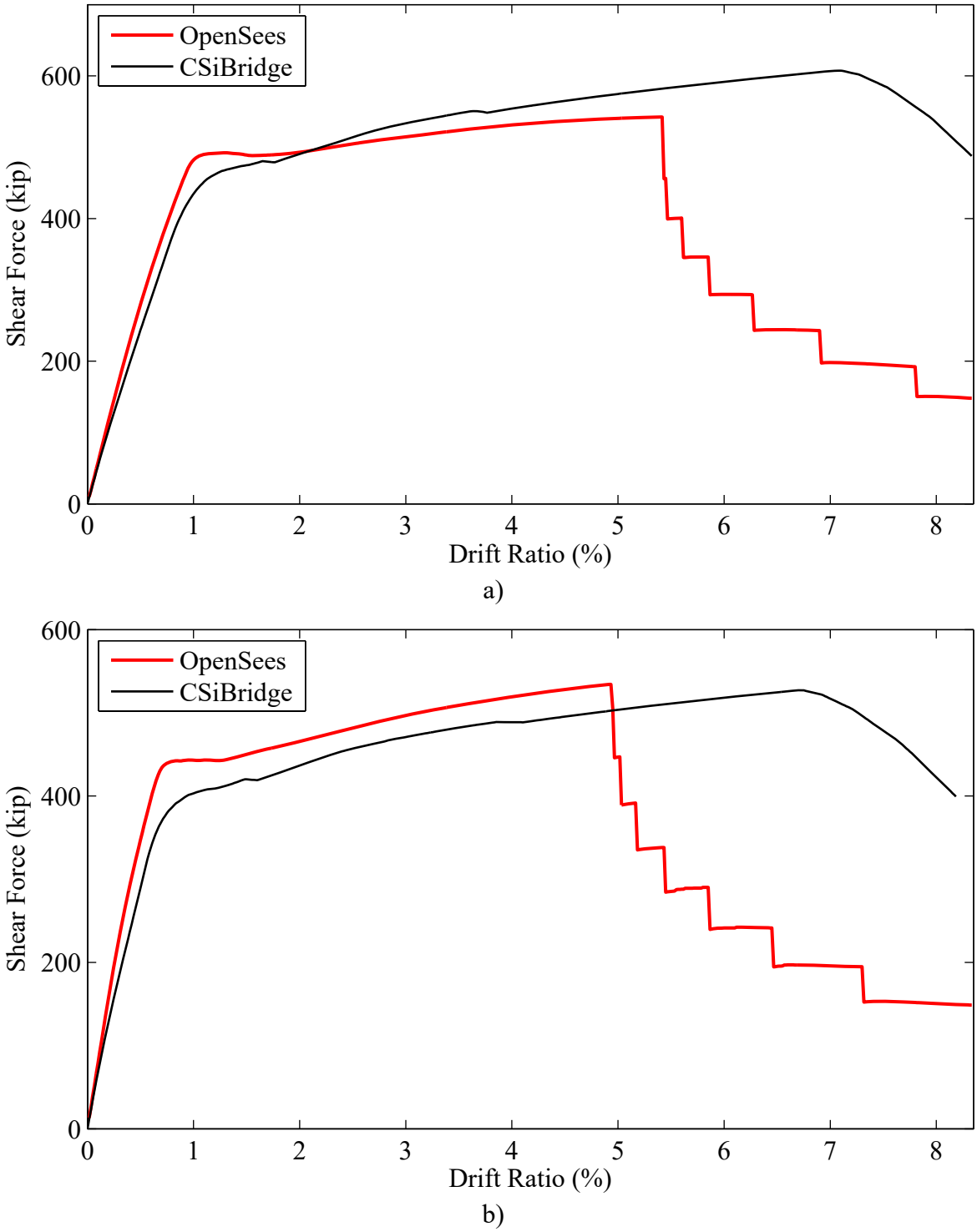

Figure 3.5 Force versus drift ratio response for each OSB1 column: a) longitudinal direction; b) transverse direction

Table 3.1. ESA Result for OSB1

Parameter	Longitudinal ESA	Transverse ESA
Displacement Demand (in)	6.5 (Roller model), 5.8 (EPP-Gap model), or 4.2 (EPP-Gap with Bearings model)	4.0

Table 3.2. Longitudinal ESA Parameters for OSB1

Parameter	Roller model	EPP-Gap model	EPP-Gap with Bearings model
Total weight calculated (kip)	4,145.27	Same	Same
Total mass calculated (kip-sec2/in)	10.73	Same	Same
Pushover load specified (kip)	207.26	Same	Same
Displacement due to pushover (in)	0.43	0.191	0.182
Calculated stiffness (kip/in)	485.78	630.70	1,095.3
Calculated period (sec)	0.93	0.62	0.61

3.4.2 ESA in the Transverse Direction

A load of 5% of the tributary weight of the bent was used for the pushover analysis. The same acceleration response spectrum (ARS) was also used in the transverse ESA. The elastic displacement demand was found to be 2.3 in (Table 3.1) in the transverse ESA. Table 3.3 lists the parameters related to this transverse ESA.

Table 3.3. Transverse ESA Parameters for OSB1

Parameter	Value
Tributary weight calculated (kip)	2,270.27
Tributary mass calculated (kip-sec2/in)	5.88
Pushover load specified (kip)	113.51
Displacement due to pushover (in)	0.168
Calculated stiffness (kip/in)	674.7
Calculated period (sec)	0.586

3.5 Nonlinear Time History Analysis

Nonlinear THA was conducted for the 50 input motions provided by Caltrans (see Appendix B for the characteristics of these 50 motions). The input motions were applied directly at the column base (note that the columns are pinned at the base for OSB1), as well as at both abutments.

Rayleigh damping was used with a 5% damping ratio (defined at periods of 1.2 and 0.7 second) in the nonlinear THA. For the time integration scheme, the Newmark average acceleration method ($\gamma = 0.5$ and $\beta = 0.25$) was employed.

In OpenSees, the variable time-stepping scheme was used in the analysis. The starting value for each time step was 0.005 second (same as the time step of the input motions) and the minimum time step was 5×10^{-5} second (upon splitting of time step when needed).

3.5.1 Maximum Deck Displacement and Acceleration

Table 3.4 lists OSB1 column top maximum displacement for the 50 motions from the nonlinear THA in OpenSees. Results for the 3 bridge models (Roller, EPP-Gap, and EPP-Gap with Bearings) are presented for comparison (Table 3.4).

In general, among the 3 models, the Roller model resulted in the largest deck maximum displacement (for both longitudinal and transverse directions). For EPP-Gap with Bearings model, the deck longitudinal maximum displacement is from 2.2 inches (ROCKS1N7) – 7.9 inches (SANDS1N1) for the motions with longitudinal component only (Motions 1-21). Note that the displacement demand from the longitudinal ESA is 4.5 inches for the same bridge model (Table 3.1).

As mentioned earlier, the EPP-Gap model was simulated in CSiBridge. Table 3.5 lists the deck maximum displacement from the OpenSees and CSiBridge analyses. The maximum displacement comparison of Table 3.5 is also presented in Bar Chart graphical form in Figures 3.6-3.9. As mentioned earlier in Chapter 1, viscous damping abutment forces are only present in the CSiBridge simulation. This difference in the abutment exerted forces accounts partially for the discrepancy (Table 3.5) in the CSiBridge and OpenSees maximum displacement estimates. Appendix K lists additional CSiBridge results (column top shear force-displacement hysteresis and bending moment time history for each input motion).

Table 3.6 displays OSB1 deck maximum acceleration (for the 3 bridge models). In general, among the 3 models, the Roller model resulted in the least deck maximum acceleration (Table 3.6).

For the EPP-Gap model, Table 3.7 lists the deck maximum acceleration from the OpenSees and CSiBridge analyses. The maximum acceleration comparison of Table 3.7 is also presented in Bar Chart graphical form in Figures 3.10-3.13.

For the OpenSees model, the maximum displacements of Table 3.4 are also shown against PGA in Figure 3.14-Figure 3.19. The maximum acceleration is also shown against in Figure 3.20-Figure 3.25.

Note that P-Delta was not considered in the CSiBridge analysis results reported herein for OSB1 (however P-Delta was considered in OpenSees analysis). Generally, inclusion of P-Delta effects in CSiBridge resulted in relatively small differences in the output, but difficulties were

encountered when input excitation was imparted in the Transverse and Longitudinal directions simultaneously (possibility a challenge only in the employed particular version of CSiBridge).

Table 3.4. OSB1 Deck Maximum Displacement (OpenSees)

(The ESA longitudinal displacement demands are 6.5 in, 5.8 in and 4.2 in for Roller, EPP-Gap, EPP-Gap with Bearings models, respectively)

Motion	Longitudinal Input	Transverse Input	Longitudinal Displacement (in)			Transverse Displacement (in)		
			Roller	EPP-Gap	EPP-Gap with Bearings	Roller	EPP-Gap	EPP-Gap with Bearings
1	ROCKS1N1 (0.7g)	-	6.8	3.8	2.5	-	-	-
2	ROCKS1N2 (0.38g)	-	4.4	3.0	2.8	-	-	-
3	ROCKS1N3 (0.32g)	-	4.8	3.3	2.3	-	-	-
4	ROCKS1N4 (0.34g)	-	6.3	3.6	3.1	-	-	-
5	ROCKS1N5 (0.53g)	-	4.3	2.8	2.9	-	-	-
6	ROCKS1N6 (0.42g)	-	4.6	3.7	2.5	-	-	-
7	ROCKS1N7 (0.36g)	-	4.5	3.8	2.2	-	-	-
8	ROCKS1P1 (0.71g)	-	7.3	4.4	2.3	-	-	-
9	ROCKS1P2 (0.44g)	-	4.1	3.2	3.0	-	-	-
10	ROCKS1P3 (0.48g)	-	5.4	2.2	2.9	-	-	-
11	ROCKS1P4 (0.32g)	-	6.8	3.3	2.9	-	-	-
12	ROCKS1P5 (0.67g)	-	5.3	4.5	2.9	-	-	-
13	ROCKS1P6 (0.41g)	-	4.7	3.5	2.5	-	-	-
14	ROCKS1P7 (0.4g)	-	6.5	4.4	3.6	-	-	-
15	SANDS1N1 (0.61g)	-	11.3	6.6	7.9	-	-	-
16	SANDS1N2 (0.51g)	-	9.0	6.2	5.5	-	-	-
17	SANDS1N3 (0.57g)	-	8.8	7.2	6.3	-	-	-
18	SANDS1N4 (0.96g)	-	10.1	9.2	6.7	-	-	-
19	SANDS1N5 (0.79g)	-	9.9	7.2	5.3	-	-	-
20	SANDS1N6 (0.67g)	-	7.1	5.9	6.1	-	-	-
21	SANDS1N7 (0.58g)	-	10.9	8.4	7.1	-	-	-
22	ROCKN1N1N (0.4g)	ROCKN1N1P (0.58g)	4.3	3.2	2.7	6.7	3.2	3.0
23	ROCKN1P1N (1.42g)	ROCKN1P1P (1.42g)	4.6	2.3	1.9	4.0	2.9	2.2
24	SANDN1N1N (0.78g)	SANDN1N1P (0.81g)	8.2	6.8	6.2	5.4	5.2	4.4
25	CLAYN1N1N (0.79g)	CLAYN1N1P (0.71g)	10.2	7.7	4.9	9.6	5.9	4.1
26	-	ROCKS1N1 (0.7g)	-	-	-	5.7	2.8	3.1
27	-	ROCKS1N2 (0.38g)	-	-	-	3.8	3.5	2.7
28	-	ROCKS1N3 (0.32g)	-	-	-	4.6	2.8	3.0
29	-	ROCKS1N4 (0.34g)	-	-	-	4.9	2.8	2.6
30	-	ROCKS1N5 (0.53g)	-	-	-	5.0	2.8	2.7
31	-	ROCKS1N6 (0.42g)	-	-	-	3.6	2.7	3.0
32	-	ROCKS1N7 (0.36g)	-	-	-	3.7	3.2	2.7
33	-	ROCKS1P1 (0.71g)	-	-	-	6.4	2.7	3.1
34	-	ROCKS1P2 (0.44g)	-	-	-	4.0	3.4	2.9
35	-	ROCKS1P3 (0.48g)	-	-	-	5.9	3.0	2.8
36	-	ROCKS1P4 (0.32g)	-	-	-	5.5	2.9	2.5
37	-	ROCKS1P5 (0.67g)	-	-	-	4.4	3.1	2.8
38	-	ROCKS1P6 (0.41g)	-	-	-	3.6	2.7	3.0
39	-	ROCKS1P7 (0.4g)	-	-	-	5.8	3.1	3.1
40	-	SANDS1N1 (0.61g)	-	-	-	10.3	4.4	3.9
41	-	SANDS1N2 (0.51g)	-	-	-	7.6	4.5	4.6
42	-	SANDS1N3 (0.57g)	-	-	-	7.8	4.5	4.3
43	-	SANDS1N4 (0.96g)	-	-	-	8.8	4.6	3.8
44	-	SANDS1N5 (0.79g)	-	-	-	8.9	4.4	4.4
45	-	SANDS1N6 (0.67g)	-	-	-	7.3	4.0	4.0
46	-	SANDS1N7 (0.58g)	-	-	-	8.9	3.5	4.0
47	ROCKN1N1P (0.58g)	ROCKN1N1N (0.4g)	7.4	2.7	2.5	3.5	3.3	3.7
48	ROCKN1P1P (1.42g)	ROCKN1P1N (1.42g)	4.6	2.3	1.9	4.0	2.9	2.2
49	SANDN1N1P (0.81g)	SANDN1N1N (0.78g)	6.0	4.7	4.6	7.6	5.0	4.5
50	CLAYN1N1P (0.71g)	CLAYN1N1N (0.79g)	10.1	7.6	6.2	8.8	4.6	4.5

Table 3.5. OSB1 Deck Maximum Displacement for EPP-Gap Model (Comparison of OpenSees and CSiBridge)

(The ESA longitudinal displacement demand is 5.8 in while the ESA transverse displacement demands is 4.0 in; Difference is relative to OpenSees result)

Motion	Longitudinal Input	Transverse Input	Longitudinal Displacement (in)			Transverse Displacement (in)		
			OpenSees	CSiBridge	Difference	OpenSees	CSiBridge	Difference
1	ROCKS1N1 (0.7g)	-	3.8	2.0	-47%	-	-	-
2	ROCKS1N2 (0.38g)	-	3.0	1.4	-53%	-	-	-
3	ROCKS1N3 (0.32g)	-	3.3	1.7	-48%	-	-	-
4	ROCKS1N4 (0.34g)	-	3.6	1.2	-67%	-	-	-
5	ROCKS1N5 (0.53g)	-	2.8	1.6	-43%	-	-	-
6	ROCKS1N6 (0.42g)	-	3.7	1.6	-57%	-	-	-
7	ROCKS1N7 (0.36g)	-	3.8	1.4	-63%	-	-	-
8	ROCKS1P1 (0.71g)	-	4.4	2.1	-52%	-	-	-
9	ROCKS1P2 (0.44g)	-	3.2	1.6	-50%	-	-	-
10	ROCKS1P3 (0.48g)	-	2.2	1.5	-32%	-	-	-
11	ROCKS1P4 (0.32g)	-	3.3	1.2	-64%	-	-	-
12	ROCKS1P5 (0.67g)	-	4.5	1.7	-62%	-	-	-
13	ROCKS1P6 (0.41g)	-	3.5	1.5	-57%	-	-	-
14	ROCKS1P7 (0.4g)	-	4.4	1.8	-59%	-	-	-
15	SANDS1N1 (0.61g)	-	6.6	4.4	-33%	-	-	-
16	SANDS1N2 (0.51g)	-	6.2	3.4	-45%	-	-	-
17	SANDS1N3 (0.57g)	-	7.2	3.6	-50%	-	-	-
18	SANDS1N4 (0.96g)	-	9.2	4.7	-49%	-	-	-
19	SANDS1N5 (0.79g)	-	7.2	4.1	-43%	-	-	-
20	SANDS1N6 (0.67g)	-	5.9	3.5	-41%	-	-	-
21	SANDS1N7 (0.58g)	-	8.4	4.2	-50%	-	-	-
22	ROCKN1N1N (0.4g)	ROCKN1N1P (0.58g)	3.2	1.3	-59%	3.2	2.9	-9%
23	ROCKN1P1N (1.42g)	ROCKN1P1P (1.42g)	2.3	1.3	-43%	2.9	2.3	-21%
24	SANDN1N1N (0.78g)	SANDN1N1P (0.81g)	6.8	4.2	-38%	5.2	4.7	-10%
25	CLAYN1N1N (0.79g)	CLAYN1N1P (0.71g)	7.7	4.1	-47%	5.9	5.0	-15%
26	-	ROCKS1N1 (0.7g)	-	-	-	2.8	2.7	-4%
27	-	ROCKS1N2 (0.38g)	-	-	-	3.5	3.0	-14%
28	-	ROCKS1N3 (0.32g)	-	-	-	2.8	2.7	-4%
29	-	ROCKS1N4 (0.34g)	-	-	-	2.8	2.4	-14%
30	-	ROCKS1N5 (0.53g)	-	-	-	2.8	2.4	-14%
31	-	ROCKS1N6 (0.42g)	-	-	-	2.7	2.4	-11%
32	-	ROCKS1N7 (0.36g)	-	-	-	3.2	2.9	-9%
33	-	ROCKS1P1 (0.71g)	-	-	-	2.7	2.6	-4%
34	-	ROCKS1P2 (0.44g)	-	-	-	3.4	3	-12%
35	-	ROCKS1P3 (0.48g)	-	-	-	3.0	2.6	-13%
36	-	ROCKS1P4 (0.32g)	-	-	-	2.9	2.4	-17%
37	-	ROCKS1P5 (0.67g)	-	-	-	3.1	2.7	-13%
38	-	ROCKS1P6 (0.41g)	-	-	-	2.7	2.4	-11%
39	-	ROCKS1P7 (0.4g)	-	-	-	3.1	2.6	-16%
40	-	SANDS1N1 (0.61g)	-	-	-	4.4	4.1	-7%
41	-	SANDS1N2 (0.51g)	-	-	-	4.5	4.3	-4%
42	-	SANDS1N3 (0.57g)	-	-	-	4.5	4.2	-7%
43	-	SANDS1N4 (0.96g)	-	-	-	4.6	4.3	-7%
44	-	SANDS1N5 (0.79g)	-	-	-	4.4	3.6	-18%
45	-	SANDS1N6 (0.67g)	-	-	-	4.0	3.8	-5%
46	-	SANDS1N7 (0.58g)	-	-	-	3.5	3.1	-11%
47	ROCKN1N1P (0.58g)	ROCKN1N1N (0.4g)	2.7	1.3	-52%	3.3	2.7	-18%
48	ROCKN1P1P (1.42g)	ROCKN1P1N (1.42g)	2.3	1.3	-43%	2.9	3.0	3%
49	SANDN1N1P (0.81g)	SANDN1N1N (0.78g)	4.7	2.7	-43%	5.0	2.7	-46%
50	CLAYN1N1P (0.71g)	CLAYN1N1N (0.79g)	7.6	4.2	-45%	4.6	2.4	-48%

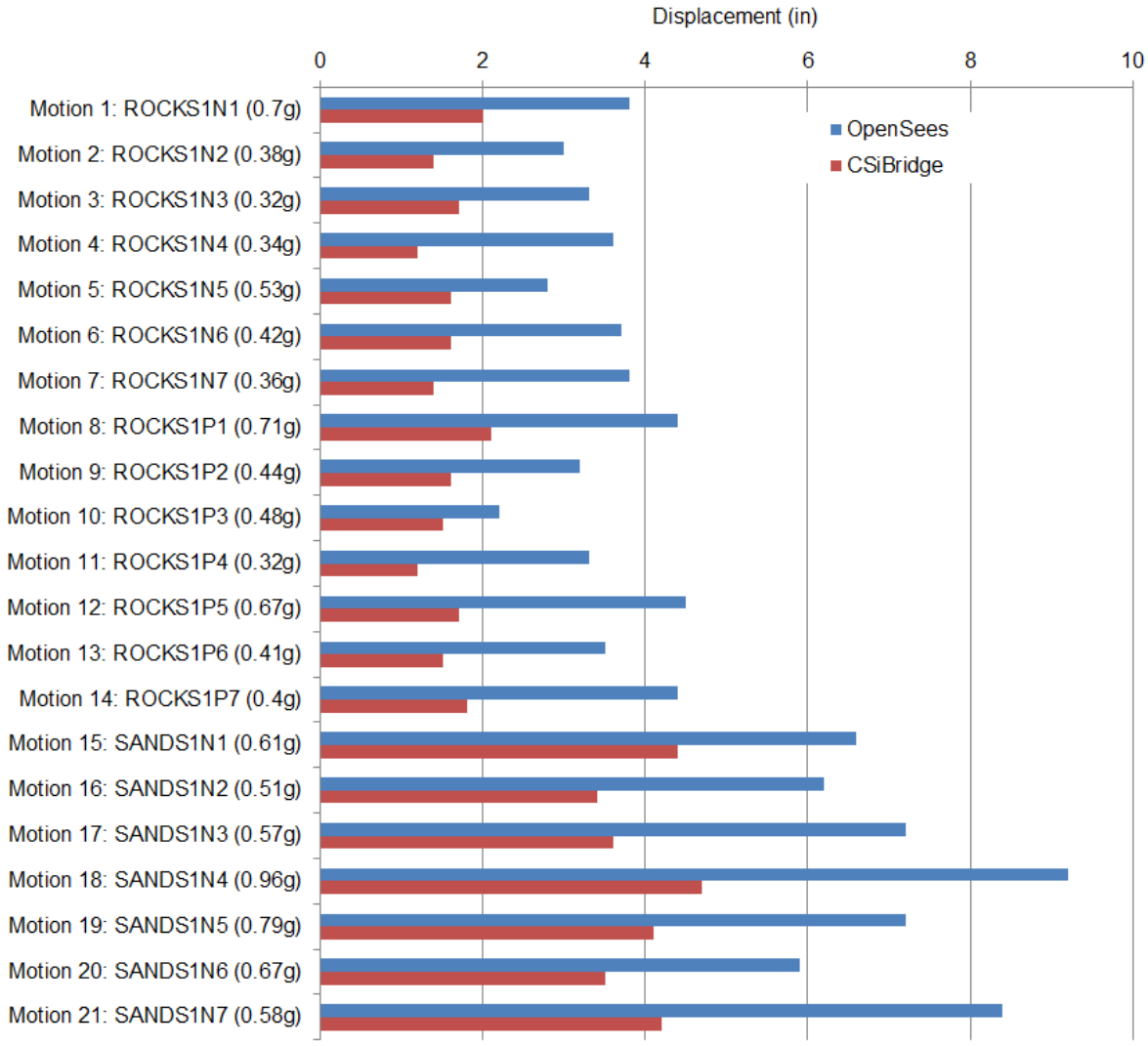

Figure 3.6 OSB1 deck maximum longitudinal displacement for Motions 1-21 (EPP-Gap model)

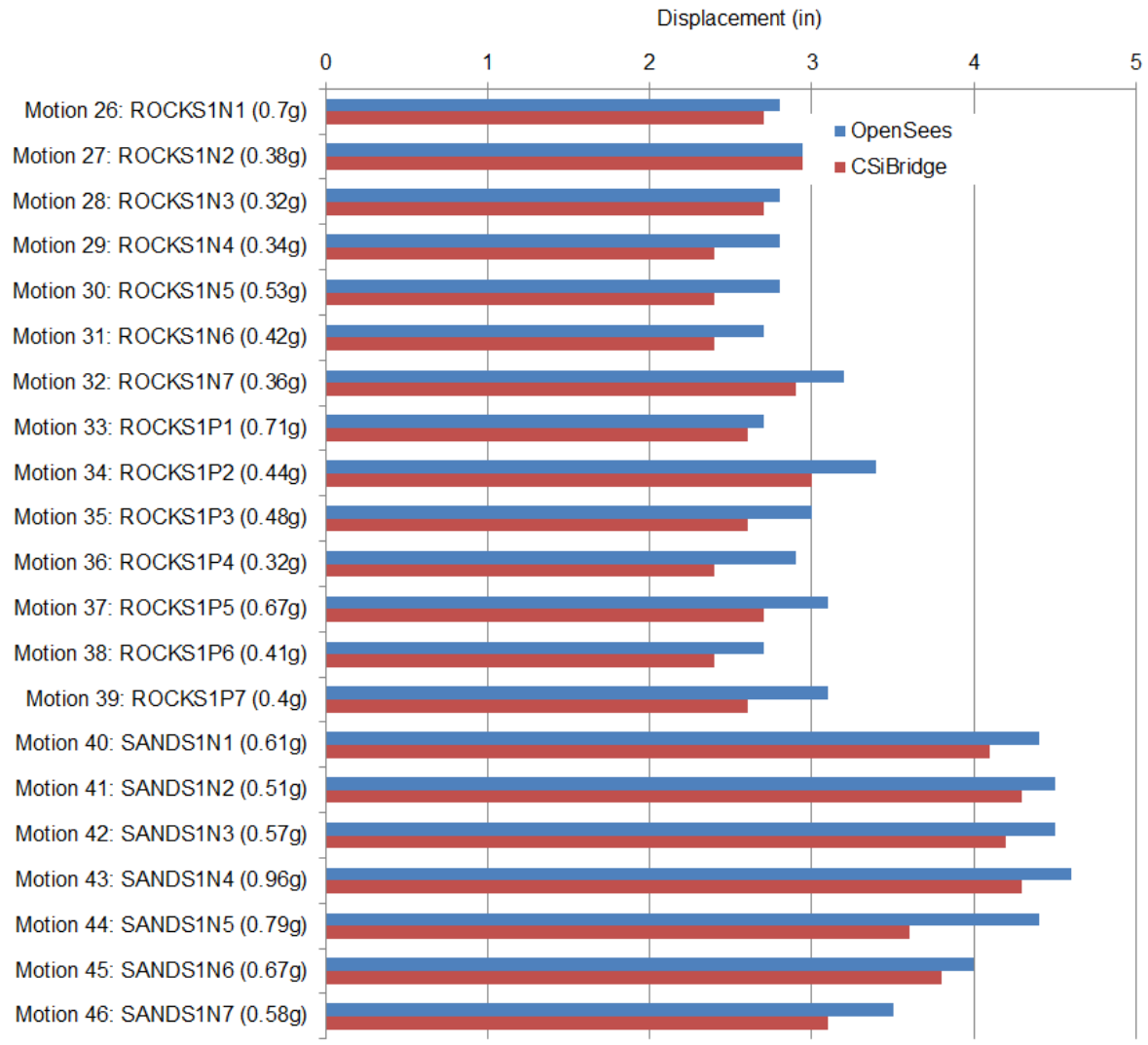

Figure 3.7 OSB1 deck maximum transverse displacement for Motions 26-46 (EPP-Gap model)

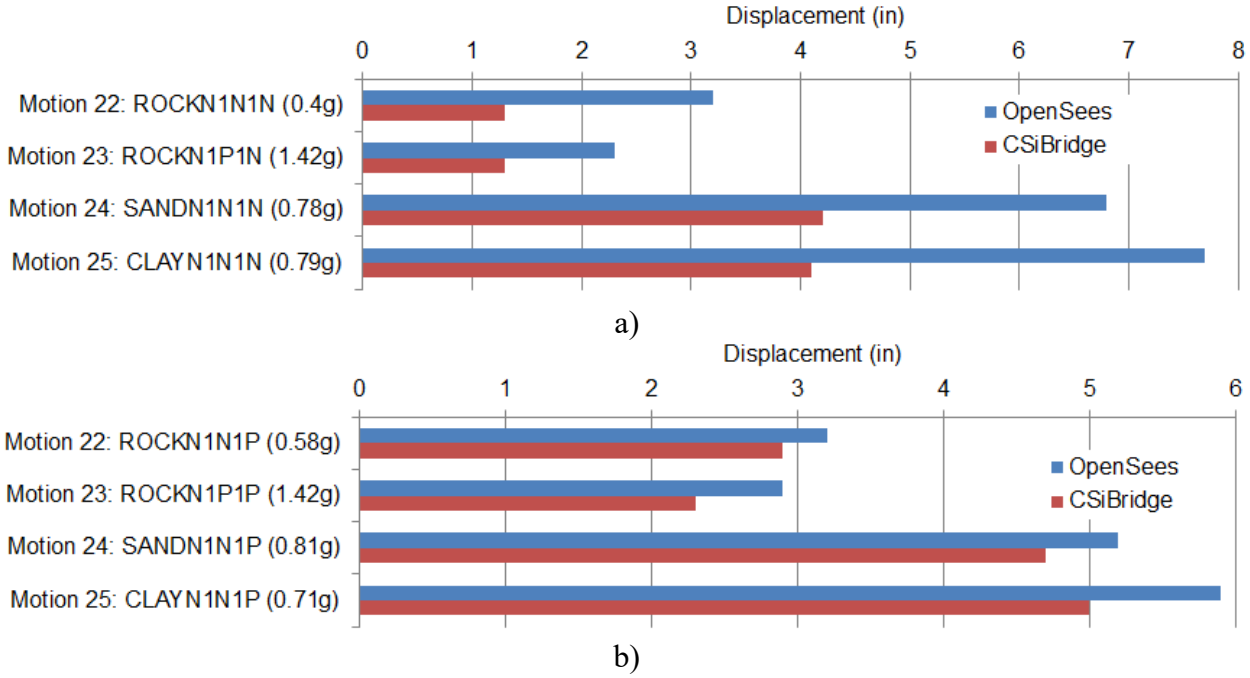

Figure 3.8 OSB1 deck maximum displacement for Motions 22-25 (EPP-Gap model): a) Lonitudinal direction; b) Transverse direction

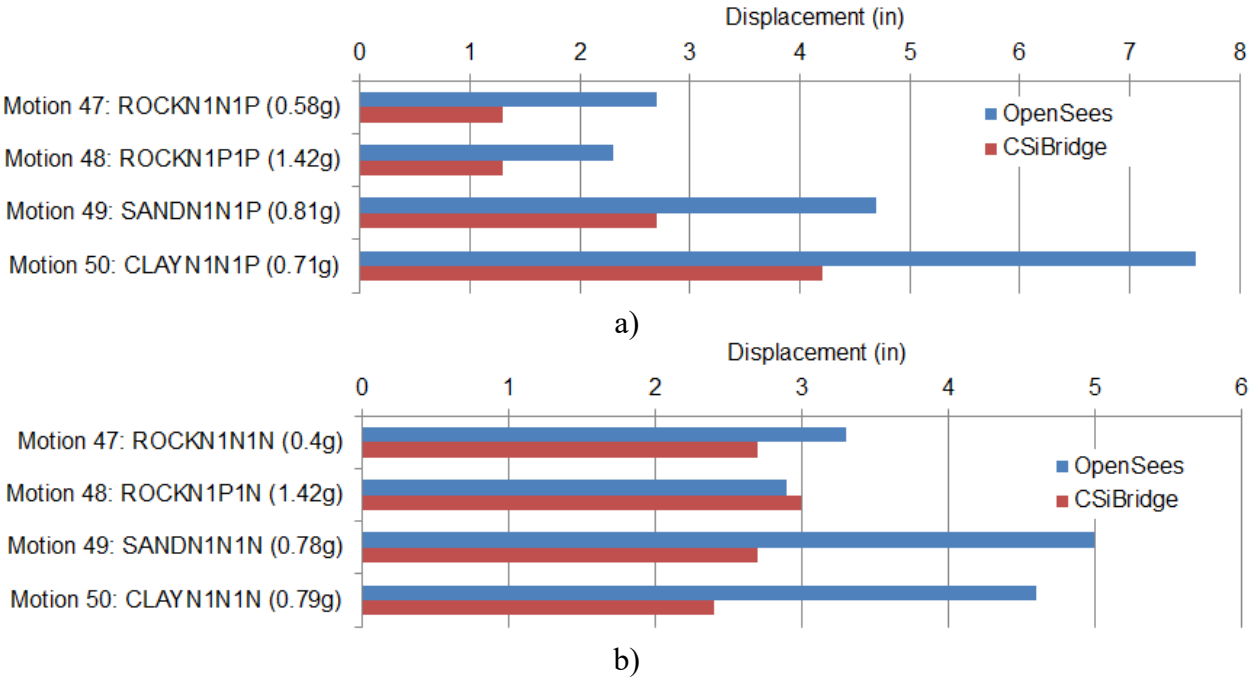

Figure 3.9 OSB1 deck maximum displacement for Motions 47-50 (EPP-Gap model): a) Lonitudinal direction; b) Transverse direction

Table 3.6. OSB1 Deck Maximum Acceleration (OpenSees)

Motion	Longitudinal Input	Transverse Input	Longitudinal Acceleration (g)			Transverse Acceleration (g)		
			Roller	EPP-Gap	EPP-Gap with Bearings	Roller	EPP-Gap	EPP-Gap with Bearings
1	ROCKS1N1 (0.7g)	-	0.38	0.87	0.86	-	-	-
2	ROCKS1N2 (0.38g)	-	0.33	0.77	0.87	-	-	-
3	ROCKS1N3 (0.32g)	-	0.34	0.79	0.84	-	-	-
4	ROCKS1N4 (0.34g)	-	0.42	0.78	0.92	-	-	-
5	ROCKS1N5 (0.53g)	-	0.34	0.76	0.85	-	-	-
6	ROCKS1N6 (0.42g)	-	0.33	0.86	0.85	-	-	-
7	ROCKS1N7 (0.36g)	-	0.34	0.90	0.83	-	-	-
8	ROCKS1P1 (0.71g)	-	0.39	0.91	0.88	-	-	-
9	ROCKS1P2 (0.44g)	-	0.32	0.79	0.88	-	-	-
10	ROCKS1P3 (0.48g)	-	0.35	0.70	0.87	-	-	-
11	ROCKS1P4 (0.32g)	-	0.43	0.81	0.90	-	-	-
12	ROCKS1P5 (0.67g)	-	0.38	0.89	0.95	-	-	-
13	ROCKS1P6 (0.41g)	-	0.33	0.83	0.86	-	-	-
14	ROCKS1P7 (0.4g)	-	0.38	0.93	0.91	-	-	-
15	SANDS1N1 (0.61g)	-	0.51	1.15	1.37	-	-	-
16	SANDS1N2 (0.51g)	-	0.48	0.99	1.19	-	-	-
17	SANDS1N3 (0.57g)	-	0.47	1.02	1.08	-	-	-
18	SANDS1N4 (0.96g)	-	0.61	1.27	1.08	-	-	-
19	SANDS1N5 (0.79g)	-	0.50	1.20	1.10	-	-	-
20	SANDS1N6 (0.67g)	-	0.42	1.05	1.30	-	-	-
21	SANDS1N7 (0.58g)	-	0.53	1.31	1.21	-	-	-
22	ROCKN1N1N (0.4g)	ROCKN1N1P (0.58g)	0.32	0.77	0.84	0.42	0.81	0.90
23	ROCKN1P1N (1.42g)	ROCKN1P1P (1.42g)	0.33	0.77	0.71	0.36	0.75	0.73
24	SANDN1N1N (0.78g)	SANDN1N1P (0.81g)	0.42	0.99	1.08	0.37	1.21	1.30
25	CLAYN1N1N (0.79g)	CLAYN1N1P (0.71g)	0.50	1.05	0.95	0.49	1.33	1.20
26	-	ROCKS1N1 (0.7g)	-	-	-	0.40	0.72	0.98
27	-	ROCKS1N2 (0.38g)	-	-	-	0.35	0.88	0.88
28	-	ROCKS1N3 (0.32g)	-	-	-	0.40	0.71	0.93
29	-	ROCKS1N4 (0.34g)	-	-	-	0.44	0.72	0.82
30	-	ROCKS1N5 (0.53g)	-	-	-	0.42	0.70	0.83
31	-	ROCKS1N6 (0.42g)	-	-	-	0.37	0.72	0.94
32	-	ROCKS1N7 (0.36g)	-	-	-	0.33	0.81	0.86
33	-	ROCKS1P1 (0.71g)	-	-	-	0.40	0.71	0.98
34	-	ROCKS1P2 (0.44g)	-	-	-	0.39	0.84	0.92
35	-	ROCKS1P3 (0.48g)	-	-	-	0.45	0.75	0.87
36	-	ROCKS1P4 (0.32g)	-	-	-	0.45	0.76	0.78
37	-	ROCKS1P5 (0.67g)	-	-	-	0.39	0.81	0.89
38	-	ROCKS1P6 (0.41g)	-	-	-	0.36	0.71	0.93
39	-	ROCKS1P7 (0.4g)	-	-	-	0.42	0.77	0.93
40	-	SANDS1N1 (0.61g)	-	-	-	0.57	1.02	1.16
41	-	SANDS1N2 (0.51g)	-	-	-	0.54	1.04	1.29
42	-	SANDS1N3 (0.57g)	-	-	-	0.47	1.06	1.26
43	-	SANDS1N4 (0.96g)	-	-	-	0.66	1.08	1.18
44	-	SANDS1N5 (0.79g)	-	-	-	0.49	1.00	1.28
45	-	SANDS1N6 (0.67g)	-	-	-	0.50	0.92	1.18
46	-	SANDS1N7 (0.58g)	-	-	-	0.53	0.81	1.18
47	ROCKN1N1P (0.58g)	ROCKN1N1N (0.4g)	0.39	0.72	0.77	0.29	0.84	1.10
48	ROCKN1P1P (1.42g)	ROCKN1P1N (1.42g)	0.33	0.76	0.71	0.36	0.75	0.73
49	SANDN1N1P (0.81g)	SANDN1N1N (0.78g)	0.36	0.88	0.99	0.47	1.10	1.22
50	CLAYN1N1P (0.71g)	CLAYN1N1N (0.79g)	0.45	1.16	1.20	0.52	0.97	1.21

Table 3.7. OSB1 Deck Maximum Acceleration for EPP-Gap Model (Comparison of OpenSees and CSiBridge)
(Difference is relative to OpenSees result)

Motion	Longitudinal Input	Transverse Input	Longitudinal Acceleration (g)			Transverse Acceleration (g)		
			OpenSees	CSiBridge	Difference	OpenSees	CSiBridge	Difference
1	ROCKS1N1 (0.7g)	-	0.87	0.60	-31%	-	-	-
2	ROCKS1N2 (0.38g)	-	0.77	0.60	-22%	-	-	-
3	ROCKS1N3 (0.32g)	-	0.79	0.56	-29%	-	-	-
4	ROCKS1N4 (0.34g)	-	0.78	0.63	-19%	-	-	-
5	ROCKS1N5 (0.53g)	-	0.76	0.62	-18%	-	-	-
6	ROCKS1N6 (0.42g)	-	0.86	0.59	-31%	-	-	-
7	ROCKS1N7 (0.36g)	-	0.90	0.85	-6%	-	-	-
8	ROCKS1P1 (0.71g)	-	0.91	0.58	-36%	-	-	-
9	ROCKS1P2 (0.44g)	-	0.79	0.6	-24%	-	-	-
10	ROCKS1P3 (0.48g)	-	0.70	0.57	-19%	-	-	-
11	ROCKS1P4 (0.32g)	-	0.81	0.63	-22%	-	-	-
12	ROCKS1P5 (0.67g)	-	0.89	0.62	-30%	-	-	-
13	ROCKS1P6 (0.41g)	-	0.83	0.63	-24%	-	-	-
14	ROCKS1P7 (0.4g)	-	0.93	0.56	-40%	-	-	-
15	SANDS1N1 (0.61g)	-	1.15	0.79	-31%	-	-	-
16	SANDS1N2 (0.51g)	-	0.99	0.79	-20%	-	-	-
17	SANDS1N3 (0.57g)	-	1.02	0.95	-7%	-	-	-
18	SANDS1N4 (0.96g)	-	1.27	0.91	-28%	-	-	-
19	SANDS1N5 (0.79g)	-	1.20	0.84	-30%	-	-	-
20	SANDS1N6 (0.67g)	-	1.05	0.86	-18%	-	-	-
21	SANDS1N7 (0.58g)	-	1.31	0.76	-42%	-	-	-
22	ROCKN1N1N (0.4g)	ROCKN1N1P (0.58g)	0.77	0.60	22%	0.81	0.78	-4%
23	ROCKN1P1N (1.42g)	ROCKN1P1P (1.42g)	0.77	0.83	8%	0.75	0.62	-17%
24	SANDN1N1N (0.78g)	SANDN1N1P (0.81g)	0.99	0.84	-15%	1.21	1.23	2%
25	CLAYN1N1N (0.79g)	CLAYN1N1P (0.71g)	1.05	0.60	-43%	1.33	1.31	-2%
26	-	ROCKS1N1 (0.7g)	-	-	-	0.72	0.70	-3%
27	-	ROCKS1N2 (0.38g)	-	-	-	0.88	0.82	-7%
28	-	ROCKS1N3 (0.32g)	-	-	-	0.71	0.71	0%
29	-	ROCKS1N4 (0.34g)	-	-	-	0.72	0.63	-13%
30	-	ROCKS1N5 (0.53g)	-	-	-	0.70	0.63	-10%
31	-	ROCKS1N6 (0.42g)	-	-	-	0.72	0.63	-13%
32	-	ROCKS1N7 (0.36g)	-	-	-	0.81	0.74	-9%
33	-	ROCKS1P1 (0.71g)	-	-	-	0.71	0.68	-4%
34	-	ROCKS1P2 (0.44g)	-	-	-	0.84	0.77	-8%
35	-	ROCKS1P3 (0.48g)	-	-	-	0.75	0.68	-9%
36	-	ROCKS1P4 (0.32g)	-	-	-	0.76	0.63	-17%
37	-	ROCKS1P5 (0.67g)	-	-	-	0.81	0.73	-10%
38	-	ROCKS1P6 (0.41g)	-	-	-	0.71	0.64	-10%
39	-	ROCKS1P7 (0.4g)	-	-	-	0.77	0.65	-16%
40	-	SANDS1N1 (0.61g)	-	-	-	1.02	1.04	2%
41	-	SANDS1N2 (0.51g)	-	-	-	1.04	1.1	6%
42	-	SANDS1N3 (0.57g)	-	-	-	1.06	1.08	2%
43	-	SANDS1N4 (0.96g)	-	-	-	1.08	1.11	3%
44	-	SANDS1N5 (0.79g)	-	-	-	1.00	0.9	-10%
45	-	SANDS1N6 (0.67g)	-	-	-	0.92	0.94	2%
46	-	SANDS1N7 (0.58g)	-	-	-	0.81	0.65	-20%
47	ROCKN1N1P (0.58g)	ROCKN1N1N (0.4g)	0.72	0.54	-25%	0.84	0.76	-10%
48	ROCKN1P1P (1.42g)	ROCKN1P1N (1.42g)	0.76	0.60	-21%	0.75	0.62	-17%
49	SANDN1N1P (0.81g)	SANDN1N1N (0.78g)	0.88	0.79	-10%	1.10	1.15	5%
50	CLAYN1N1P (0.71g)	CLAYN1N1N (0.79g)	1.16	0.89	-23%	0.97	1.01	4%

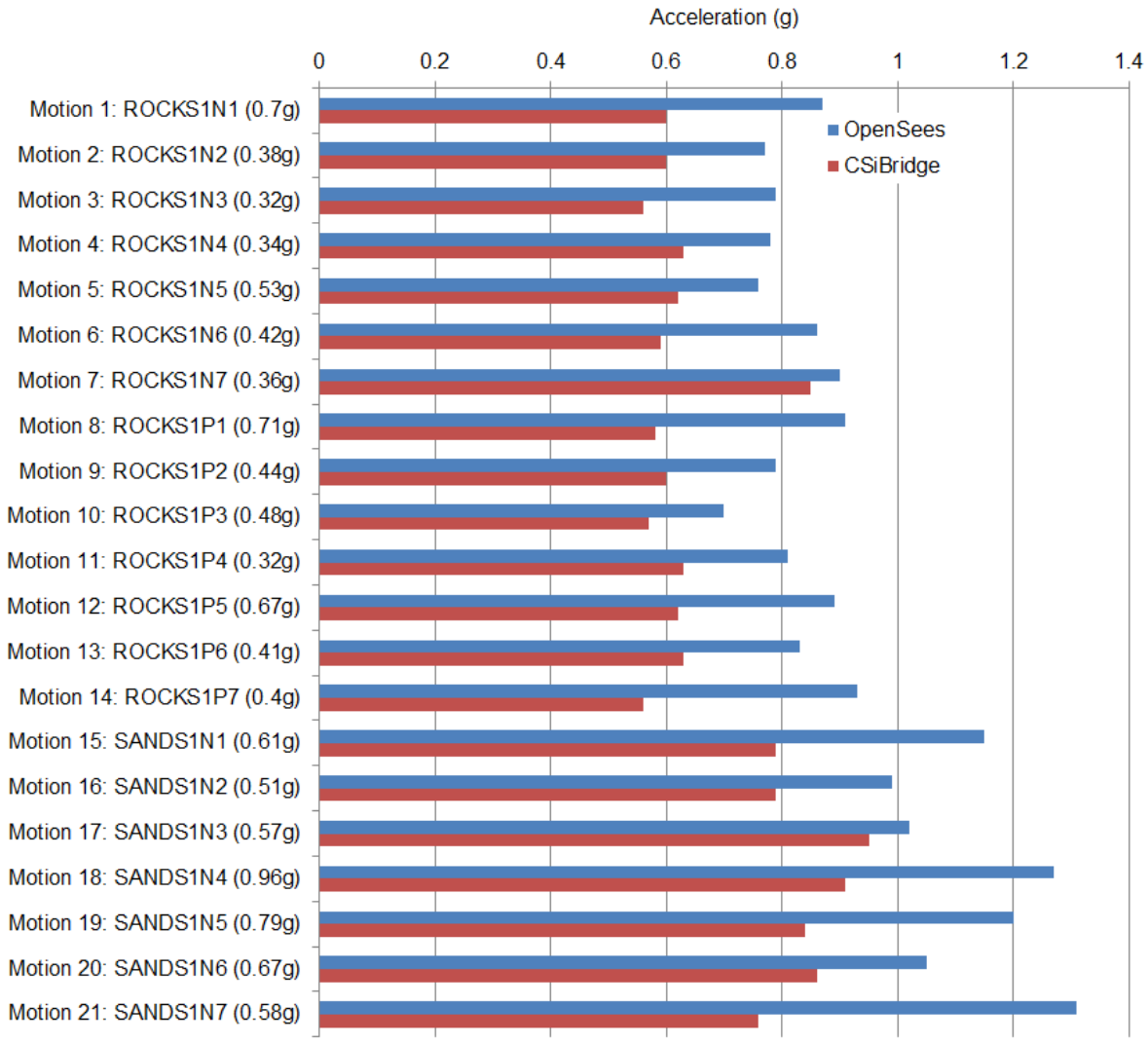

Figure 3.10 OSB1 deck maximum longitudinal acceleration for Motions 1-21 (EPP-Gap model)

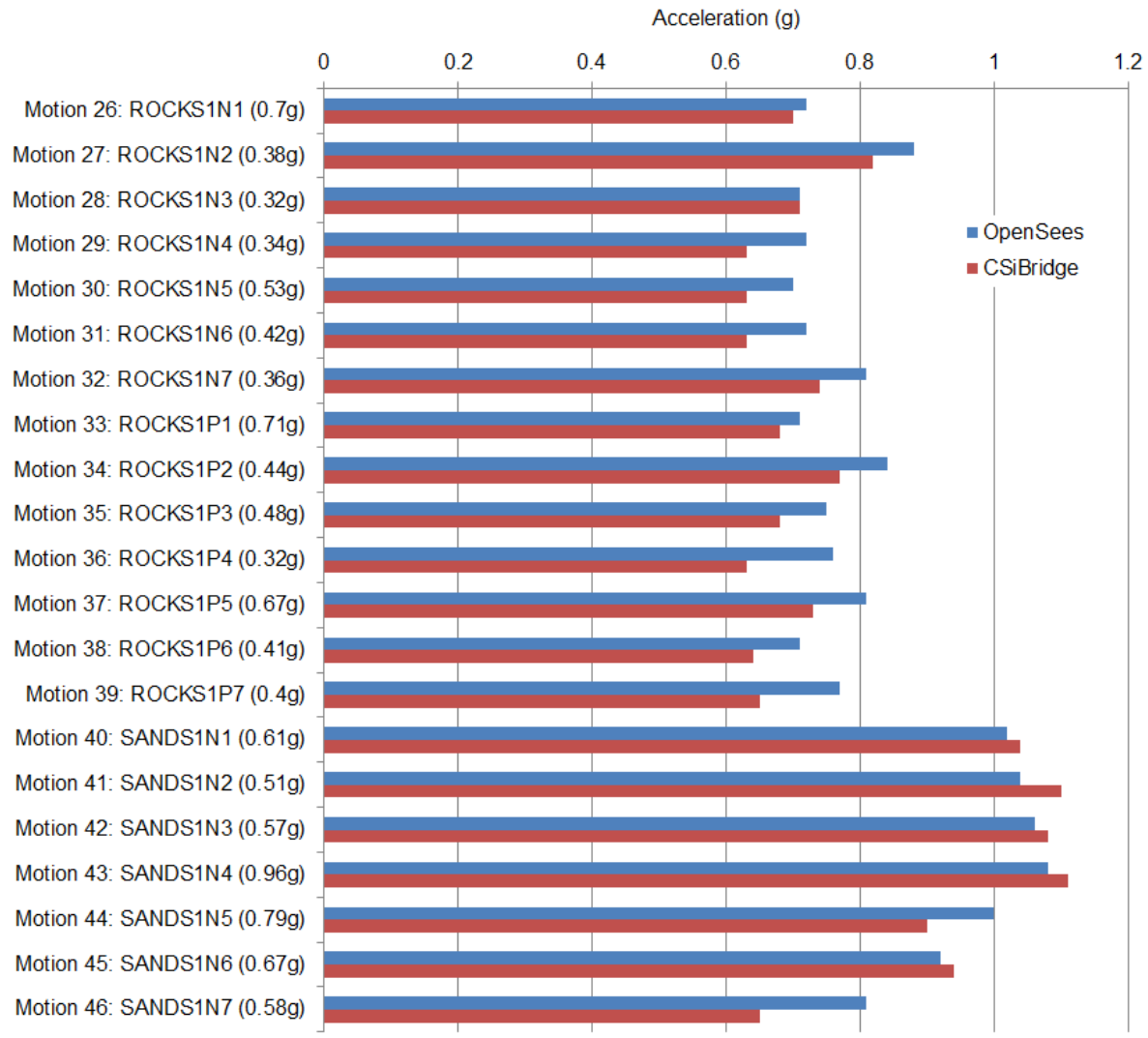

Figure 3.11 OSB1 deck maximum transverse acceleration for Motions 26-46 (EPP-Gap model)

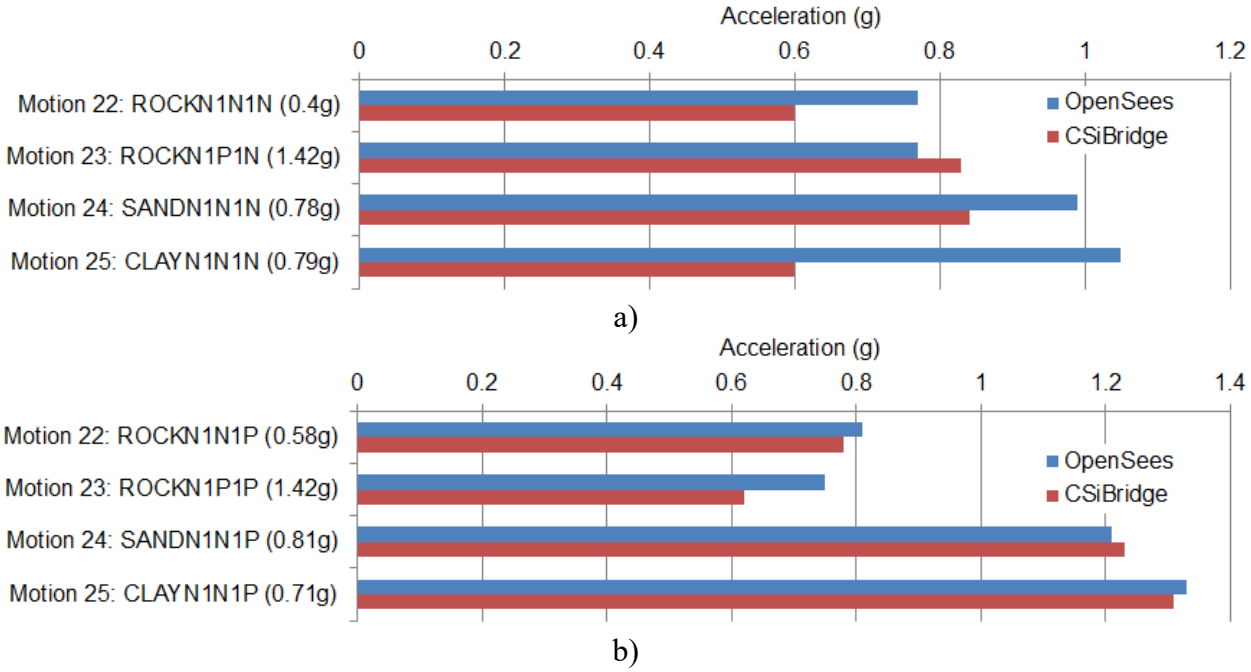

Figure 3.12 OSB1 deck maximum acceleration for Motions 22-25 (EPP-Gap model): a) Lonitudinal direction; b) Transverse direction

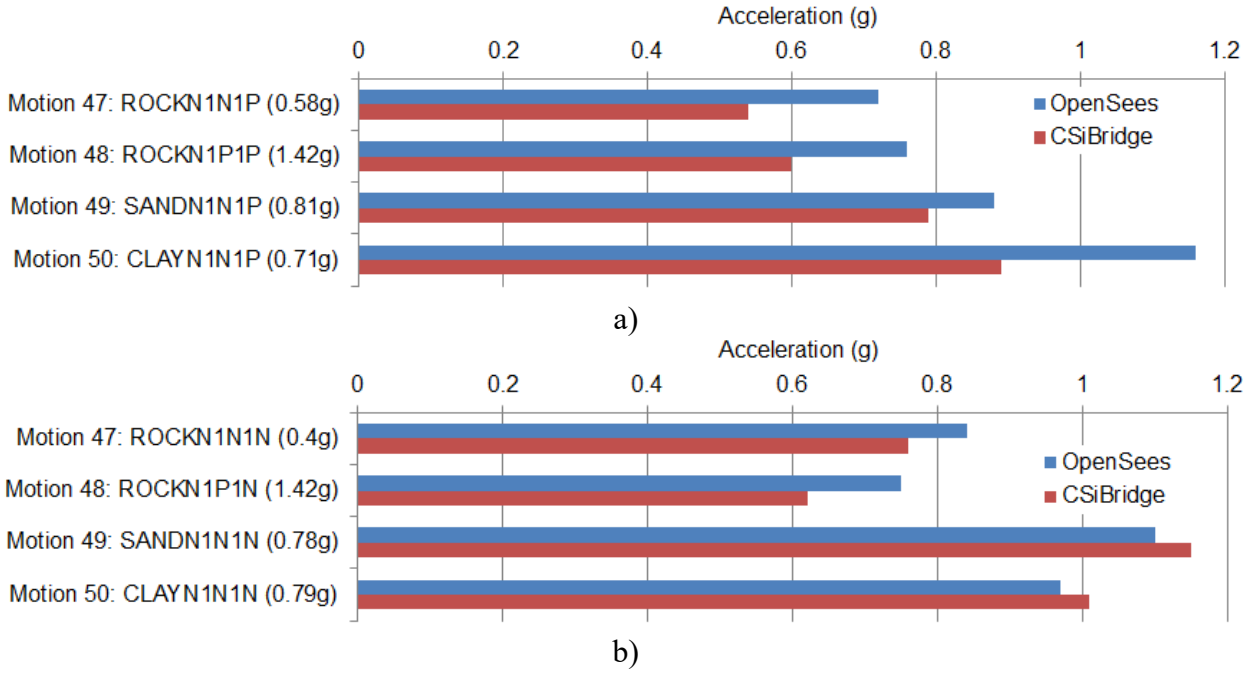

Figure 3.13 OSB1 deck maximum acceleration for Motions 47-50 (EPP-Gap model): a) Lonitudinal direction; b) Transverse direction

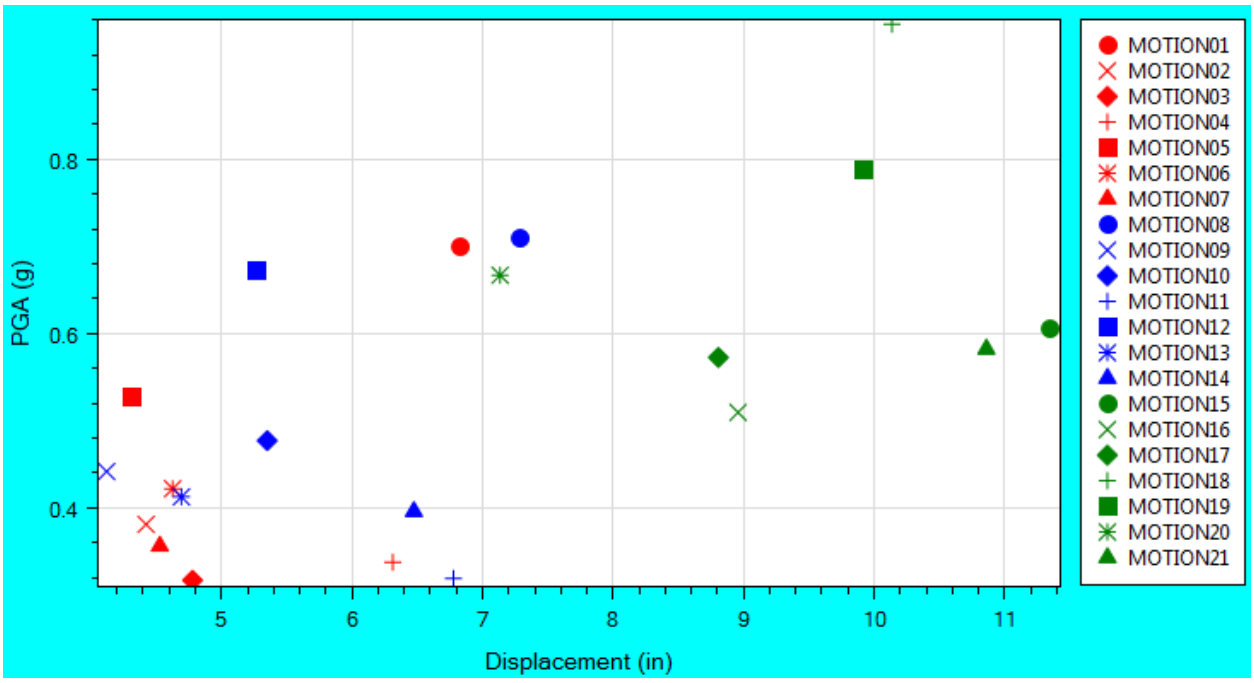

Figure 3.14 OSB1 deck maximum longitudinal displacement in OpenSees (Motions 1-21; Roller model)

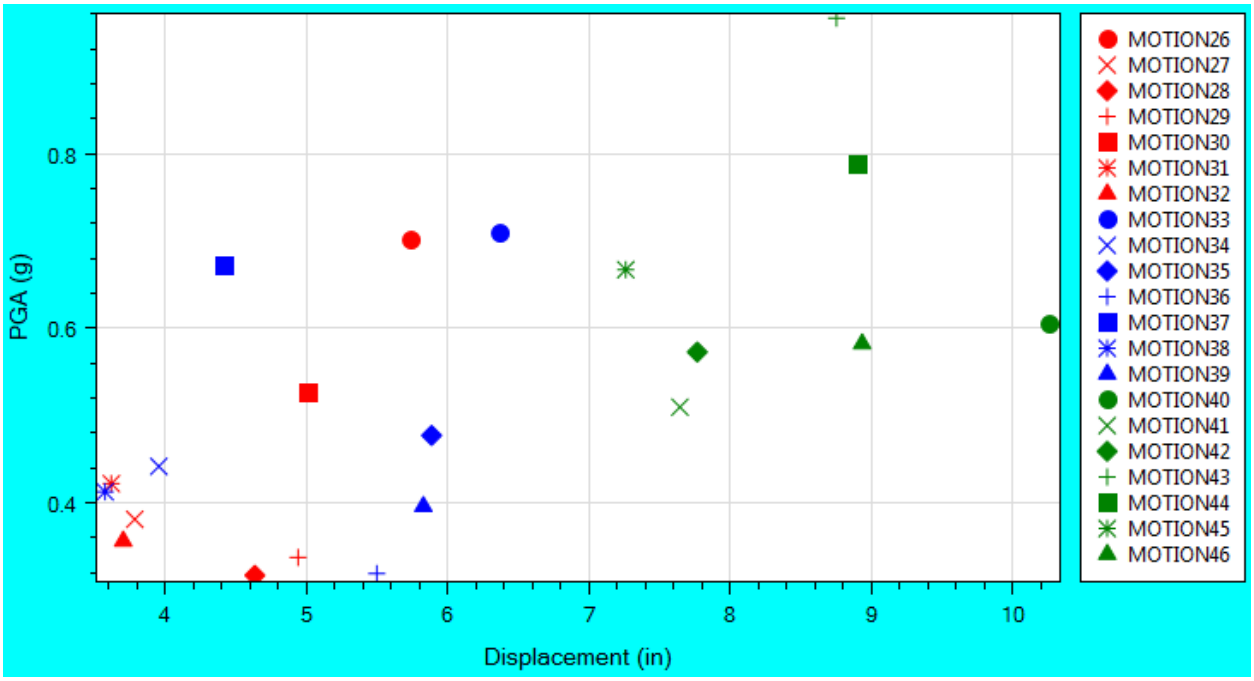

Figure 3.15 OSB1 deck maximum transverse displacement in OpenSees (Motions 26-46; Roller model)

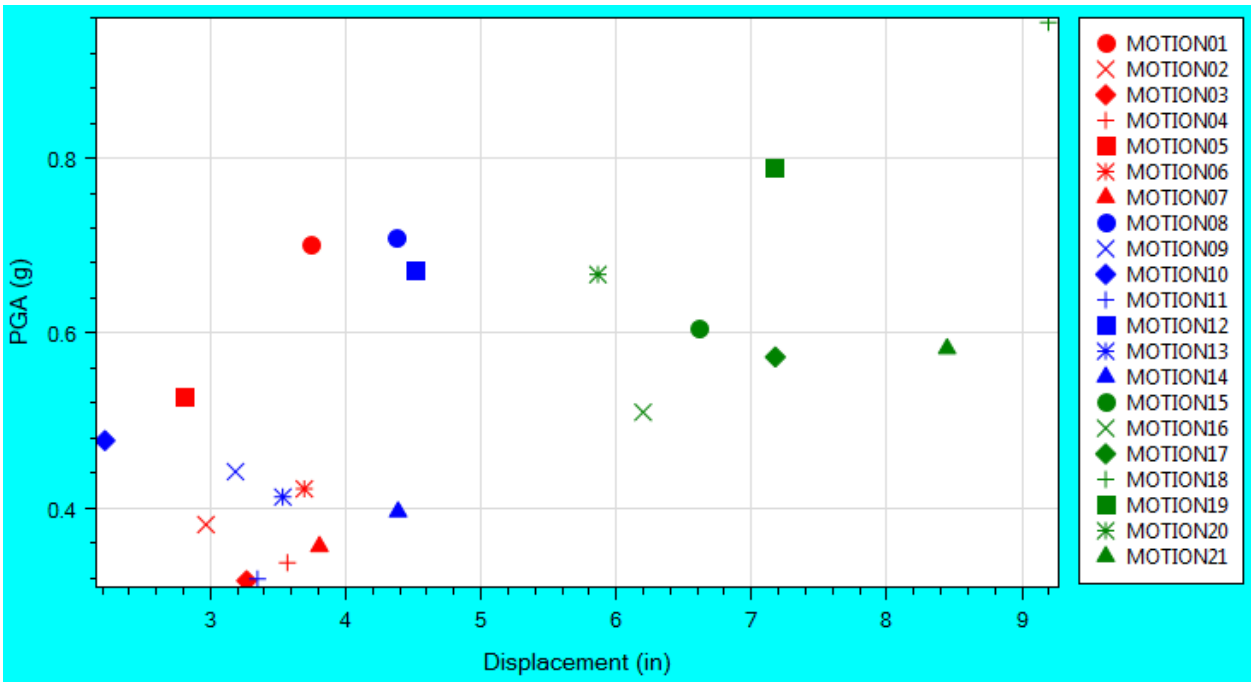

Figure 3.16 OSB1 deck maximum longitudinal displacement in OpenSees (Motions 1-21; EPP-Gap model)

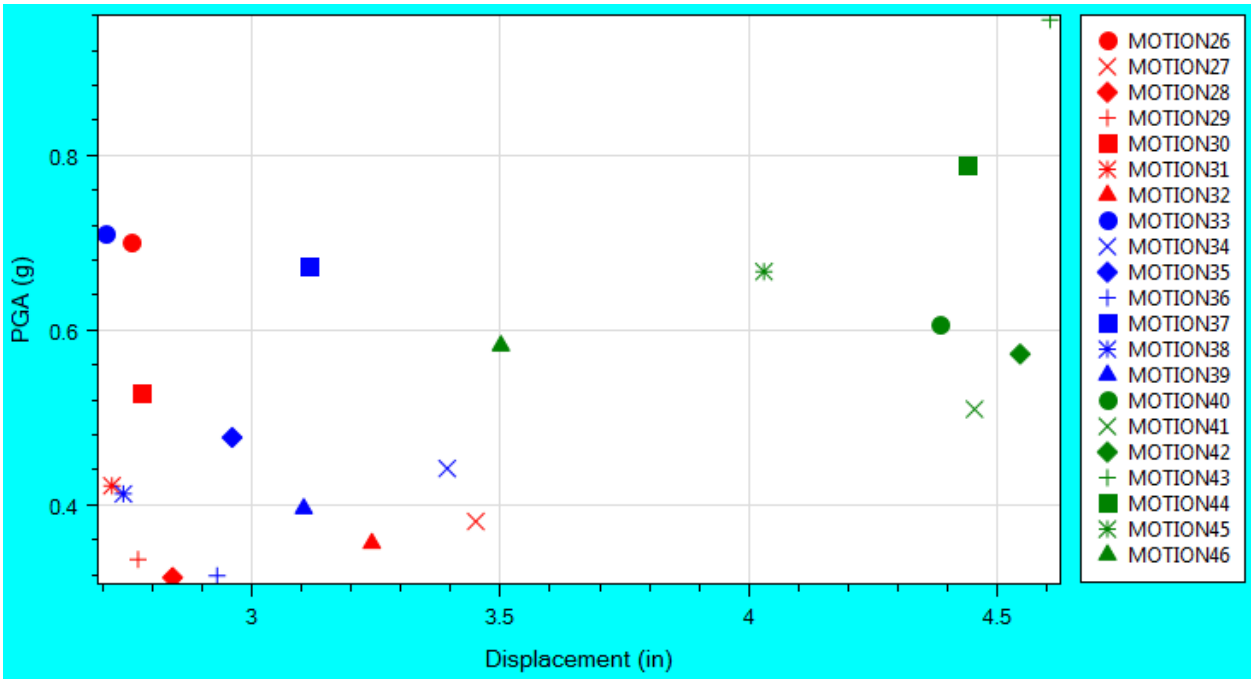

Figure 3.17 OSB1 deck maximum transverse displacement in OpenSees (Motions 26-46; EPP-Gap model)

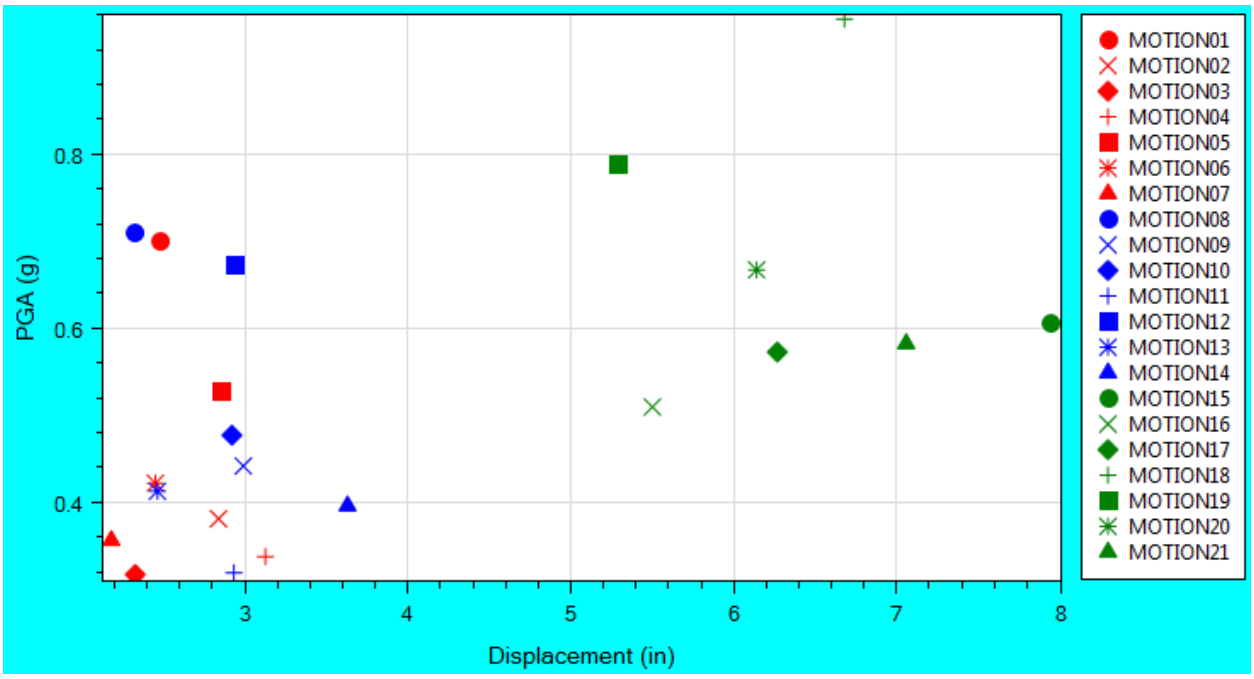

Figure 3.18 OSB1 deck maximum longitudinal displacement in OpenSees (Motions 1-21; EPP-Gap with Bearings model)

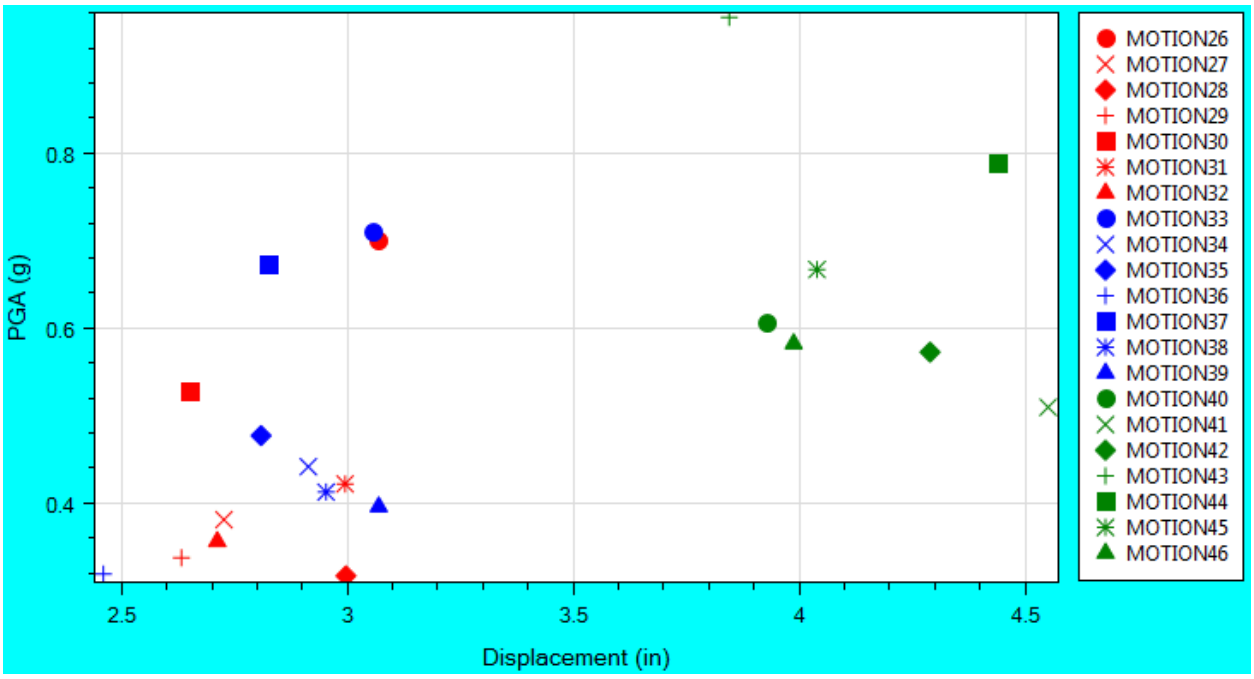

Figure 3.19 OSB1 deck maximum transverse displacement in OpenSees (Motions 26-46; EPP-Gap with Bearings model)

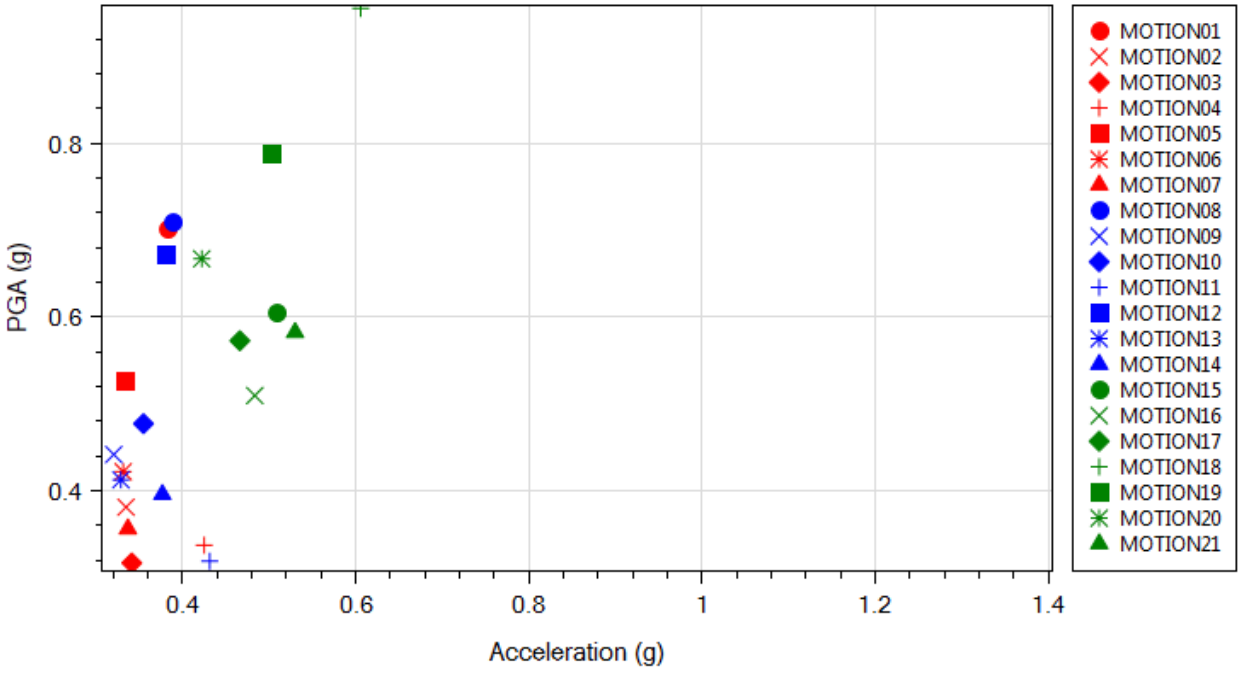

Figure 3.20 OSB1 deck maximum longitudinal acceleration in OpenSees (Motions 1-21; Roller model)

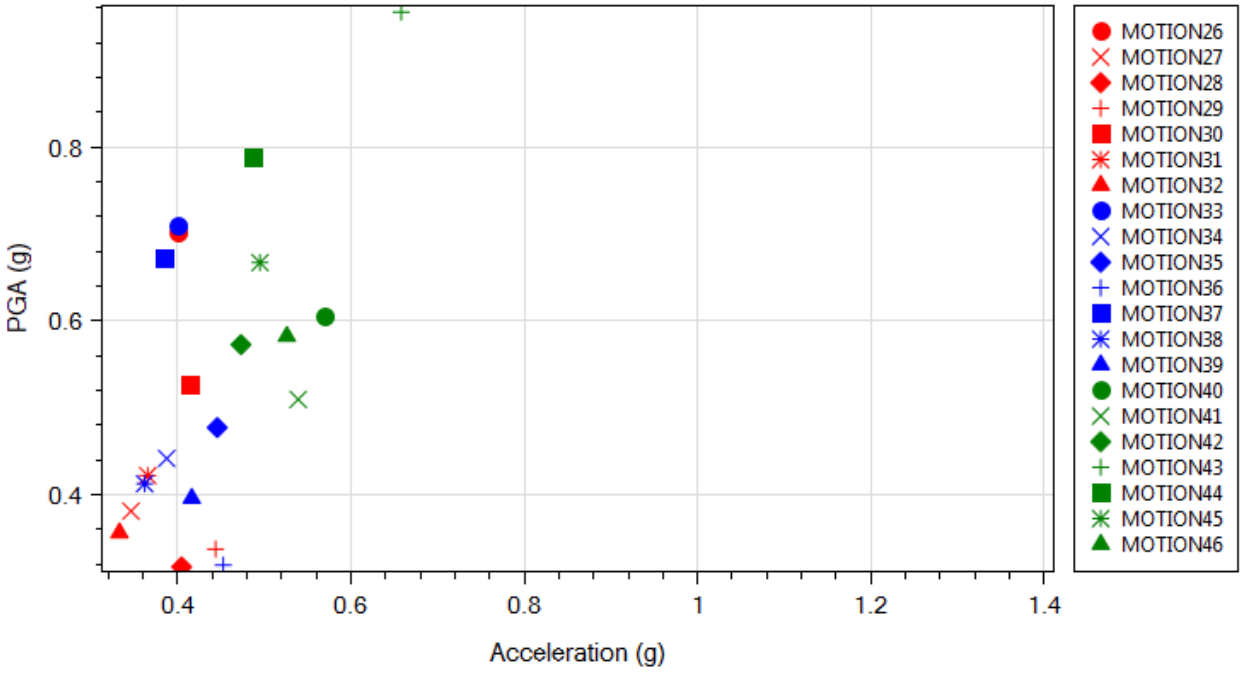

Figure 3.21 OSB1 deck maximum transverse acceleration in OpenSees (Motions 26-46; Roller model)

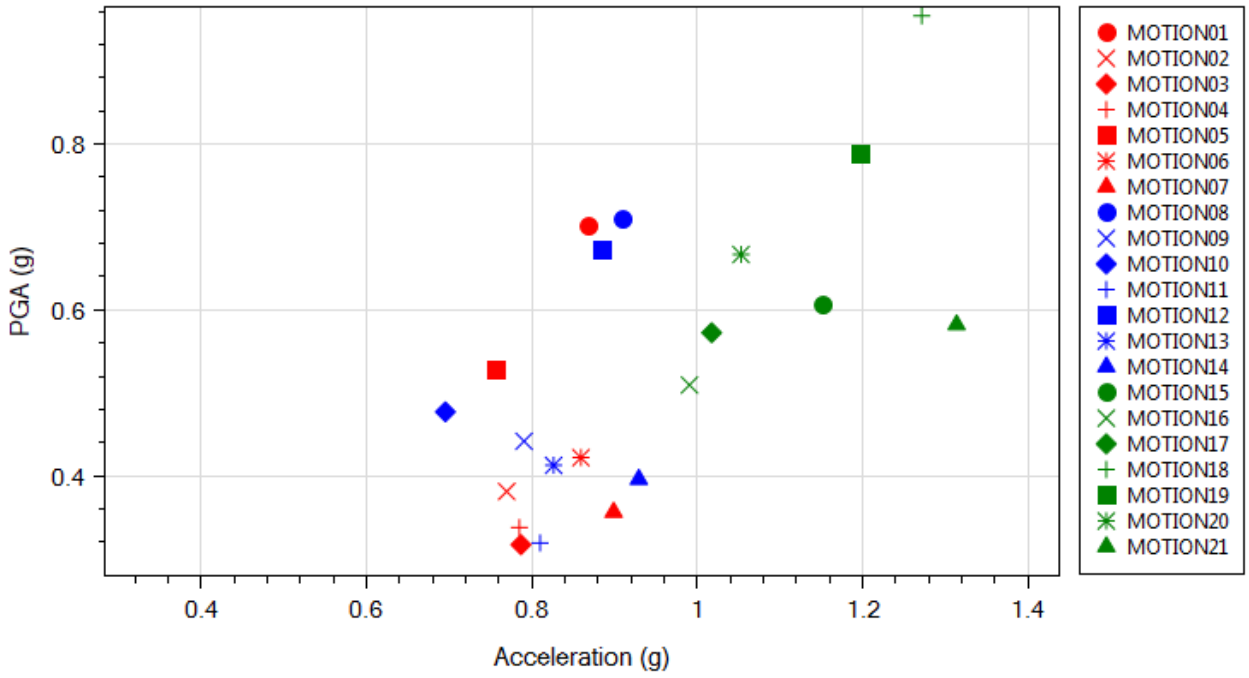

Figure 3.22 OSB1 deck maximum longitudinal acceleration in OpenSees (Motions 1-21; EPP-Gap model)

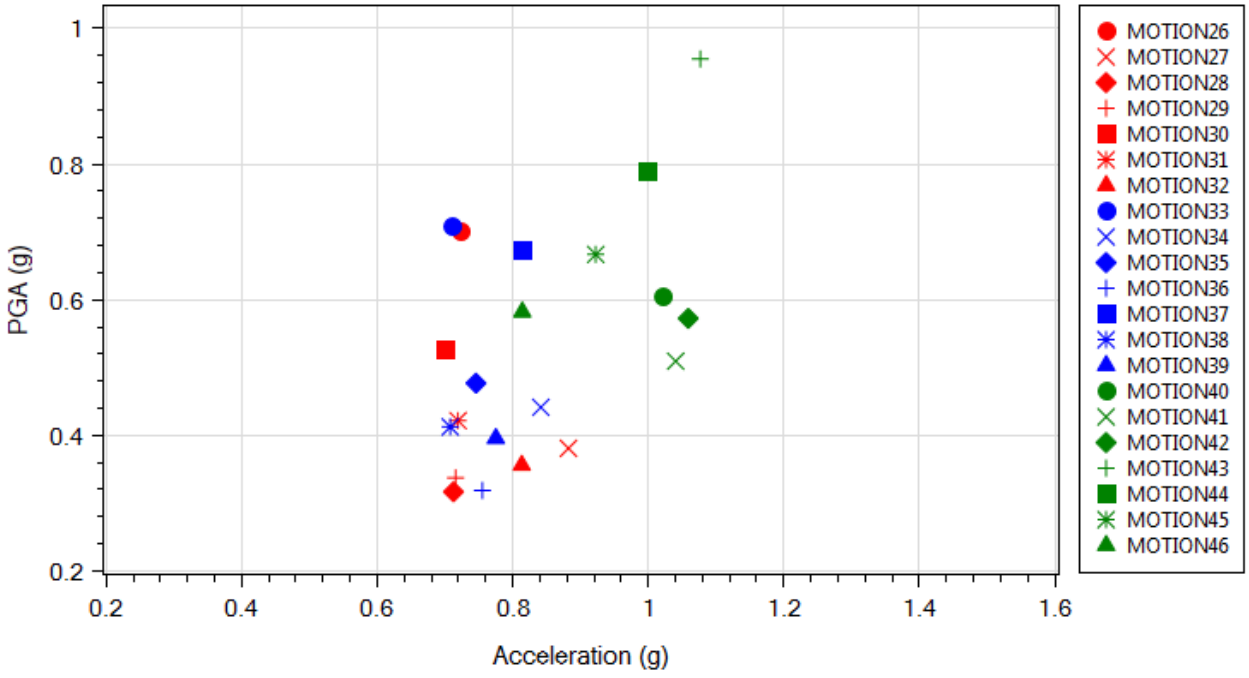

Figure 3.23 OSB1 deck maximum transverse acceleration in OpenSees (Motions 26-46; EPP-Gap model)

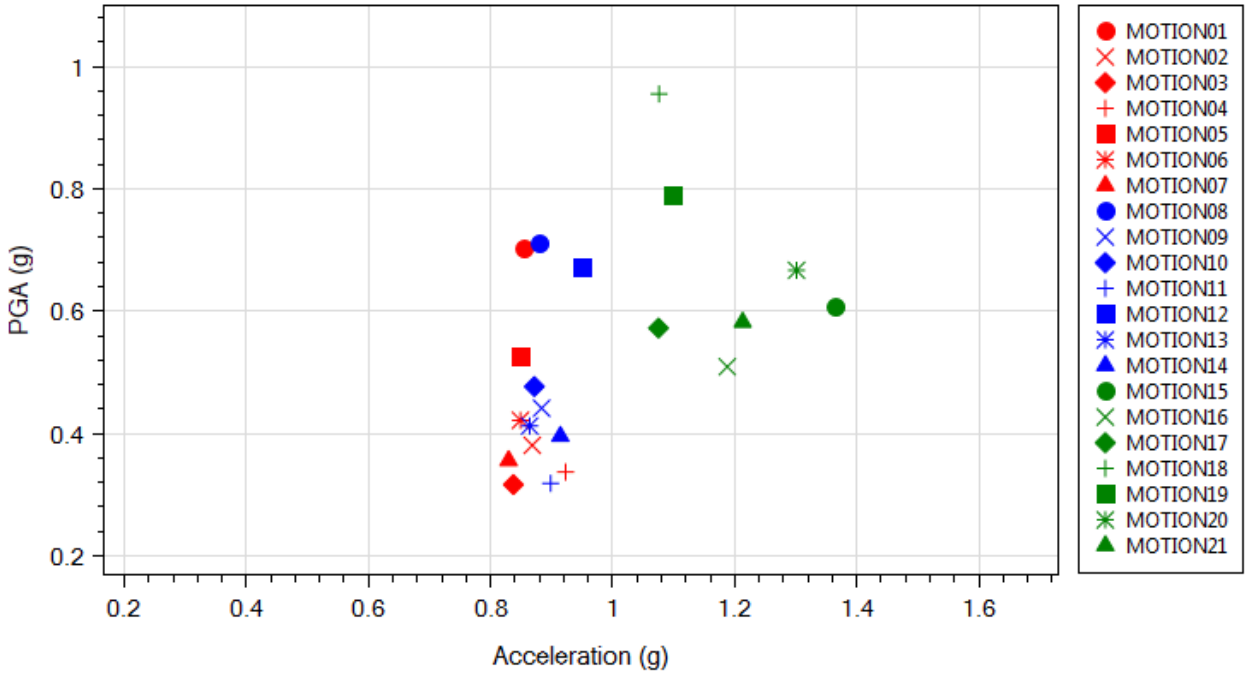

Figure 3.24 OSB1 deck maximum longitudinal acceleration in OpenSees (Motions 1-21; EPP-Gap with Bearings model)

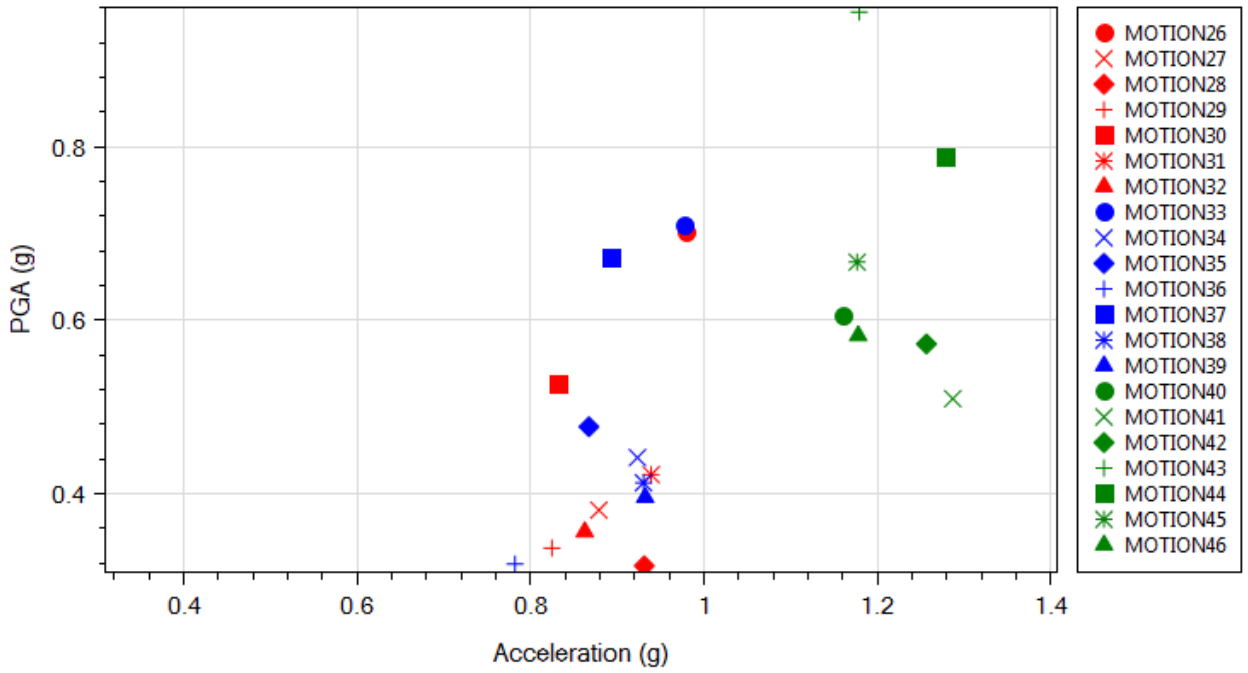

Figure 3.25 OSB1 deck maximum transverse acceleration in OpenSees (Motions 26-46; EPP-Gap with Bearings model)

3.5.2 Response Time History (OpenSees)

In this section, OSB1 OpenSees response time histories for 2 representative input motions (Motions 1 and 15) for the EPP-Gap with Bearings model are presented. Note that the CSiBridge analysis for OSB1 (see Table 3.5 and Table 3.7) was conducted for a different bridge model (the EPP-Gap model, without abutment bearing pads). As such, no CSiBridge output is available to compare with the OpenSees result presented in this section.

1) Motion 1 ROCKS1N1

For Motion 1, the deck maximum displacement is 2.5 in (Table 3.4) which is essentially the smallest among the 21 longitudinal motion cases (Motions 1-21). Figure 3.26 displays OSB1 column response time history for Motion 1 (ROCKS1N1). The input motion ROCKS1N1 is also included for reference (Figure 3.26d).

The column and abutment force-displacement response is displayed in Figure 3.27. The abutment force-displacement response curves (Figure 3.27c and Figure 3.27d) show that the embankment was fully mobilized (the yield force of -1,555 kip was reached) during the shaking event. The straight line segments with the smaller slope indicate that only the bearings were in effect at that time (the specified longitudinal gap is 0.14 ft in this case). This small slope is actually the combined initial elastic stiffness of all 6 bearings.

Figure 3.28 displays the moment-curvature response at the column top. The bending moment reached 9,500 kip-ft, bordering on the phase of significant yielding (the yield bending moment is 11,000 kip-ft, see Appendix D).

2) Motion 15 SANDS1N1

Motion 15 resulted in the largest maximum displacement among the motions with longitudinal components only (Motions 1-21). Figure 3.29 shows OSB1 column response time history for the EPP-Gap with Bearings abutment model.

The column and abutment force-displacement response are displayed in Figure 3.30. It is seen that the embankment was fully mobilized (the yield force of -1,555 kip was reached) during the shaking event in this case.

Figure 3.31 displays the moment-curvature response at the column top for Motion 15. The maximum curvature is 0.00055 rad/in (reached at the maximum bending moment of 11,000 kip-ft as shown in Figure 2.31).

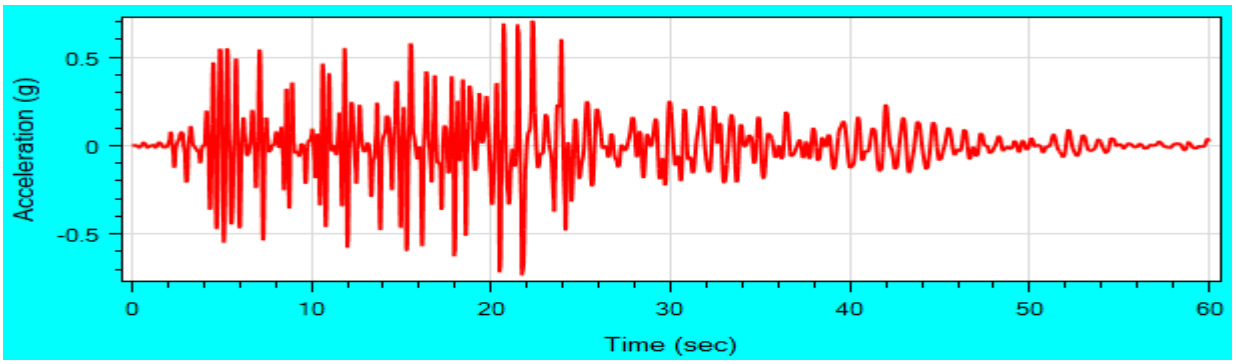

a)

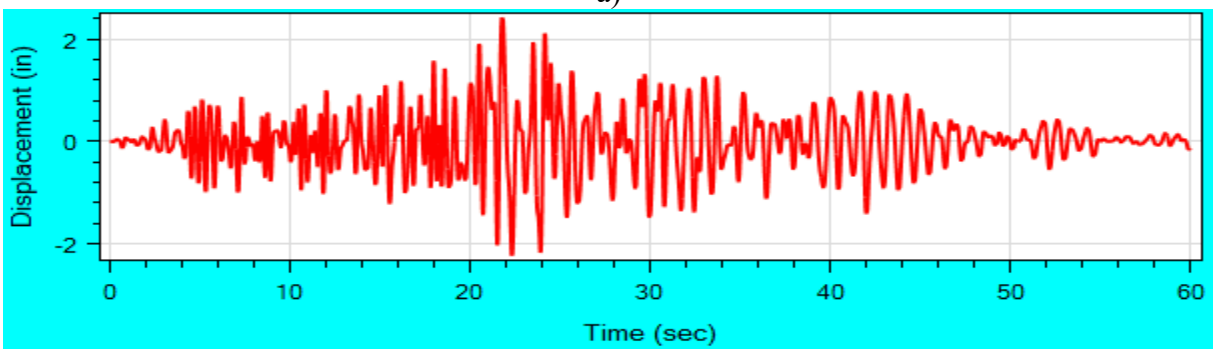

b)

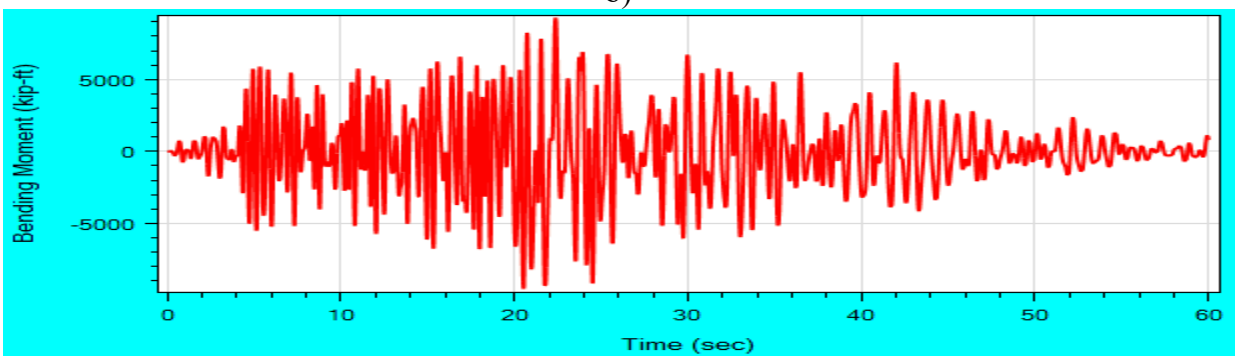

c)

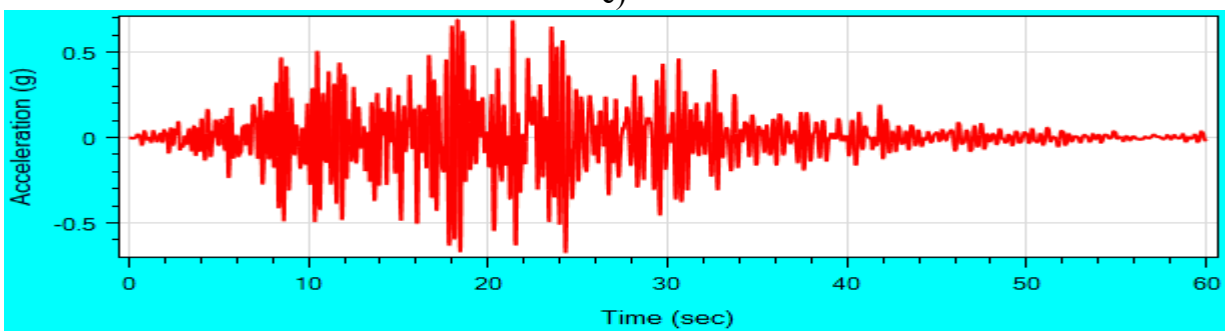

d)

Figure 3.26 OSB1 column top longitudinal response time histories for Motion 1 ROCKS1N1 (EPP-Gap with Bearings model): a) acceleration; b) displacement; c) bending moment; d) base excitation ROCKS1N1

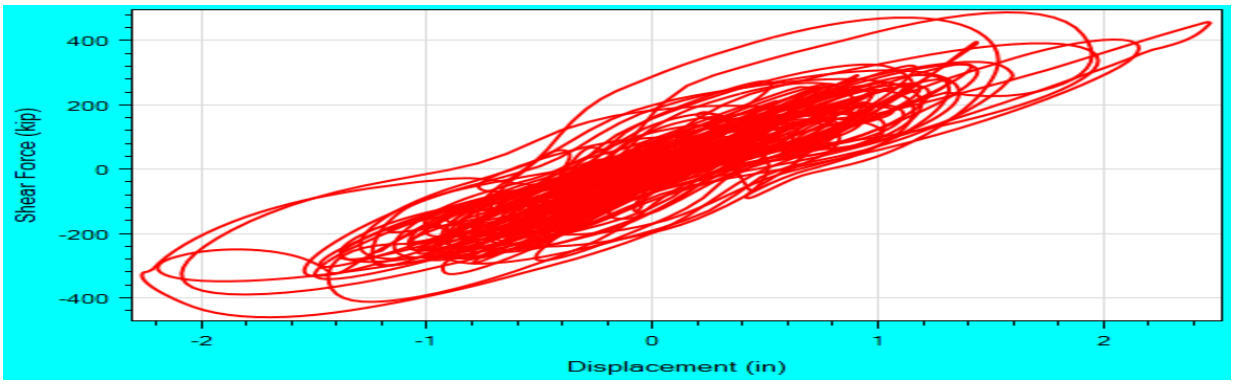

a)

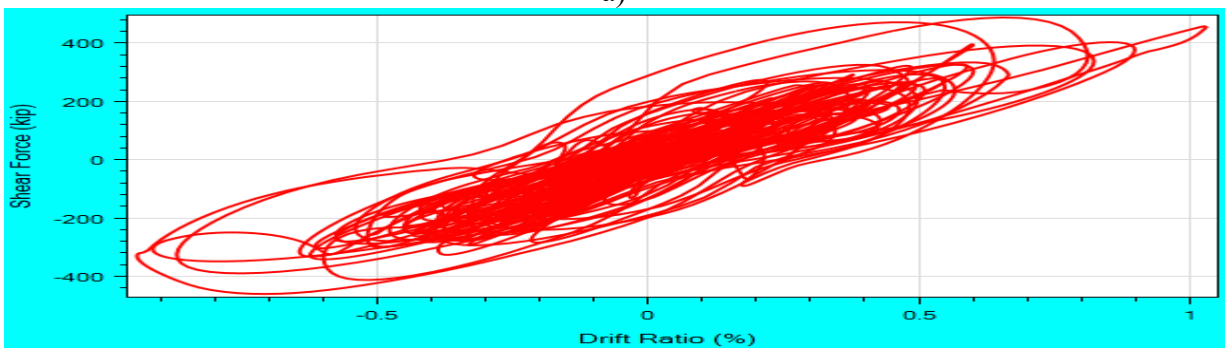

b)

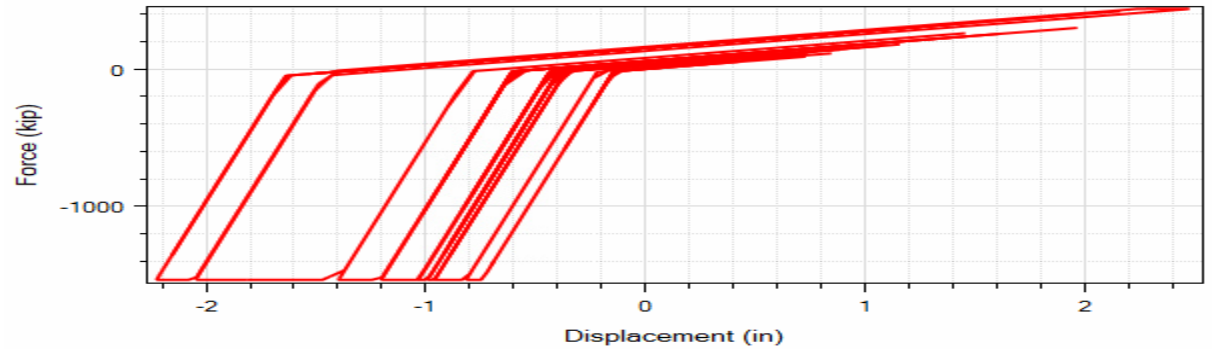

c)

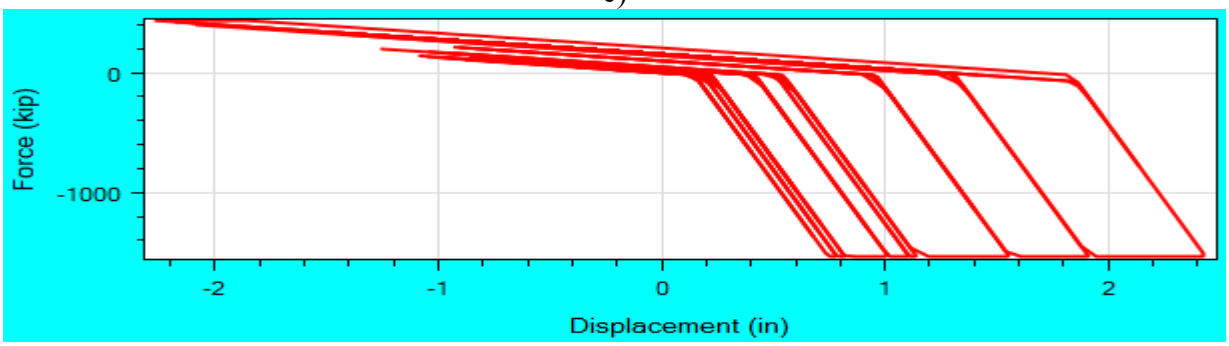

d)

Figure 3.27 OSB1 longitudinal force-displacement response for Motion 1 ROCKS1N1 (EPP-Gap with Bearings model): a) column top force-displacement; b) column top force-drift ratio; c) left abutment force-displacement response; d) right abutment force-displacement response

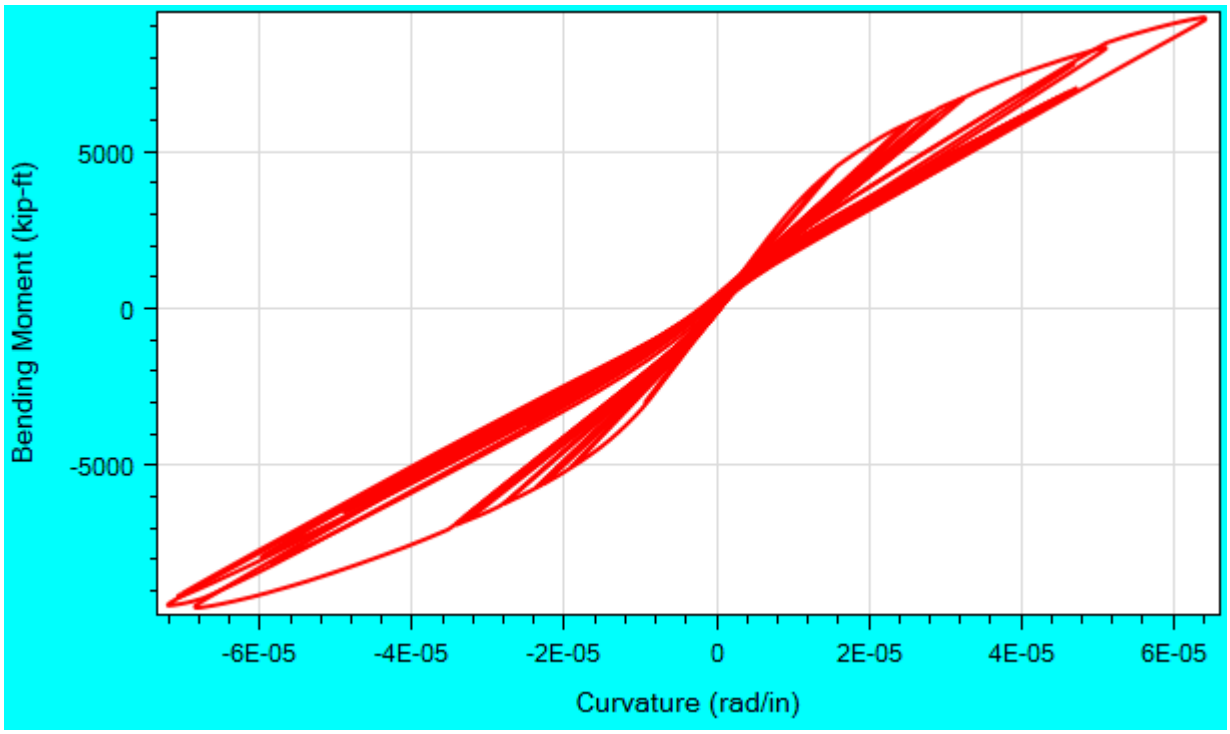

Figure 3.28 OSB1 column top longitudinal moment-curvature response for Motion 1 ROCKS1N1 (EPP-Gap with Bearings model)

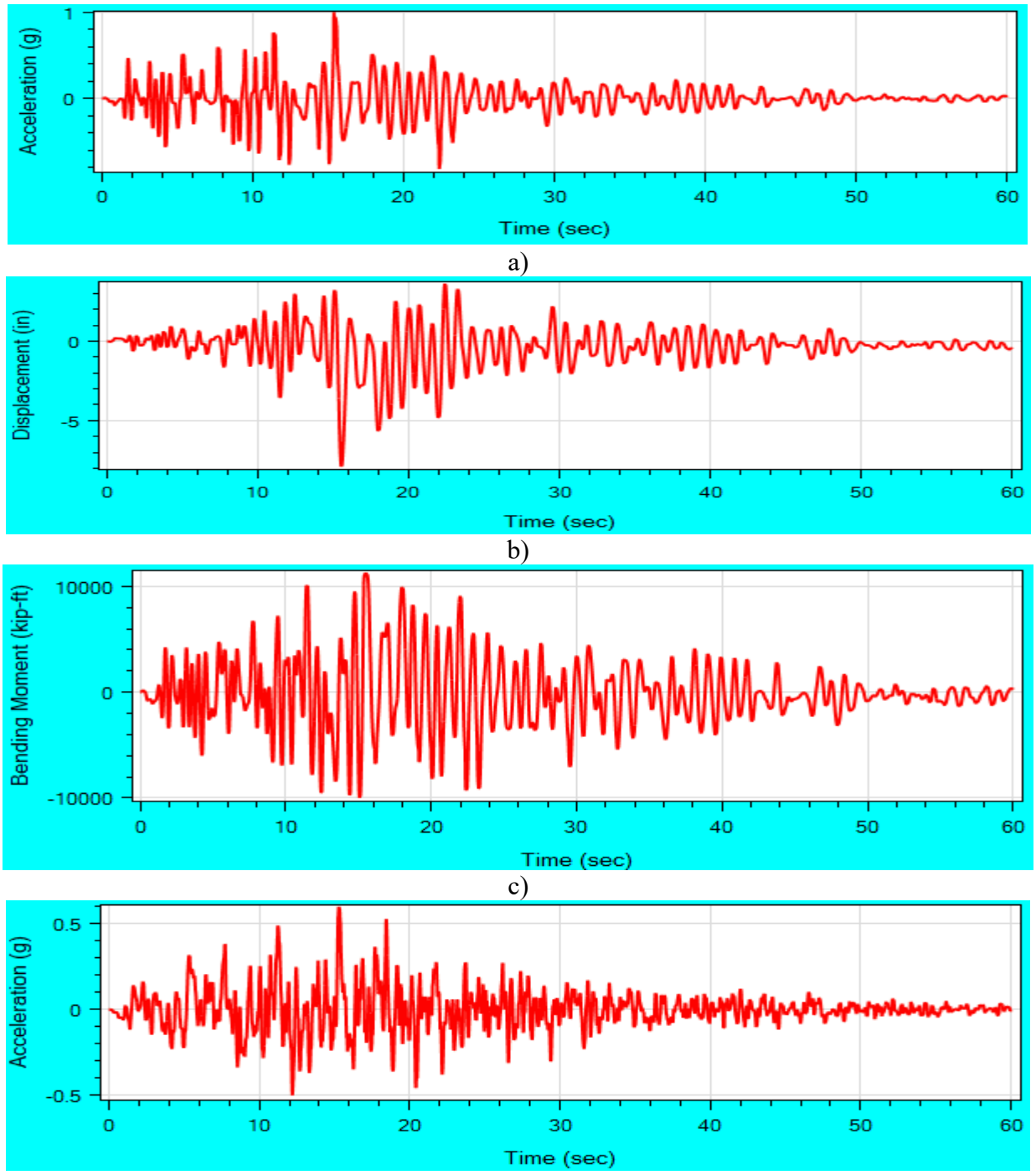

Figure 3.29 OSB1 column top longitudinal response time histories for Motion 15 SANDS1N1 (EPP-Gap with Bearings model): a) acceleration; b) displacement; c) bending moment; d) base excitation SANDS1N1

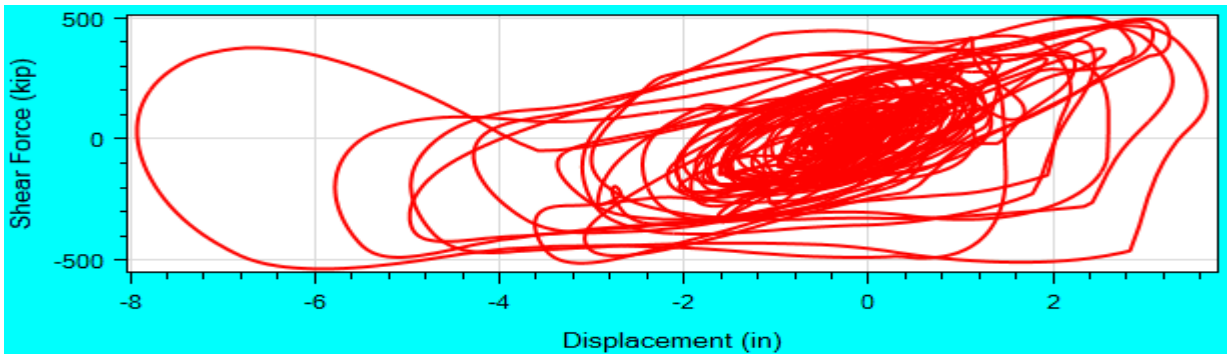

a)

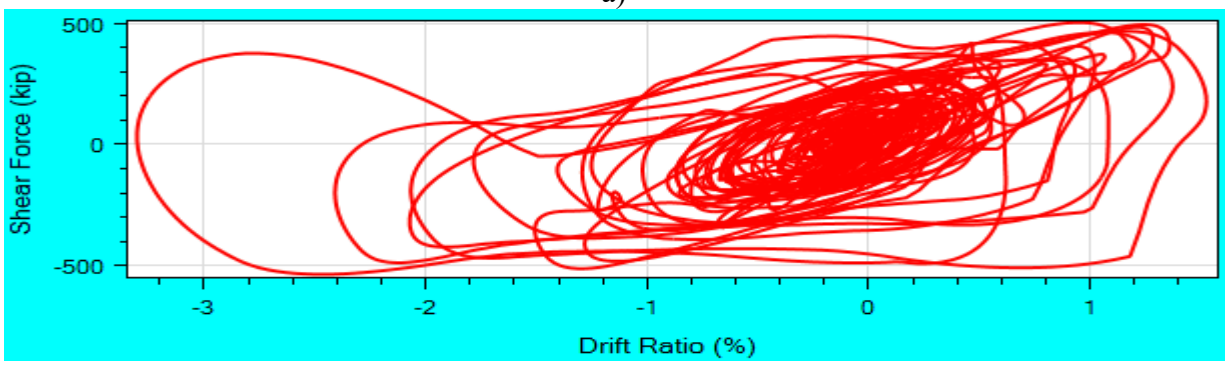

b)

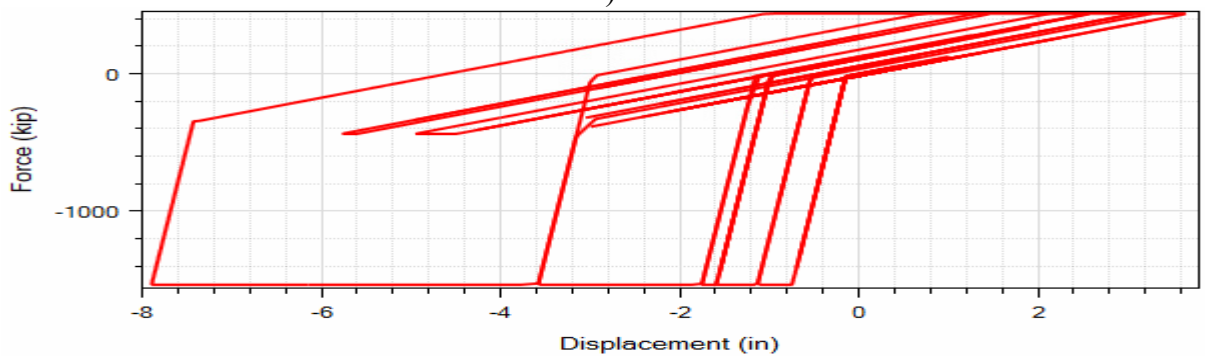

c)

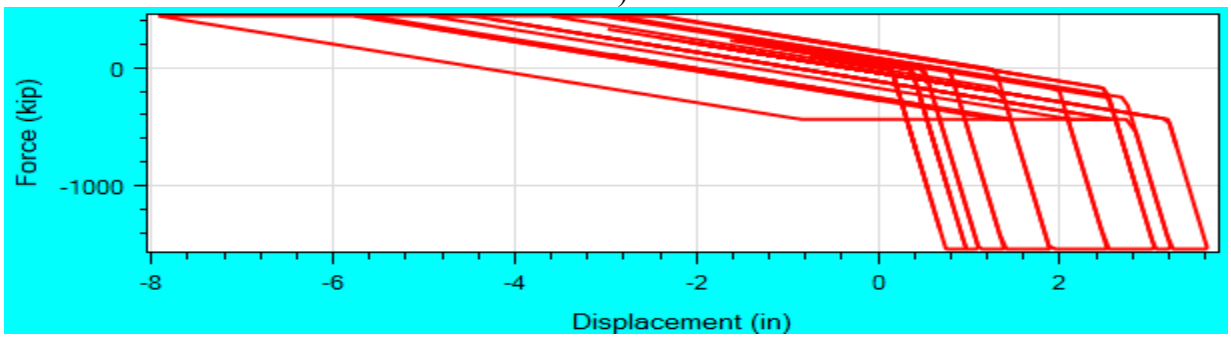

d)

Figure 3.30 OSB1 longitudinal force-displacement response for Motion 15 SANDS1N1 (EPP-Gap with Bearings model): a) column top force-displacement; b) column top force-drift ratio; c) left abutment force-displacement response; d) right abutment force-displacement response

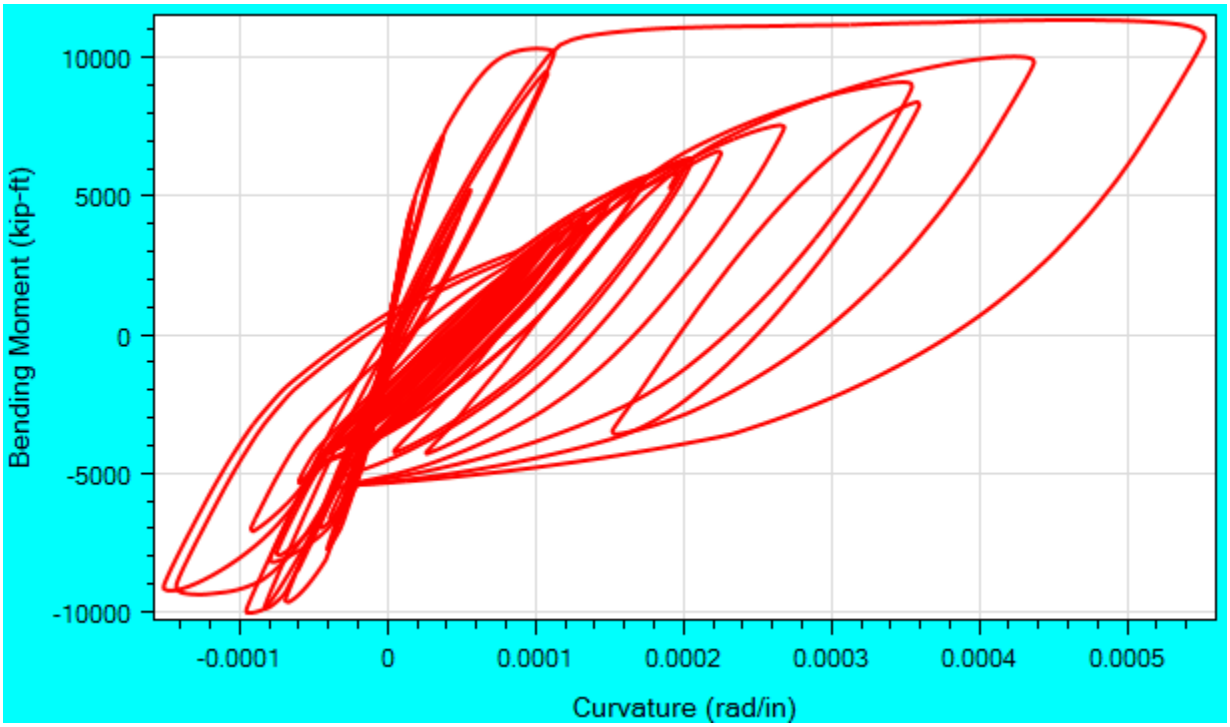

Figure 3.31 OSB1 column top longitudinal moment-curvature response for Motion 15 SANDS1N1 (EPP-Gap with Bearings model)

3.6 Summary

OSB1 was modeled in OpenSees and CSiBridge. Nonlinear THA of OSB1 was conducted for the 50 motions provided by Caltrans. Three types of abutment models (Roller, EPP-Gap, and EPP-Gap with Bearings) were addressed. For the EPP-Gap with Bearings model, the maximum displacement was 1.9-7.9 inches in the bridge longitudinal direction and 2.2-4.5 inches in the transverse direction. Only the case with the EPP-Gap model (without abutment bearing pads) was simulated in CSiBridge.

ESA was also conducted for OSB1 using MSBridge. The longitudinal ESA shows the displacement demand to be 4.2 inches for the EPP-Gap with Bearings model. The displacement demand was 4.0 inches from the transverse ESA.

3.7 Conclusions

1. For the employed ESA spectrum, column drift ratio demand was about 1.8% and 1.7% in the longitudinal (EPP-Gap with Bearings model) and in the transverse directions, respectively.

2. For the investigated set of ground motions in OpenSees (EPP-Gap with Bearings model):

2.1. In the longitudinal direction, about 20% of the shaking events resulted in column drift demand that exceeded that of the ESA. This demand reached a maximum of 75% in excess of that from the corresponding ESA (peak column drift ratio of about 3.5%). With the 0.14 in gap, the abutment reduced the peak maximum displacement from 11.3 in (for the Roller model) to 7.9 in (for the EPP-Gap with Bearings model).

2.2. In the transverse direction, about 20% of the shaking events resulted in column drift demand that exceeded that of the ESA. This demand reached a maximum of 15% in excess of that from the corresponding ESA (peak column drift ratio of about 2%). With the elastic response in the transverse direction, the abutment reduced the peak maximum displacement from 10.3 in (for the Roller model) to 4.5 in (for the EPP-Gap with Bearings model).

3. For the OpenSees model, the ground input motions of the SANDS1 group (Figure B.4, Figure B.8 and Table 3.4) appear to result consistently in a larger longitudinal and transverse displacement demand (Figures 3.14-3.19).

4. For the EPP-Gap model (without abutment bearing pads), the shaking events of the ROCKS1N and SANDS1 groups resulted in lower maximum displacement in CSiBridge, compared to the OpenSees result (Table 3.5), while the ROCKS1P group resulted in larger maximum displacement in CSiBridge. The maximum displacement difference between the OpenSees and CSibridge results is relatively large in general for the input motions of the SANDS1 group, compared to the ROCKS1N and ROCKS1P groups. In the longitudinal direction, the difference (between OpenSees and CSiBridge) is within 67% for the input motions of the ROCKS1N and ROCKS1P groups and 68%-87% for the SANDS1 group (Table 3.5 and Figure 3.6). In the transverse direction, the difference is within 52% for the input motions of the ROCKS1N and ROCKS1P groups and 26%-48% for the SANDS1 group (Table 3.5 and Figure 3.7).

4 OSB STUDY BRIDGE 4

4.1 Bridge Description

OSB Study Bridge 4 (hereinafter referred to as "OSB4") is a single bent PC/PS wide flange girder bridge with two spans of 150 feet in length. The single-bent is composed of one circular Pre-cast column with 2 isolation bearings at column top In addition, 2 isolation bearings are located on top of the each abutment. Figure 4.1 shows the general geometries of OSB4.

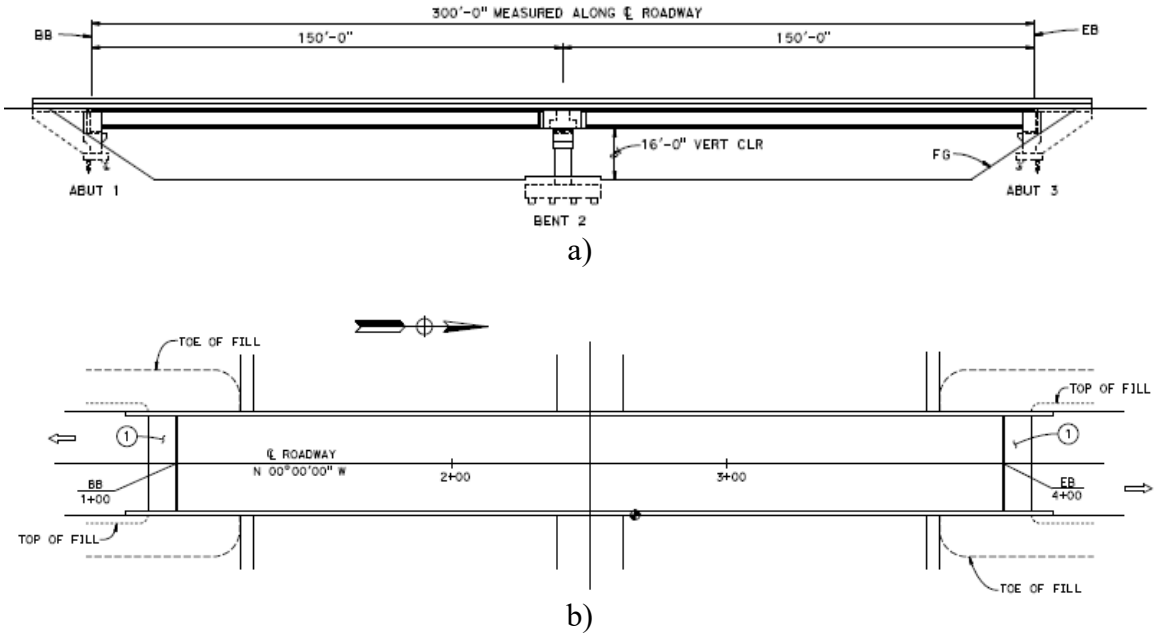

Figure 4.1 Schematic of OSB4 (drawings provided by Caltrans): (a) Elevation view; (b) Plan view

4.2 Geometric Configuration

Figure 4.2 shows the elevation view of OSB4 along with the column reinforcement details. The PC/PS wide flange girder is 37.5 feet wide by 6.33 feet deep. The column is 16 feet high with a diameter of 66 inches. The column is fixed both at top and at the base. The bentcap was assumed to be rigid but weightless/massless in this study (due to limitations in the current version of MSBridge).

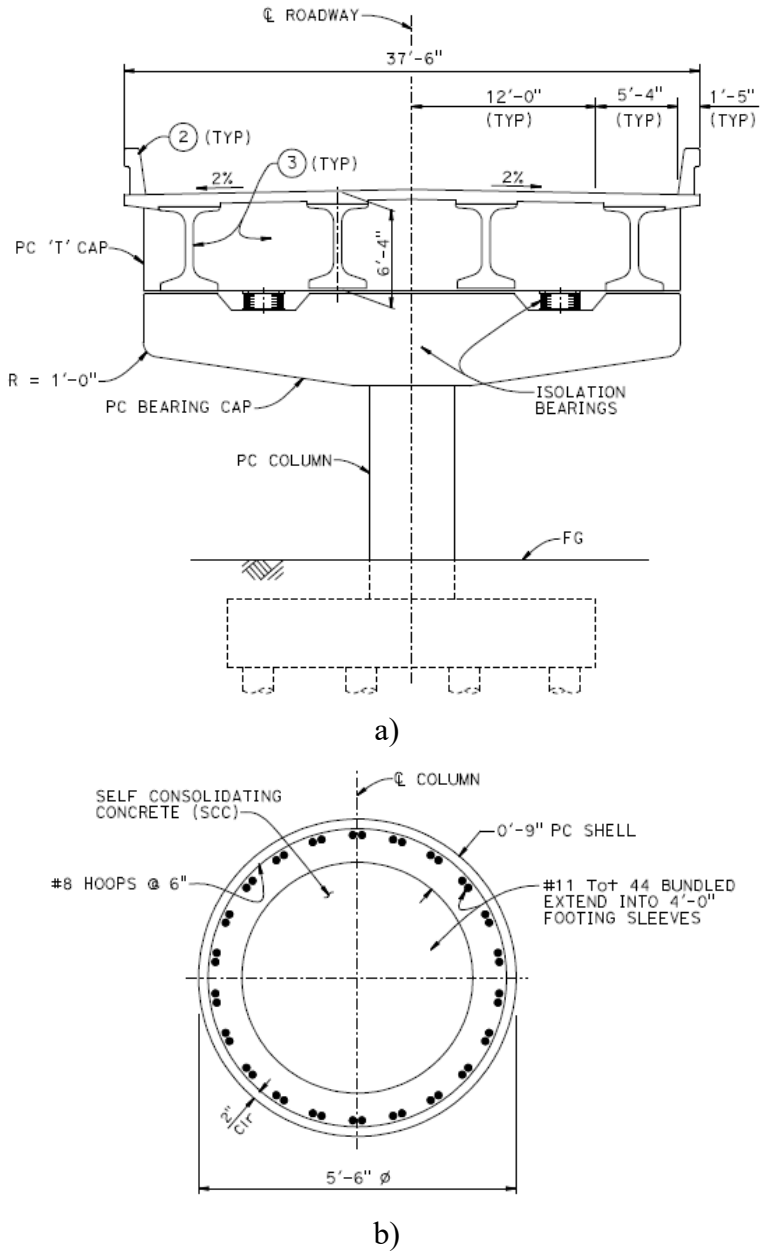

Figure 4.2 Elevation and sectional details of OSB4: (a) deck; (b) circular section (Caltrans 2012)

4.3 OSB4 OpenSees Modeling and Response

4.3.1 Finite Element Model

The employed modeling techniques and associated model properties are presented in Appendix E. To facilitate the conducted analyses in OpenSees, a recently developed user interface MSBridge

was employed (please see Appendix A for more information about MSBridge). Figure 4.3 shows the OSB4 model created in MSBridge and CSiBridge.

The forceBeamColumn element (with the distributed plasticity integration method) in OpenSees was used to model the column. The deck was considered linearly elastic (see Appendix E for the deck geometric and material properties).

As shown in Figure 4.3, two equal-length elements were used for the column (the column height is 16 ft). The offset between the column top and the deck was not considered (due to limitations in the current version of MSBridge). No rotation around the bridge longitudinal direction is allowed for the deck (at the abutments).

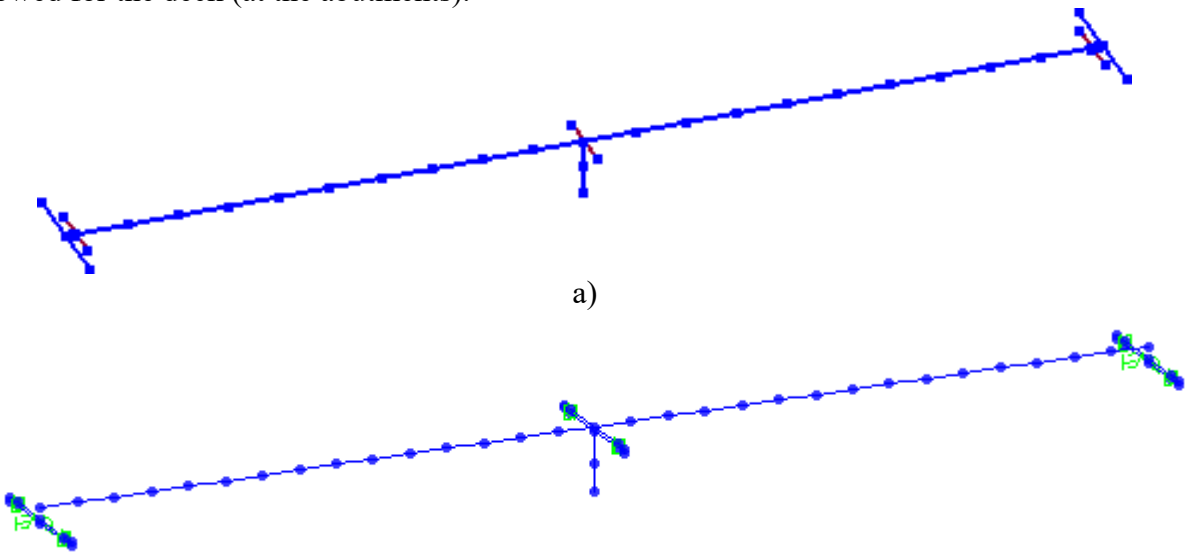

a)

b)

Figure 4.3 OSB4 model (3D view) created in: a) MSBridge; b) CSiBridge

Two types of abutment models were employed in this study:

i) Roller with Isolation Bearings, and
ii) EPP-Gap with Isolation Bearings.

The resulting OSB4 bridge models will be hereinafter referred to as "Roller with Isolation Bearings" and "EPP-Gap with Isolation Bearings", respectively. The first natural periods for OSB4 with the 2 bridge models are both 0.96 second. For detailed information about the above abutment models, please see Appendix E. As suggested by Caltrans, only the EPP_Gap with Isolation Bearings model was simulated in CSiBridge.

4.3.2 Isolation Bearing and Abutment Response

Pushover analysis was conducted in OpenSees to document the corresponding isolation bearing response. The pushover load was applied at the deck center (in the longitudinal & transverse directions). Figure 4.4 shows the isolation bearing force-displacement response due to pushover loading.

Figure 4.5 shows the right abutment force-displacement response due to pushover loading in the longitudinal (Figure 4.5a) and transverse (Figure 4.5b) directions.

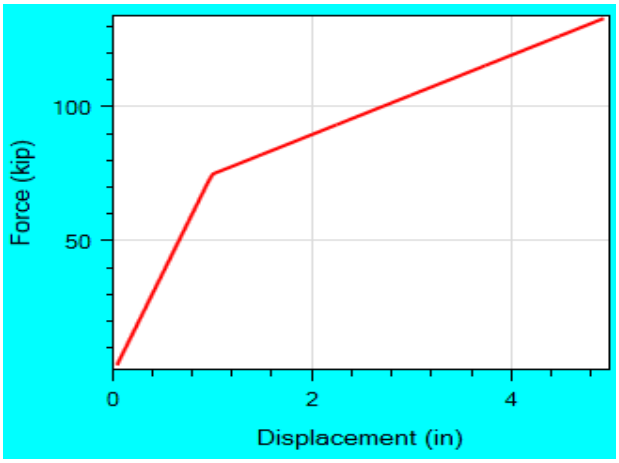

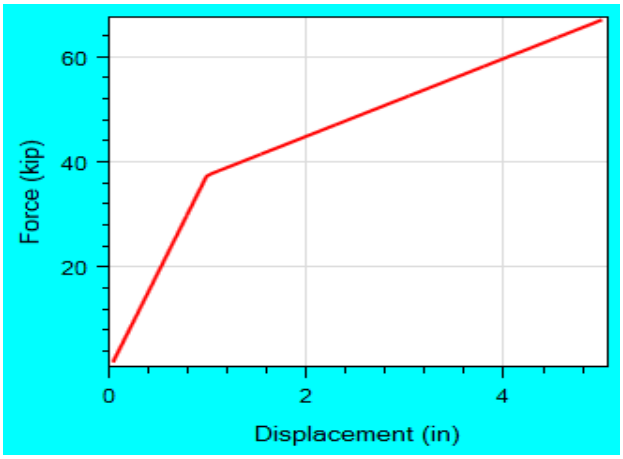

a) b)

Figure 4.4 OSB4 isolation bearing longtudinal and transverse response (only up to 5 inches of pushover displacement is shown) for: a) bent isolation bearing; b) abutment isolation bearing

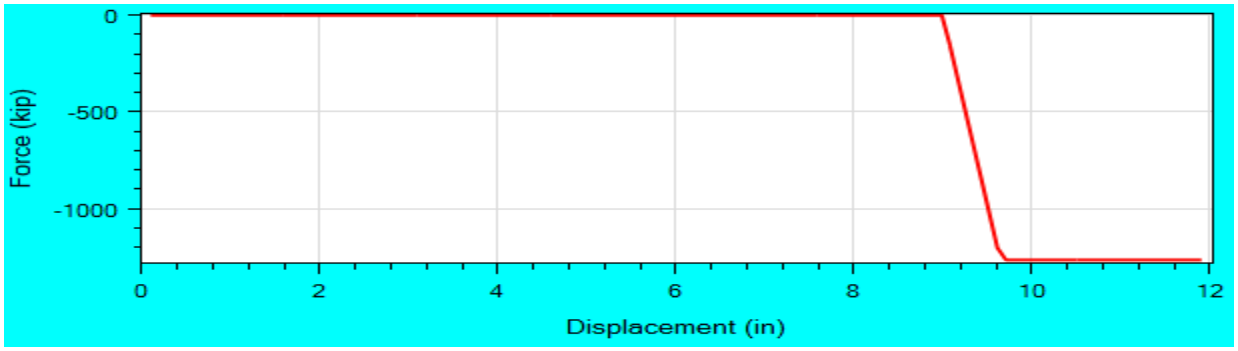

a)

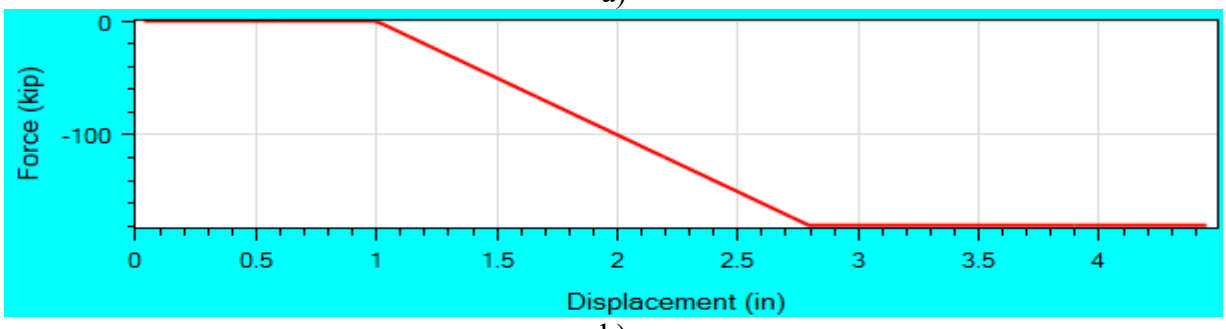

b)

Figure 4.5 OSB4 abutment force-displacement response (in EPP-Gap with Isolation Bearings abutment model only): a) longitudinal response; b) transverse response

4.4 Equivalent Static Analysis (ESA)

ESA was conducted for OSB4 in the bridge longitudinal and transverse directions. For the procedure to conduct ESA in MSBridge, please refer to the MSBridge user manual (Elgamal et al. 2014).

4.4.1 ESA in the Longitudinal Direction

A load of 5% of the total bridge weight was used for longitudinal pushover analysis. For the acceleration response spectrum (ARS) employed in the ESA, please see Appendix C.

Table 4.1 shows the ESA result for OSB4. The final elastic displacement demand is 6.7 in. Table 4.2 lists the parameters related to this longitudinal ESA.

4.4.2 ESA in the Transverse Direction

A load of 1% of the tributary weight of the bent was used for the (transverse) pushover analysis. The same acceleration response spectrum (ARS) was used in the transverse ESA.

The elastic displacement demand was found to be 6.8 in (Table 4.1) in the transverse ESA. Table 4.3 lists the parameters related to this transverse ESA.

Table 4.1. ESA Result for OSB4

Parameter	Longitudinal Direction	Transverse Direction
Displacement Demand (in)	6.7	6.8

Table 4.2. Longitudinal ESA Parameters for OSB4

Parameter	Value
Total weight calculated (kip)	2,668
Total mass calculated (kip-sec^2/in)	6.9
Pushover load specified (kip)	133.38
Displacement due to pushover (in)	0.45
Calculated stiffness (kip/in)	294
Calculated period (sec)	0.96

Table 4.3. Transverse ESA Parameters for OSB4

Parameter	Value
Tributary weight calculated (kip)	1,320
Tributary mass calculated (kip-sec^2/in)	3.42
Pushover load specified (kip)	13.2
Displacement due to pushover (in)	0.095
Calculated stiffness (kip/in)	138.3
Calculated period (sec)	0.99

4.5 Nonlinear Time History Analysis

Nonlinear Time History Analysis (THA) was conducted for the 50 input motions provided by Caltrans (see Appendix B for the characteristics of the 50 motions). The input motions were applied directly at the column base as well as both abutments.

Rayleigh damping was used with a 5% damping ratio (defined at periods of 0.2 and 2.3 second) in the nonlinear THA. For the time integration scheme, the Newmark's average acceleration method ($\gamma = 0.5$ and $\beta = 0.25$) was employed.

In OpenSees, the variable time-stepping scheme was used in the analysis. The starting value for each time step was 0.005 second (same as the time step of the input motions) and the minimum time step was 5×10^{-5} second (upon splitting of time step).

4.5.1 Maximum Displacement and Acceleration

Table 4.4 lists OSB4 deck maximum displacement for the 50 motions from the nonlinear THA in OpenSees. Note that the Roller with Isolation Bearings and EPP-Gap with Isolation Bearings models gave the same maximum longitudinal displacement when the displacement is around 9 inches or less (Table 4.4). This is because the specified longitudinal gap is 9 inches in the EPP-Gap with Isolation Bearings model. As such, both OSB4 models (Roller with Isolation Bearings and EPP-Gap with Isolation Bearings) essentially behave in the same way under longitudinal loading, when the gap is not closed.

As mentioned earlier, the case with the EPP-Gap with Isolation Bearings model was simulated in CSiBridge. Table 4.5 lists the deck maximum displacement from the OpenSees and CSiBridge analyses. The maximum displacement comparison of Table 4.5 is also presented in Bar Chart graphical form in Figures 4.6-4.9. As mentioned earlier in Chapter 1, viscous damping abutment forces are only present in the CSiBridge simulation. This difference in the abutment exerted forces accounts partially for the discrepancy (Table 4.5) in the CSiBridge and OpenSees maximum displacement estimates.

Table 4.6 displays OSB4 deck maximum acceleration from OpenSees nonlinear THA. For the EPP-Gap with Isolation Bearings model, Table 4.7 lists the column top maximum acceleration from the OpenSees and CSiBridge analyses. The maximum acceleration comparison of Table 4.7 is also presented in Bar Chart graphical form in Figures 4.10-4.13.

For the OpenSees model, the maximum displacements of Table 4.4 are also shown in graphical form against Peak Ground Acceleration (PGA) in Figure 4.14-Figure 4.17. The maximum acceleration is also shown graphically against PGA in in Figure 4.18-Figure 4.21.

Note that P-Delta was not considered in CSiBridge analysis for OSB4 (but P-Delta was considered in OpenSees analysis). Generally, inclusion of P-Delta effects in CSiBridge resulted in relatively small differences in the output.

Table 4.4. OSB4 Deck Maximum Displacement (OpenSees)
(The ESA longitudinal displacement demands are 6.7 in for
Roller with Isolation Bearings, and EPP-Gap with Isolation Bearings models)

Motion	Longitudinal Input	Transverse Input	Longitudinal Displacement (in)		Transverse Displacement (in)	
			Roller with Isolation Bearings	EPP-Gap with Isolation Bearings	Roller with Isolation Bearings	EPP-Gap with Isolation Bearings
1	ROCKS1N1 (0.7g)	-	9.4	9.3	-	-
2	ROCKS1N2 (0.38g)	-	6.6	6.6	-	-
3	ROCKS1N3 (0.32g)	-	5.6	5.6	-	-
4	ROCKS1N4 (0.34g)	-	8.9	8.9	-	-
5	ROCKS1N5 (0.53g)	-	5.7	5.7	-	-
6	ROCKS1N6 (0.42g)	-	6.8	6.8	-	-
7	ROCKS1N7 (0.36g)	-	7.3	7.3	-	-
8	ROCKS1P1 (0.71g)	-	10.2	9.9	-	-
9	ROCKS1P2 (0.44g)	-	6.8	6.8	-	-
10	ROCKS1P3 (0.48g)	-	7.6	7.6	-	-
11	ROCKS1P4 (0.32g)	-	8.1	8.1	-	-
12	ROCKS1P5 (0.67g)	-	7.3	7.3	-	-
13	ROCKS1P6 (0.41g)	-	6.8	6.8	-	-
14	ROCKS1P7 (0.4g)	-	8.1	8.1	-	-
15	SANDS1N1 (0.61g)	-	16.6	14.0	-	-
16	SANDS1N2 (0.51g)	-	16.0	12.6	-	-
17	SANDS1N3 (0.57g)	-	18.3	13.0	-	-
18	SANDS1N4 (0.96g)	-	14.8	11.6	-	-
19	SANDS1N5 (0.79g)	-	18.4	15.4	-	-
20	SANDS1N6 (0.67g)	-	15.9	12.9	-	-
21	SANDS1N7 (0.58g)	-	23.9	17.5	-	-
22	ROCKN1N1N (0.4g)	ROCKN1N1P (0.58g)	6.7	6.7	12.0	6.4
23	ROCKN1P1N (1.42g)	ROCKN1P1P (1.42g)	5.2	5.2	5.2	4.1
24	SANDN1N1N (0.78g)	SANDN1N1P (0.81g)	17.3	13.7	11.8	10.6
25	CLAYN1N1N (0.79g)	CLAYN1N1P (0.71g)	25.7	16.7	21.1	16.0
26	-	ROCKS1N1 (0.7g)	-	-	9.4	8.1
27	-	ROCKS1N2 (0.38g)	-	-	6.6	4.2
28	-	ROCKS1N3 (0.32g)	-	-	5.6	5.2
29	-	ROCKS1N4 (0.34g)	-	-	9.0	7.4
30	-	ROCKS1N5 (0.53g)	-	-	5.7	6.1
31	-	ROCKS1N6 (0.42g)	-	-	6.8	3.9
32	-	ROCKS1N7 (0.36g)	-	-	7.4	4.5
33	-	ROCKS1P1 (0.71g)	-	-	10.3	8.8
34	-	ROCKS1P2 (0.44g)	-	-	6.8	4.4
35	-	ROCKS1P3 (0.48g)	-	-	7.6	7.0
36	-	ROCKS1P4 (0.32g)	-	-	8.1	7.6
37	-	ROCKS1P5 (0.67g)	-	-	7.3	5.2
38	-	ROCKS1P6 (0.41g)	-	-	6.9	3.9
39	-	ROCKS1P7 (0.4g)	-	-	8.2	6.9
40	-	SANDS1N1 (0.61g)	-	-	16.6	15.0
41	-	SANDS1N2 (0.51g)	-	-	16.1	10.3
42	-	SANDS1N3 (0.57g)	-	-	18.3	15.8
43	-	SANDS1N4 (0.96g)	-	-	14.8	11.9
44	-	SANDS1N5 (0.79g)	-	-	18.5	17.2
45	-	SANDS1N6 (0.67g)	-	-	16.1	12.7
46	-	SANDS1N7 (0.58g)	-	-	23.9	22.5
47	ROCKN1N1P (0.58g)	ROCKN1N1N (0.4g)	11.9	10.7	6.7	4.1
48	ROCKN1P1P (1.42g)	ROCKN1P1N (1.42g)	5.2	5.2	5.2	4.1
49	SANDN1N1P (0.81g)	SANDN1N1N (0.78g)	11.8	10.6	17.3	15.8
50	CLAYN1N1P (0.71g)	CLAYN1N1N (0.79g)	21.0	13.8	25.8	22.6

Table 4.5. OSB4 Deck Maximum Displacement for EPP-Gap with Isolation Bearings Model (Comparison of OpenSees and CSiBridge)

(The ESA longitudinal displacement demand is 6.7 in while the ESA transverse displacement demands is 6.8 in; Difference is relative to OpenSees result)

Motion	Longitudinal Input	Transverse Input	Longitudinal Displacement (in)			Transverse Displacement (in)		
			OpenSees	CSiBridge	Difference	OpenSees	CSiBridge	Difference
1	ROCKS1N1 (0.7g)	-	9.3	9.2	-1%	-	-	-
2	ROCKS1N2 (0.38g)	-	6.6	7.7	17%	-	-	-
3	ROCKS1N3 (0.32g)	-	5.6	6.4	14%	-	-	-
4	ROCKS1N4 (0.34g)	-	8.9	8.3	-7%	-	-	-
5	ROCKS1N5 (0.53g)	-	5.7	5.6	-2%	-	-	-
6	ROCKS1N6 (0.42g)	-	6.8	7.2	6%	-	-	-
7	ROCKS1N7 (0.36g)	-	7.3	9.2	26%	-	-	-
8	ROCKS1P1 (0.71g)	-	9.9	10	1%	-	-	-
9	ROCKS1P2 (0.44g)	-	6.8	7.9	16%	-	-	-
10	ROCKS1P3 (0.48g)	-	7.6	6.1	-20%	-	-	-
11	ROCKS1P4 (0.32g)	-	8.1	8.3	2%	-	-	-
12	ROCKS1P5 (0.67g)	-	7.3	8.5	16%	-	-	-
13	ROCKS1P6 (0.41g)	-	6.8	7	3%	-	-	-
14	ROCKS1P7 (0.4g)	-	8.1	7.8	-4%	-	-	-
15	SANDS1N1 (0.61g)	-	14	9.6	-31%	-	-	-
16	SANDS1N2 (0.51g)	-	12.6	10.3	-18%	-	-	-
17	SANDS1N3 (0.57g)	-	13	9.4	-28%	-	-	-
18	SANDS1N4 (0.96g)	-	11.6	11.6	0%	-	-	-
19	SANDS1N5 (0.79g)	-	15.4	15.2	-1%	-	-	-
20	SANDS1N6 (0.67g)	-	12.9	9.3	-28%	-	-	-
21	SANDS1N7 (0.58g)	-	17.5	13.3	-24%	-	-	-
22	ROCKN1N1N (0.4g)	ROCKN1N1P (0.58g)	6.7	7.6	13%	6.4	9.5	48%
23	ROCKN1P1N (1.42g)	ROCKN1P1P (1.42g)	5.2	4.1	-21%	4.1	5.2	27%
24	SANDN1N1N (0.78g)	SANDN1N1P (0.81g)	13.7	13.7	0%	10.6	8.3	-22%
25	CLAYN1N1N (0.79g)	CLAYN1N1P (0.71g)	16.7	10.7	-36%	16	15.1	-6%
26	-	ROCKS1N1 (0.7g)	-	-	-	8.1	8.1	0%
27	-	ROCKS1N2 (0.38g)	-	-	-	4.2	4.5	7%
28	-	ROCKS1N3 (0.32g)	-	-	-	5.2	5	-4%
29	-	ROCKS1N4 (0.34g)	-	-	-	7.4	6.8	-8%
30	-	ROCKS1N5 (0.53g)	-	-	-	6.1	6.5	7%
31	-	ROCKS1N6 (0.42g)	-	-	-	3.9	4	3%
32	-	ROCKS1N7 (0.36g)	-	-	-	4.5	5	11%
33	-	ROCKS1P1 (0.71g)	-	-	-	8.8	8.6	-2%
34	-	ROCKS1P2 (0.44g)	-	-	-	4.4	5	14%
35	-	ROCKS1P3 (0.48g)	-	-	-	7	7.9	13%
36	-	ROCKS1P4 (0.32g)	-	-	-	7.6	7	-8%
37	-	ROCKS1P5 (0.67g)	-	-	-	5.2	5.5	6%
38	-	ROCKS1P6 (0.41g)	-	-	-	3.9	4.3	10%
39	-	ROCKS1P7 (0.4g)	-	-	-	6.9	6.9	0%
40	-	SANDS1N1 (0.61g)	-	-	-	15	14.4	-4%
41	-	SANDS1N2 (0.51g)	-	-	-	10.3	11.8	15%
42	-	SANDS1N3 (0.57g)	-	-	-	15.8	12.4	-22%
43	-	SANDS1N4 (0.96g)	-	-	-	11.9	13.4	13%
44	-	SANDS1N5 (0.79g)	-	-	-	17.2	14.5	-16%
45	-	SANDS1N6 (0.67g)	-	-	-	12.7	10.4	-18%
46	-	SANDS1N7 (0.58g)	-	-	-	22.5	19.1	-15%
47	ROCKN1N1P (0.58g)	ROCKN1N1N (0.4g)	10.7	10.2	-5%	4.1	5.9	44%
48	ROCKN1P1P (1.42g)	ROCKN1P1N (1.42g)	5.2	4.1	-21%	4.1	5.2	27%
49	SANDN1N1P (0.81g)	SANDN1N1N (0.78g)	10.6	10	-6%	15.8	11.6	-27%
50	CLAYN1N1P (0.71g)	CLAYN1N1N (0.79g)	13.8	14.5	5%	22.6	18.7	-17%

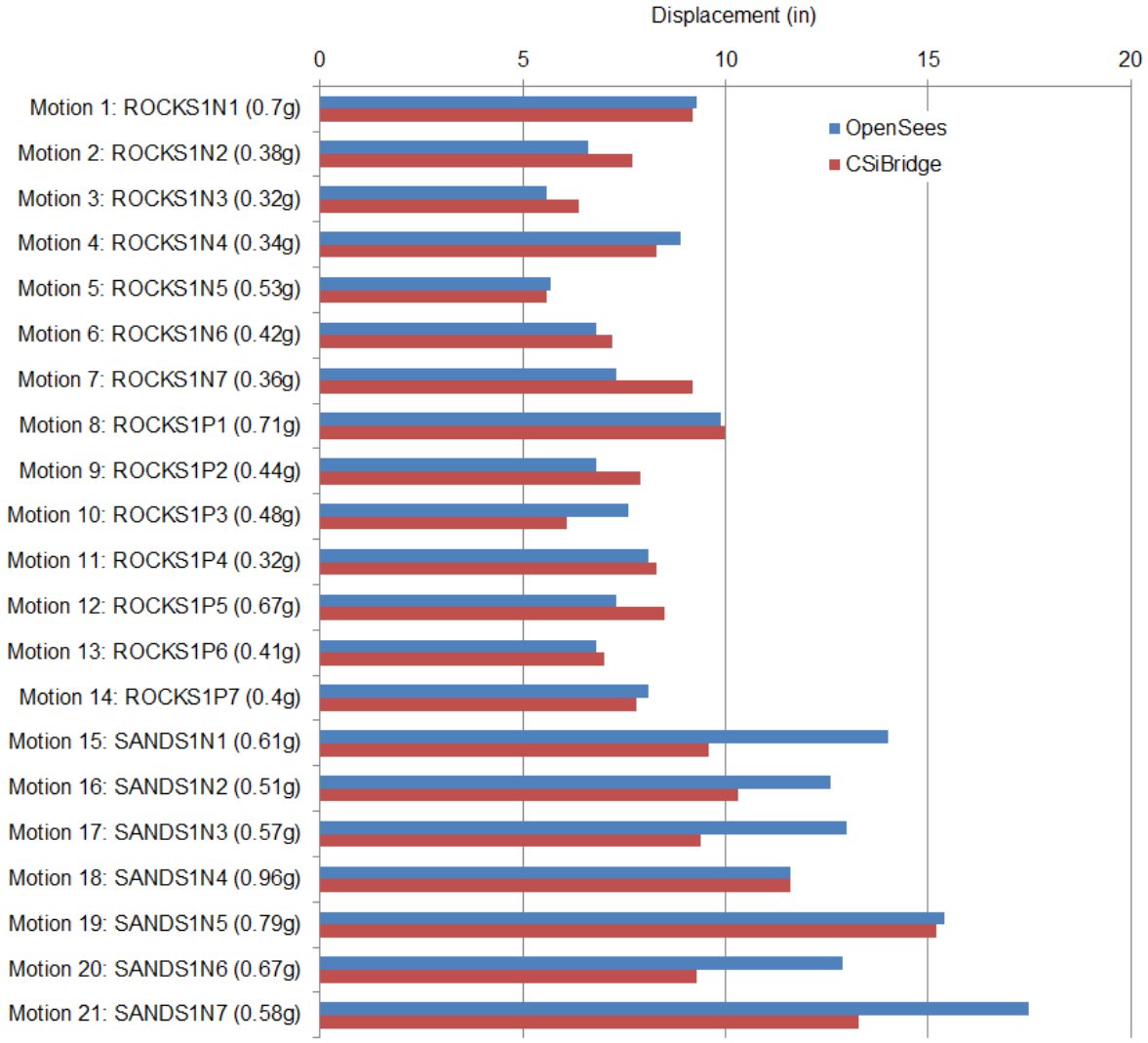

Figure 4.6 OSB4 deck maximum longitudinal displacement for Motions 1-21 (EPP-Gap with Isolation Bearings model)

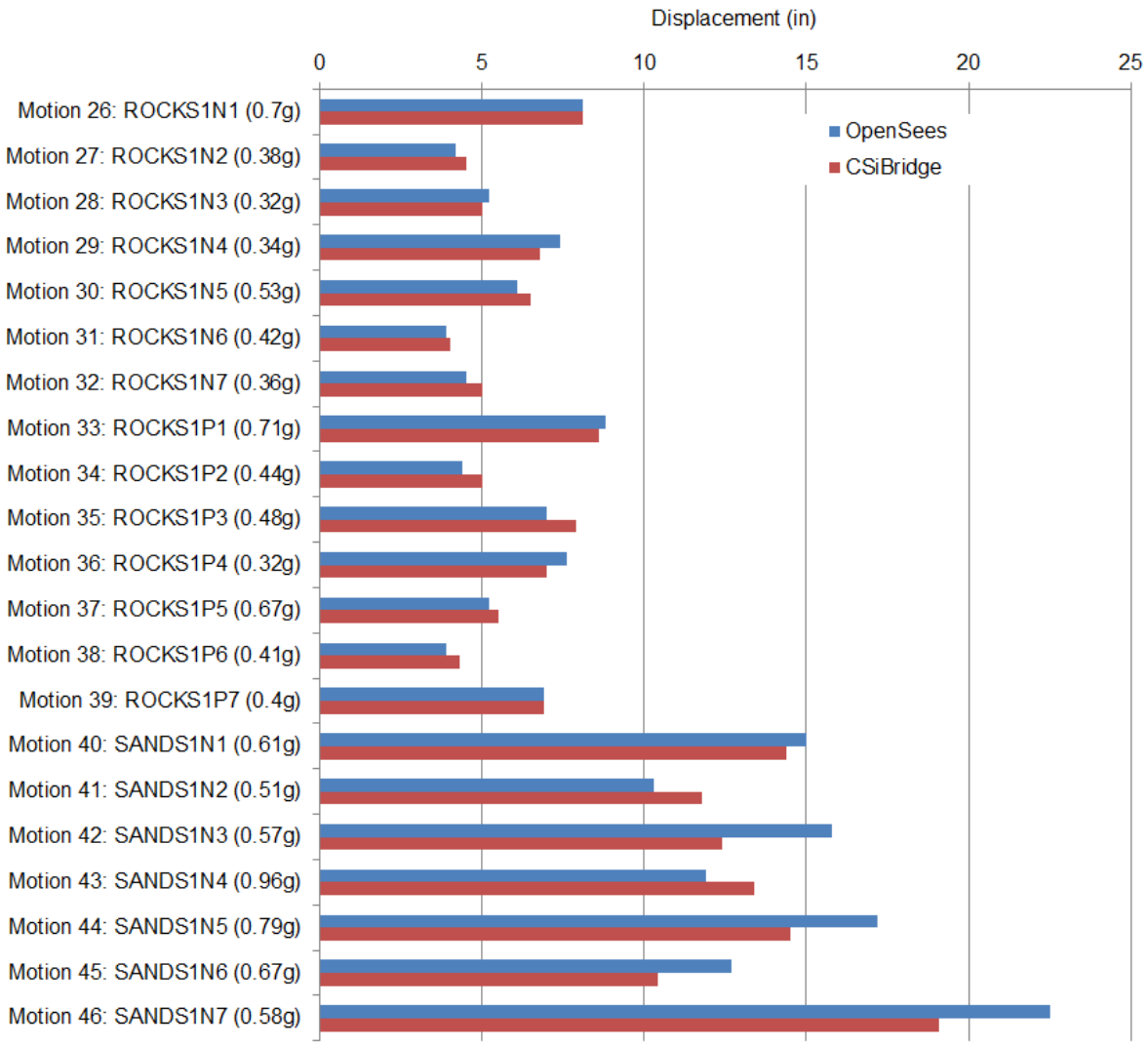

Figure 4.7 OSB4 deck maximum transverse displacement for Motions 26-46 (EPP-Gap with Isolation Bearings model)

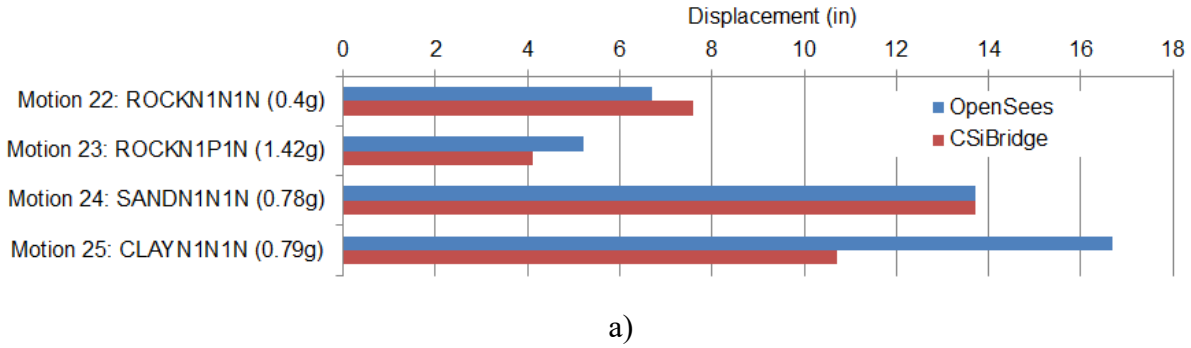

a)

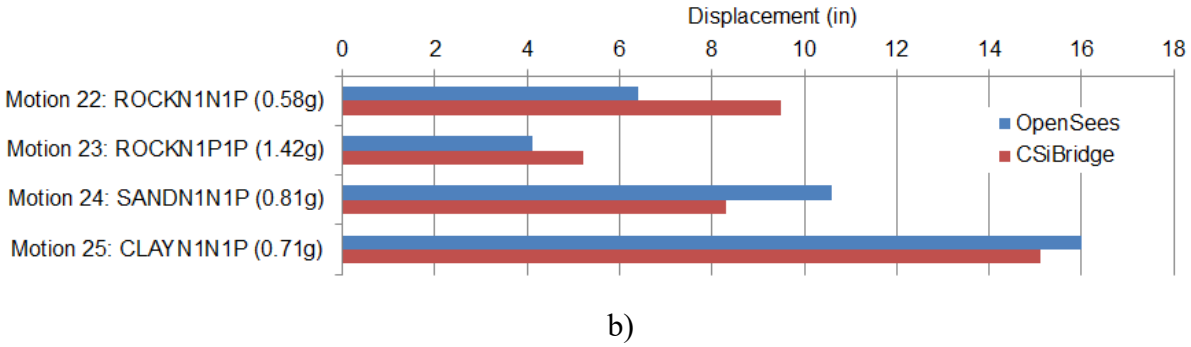

b)

Figure 4.8 OSB4 deck maximum displacement for Motions 22-25 (EPP-Gap with Isolation Bearings model): a) Lonitudinal direction; b) Transverse direction

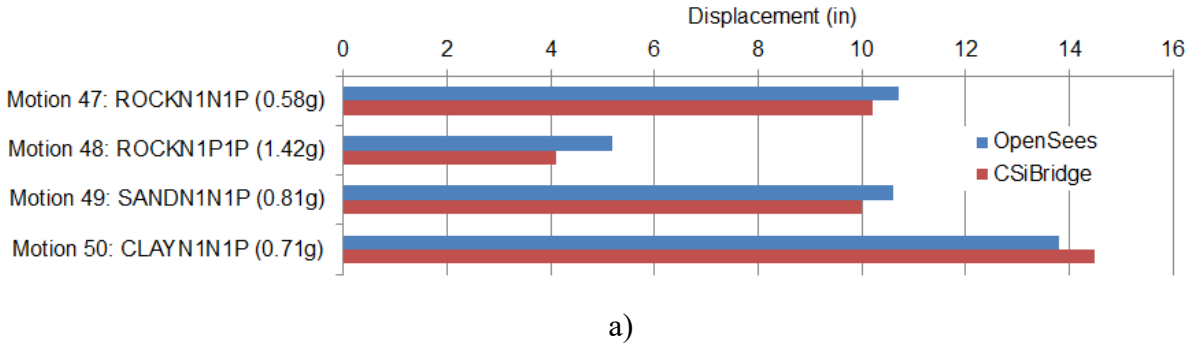

a)

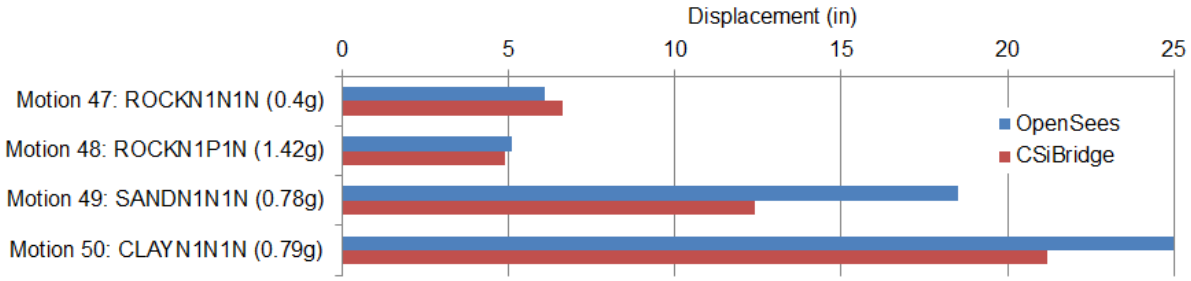

b)

Figure 4.9 OSB4 deck maximum displacement for Motions 47-50 (EPP-Gap with Isolation Bearings model): a) Lonitudinal direction; b) Transverse direction

Table 4.6. OSB4 Deck Maximum Acceleration (OpenSees)

Motion	Longitudinal Input	Transverse Input	Longitudinal Acceleration (g)		Transverse Acceleration (g)	
			Roller with Isolation Bearings	EPP-Gap with Isolation Bearings	Roller with Isolation Bearings	EPP-Gap with Isolation Bearings
1	ROCKS1N1 (0.7g)	-	0.70	0.70	-	-
2	ROCKS1N2 (0.38g)	-	0.38	0.38	-	-
3	ROCKS1N3 (0.32g)	-	0.41	0.41	-	-
4	ROCKS1N4 (0.34g)	-	0.37	0.37	-	-
5	ROCKS1N5 (0.53g)	-	0.55	0.55	-	-
6	ROCKS1N6 (0.42g)	-	0.42	0.42	-	-
7	ROCKS1N7 (0.36g)	-	0.38	0.38	-	-
8	ROCKS1P1 (0.71g)	-	0.71	1.02	-	-
9	ROCKS1P2 (0.44g)	-	0.44	0.44	-	-
10	ROCKS1P3 (0.48g)	-	0.61	0.61	-	-
11	ROCKS1P4 (0.32g)	-	0.50	0.50	-	-
12	ROCKS1P5 (0.67g)	-	0.67	0.67	-	-
13	ROCKS1P6 (0.41g)	-	0.41	0.41	-	-
14	ROCKS1P7 (0.4g)	-	0.51	0.51	-	-
15	SANDS1N1 (0.61g)	-	0.84	1.66	-	-
16	SANDS1N2 (0.51g)	-	0.58	1.43	-	-
17	SANDS1N3 (0.57g)	-	0.63	1.56	-	-
18	SANDS1N4 (0.96g)	-	1.24	1.29	-	-
19	SANDS1N5 (0.79g)	-	0.80	1.48	-	-
20	SANDS1N6 (0.67g)	-	0.67	1.42	-	-
21	SANDS1N7 (0.58g)	-	0.63	1.95	-	-
22	ROCKN1N1N (0.4g)	ROCKN1N1P (0.58g)	0.40	0.40	0.57	0.57
23	ROCKN1P1N (1.42g)	ROCKN1P1P (1.42g)	1.46	1.46	1.58	1.58
24	SANDN1N1N (0.78g)	SANDN1N1P (0.81g)	0.78	1.47	0.83	0.82
25	CLAYN1N1N (0.79g)	CLAYN1N1P (0.71g)	0.89	1.94	1.09	1.04
26	-	ROCKS1N1 (0.7g)	-	-	0.70	0.76
27	-	ROCKS1N2 (0.38g)	-	-	0.44	0.48
28	-	ROCKS1N3 (0.32g)	-	-	0.57	0.57
29	-	ROCKS1N4 (0.34g)	-	-	0.55	0.47
30	-	ROCKS1N5 (0.53g)	-	-	0.70	0.55
31	-	ROCKS1N6 (0.42g)	-	-	0.43	0.59
32	-	ROCKS1N7 (0.36g)	-	-	0.53	0.49
33	-	ROCKS1P1 (0.71g)	-	-	0.71	0.71
34	-	ROCKS1P2 (0.44g)	-	-	0.44	0.48
35	-	ROCKS1P3 (0.48g)	-	-	0.72	0.58
36	-	ROCKS1P4 (0.32g)	-	-	0.56	0.47
37	-	ROCKS1P5 (0.67g)	-	-	0.67	0.86
38	-	ROCKS1P6 (0.41g)	-	-	0.44	0.52
39	-	ROCKS1P7 (0.4g)	-	-	0.65	0.62
40	-	SANDS1N1 (0.61g)	-	-	1.09	1.01
41	-	SANDS1N2 (0.51g)	-	-	0.74	0.65
42	-	SANDS1N3 (0.57g)	-	-	0.78	0.74
43	-	SANDS1N4 (0.96g)	-	-	1.43	1.37
44	-	SANDS1N5 (0.79g)	-	-	0.84	0.82
45	-	SANDS1N6 (0.67g)	-	-	0.71	0.97
46	-	SANDS1N7 (0.58g)	-	-	0.87	0.84
47	ROCKN1N1P (0.58g)	ROCKN1N1N (0.4g)	0.58	1.33	0.47	0.46
48	ROCKN1P1P (1.42g)	ROCKN1P1N (1.42g)	1.46	1.46	1.58	1.58
49	SANDN1N1P (0.81g)	SANDN1N1N (0.78g)	0.82	1.11	0.97	1.97
50	CLAYN1N1P (0.71g)	CLAYN1N1N (0.79g)	0.93	1.40	1.02	0.85

Table 4.7. OSB4 Deck Maximum Acceleration for EPP-Gap with Isolation Bearings Model (Comparison of OpenSees and CSiBridge)

(Difference is relative to OpenSees result)

Motion	Longitudinal Input	Transverse Input	Longitudinal Acceleration (g)			Transverse Acceleration (g)		
			OpenSees	CSiBridge	Difference	OpenSees	CSiBridge	Difference
1	ROCKS1N1 (0.7g)	-	0.7	0.59	-16%	-	-	-
2	ROCKS1N2 (0.38g)	-	0.38	0.44	16%	-	-	-
3	ROCKS1N3 (0.32g)	-	0.41	0.25	-39%	-	-	-
4	ROCKS1N4 (0.34g)	-	0.37	0.51	38%	-	-	-
5	ROCKS1N5 (0.53g)	-	0.55	0.17	-69%	-	-	-
6	ROCKS1N6 (0.42g)	-	0.42	0.36	-14%	-	-	-
7	ROCKS1N7 (0.36g)	-	0.38	0.57	50%	-	-	-
8	ROCKS1P1 (0.71g)	-	1.02	0.63	-38%	-	-	-
9	ROCKS1P2 (0.44g)	-	0.44	0.37	-16%	-	-	-
10	ROCKS1P3 (0.48g)	-	0.61	0.23	-62%	-	-	-
11	ROCKS1P4 (0.32g)	-	0.5	0.5	0%	-	-	-
12	ROCKS1P5 (0.67g)	-	0.67	0.4	-40%	-	-	-
13	ROCKS1P6 (0.41g)	-	0.41	0.25	-39%	-	-	-
14	ROCKS1P7 (0.4g)	-	0.51	0.38	-25%	-	-	-
15	SANDS1N1 (0.61g)	-	1.66	0.63	-62%	-	-	-
16	SANDS1N2 (0.51g)	-	1.43	0.65	-55%	-	-	-
17	SANDS1N3 (0.57g)	-	1.56	0.62	-60%	-	-	-
18	SANDS1N4 (0.96g)	-	1.29	0.67	-48%	-	-	-
19	SANDS1N5 (0.79g)	-	1.48	0.73	-51%	-	-	-
20	SANDS1N6 (0.67g)	-	1.42	0.62	-56%	-	-	-
21	SANDS1N7 (0.58g)	-	1.95	0.71	-64%	-	-	-
22	ROCKN1N1N (0.4g)	ROCKN1N1P (0.58g)	0.4	0.36	-10%	0.57	0.36	-37%
23	ROCKN1P1N (1.42g)	ROCKN1P1P (1.42g)	1.46	0.15	-90%	1.58	0.3	-81%
24	SANDN1N1N (0.78g)	SANDN1N1P (0.81g)	1.47	0.7	-52%	0.82	0.34	-59%
25	CLAYN1N1N (0.79g)	CLAYN1N1P (0.71g)	1.94	0.64	-67%	1.04	0.47	-55%
26	-	ROCKS1N1 (0.7g)	-	-	-	0.76	0.38	-50%
27	-	ROCKS1N2 (0.38g)	-	-	-	0.48	0.32	-33%
28	-	ROCKS1N3 (0.32g)	-	-	-	0.57	0.32	-44%
29	-	ROCKS1N4 (0.34g)	-	-	-	0.47	0.32	-32%
30	-	ROCKS1N5 (0.53g)	-	-	-	0.55	0.36	-35%
31	-	ROCKS1N6 (0.42g)	-	-	-	0.59	0.31	-47%
32	-	ROCKS1N7 (0.36g)	-	-	-	0.49	0.31	-37%
33	-	ROCKS1P1 (0.71g)	-	-	-	0.71	0.41	-42%
34	-	ROCKS1P2 (0.44g)	-	-	-	0.48	0.4	-17%
35	-	ROCKS1P3 (0.48g)	-	-	-	0.58	0.38	-34%
36	-	ROCKS1P4 (0.32g)	-	-	-	0.47	0.32	-32%
37	-	ROCKS1P5 (0.67g)	-	-	-	0.86	0.36	-58%
38	-	ROCKS1P6 (0.41g)	-	-	-	0.52	0.34	-35%
39	-	ROCKS1P7 (0.4g)	-	-	-	0.62	0.33	-47%
40	-	SANDS1N1 (0.61g)	-	-	-	1.01	0.53	-48%
41	-	SANDS1N2 (0.51g)	-	-	-	0.65	0.41	-37%
42	-	SANDS1N3 (0.57g)	-	-	-	0.74	0.41	-45%
43	-	SANDS1N4 (0.96g)	-	-	-	1.37	0.45	-67%
44	-	SANDS1N5 (0.79g)	-	-	-	0.82	0.46	-44%
45	-	SANDS1N6 (0.67g)	-	-	-	0.97	0.38	-61%
46	-	SANDS1N7 (0.58g)	-	-	-	0.84	0.51	-39%
47	ROCKN1N1P (0.58g)	ROCKN1N1N (0.4g)	1.33	0.64	-52%	0.46	0.35	-24%
48	ROCKN1P1P (1.42g)	ROCKN1P1N (1.42g)	1.46	0.15	-90%	1.58	0.3	-81%
49	SANDN1N1P (0.81g)	SANDN1N1N (0.78g)	1.11	0.63	-43%	1.97	0.37	-81%
50	CLAYN1N1P (0.71g)	CLAYN1N1N (0.79g)	1.4	0.72	-49%	0.85	0.52	-39%

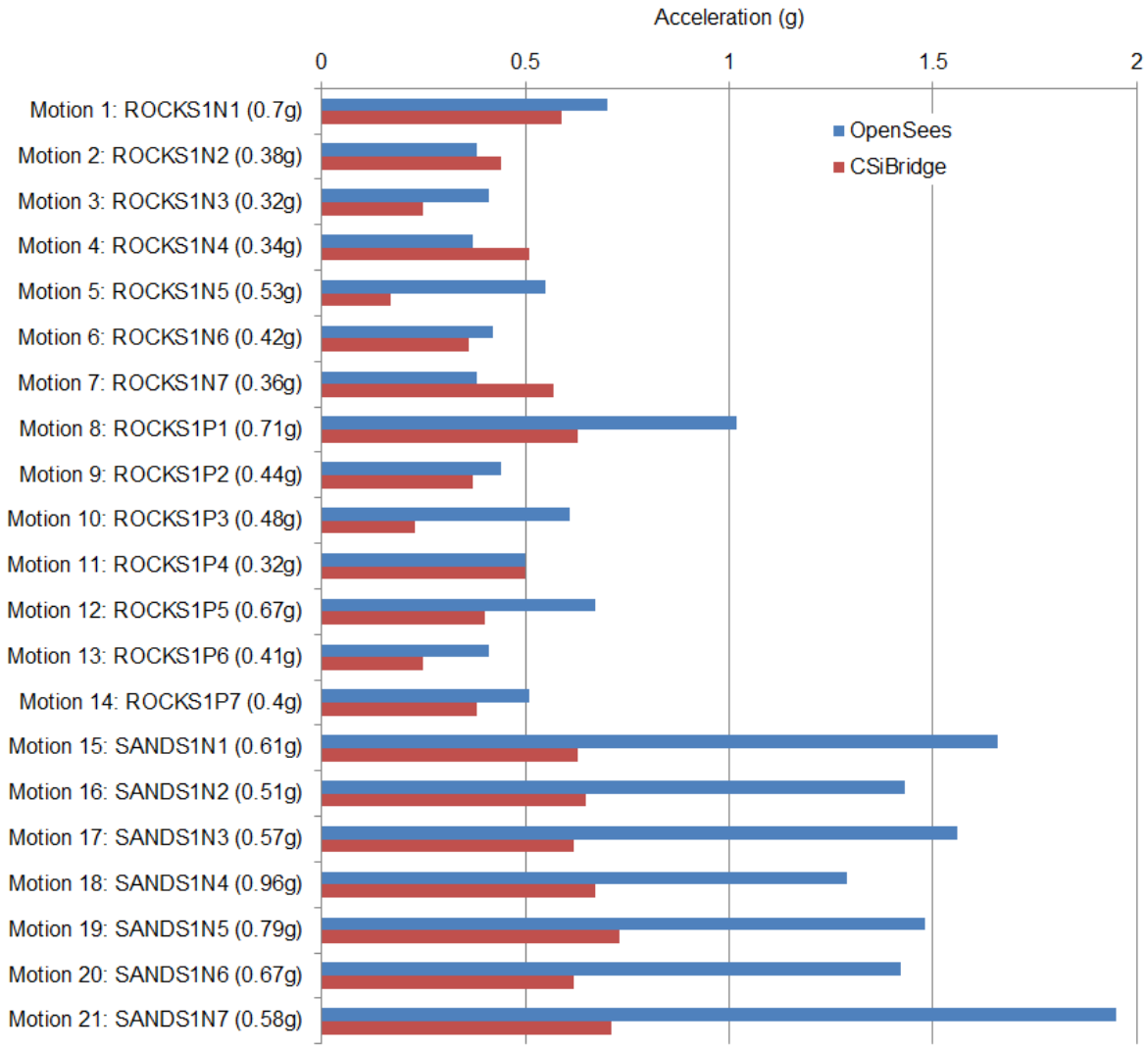

Figure 4.10 OSB4 deck maximum longitudinal acceleration for Motions 1-21 (EPP-Gap with Isolation Bearings model)

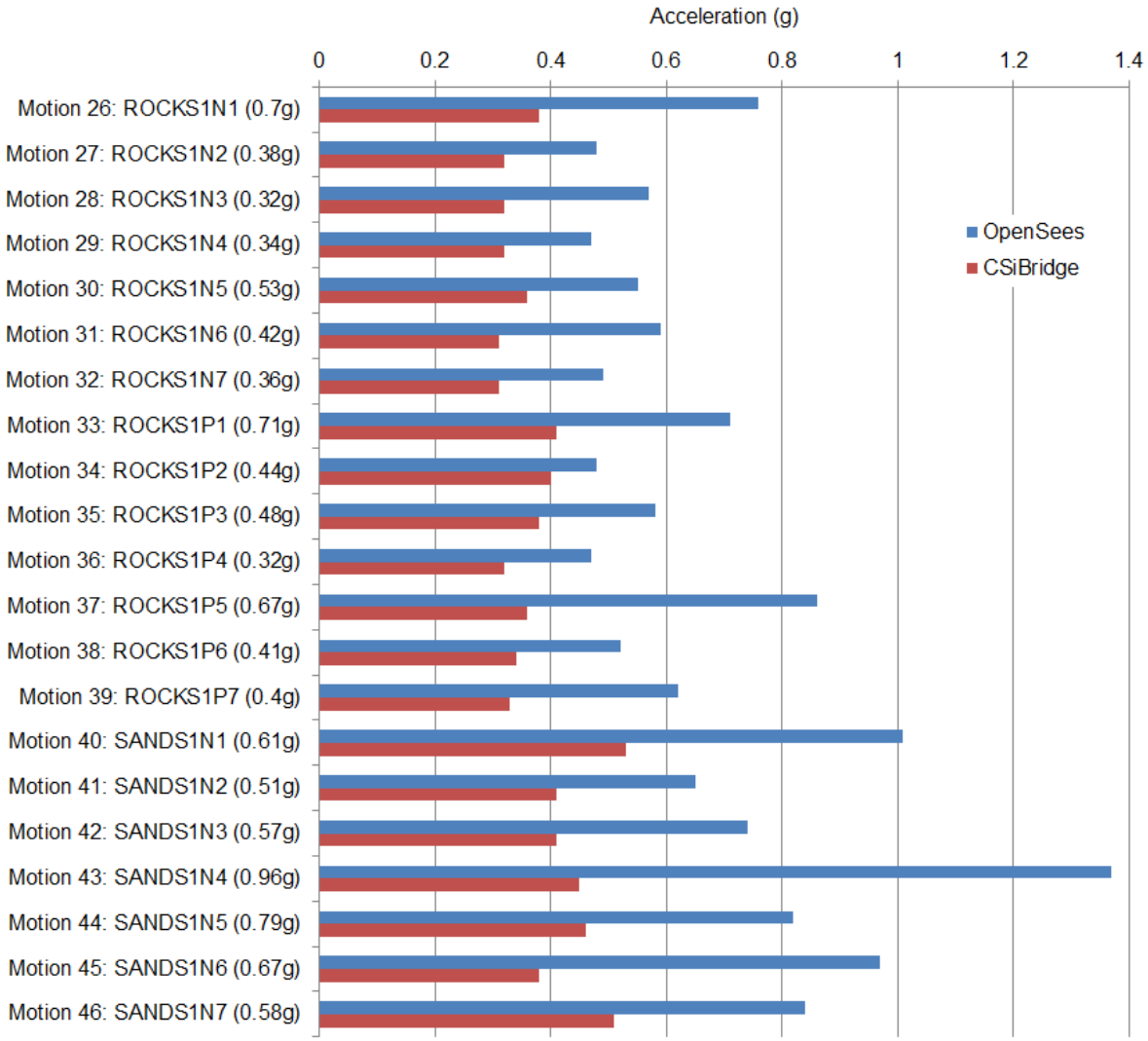

Figure 4.11 OSB4 deck maximum transverse acceleration for Motions 26-46 (EPP-Gap with Isolation Bearings model)

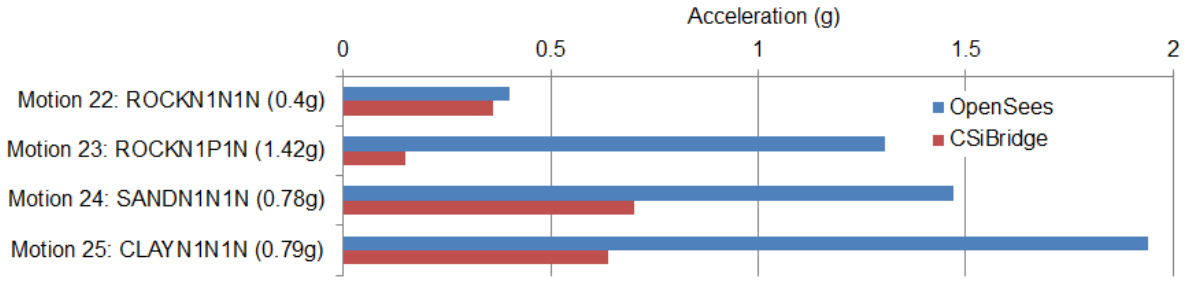

a)

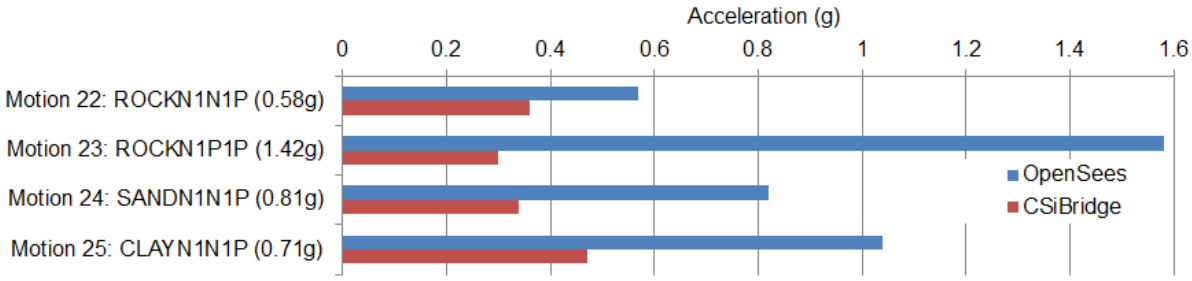

b)

Figure 4.12 OSB4 deck maximum acceleration for Motions 22-25 (EPP-Gap with Isolation Bearings model): a) Lonitudinal direction; b) Transverse direction

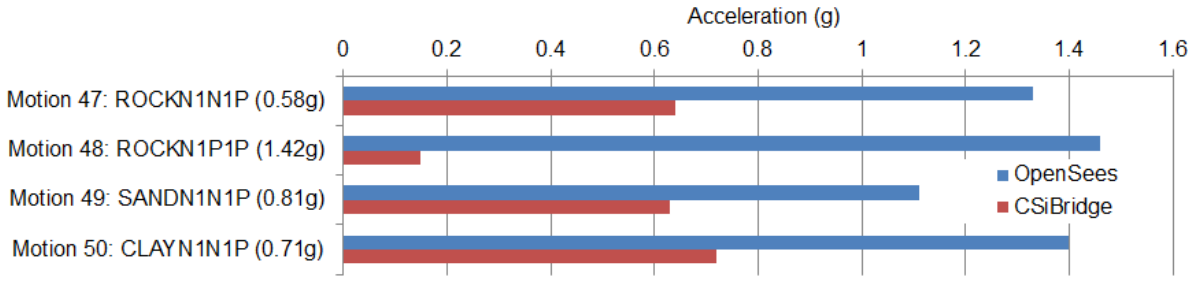

a)

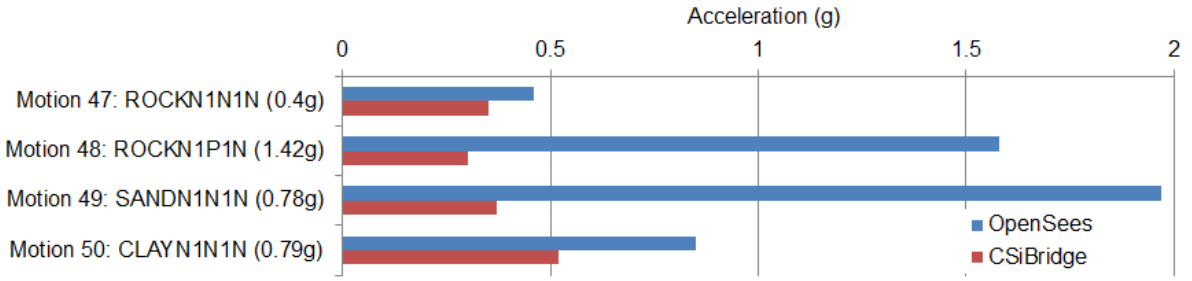

b)

Figure 4.13 OSB4 deck maximum acceleration for Motions 47-50 (EPP-Gap with Isolation Bearings model): a) Lonitudinal direction; b) Transverse direction

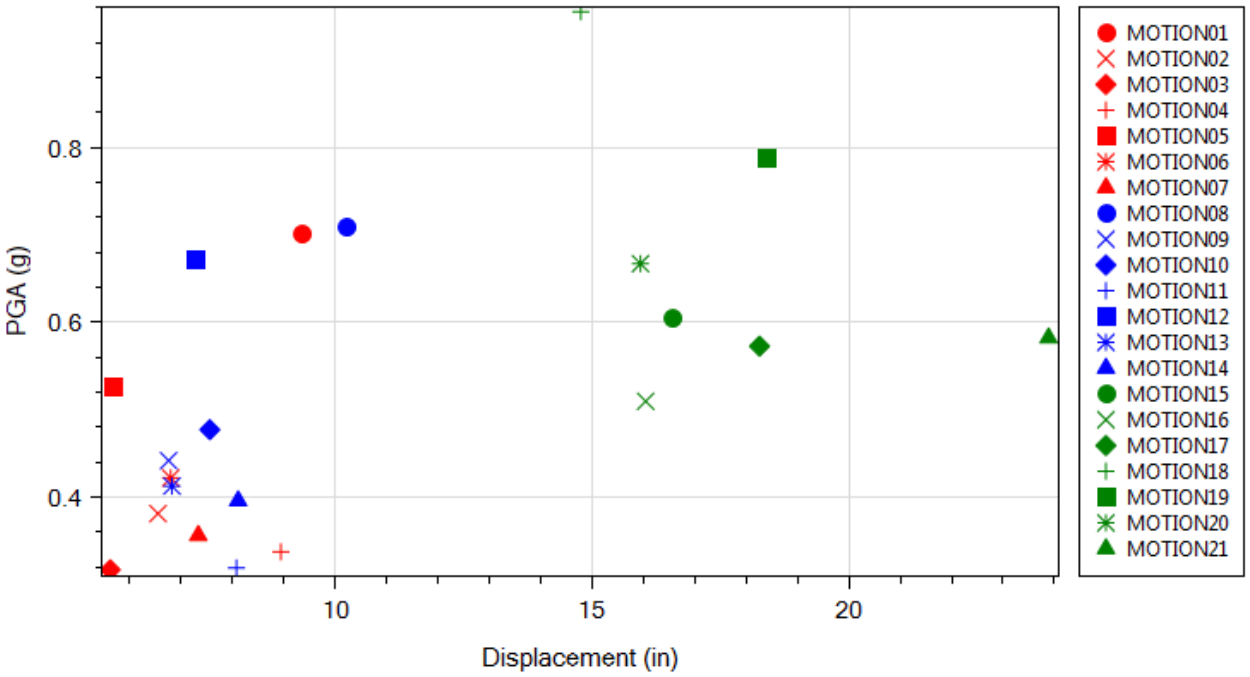

Figure 4.14 OSB4 deck maximum longitudinal displacement in OpenSees (Motions 1-21; Roller with Isolation Bearings model)

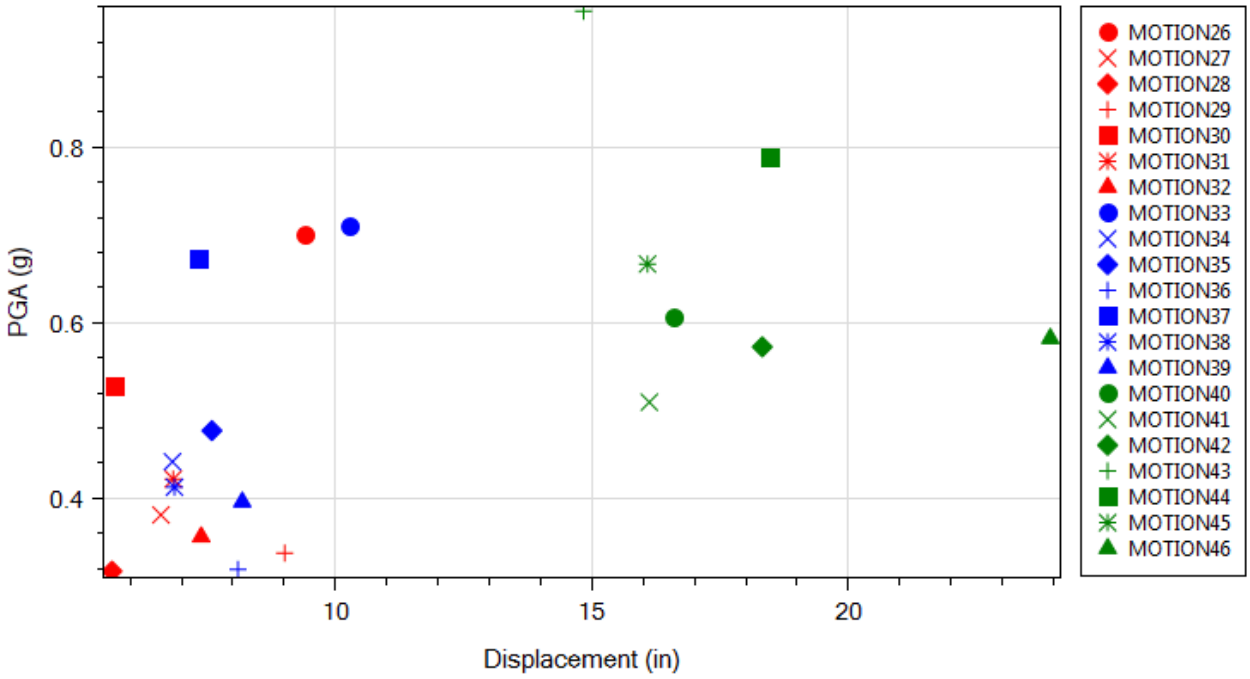

Figure 4.15 OSB4 deck maximum transverse displacement in OpenSees (Motions 26-46; Roller with Isolation Bearings model)

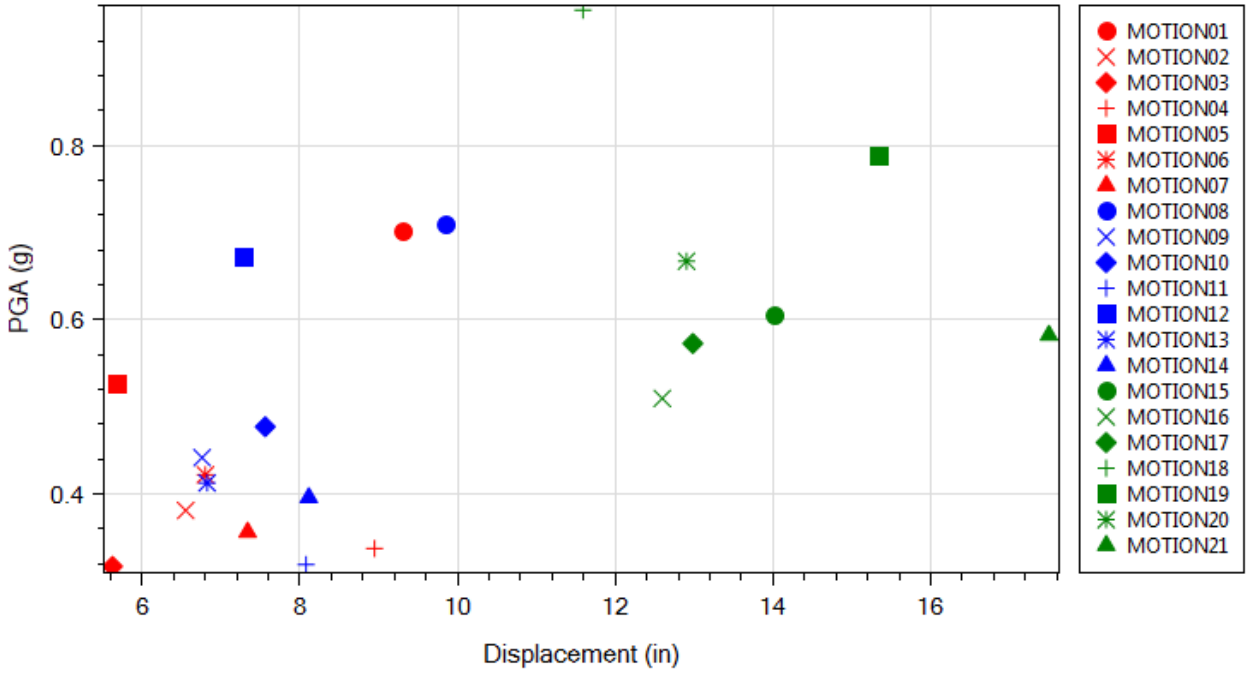

Figure 4.16 OSB4 deck maximum longitudinal displacement in OpenSees (Motions 1-21; EPP-Gap with Isolation Bearings model)

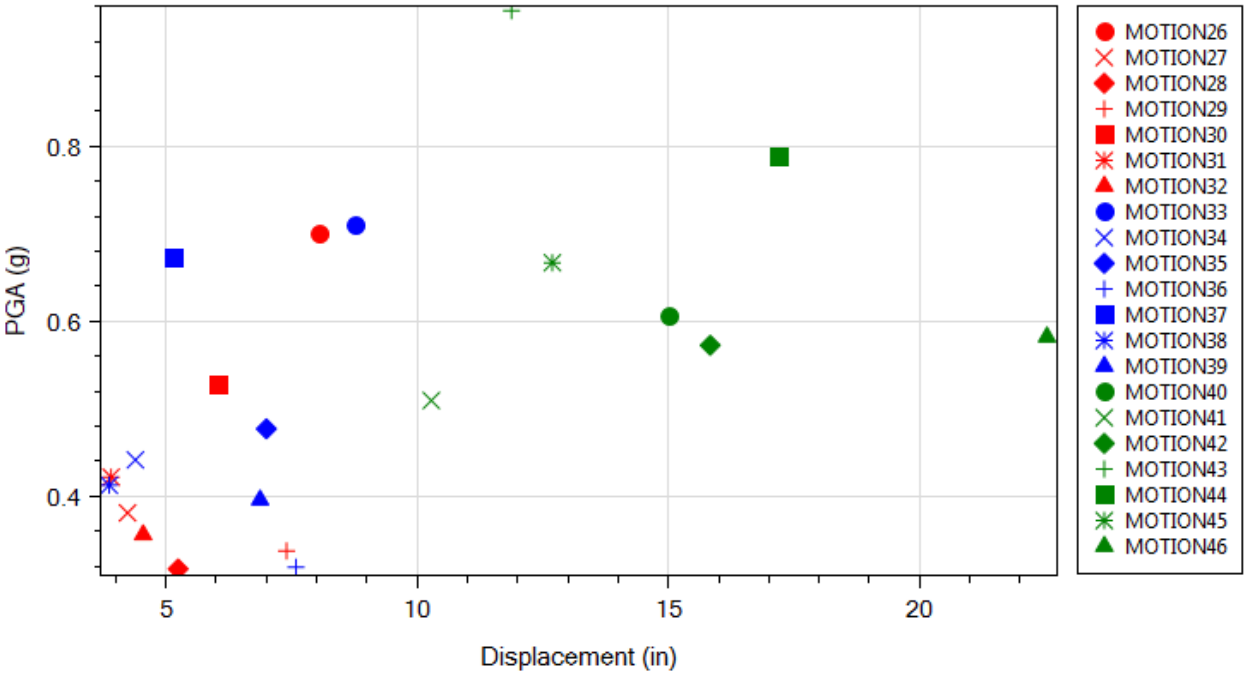

Figure 4.17 OSB4 deck maximum transverse displacement in OpenSees (Motions 26-46; EPP-Gap with Isolation Bearings model)

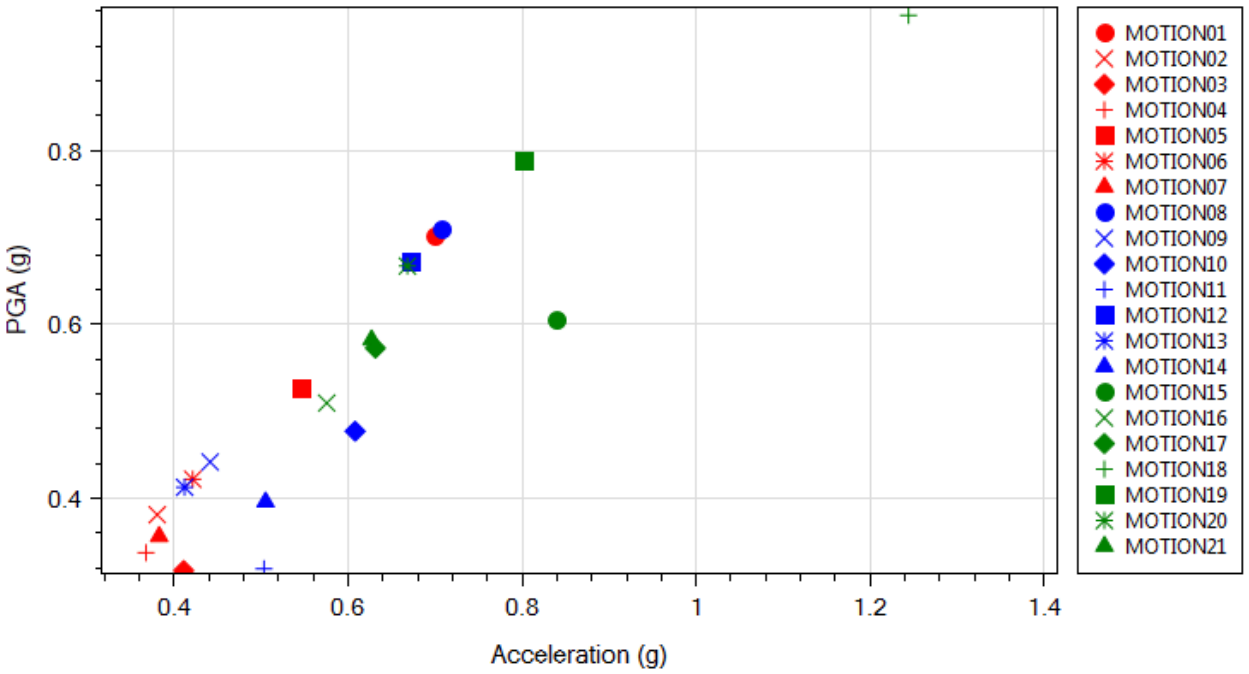

Figure 4.18 OSB4 deck maximum longitudinal acceleration in OpenSees (Motions 1-21; Roller with Isolation Bearings model)

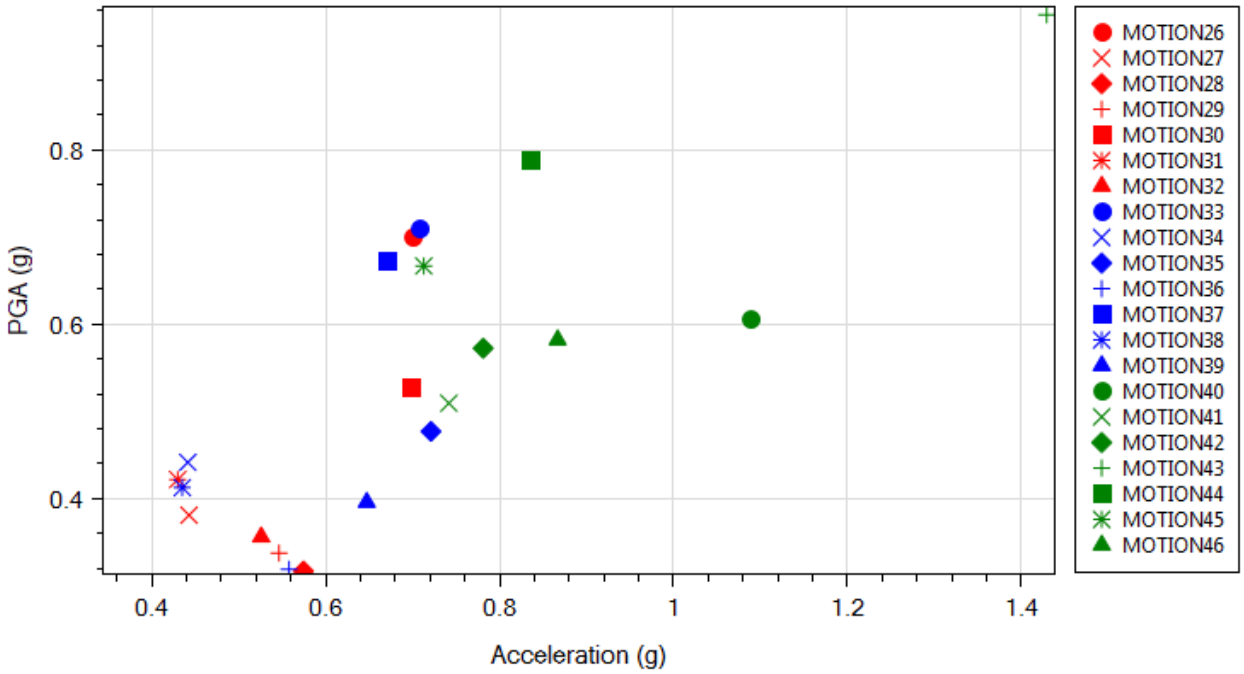

Figure 4.19 OSB4 deck maximum transverse acceleration in OpenSees (Motions 26-46; Roller with Isolation Bearings model)

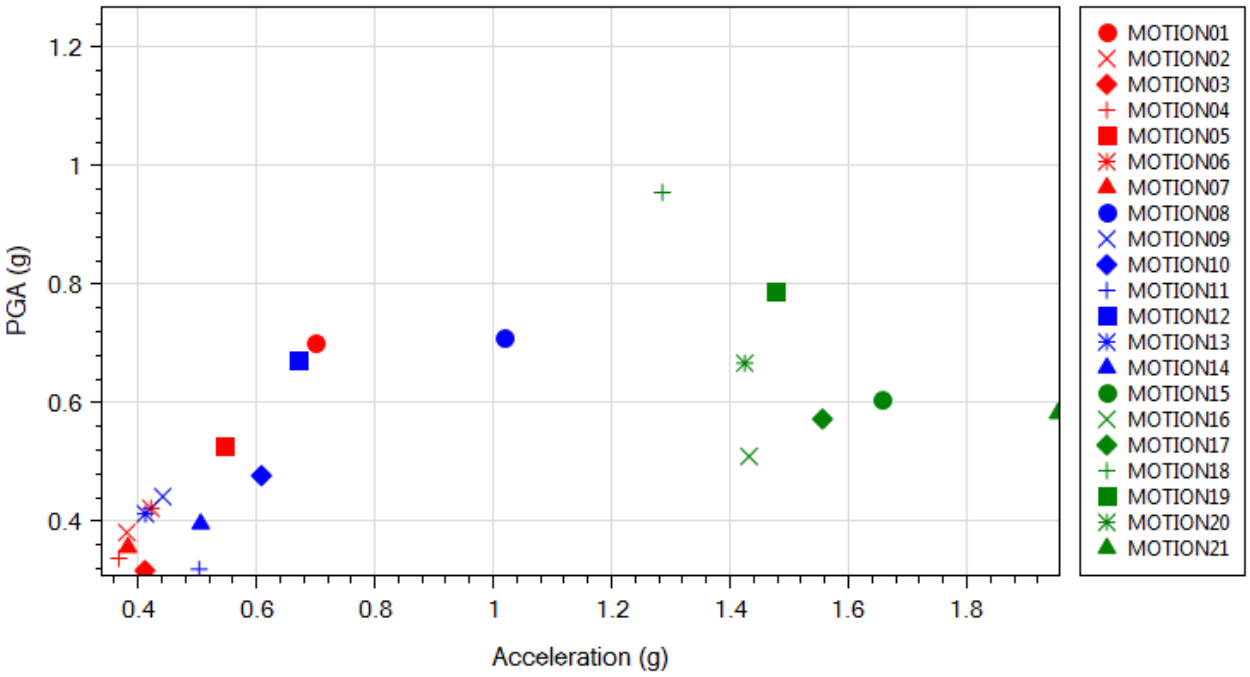

Figure 4.20 OSB4 deck maximum longitudinal acceleration in OpenSees (Motions 1-21; EPP-Gap with Isolation Bearings model)

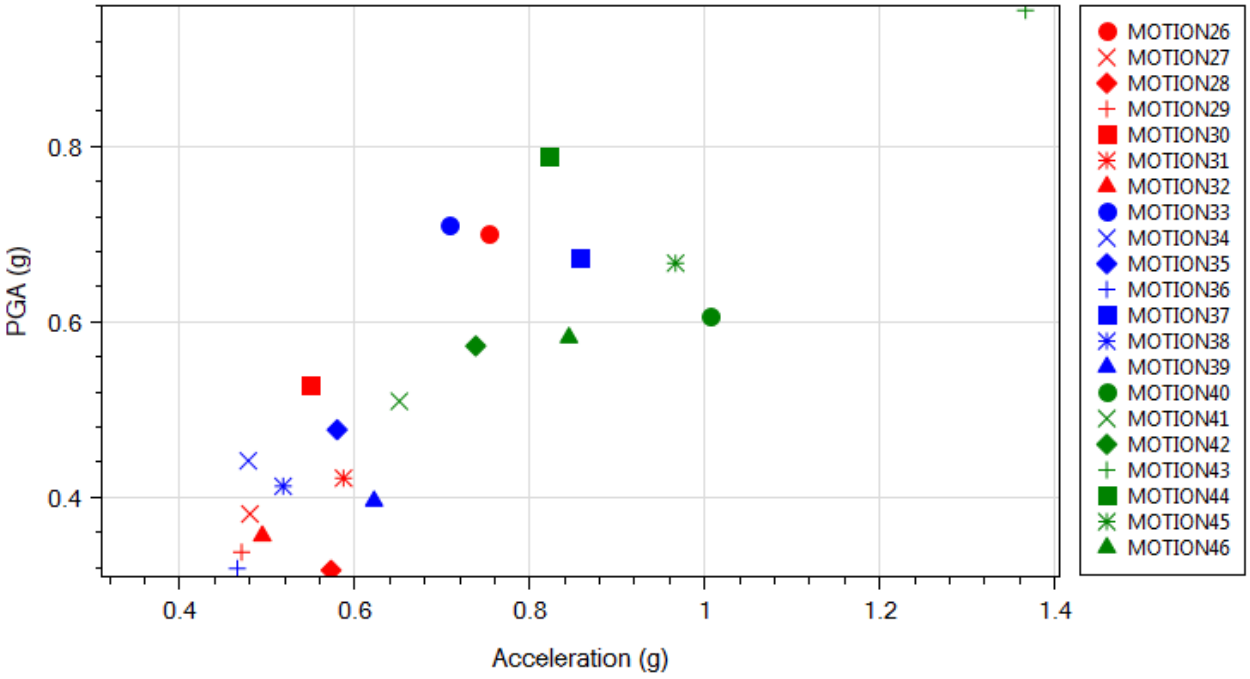

Figure 4.21 OSB4 deck maximum transverse acceleration in OpenSees (Motions 26-46; EPP-Gap with Isolation Bearings model)

4.5.2 Response Time History (OpenSees)

In this section, response time histories from 2 motions (Motions 1 and 15) from OpenSees nonlinear THA are presented (for the EPP-Gap with Isolation Bearings model).

1) Motion 1 ROCKS1N1

For Motion 1, the deck maximum displacement is 9.3 in (Table 4.4). Figure 4.22 displays OSB4 longitudinal response time history for Motion 1 (ROCKS1N1). The input motion ROCKS1N1 is shown in Figure 4.22d for reference.

The column and isolation bearing force-displacement response is displayed in Figure 4.23. Note that the right abutment resisting force was essentially zero since the longitudinal gap (9 in) was not closed. Figure 4.24 displays the column top longitudinal moment-curvature response which is essentially linear.

2) Motion 15 SANDS1N1

Figure 4.25 shows OSB4 longitudinal response time history. The column and isolation bearing force-displacement response is displayed in Figure 4.26. Figure 4.27 displays the column top longitudinal moment-curvature response which is also essentially linear.

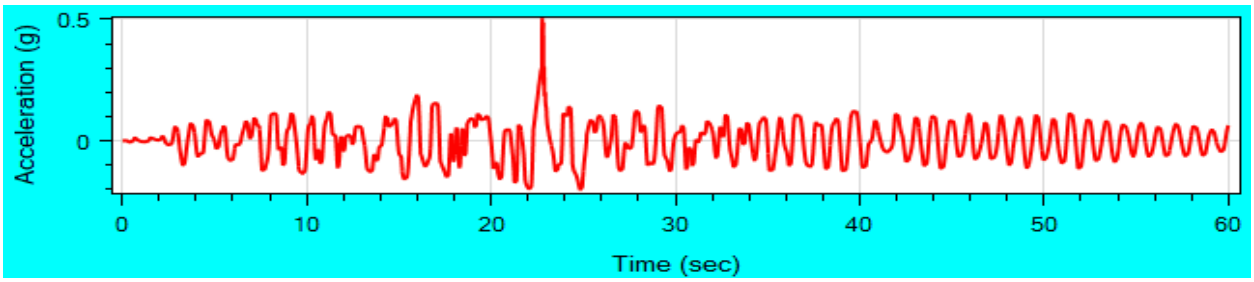

a)

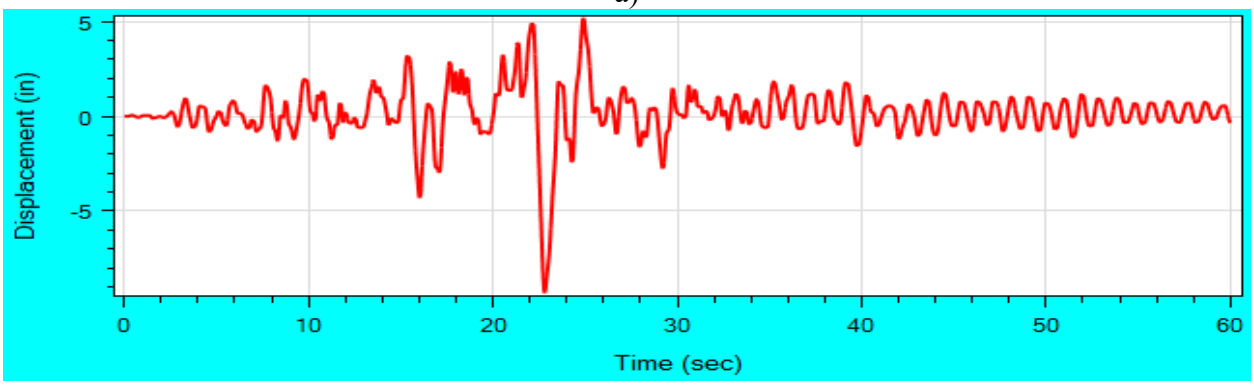

b)

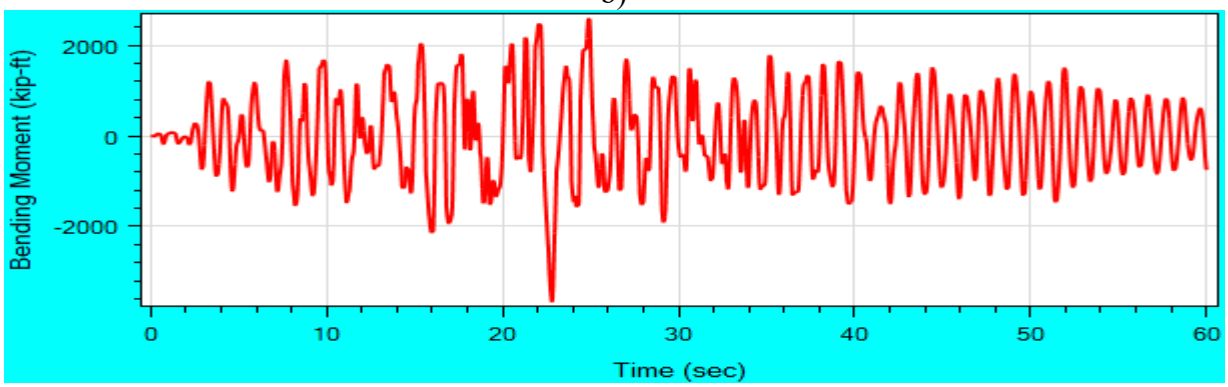

c)

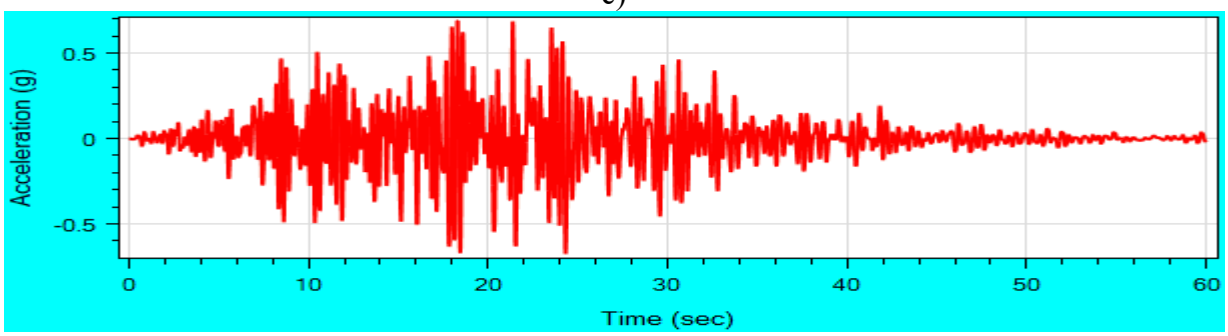

d)

Figure 4.22 OSB4 longitudinal response time histories for Motion 1 ROCKS1N1 (EPP-Gap with Isolation Bearings model): a) deck acceleration; b) deck displacement; c) column base bending moment; d) base excitation ROCKS1N1

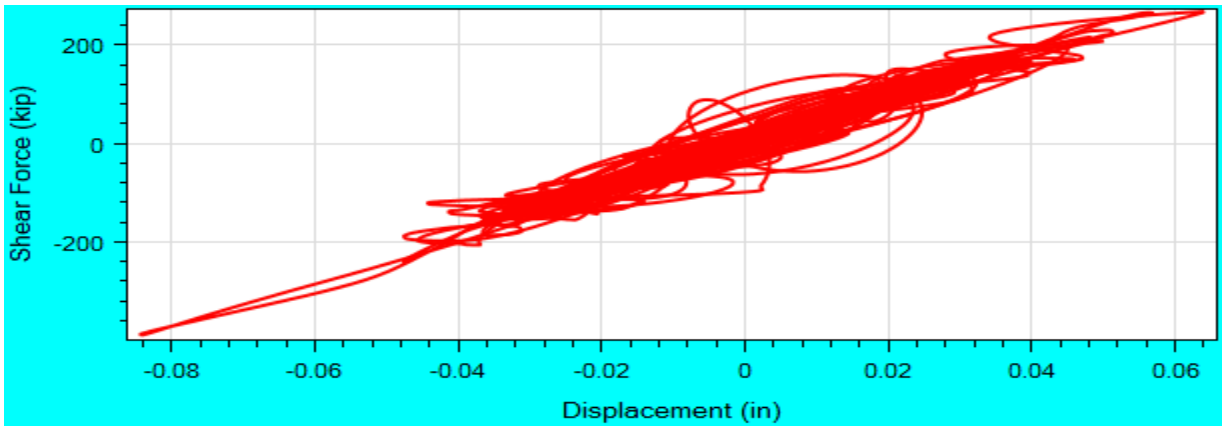

a)

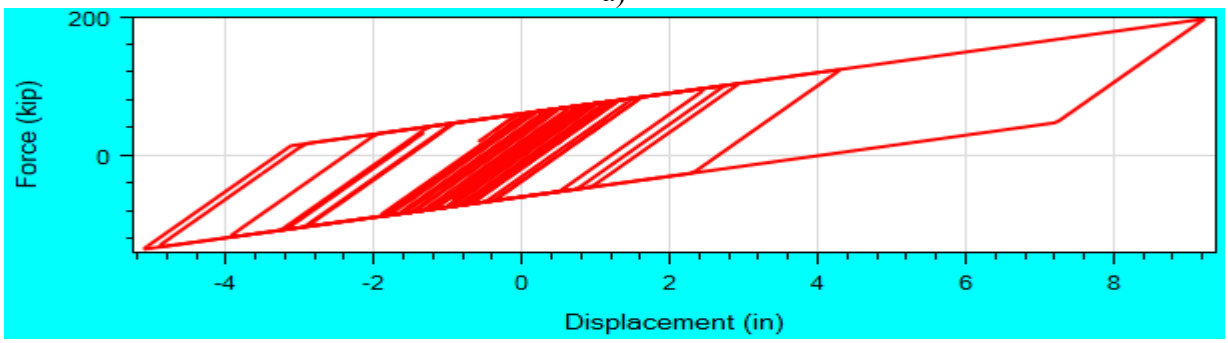

b)

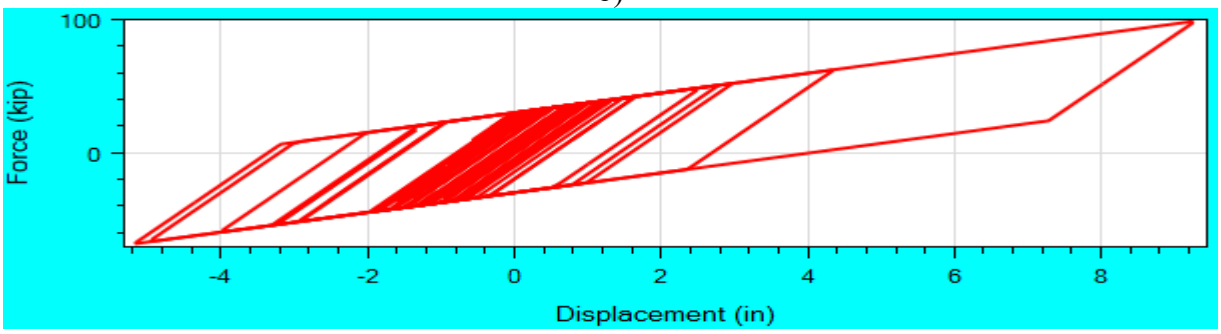

c)

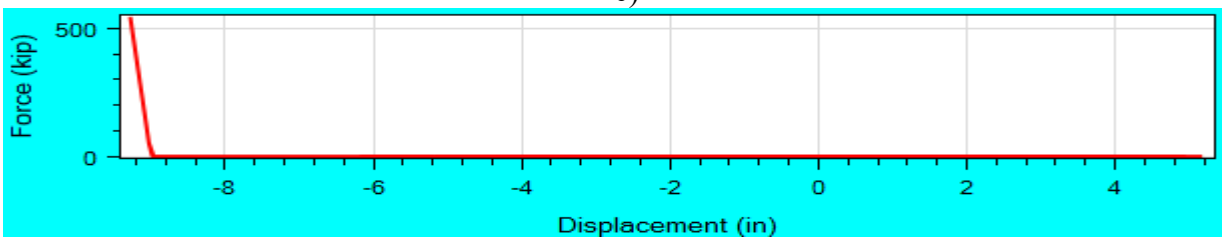

d)

Figure 4.23 OSB4 longitudinal force-displacement response for Motion 1 ROCKS1N1 (EPP-Gap with Isolation Bearings model): a) column top force-displacement; b) bent isolation bearing force-displacement response; c) left abutment isolation bearing force-displacement response; d) left abutment embankment response

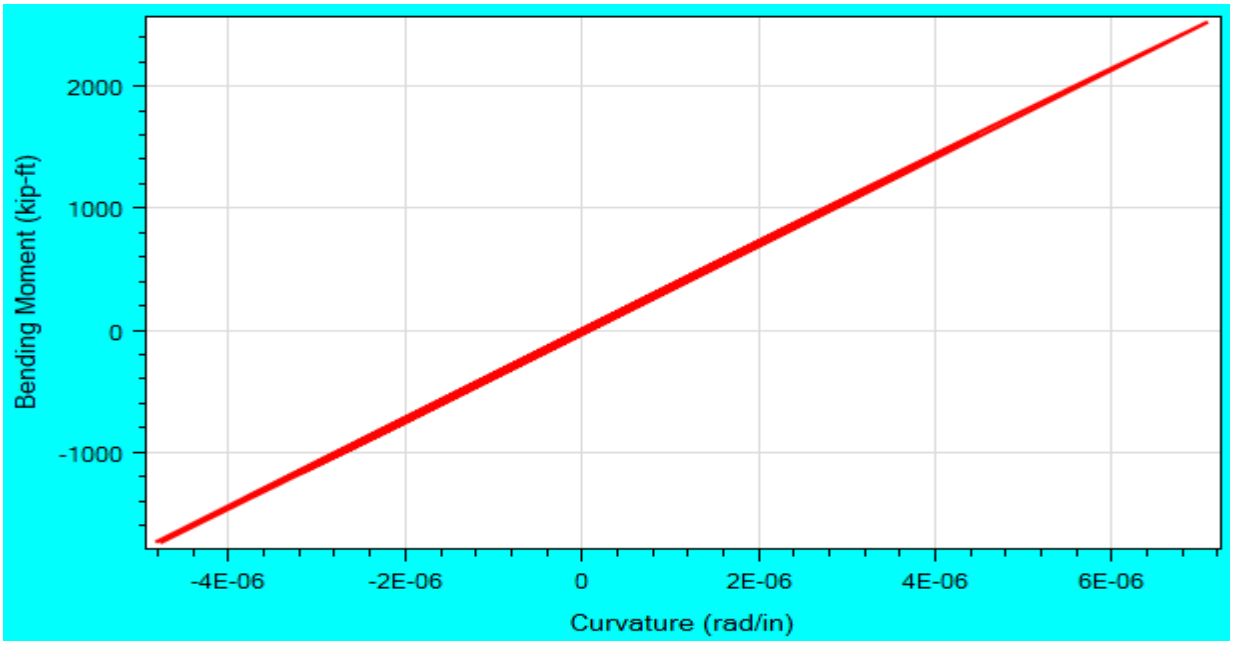

a)

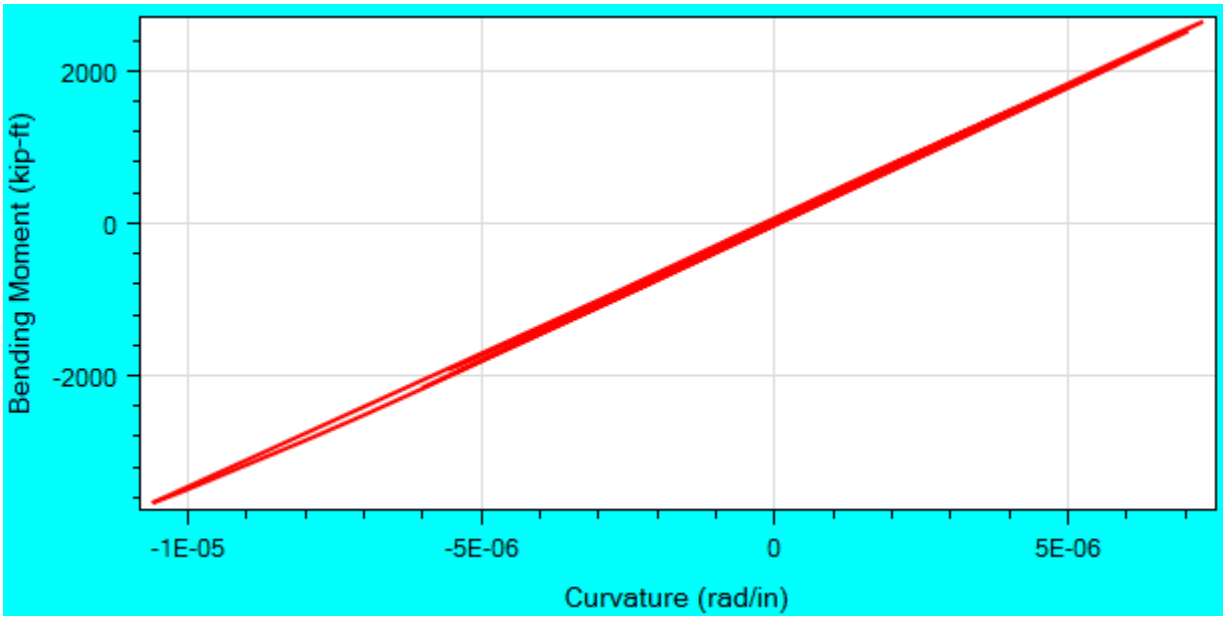

b)

Figure 4.24 OSB4 longitudinal moment-curvature response for Motion 1 ROCKS1N1 (EPP-Gap with Isolation Bearings model) at: a) column top; b) column base

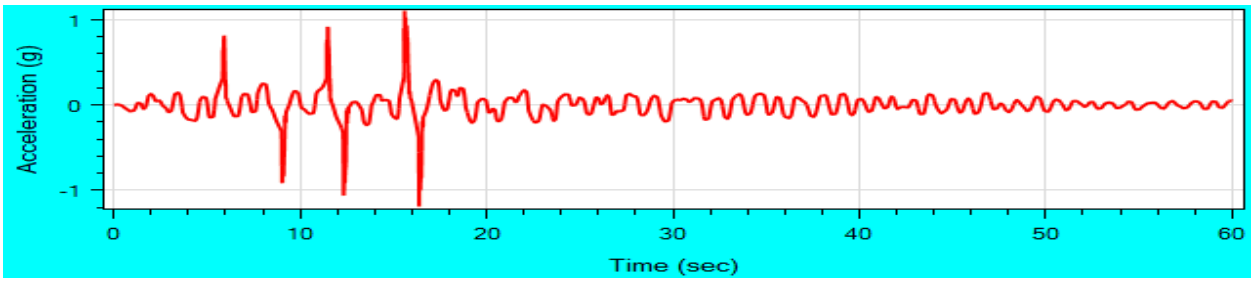

a)

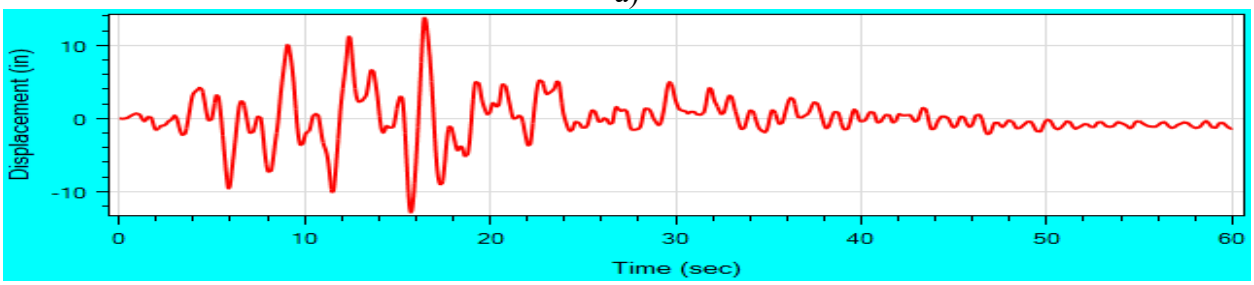

b)

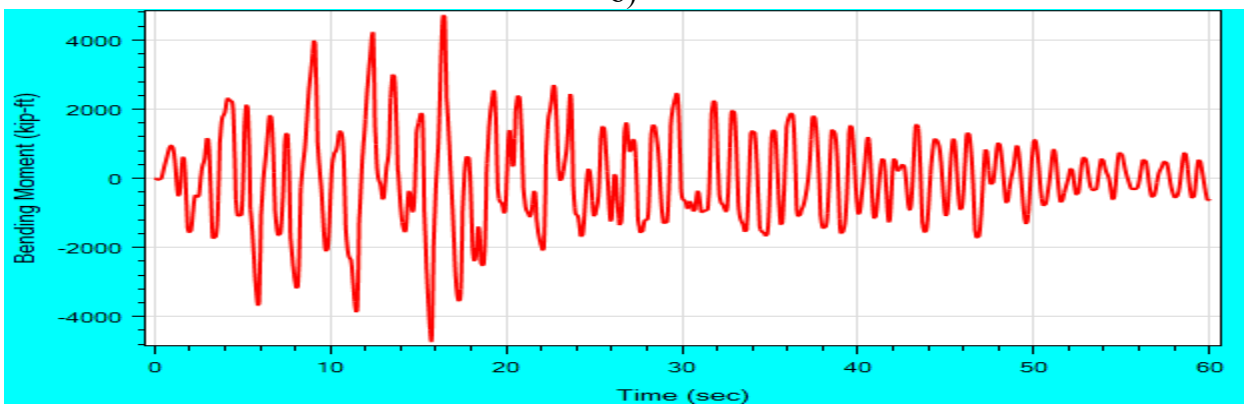

c)

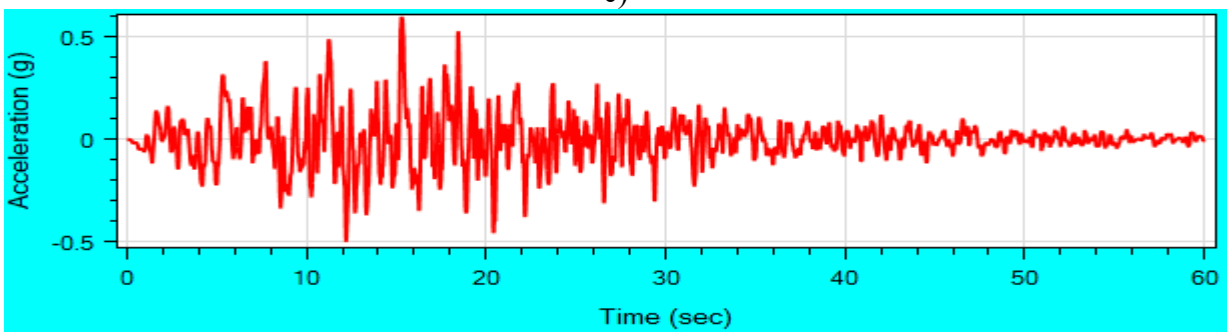

d)

Figure 4.25 OSB4 longitudinal response time histories for Motion 15 SANDS1N1 (EPP-Gap with Isolation Bearings model): a) deck acceleration; b) deck displacement; c) column base bending moment; d) base excitation SANDS1N1

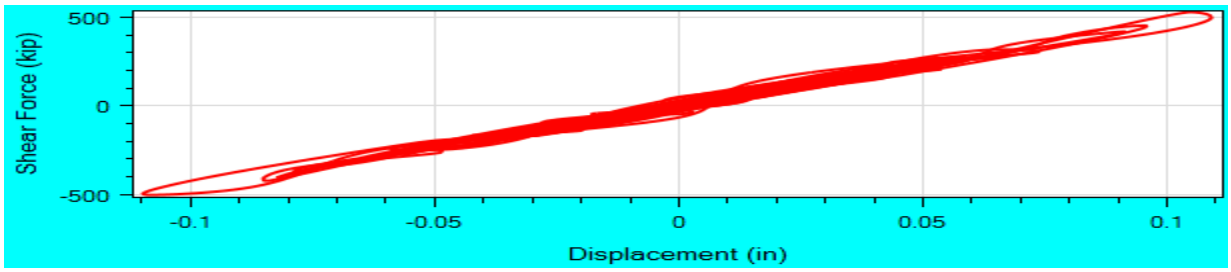

a)

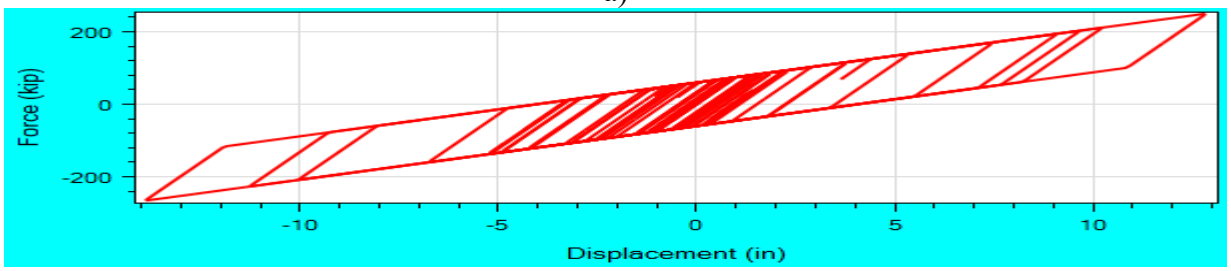

b)

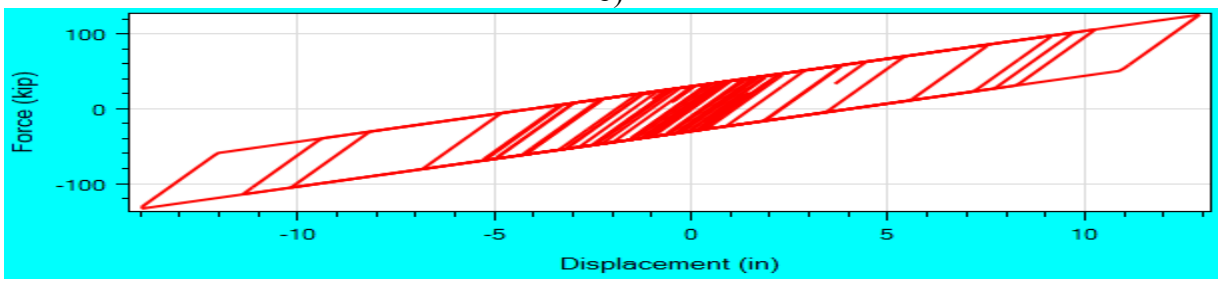

c)

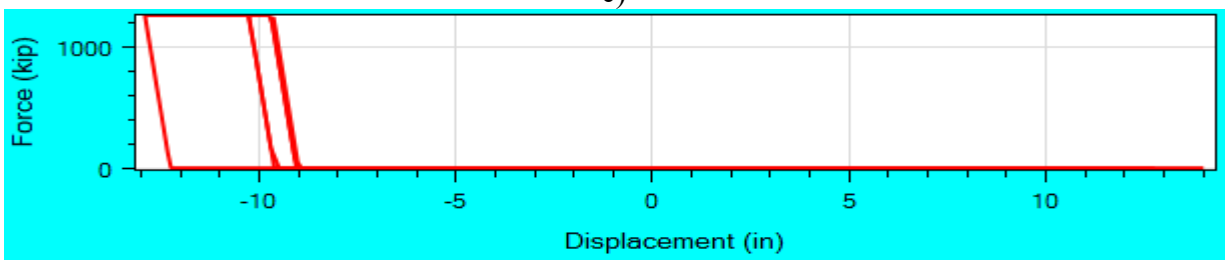

d)

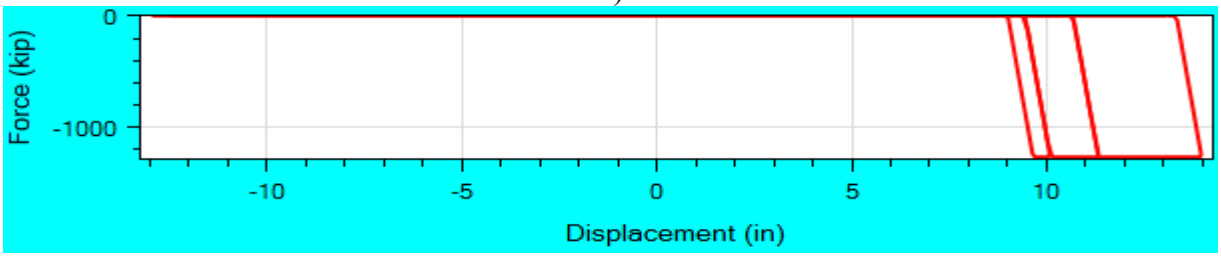

e)

Figure 4.26 OSB4 longitudinal force-displacement response for Motion 15 SANDS1N1 (EPP-Gap with Isolation Bearings model): a) column top force-displacement; b) bent isolation bearing force-displacement response; c) left abutment isolation bearing force-displacement response; d) left abutment embankment response; e) right abutment embankment response

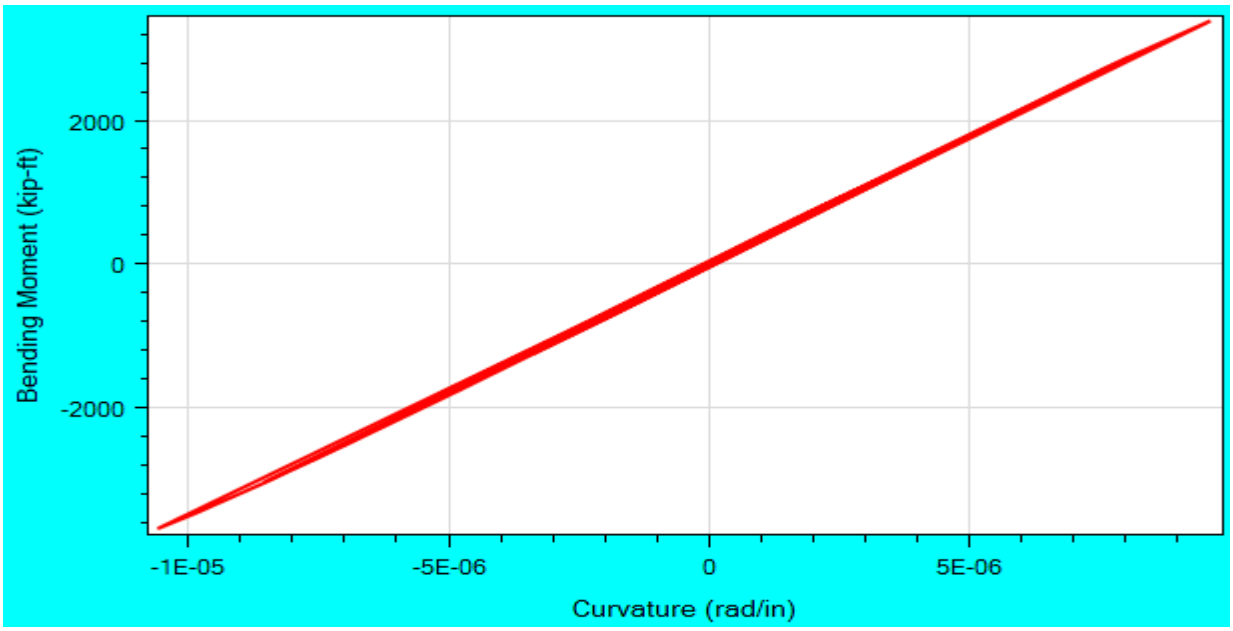

a)

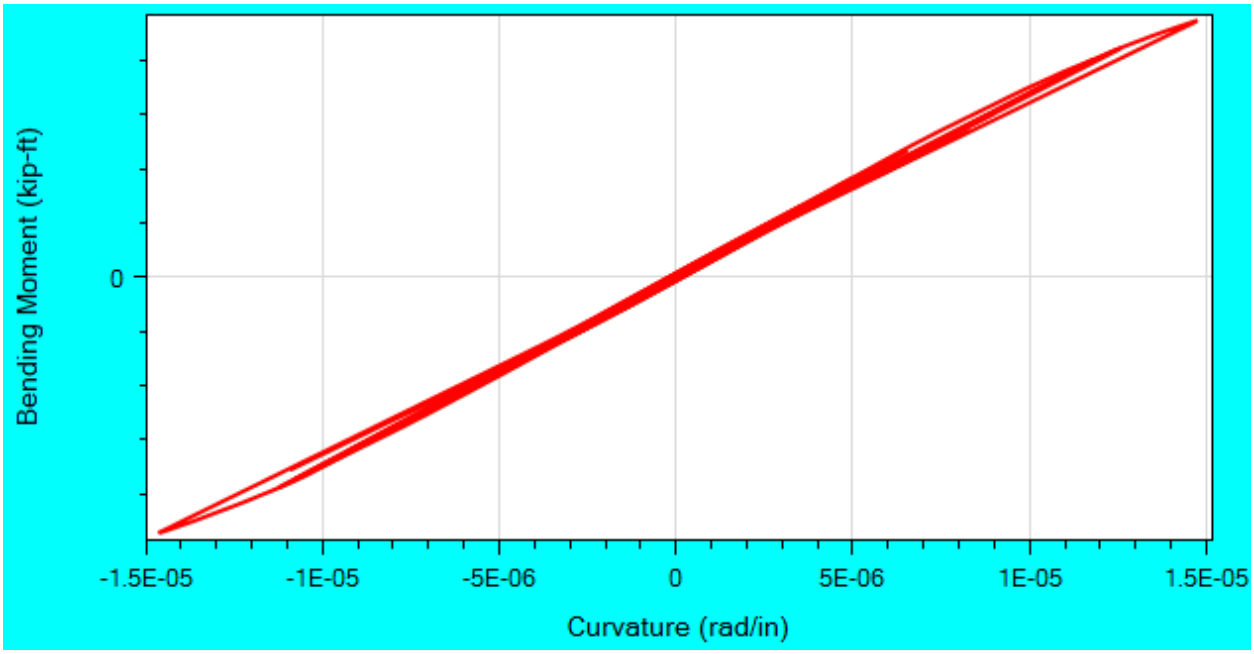

b)

Figure 4.27 OSB4 longitudinal moment-curvature response for Motion 15 SANDS1N1 (EPP-Gap with Isolation Bearings model) at: a) column top; b) column base

4.6 Summary

OSB4 was modeled in OpenSees and CSiBridge. A recently developed user interface MSBridge was employed for pre- and post-processing.

Nonlinear THA was conducted for the 50 motions provided by Caltrans. Two types of abutment models (Roller with Isolation Bearings, and EPP-Gap with Isolation Bearings) were addressed in OpenSees. For the EPP-Gap with Isolation Bearings model, the maximum displacement is 5.6-17.5 inches in the bridge longitudinal direction and 3.9-22.6 inches in the transverse direction. In CSiBridge, only the EPP-Gap with Isolation Bearings model was simulated.

ESA was also conducted for OSB4 using MSBridge. The longitudinal ESA shows the displacement demand to be 6.7 inches. The displacement demand was 6.8 inches from the transverse ESA.

4.7 Conclusions

1. For the investigated set of ground motions in the OpenSees model (EPP-Gap with Isolation Bearings model):

1.1. In the longitudinal direction, about 50% of the shaking events resulted in deck displacement demand that exceeded that of the ESA (6.7 in). This demand reached a maximum of 160% in excess of that from the corresponding ESA. With the 9 in gap, the abutment reduced the peak maximum displacement from 25.7 in (for the Roller with Isolation Bearings model) to 16.7 in (for the EPP-Gap with Isolation Bearings model).

1.2. In the transverse direction, about 35% of the shaking events resulted in deck displacement demand that exceeded that of the ESA (6.8 in). This demand reached a maximum of 240% in excess of that from the corresponding ESA. With the 1 in gap, the abutment reduced the peak maximum displacement from 25.8 in (for the Roller with Isolation Bearings model) to 22.6 in (for the EPP-Gap with Isolation Bearings model).

2. For the OpenSees model, the ground input motions of the SANDS1 group (Figure B.4, Figure B.8 and Table 4.4) appear to result consistently in a larger longitudinal and transverse displacement demand (Figures 4.14-4.17).

3. For the EPP-Gap with Isolation Bearings model, in the longitudinal direction, the maximum displacement difference between the OpenSees and CSibridge results is within 20% for about 4/5 of shaking events (Table 4.5). In the transverse direction, the difference is 20% for about 2/3 of shaking events (Table 4.5).

5 OSB STUDY BRIDGE 3

5.1 Bridge Description

OSB Study Bridge 3 (hereinafter referred to as "OSB3") is a single bent PC/PS wide flange girder bridge with two spans of 150 feet in length. The single-bent is composed of two circular Pre-cast columns with 2 isolation bearings at column top. In addition, 2 isolation bearings are located on top of the each abutment. Figure 5.1 shows the general geometries of OSB3.

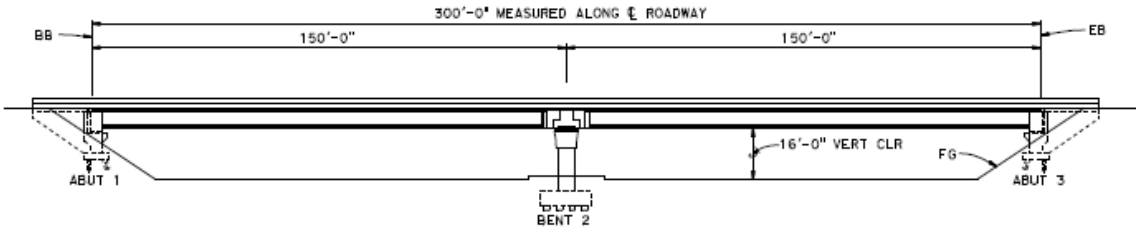

a)

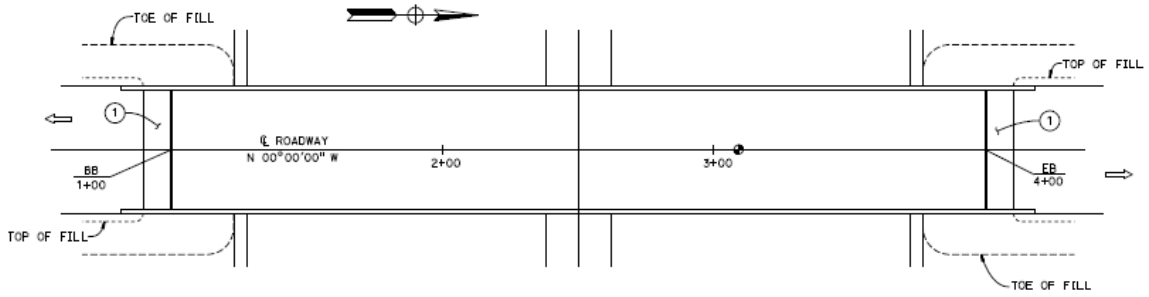

b)

Figure 5.1 Schematic of OSB3 (drawings provided by Caltrans): (a) Elevation view; (b) Plan view

5.2 Geometric Configuration

Figure 5.2 shows the elevation view of OSB3 along with the column reinforcement details. The PC/PS wide flange girder is 47 feet wide by 6.33 feet deep. The bentcap is assumed to be rigid. The column is 16 feet high with a diameter of 66 inches.

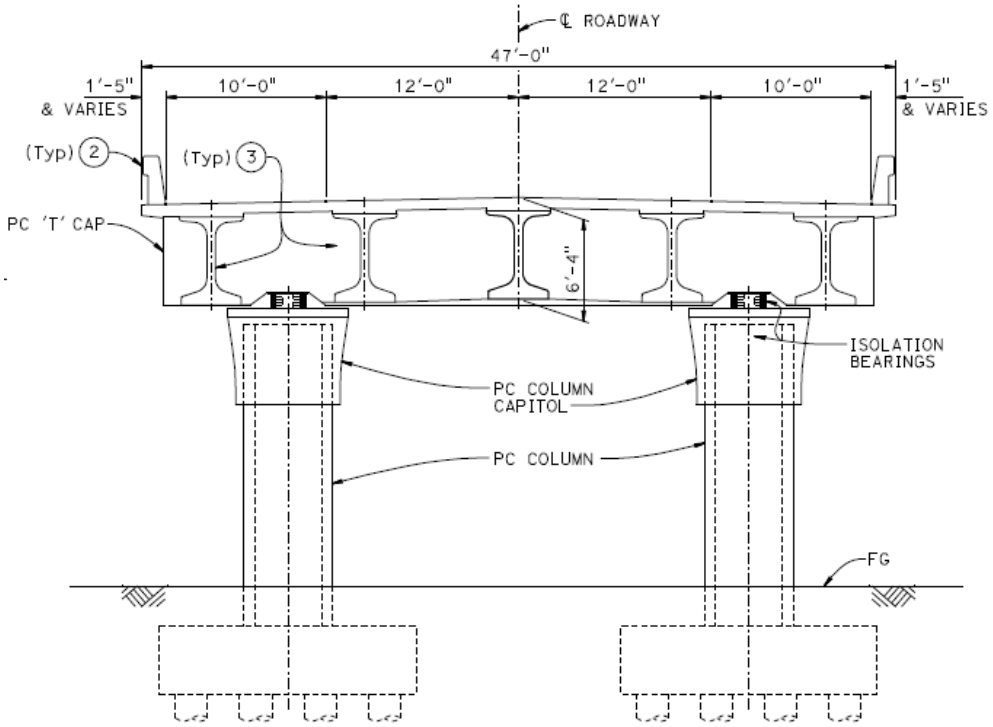

a)

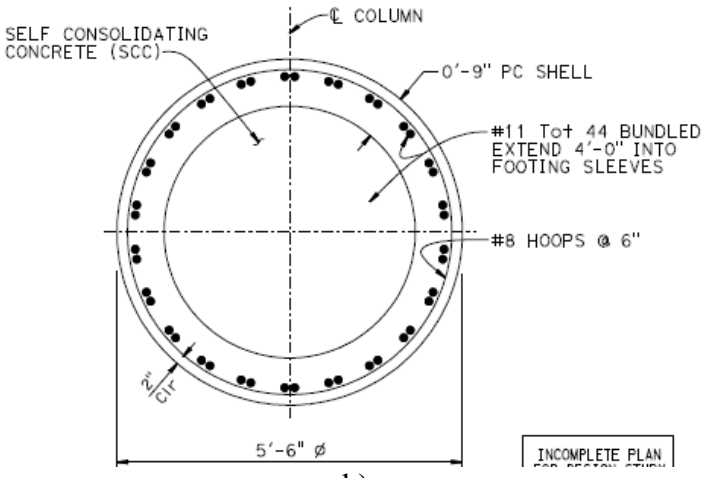

b)

Figure 5.2 Elevation and sectional details of OSB3: (a) deck; (b) circular section (Caltrans 2012)

5.3 OSB3 OpenSees Modeling and Response

5.3.1 Finite Element Model

The employed modeling techniques and associated model properties are presented in Appendix F. To facilitate the conducted analyses, a recently developed user interface MSBridge was employed (please see Appendix A for more information about MSBridge). Figure 5.3 shows the OSB3 model created in MSBridge and CSiBridge.

The forceBeamColumn element (with the distributed plasticity integration method) in OpenSees was used to model the column. The deck was considered linearly elastic (see Appendix E for the deck geometric and material properties).

As shown in Figure 5.3, two equal-length elements were used for the column (the column height is 16 ft). The column is pinned at top and assumed fixed at base. The offset between the column top and the deck was not considered (due to limitations in the current version of MSBridge). No rotation around the bridge longitudinal direction is allowed for the deck (at the abutments).

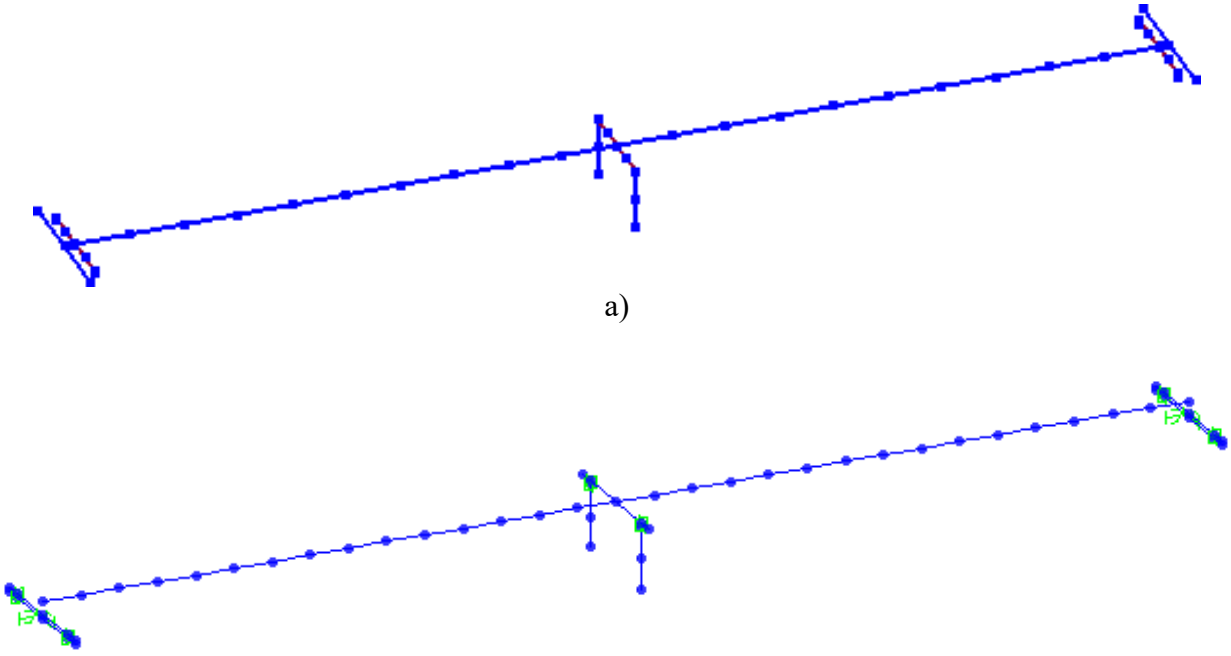

a)

b)

Figure 5.3 OSB3 model (3D view) created in: a) MSBridge; b) CSiBridge

Two types of abutment models were employed in this study:

i) Roller with Isolation Bearings abutment model, and
ii) EPP-Gap with Isolation Bearings abutment model.

The resulting OSB3 bridge models will be hereinafter referred to as "Roller with Isolation Bearings" and "EPP-Gap with Isolation Bearings", respectively. The first natural periods for OSB3 with the 2 bridge models are both 1.07 second. For detailed information about the above abutment models, please see Appendix F. As suggested by Caltrans, only the EPP-Gap with Isolation Bearings model was simulated in the CSiBridge nonlinear THA.

5.3.2 Isolation Bearing and Abutment Response

Pushover analysis was conducted in OpenSees to document the corresponding isolation bearing response. The pushover load was applied at the deck center (in the longitudinal & transverse directions). Figure 5.4 shows the isolation bearing force-displacement response due to pushover loading. Figure 5.5 shows the right abutment force-displacement response due to pushover loading in the longitudinal (Figure 5.5a) and transverse (Figure 5.5b) directions.

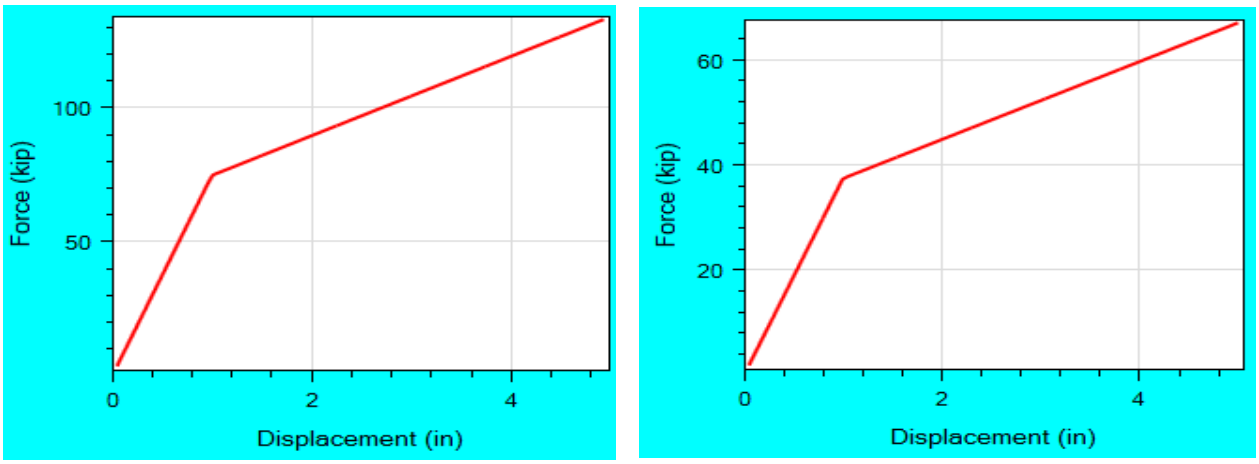

a) b)

Figure 5.4 OSB3 isolation bearming lateral response response (only up to 5 inches of pushover displacement is shown) for: a) bent isolation bearing; b) abutment isolation bearing

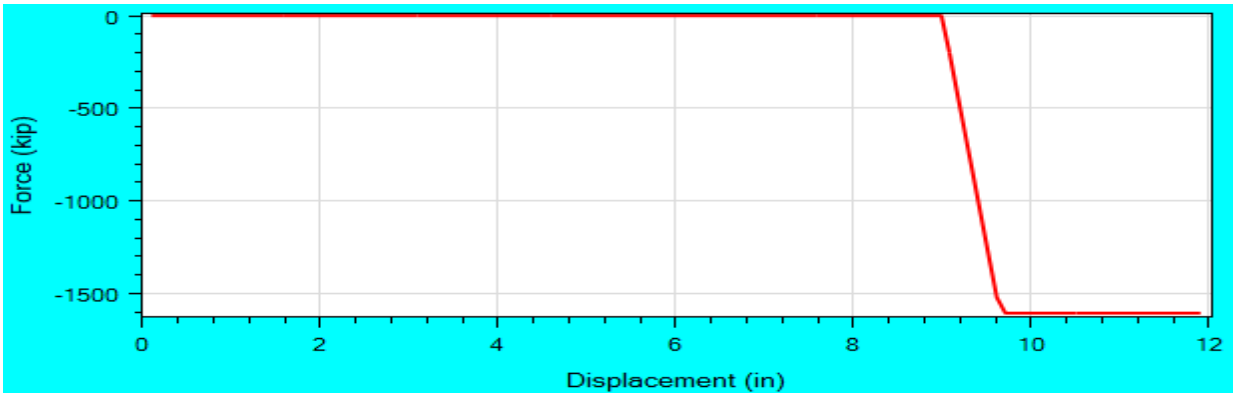

a)

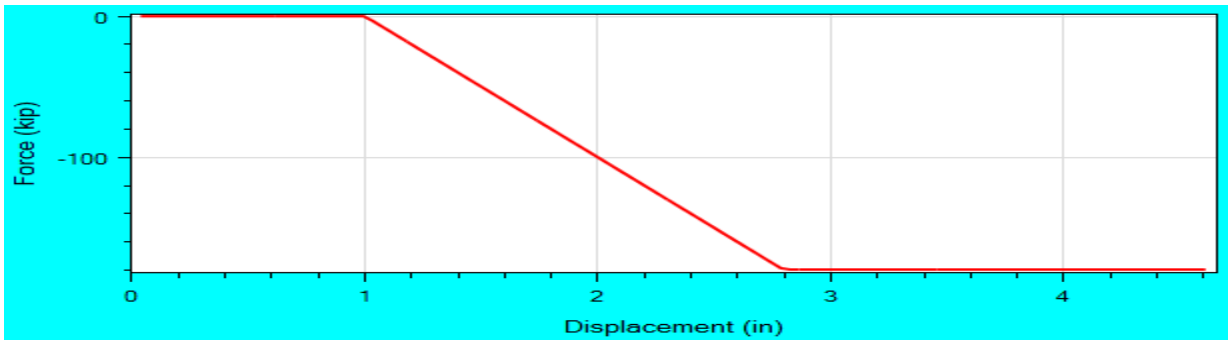

b)

Figure 5.5 OSB3 abutment force-displacement response (for EPP-Gap with Isolation Bearings abutment model only): a) longitudinal response; b) transverse response

5.4 Equivalent Static Analysis (ESA) in OpenSees

ESA was conducted in OpenSees for OSB3 in the bridge longitudinal and transverse directions. For the procedure to conduct ESA in MSBridge, please refer to the MSBridge user manual (Elgamal et al. 2014).

5.4.1 ESA in the Longitudinal Direction

A load of 5% of the total bridge weight was used for longitudinal pushover analysis. The pushover load was applied at the deck center at the bent (along the bridge longitudinal direction). For the acceleration response spectrum (ARS) employed in the ESA, please see Appendix C.

Table 5.1 shows the ESA result for OSB3. The final elastic displacement demand is 8.7 in. Table 5.2 lists the parameters related to this longitudinal ESA.

5.4.2 ESA in the Transverse Direction

A load of 1% of the tributary weight of the bent was used for the (transverse) pushover analysis. The same acceleration response spectrum (ARS) was used in the transverse ESA.

The elastic displacement demand was found to be 8.4 in (Table 5.1) in the transverse ESA. Table 5.3 lists the parameters related to this transverse ESA.

Table 5.1. ESA Result for OSB3

Parameter	Longitudinal Direction	Transverse Direction
Displacement Demand (in)	8.7	8.4

Table 5.2. Longitudinal ESA Parameters for OSB3

Parameter	Value
Total weight calculated (kip)	4,341.18
Total mass calculated (kip-sec^2/in)	11.23
Pushover load specified (kip)	217.06
Displacement due to pushover (in)	0.742
Calculated stiffness (kip/in)	292.7
Calculated period (sec)	1.2

Table 5.3. Transverse ESA Parameters for OSB3

Parameter	Value
Tributary weight calculated (kip)	1,999
Tributary mass calculated (kip-sec^2/in)	5.17
Pushover load specified (kip)	20
Displacement due to pushover (in)	0.139
Calculated stiffness (kip/in)	143.75
Calculated period (sec)	1.19

5.5 Nonlinear Time History Analysis

Nonlinear Time History Analysis (THA) was conducted for the 50 input motions provided by Caltrans (see Appendix B for the characteristics of the 50 motions). The input motions were applied directly at the column base as well as both abutments.

Rayleigh damping was used with a 5% damping ratio (defined at periods of 0.2 and 2.3 second) in the nonlinear THA. For the time integration scheme, the Newmark's average acceleration method ($\gamma = 0.5$ and $\beta = 0.25$) was employed.

In OpenSees, the variable time-stepping scheme was used in the analysis. The starting value for each time step was 0.005 second (same as the time step of the input motions) and the minimum time step was 5×10^{-5} second (upon splitting of time step).

5.5.1 Maximum Displacement and Acceleration

Table 5.4 lists OSB3 deck maximum displacement for the 50 motions from the OpenSees nonlinear THA. Note that the Roller with Isolation Bearings and EPP-Gap with Isolation Bearings models gave the same maximum longitudinal displacement when the displacement is around 9 inches or less (Table 5.4). This is because the specified longitudinal gap is 9 inches in the EPP-Gap abutment model. As such, both OSB3 models (Roller with Isolation Bearings and EPP-Gap with Isolation Bearings) essentially behave in the same way under longitudinal loading, when the gap is not closed.

As mentioned earlier, the EPP-Gap with Isolation Bearings model was simulated in CSiBridge. Table 5.5 lists the deck maximum displacement from the OpenSees and CSiBridge analyses. The maximum displacement comparison of Table 5.5 is also presented in Bar Chart graphical form in Figures 5.6-5.9.

Table 5.6 displays OSB3 deck maximum acceleration from OpenSees nonlinear THA. For the EPP-Gap abutment model, Table 5.7 lists the deck maximum acceleration from the OpenSees and CSiBridge analyses. The maximum acceleration comparison of Table 5.7 is also presented in Bar Chart graphical form in Figures 5.10-5.13. As mentioned earlier in Chapter 1, viscous damping abutment forces are only present in the CSiBridge simulation. This difference in the abutment exerted forces accounts partially for the discrepancy (Table 5.7) in the CSiBridge and OpenSees maximum displacement estimates.

For the OpenSees model, the maximum displacements of Table 5.4 are also shown in graphical form against Peak Ground Acceleration (PGA) in Figure 5.14-Figure 5.17.The maximum acceleration is also shown graphically against PGA in in Figure 5.18-Figure 5.21.

Note that P-Delta was not considered in CSiBridge analysis for OSB3 (but P-Delta was considered in OpenSees analysis). Generally, inclusion of P-Delta effects in CSiBridge resulted in relatively small differences in the output.

Table 5.4. OSB3 Deck Maximum Displacement (OpenSees)
(The ESA longitudinal displacement demands are 8.7 in for
Roller with Isolation Bearings, and EPP-Gap with Isolation Bearings models)

Motion	Longitudinal Input	Transverse Input	Longitudinal Displacement (in)		Transverse Displacement (in)	
			Roller with Isolation Bearings	EPP-Gap with Isolation Bearings	Roller with Isolation Bearings	EPP-Gap with Isolation Bearings
1	ROCKS1N1 (0.7g)	-	10.6	9.6	-	-
2	ROCKS1N2 (0.38g)	-	8.8	8.8	-	-
3	ROCKS1N3 (0.32g)	-	6.8	6.8	-	-
4	ROCKS1N4 (0.34g)	-	11.6	9.9	-	-
5	ROCKS1N5 (0.53g)	-	6.4	6.4	-	-
6	ROCKS1N6 (0.42g)	-	7.7	7.7	-	-
7	ROCKS1N7 (0.36g)	-	9.4	9.3	-	-
8	ROCKS1P1 (0.71g)	-	12.0	10.3	-	-
9	ROCKS1P2 (0.44g)	-	8.9	8.9	-	-
10	ROCKS1P3 (0.48g)	-	8.3	8.3	-	-
11	ROCKS1P4 (0.32g)	-	10.2	9.6	-	-
12	ROCKS1P5 (0.67g)	-	9.1	9.1	-	-
13	ROCKS1P6 (0.41g)	-	7.7	7.7	-	-
14	ROCKS1P7 (0.4g)	-	9.9	9.6	-	-
15	SANDS1N1 (0.61g)	-	17.3	15.5	-	-
16	SANDS1N2 (0.51g)	-	18.4	14.4	-	-
17	SANDS1N3 (0.57g)	-	20.1	13.1	-	-
18	SANDS1N4 (0.96g)	-	17.1	12.4	-	-
19	SANDS1N5 (0.79g)	-	20.8	17.6	-	-
20	SANDS1N6 (0.67g)	-	18.7	14.6	-	-
21	SANDS1N7 (0.58g)	-	24.8	19.9	-	-
22	ROCKN1N1N (0.4g)	ROCKN1N1P (0.58g)	7.8	7.8	15.5	9.1
23	ROCKN1P1N (1.42g)	ROCKN1P1P (1.42g)	4.9	4.9	4.9	5.1
24	SANDN1N1N (0.78g)	SANDN1N1P (0.81g)	18.1	15.6	13.3	13.2
25	CLAYN1N1N (0.79g)	CLAYN1N1P (0.71g)	28.5	18.7	28.2	22.8
26	-	ROCKS1N1 (0.7g)	-	-	10.6	9.6
27	-	ROCKS1N2 (0.38g)	-	-	8.8	5.3
28	-	ROCKS1N3 (0.32g)	-	-	6.8	5.9
29	-	ROCKS1N4 (0.34g)	-	-	11.6	8.3
30	-	ROCKS1N5 (0.53g)	-	-	6.4	6.3
31	-	ROCKS1N6 (0.42g)	-	-	7.7	6.1
32	-	ROCKS1N7 (0.36g)	-	-	9.4	8.2
33	-	ROCKS1P1 (0.71g)	-	-	12.0	10.9
34	-	ROCKS1P2 (0.44g)	-	-	8.9	5.9
35	-	ROCKS1P3 (0.48g)	-	-	8.3	7.5
36	-	ROCKS1P4 (0.32g)	-	-	10.2	8.6
37	-	ROCKS1P5 (0.67g)	-	-	9.1	5.9
38	-	ROCKS1P6 (0.41g)	-	-	7.7	6.1
39	-	ROCKS1P7 (0.4g)	-	-	9.9	8.4
40	-	SANDS1N1 (0.61g)	-	-	17.3	17.2
41	-	SANDS1N2 (0.51g)	-	-	18.4	14.6
42	-	SANDS1N3 (0.57g)	-	-	20.1	18.0
43	-	SANDS1N4 (0.96g)	-	-	17.1	14.3
44	-	SANDS1N5 (0.79g)	-	-	20.8	20.1
45	-	SANDS1N6 (0.67g)	-	-	18.7	15.8
46	-	SANDS1N7 (0.58g)	-	-	24.8	24.6
47	ROCKN1N1P (0.58g)	ROCKN1N1N (0.4g)	15.5	12.1	7.8	6.1
48	ROCKN1P1P (1.42g)	ROCKN1P1N (1.42g)	4.9	4.9	4.9	5.1
49	SANDN1N1P (0.81g)	SANDN1N1N (0.78g)	13.3	11.4	18.1	18.5
50	CLAYN1N1P (0.71g)	CLAYN1N1N (0.79g)	28.2	16.8	28.6	25.0

Table 5.5. OSB3 Deck Maximum Displacement for EPP-Gap with Bearings Model (Comparison of OpenSees and CSiBridge)

(The ESA longitudinal displacement demand is 8.7 in while the ESA transverse displacement demands is 8.4; Difference is relative to OpenSees result)

Motion	Longitudinal Input	Transverse Input	Longitudinal Displacement (in)			Transverse Displacement (in)		
			OpenSees	CSiBridge	Difference	OpenSees	CSiBridge	Difference
1	ROCKS1N1 (0.7g)	-	9.6	9.4	-2%	-	-	-
2	ROCKS1N2 (0.38g)	-	8.8	9.4	7%	-	-	-
3	ROCKS1N3 (0.32g)	-	6.8	8.2	21%	-	-	-
4	ROCKS1N4 (0.34g)	-	9.9	10.3	4%	-	-	-
5	ROCKS1N5 (0.53g)	-	6.4	9.3	45%	-	-	-
6	ROCKS1N6 (0.42g)	-	7.7	8.5	10%	-	-	-
7	ROCKS1N7 (0.36g)	-	9.3	10.6	14%	-	-	-
8	ROCKS1P1 (0.71g)	-	10.3	10	-3%	-	-	-
9	ROCKS1P2 (0.44g)	-	8.9	8.5	-4%	-	-	-
10	ROCKS1P3 (0.48g)	-	8.3	8.5	2%	-	-	-
11	ROCKS1P4 (0.32g)	-	9.6	9.8	2%	-	-	-
12	ROCKS1P5 (0.67g)	-	9.1	9.1	0%	-	-	-
13	ROCKS1P6 (0.41g)	-	7.7	8.3	8%	-	-	-
14	ROCKS1P7 (0.4g)	-	9.6	7.9	-18%	-	-	-
15	SANDS1N1 (0.61g)	-	15.5	9.9	-36%	-	-	-
16	SANDS1N2 (0.51g)	-	14.4	9.4	-35%	-	-	-
17	SANDS1N3 (0.57g)	-	13.1	9.5	-27%	-	-	-
18	SANDS1N4 (0.96g)	-	12.4	12.4	0%	-	-	-
19	SANDS1N5 (0.79g)	-	17.6	17.2	-2%	-	-	-
20	SANDS1N6 (0.67g)	-	14.6	11	-25%	-	-	-
21	SANDS1N7 (0.58g)	-	19.9	13.4	-33%	-	-	-
22	ROCKN1N1N (0.4g)	ROCKN1N1P (0.58g)	7.8	8.4	8%	9.1	11.5	26%
23	ROCKN1P1N (1.42g)	ROCKN1P1P (1.42g)	4.9	4.3	-12%	5.1	4.9	-4%
24	SANDN1N1N (0.78g)	SANDN1N1P (0.81g)	15.6	14.4	-8%	13.2	8.8	-33%
25	CLAYN1N1N (0.79g)	CLAYN1N1P (0.71g)	18.7	12	-36%	22.8	16.8	-26%
26	-	ROCKS1N1 (0.7g)	-	-	-	9.6	8.5	-11%
27	-	ROCKS1N2 (0.38g)	-	-	-	5.3	4.9	-8%
28	-	ROCKS1N3 (0.32g)	-	-	-	5.9	5.4	-8%
29	-	ROCKS1N4 (0.34g)	-	-	-	8.3	6.9	-17%
30	-	ROCKS1N5 (0.53g)	-	-	-	6.3	6.6	5%
31	-	ROCKS1N6 (0.42g)	-	-	-	6.1	5.1	-16%
32	-	ROCKS1N7 (0.36g)	-	-	-	8.2	6	-27%
33	-	ROCKS1P1 (0.71g)	-	-	-	10.9	9.4	-14%
34	-	ROCKS1P2 (0.44g)	-	-	-	5.9	4.7	-20%
35	-	ROCKS1P3 (0.48g)	-	-	-	7.5	8.4	12%
36	-	ROCKS1P4 (0.32g)	-	-	-	8.6	7.1	-17%
37	-	ROCKS1P5 (0.67g)	-	-	-	5.9	6.1	3%
38	-	ROCKS1P6 (0.41g)	-	-	-	6.1	5	-18%
39	-	ROCKS1P7 (0.4g)	-	-	-	8.4	7.9	-6%
40	-	SANDS1N1 (0.61g)	-	-	-	17.2	15.4	-10%
41	-	SANDS1N2 (0.51g)	-	-	-	14.6	14.1	-3%
42	-	SANDS1N3 (0.57g)	-	-	-	18	14.6	-19%
43	-	SANDS1N4 (0.96g)	-	-	-	14.3	15.1	6%
44	-	SANDS1N5 (0.79g)	-	-	-	20.1	15.9	-21%
45	-	SANDS1N6 (0.67g)	-	-	-	15.8	11.3	-28%
46	-	SANDS1N7 (0.58g)	-	-	-	24.6	20	-19%
47	ROCKN1N1P (0.58g)	ROCKN1N1N (0.4g)	12.1	9.9	-18%	6.1	6.6	8%
48	ROCKN1P1P (1.42g)	ROCKN1P1N (1.42g)	4.9	4.3	-12%	5.1	4.9	-4%
49	SANDN1N1P (0.81g)	SANDN1N1N (0.78g)	11.4	8.1	-29%	18.5	12.4	-33%
50	CLAYN1N1P (0.71g)	CLAYN1N1N (0.79g)	16.8	14.5	-14%	25	21.2	-15%

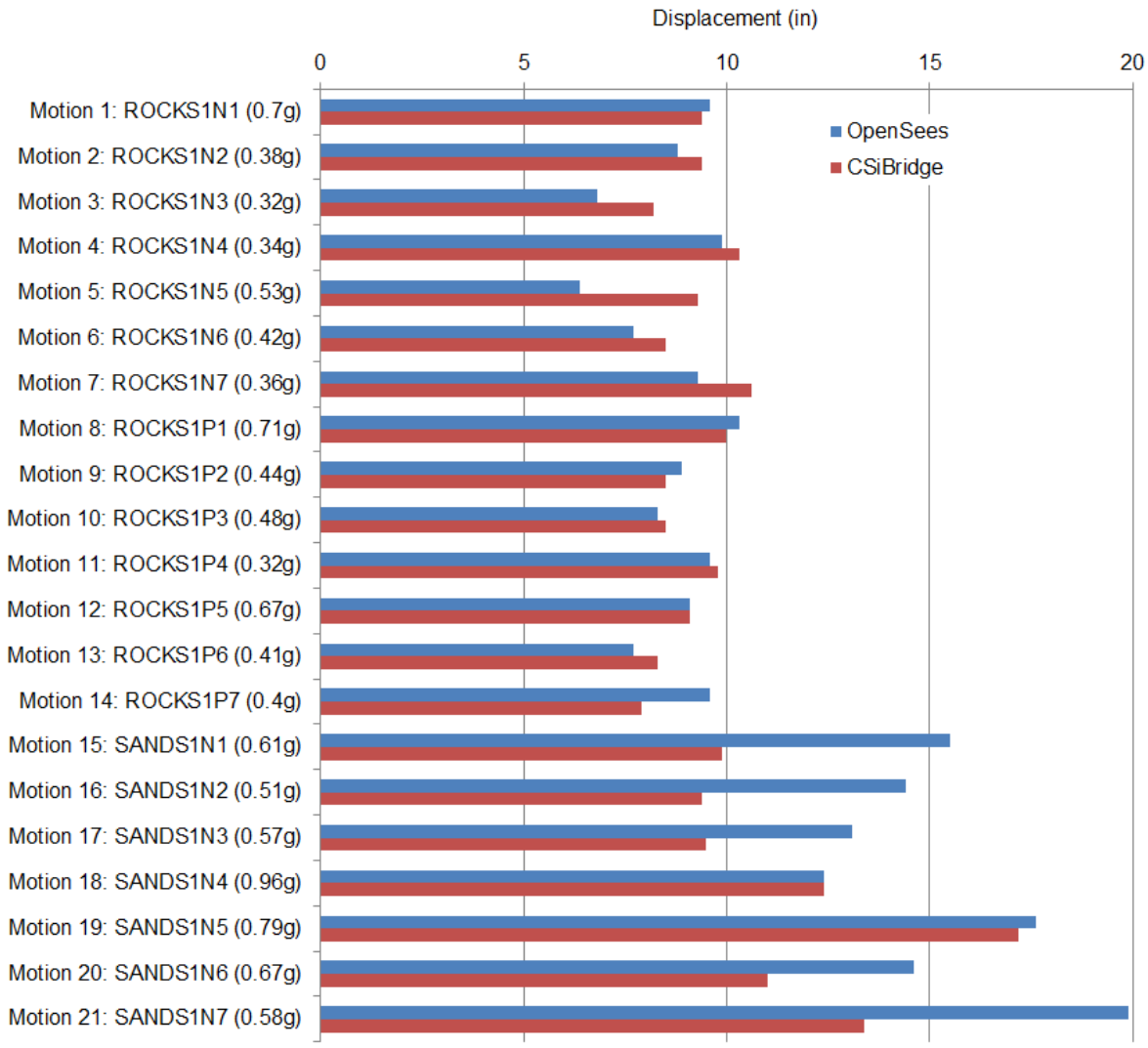

Figure 5.6 OSB3 deck maximum longitudinal displacement for Motions 1-21 (EPP-Gap with Isolation Bearings model)

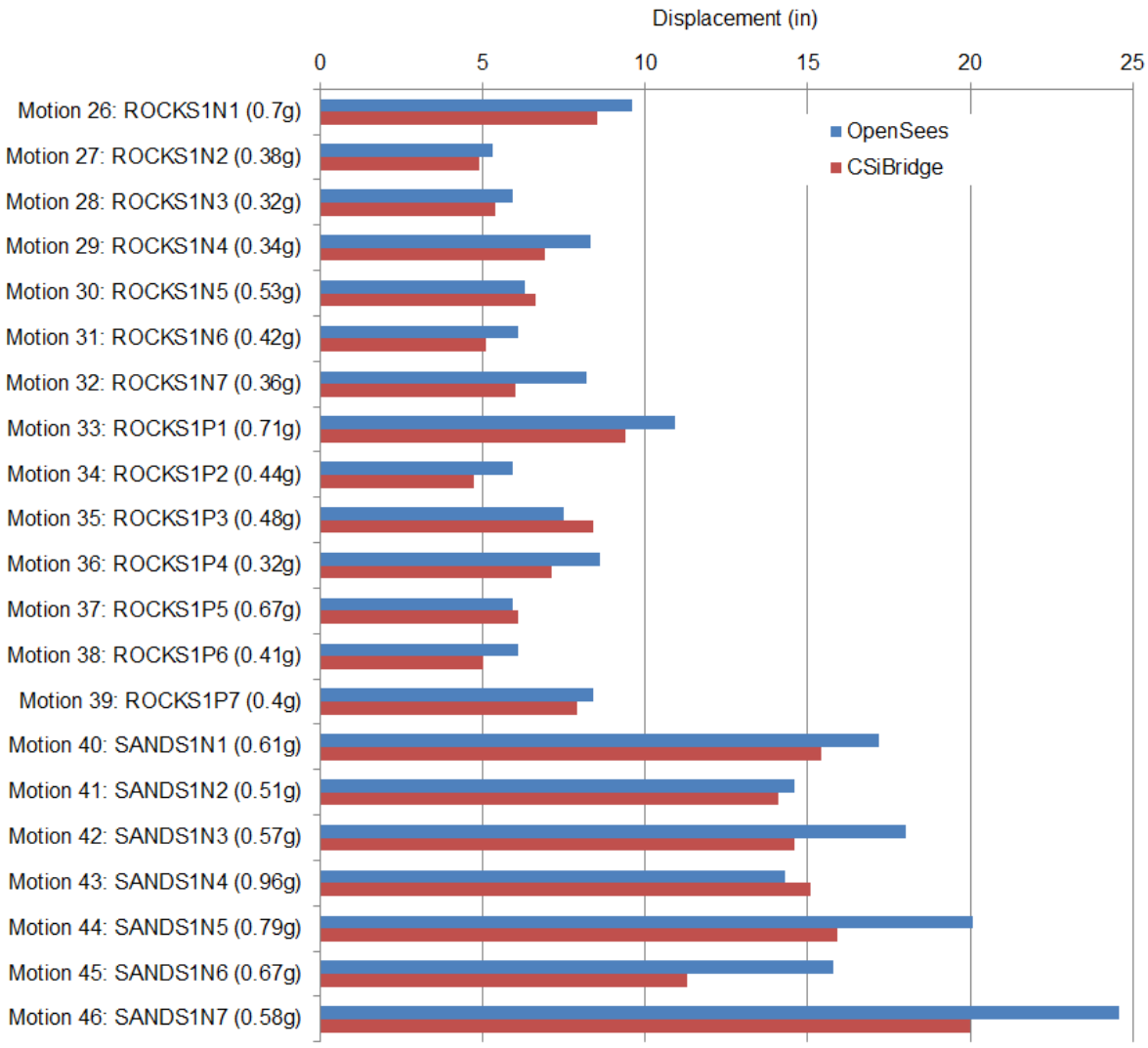

Figure 5.7 OSB3 deck maximum transverse displacement for Motions 26-46 (EPP-Gap with Isolation Bearings model)

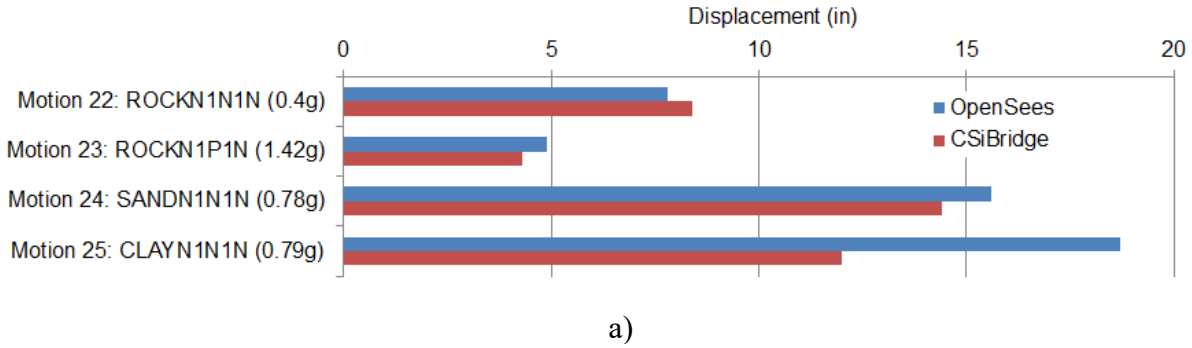

a)

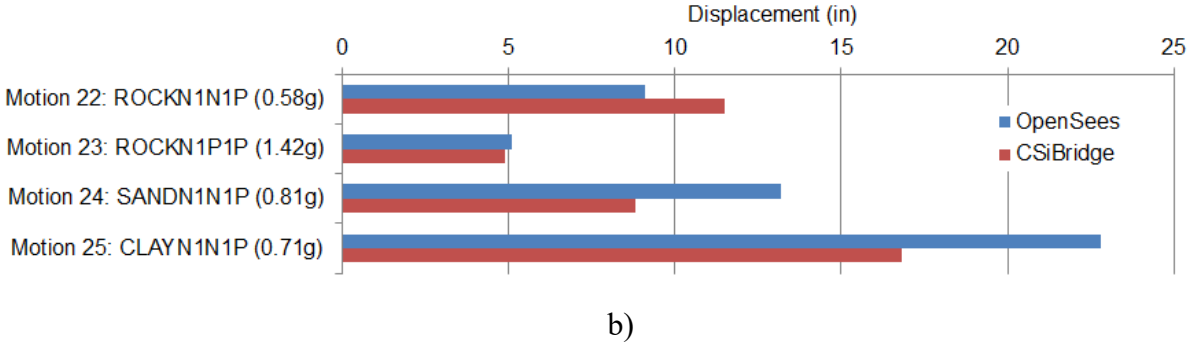

b)

Figure 5.8 OSB3 deck maximum displacement for Motions 22-25 (EPP-Gap with Isolation Bearings model): a) Lonitudinal direction; b) Transverse direction

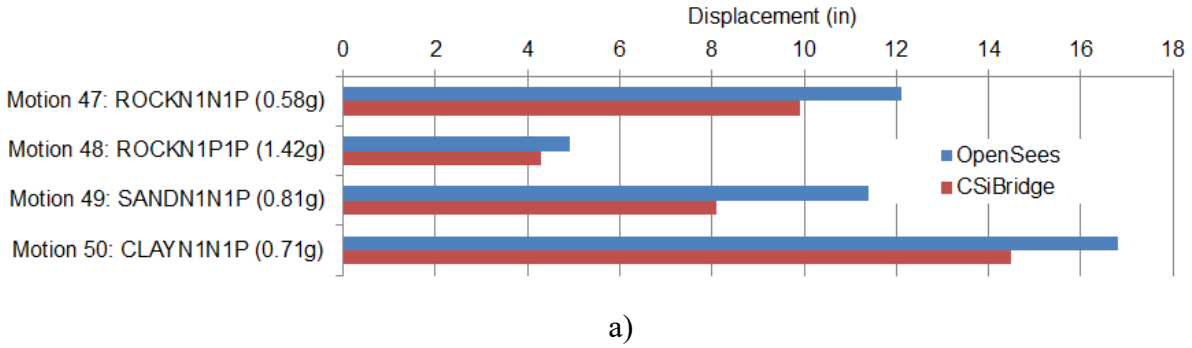

a)

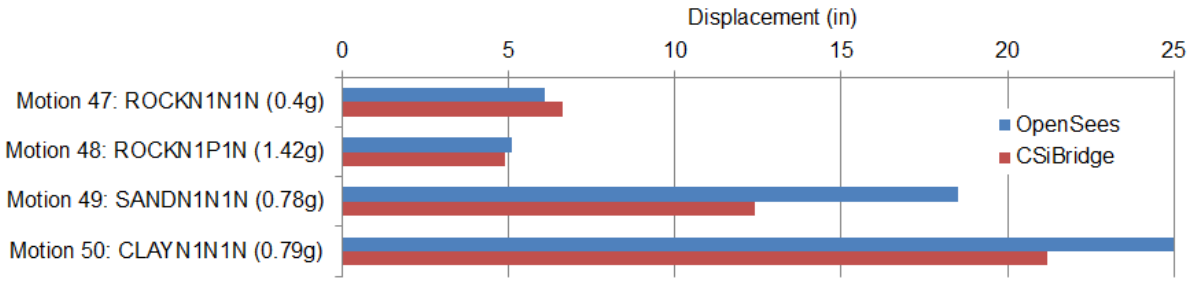

b)

Figure 5.9 OSB3 deck maximum displacement for Motions 47-50 (EPP-Gap with Isolation Bearings model): a) Lonitudinal direction; b) Transverse direction

Table 5.6. OSB3 Deck Maximum Acceleration (OpenSees)

Motion	Longitudinal Input	Transverse Input	Longitudinal Acceleration (g)		Transverse Acceleration (g)	
			Roller with Isolation Bearings	EPP-Gap with Isolation Bearings	Roller with Isolation Bearings	EPP-Gap with Isolation Bearings
1	ROCKS1N1 (0.7g)	-	0.80	0.82	-	-
2	ROCKS1N2 (0.38g)	-	0.39	0.39	-	-
3	ROCKS1N3 (0.32g)	-	0.40	0.40	-	-
4	ROCKS1N4 (0.34g)	-	0.40	0.83	-	-
5	ROCKS1N5 (0.53g)	-	0.63	0.63	-	-
6	ROCKS1N6 (0.42g)	-	0.55	0.55	-	-
7	ROCKS1N7 (0.36g)	-	0.45	0.46	-	-
8	ROCKS1P1 (0.71g)	-	0.83	1.18	-	-
9	ROCKS1P2 (0.44g)	-	0.45	0.45	-	-
10	ROCKS1P3 (0.48g)	-	0.62	0.62	-	-
11	ROCKS1P4 (0.32g)	-	0.47	0.68	-	-
12	ROCKS1P5 (0.67g)	-	0.82	0.82	-	-
13	ROCKS1P6 (0.41g)	-	0.55	0.55	-	-
14	ROCKS1P7 (0.4g)	-	0.43	0.71	-	-
15	SANDS1N1 (0.61g)	-	0.65	1.42	-	-
16	SANDS1N2 (0.51g)	-	0.61	1.44	-	-
17	SANDS1N3 (0.57g)	-	0.69	1.36	-	-
18	SANDS1N4 (0.96g)	-	1.01	1.28	-	-
19	SANDS1N5 (0.79g)	-	1.11	1.56	-	-
20	SANDS1N6 (0.67g)	-	0.75	1.43	-	-
21	SANDS1N7 (0.58g)	-	0.66	2.18	-	-
22	ROCKN1N1N (0.4g)	ROCKN1N1P (0.58g)	0.53	0.53	0.75	0.75
23	ROCKN1P1N (1.42g)	ROCKN1P1P (1.42g)	2.10	2.11	2.10	2.09
24	SANDN1N1N (0.78g)	SANDN1N1P (0.81g)	1.31	1.40	1.35	1.35
25	CLAYN1N1N (0.79g)	CLAYN1N1P (0.71g)	1.63	1.95	1.28	1.27
26	-	ROCKS1N1 (0.7g)	-	-	0.80	0.86
27	-	ROCKS1N2 (0.38g)	-	-	0.39	0.44
28	-	ROCKS1N3 (0.32g)	-	-	0.40	0.39
29	-	ROCKS1N4 (0.34g)	-	-	0.40	0.41
30	-	ROCKS1N5 (0.53g)	-	-	0.63	0.66
31	-	ROCKS1N6 (0.42g)	-	-	0.55	0.53
32	-	ROCKS1N7 (0.36g)	-	-	0.45	0.42
33	-	ROCKS1P1 (0.71g)	-	-	0.82	0.82
34	-	ROCKS1P2 (0.44g)	-	-	0.45	0.46
35	-	ROCKS1P3 (0.48g)	-	-	0.62	0.69
36	-	ROCKS1P4 (0.32g)	-	-	0.47	0.41
37	-	ROCKS1P5 (0.67g)	-	-	0.82	0.84
38	-	ROCKS1P6 (0.41g)	-	-	0.55	0.53
39	-	ROCKS1P7 (0.4g)	-	-	0.43	0.47
40	-	SANDS1N1 (0.61g)	-	-	0.65	0.71
41	-	SANDS1N2 (0.51g)	-	-	0.61	0.55
42	-	SANDS1N3 (0.57g)	-	-	0.69	0.67
43	-	SANDS1N4 (0.96g)	-	-	1.00	1.00
44	-	SANDS1N5 (0.79g)	-	-	1.11	1.07
45	-	SANDS1N6 (0.67g)	-	-	0.75	0.72
46	-	SANDS1N7 (0.58g)	-	-	0.66	0.68
47	ROCKN1N1P (0.58g)	ROCKN1N1N (0.4g)	0.75	1.39	0.54	0.52
48	ROCKN1P1P (1.42g)	ROCKN1P1N (1.42g)	2.10	2.11	2.10	2.09
49	SANDN1N1P (0.81g)	SANDN1N1N (0.78g)	1.35	1.35	1.31	1.36
50	CLAYN1N1P (0.71g)	CLAYN1N1N (0.79g)	1.28	1.45	1.63	1.54

Table 5.7. OSB3 Deck Maximum Acceleration for EPP-Gap with Bearings Model (Comparison of OpenSees and CSiBridge)

Motion	Longitudinal Input	Transverse Input	Longitudinal Acceleration (g)			Transverse Acceleration (g)		
			OpenSees	CSiBridge	Difference	OpenSees	CSiBridge	Difference
1	ROCKS1N1 (0.7g)	-	0.82	0.58	-29%	-	-	-
2	ROCKS1N2 (0.38g)	-	0.39	0.58	49%	-	-	-
3	ROCKS1N3 (0.32g)	-	0.4	0.47	18%	-	-	-
4	ROCKS1N4 (0.34g)	-	0.83	0.63	-24%	-	-	-
5	ROCKS1N5 (0.53g)	-	0.63	0.56	-11%	-	-	-
6	ROCKS1N6 (0.42g)	-	0.55	0.5	-9%	-	-	-
7	ROCKS1N7 (0.36g)	-	0.46	0.64	39%	-	-	-
8	ROCKS1P1 (0.71g)	-	1.18	0.62	-47%	-	-	-
9	ROCKS1P2 (0.44g)	-	0.45	0.44	-2%	-	-	-
10	ROCKS1P3 (0.48g)	-	0.62	0.54	-13%	-	-	-
11	ROCKS1P4 (0.32g)	-	0.68	0.61	-10%	-	-	-
12	ROCKS1P5 (0.67g)	-	0.82	0.49	-40%	-	-	-
13	ROCKS1P6 (0.41g)	-	0.55	0.48	-13%	-	-	-
14	ROCKS1P7 (0.4g)	-	0.71	0.38	-46%	-	-	-
15	SANDS1N1 (0.61g)	-	1.42	0.62	-56%	-	-	-
16	SANDS1N2 (0.51g)	-	1.44	0.59	-59%	-	-	-
17	SANDS1N3 (0.57g)	-	1.36	0.62	-54%	-	-	-
18	SANDS1N4 (0.96g)	-	1.28	0.66	-48%	-	-	-
19	SANDS1N5 (0.79g)	-	1.56	0.73	-53%	-	-	-
20	SANDS1N6 (0.67g)	-	1.43	0.64	-55%	-	-	-
21	SANDS1N7 (0.58g)	-	2.18	0.67	-69%	-	-	-
22	ROCKN1N1N (0.4g)	ROCKN1N1P (0.58g)	0.53	0.53	0%	0.75	0.36	-52%
23	ROCKN1P1N (1.42g)	ROCKN1P1P (1.42g)	2.11	0.13	-94%	2.09	0.23	-89%
24	SANDN1N1N (0.78g)	SANDN1N1P (0.81g)	1.4	0.69	-51%	1.35	0.31	-77%
25	CLAYN1N1N (0.79g)	CLAYN1N1P (0.71g)	1.95	0.64	-67%	1.27	0.4	-69%
26	-	ROCKS1N1 (0.7g)	-	-	-	0.86	0.28	-67%
27	-	ROCKS1N2 (0.38g)	-	-	-	0.44	0.31	-30%
28	-	ROCKS1N3 (0.32g)	-	-	-	0.39	0.28	-28%
29	-	ROCKS1N4 (0.34g)	-	-	-	0.41	0.27	-34%
30	-	ROCKS1N5 (0.53g)	-	-	-	0.66	0.29	-56%
31	-	ROCKS1N6 (0.42g)	-	-	-	0.53	0.27	-49%
32	-	ROCKS1N7 (0.36g)	-	-	-	0.42	0.26	-38%
33	-	ROCKS1P1 (0.71g)	-	-	-	0.82	0.29	-65%
34	-	ROCKS1P2 (0.44g)	-	-	-	0.46	0.36	-22%
35	-	ROCKS1P3 (0.48g)	-	-	-	0.69	0.3	-57%
36	-	ROCKS1P4 (0.32g)	-	-	-	0.41	0.26	-37%
37	-	ROCKS1P5 (0.67g)	-	-	-	0.84	0.37	-56%
38	-	ROCKS1P6 (0.41g)	-	-	-	0.53	0.28	-47%
39	-	ROCKS1P7 (0.4g)	-	-	-	0.47	0.31	-34%
40	-	SANDS1N1 (0.61g)	-	-	-	0.71	0.43	-39%
41	-	SANDS1N2 (0.51g)	-	-	-	0.55	0.37	-33%
42	-	SANDS1N3 (0.57g)	-	-	-	0.67	0.37	-45%
43	-	SANDS1N4 (0.96g)	-	-	-	1	0.42	-58%
44	-	SANDS1N5 (0.79g)	-	-	-	1.07	0.4	-63%
45	-	SANDS1N6 (0.67g)	-	-	-	0.72	0.35	-51%
46	-	SANDS1N7 (0.58g)	-	-	-	0.68	0.45	-34%
47	ROCKN1N1P (0.58g)	ROCKN1N1N (0.4g)	1.39	0.6	-57%	0.52	0.29	-44%
48	ROCKN1P1P (1.42g)	ROCKN1P1N (1.42g)	2.11	0.13	-94%	2.09	0.23	-89%
49	SANDN1N1P (0.81g)	SANDN1N1N (0.78g)	1.35	0.54	-60%	1.36	0.35	-74%
50	CLAYN1N1P (0.71g)	CLAYN1N1N (0.79g)	1.45	0.69	-52%	1.54	0.44	-71%

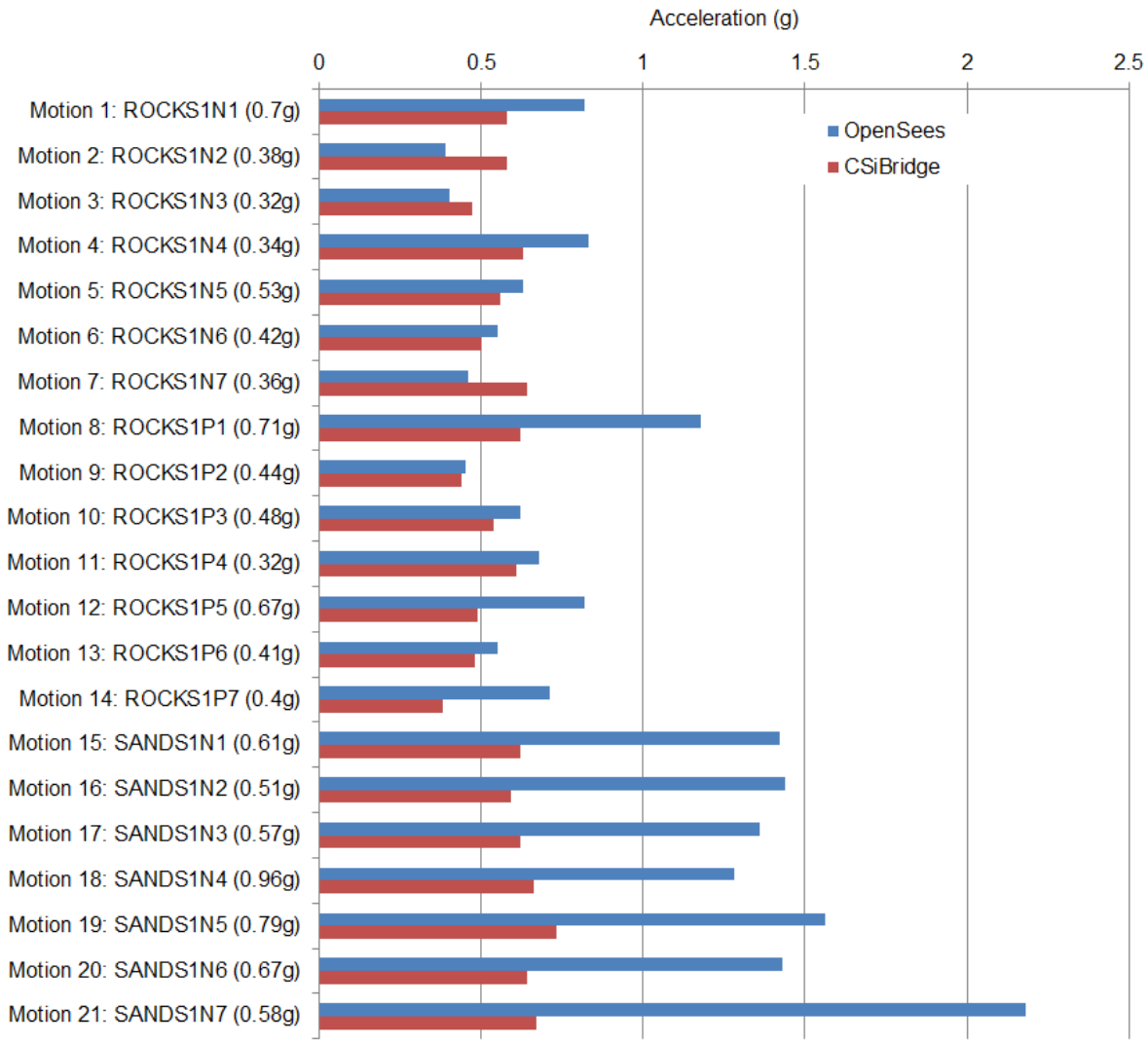

Figure 5.10 OSB3 deck maximum longitudinal acceleration for Motions 1-21 (EPP-Gap with Isolation Bearings model)

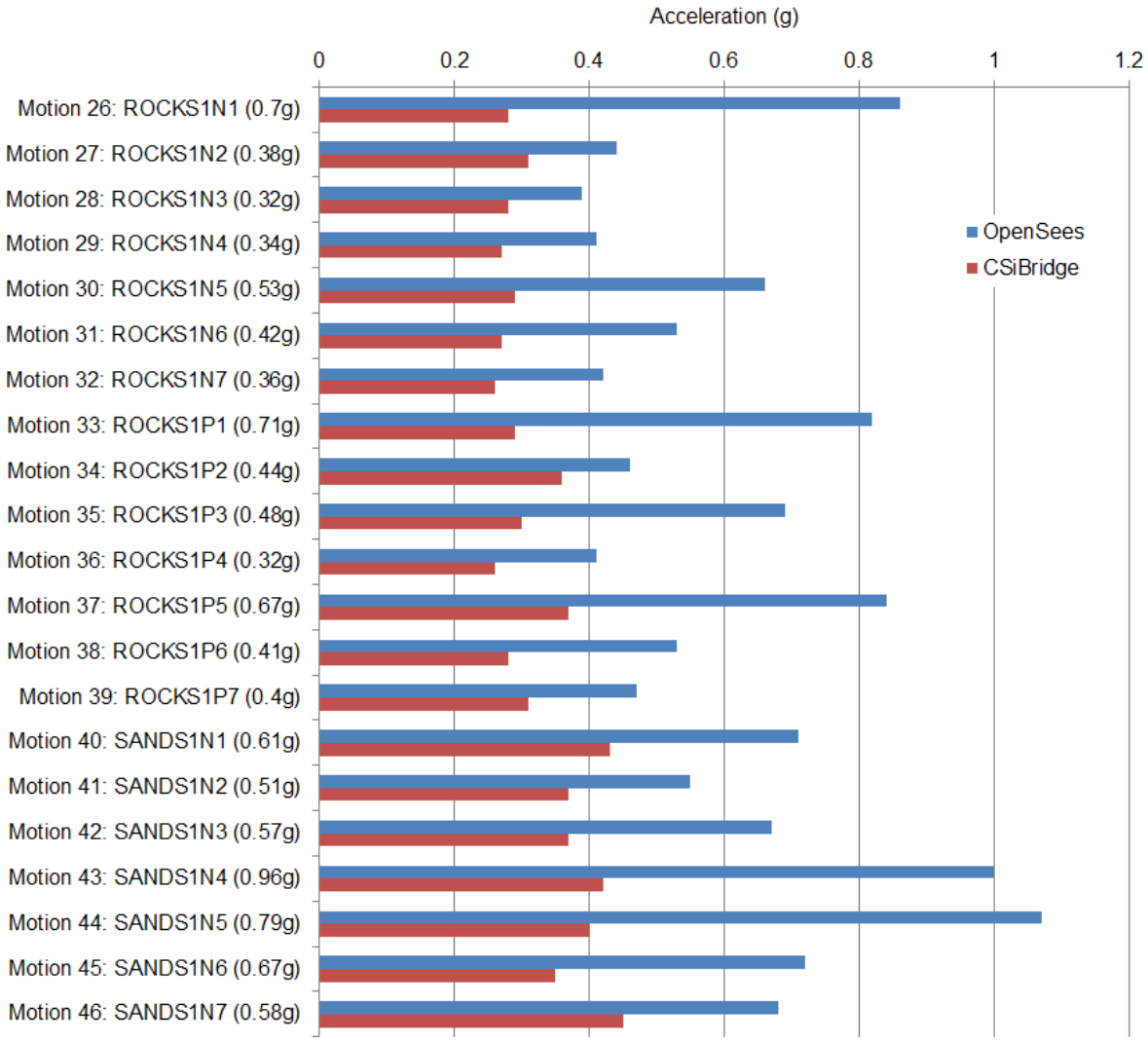

Figure 5.11 OSB3 deck maximum transverse acceleration for Motions 26-46 (EPP-Gap with Isolation Bearings model)

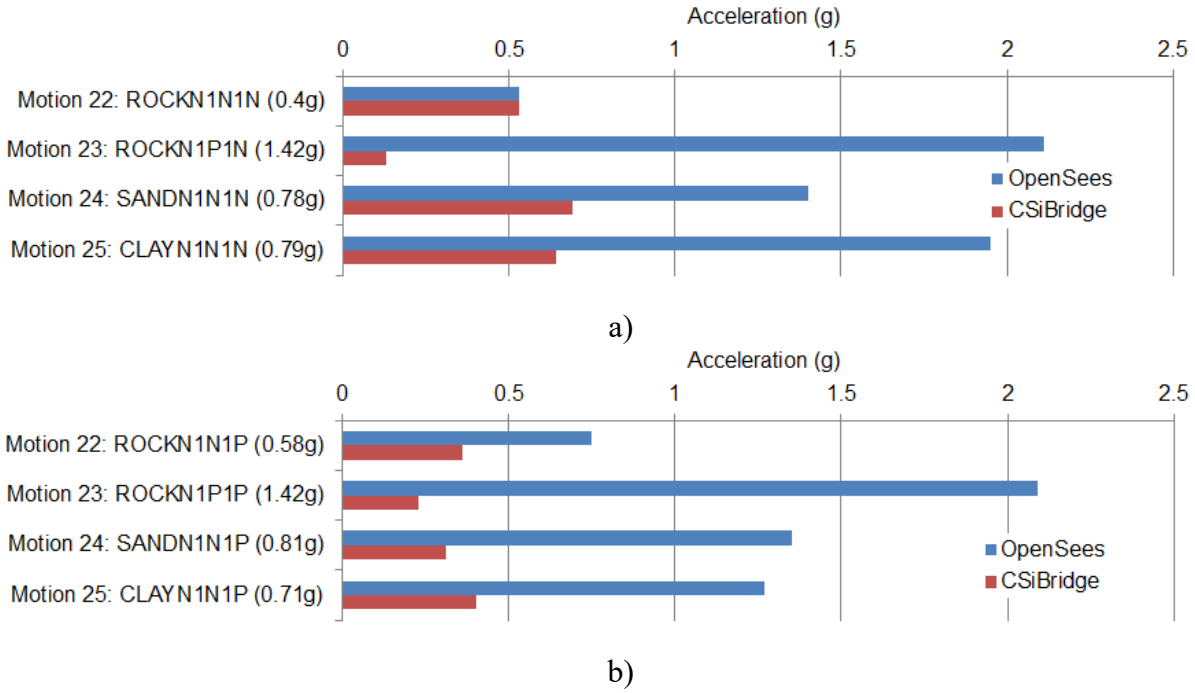

Figure 5.12 OSB3 deck maximum acceleration for Motions 22-25 (EPP-Gap with Isolation Bearings model): a) Lonitudinal direction; b) Transverse direction

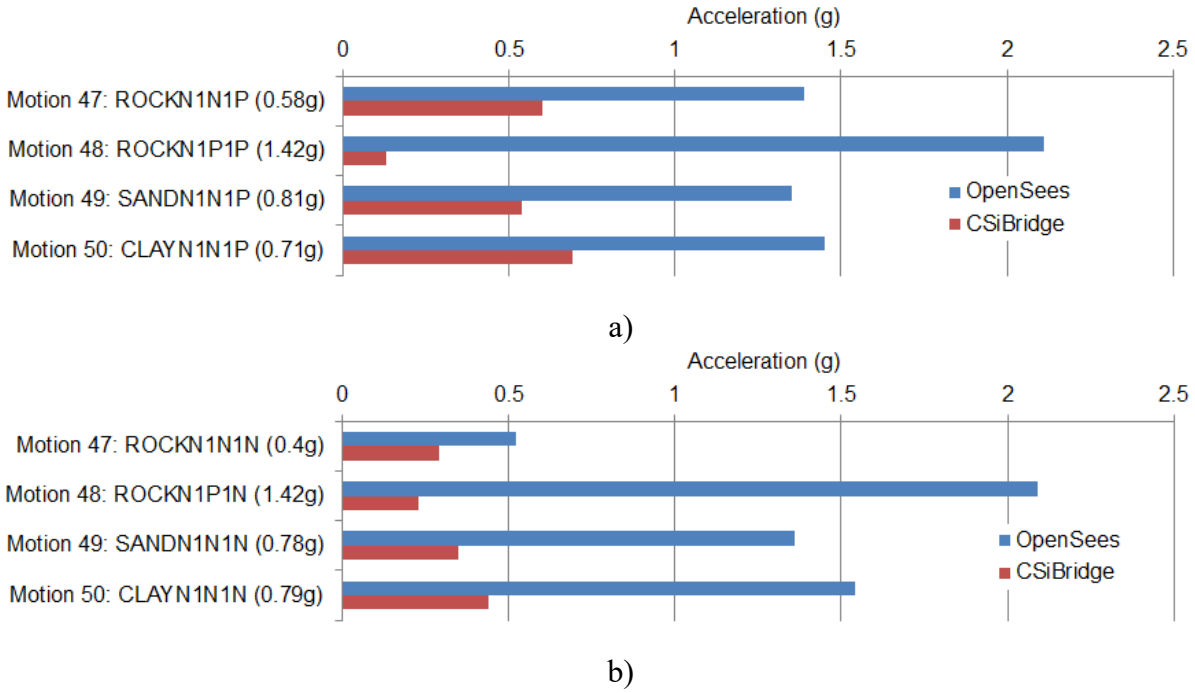

Figure 5.13 OSB3 deck maximum acceleration for Motions 47-50 (EPP-Gap with Isolation Bearings model): a) Lonitudinal direction; b) Transverse direction

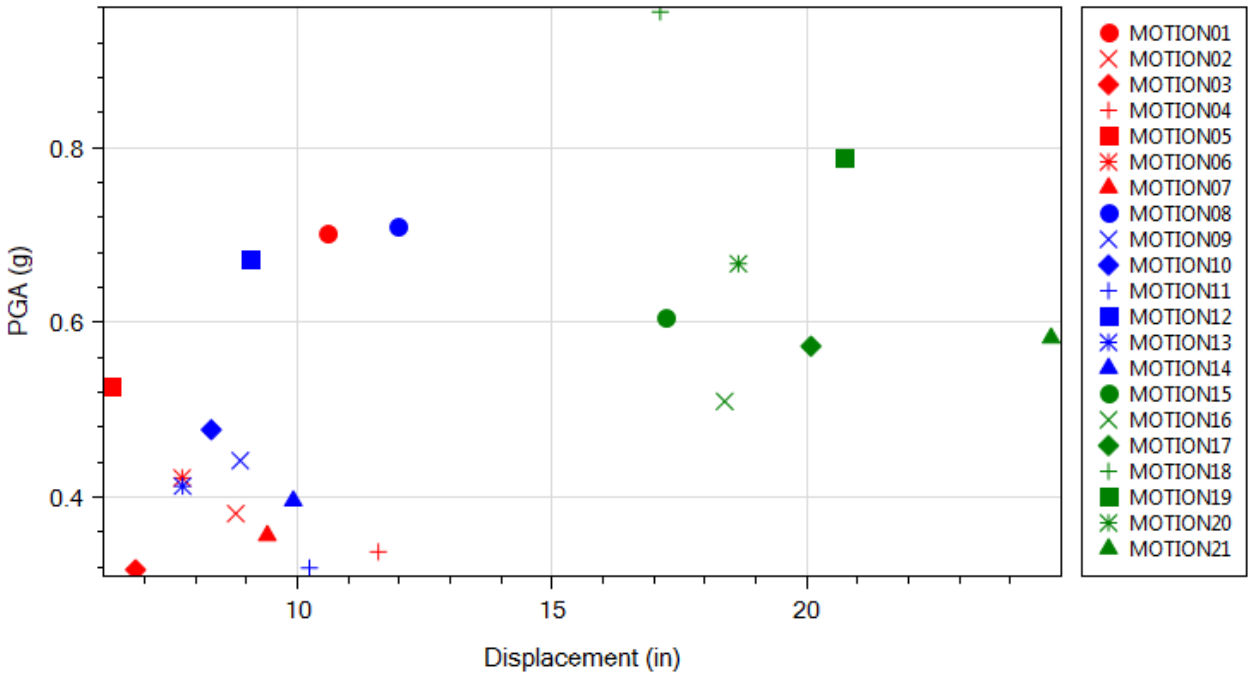

Figure 5.14 OSB3 deck maximum longitudinal displacement in OpenSees (Motions 1-21; Roller with Isolation Bearings model)

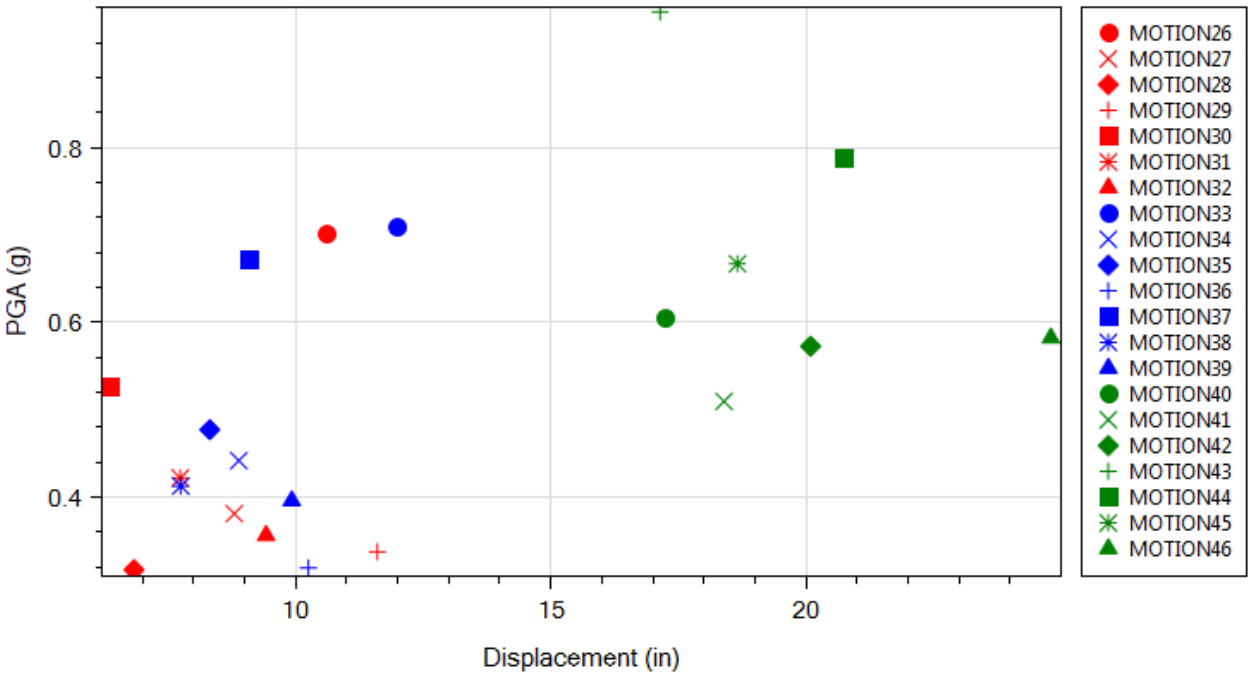

Figure 5.15 OSB3 deck maximum transverse displacement in OpenSees (Motions 26-46; Roller with Isolation Bearings model)

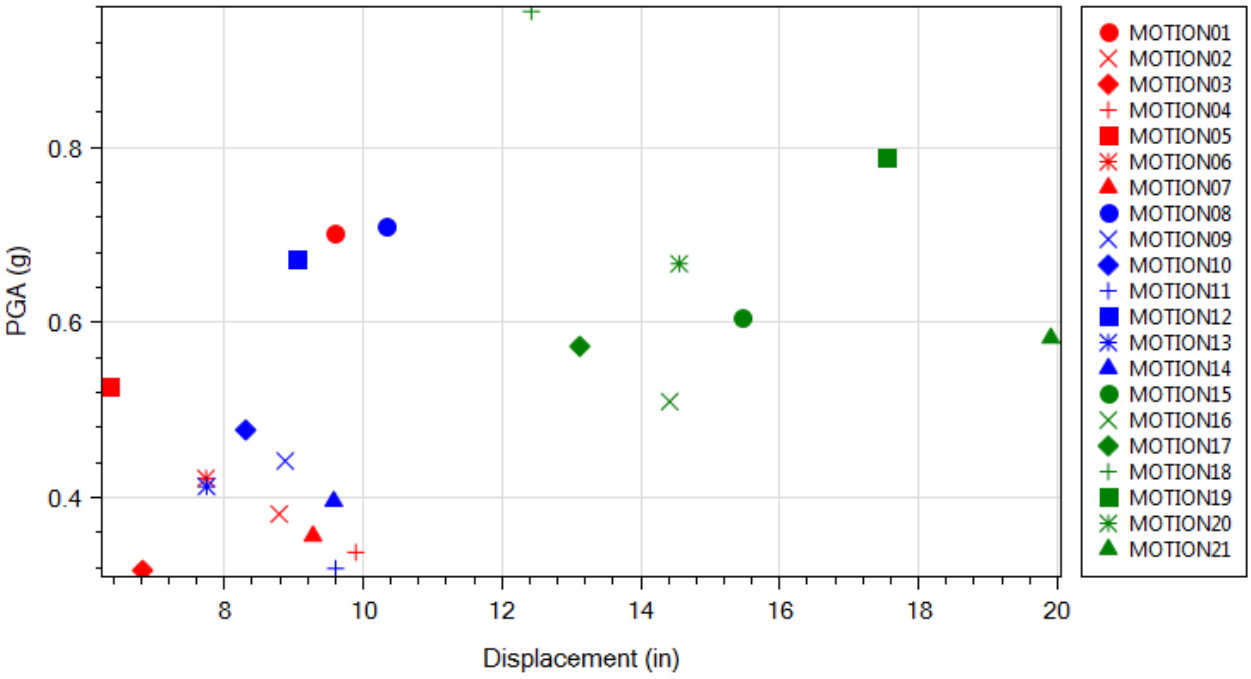

Figure 5.16 OSB3 deck maximum longitudinal displacement in OpenSees (Motions 1-21; EPP-Gap with Isolation Bearings model)

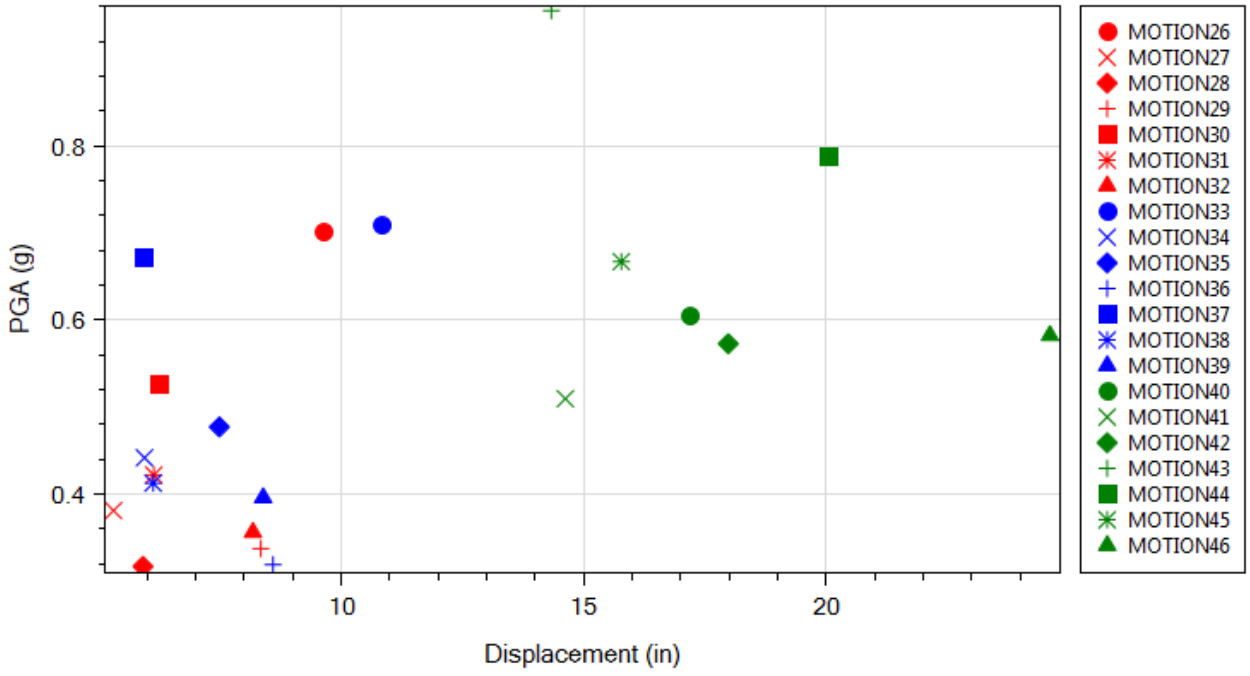

Figure 5.17 OSB3 deck maximum transverse displacement in OpenSees (Motions 26-46; EPP-Gap with Isolation Bearings model)

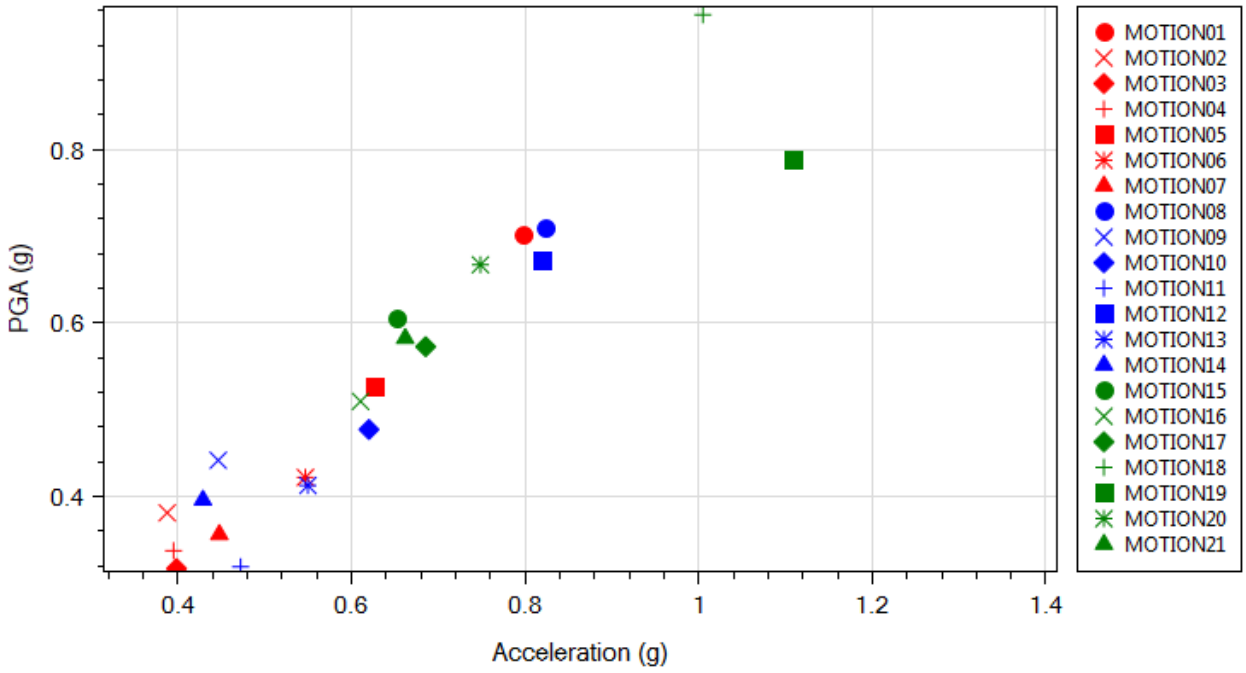

Figure 5.18 OSB3 deck maximum longitudinal acceleration in OpenSees (Motions 1-21; Roller with Isolation Bearings model)

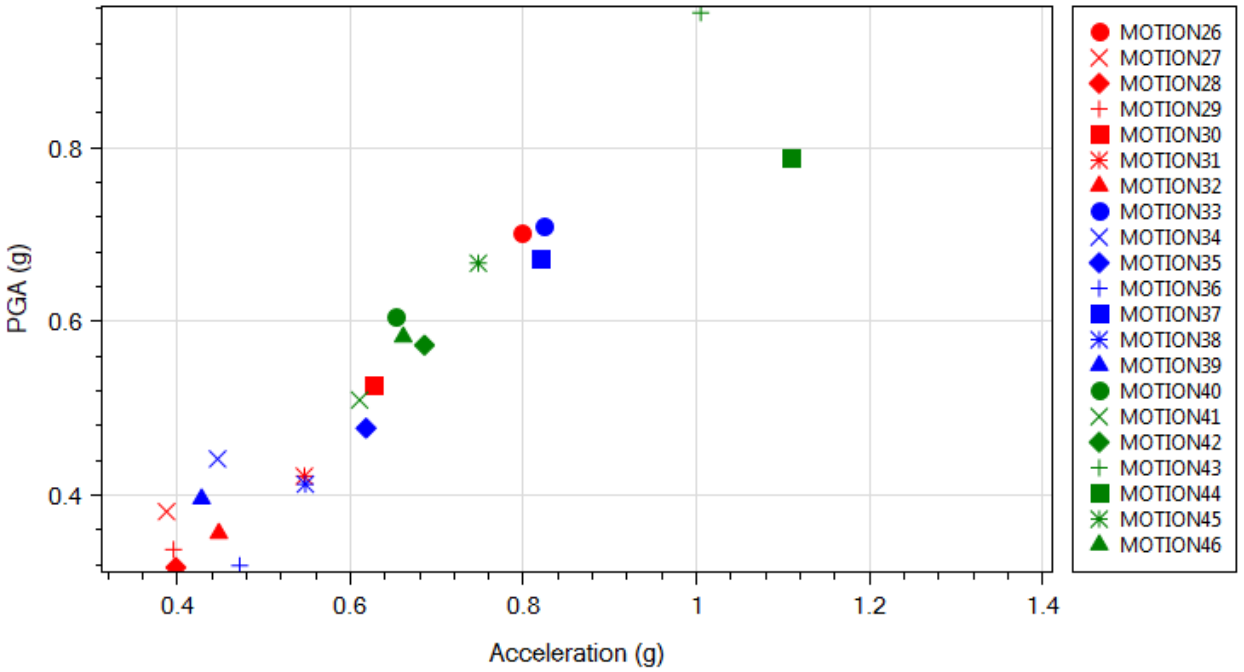

Figure 5.19 OS OSB3 deck maximum transverse acceleration in OpenSees (Motions 26-46; Roller with Isolation Bearings model)

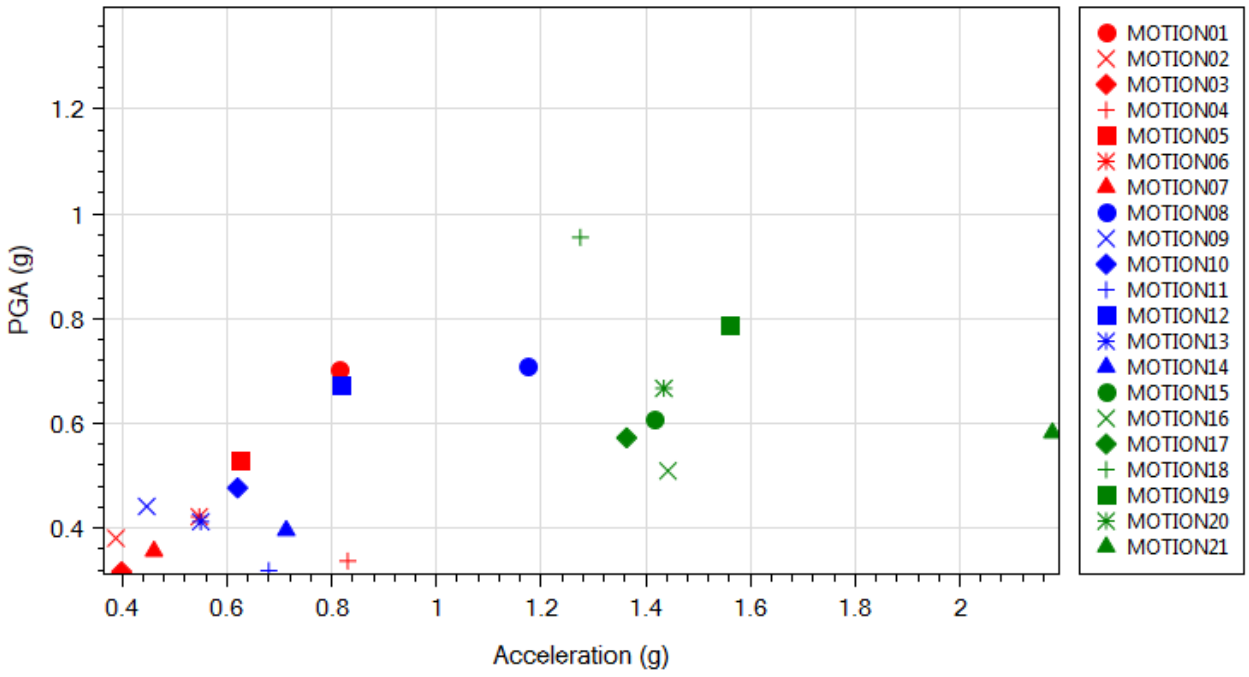

Figure 5.20 OSB3 deck maximum longitudinal acceleration in OpenSees (Motions 1-21; EPP-Gap with Isolation Bearings model)

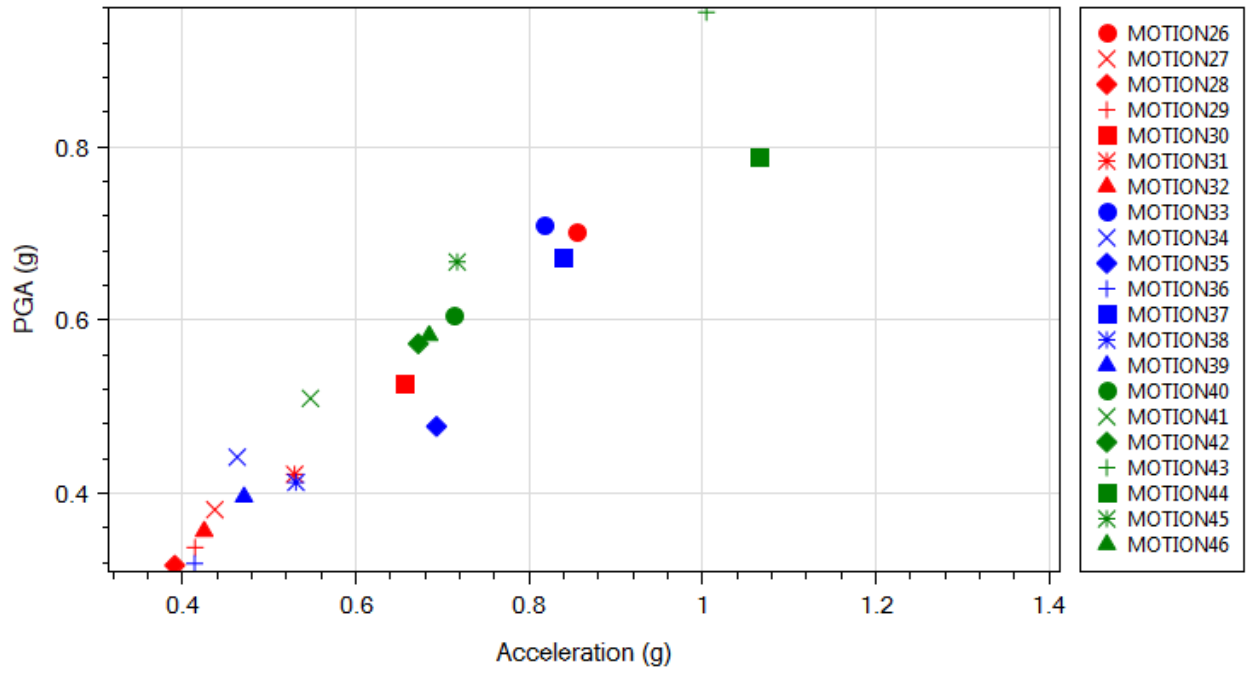

Figure 5.21 OSB3 deck maximum transverse acceleration in OpenSees (Motions 26-46; EPP-Gap with Isolation Bearings model)

5.5.2 Response Time History (OpenSees)

In this section, response time histories from 2 motions (Motions 1 and 15) from OpenSees nonlinear THA are presented (for the EPP-Gap with Isolation Bearings model).

1) Motion 1 ROCKS1N1

For Motion 1, the deck maximum displacement is 11 in (Table 5.4). Figure 5.22 displays OSB3 longitudinal response time history for Motion 1 (ROCKS1N1). The input motion ROCKS1N1 is shown in Figure 5.22d for reference. The column and isolation bearing force-displacement response is displayed in Figure 5.23. Figure 5.24 displays the column top longitudinal moment-curvature response which is essentially linear.

2) Motion 15 SANDS1N1

Figure 5.25 shows OSB3 longitudinal response time history. The column and isolation bearing force-displacement response is displayed in Figure 5.26. Figure 5.27 displays longitudinal moment-curvature response which is also essentially linear.

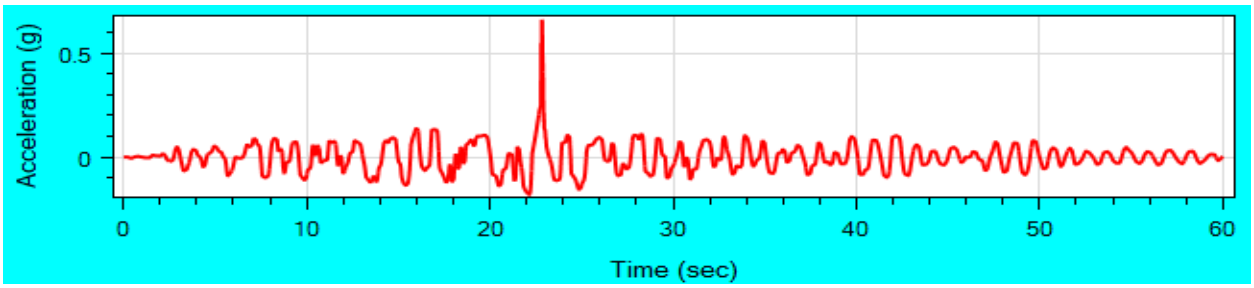

a)

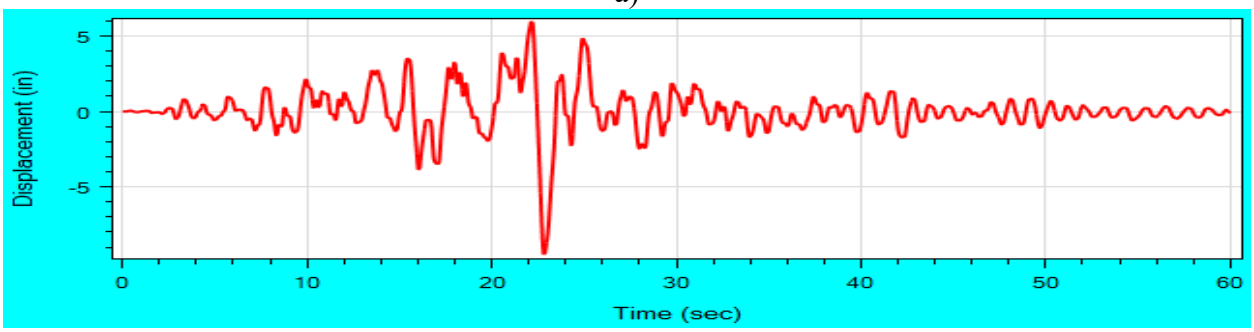

b)

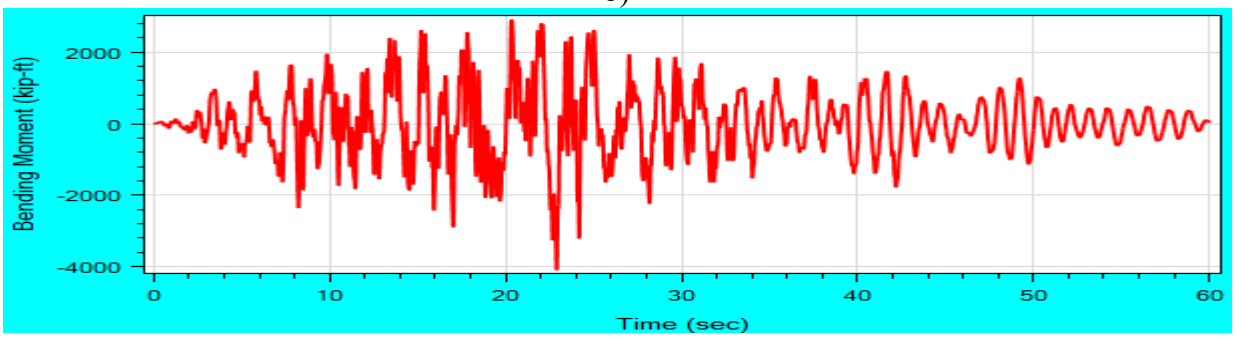

c)

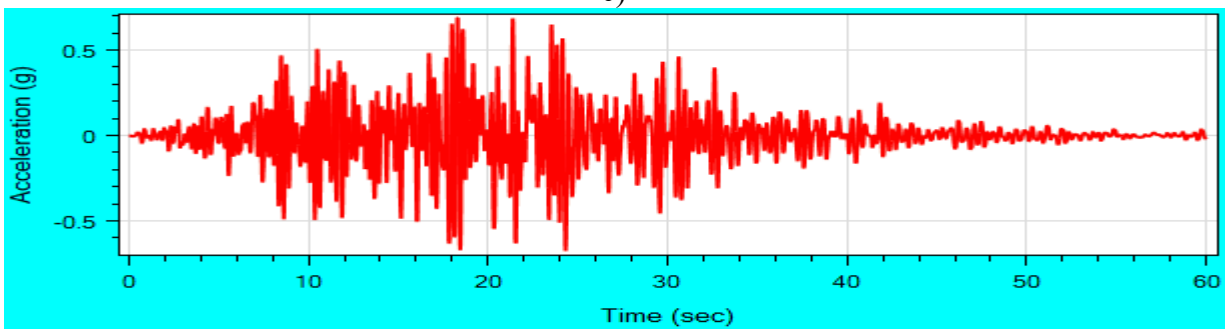

d)

Figure 5.22 OSB3 longitudinal response time histories for Motion 1 ROCKS1N1 (EPP-Gap with Isolation Bearings model): a) deck acceleration; b) deck displacement; c) column base bending moment; d) base excitation ROCKS1N1

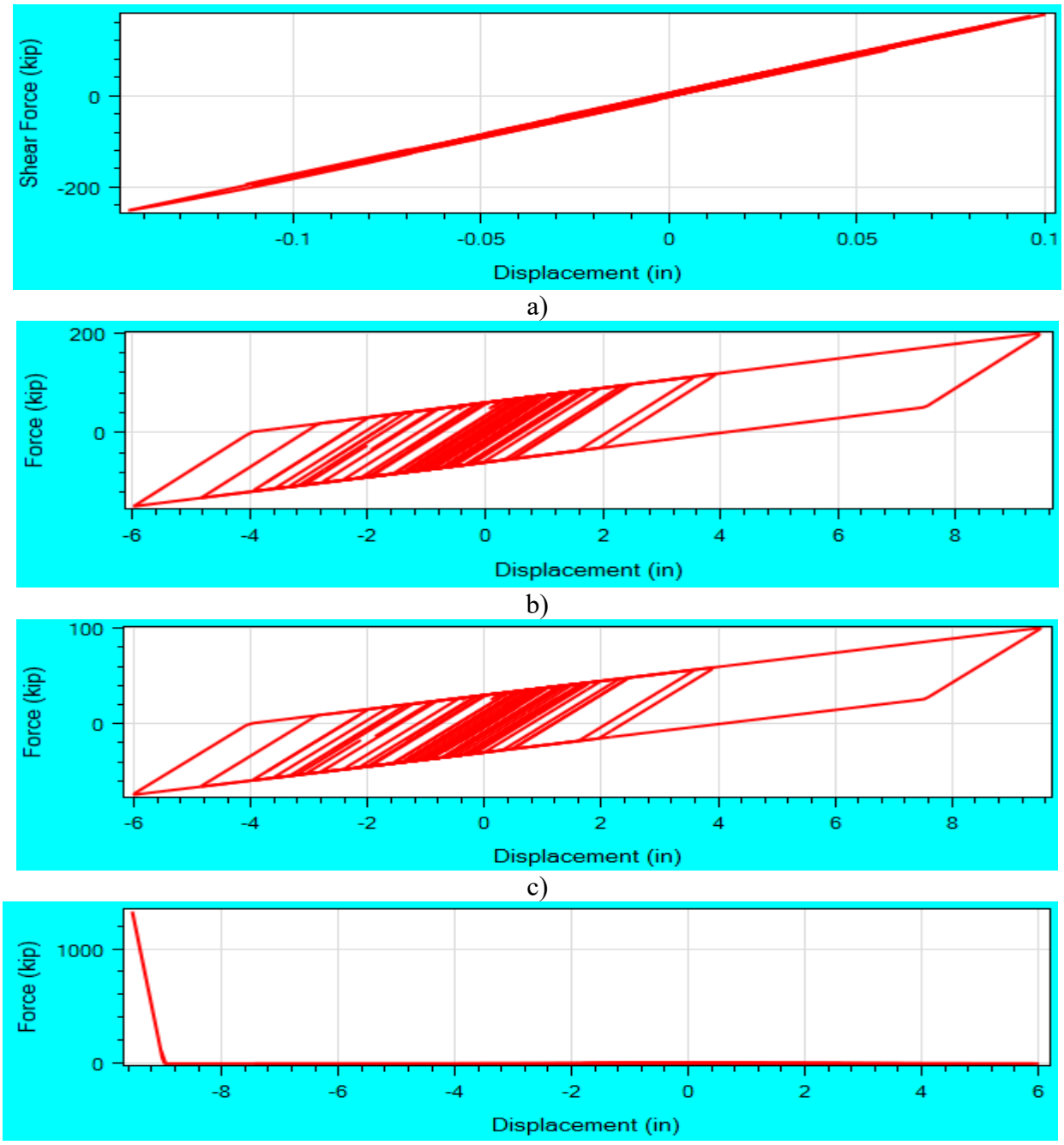

Figure 5.23 OSB3 longitudinal force-displacement response for Motion 1 ROCKS1N1 ROCKS1N1 (EPP-Gap with Isolation Bearings model): a) column top force-displacement; b) bent isolation bearing force-displacement response; c) left abutment isolation bearing force-displacement response; d) left abutment embankment response

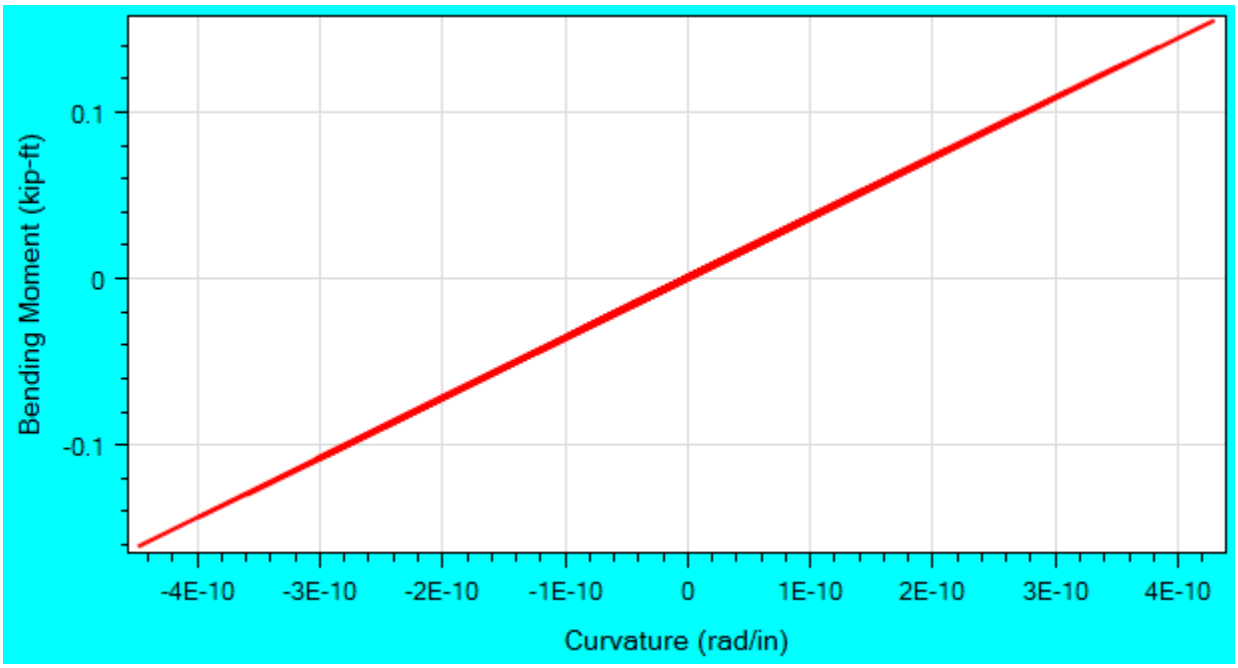

a)

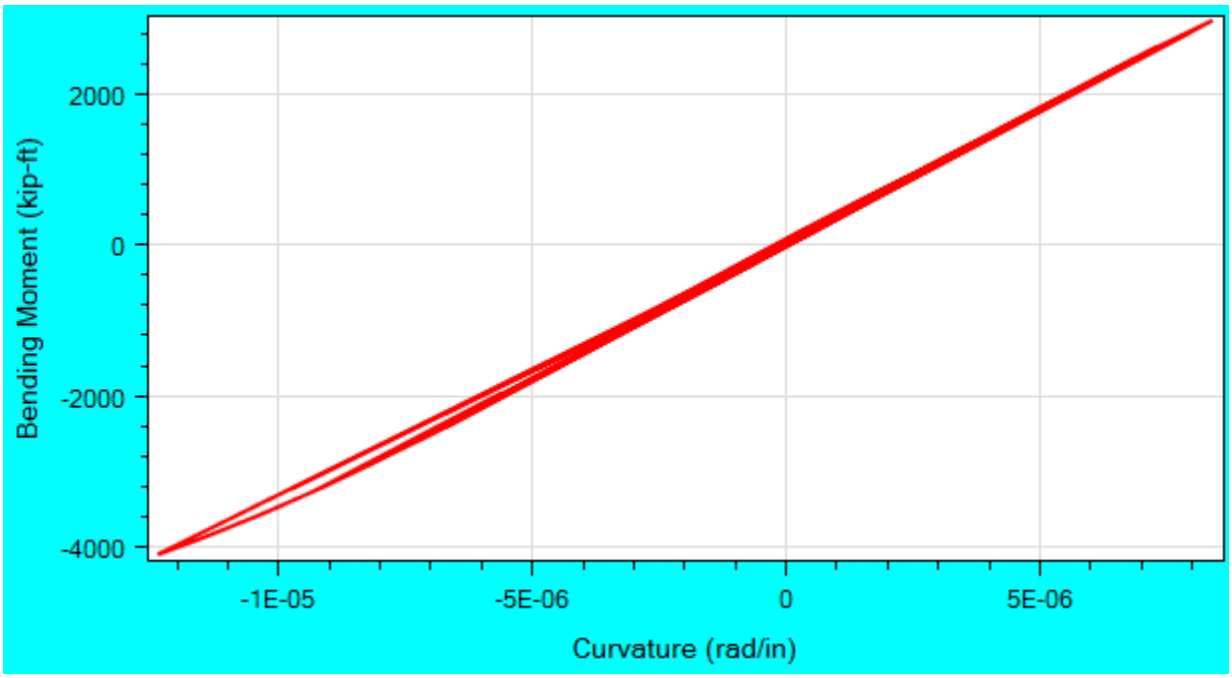

b)

Figure 5.24 OSB3 longitudinal moment-curvature response for Motion 1 ROCKS1N1 (EPP-Gap with Isolation Bearings model) at: a) column top; b) column base

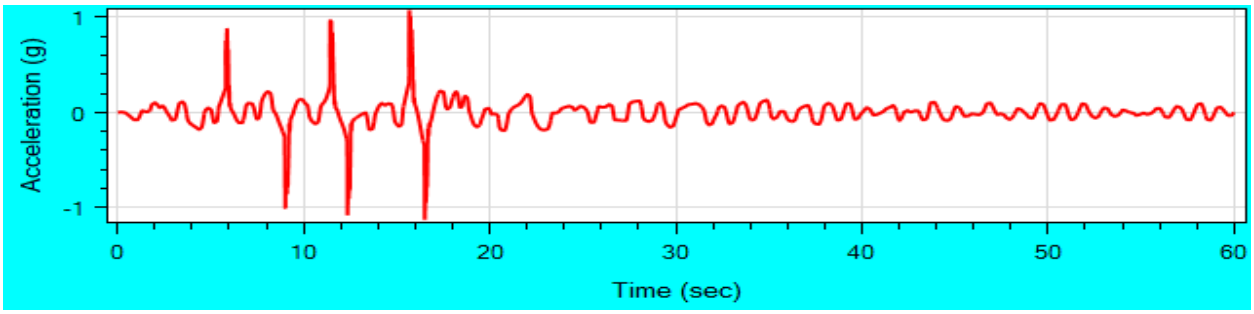

a)

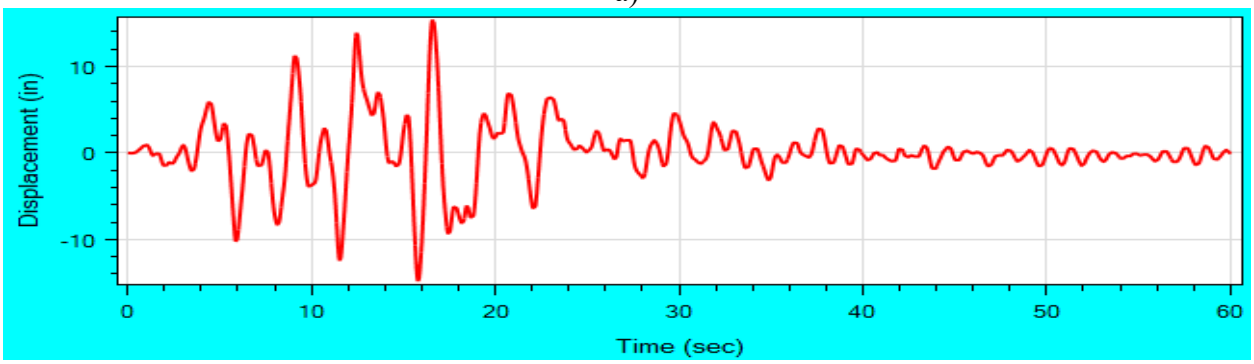

b)

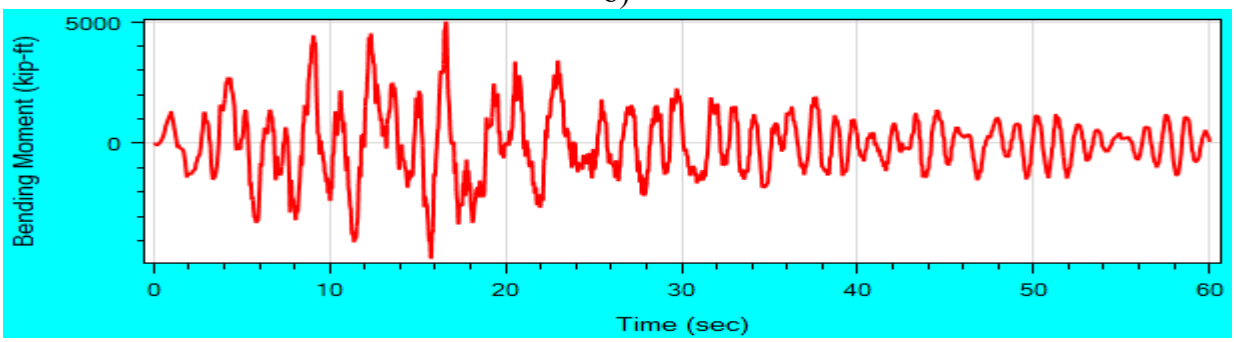

c)

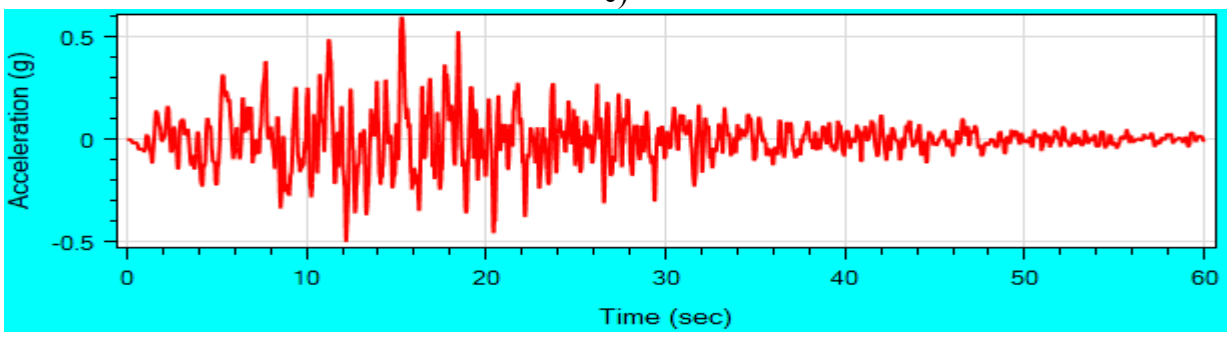

d)

Figure 5.25 OSB3 longitudinal response time histories for Motion 15 SANDS1N1 (EPP-Gap with Isolation Bearings model): a) deck acceleration; b) deck displacement; c) column base bending moment; d) base excitation SANDS1N1

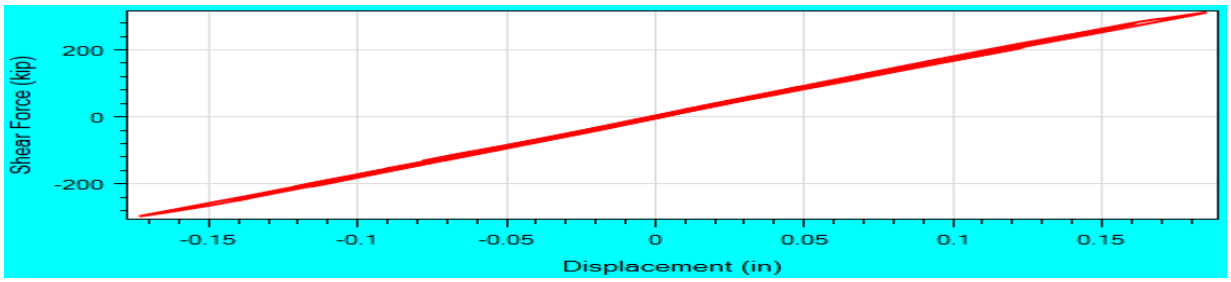

a)

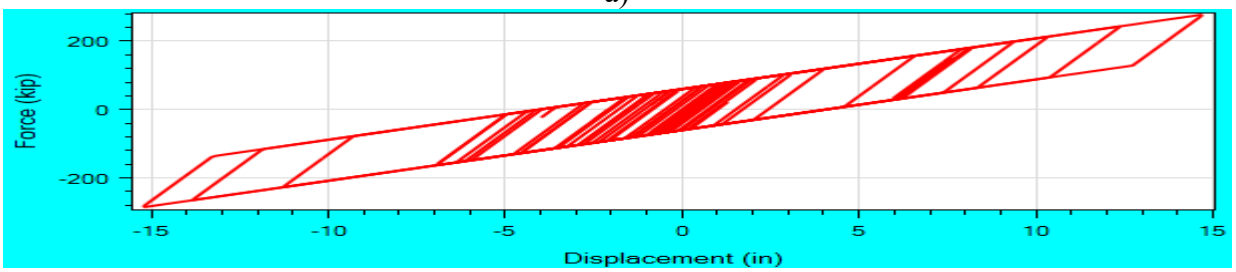

b)

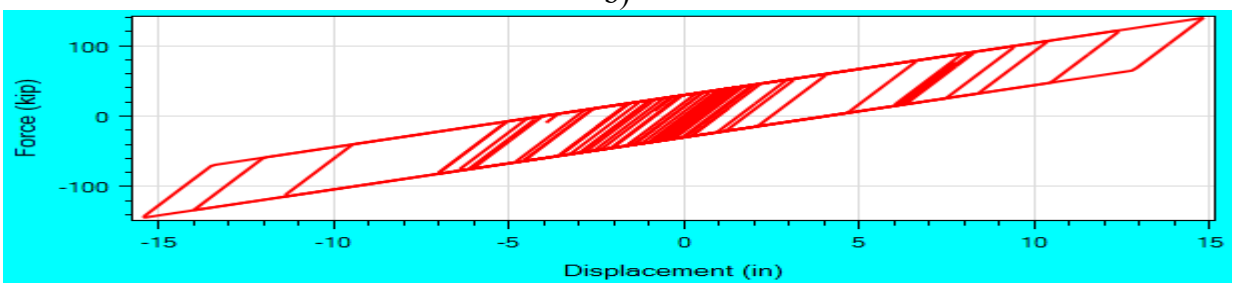

c)

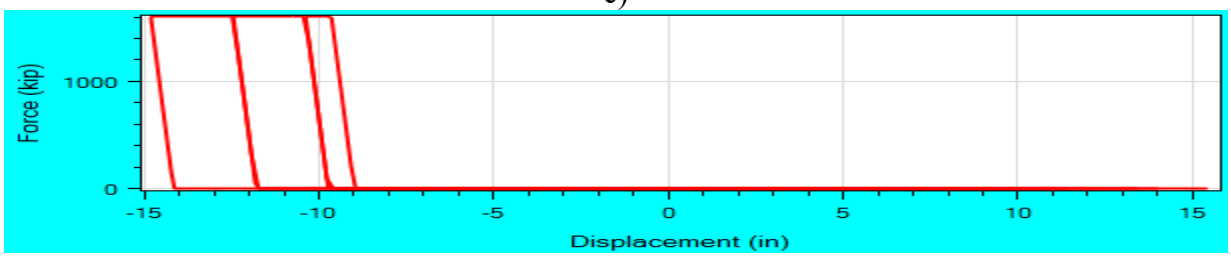

d)

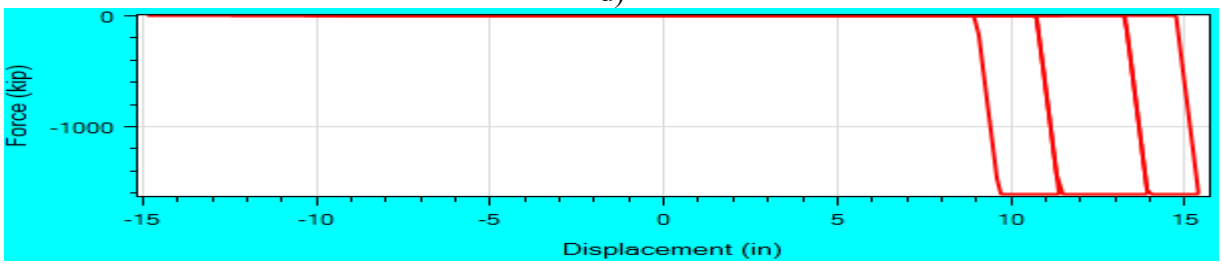

e)

Figure 5.26 OSB3 longitudinal force-displacement response for Motion 15 SANDS1N1 (EPP-Gap with Isolation Bearings model): a) column top force-displacement; b) bent isolation bearing force-displacement response; c) left abutment isolation bearing force-displacement response; d) left abutment embankment response; e) right abutment embankment response

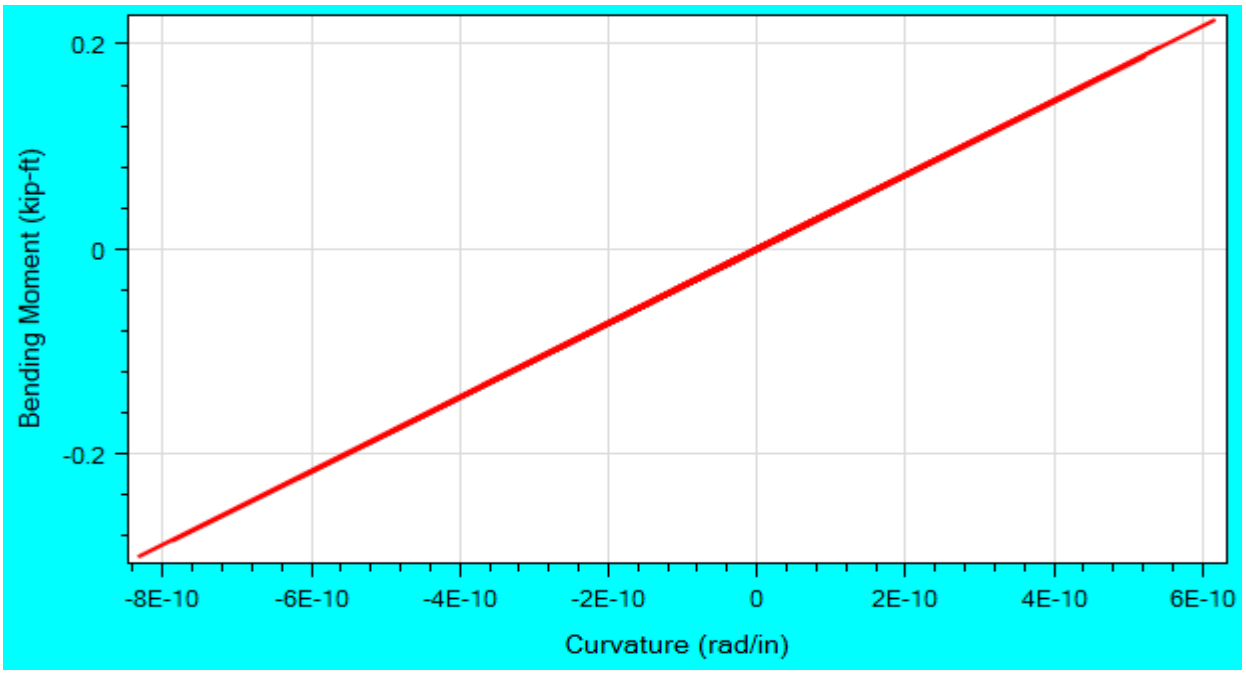

a)

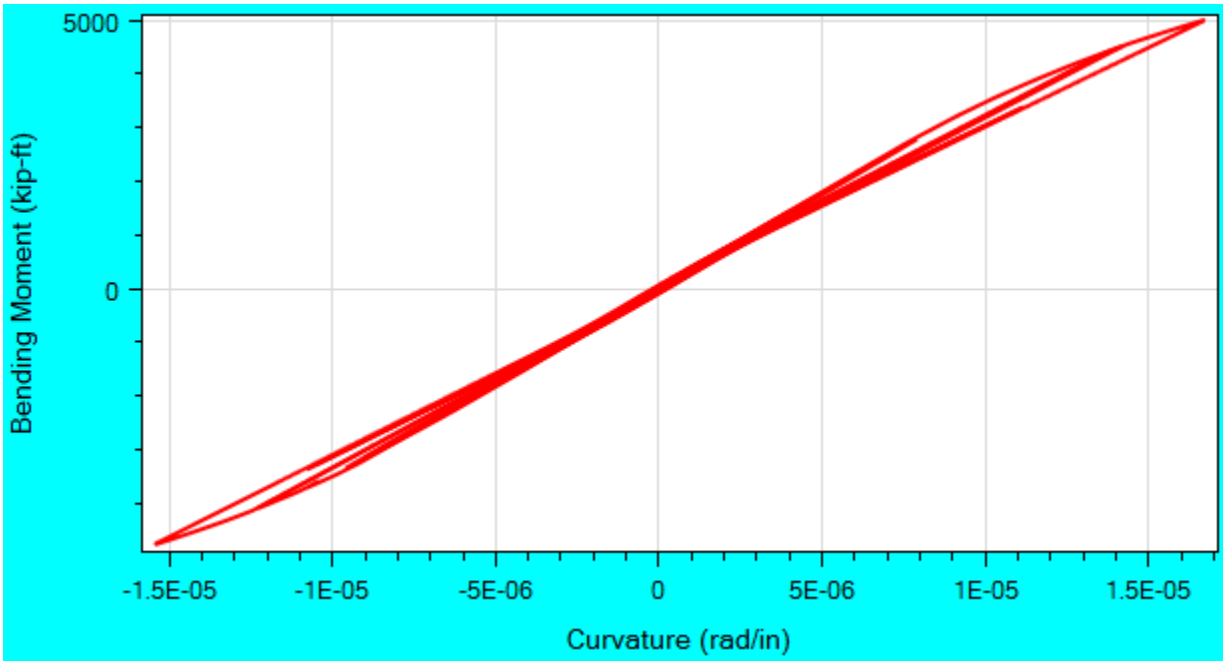

b)

Figure 5.27 OSB3 longitudinal moment-curvature response for Motion 15 SANDS1N1 (EPP-Gap with Isolation Bearings abutment model) at: a) column top; b) column base

5.6 Summary

OSB3 was modeled in OpenSees and CSiBridge. A recently developed user interface MSBridge was employed for pre- and post-processing.

Nonlinear THA was conducted for the 50 motions provided by Caltrans. Two types of abutment models (Roller with Isolation Bearings, and EPP-Gap with Isolation Bearings) were addressed. For the EPP-Gap with Isolation Bearings model, the maximum displacement is 6.4-19.9 inches in the bridge longitudinal direction and 5.1-25 inches in the transverse direction. In CSiBridge, only the EPP-Gap abutment model was simulated.

ESA was also conducted for OSB3 in OpenSees using MSBridge. The longitudinal ESA show the displacement demand to be 7.6 in. The displacement demand was 8.4 in from the transverse ESA.

5.7 Conclusions

1. For the investigated set of ground motions in the OpenSees model (EPP-Gap with Isolation Bearings model):

1.1. In the longitudinal direction, about 50% of the shaking events resulted in deck displacement demand that exceeded that of the ESA (8.7 in). This demand reached a maximum of 160% in excess of that from the corresponding ESA. With the 9 in gap, the abutment reduced the peak maximum displacement from 28.5 in (for the Roller with Isolation Bearings model) to 19.9 in (for the EPP-Gap with Isolation Bearings model).

1.2. In the transverse direction, about 35% of the shaking events resulted in deck displacement demand that exceeded that of the ESA (8.4 in). This demand reached a maximum of 200% in excess of that from the corresponding ESA. With the 1 in gap, the abutment reduced the peak maximum displacement from 28.6 in (for the Roller with Isolation Bearings model) to 25 in (for the EPP-Gap with Isolation Bearings model).

2. For the OpenSees model, the ground input motions of the SANDS1 group (Figure B.4, Figure B.8 and Table 5.4) appear to result consistently in a larger longitudinal and transverse displacement demand (Figures 5.14-5.16).

3. For the EPP-Gap with Isolation Bearings model, in the longitudinal direction, the maximum displacement difference between the OpenSees and CSibridge results is within 20% for about 2/3 of the shaking events (Table 5.5). In the transverse direction, the difference is also within 20% for about 2/3 of the shaking events (Table 5.5).

6 SUMMARY AND CONCLUSIONS

6.1 Summary

Four OSB (Ordinary Standard Bridge) Study Bridges (OSB1, OSB2, OSB3 and OSB4) were studied using OpenSees and CSiBridge. The analysis procedures and results were presented in this report.

For OSB1 & OSB2 in OpenSees analysis, three types of abutment models (Roller, EPP-Gap and EPP-Gap with Bearings) were addressed. The forceBeamColumn (BeamWithHinges) element in OpenSees was employed to model the column while the deck was considered linearly elastic and the bentcap was assumed rigid. As suggested by Caltrans, only the EPP-Gap model (without abutment bearing pads) was simulated in the CSiBrige nonlinear THA.

For OSB3 & OSB4 in OpenSees analysis, two types of abutment models (Roller with Isolation Bearings, and EPP-Gap with Isolation Bearings) were addressed. The forceBeamColumn (with the distributed plasticity integration method) element in OpenSees was employed to model the column while the deck was considered linearly elastic and the bentcap was assumed rigid. As suggested by Caltrans, only the EPP-Gap with Isolation Bearings model was simulated in the CSiBridge nonlinear THA.

To facilitate the conducted analyses in OpenSees, a recently developed user interface MSBridge was employed. Nonlinear THA was conducted for 50 input motions provided by Caltrans. ESA (Equivalent Static Analysis) was performed in OpenSees as well using MSBridge.

6.2 Conclusions

1. In general, the Roller model resulted in the largest maximum deck displacement, and corresponding lower bridge peak acceleration.

2. In the longitudinal direction (OpenSees model), for the bridges without isolation bearings (OSB1 and OBS2), the majority (80%) of the shaking events resulted in column drift demand that is within that of the ESA. Exceedance of the ESA demand reached as much as 75% for OSB1 and 40% for OSB2.

3. In the transverse direction (OpenSees model), for OSB1, 80% of the shaking events resulted in column drift demand that is within that of the ESA, while for OSB2, all of the shaking events resulted in column drift demand that exceeds that of the ESA. Exceedance of the ESA demand reached as much as 15% for OSB1 and 250% for OSB2.

4. For the bridges with isolation bearings (OSB3 and OSB4), in the longitudinal direction (OpenSees model), about 50% of the shaking events resulted in deck displacement demand that is within that of the ESA. Exceedance of the ESA demand reached as much as 160% for OSB3 and OSB4.

5. In the transverse direction (OpenSees model), for OSB3 and OSB4, 65% of the shaking events resulted in column drift demand that is within that of the ESA. Exceedance of the ESA demand reached as much as 200% for OSB3 and 240% for OSB4.

6. The ground input motions of the SANDS1 group appear to result consistently in a larger longitudinal and transverse displacement demand.

7. Comparison of OpenSees and CSiBridge shows that initial column stiffness appears to be different between CSiBridge and OpenSees (lower than expected in the employed CSiBridge beam with hinge model). In addition, the "Hinge Location" in CSiBridge may be difficult to use for reproduction of the OpenSees "Plastic Hinge Length" (as "Hinge Location" in CSiBridge and "Plastic Hinge Length") in OpenSees are not related in any straightforward fashion.

8. For the EPP-Gap abutment model, the difference between the OpenSees and CSibridge results is relatively large in general for the input motions of the SANDS1 group, compared to the ROCKS1N and ROCKS1P groups.

6.3 Future Work

Suggested future work includes:

1. Parametric studies of multi-span OSB bridges.

2. Inclusion of capabilities to represent foundations and related to soil-structure interaction.

3. Further comparison with other relevant computer software packages.

4. Closer investigation of the SANDS1 group input motion characteristics in view of the consistently larger displacement demands for the four investigated OSB bridge configurations.

APPENDIX A: MSBRIDGE: MULTI-SPAN BRIDGE ANALYSIS

MSBridge is a PC-based graphical pre- and post-processor (user-interface) for conducting nonlinear Finite Element (FE) studies for multi-span multi-column bridge systems. This research project was funded by California Department of Transportation (Caltrans). Main features of MSBridge include:

i) Automatic mesh generation of multi-span (straight or curved) bridge systems
ii) Options of foundation soil springs and foundation matrix
iii) Options of deck hinges, isolation bearings, and steel jackets
iv) Management of ground motion suites
v) Simultaneous execution of nonlinear time history analyses for multiple motions
vi) Visualization and animation of response time histories

Finite element computations in MSBridge are conducted using OpenSees (currently ver. 2.4.0 is employed). OpenSees is an open source software framework (McKenna et al. 2010, Mazzoni et al. 2009) for simulating the seismic response of structural and geotechnical systems. OpenSees has been developed as the computational platform for research in performance-based earthquake engineering at the Pacific Earthquake Engineering Research (PEER) Center. For more information about OpenSees, please visit http://opensees.berkeley.edu/.

The analysis options available in MSBridge include:

i) Pushover Analysis
ii) Mode Shape Analysis
iii) Single 3D Base Input Acceleration Analysis
iv) Multiple 3D Base Input Acceleration Analysis
v) Equivalent Static Analysis (ESA)

MSBridge supports analysis in both the US/English and SI unit systems. The default unit system is US/English units. This unit option can be interchanged during model creation, and MSBridge will convert all input data to the desired unit system.

The global coordinate system employed in MSBridge is shown in Figure A.1. The origin is located at the left deck-end of the bridge. The bridge deck direction in a straight bridge is referred to as “longitudinal direction (X)”, while the horizontal direction perpendicular to the longitudinal direction is referred to as “transverse direction (Y)”. At any time, “Z” denotes the vertical direction.

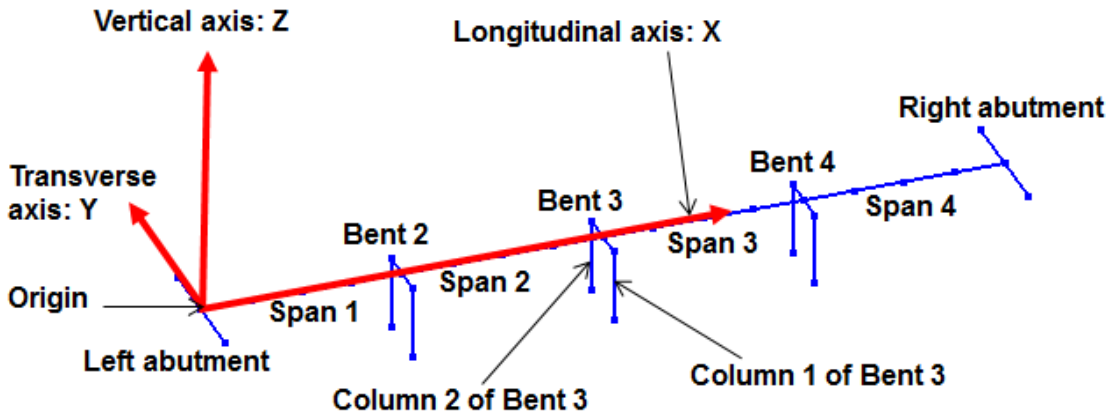

Figure A.1 Global coordinate system employed in MSBridge

MSBridge was written in Microsoft .NET Framework (Windows Presentation Foundation or WPF). OpenTK (OpenGL) library (website: http://www.opentk.com/) was used for visualization of FE mesh and the OxyPlot package (http://oxyplot.codeplex.com/) was employed for x-y plotting.

For more information about MSBridge, please refer to the MSBridge user manual (Elgamal et al. 2014). For information on how to download and install MSBridge, please visit the MSBridge website (http://soilquake.net/msbridge/).

APPENDIX B: BASE INPUT MOTIONS

Table B-1 lists the 50 input motions employed in the study. These motion files were provided by Caltrans.

The motion names (Table B-1) have 8 or 9 character with naming convention as follows:

TypeAiBjC , where

Type = ROCK, SAND, or CLAY
A = S for Synthetic, N for Natural
i = 1 for base record (1000 year return)
B = P for pulse-like motion, N for non-pulse-like motion
j = Record number for records of same TypeAiB
C = N for normal component, P for Parallel component, nonexistent for one component synthetic

Note that the vertical acceleration input is zero for all motions.

Figure B.1 shows the longitudinal PGA histograms for the input motions (the same plot also applies to the transverse direction). Most motions are within 0.28g – 0.99g whereas 2 motions (i.e., Motions 23 & 48) are between 1.28g – 1.42g.

Table B-2 and Table B-3 display the Intensity Measures of the motions with the longitudinal component only, and the 2 horizontal components, respectively. Note that Motions 26-50 are obtained from Motions 1-25, respectively, by switching the 2 horizontal acceleration components. Therefore, Table B-2 also applies to the motions with the transverse component only (Motions 26-46). The acceleration time histories of the input motion components are shown in Figure B.2-Figure B.5. The Pseudo-Spectral Accelerations of the input motions are displayed in Figure B.6-Figure B.9.

Table B-1. Input Motions Employed in the THA

Motion No.	Longitudinal Input		Transverse Input	
	Name	Max. Acc. (g)	Name	Max. Acc. (g)
Motion 1	ROCKS1N1	0.70	-	-
Motion 2	ROCKS1N2	0.38	-	-
Motion 3	ROCKS1N3	0.32	-	-
Motion 4	ROCKS1N4	0.34	-	-
Motion 5	ROCKS1N5	0.53	-	-
Motion 6	ROCKS1N6	0.42	-	-
Motion 7	ROCKS1N7	0.36	-	-
Motion 8	ROCKS1P1	0.71	-	-
Motion 9	ROCKS1P2	0.44	-	-
Motion 10	ROCKS1P3	0.48	-	-
Motion 11	ROCKS1P4	0.32	-	-
Motion 12	ROCKS1P5	0.67	-	-
Motion 13	ROCKS1P6	0.41	-	-
Motion 14	ROCKS1P7	0.40	-	-
Motion 15	SANDS1N1	0.61	-	-
Motion 16	SANDS1N2	0.51	-	-
Motion 17	SANDS1N3	0.57	-	-
Motion 18	SANDS1N4	0.96	-	-
Motion 19	SANDS1N5	0.79	-	-
Motion 20	SANDS1N6	0.67	-	-
Motion 21	SANDS1N7	0.58	-	-
Motion 22	ROCKN1N1N	0.40	ROCKN1N1P	0.58
Motion 23	ROCKN1P1N	1.42	ROCKN1P1P	1.42
Motion 24	SANDN1N1N	0.78	SANDN1N1P	0.81
Motion 25	CLAYN1N1N	0.79	CLAYN1N1P	0.71
Motion 26	-	-	ROCKS1N1	0.70
Motion 27	-	-	ROCKS1N2	0.38
Motion 28	-	-	ROCKS1N3	0.32
Motion 29	-	-	ROCKS1N4	0.34
Motion 30	-	-	ROCKS1N5	0.53
Motion 31	-	-	ROCKS1N6	0.42
Motion 32	-	-	ROCKS1N7	0.36
Motion 33	-	-	ROCKS1P1	0.71
Motion 34	-	-	ROCKS1P2	0.44
Motion 35	-	-	ROCKS1P3	0.48
Motion 36	-	-	ROCKS1P4	0.32
Motion 37	-	-	ROCKS1P5	0.67
Motion 38	-	-	ROCKS1P6	0.41
Motion 39	-	-	ROCKS1P7	0.40
Motion 40	-	-	SANDS1N1	0.61
Motion 41	-	-	SANDS1N2	0.51
Motion 42	-	-	SANDS1N3	0.57
Motion 43	-	-	SANDS1N4	0.96
Motion 44	-	-	SANDS1N5	0.79
Motion 45	-	-	SANDS1N6	0.67
Motion 46	-	-	SANDS1N7	0.58
Motion 47	ROCKN1N1P	0.58	ROCKN1N1N	0.40
Motion 48	ROCKN1P1P	1.42	ROCKN1P1N	1.42
Motion 49	SANDN1N1P	0.81	SANDN1N1N	0.78
Motion 50	CLAYN1N1P	0.71	CLAYN1N1N	0.79

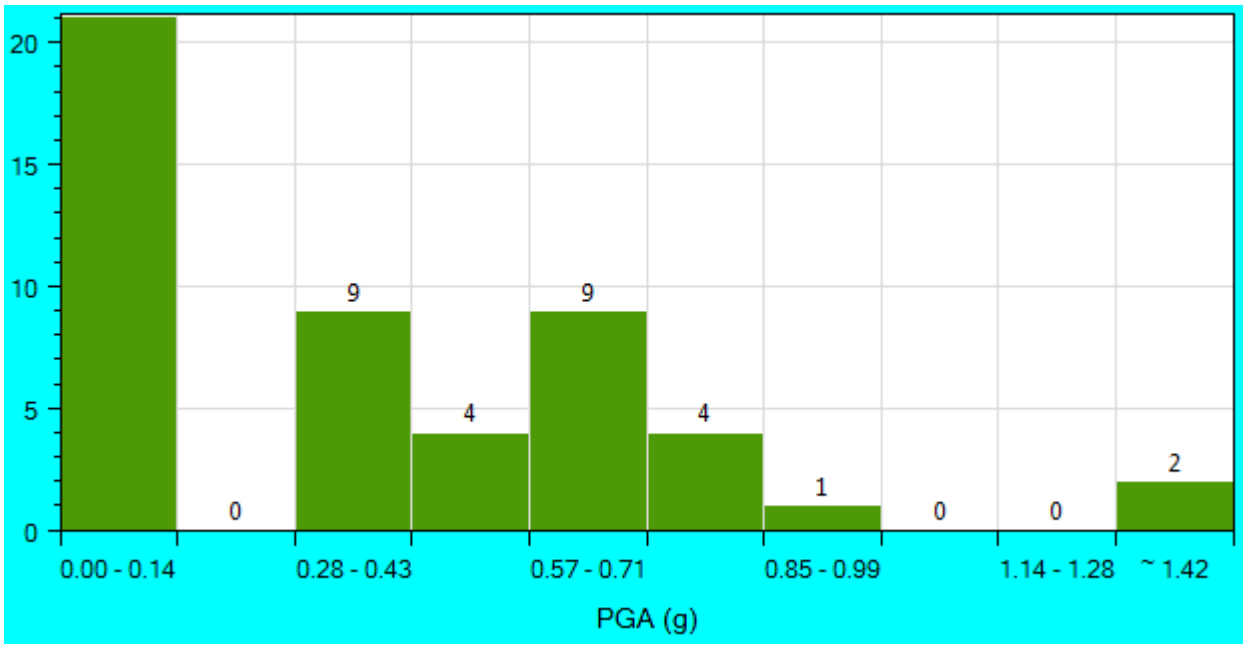

Figure B.1 Longitudinal PGA histograms of the input motions (the bar on the left shows zero input for those motions with the longitudinal component only)

Table B-2. Intensity Measures of Motions 1-21 (Longitudinal Component only)

Motion #	PGA (g)	PGV (in/sec)	PGD (in)	D(5-95) (sec)	CAV (in/sec)	Arias Intensity (in/sec)	SD (in)*	PSA (g)*	PSV (in/sec)*
1	0.7	35.231	21.634	86.875	2409.428	844.027	6.369	0.651	40.02
2	0.381	32.859	22.431	86.295	834.813	131.109	7.203	0.736	45.255
3	0.317	29.943	16.469	89.285	794.067	115.058	6.191	0.632	38.897
4	0.337	35.984	43.945	87.145	909.658	146.66	8.242	0.842	51.783
5	0.526	28.869	25.416	83.895	1071.14	195.452	6.887	0.704	43.275
6	0.422	25.616	37.547	83.82	1226.601	219.001	5.642	0.576	35.449
7	0.356	35.106	41.365	88.025	1033.964	170.179	6.74	0.689	42.348
8	0.709	44.435	45.36	86.87	2404.713	835.79	6.606	0.675	41.506
9	0.441	41.297	51.113	85.52	840.053	139.417	7.039	0.719	44.227
10	0.477	45.129	40.75	83.885	1077.207	199.85	7.259	0.742	45.609
11	0.319	40.454	71.431	87.08	922.947	152.089	8.282	0.846	52.04
12	0.672	53.511	60.915	87.95	1442.94	406.681	8.351	0.853	52.473
13	0.412	24.455	37.643	83.83	1228.427	219.589	5.656	0.578	35.538
14	0.396	55.165	53.625	89.09	815.733	125.978	6.228	0.636	39.132
15	0.605	51.621	60.864	104.745	1898.466	465.928	10.434	1.066	65.558
16	0.509	41.307	51.014	102.25	1247.759	259.706	11.418	1.167	71.74
17	0.573	69.702	78.069	97.875	1852.573	476.356	12.49	1.276	78.477
18	0.955	50.053	48.708	98.915	2375.957	674.228	11.423	1.167	71.772
19	0.788	66.319	144.299	104.635	2533.877	865.91	11.223	1.147	70.517
20	0.667	59.739	53.132	103.115	1639.337	403.652	8.306	0.849	52.189
21	0.582	57.799	93.529	100.01	1701.943	390.457	15.226	1.556	95.666

*For period = 1 sec

Table B-3. Intensity Measures of the Motions with 2 Components

Motion #	PGA (g)	PGV (in/sec)	PGD (in)	D(5-95) (sec)	CAV (in/sec)	Arias Intensity (in/sec)	SD (in)*	PSA (g)*	PSV (in/sec) *
(Longitudinal component)									
22	0.399	23.329	10.141	27.245	697.522	144.311	7.466	0.763	46.91
23	1.419	25.312	68.094	40.625	1759.223	796.492	5.618	0.574	35.299
24	0.784	33.996	13.136	59.25	2739.835	925.332	12.734	1.301	80.007
25	0.788	40.948	22.75	37.15	1563.352	509.352	10.74	1.097	67.483
47	0.576	30.715	17.666	27.32	792.318	209.257	7.153	0.731	44.941
48	1.419	25.312	68.094	40.625	1759.223	796.492	5.618	0.574	35.299
49	0.812	26.761	12.099	59.855	2666.164	869.965	9.404	0.961	59.087
50	0.706	42.57	37.775	36.835	1618.51	535.308	13.025	1.331	81.841
(Transverse component)									
22	0.576	30.715	17.666	27.32	792.318	209.257	7.153	0.731	44.941
23	1.419	25.312	68.094	40.625	1759.223	796.492	5.618	0.574	35.299
24	0.812	26.761	12.099	59.855	2666.164	869.965	9.404	0.961	59.087
25	0.706	42.57	37.775	36.835	1618.51	535.308	13.025	1.331	81.841
47	0.399	23.329	10.141	27.245	697.522	144.311	7.466	0.763	46.91
48	1.419	25.312	68.094	40.625	1759.223	796.492	5.618	0.574	35.299
49	0.784	33.996	13.136	59.25	2739.835	925.332	12.734	1.301	80.007
50	0.788	40.948	22.75	37.15	1563.352	509.352	10.74	1.097	67.483

*For period = 1 sec

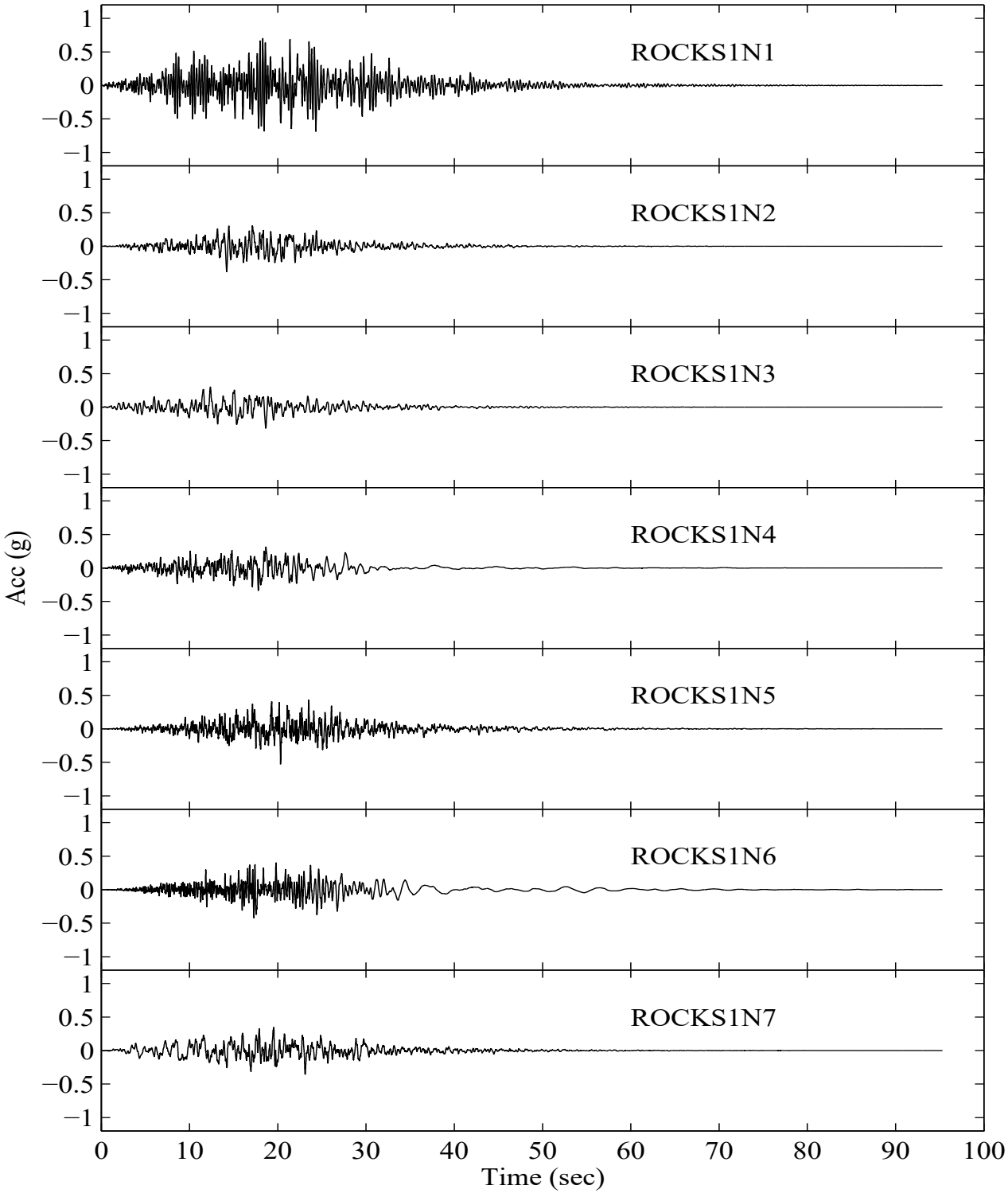

Figure B.2 Acceleration time histories of the input motion components for Rock site (non-pulse-like motions)

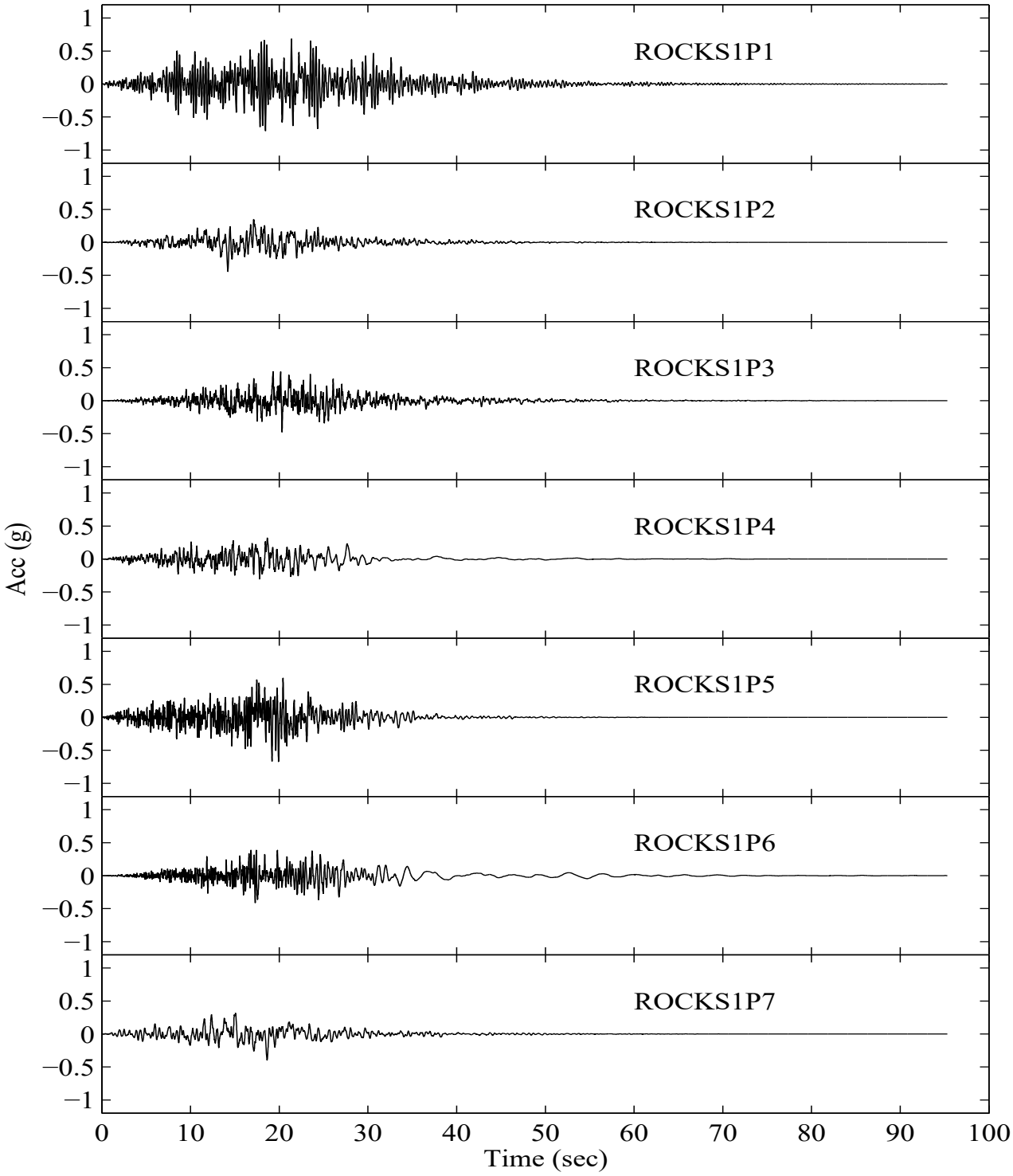

Figure B.3 Acceleration time histories of the input motion components for Rock site (pulse-like motions)

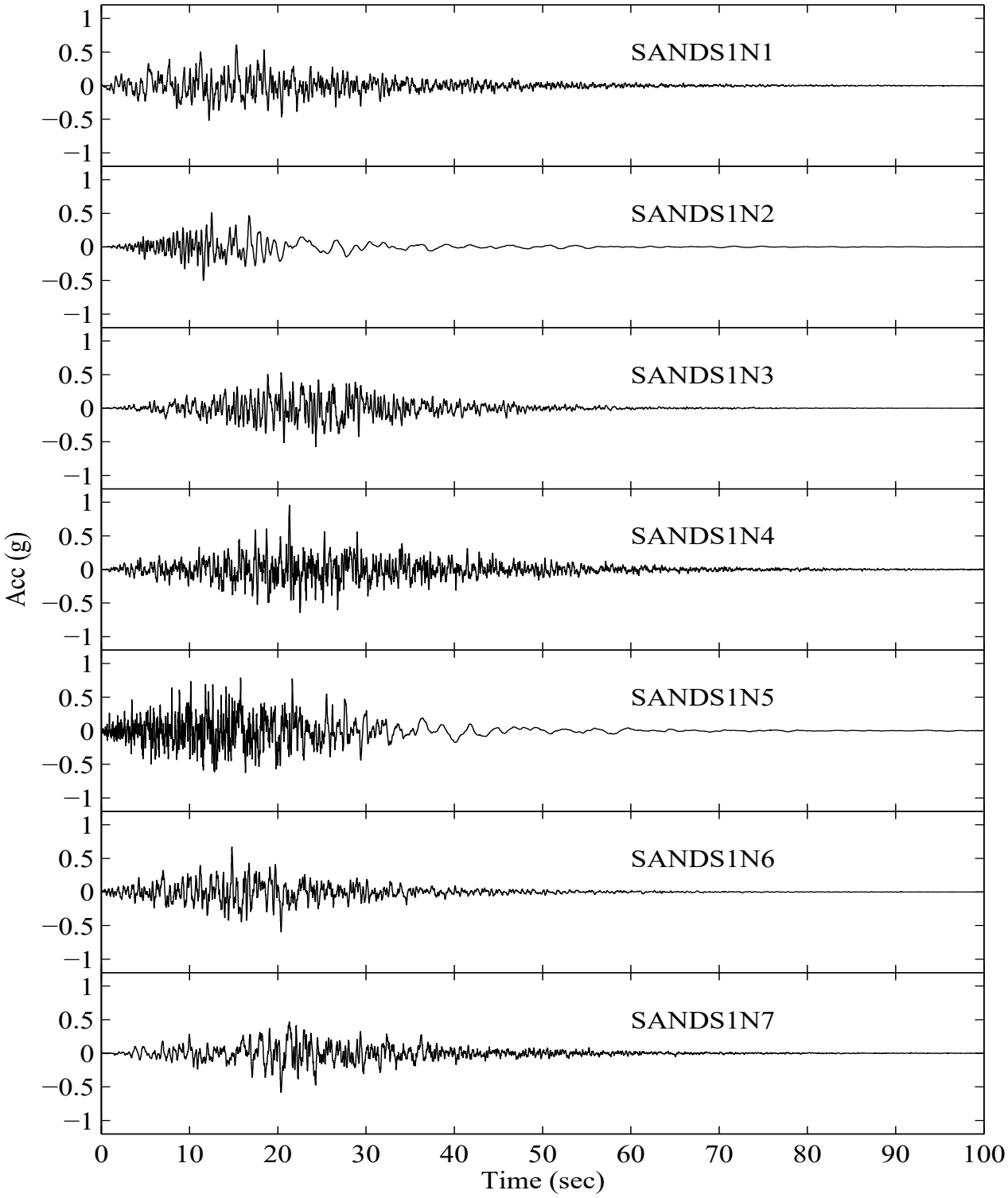

Figure B.4 Acceleration time histories of the input motion components for Sand site (non-pulse-like motions)

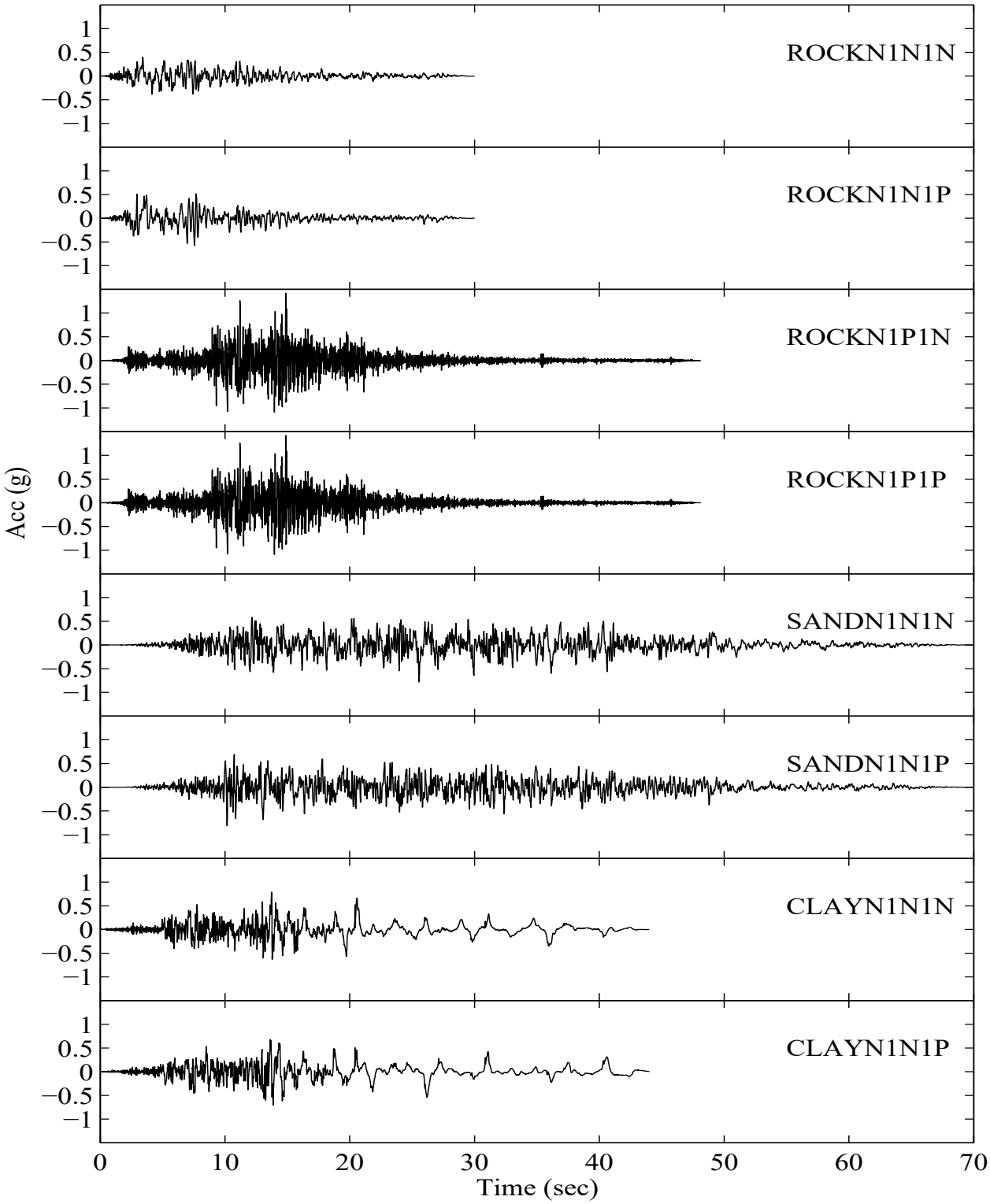

Figure B.5 Acceleration time histories of the input motions with 2 horizontal components

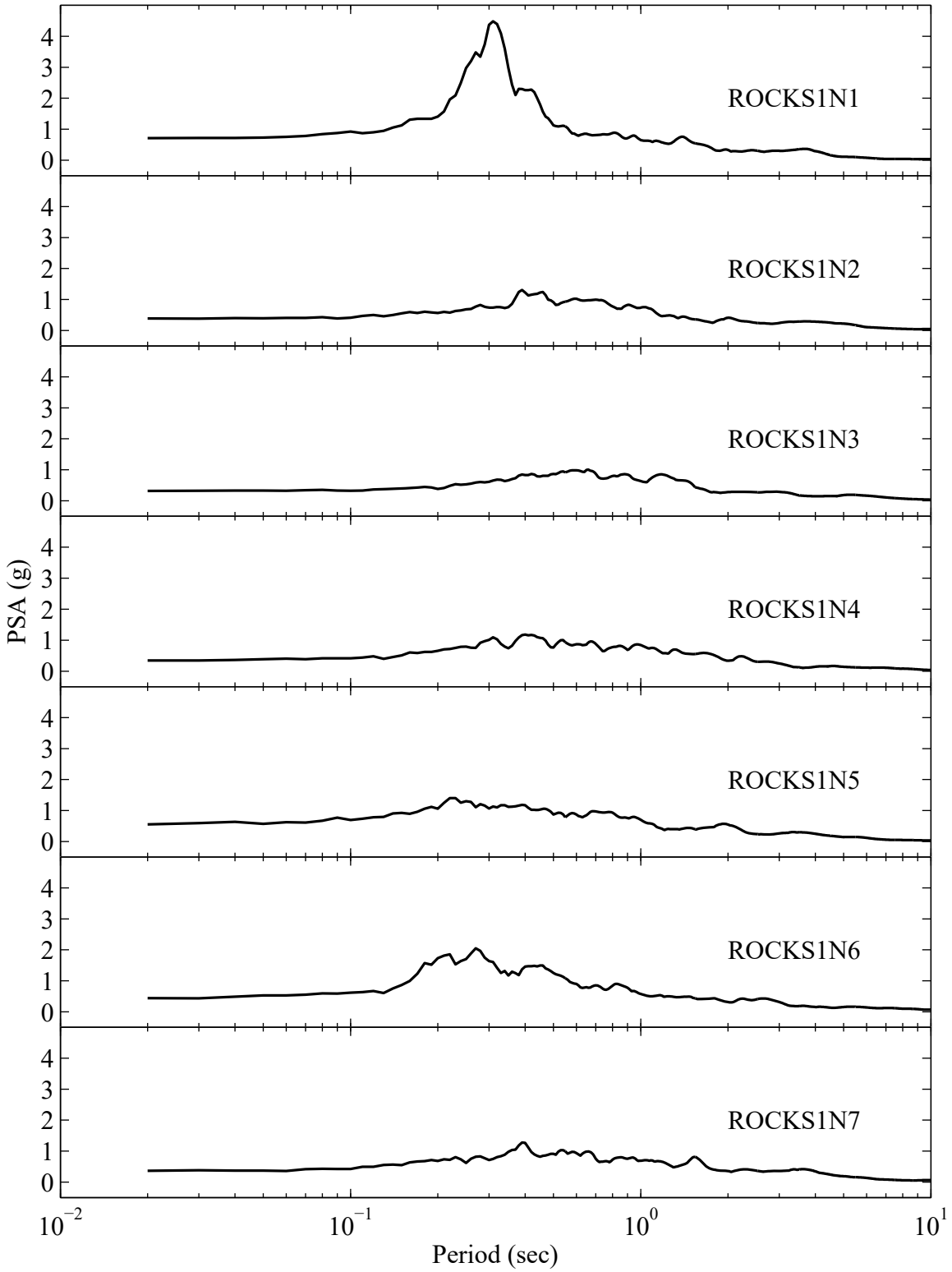

Figure B.6 Pseudo-Spectral Acceleration for Rock site (non-pulse-like motions)

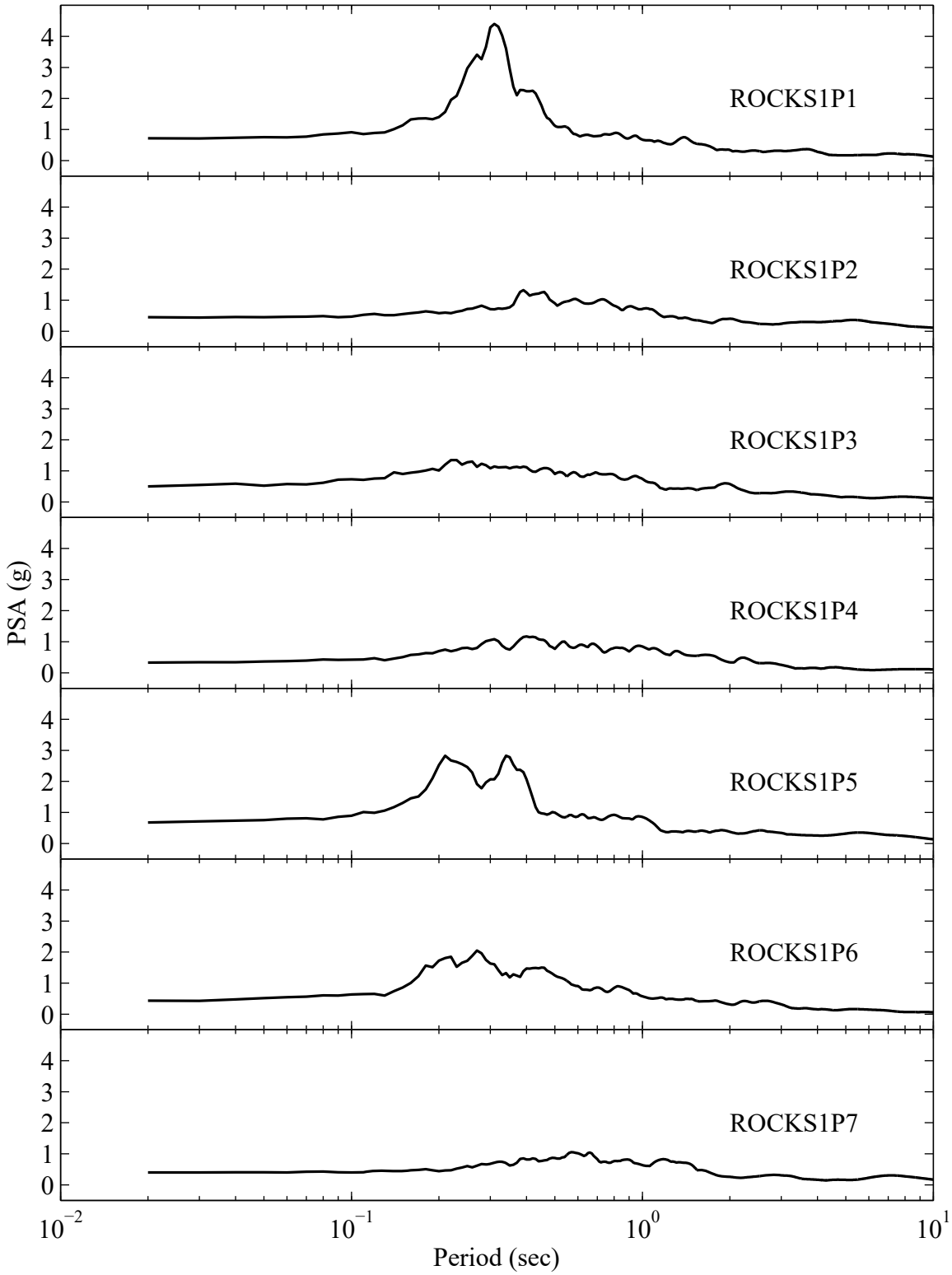

Figure B.7 Pseudo-Spectral Acceleration for Rock site (pulse-like motions)

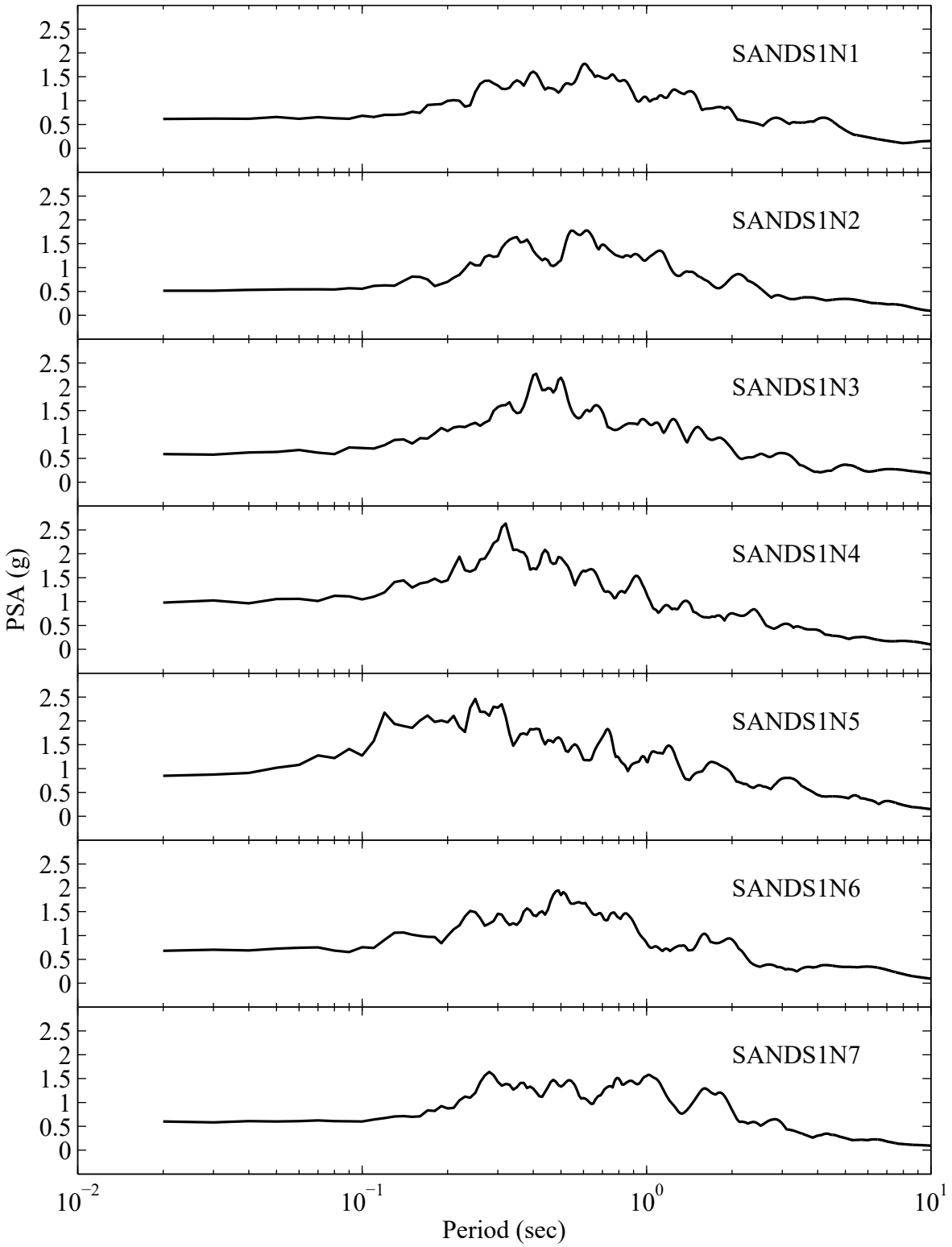

Figure B.8 Pseudo-Spectral Acceleration for Sand site (non-pulse-like motions)

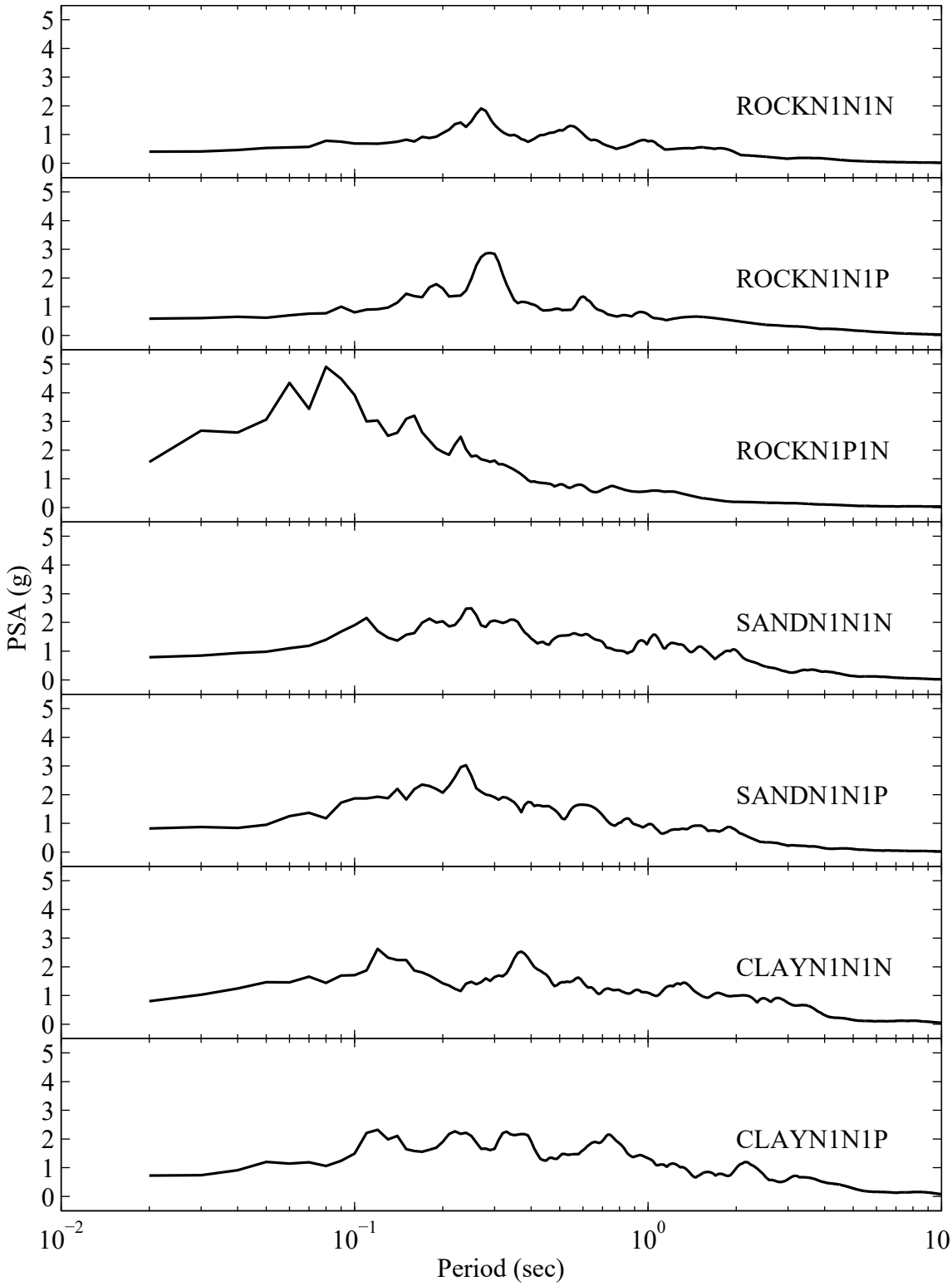

Figure B.9 Pseudo-Spectral Acceleration of the input motions with 2 horizontal components (ROCKN1P1P and ROCKN1P1N are identical)

APPENDIX C: OSB2 MODELING DETAILS

Column

Nonlinear Fiber Section in OpenSees was used to model the circular column section. The reinforced concrete (RC) section properties are listed in Table C-4.

Table C-4. OSB2 Column Reinforced Concrete Properties

Parameter	Value
Number of longitudinal bars	44
Longitudinal bar size (US #)	11
Longitudinal steel %	2
Transverse bar size (US #)	8
Transverse steel %	0.84
Transverse bar spacing (in)	6
Steel unit weight (kcf)	0.49
Steel yield strength (ksi)	66
Steel strain limit	0.06
Concrete unit weight (kcf)	0.15
Concrete unconfined strength (ksi)	4

1) Steel

According to SDC (2013), reinforcing steel shall be modeled with a stress-strain relationship that exhibits an initial linear elastic portion, a yield plateau, and a strain hardening range in which the stress increases with strain. Thus, the ReinforcingSteel material in OpenSees (Table C-5) was used for the longitudinal rebars. A strain limit of 0.06 (shown in Table C-4) was used (for #11 longitudinal rebars according to SDC 2013). Figure C.1 shows the stress-strain curve for the ReinforcingSteel material.

Table C-5. ReinforcingSteel Material Properties Employed for the OSB2 Column

Parameter	Value
Young's modulus (ksi)	29,000
Ultimate stress (ksi)	99
Youngs modulus at initial stress-hardening (ksi)	1,200
Strain at initial stress-hardening	0.01
Strain at peak stress	0.09

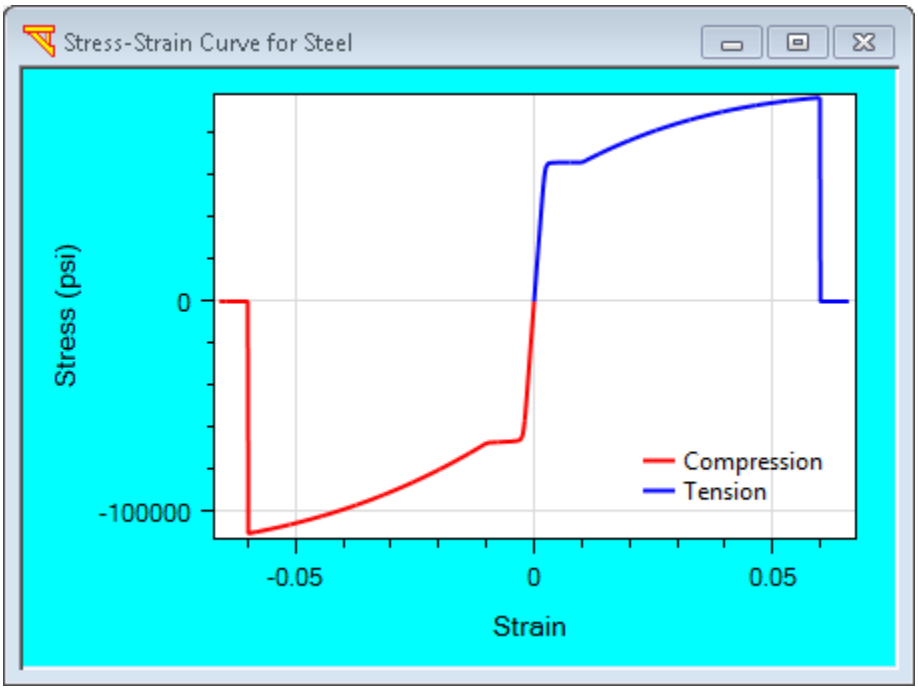

Figure C.1 Stress-strain curve of the ReinforcingSteel material for the OSB2 column

2) Concrete

The Concrete02 material as shown in Table C-6 was used for the cover and core concrete. Figure C.2 shows the stress-strain curve of the Concrete02 material.

Table C-6. Concrete02 Material Properties Employed for the OSB2 Column

Parameter	Core	Cover
Compressive strength (ksi)	-5.549	-4
Strain at maximum strength	-0.0029	-0.002
Crushing strength (ksi)	-5.205	0
Strain at crushing strength	-0.02	-0.006
Ratio between unloading slope	0.1	0.1
Tensile strength (ksi)	0.777	0.56
Tensile softening stiffness (ksi)	268.398	280

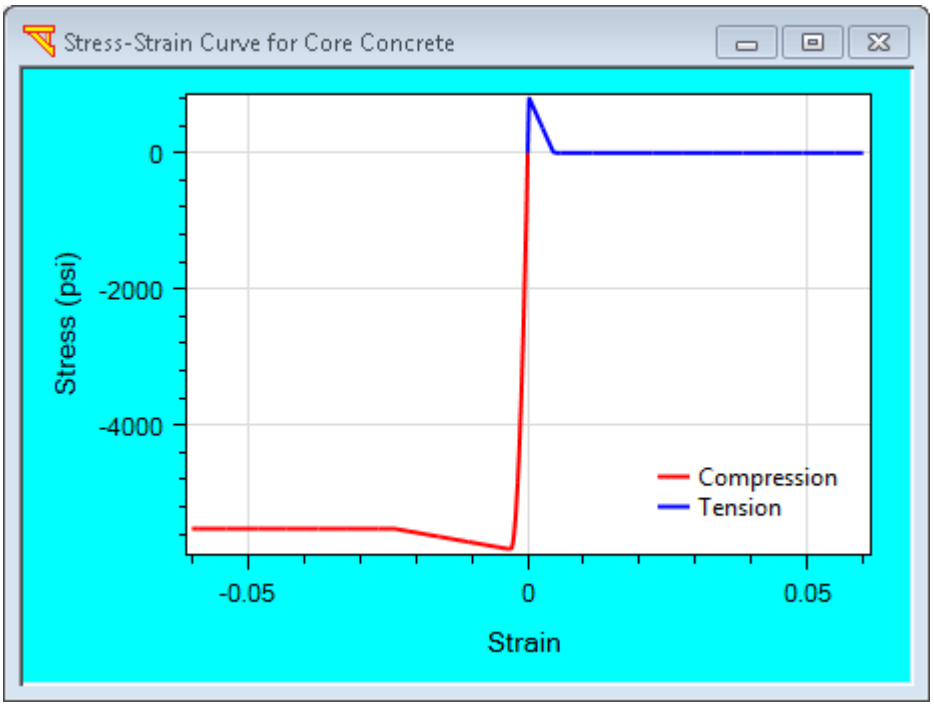

a)

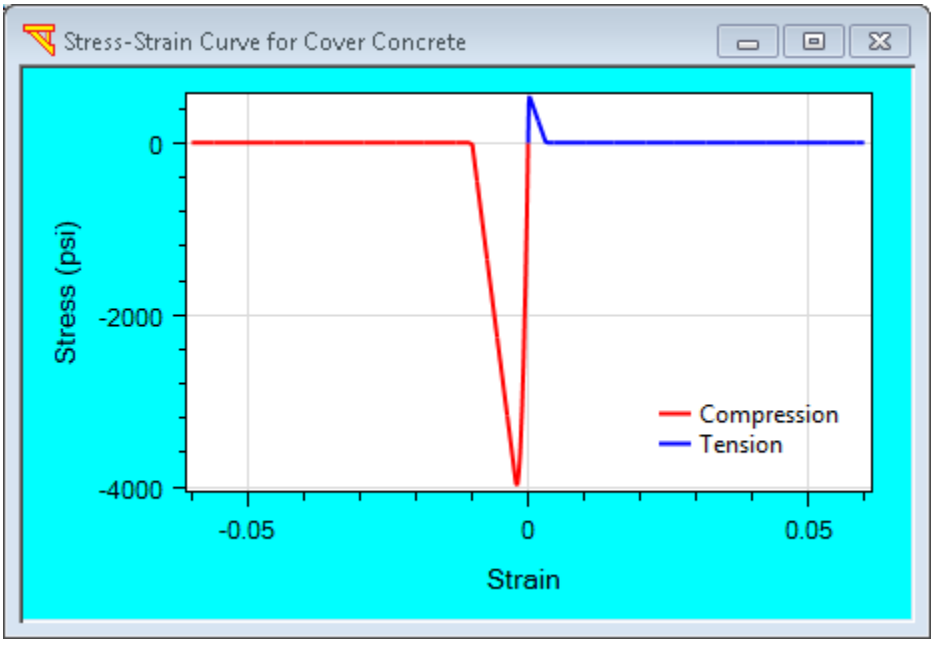

b)

Figure C.2 Stress-strain curves of the Concrete02 material for the OSB2 column: a) Core (confined); (b) Cover (unconfined)

3) Moment-Curvature Relationship

The moment-curvature response of the column Fiber section obtained from **OpenSees** is shown in Figure C.3, along with the result from **XSECTION** for comparison. An axial compressive load of 1991 kip, which is equal to the deadload applied at the column top in the actual case of OSB2, was applied in the moment-curvature analysis.

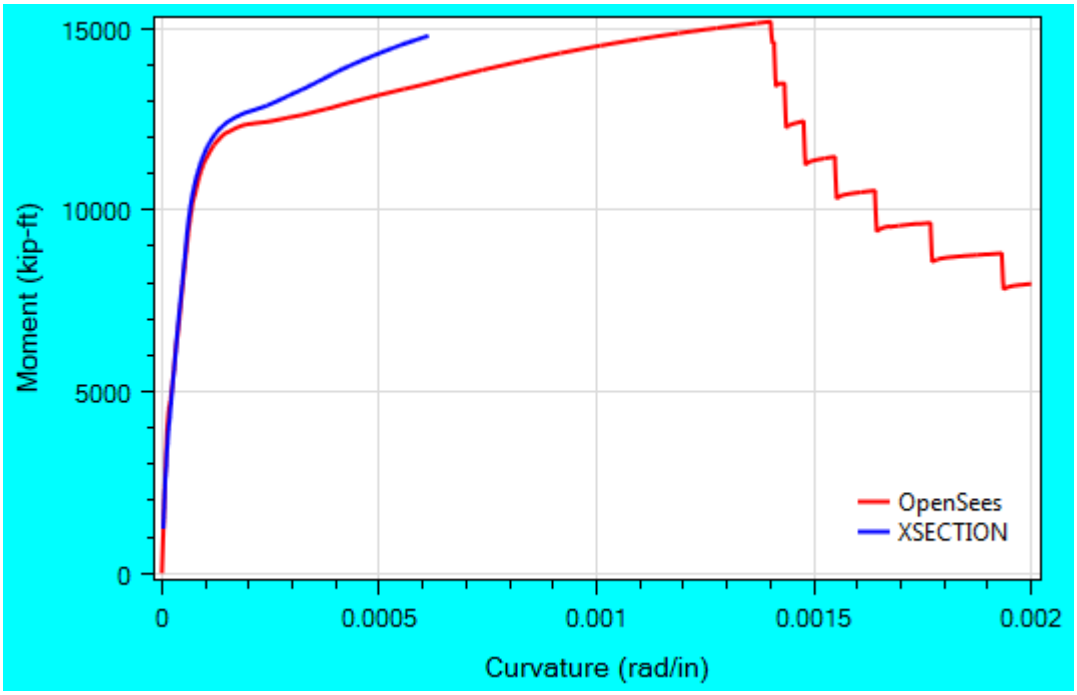

Figure C.3 Moment-curvature relationships of the circular column section for OSB2 (an axial compressive load of 1991 kip was applied)

4) Beam-column element

The forceBeamColumn (BeamWithHinges) element in **OpenSees** was used to model the column. When the BeamWithHinges element was used, a plastic hinge length (L_p) was required. The calculation of the plastic hinge length for the column was based on Eq. 7.6.2.1-1 of SDC (2013):

$$L_p = \begin{cases} 0.08L + 0.15 f_{ye} d_{bl} \geq 0.3 f_{ye} d_{bl} & (\text{in, ksi}) \\ 0.08L + 0.022 f_{ye} d_{bl} \geq 0.044 f_{ye} d_{bl} & (\text{mm, MPa}) \end{cases} \quad \text{(C-1)}$$

Where L is the column height, f_{ye} is the steel yield strength, d_{bl} is the longitudinal bar size.

For OSB2 Column, L = 20 ft, f_{ye} = 66 ksi (Table C-4), and d_{bl} = 11. Therefore, the plastic hinge length L_p = 2.8 ft.

In addition, the column interior section was assumed to be linearly elastic when the BeamWithHinges element was used. Table C-7 shows the material and section properties of the interior elastic section of the Beam-With-Hinges element.

Table C-7. Material and Section Properties of the Interior Elastic Section for the OSB2 Column

Parameter	Value
Young's modulus (ksi)	4,287
Shear modulus (ksi)	1,786.25
Unit weight (kcf)	0.15
Area of cross section (ft^2)	23.76
Gross Moment of inertia @ longitudinal axis (ft^4)	44.92
Gross Moment of inertia @ transverse axis (ft^4)	44.92
Cracked Section Property Factor (for Moment of Inertia)	0.35
Torsion constant (ft^4)	89.84

Deck

The material and section properties of the box-girder are listed in Table C-8. The weight of the bridge deck per unit length is 10.62 kip/ft (= 70.8 ft^2 x 0.15 kcf).

Table C-8. OSB2 Deck Material and Section Properties

Parameter	Value
Young's modulus (ksi)	3,420
Shear modulus (ksi)	1,425
Unit weight (kcf)	0.15
Area of cross section (ft^2)	70.8
Moment of inertia @ horizontal axis (ft^4)	310.9
Moment of inertia @ vertical axis (ft^4)	7097.9
Torsion constant (ft^4)	777.43

Abutment

Three types of abutment models were employed.

i) Roller;

ii) EPP-Gap;

In the EPP-Gap model, a compression-only ElasticPPGap material in OpenSees was used for the longitudinal direction (Figure C.4a). The effective stiffness was 1,781 kip/in and the yield force

was -1,031 kip. The longitudinal gap was 2 in (Figure C.4a). For the transverse direction (Figure C.4b), a compression-only ElasticPPGap material in OpenSees was also used, in which the effective stiffness was 100 kip/in and yield force was -179.4 kip and the gap was 1 in (Figure C.4b). The vertical direction was assumed to be fixed.

iii) EPP-Gap w/ Bearings

Four elastomeric bearing pads (Table C-9) were included in addition to those described in the EPP-Gap model (Aviram et al 2008a). The pad length is 18 in and the pad height is 2.25 in. Figure C.5 shows the force-displacement relationships of this abutment model.

Table C-9. Bearing Pad Geometric and Material Properties

Parameter	Value
Young's modulus *E* (ksi)	5
Shear modulus *G* (ksi)	0.15
Yield Strain	150% shear strain
Pad length (in)	18
Pad height *h* (in)	2.25
Lateral Stiffness	*GA / h* (where *A* is the cross-section area and *h* is the pad height)
Hardening Ratio	1%
Vertical Stiffness	*EA / h*
Vertical Yield Strength (ksi)	2.25

ESA

The ESA was conducted in the longitudinal and transverse directions. Figure C.6 shows the acceleration response spectrum (ARS) used in the ESA throughout this study. It is noted herein that the user interface MSBridge allows the ESA to be based on the ARS of the specific input motions that the user specifies. However, in this report, ESA was always based on the ARS of Figure C.6.

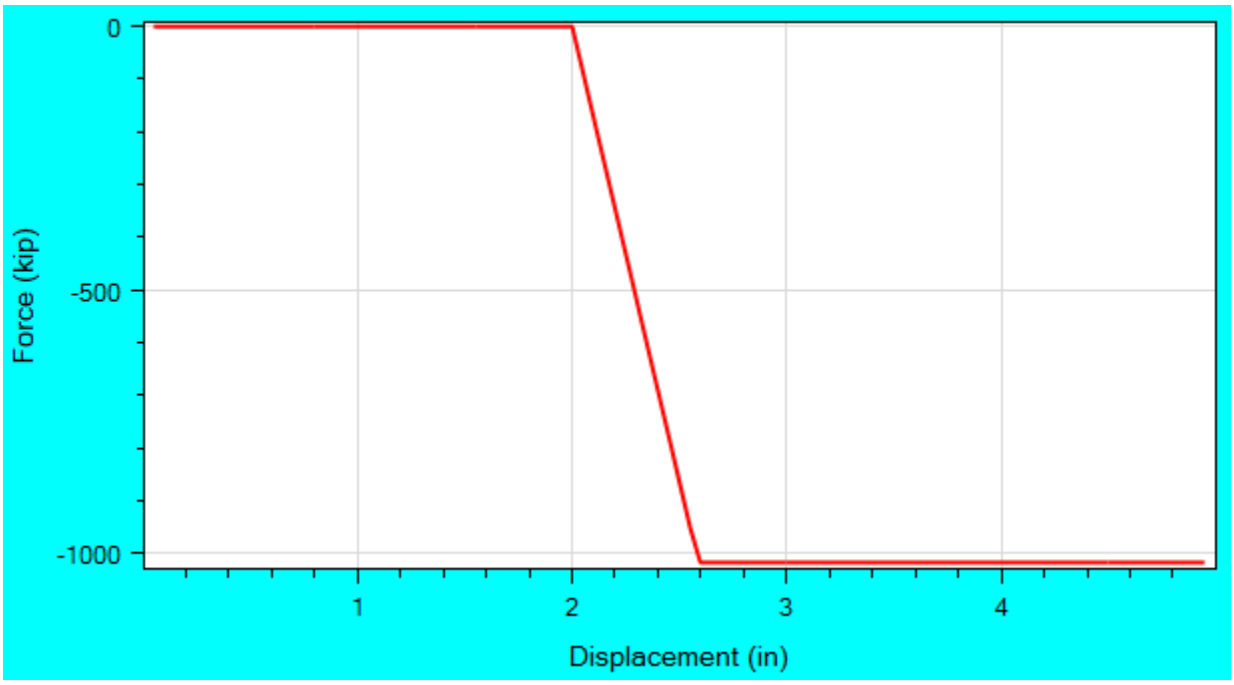

a)

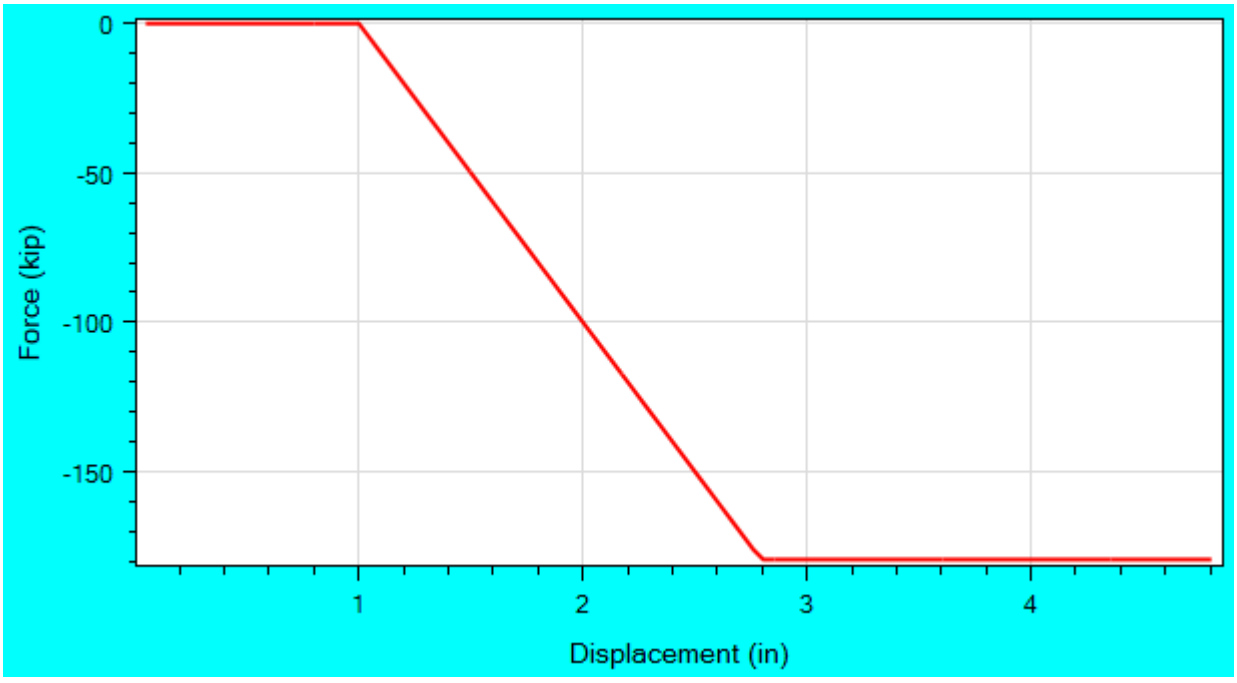

b)

Figure C.4 Abutment force-displacement responses for EPP-Gap model: a) longitudinal direction; b) transverse direction

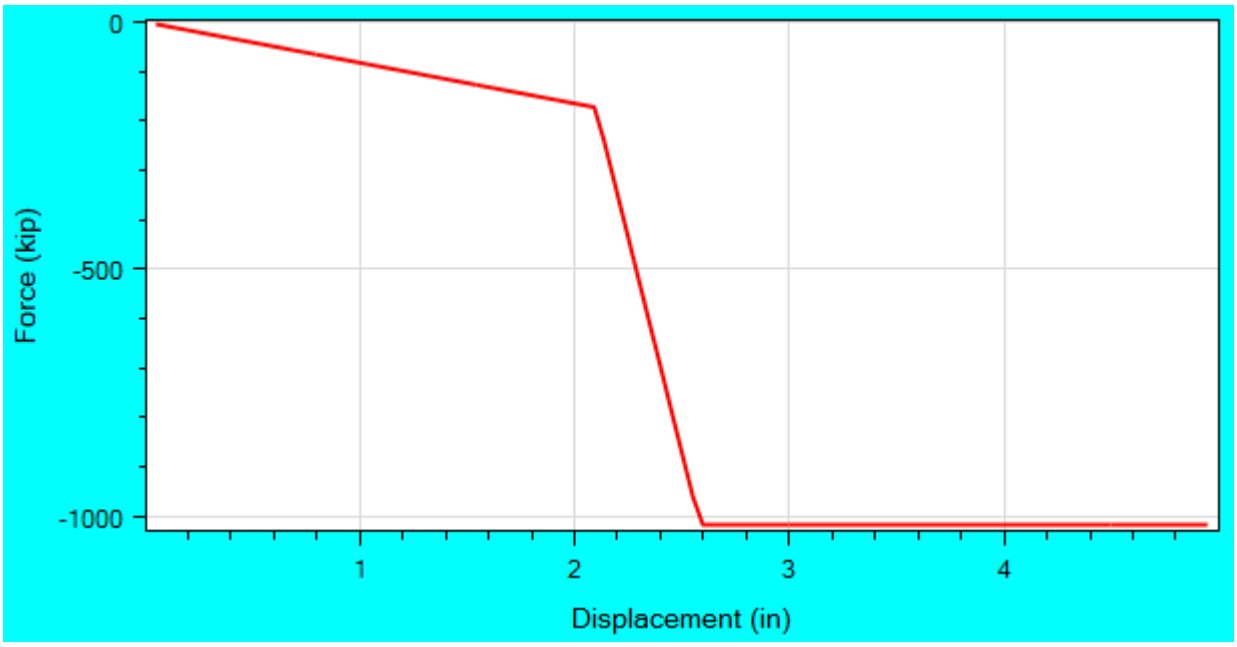

a)

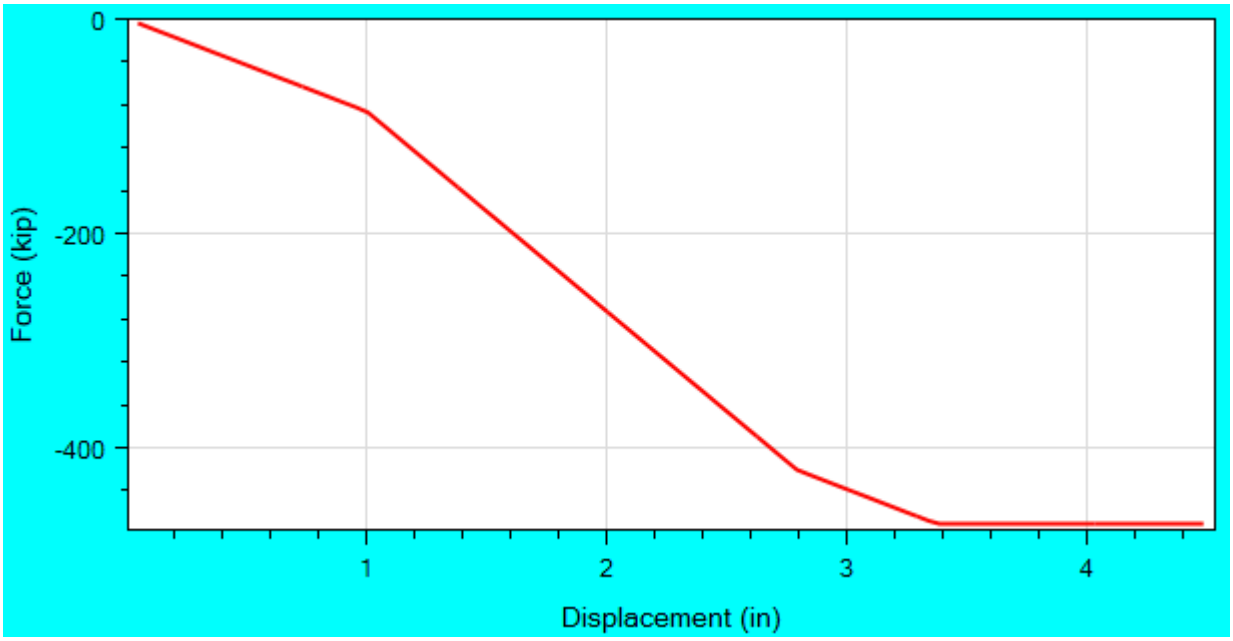

b)

Figure C.5 Abutment force-displacement responses for the EPP-Gap model with Bearings: a) longitudinal direction; b) transverse direction

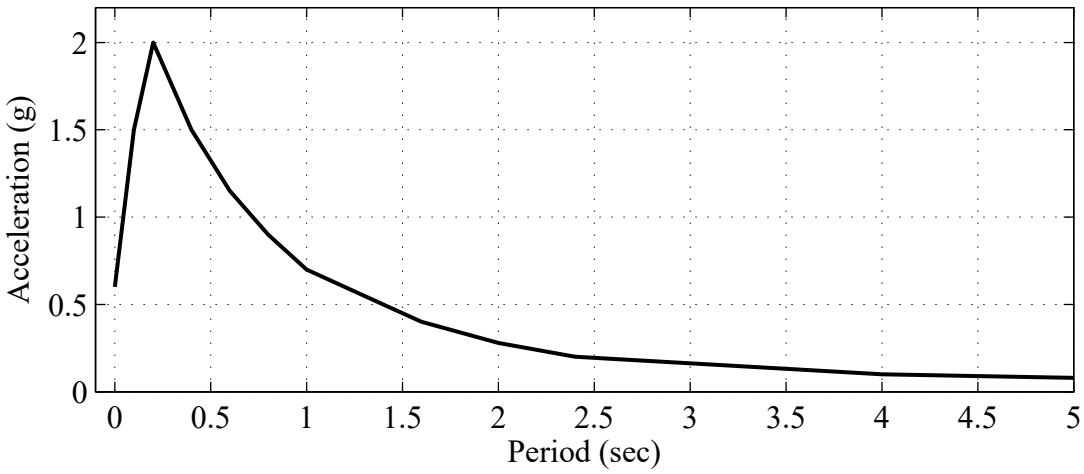

Figure C.6 Acceleration response spectrum employed in the ESA

APPENDIX D: OSB1 MODELING DETAILS

Column

The single-bent in OSB1 is composed of two circular reinforced concrete columns. Each column is 20 ft high with a diameter of 66 in. The columns are fixed at top and pinned at the base. Nonlinear Fiber Section in OpenSees was used to model the circular column section. The reinforced concrete (RC) section properties are listed in Table D-10.

Table D-10. OSB1 Column Reinforced Concrete Properties

Parameter	Value
Number of longitudinal bars	36
Longitudinal bar size (US #)	11
Longitudinal steel %	1.64
Transverse bar size (US #)	8
Transverse steel %	0.84
Transverse bar spacing (in)	6
Steel unit weight (kcf)	0.49
Steel yield strength (ksi)	66
Steel strain limit	0.06
Concrete unit weight (kcf)	0.15
Concrete unconfined strength (ksi)	3.6

1) Steel

Thus, the ReinforcingSteel material in OpenSees (Same as OSB2 as shown in Table C-5 and Figure C.1) was used for the longitudinal rebars. A strain limit of 0.06 (shown in Table D-10) also was used (for #11 longitudinal rebars according to SDC 2013).

2) Concrete

The Concrete02 material as shown in Table D-11 was used for the cover and core concrete. Figure D.1 shows the stress-strain curve of the Concrete02 material.

Table D-11. Concrete02 Material Properties Employed for the OSB1 Column

Parameter	Core	Cover
Compressive strength (ksi)	-5.129	-3.6
Strain at maximum strength	-0.0028	-0.002
Crushing strength (ksi)	-4.806	0
Strain at crushing strength	-0.023	-0.006
Ratio between unloading slope	0.1	0.1
Tensile strength (ksi)	0.718	0.5
Tensile softening stiffness (ksi)	254.624	252

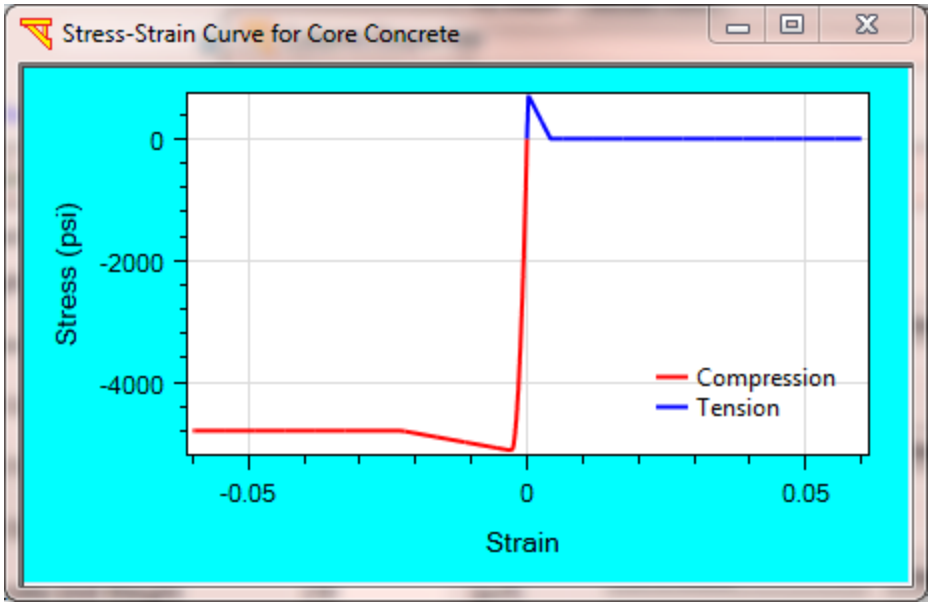

a)

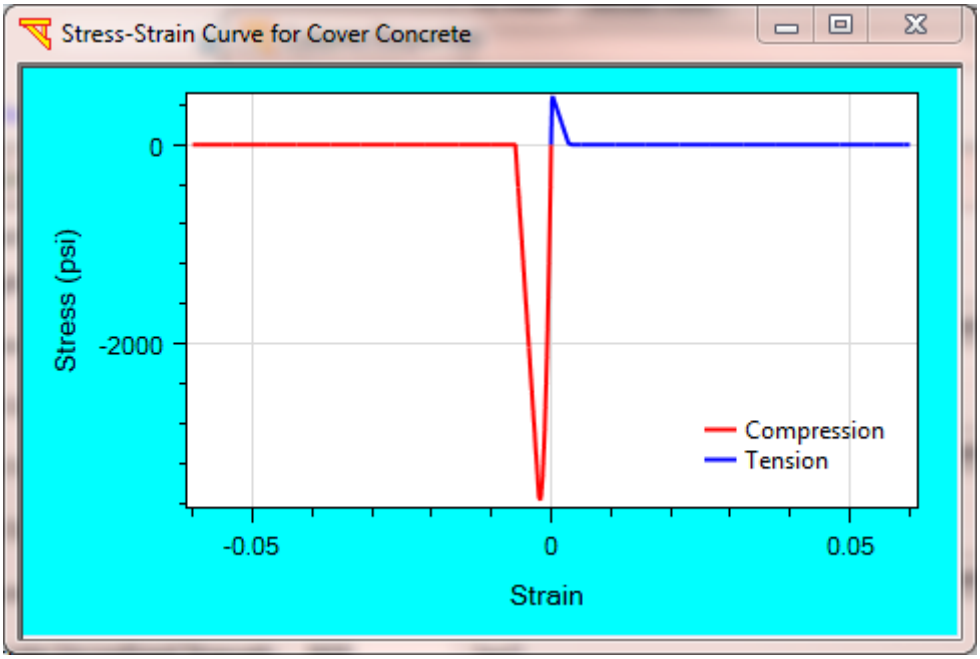

b)

Figure D.1 Stress-strain curves of the Concrete02 material for the OSB1 columns: a) Core (confined); (b) Cover (unconfined)

3) Moment-Curvature Relationship

The moment-curvature response of the column Fiber section obtained from OpenSees is shown in Figure D.2, along with the result from XSECTION for comparison. An axial load of 1333 kip, which is equal to the deadload applied at the column top in the actual case of OSB1, was applied in the moment-curvature analysis.

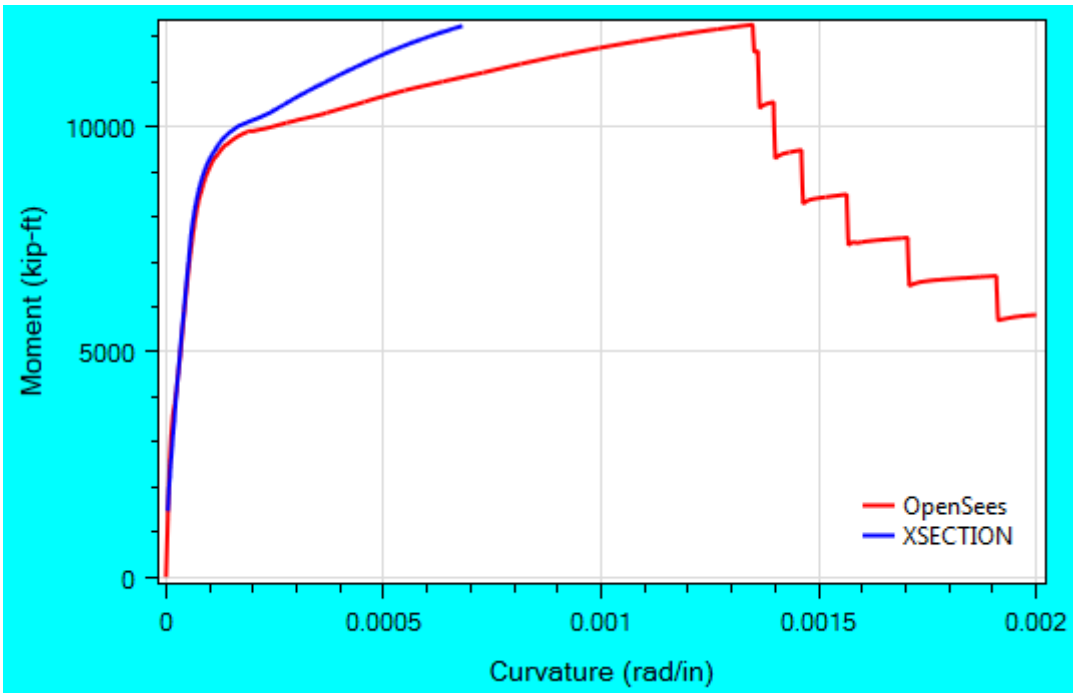

Figure D.2 Moment-curvature relationships of the circular column section for OSB1 (an axial load of 1333 kip was applied)

4) Beam-column element

The forceBeamColumn (BeamWithHinges) element in OpenSees was used to model the column. When the BeamWithHinges element was used, a plastic hinge length (L_p) was required. The calculation of the plastic hinge length for the column was based on Eq. 7.6.2.1-1 of SDC (2013). For each OSB1 Column, the (calculated) plastic hinge length is also the same as that of OSB2 (i.e., L_p = 2.8 ft).

In addition, the column interior section was assumed to be linearly elastic when the BeamWithHinges element was used. Table D-12 shows the material and section properties of the interior elastic section of the BeamWithHinges element.

Table D-12. Material and Section Properties of the Interior Elastic Section for the OSB2 Column

Parameter	Value
Young's modulus (ksi)	3,420
Shear modulus (ksi)	1,425
Unit weight (kcf)	0.15
Area of cross section (ft^2)	23.76
Gross Moment of inertia @ longitudinal axis (ft^4)	44.92
Gross Moment of inertia @ transverse axis (ft^4)	44.92
Cracked Section Property Factor (for Moment of Inertia)	0.35
Torsion constant (ft^4)	89.84

Deck

The material and section properties of the box-girder are listed in Table D-13. The weight of the bridge deck per unit length is 12.5 kip/ft (= 83.3 ft^2 x 0.15 kcf).

Table D-13. OSB1 Deck Material and Section Properties

Parameter	Value
Young's modulus (ksi)	3,420
Shear modulus (ksi)	1,425
Unit weight (kcf)	0.15
Area of cross section (ft^2)	83.3
Moment of inertia @ horizontal axis (ft^4)	444.0
Moment of inertia @ vertical axis (ft^4)	15087.1
Torsion constant (ft^4)	1283

Bentcap

The bentcap is assumed to be rigid. The weight of the bentcap per unit length is 13.5 kip/ft.

Abutment

Three types of abutment models were employed:

i) Roller;

ii) EPP-Gap;

In the EPP-Gap model, a compression-only ElasticPPGap material in OpenSees was used for the longitudinal direction (Figure D.3a). The effective stiffness was 2,591 kip/in and the yield force was -1,555 kip. The longitudinal gap was 0.14 in. Linear elastic behavior was assumed for the abutment transverse and vertical directions. The effective stiffness was 315 kip/in and 83,333 kip/in, respectively, for the transverse and vertical direction.

iii) EPP-Gap with Bearings

Six elastomeric bearing pads (Table D-14) were included in addition to those described in the EPP-Gap model (Aviram et al 2008a). The pad length is 18 in and the pad height is 2.25 in. Figure D.3b shows the longitudinal force-displacement relationship of this abutment model.

Table D-14. Bearing Pad Geometric and Material Properties

Parameter	Value
Young's modulus E (ksi)	5
Shear modulus G (ksi)	0.15
Yield Strain	150% shear strain
Pad length (in)	18
Pad height h (in)	2.25
Lateral Stiffness	GA / h (where A is the cross-section area and h is the pad height)
Hardening Ratio	1%
Vertical Stiffness	EA / h
Vertical Yield Strength (ksi)	2.25

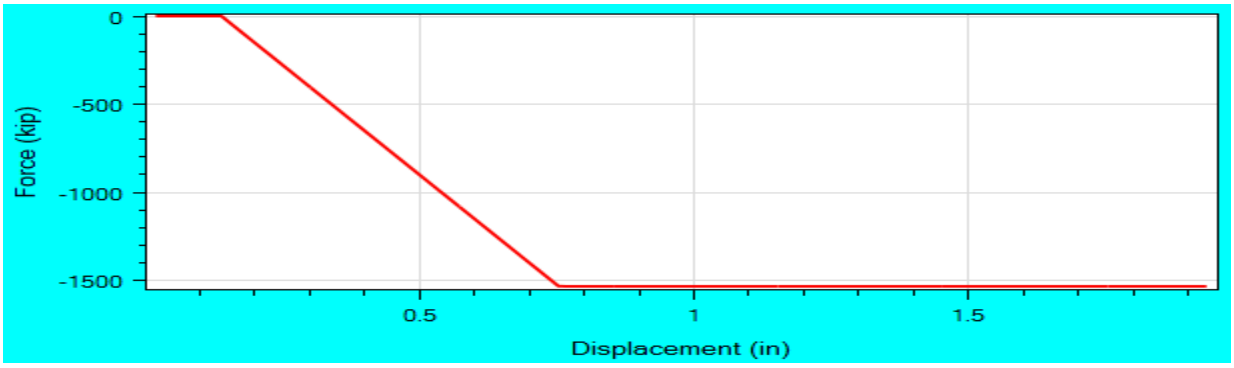

a)

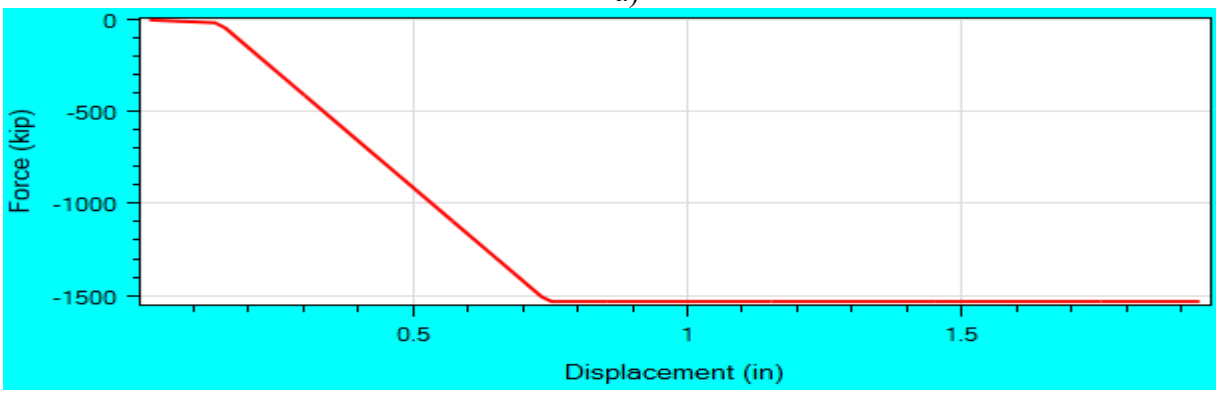

b)

Figure D.3 Abutment longitudinal force-displacement response (due to longitudinal pushover): a) EPP-Gap model; b) EPP-Gap model with Bearings

APPENDIX E: OSB4 MODELING DETAILS

Column

Nonlinear Fiber Section in OpenSees was used to model the circular column section. The reinforced concrete (RC) section properties are listed in Table E-15.

Table E-15. OSB4 Column Reinforced Concrete Properties

Parameter	Value
Number of longitudinal bars	44
Longitudinal bar size (US #)	11
Longitudinal steel %	2
Transverse bar size (US #)	8
Transverse steel %	0.84
Transverse bar spacing (in)	6
Steel unit weight (kcf)	0.49
Steel yield strength (ksi)	66
Steel strain limit	0.06
Concrete unit weight (kcf)	0.15
Concrete unconfined strength (ksi)	4

1) Steel

The ReinforcingSteel material in OpenSees (Table E-16) was used for the longitudinal rebars. A strain limit of 0.06 (shown in Table C-4) was used (for #11 longitudinal rebars according to SDC 2013). Figure E.1 shows the stress-strain curve for the ReinforcingSteel material.

Table E-16. ReinforcingSteel Material Properties Employed for the OSB4 Column

Parameter	Value
Young's modulus (ksi)	29,000
Ultimate stress (ksi)	99
Youngs modulus at initial stress-hardening (ksi)	1,200
Strain at initial stress-hardening	0.0115
Strain at peak stress	0.09

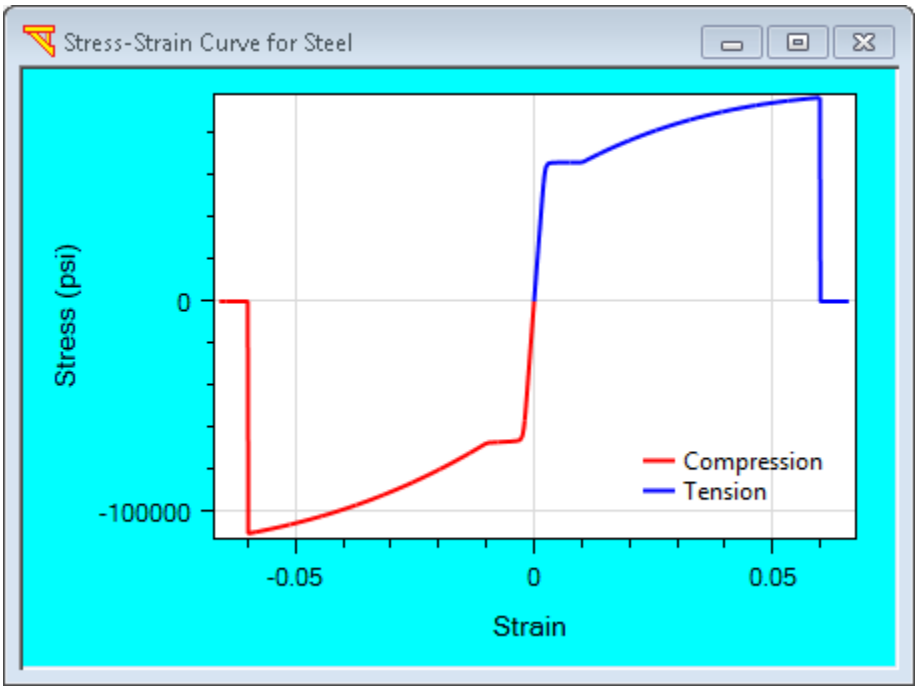

Figure E.1 Stress-strain curve of the ReinforcingSteel material for the OSB4 column

2) Concrete

The Concrete02 material as shown in Table E-17 was used for the cover and core concrete. Figure E.2 shows the stress-strain curve of the Concrete02 material.

Table E-17. Concrete02 Material Properties Employed for the OSB4 Column

Parameter	Core	Cover
Compressive strength (ksi)	-5.549	-4
Strain at maximum strength	-0.0029	-0.002
Crushing strength (ksi)	-5.205	0
Strain at crushing strength	-0.02	-0.006
Ratio between unloading slope	0.1	0.1
Tensile strength (ksi)	0.777	0.56
Tensile softening stiffness (ksi)	268.398	280

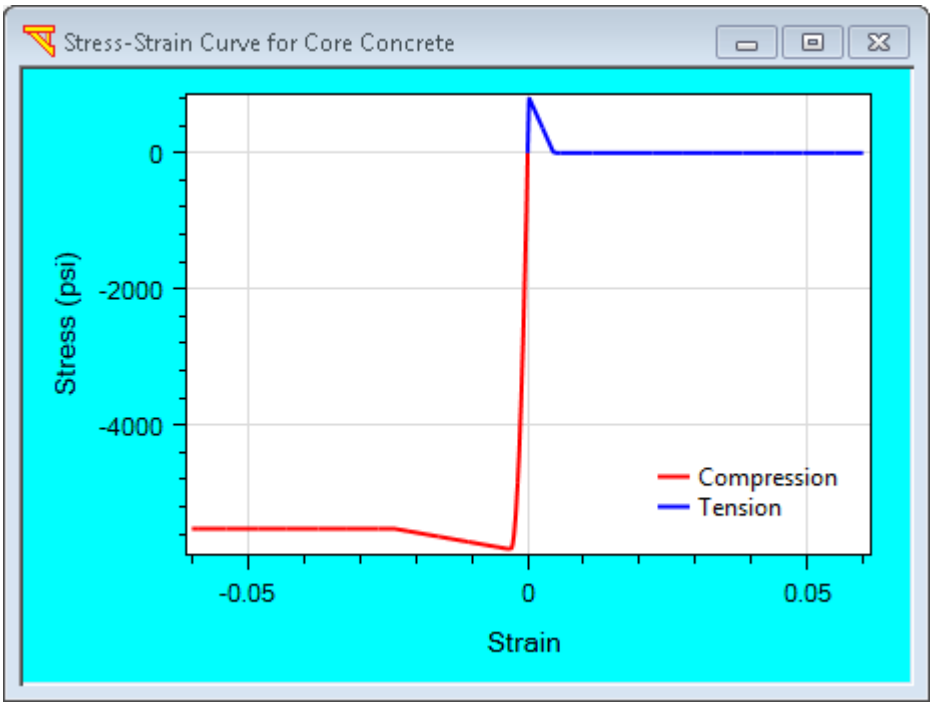

a)

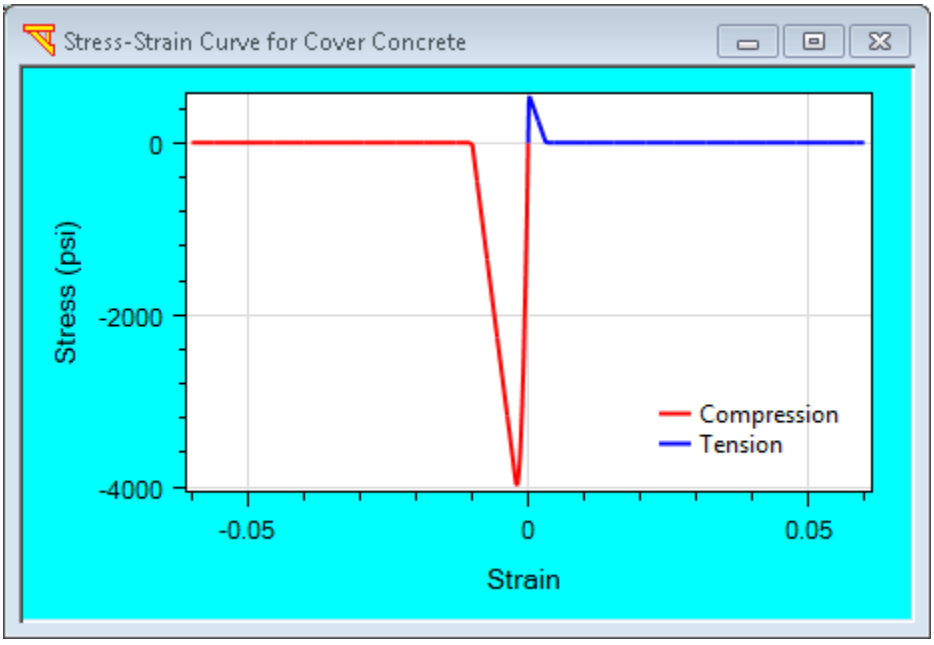

b)

Figure E.2 Stress-strain curves of the Concrete02 material for the OSB4 column: a) Core (confined); (b) Cover (unconfined)

3) Moment-Curvature Relationship

The moment-curvature response of the column Fiber section obtained from **OpenSees** is shown in Figure C.3, along with the result from **XSECTION** for comparison. An axial compressive load of 1600 kip, which is equal to the deadload applied at the column top in the actual case of OSB4, was applied in the moment-curvature analysis.

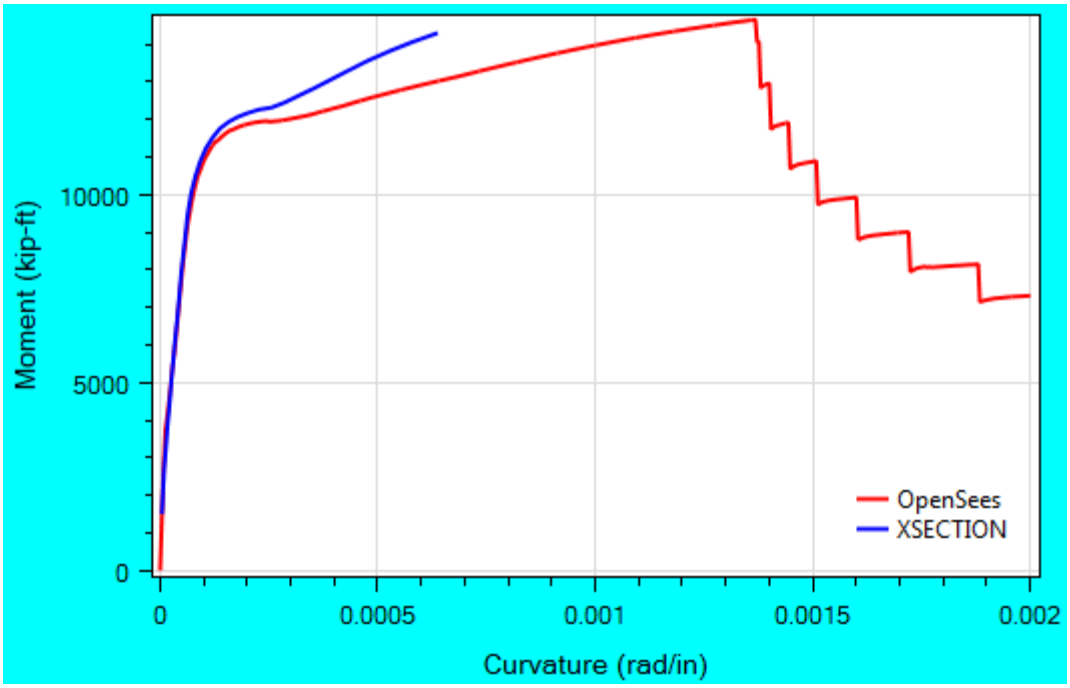

Figure E.3 Moment-curvature relationships of the circular column section for OSB4 (an axial compressive load of 1600 kip was applied)

4) Beam-column element

The forceBeamColumn (with the distributed plasticity integration method) element in **OpenSees** was used to model the column.

Deck

The material and section properties of the box-girder are listed in Table E-18. The weight of the bridge deck per unit length is 8.785 kip/ft (= 58.56 ft^2 x 0.15 kcf).

Table E-18. OSB4 Deck Material and Section Properties

Parameter	Value
Young's modulus (ksi)	3,420
Shear modulus (ksi)	1,425
Unit weight (kcf)	0.15
Area of cross section (ft^2)	58.56
Moment of inertia @ horizontal axis (ft^4)	353.39
Moment of inertia @ vertical axis (ft^4)	6359.8
Torsion constant (ft^4)	800

Isolation Bearings

There are 2 isolation bearings at column top as well as at each abutment. The isolation bearing properties (which were provided by Caltrans) are shown in Table E-19 and Table E-20.

Table E-19. OSB4 Bent Isolation Bearing Material Properties

Parameter	Value
Yield strength (kip)	74.8
Initial elastic stiffness (kip/in)	74.8
Post-yield stiffness ratio	0.1981

Table E-20. OSB4 Abutment Isolation Bearing Material Properties

Parameter	Value
Yield strength (kip)	37.4
Initial elastic stiffness (kip/in)	37.4
Post-yield stiffness ratio	0.1981

Abutment

Two types of abutment models were employed.

i) Roller with Isolation Bearings;

ii) EPP-Gap with Isolation Bearings;

In the EPP-Gap with Isolation Bearings model, a compression-only MultiLinear Plastic (Nonlinear) was used for the longitudinal direction of the abutment. The effective stiffness is 2,024.64 kip/in and the yield force is -1,282 kip. The longitudinal gap is 9 in.

A compression-only MultiLinear Plastic (Nonlinear) was also used for the transverse direction of the abutment. The effective stiffness is 100 kip/in and the yield force is -179.4 kip. The gap is 1 in. The vertical direction is fixed.

ESA

The ESA was conducted in the longitudinal and transverse directions. Figure C.6 shows the acceleration response spectrum (ARS) used in the ESA of OSB2 and OSB1.

APPENDIX F: OSB3 MODELING DETAILS

Column

The single-bent in OSB3 is composed of two circular reinforced concrete columns. Each column is 16 ft high with a diameter of 66 in. The columns are fixed at top and pinned at the base. Nonlinear Fiber Section in OpenSees was used to model the circular column section. The reinforced concrete (RC) section properties are listed in Table F-21.

Table F-21. OSB3 Column Reinforced Concrete Properties

Parameter	Value
Number of longitudinal bars	44
Longitudinal bar size (US #)	11
Longitudinal steel %	2
Transverse bar size (US #)	8
Transverse steel %	0.84
Transverse bar spacing (in)	6
Steel unit weight (kcf)	0.49
Steel yield strength (ksi)	66
Steel strain limit	0.06
Concrete unit weight (kcf)	0.15
Concrete unconfined strength (ksi)	4

1) Steel

Thus, the ReinforcingSteel material in OpenSees (Same as OSB4 as shown in Table E-16 and Figure E.1) was used for the longitudinal rebars. A strain limit of 0.06 (shown in Table F-21) also was used (for #11 longitudinal rebars according to SDC 2013).

2) Concrete

The Concrete02 material as shown in Table F-22 was used for the cover and core concrete. Figure F.1 shows the stress-strain curve of the Concrete02 material.

Table F-22. Concrete02 Material Properties Employed for the OSB3 Column

Parameter	Core	Cover
Compressive strength (ksi)	-5.556	-4
Strain at maximum strength	-0.0029	-0.002
Crushing strength (ksi)	-5.215	0
Strain at crushing strength	-0.021	-0.006
Ratio between unloading slope	0.1	0.1
Tensile strength (ksi)	0.778	0.56
Tensile softening stiffness (ksi)	268.398	280

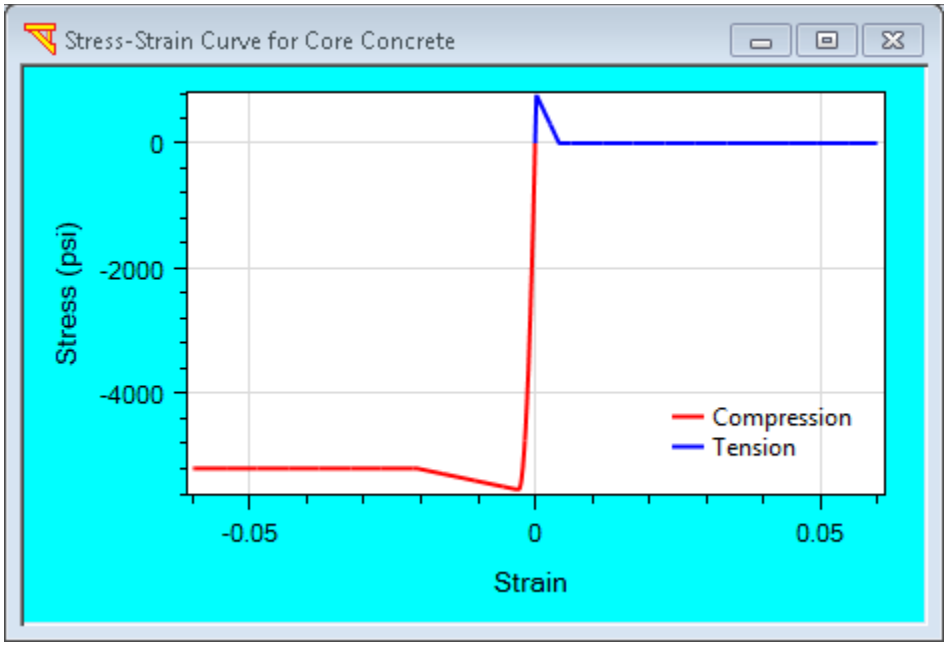

a)

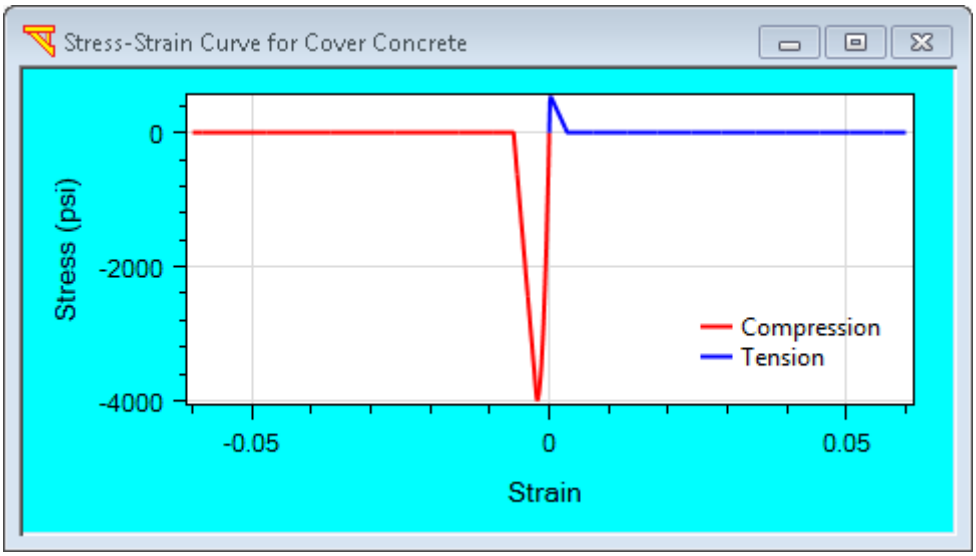

b)

Figure F.1 Stress-strain curves of the Concrete02 material for the OSB3 columns: a) Core (confined); (b) Cover (unconfined)

3) Moment-Curvature Relationship

The moment-curvature response of the column Fiber section obtained from OpenSees is shown in Figure F.2, along with the result from XSECTION for comparison. An axial load of 1000 kip, which is equal to the deadload applied at the column top in the actual case of OSB3, was applied in the moment-curvature analysis.

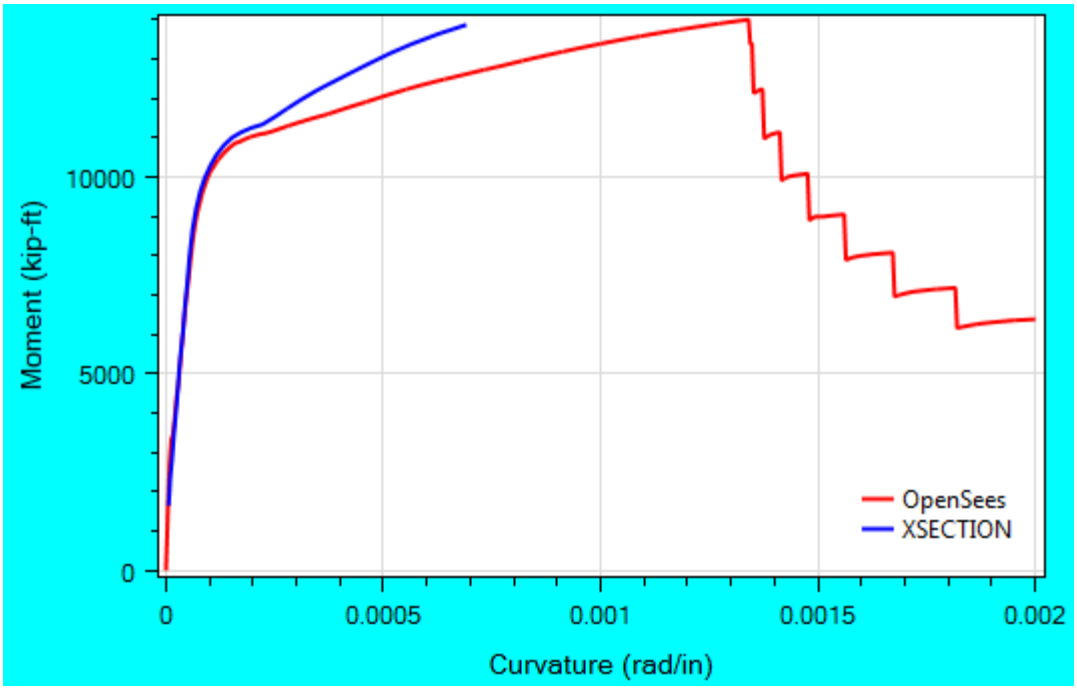

Figure F.2 Moment-curvature relationships of the circular column section for OSB3 (an axial load of 1000 kip was applied).

4) Beam-column element

The forceBeamColumn element (with the distributed plasticity integration method) in OpenSees was used to model the column.

Deck

The material and section properties of the box-girder are listed in Table D-13. The weight of the bridge deck per unit length is 10.95 kip/ft (= 73 ft^2 x 0.15 kcf).

Bentcap

The bentcap is assumed to be rigid. The weight of the bentcap per unit length is 11.39 kip/ft.

Table F-23. OSB1 Deck Material and Section Properties

Parameter	Value
Young's modulus (ksi)	3,420
Shear modulus (ksi)	1,425
Unit weight (kcf)	0.15
Area of cross section (ft^2)	73
Moment of inertia @ horizontal axis (ft^4)	364.51
Moment of inertia @ vertical axis (ft^4)	12727.11
Torsion constant (ft^4)	880.48

Isolation Bearings

There are 2 isolation bearings at column top as well as at each abutment. The isolation bearing properties (provided by Caltrans) are shown in Table F-24 and Table F-25.

Table F-24. OSB3 Bent Isolation Bearing Material Properties

Parameter	Value
Yield strength (kip)	74.8
Initial elastic stiffness (kip/in)	74.8
Post-yield stiffness ratio	0.1981

Table F-25. OSB3 Abutment Isolation Bearing Material Properties

Parameter	Value
Yield strength (kip)	37.4
Initial elastic stiffness (kip/in)	37.4
Post-yield stiffness ratio	0.1981

Abutment

Two types of abutment models were employed.

i) Roller with Isolation Bearings;

ii) EPP-Gap with Isolation Bearings;

In the EPP-Gap with Isolation Bearings model, a compression-only MultiLinear Plastic (Nonlinear) was used for the longitudinal direction of the abutment. The effective stiffness is 2,572 kip/in and the yield force is -1,629 kip. The longitudinal gap is 9 in.

A compression-only MultiLinear Plastic (Nonlinear) was also used for the transverse direction of the abutment. The effective stiffness is 100 kip/in and the yield force is -179.4 kip. The gap is 1 in. The vertical direction is fixed.

ESA

The ESA was conducted in the longitudinal and transverse directions. Figure C.6 shows the acceleration response spectrum (ARS) used in the ESA of OSB3.

APPENDIX G: OPENSEES AND CSIBRIDGE COMPARISON

This section presents modeling of OSB2 and OSB1 using CSiBridge (CSI 2015a) and MSBridge. Roller abutment model was assumed. Linear and nonlinear response was addressed.

G.1 Linear Response

G.1.1 OSB2 Linear Response

Figure G.1 shows the models of OSB2 created in CSiBridge and MSBridge. As shown in Figure G.1, two equal-length elements were used for the column (the column height is 20 ft). Both column top and base are fixed. The offset between the column top and the deck is not considered at this point (to maintain similarity between the two modeling techniques). No rotation around the bridge longitudinal direction is allowed for the deck (at the abutments).

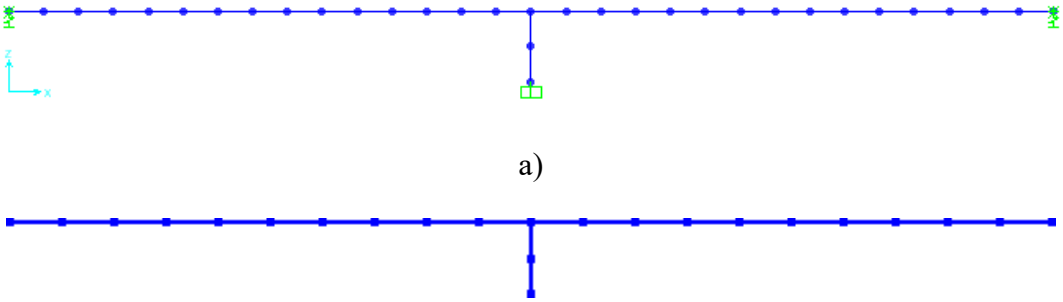

a)

b)

Figure G.1 OSB2 model (side view): (a) CSiBridge; (b) MSBridge

G.1.1.1 OSB2 Pushover Analysis

G.1.1.1.1 Pushover in the Longitudinal Direction

Three cases were studied: i) soft deck (i.e., cantilever column response; ii) rigid deck (i.e., fixed-fixed column response); and iii) actual deck stiffness (column boundary condition at the deck is compliant to some degree as dictated by the effective overall deck stiffness, its length to the abutments, and its boundary condition at the abutments). The soft deck case is equivalent to a cantilever beam while the rigid deck case is equivalent to a beam with both end fixed. A load of 1000 kip was applied at the column top along the longitudinal direction.

Table G-26 shows the effective column stiffness calculated based on observed shear force and column top longitudinal displacement obtained from the pushover analysis. The values in the "Theoretical" column in Table G-26 are based on the elastic solution (cantilever stiffness $3EI/L^3$ and fixed-fixed condition stiffness $12EI/L^3$ of a bending beam). It can be seen that CSiBridge and

OpenSees match the elastic solution for the linear case.

Table G-26. Effective Column Stiffness in the Longitudinal Direction for OSB2

Deck Type	Effective Column Stiffness (kip/in)		
	CSiBridge*	OpenSees	Theoretical
Soft Deck	855	855	855
Rigid Deck	3,425	3,425	3,425
Actual Deck	2,212	2,212	N/A

*Zero shear areas for column were assumed (use of the shear area values provided for use in CSiBridge makes a difference of about 5%).

G.1.1.1.2 Pushover in the Transverse Direction

Similarly, 3 cases were analyzed. A load of 1000 kip was applied at the column top along the transverse direction. Table G-27 shows the effective column stiffness calculated in the transverse pushover analysis. Again, this shows that CSiBridge and OpenSees match the elastic solution for the linear case.

Table G-27. Effective Column Stiffness in the Transverse Direction for OSB2

Deck Type	Effective Column Stiffness (kip/in)		
	CSiBridge	OpenSees	Theoretical
Soft Deck	855	855	855
Rigid Deck*	3,425	3,425	3,425
Actual Deck*	1,575	1,575	N/A

*No rotation around the bridge longitudinal direction was assumed for the deck.

G.1.1.2 OSB2 Linear Time History Analysis

Input motion ROCKS1N1 (bottom graph of Figure G.2) was employed in the longitudinal and transverse directions (For more information about the input motions, please see Appendix B).

Rayleigh damping was used with a 5% damping ratio (defined at periods of 0.889 and 0.692 second) in the THA. For the time integration scheme, the Newmark's average acceleration method ($\gamma = 0.5$ and $\beta = 0.25$) was employed. The analysis time step was 0.005 second (same as the time step of the input motion).

Figure G.2 shows the bridge deck longitudinal acceleration and displacement response time histories at column top (Figure G.3 shows the transverse response). In this case, the columns are assumed to be linearly elastic and the abutment has no longitudinal resistance (Roller-type).

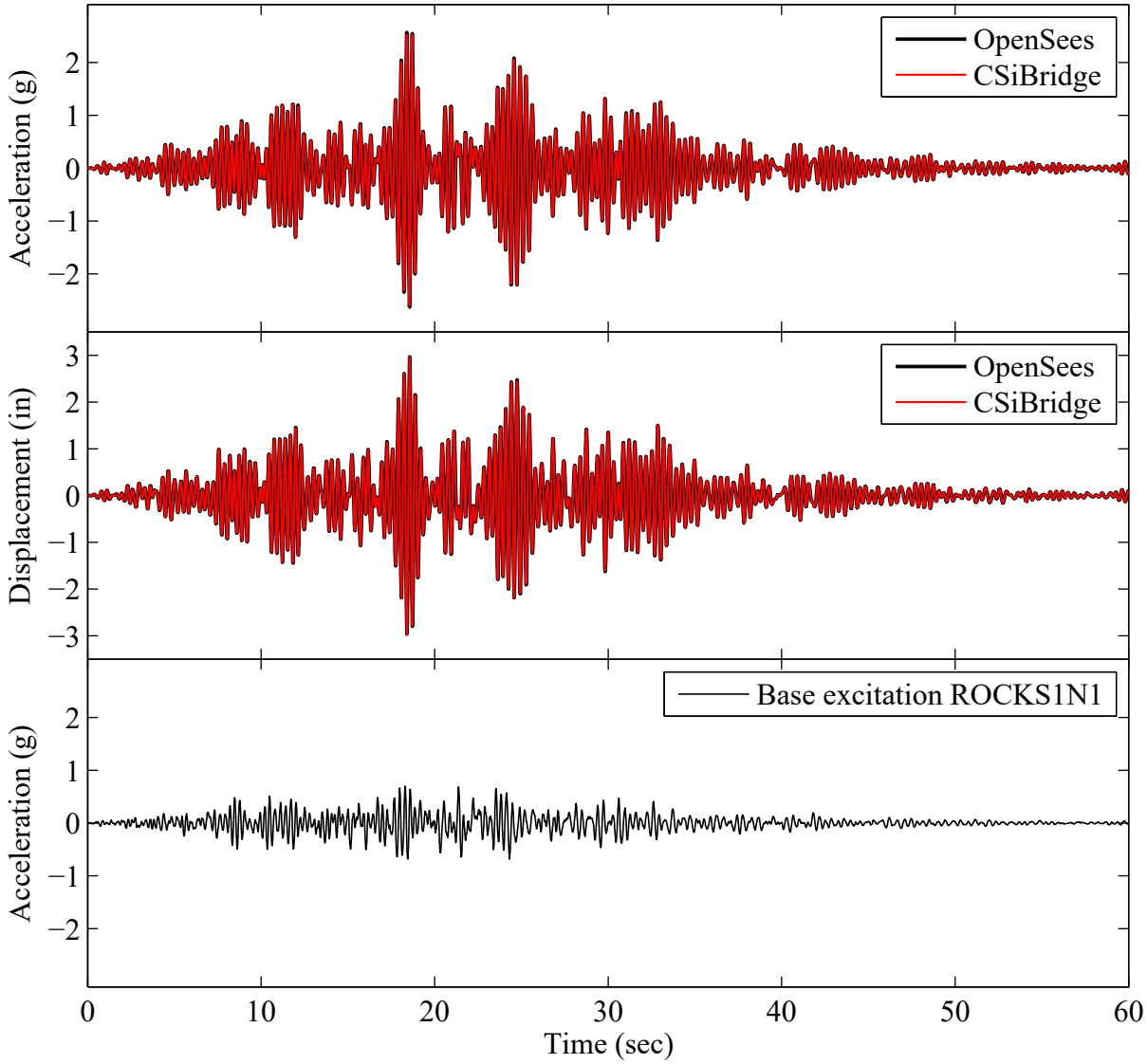

Figure G.2 Longitudinal acceleration (top graph) and displacement (middle graph) response time histories at column top for OSB2

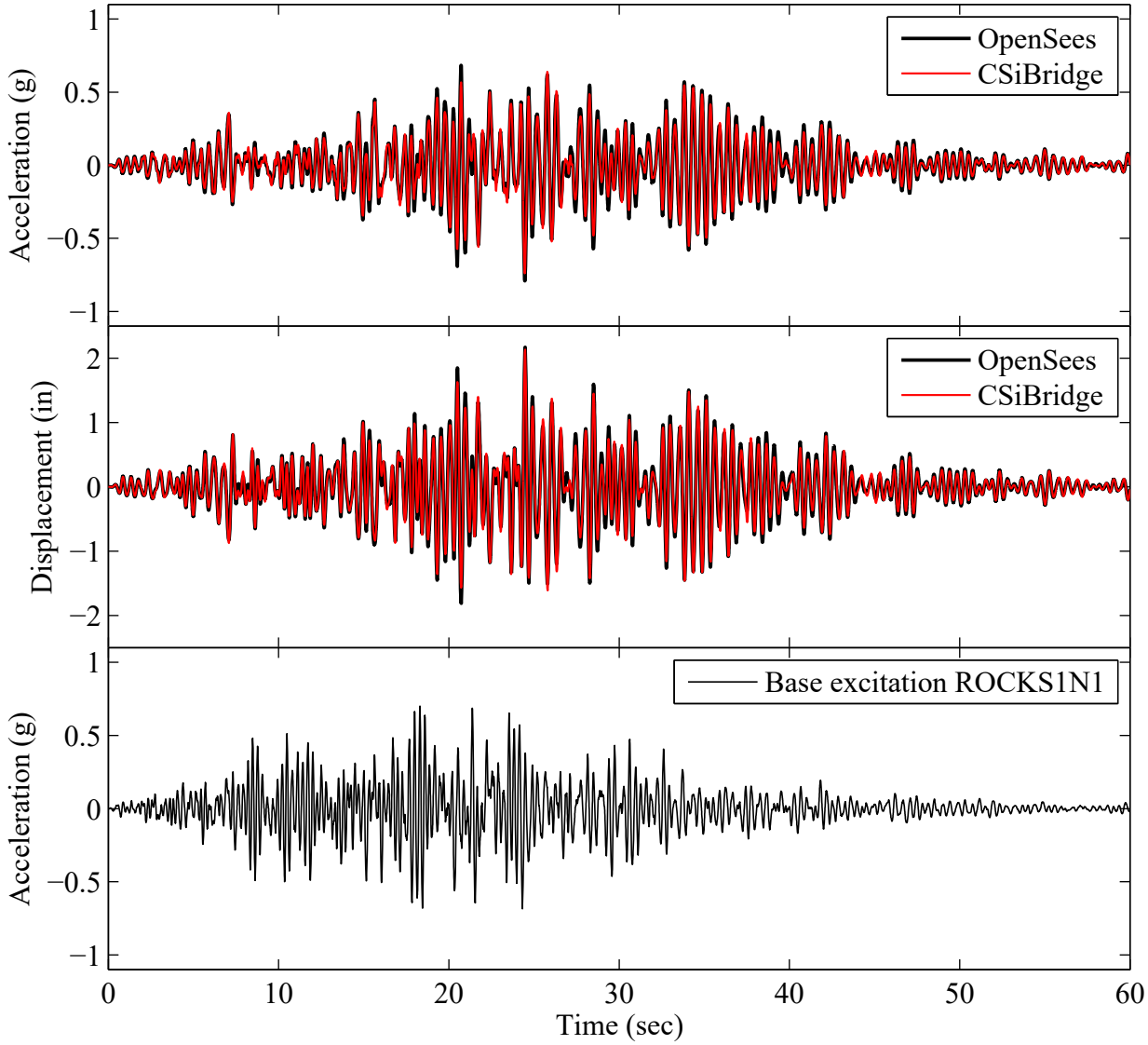

Figure G.3 Transverse acceleration (top graph) and displacement (middle graph) response time histories at column top for OSB2

G.1.2 OSB1 Linear Response

OSB1 was modeled using CSiBridge and MSBridge. Please see Appendix D for the employed modeling techniques and associated model properties. Figure G.4 shows the models of OSB1 created in CSiBridge and MSBridge, respectively. The offset (3 ft) between column top and the deck was not represented in this study.

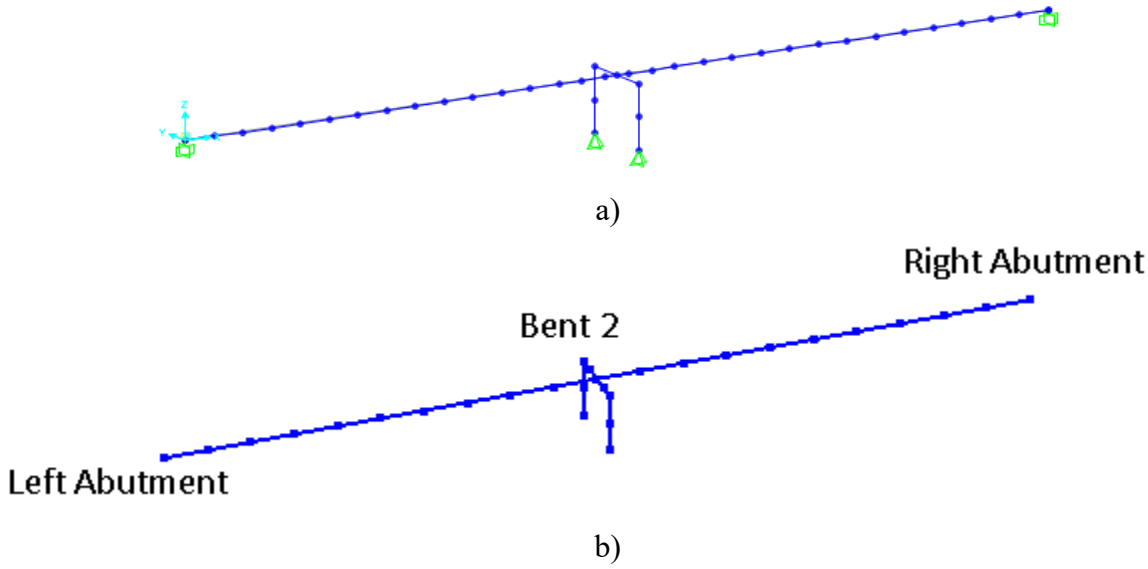

Figure G.4 OSB1 model (3D view) created in: a) CSiBridge; b) MSBridge

G.1.2.1 OSB1 Pushover Analysis

G.1.2.1.1 Pushover in the Longitudinal Direction

Two cases were studied: i) rigid deck (i.e., fixed-fixed column response); and ii) actual deck stiffness (column boundary condition at the deck is compliant to some degree as dictated by the effective overall deck stiffness, its length to the abutments, and its boundary condition at the abutments). The rigid deck case is equivalent to a beam with both end fixed. A load of 1000 kip was applied at the bent top (deck center) along the longitudinal direction.

Table G-28 shows the effective column stiffness calculated based on observed shear force and column top longitudinal displacement obtained from the pushover analysis. The values in the "Theoretical" column in Table G-28 are based on the elastic solution (cantilever stiffness $3EI/L^3$). The result shows CSiBridge and OpenSees match the elastic solution for the linear case.

Table G-28. Effective Column Stiffness in the Longitudinal Direction for OSB1

Deck Type	Effective Column Stiffness (kip/in)		
	CSiBridge*	OpenSees	Theoretical
Rigid Deck	682.5	682.5	682.5
Actual Deck	389.7	390.0	N/A

*Zero shear areas for columns were assumed (use of the shear area values provided for use in CSiBridge makes a difference of about 5%).

G.1.2.1.1 Pushover in the Transverse Direction

Similarly, 2 cases were also analyzed. A load of 1000 kip was applied at the column top along the transverse direction. Table G-29 shows the effective column stiffness calculated in the transverse pushover analysis. Again, the result shows CSiBridge and OpenSees match the elastic solution for the linear case.

Table G-29. Effective Column Stiffness in the Transverse Direction for OSB1

Deck Type	Effective Column Stiffness (kip/in)		
	CSiBridge*	OpenSees	Theoretical
Rigid Deck	682.5	682.5	682.5
Actual Deck	657.3	657.5	N/A

*No rotation around the bridge longitudinal direction was assumed for the deck.

G.1.2.2 OSB1 Linear Time History Analysis

Input motion ROCKS1N1 (bottom graph of Figure G.5) was employed in the longitudinal and transverse directions (For more information about the input motions, please see Appendix B). Rayleigh damping was used with a 5% damping ratio (defined at periods of 1.2 and 0.7 second) in the THA. For the time integration scheme, the Newmark's average acceleration method (γ = 0.5 and β = 0.25) was employed. The analysis time step was 0.005 second (same as the time step of the input motion).

Figure G.5 shows the bridge deck longitudinal acceleration response time histories at column top (Figure G.6 shows the transverse response). In this case, the columns are assumed to be linearly elastic and the abutment has no longitudinal resistance.

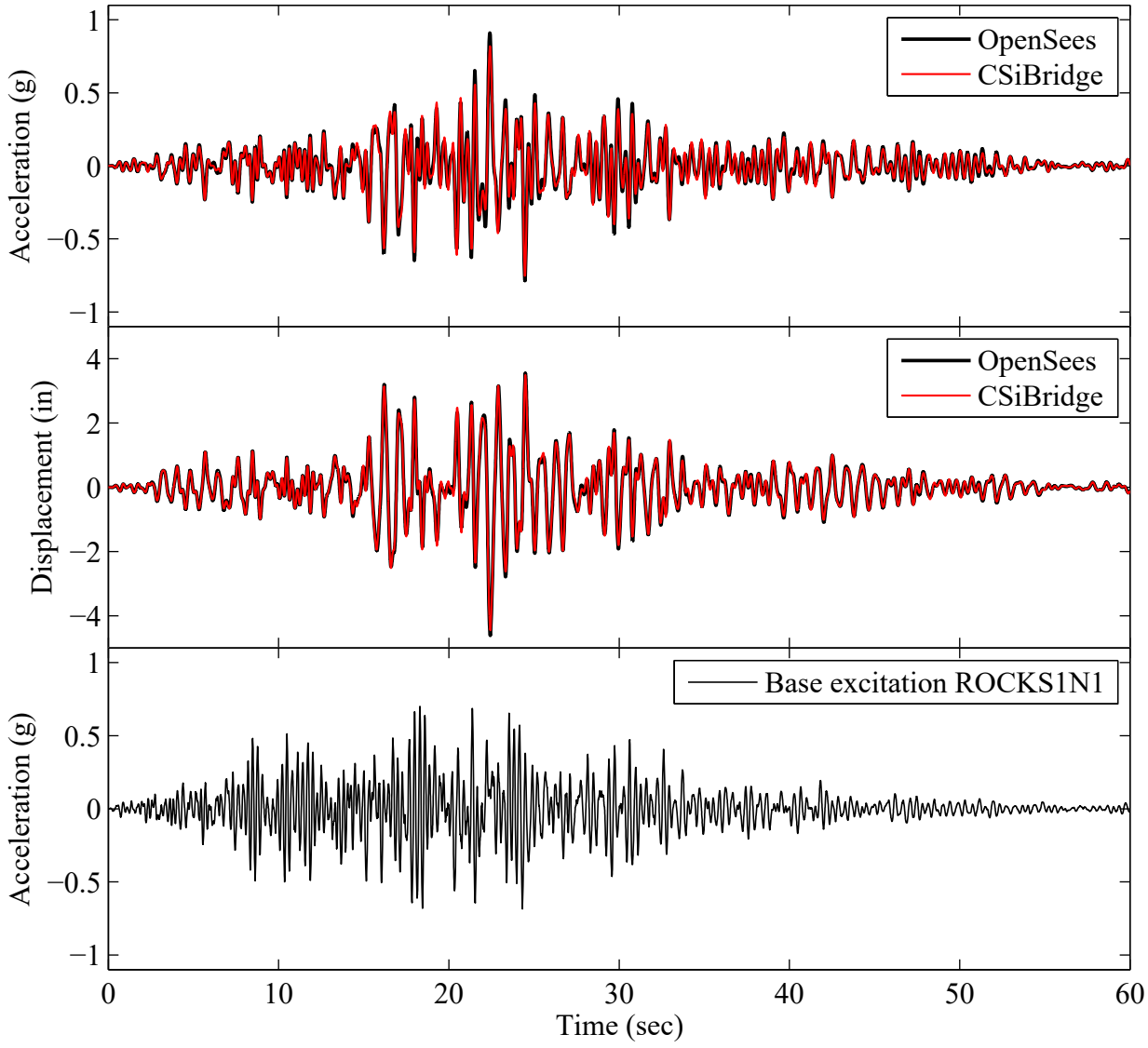

Figure G.5 OSB1 deck longitudinal acceleration (top graph) and displacement (middle graph) response time histories

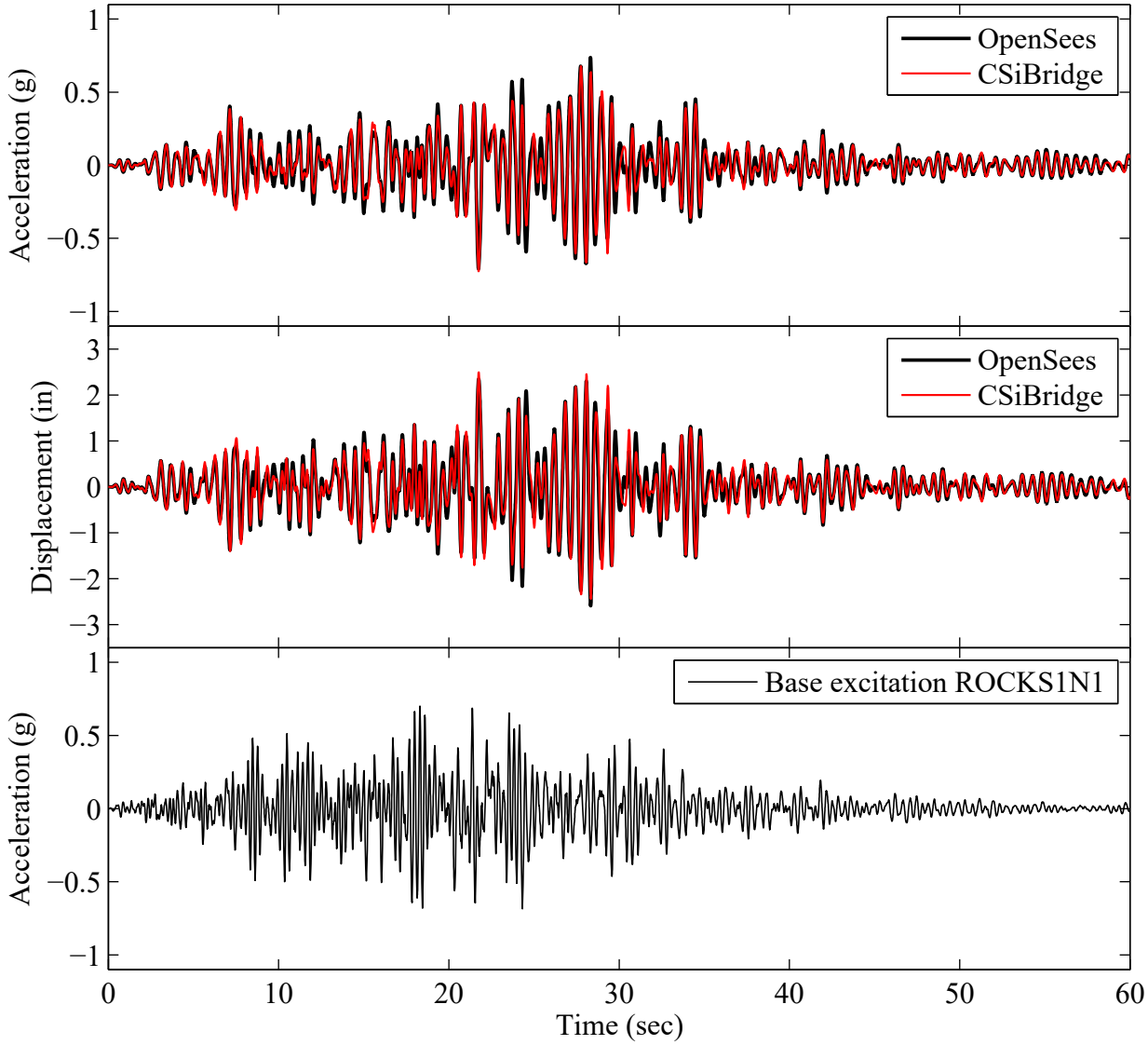

Figure G.6 OSB1 deck transverse acceleration (top graph) and displacement (middle graph) response time histories

G.2 Nonlinear Response

G.2.1 OSB2 Nonlinear Response

G.2.1.1 Pushover Analysis of OSB2 Single Column

In this section, only the OSB2 single column was studied (deck was not considered). The column height is 20 ft in this essentally fixed-fixed single column model. An axial compressive load of 1991 kip, which is equal to the deadload applied at the column top in the actual case of OSB2,

was applied before applying the horizontal pushover displcement. A horizontal pushover displacement of 20 inches was applied at the column top in 500 steps.

Figure G.7 shows the moment-curvature relationships of the circular column section obtained from OpenSees, CSiBridge and xSection (Caltrans 1999). An axial compressive load of 1991 kip was applied for this moment-curvature analysis.

Figure G.8 shows the column force-displacement responses from OpenSees and CSiBridge analyses. Figure G.8a shows the plot up to 20 in of pushover displacement while Figure G.8b shows the plot only up to 2 in of pushover displacement (for clarity). A line with a slope of k = 3,425 kip/in (which is equal to the linear fixed-fixed condition stiffness $12EI/L^3$ of a bending beam) as well as a line with a slope of 0.35 k (factor currently spcified for cracked section) are also included in the figure for reference. In addition to the OpenSees force-based fiber element (forceBeamColumn), the BeamWithHinges element (Scott and Fenves 2006; Scott and Ryan, 2013) was also used in the reported OpenSees analysis.

1) Column shear strength

First, it is noted that hinge "*Location*" as used in CSiBridge and hinge "*Length*" as implemented in the OpenSees element beam-column "with Hinges" are two different things, not related in any straightforward way. Because the OpenSees formulation represents the hinge at the element ends (nodes), a closer CSiBridge match to shear strength can be achieved if hinge "*Location*" in CSiBridge is essentially defined as zero or a very small number such as 0.1 ft for instance. Large values of hinge location (e.g., 2.8 ft as currently specified) cause the hinges to reduce the effective fixed-fixed column height from the original 20 ft to 20-2x2.8 = 14.4 ft.

2) Initial column stiffness

Initial column stiffness appears also to be different between CSiBridge and OpenSees. CSiBridge appears to reduce the initial stiffness much more than expected (please see Figure G.8a and Figure G.8b). The report by Aviram et al. (2008b) also discussed a similar finding (see page 34). Of relevance as well, the CSi Knowledge Base (2015b) website https://wiki.csiamerica.com/display/kb/Elastic+softening+from+fiber+hinges also discusses the elastic softening behavior from fiber hinges:

*"**Question**: Fiber hinges seem to introduce artificial flexibility to the model, though hinges are a plastic mechanism which should not influence elastic behavior. Is it possible to implement fiber hinges without introducing softening?*

***Answer**: This softening behavior may be attributed to calculation of the fiber-hinge response curve, which proceeds directly from the axial response of individual section fibers. During linear response, fiber elasticity is added to element elasticity, causing softening. To avoid elastic softening, users should divide frame members at hinge locations such that a smaller segment is positioned along the hinge length. A large area property modifier should then be assigned to small sections, using the Assign > Frame > Property Modifiers menu."*

As such, for this report, only OpenSees was used to conduct time history analysis (as present in Chapters 2 & 3).

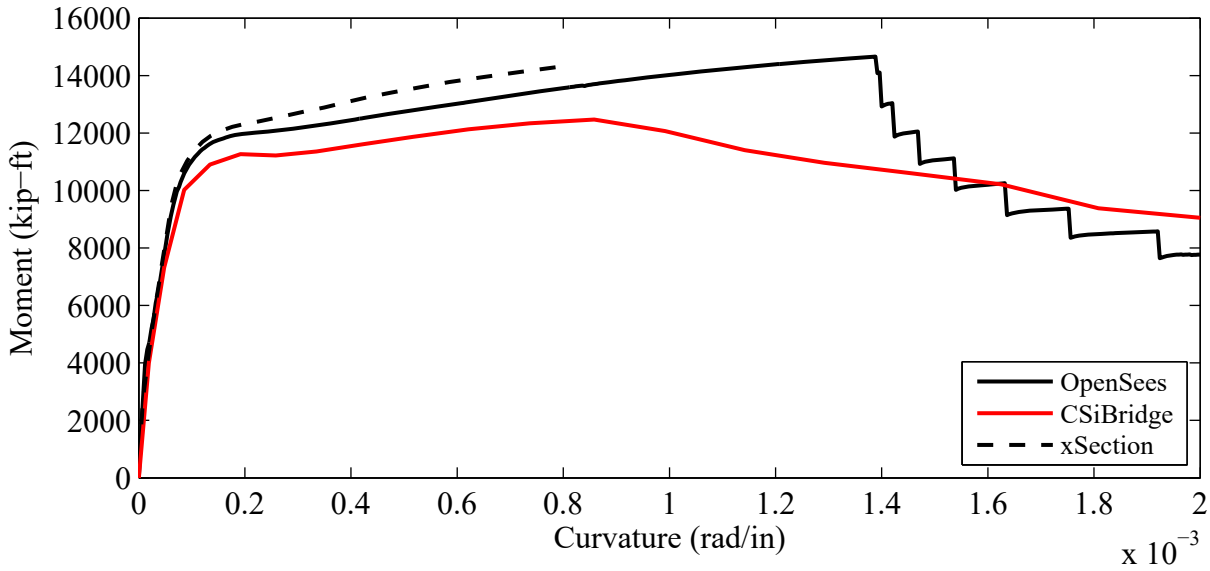

Figure G.7 Moment-curvature relationships of the fixed-fixed circular column section (axial compressive load = 1991 kip)

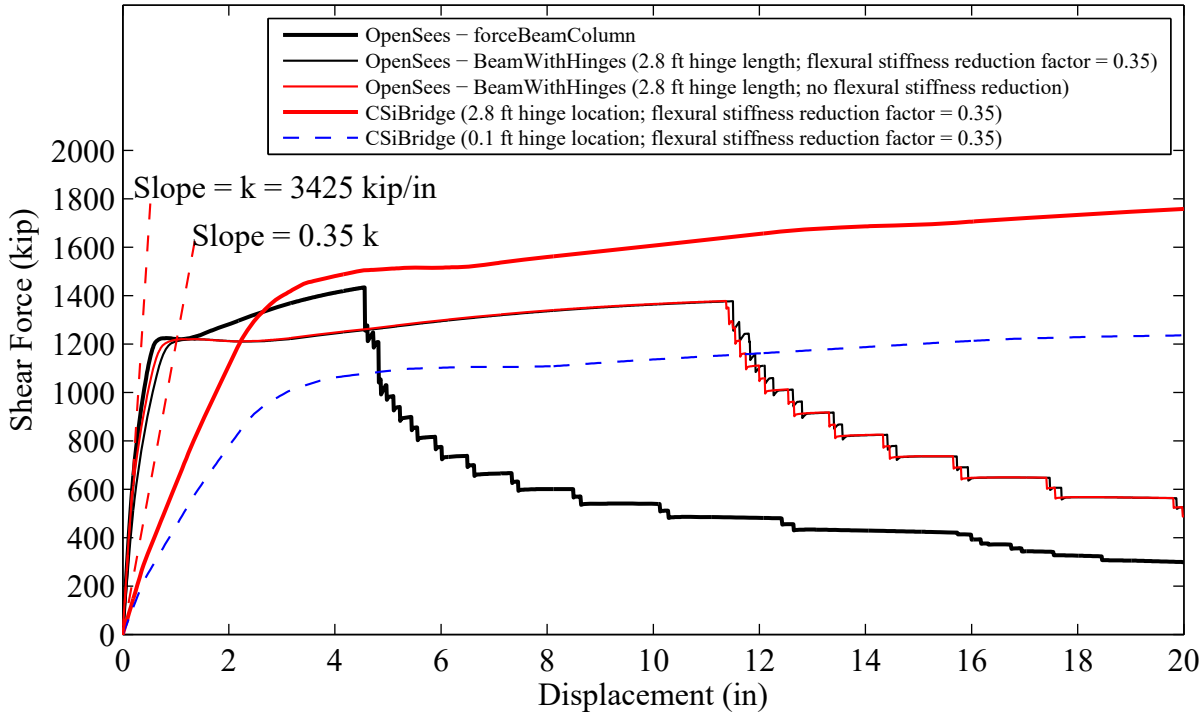

a)

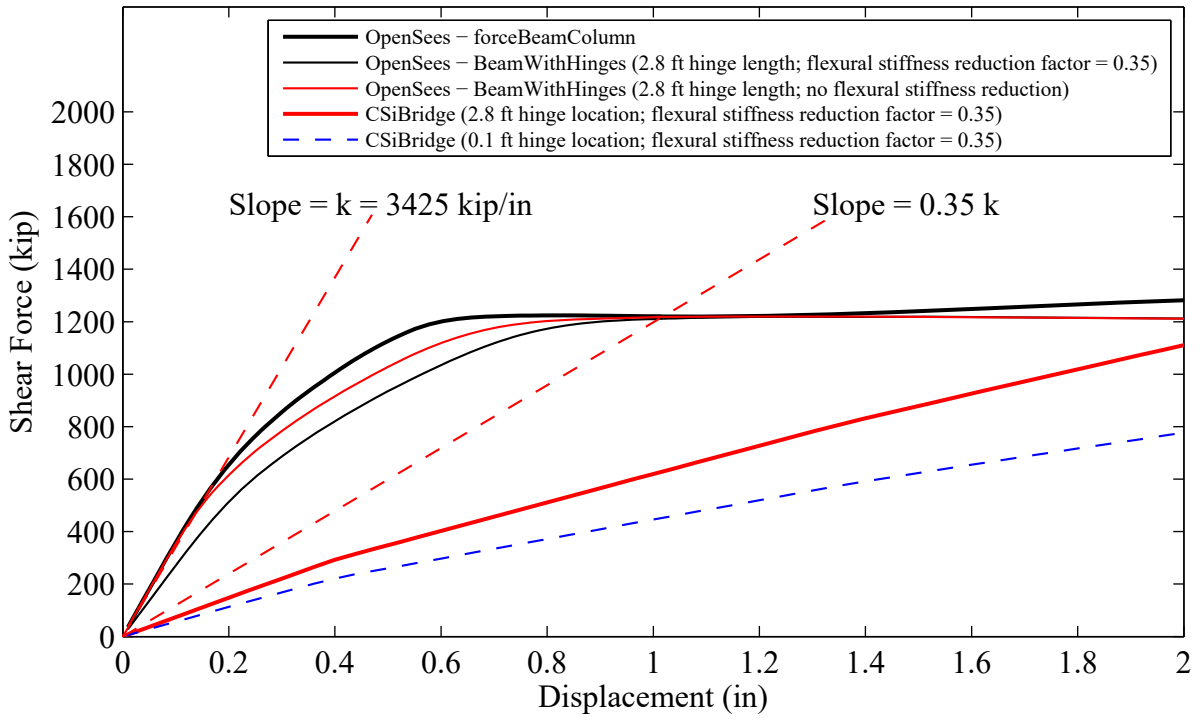

b)

Figure G.8 OSB2 column top force-displacement response: a) plot up to 20 in of pushover displacement; b) plot up to 2 in of pushover displacement

G.2.1.2 Pushover Analysis of OSB2 (Whole Model)

In this case, the roller abutment model was employed. The nonlinear column response was considered and the cracked section properties were employed for the elastic section (a cracked section property factor of 0.35 was used). Dead load was applied in this case.

G.2.1.2.1 Pushover in the Longitudinal Direction

A pushover displacement of 20 inches was applied at the column top along the longitudinal direction (in 500 steps). Figure G.9 shows the column force-displacement responses from OpenSees, along with the CSiBridge results for comparison (2.8 ft plastic hinge length in OpenSees, and 2.8 ft hinge location in CSiBridge).

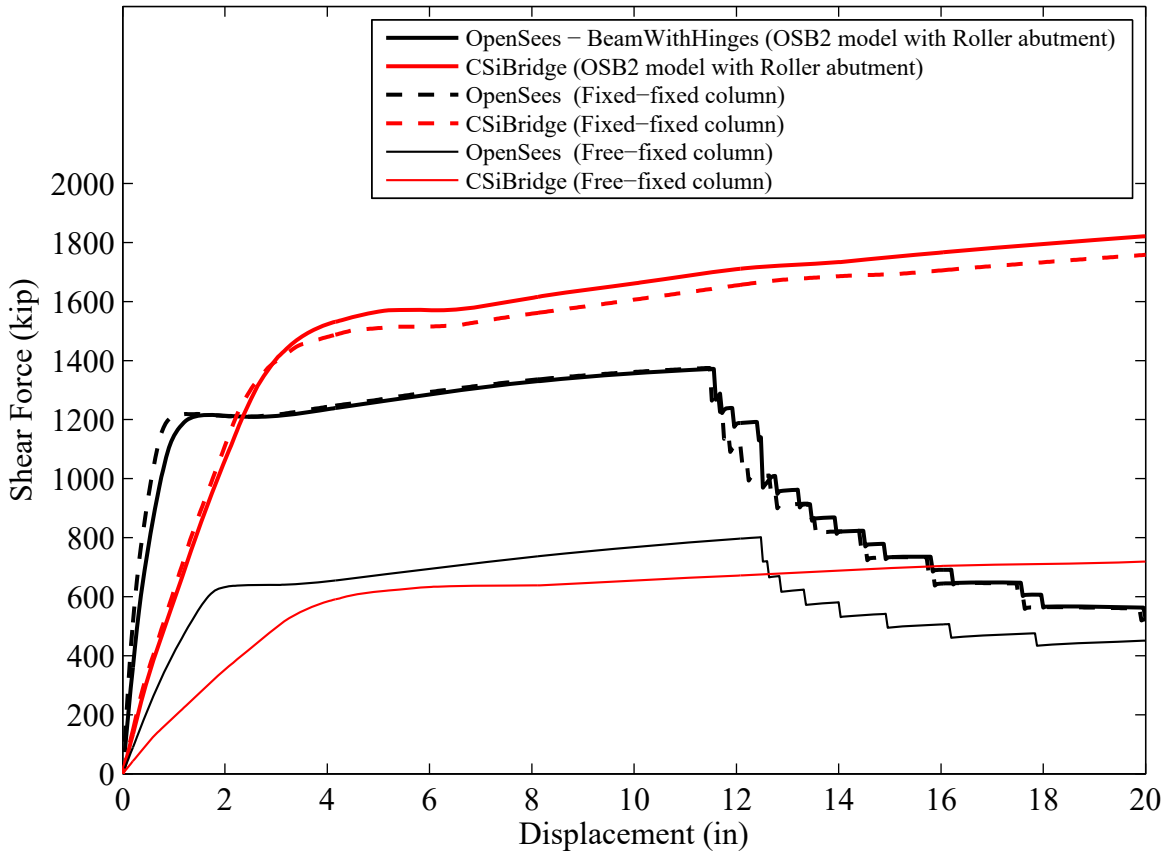

Figure G.9 Column top force-displacement responses (flexural stiffness reduction factor = 0.35; plastic hinge length = 2.8 ft for OpenSees and hinge location = 2.8 ft for CSiBridge)

G.2.1.2.1 Pushover in the Transverse Direction

A pushover displacement of 20 inches was applied at the column top along the transverse direction (in 500 steps).

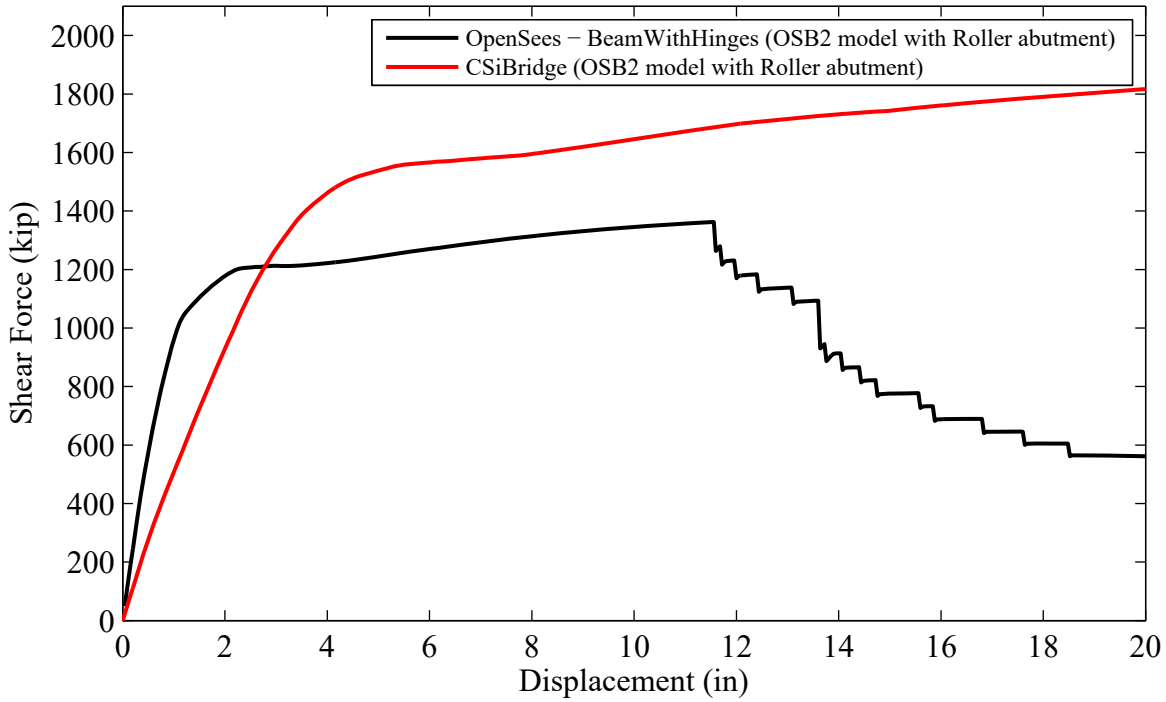

Figure G.10 Column top transverse force-displacement responses (flexural stiffness reduction factor = 0.35; plastic hinge length = 2.8 ft for OpenSees and hinge location = 2.8 ft for CSiBridge)

G.2.1.2 OSB2 Nonlinear Time History Analysis

Nonlinear THA was conducted for OSB2 in CSiBridge and OpenSees. Motion 1 ROCKS1N1 was employed. Rayleigh damping was used with a 5% damping ratio (defined at periods of 0.889 and 0.692 second) in the nonlinear THA. For the time integration scheme, the Newmark's average acceleration method (γ = 0.5 and β = 0.25) was employed. A variable time-stepping scheme was used in the analysis. The initial time step at each step was 0.005 second (same as the time step of the input motion) and the minimum time step was 5 $\times 10^{-5}$ second (upon splitting of time step).

Figure G.11 shows the column top longitudinal acceleration and displacement response time histories for OpenSees and CSiBridge. In light of the differences above in column stiffness and yield strength, the responses in Figure G.11are not close.

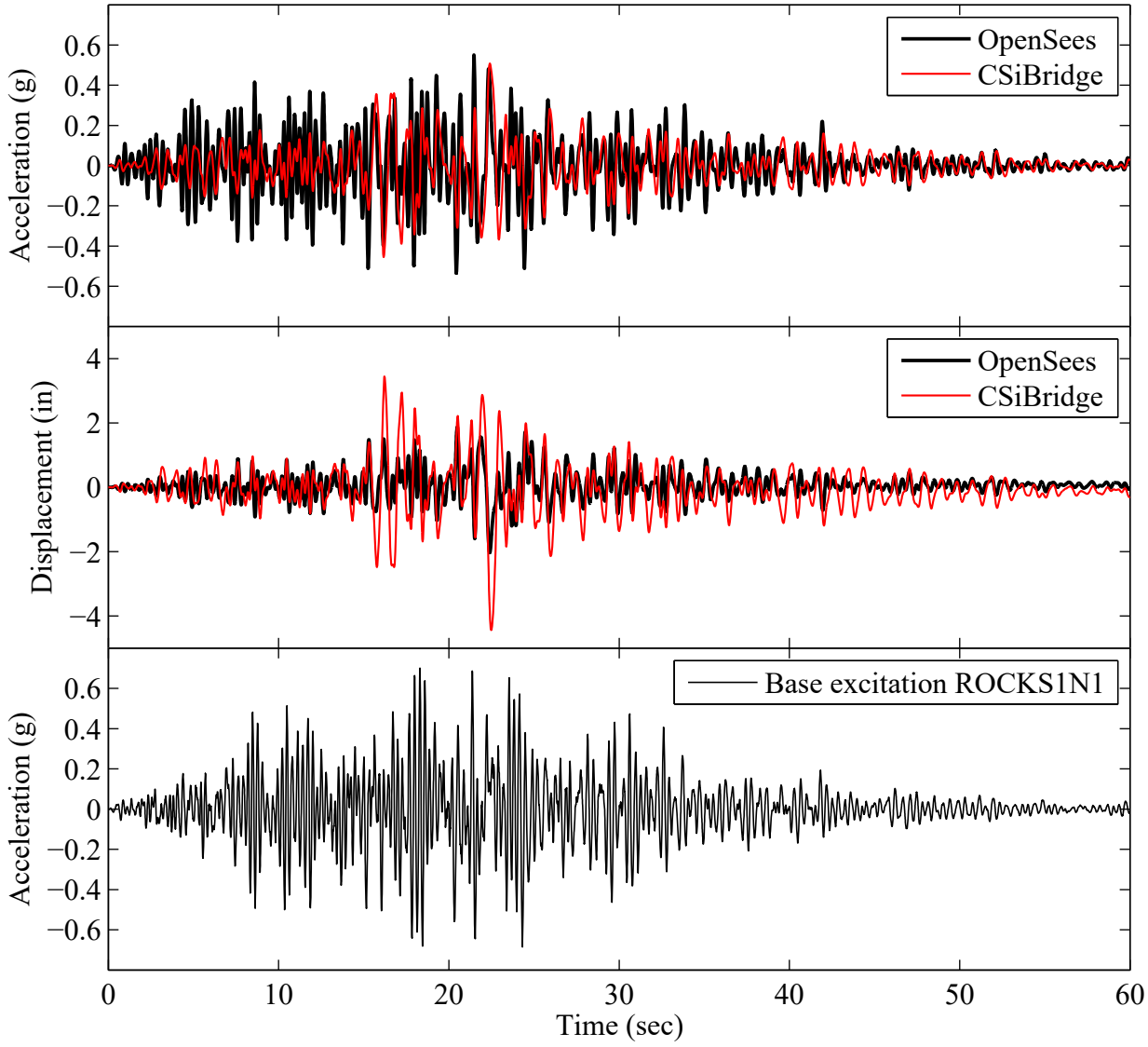

Figure G.11 OSB2 column top longitudinal acceleration (top graph) and displacement (middle graph) response time histories for Motion 1 ROCKS1N1

G.2.2 OSB1 Nonlinear Response

In this case, the roller abutment model was also employed. The nonlinear column response was considered and the cracked section properties were employed for the elastic section (a cracked section property factor of 0.35 was used). Dead load was applied in this case.

G.2.2.1 OSB1 Pushover Analysis

A pushover displacement of 20 inches was applied at the deck center along the longitudinal or transverse direction (in 500 steps). Figure G.12 shows the column top force-displacement responses from OpenSees, along with the CSiBridge results for comparison.

G.2.2.2 OSB1 Nonlinear Time History Analysis

Nonlinear THA was conducted for OSB1 in CSiBridge and OpenSees. Motion 1 ROCKS1N1 was employed. Rayleigh damping was used with a 5% damping ratio (defined at periods of 1.2 and 0.7 second) in the nonlinear THA. For the time integration scheme, the Newmark's average acceleration method ($\gamma = 0.5$ and $\beta = 0.25$) was employed. A variable time-stepping scheme was used in the analysis. The initial time step at each step was 0.005 second (same as the time step of the input motion) and the minimum time step was 5×10^{-5} second (upon splitting of time step).

Figure G.13 shows the deck center longitudinal acceleration and displacement response time histories for OpenSees and CSiBridge. A relatively close match is observed in this case, possibly in view of the closer match in column lateral response (Figure G.12).

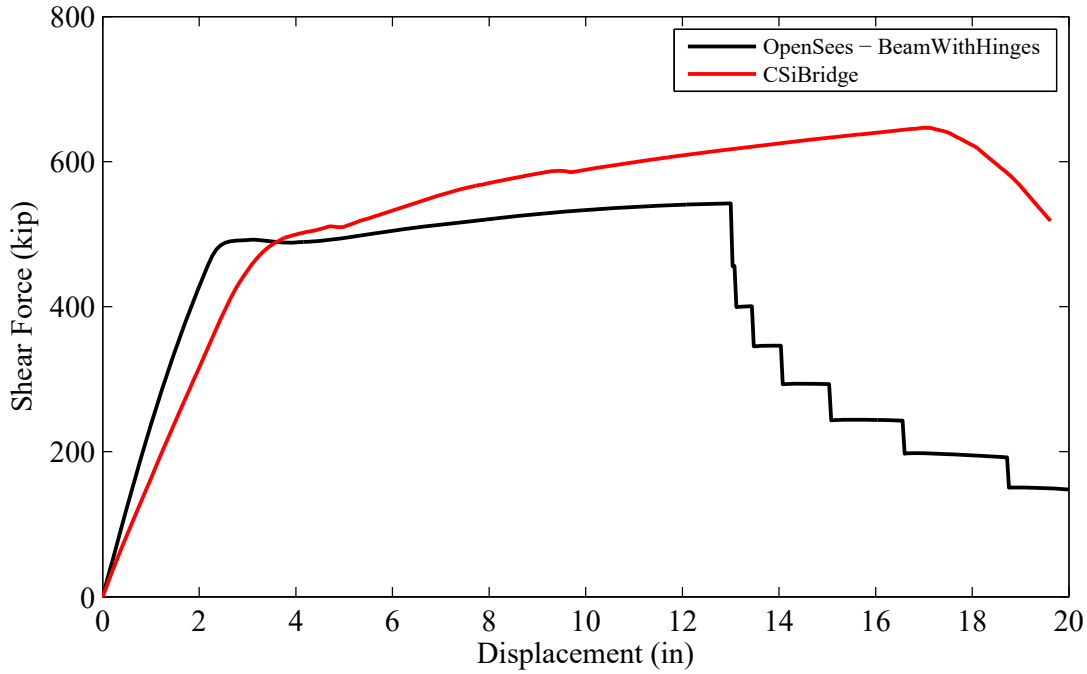

a)

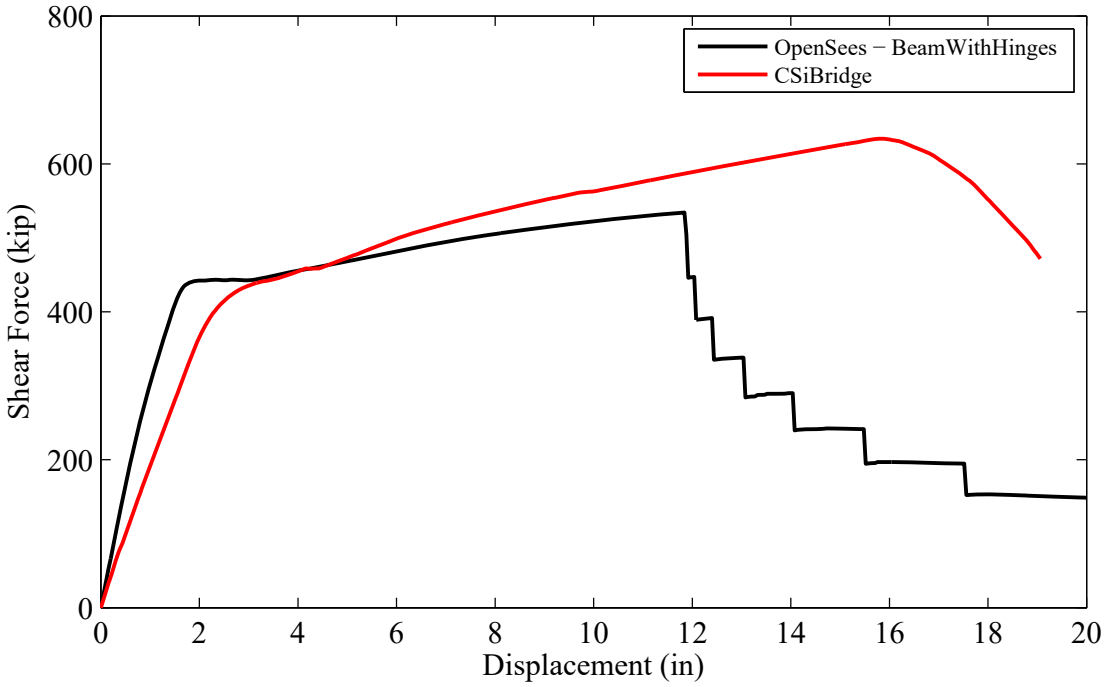

b)

Figure G.12 Column top force-displacement responses (flexural stiffness reduction factor = 0.35; plastic hinge length = 2.8 ft for OpenSees and hinge location = 2.8 ft for CSiBridge): a) longitudinal direction; b) transverse direction

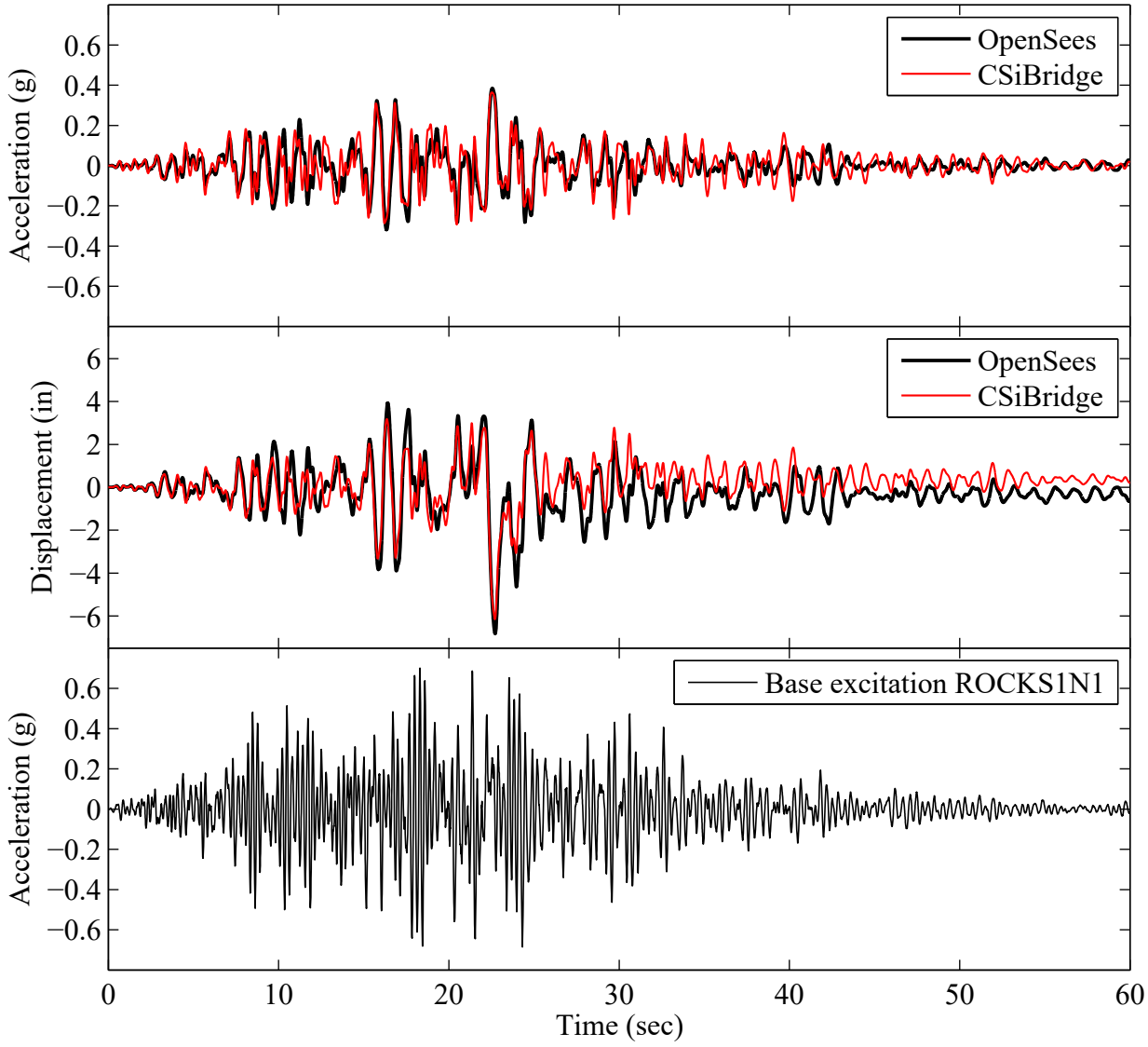

Figure G.13 OSB1 deck center longitudinal acceleration (top graph) and displacement (middle graph) response time histories for Motion 1 ROCKS1N1

APPENDIX H: COLUMN MODELING APPROACH FOR OSB2 STUDY USING CSIBRIDGE

H.1 Column Modeling Approach

To address the initial column stiffness/strength issues for the Fiber section in CSiBridge discussed in Appendix G, a special column modeling approach was proposed by Caltrans. The procedure in this approach involves:

i) Discretize the column into at least two elements (one for the hinge length centered at the hinge position and the other(s) for the remainder of the column);
ii) Place the hinge at the center of the hinge length element;
iii) Add a stiff section modifier to the hinge length element (increase the element Moment of Inertia) to avoid double counting the elastic deformation over the hinge length;
iv) As usual, assign cracked section modifiers to all elements in the column except the hinge region.

H.2 CSiBridge OSB2 Study based on the Employed Column Modeling Approach

The above-mentioned modeling approach proposed by Caltrans was employed to model the bridge column in CSiBridge.

In this study, the OSB2 column was discretized into 4 elements (see Fig. H.1). Both the top and bottom elements of the column were 2.8 ft long (this length is equal to the plastic hinge length obtained based on SDC). A hinge was placed at the center of the top element as well as the bottom element. A cracked section property modifier of 0.35 was assigned to the middle 2 elements. Moment curvature is shown in Fig. H.2 Roller abutment model was assumed.

H.2.1 OSB2 Column Shear Force-Displacement Response Due to Pushover

Figs. H.3 and H.4 show the column shear force-displacement response due to pushover loading for different section property modifier for the hinge length element (k = 3,425 kip/in is the linear fixed-fixed condition stiffness $12EI/L^3$).

H.2.2 Base Shaking

A series of earthquake excitation cases using input motion ROCKS1N1 were analyzed in CSiBridge by varying the section property modifier and the damping ratio (Rayleigh damping). The column shear force-displacement response for each case is shown in Figs. H.6-18. It appears possibly that the damping force is included in the recorded element shear force in CSiBridge though we are not sure.

Figs. H.4 and H.7 show that a section modifier of 3 for the hinge length element gave reasonable overall initial column stiffness/strength response. Therefore, the section modifier of 3 was used in all the CSiBridge analyses for OSB1 (Chapter 3) and OSB2 (Chapter 2). Note that in the report by Aviram et al. (2008b), a section property modifier in the range of 1-3 was suggested.

H.3 Additional Remarks

In the static pushover analysis, the element shear force looks reasonable (Figs. H.3 and H.4).

When performing earthquake shaking computations, we found that the response graph of the element shear force appears to be damping-dependent. In some of the cases we ran (e.g., when the section property modifier of the hinge length element is 100 or larger), the element shear force reached over 6,000 kip while the push-over column response shows yielding at around 1,200 kip.

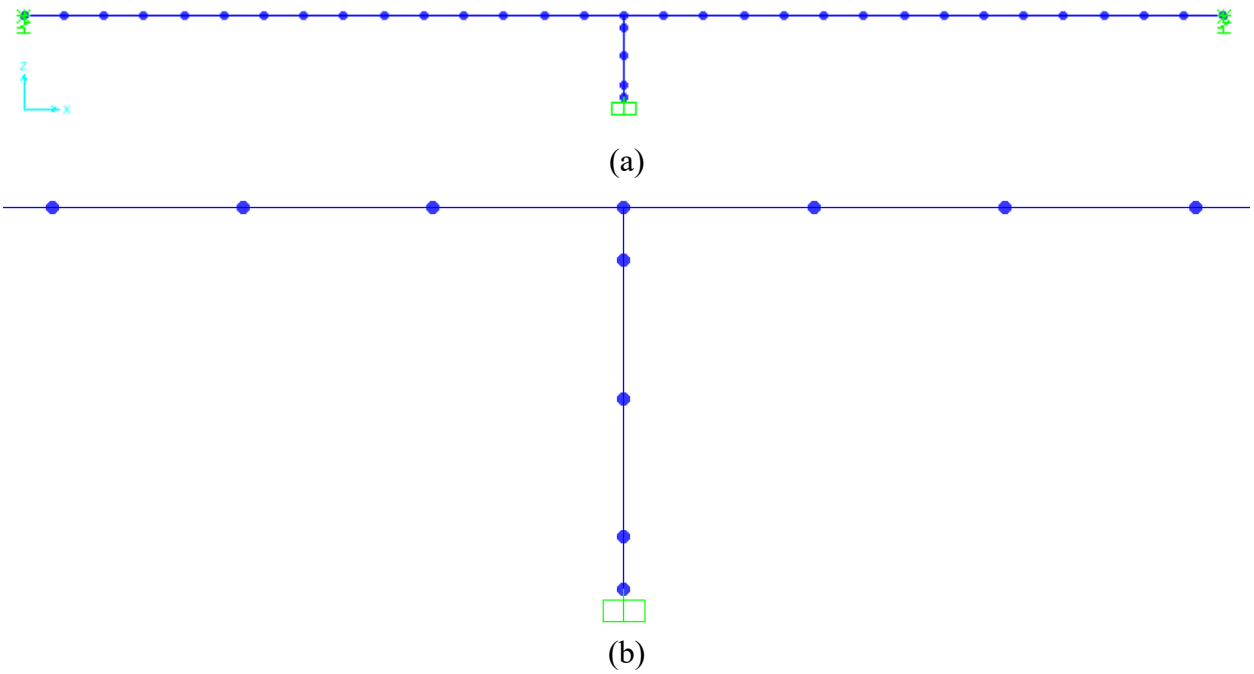

Figure H.1 OSB2 model created in CSiBridge: (a) entire model; (b) close-up of column

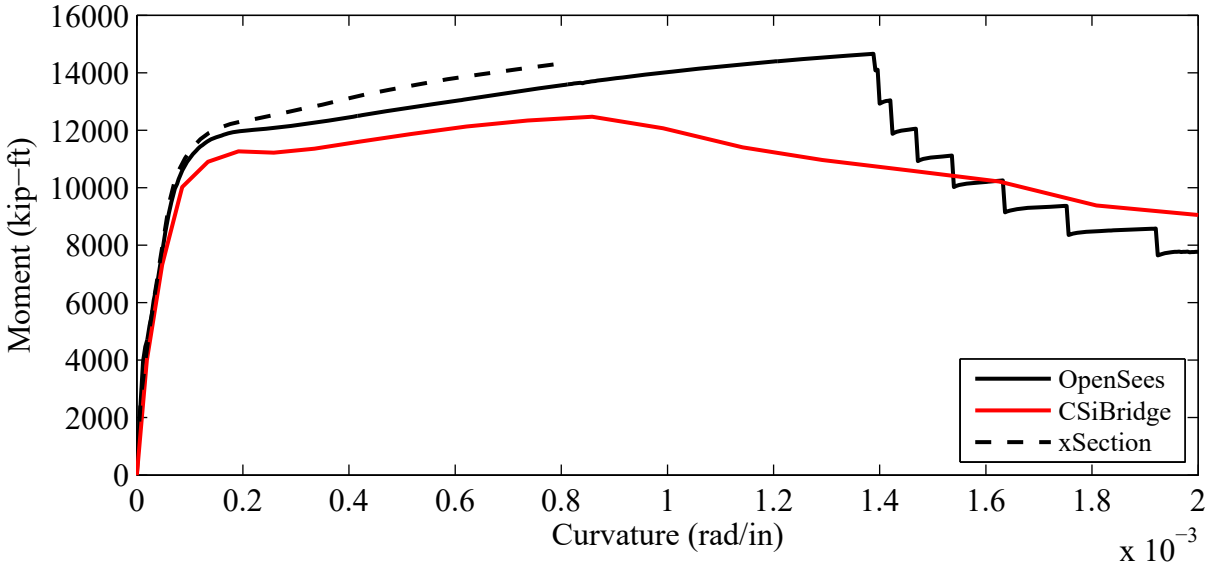

Figure H.2 Moment-curvature response of circular column section (axial compressive load = 1991 kip)

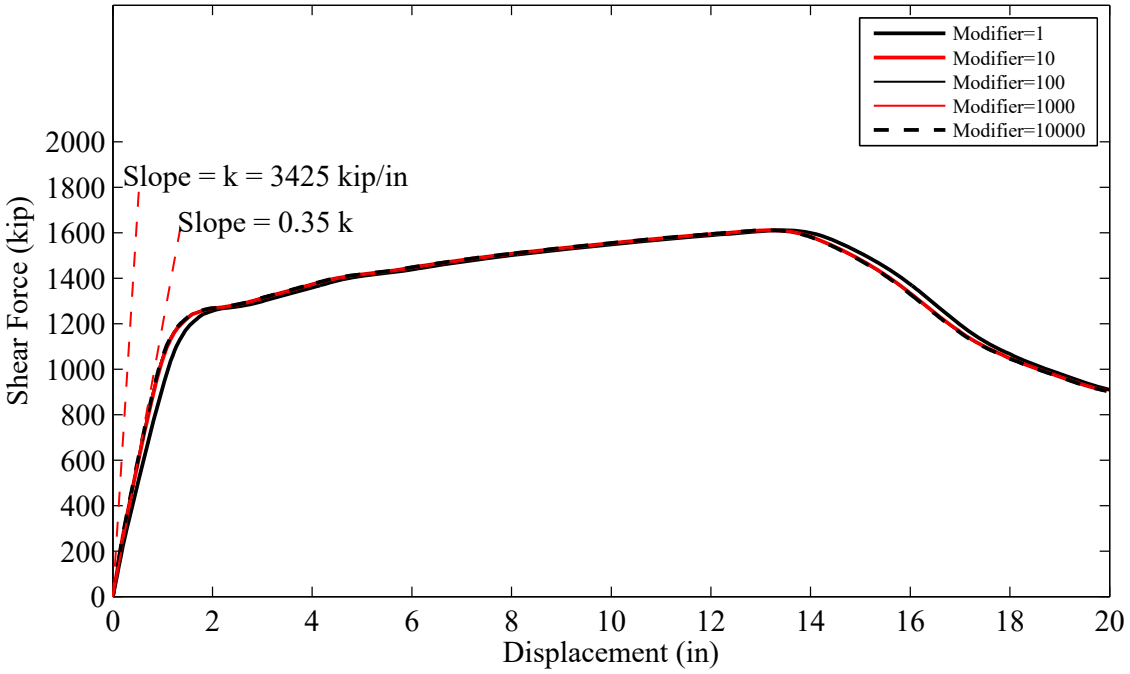

(a)

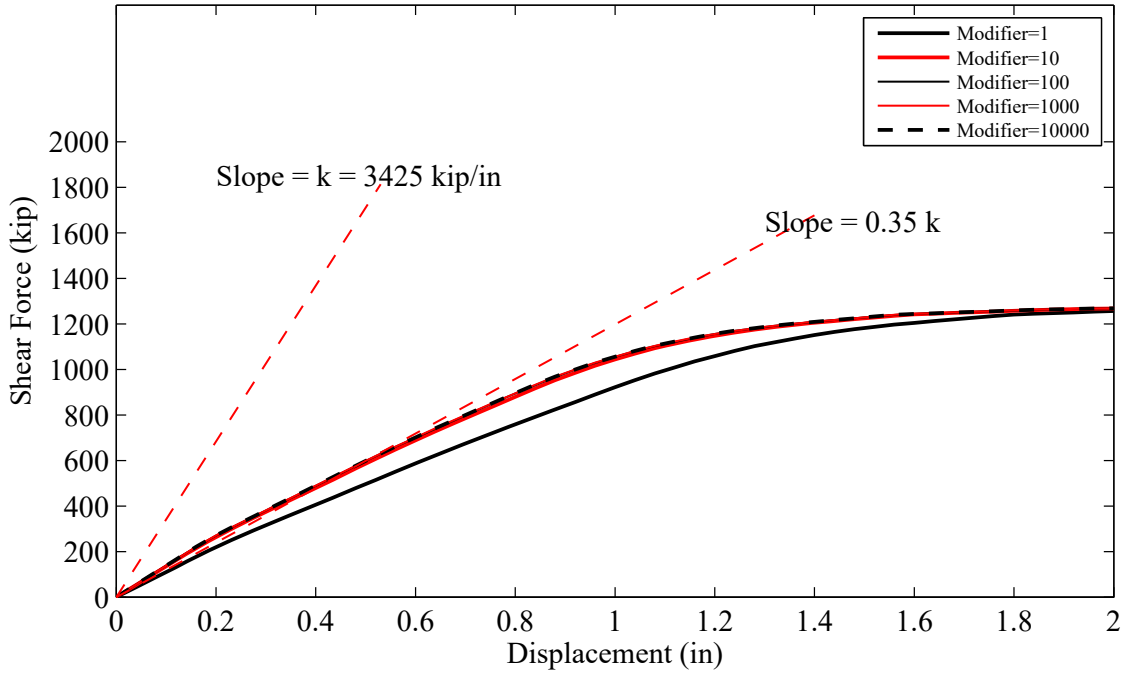

(b)

Figure H.3 CSiBridge column shear force-displacement response due to pushover: (a) plot up to 20 in of pushover displacement; (b) close-up plot up to 2 in of pushover displacement

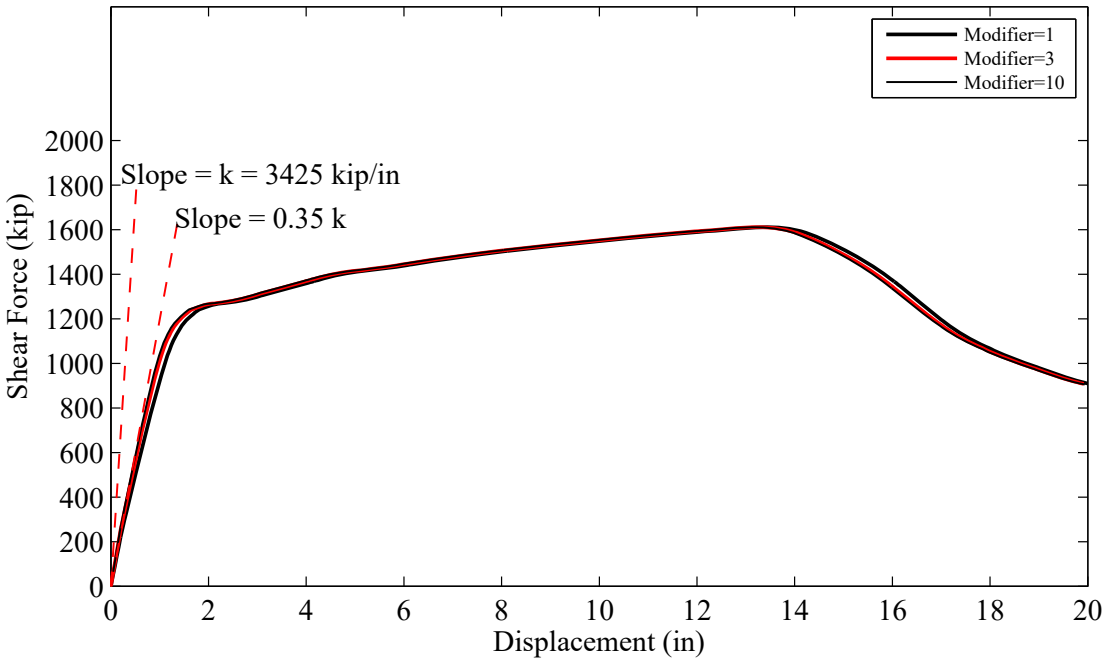

(a)

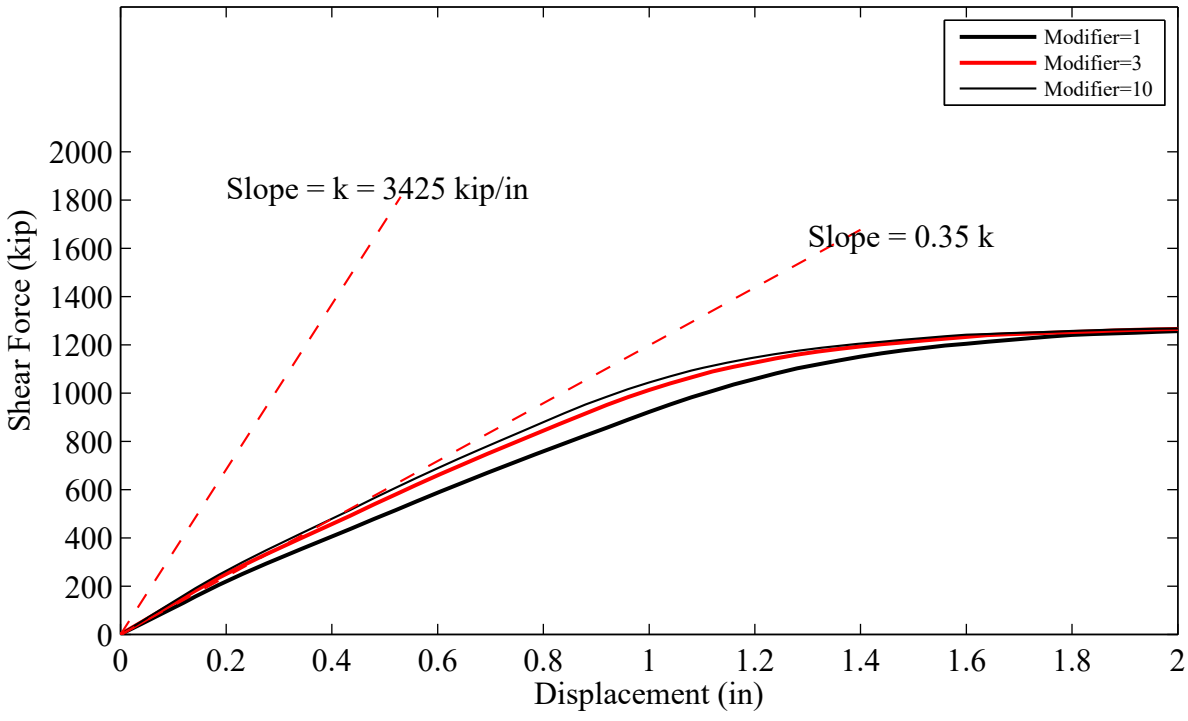

(b)

Figure H.4 Column shear force-displacement response due to pushover: (a) plot up to 20 in of pushover displacement; (b) plot up to 2 in of pushover displacement

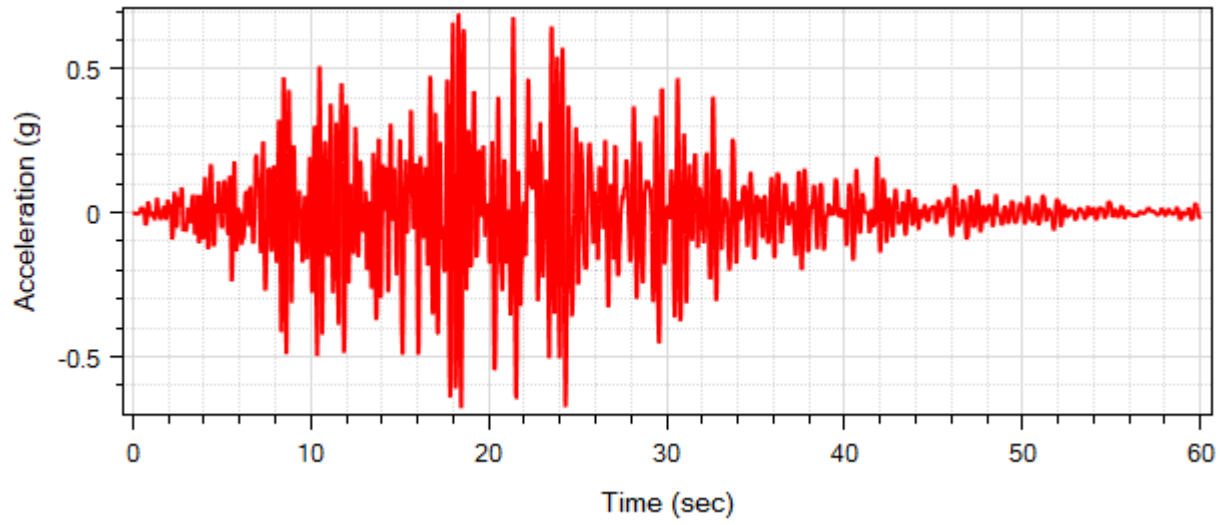

Figure H.5 Input motion ROCKS1N1

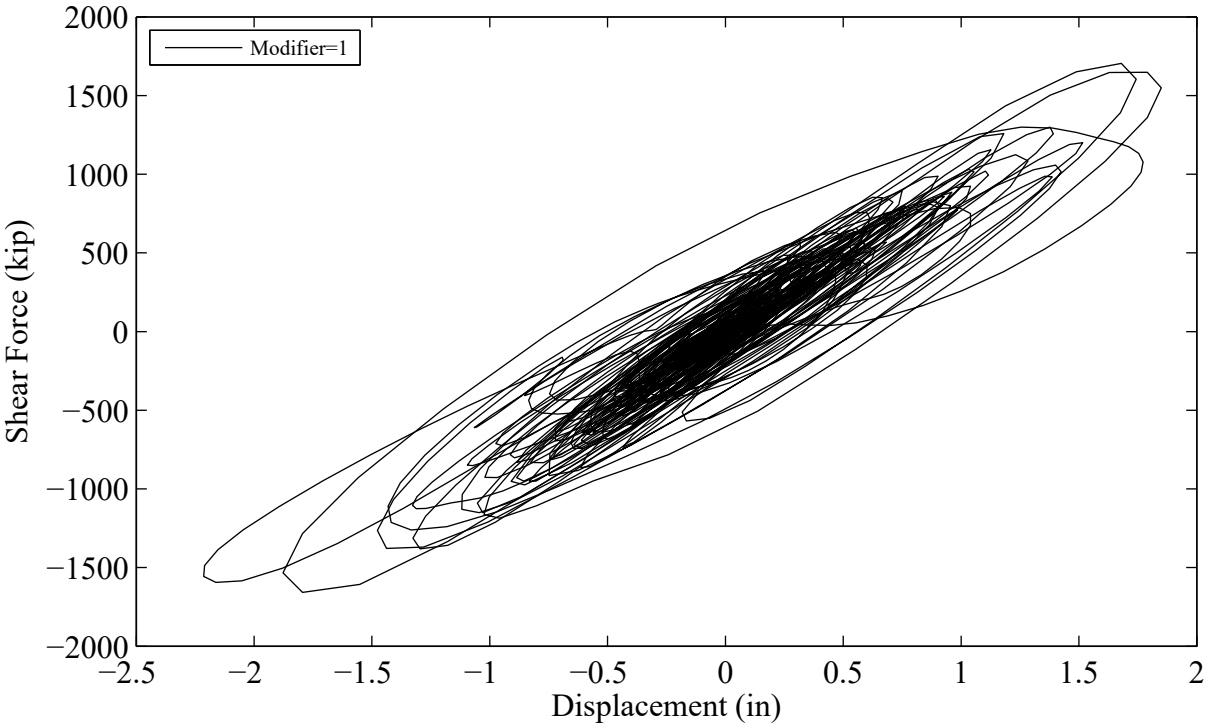

Figure H.6 Column shear force-displacement response due to shaking for section property modifier = 1 (Damping ratio = 5%)

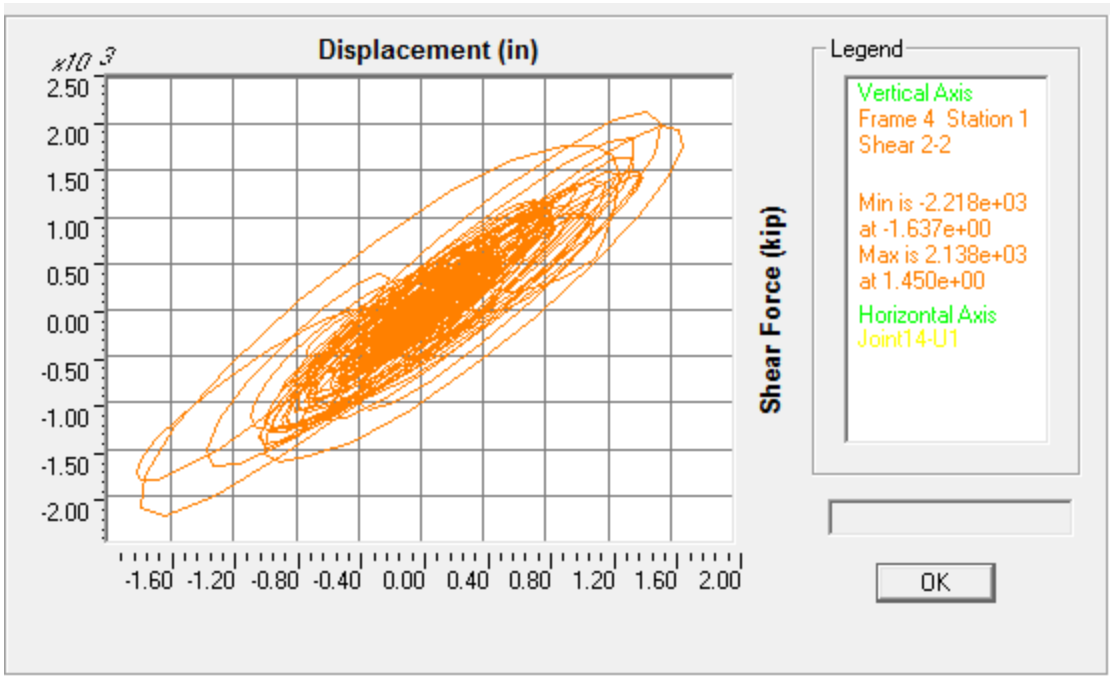

Figure H.7 Column shear force-displacement response due to shaking for section property modifier = 3 (Damping ratio = 5%)

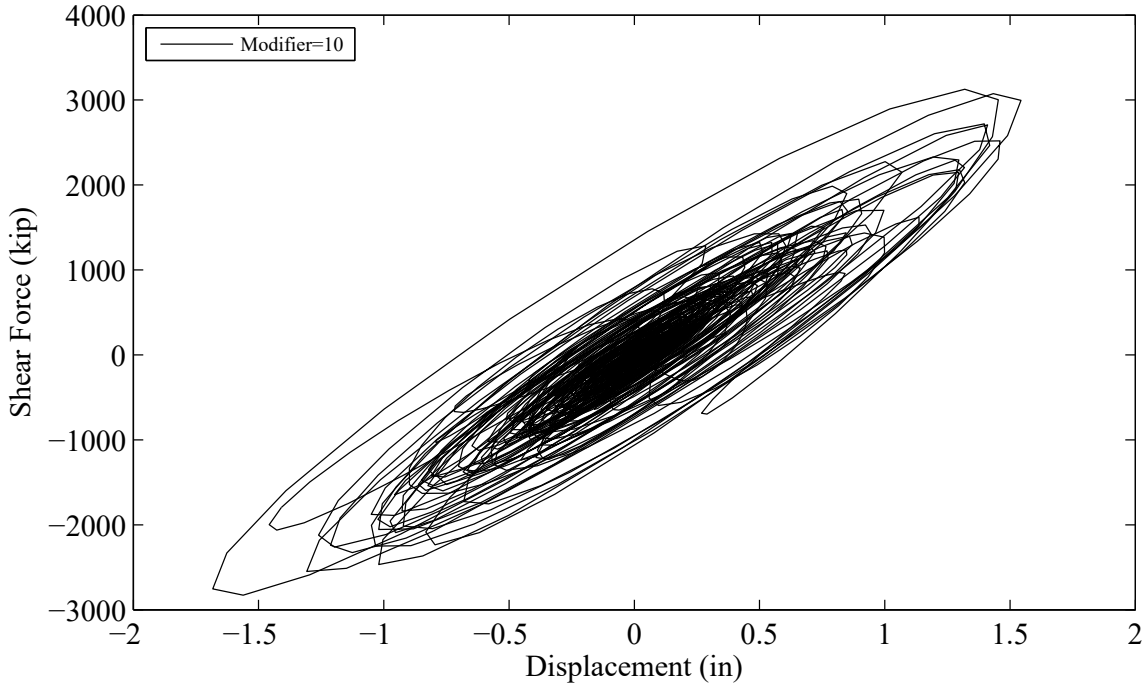

Figure H.8 Column shear force-displacement response due to shaking for section property modifier = 10 (Damping ratio = 5%)

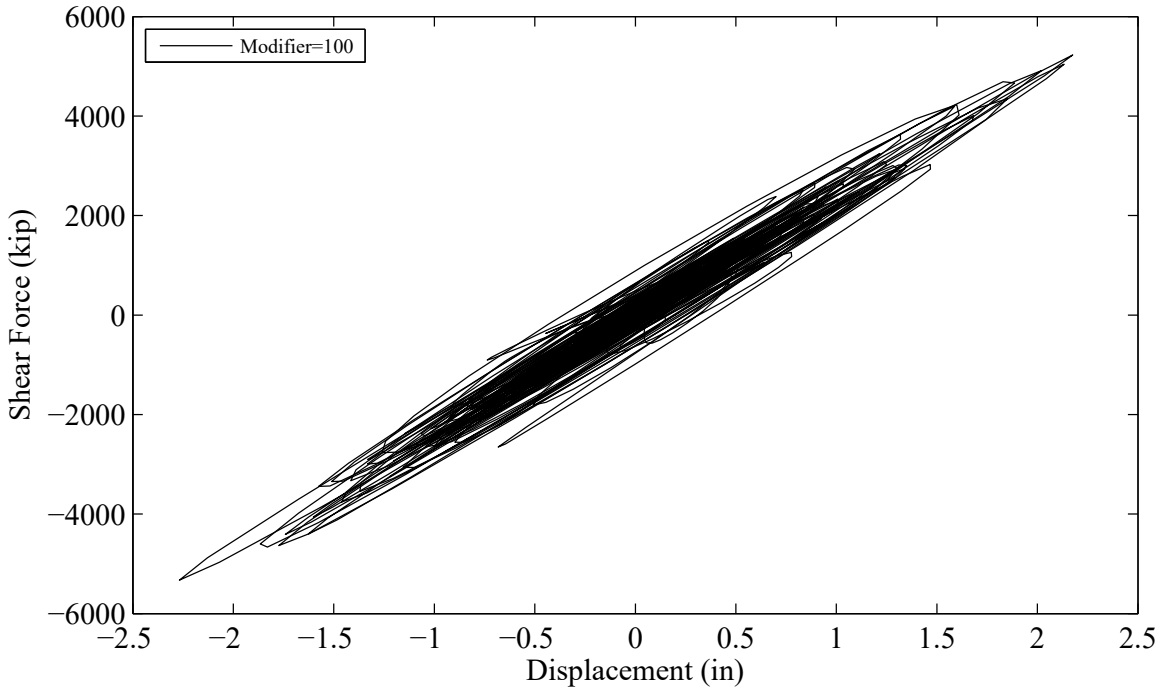

Figure H.9 Column shear force-displacement response due to shaking for section property modifier = 100 (Damping ratio = 5%)

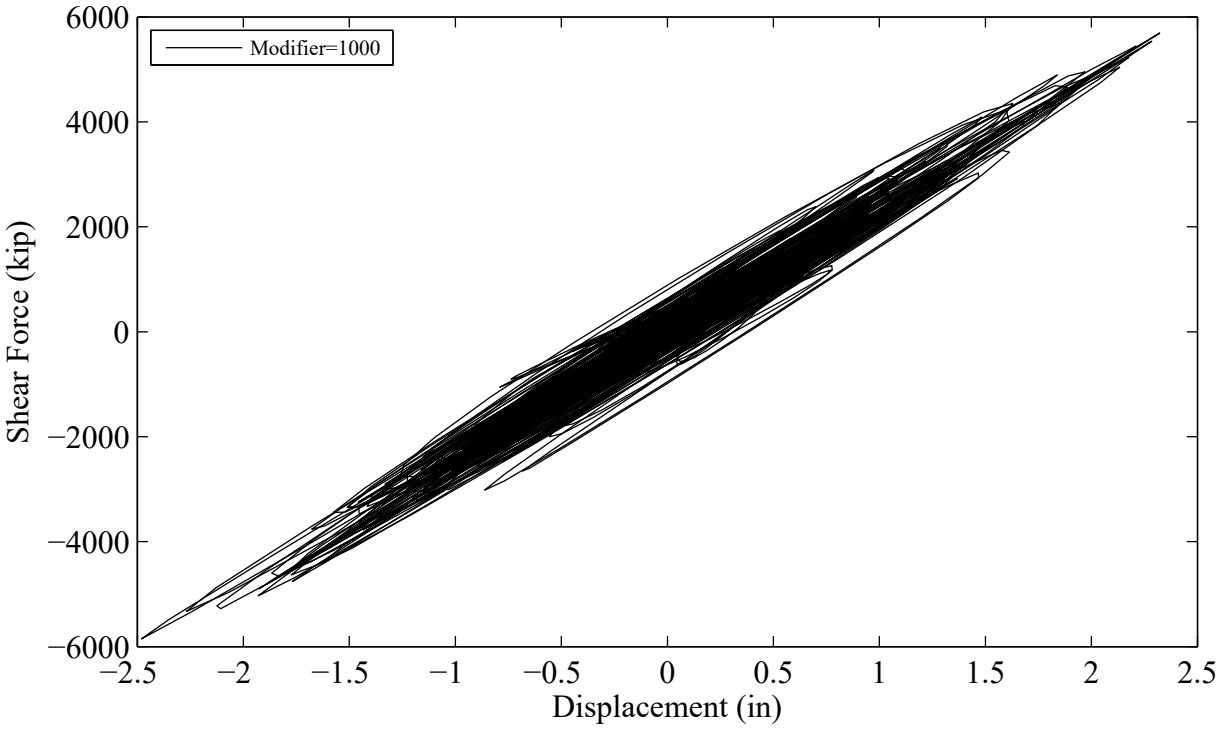

Figure H.10 Column shear force-displacement response due to shaking for section property modifier = 1,000 (Damping ratio = 5%)

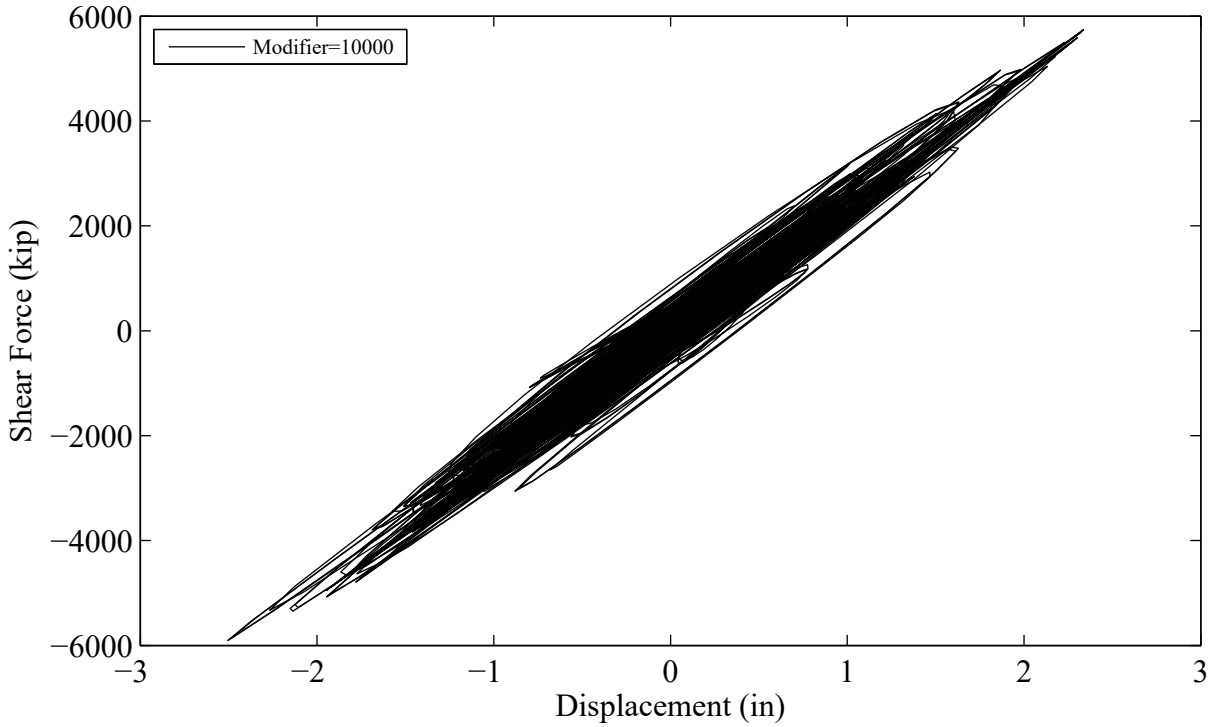

Figure H.11 Column shear force-displacement response due to shaking for section property modifier = 10,000 (Damping ratio = 5%)

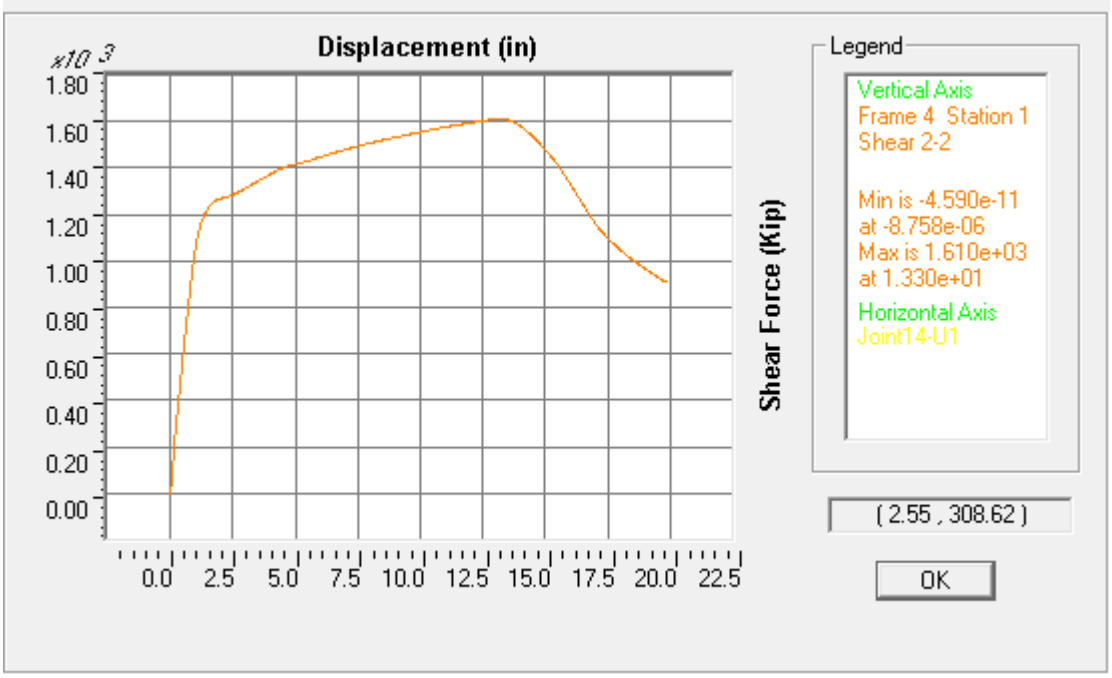

Figure H.12 Column shear force-displacement response due to pushover (For damping ratio = 0, 0.001%, 0.01%, 0.1%, 1% and 5%, and Section property modifier = 10,000)

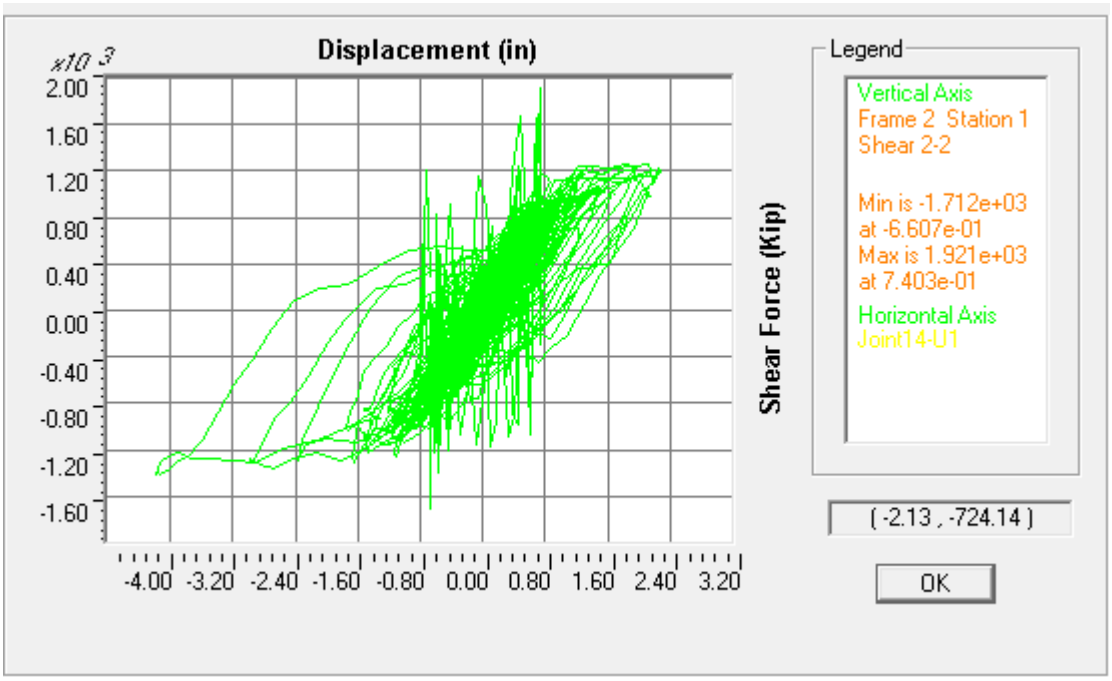

Figure H.13 Column shear force-displacement response due to shaking for damping ratio = 0 % (Section property modifier = 10,000)

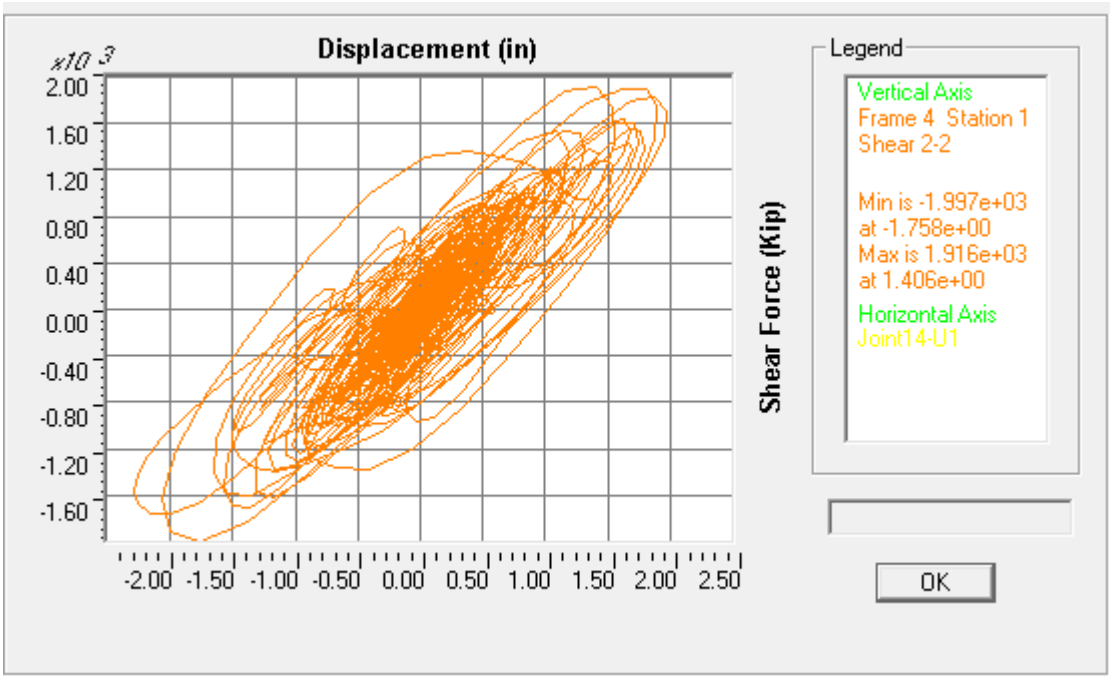

Figure H.14 Column shear force-displacement response due to shaking for damping ratio = 0.001% (Section property modifier = 10,000)

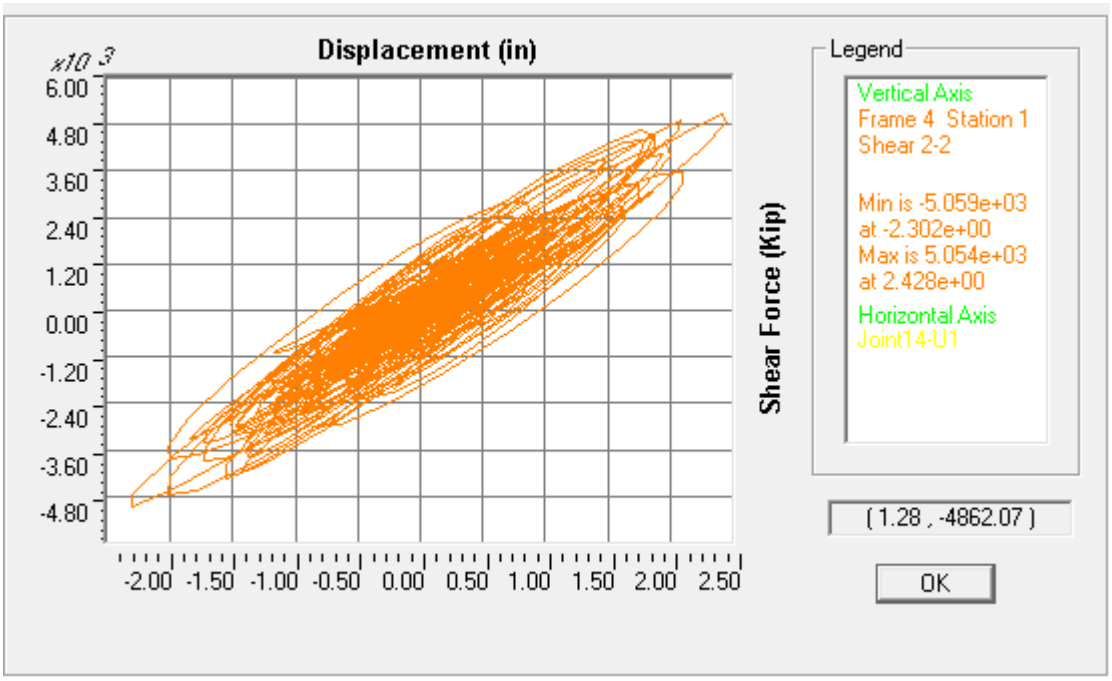

Figure H.15 Column shear force-displacement response due to shaking for damping ratio = 0.01% (Section property modifier = 10,000)

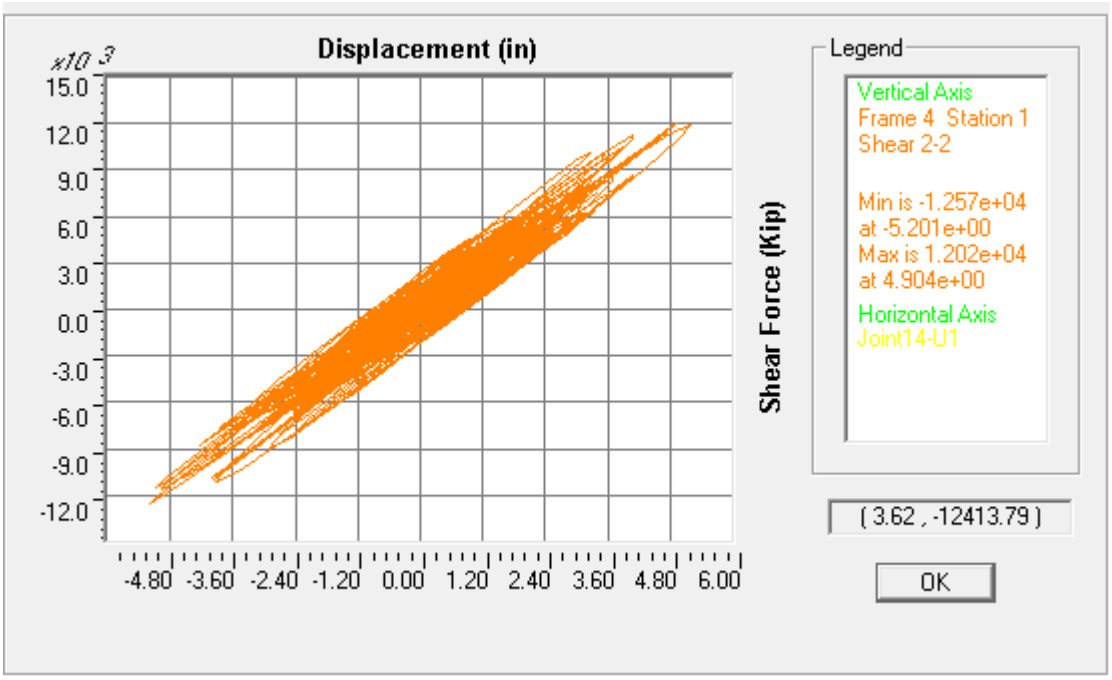

Figure H.16 Column shear force-displacement response due to shaking for damping ratio = 0.1% (Section property modifier = 10,000)

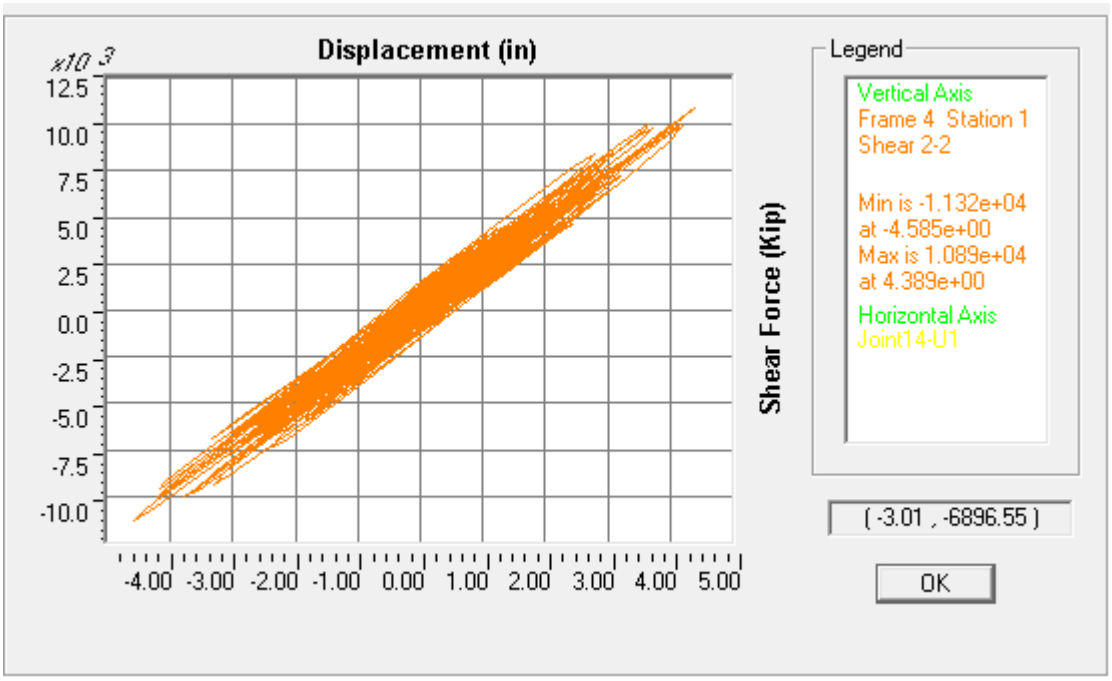

Figure H.17 Column shear force-displacement response due to shaking for damping ratio = 1% (Section property modifier = 10,000)

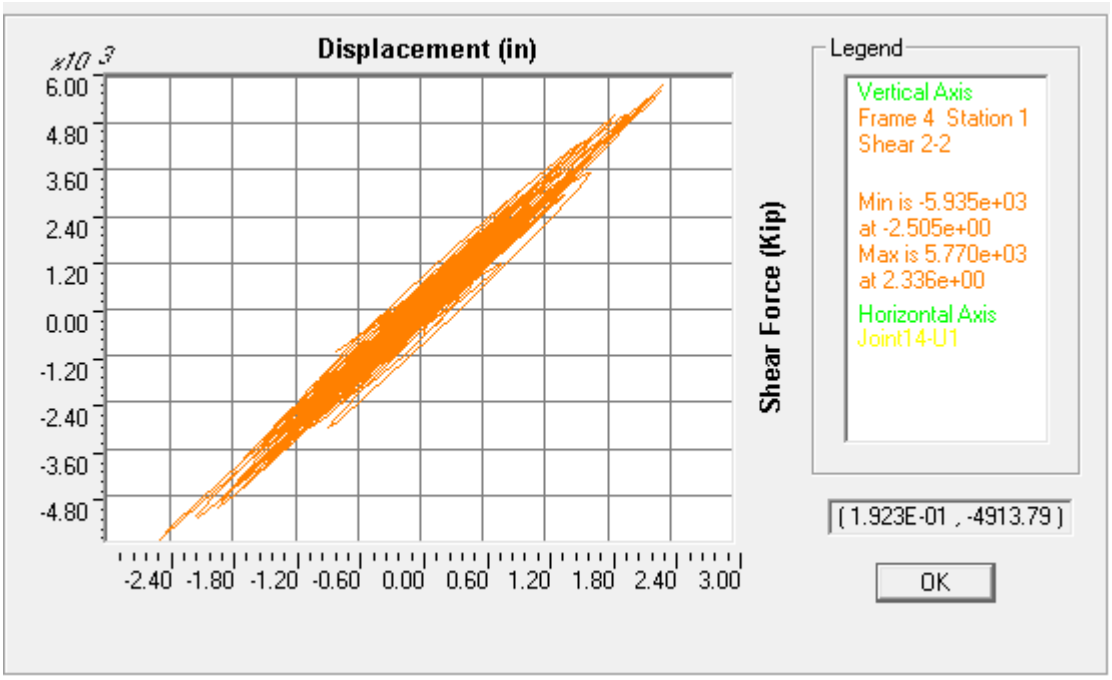

Figure H.18 Column shear force-displacement response due to shaking for damping ratio = 5% (Section property modifier = 10,000)

APPENDIX I: VISCOUS DAMPING: COMPARISON OF OPENSEES AND CSIBRIDGE OSB1 SEISMIC LONGITUDINAL RESPONSE

I.1 Summary

OSB1 (Fig. I.1) seismic longitudinal response was studied using OpenSees and CSiBridge for a number of abutment models (Roller, Elastic spring, and EPP-Gap). The columns were assumed to be linearly elastic and the deck and bentcap were considered rigid (to simply illustrate the difference in response between the two programs OpenSees and CSiBridge as shown in Table 3.5).

When performing earthquake shaking computations, it was found that the response from OpenSees and CSiBridge is quite different (Elastic spring and EPP-Gap models). However, both programs gave the same results for the Roller model. The results are presented in Sections I.2-I.5.

When the specified viscous damping was removed (i.e. zero damping), the shaking results (not shown in this report) from OpenSees and CSiBridge are identical for the 3 abutment models (i.e., Roller, Elastic spring, and EPP-Gap). This indicates that viscous damping may be the main reason causing the discrepancy between the 2 programs.

Note that pushover and mode shape analyses have been conducted for the 3 abutment models. The results (again, not shown in this document) from OpenSees and CSiBridge are identical.

I.2 OSB1 Modeling Details

Span length = 150 ft
Column height = 20 ft
Rigid links (3 ft in height) activated at column top
Rigid link (0.3 ft in height) activated between bentcap and deck
Linear column + Rigid deck + Rigid bentcap (to simply illustrate the issue)

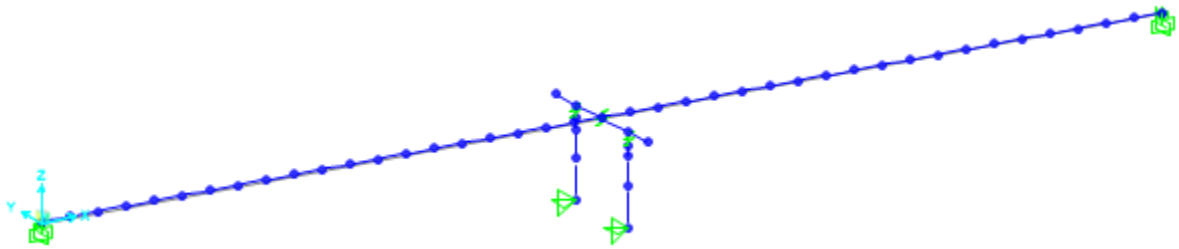

Figure I.1 OSB1 FE mesh

Motion ROCKS1N1 was employed for the dynamic shaking. Rayleigh damping was used with a 5% damping ratio defined at the periods of 1.2 and 0.7 second (unless otherwise stated).

The EPP-Gap model when engaged in compression, has an effective stiffness of 2,591 kip/in and a yield force at -1,555 kip. In the Elastic spring abutment model, the stiffness (of each abutment) was selected to be 1295.5 kip/in, which is half of the effective stiffness of EPP-Gap model (just for the purposes of illustration).

I.3 Roller Abutment Model

Column shear force-displacement response is shown below (essentially identical response is seen for CSiBridge and OpenSees).

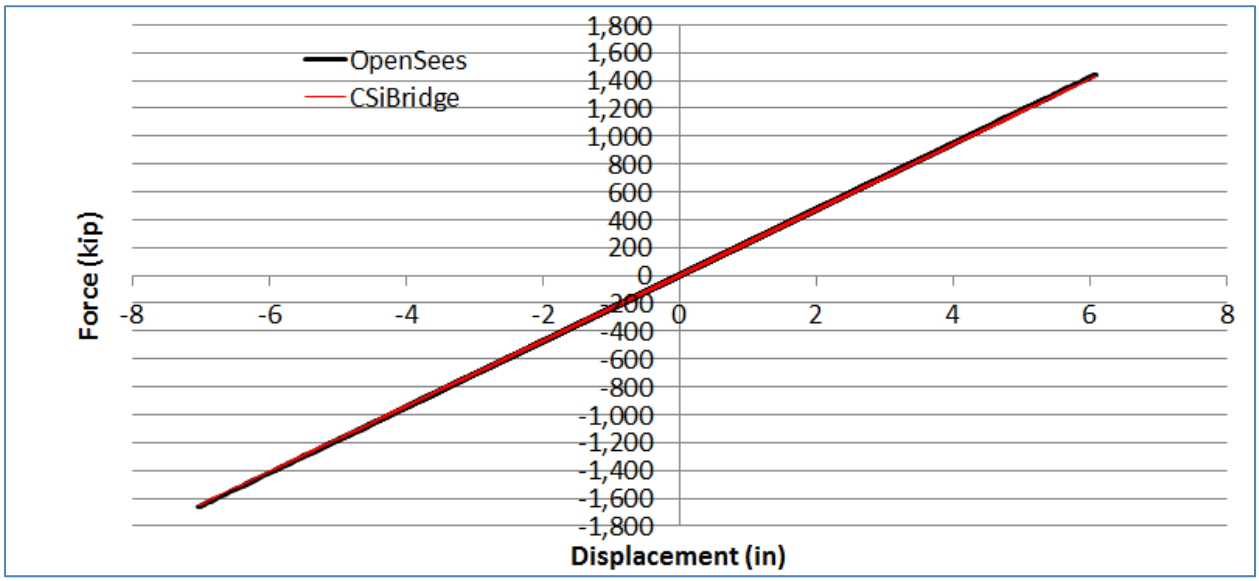

Figure I.2 Column shear force-displacement response

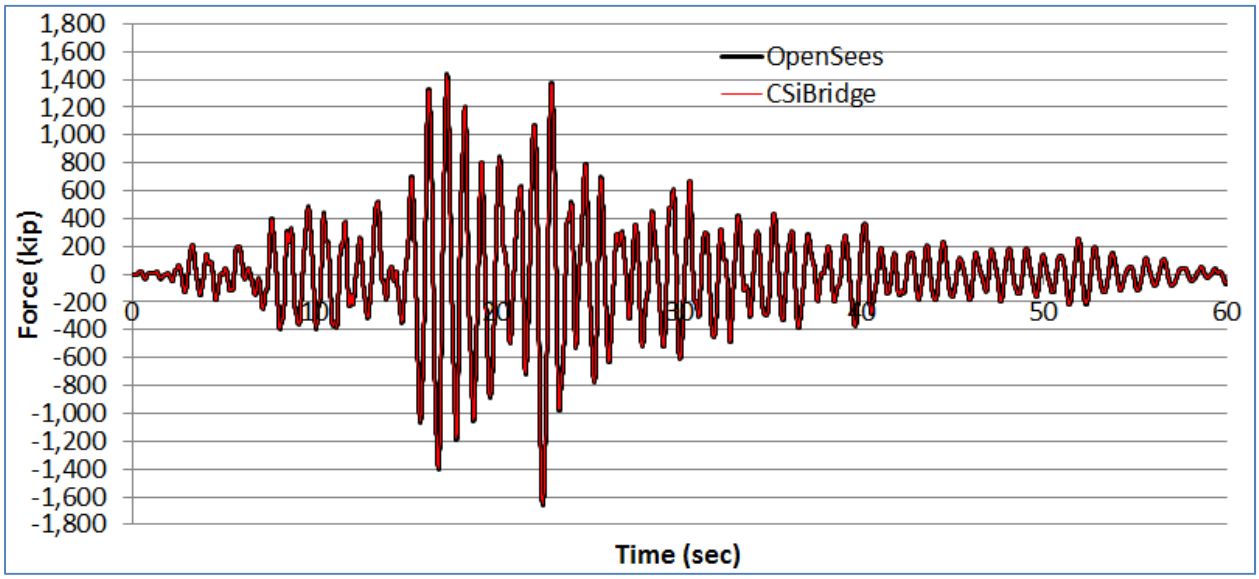

Figure I.3 Column shear force response time history

Left deck-end and right deck-end axial force response time history (slight fluctuation below because of inertia force of the outmost element). Otherwise, should be just zero all through in this roller abutment case.

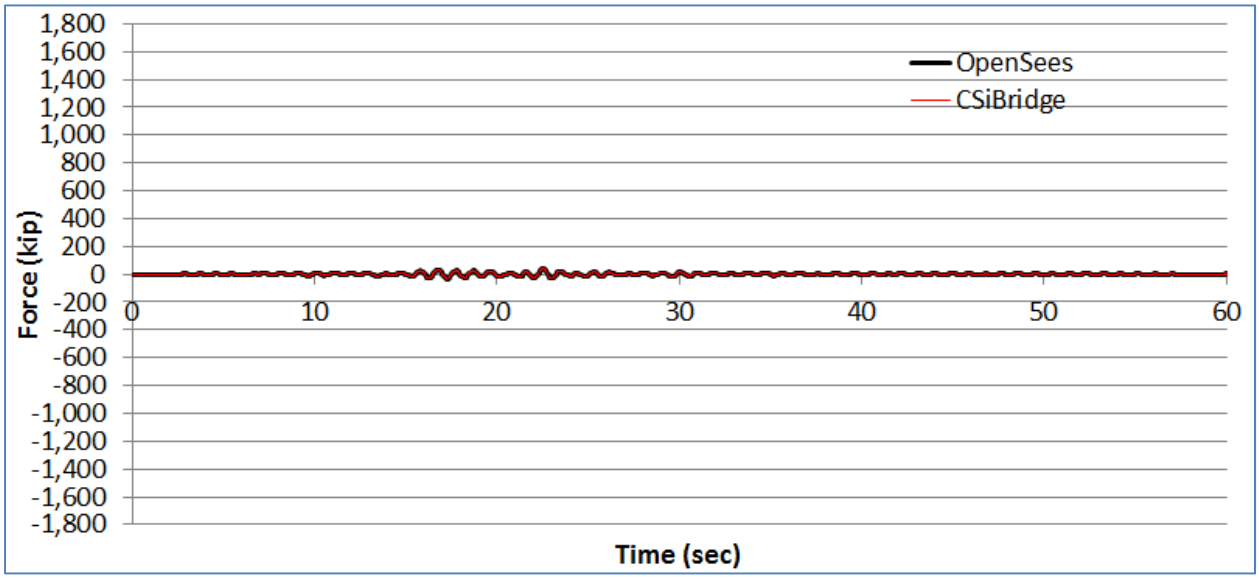

Figure I.4 Left deck-end axial force response time history

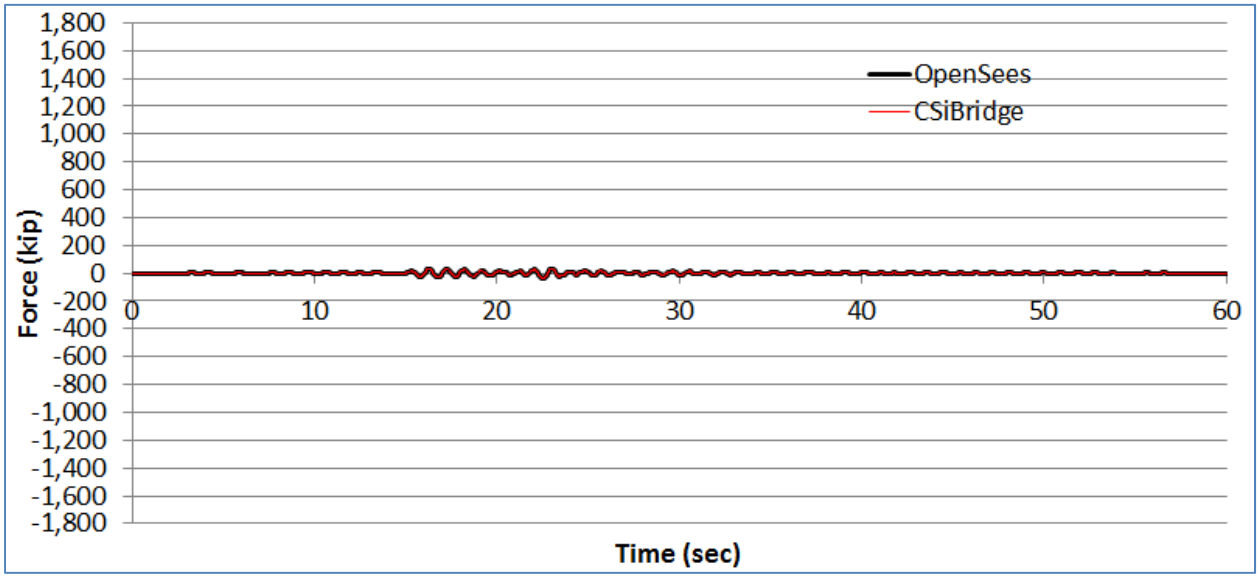

Figure I.5 Right deck-end axial force response time history

I.4 Elastic Spring Abutment Model

In the Elastic spring abutment model, the spring stiffness (1295.5 kip/in) of each abutment is half of the effective stiffness (2591 kip/in) of EPP-Gap model (just for the purposes of illustration).

I.4.1 Bridge Column

Column shear force displacement response (still with the same viscous damping and everything else as above). Now, the response is quite different as shown below.

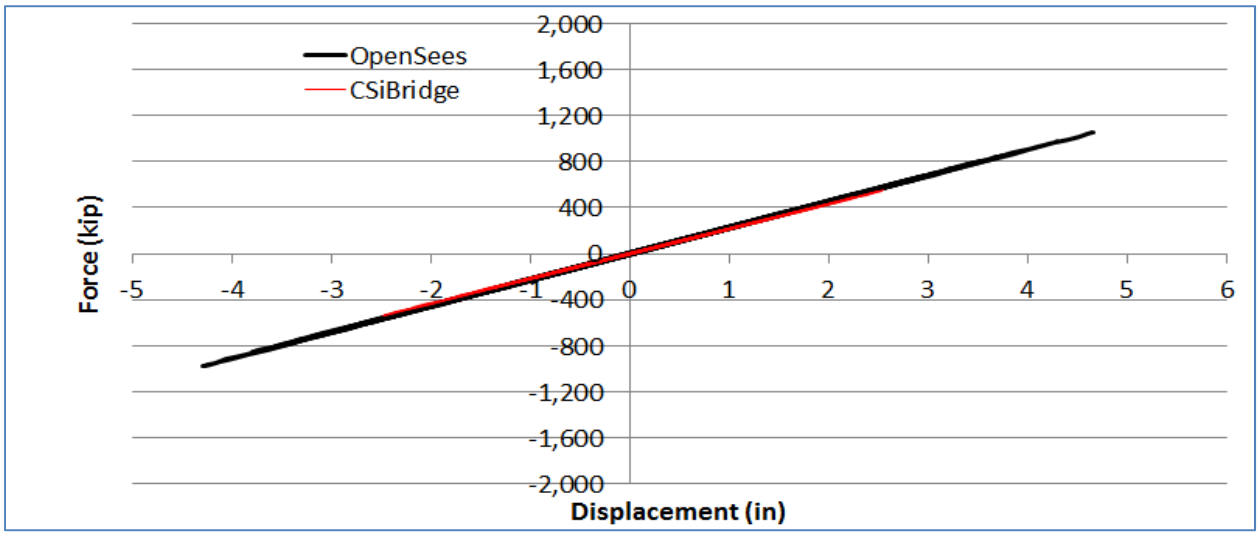

Figure I.6 Column shear force-displacement response

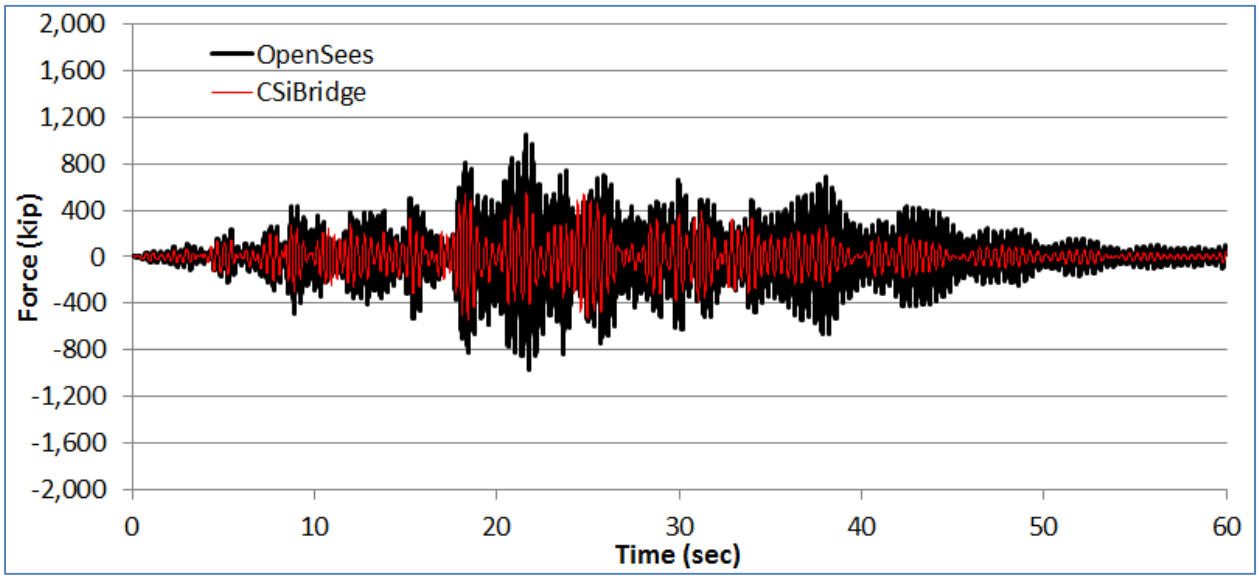

Figure I.7 Column shear force response time history

I.4.2 Left Abutment

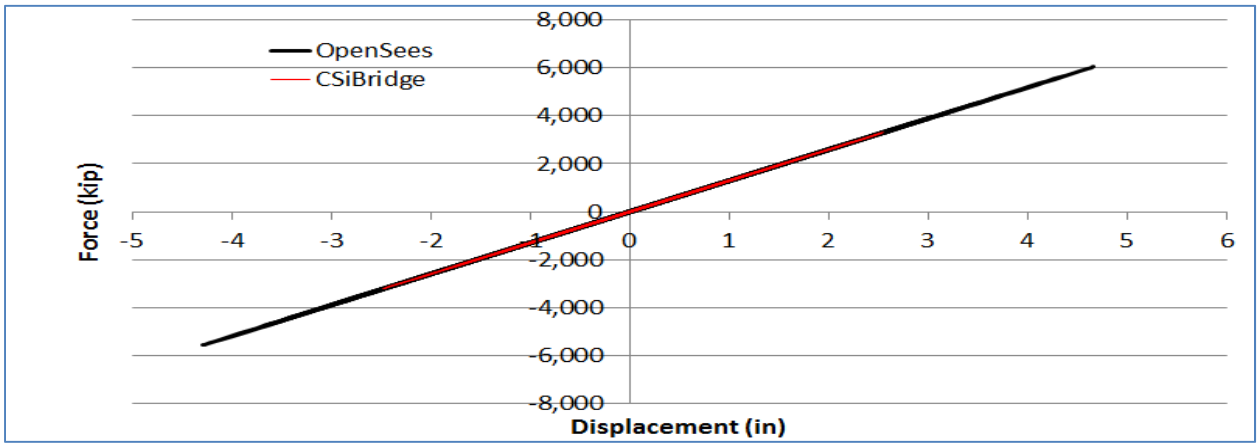

Figure I.8 Left abutment Elastic spring model force-displacement response

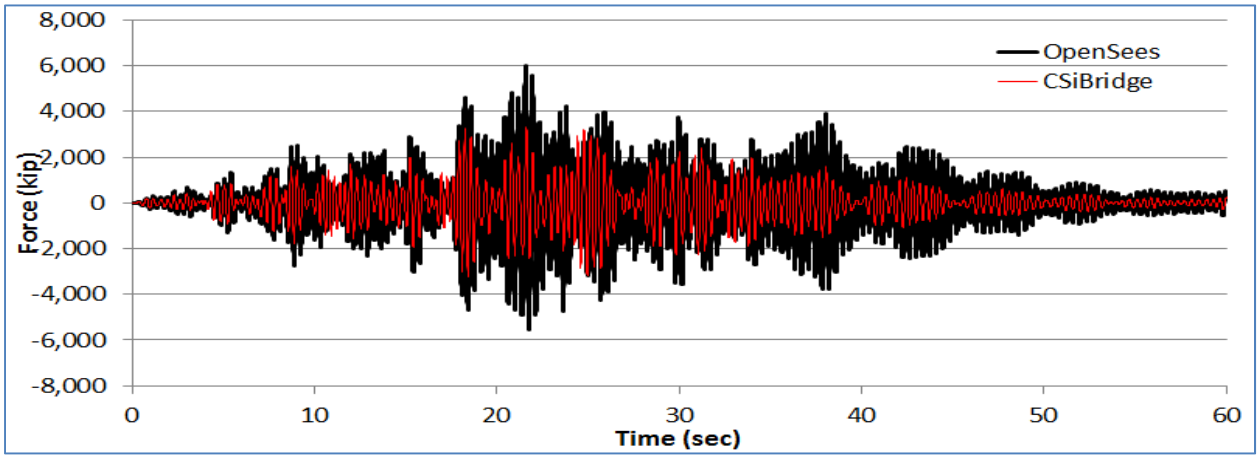

Figure I.9 Left abutment Elastic spring model force response time history

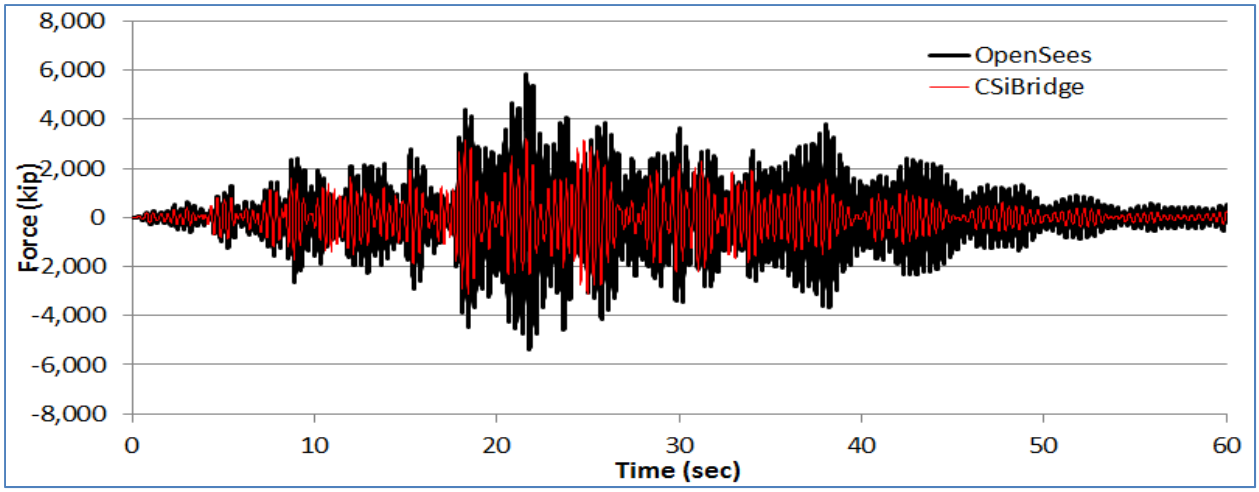

Figure I.10 Left deck-end axial force response time history

I.4.3 Right Abutment

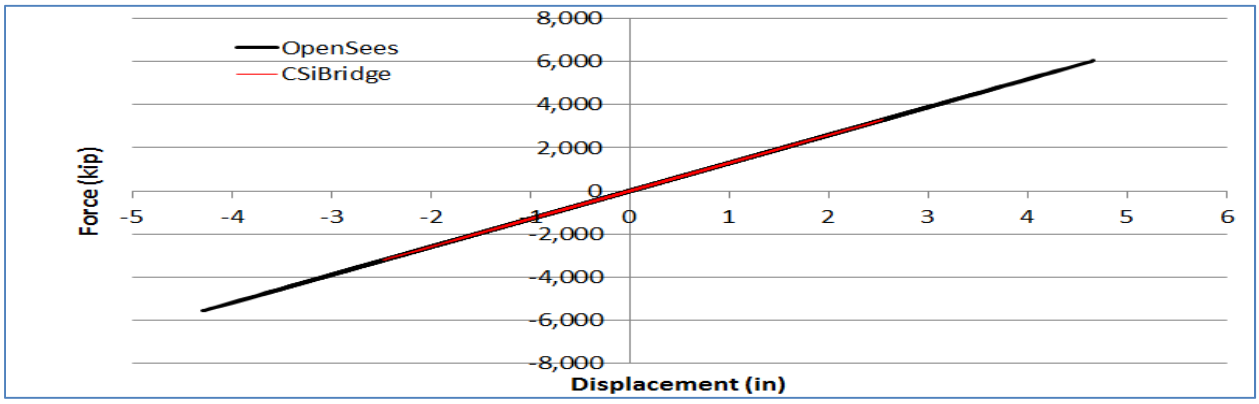

Figure I.11 Right abutment Elastic spring model force-displacement response

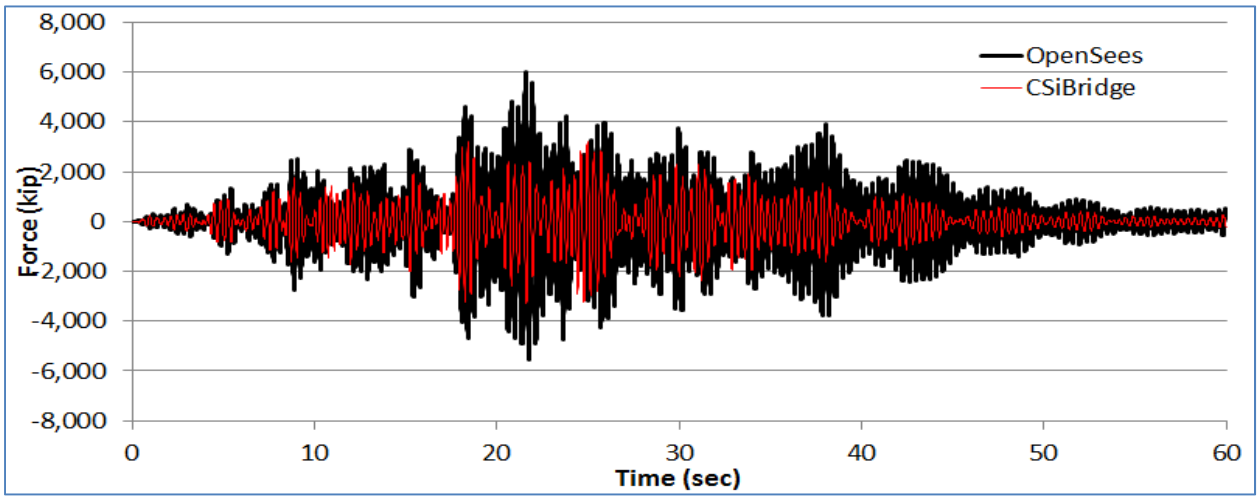

Figure I.12 Right abutment Elastic spring model force response time history

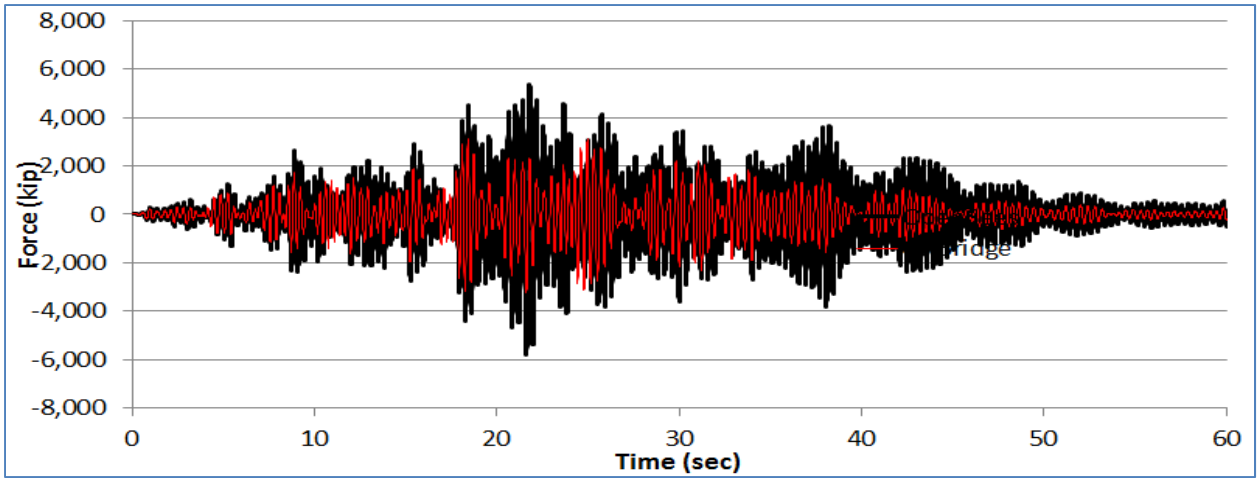

Figure I.13 Right deck-end axial force response time history

I.5 EPP-Gap Abutment Model

I.5.1 Stiffness and Mass – Proportional Damping Coefficients Included

I.5.1.1 Bridge Column

Column shear force displacement response is shown below (still with the same viscous damping and everything else as above). Now the response is quite different as shown below:

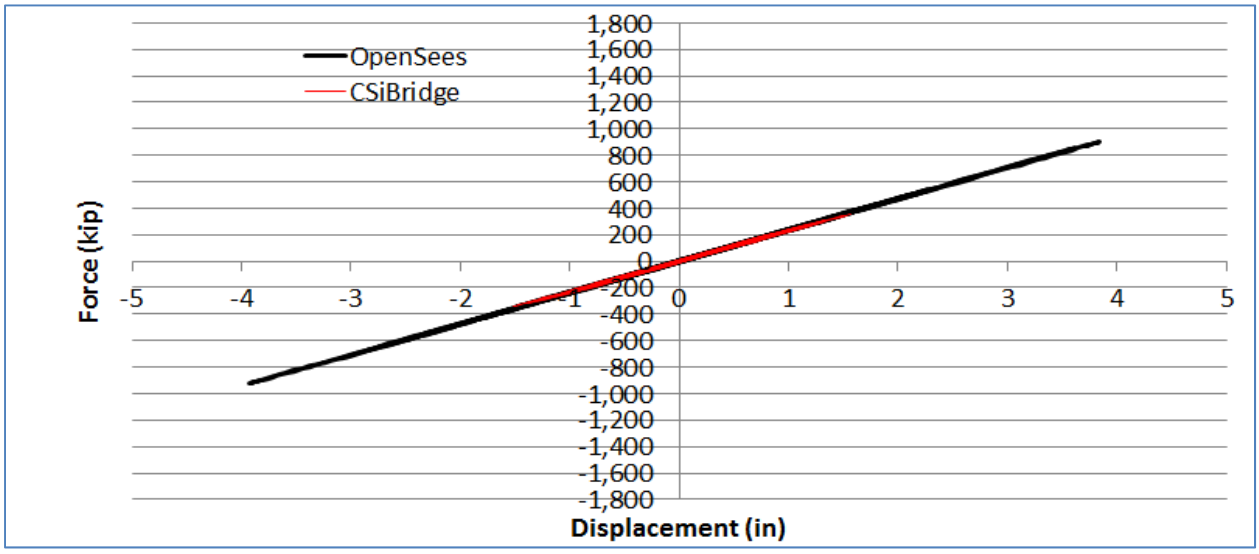

Figure I.14 Column shear force-displacement response

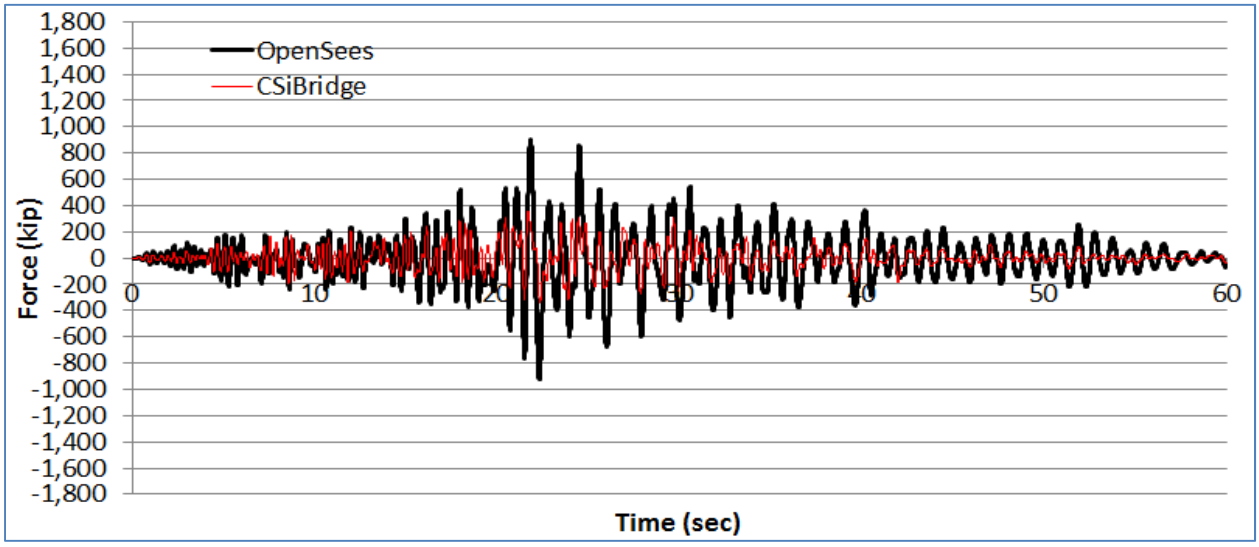

Figure I.15 Column shear force response time history

I.5.1.2 Left Abutment

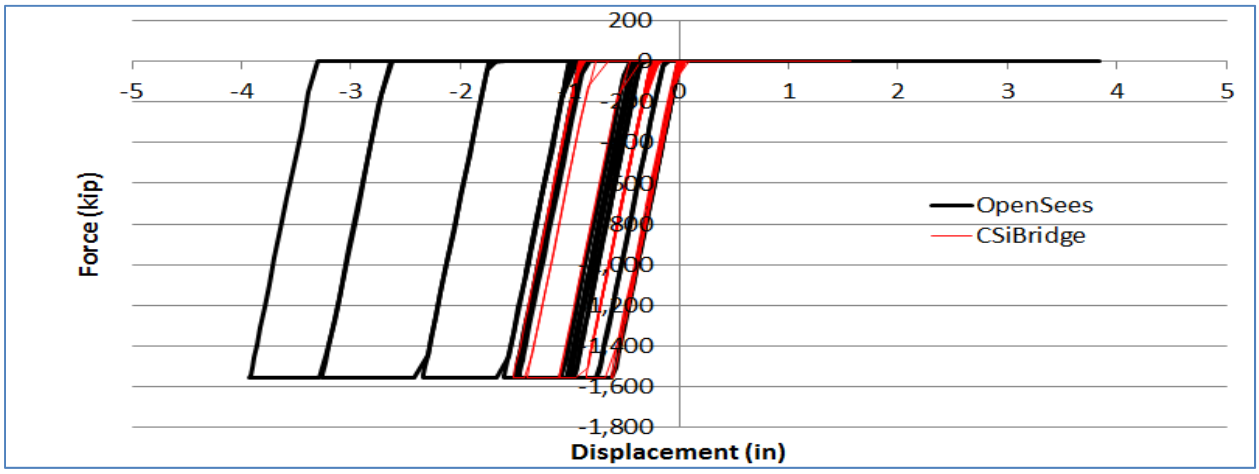

Figure I.16 Left abutment EPP-Gap model force-displacement response

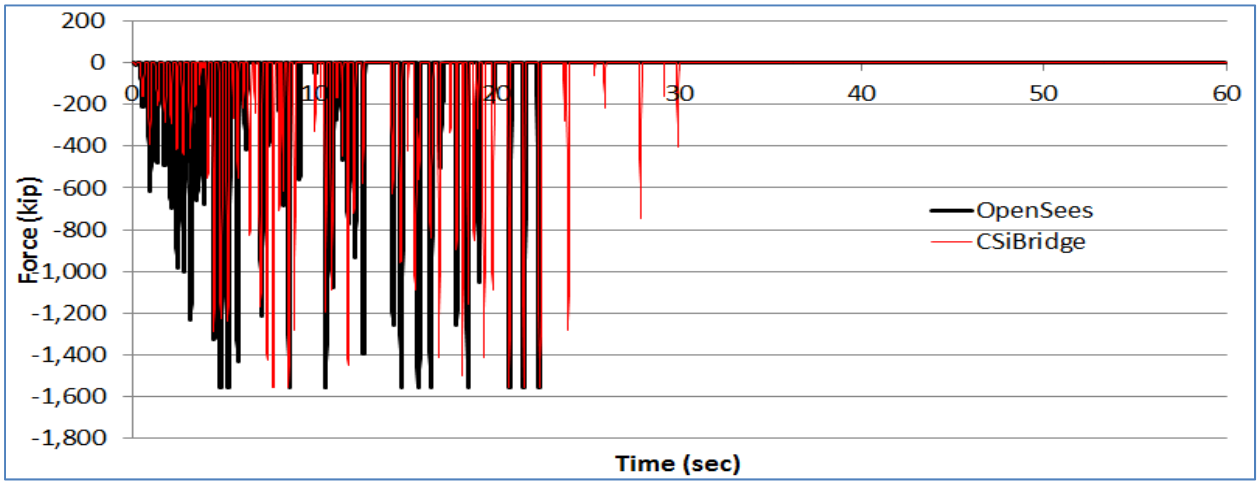

Figure I.17 Left abutment EPP- Gap model force response time history

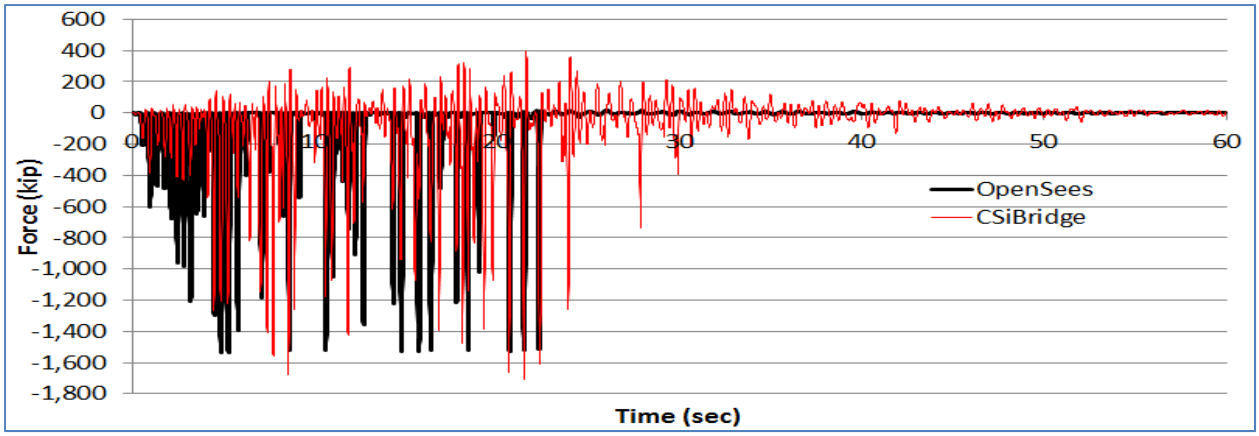

Figure I.18 Left deck-end axial force response time history

I.5.1.3 Right Abutment

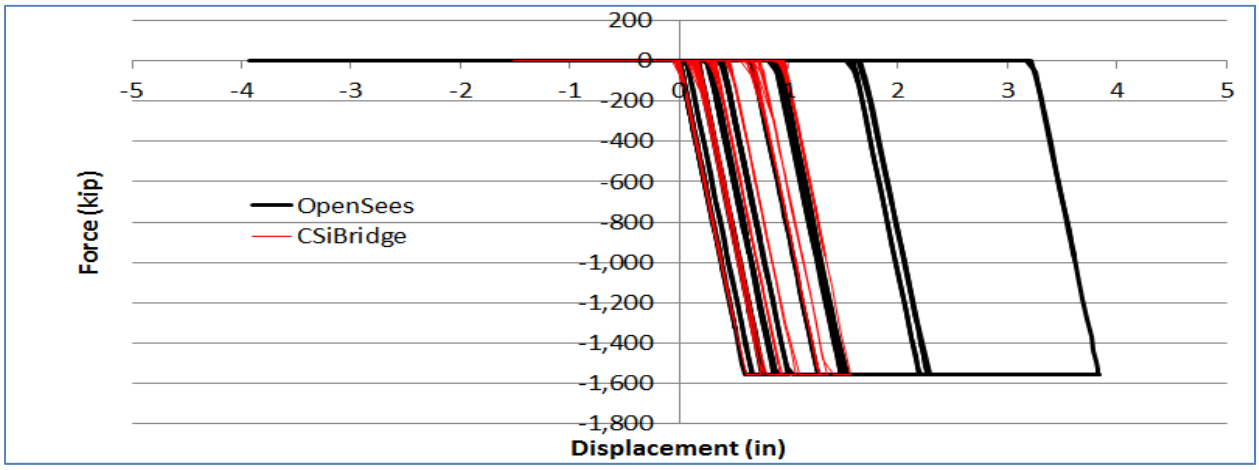

Figure I.19 Right abutment EPP-Gap model force-displacement response

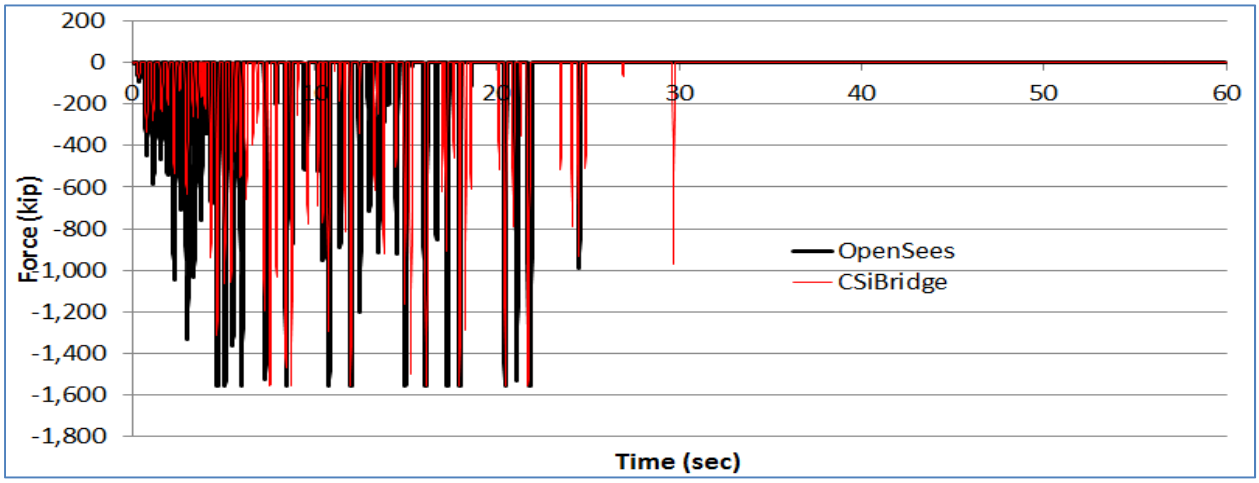

Figure I.20 Right abutment EPP-Gap model force response time history

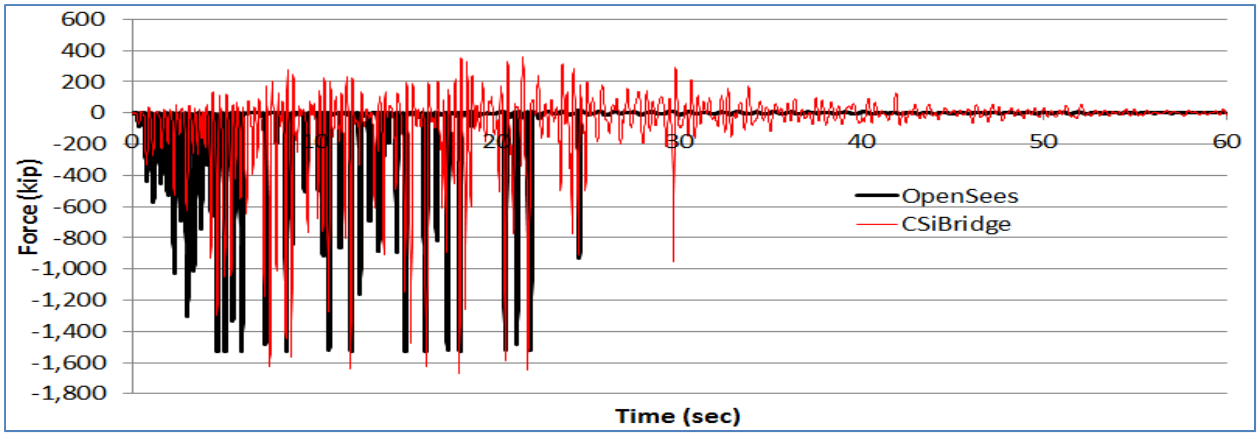

Figure I.21 Right deck-end axial force response time history

As shown above:

1) In OpenSees, we still see that the axial force at the end of the deck essentially matches the force exerted by the abutment as expected (Figure I.18 and Figure I.21).

2) In CSiBridge, now the axial force in the deck end is not the same as that exerted by the abutment (Figure I.18 and Figure I.21). Note in particular the positive (tensile) parts of Figure I.21 (CSiBridge), which are unexpected (because of the no-tension nature of the abutment EPP-Gap model).

Two additional EPP-gap models are shown below in an attempt to isolate the effects of the mass proportional and stiffness proportional components of the viscous damping formulation. As shown below, the stiffness proportional damping case is quite off. In the mass proportional damping case, we do not see the unexpected tensile force instants at the ends of the deck (matches expectation), and the result overall is much closer to that of OpenSees.

I.5.2 Stiffness-Proportional Damping Only

The case below was analyzed using the following Rayleigh damping coefficients (just 5% damping at the first frequency): Stiffness-proportional damping coefficient = 0.0191, and Mass-proportional damping coefficient = 0.

I.5.2.1 Bridge Column

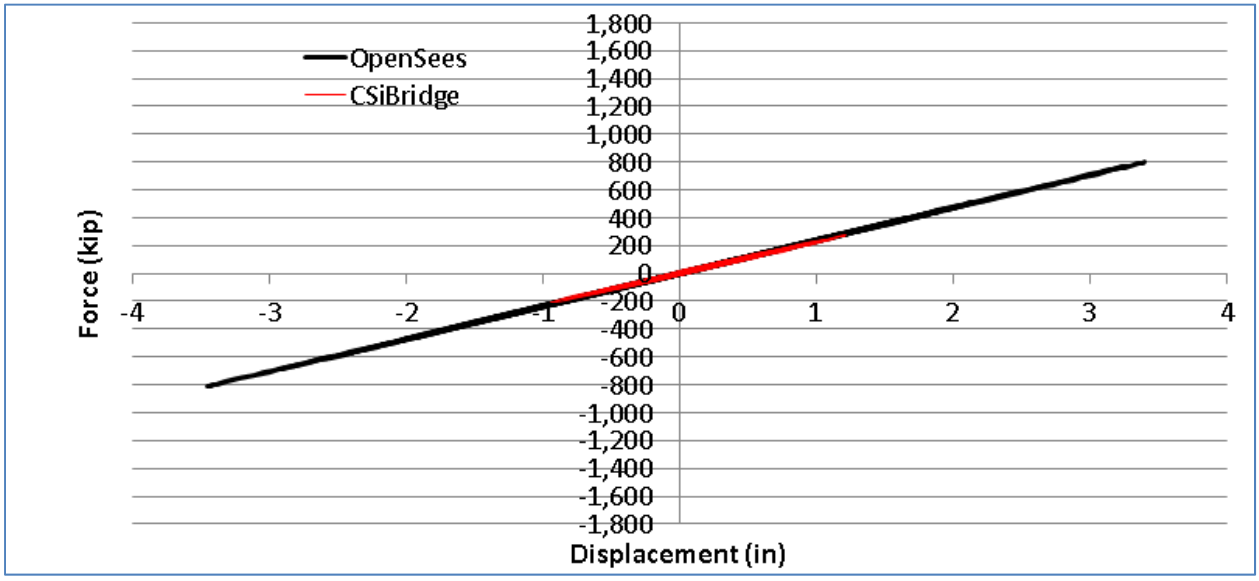

Figure I.22 Column shear force displacement response

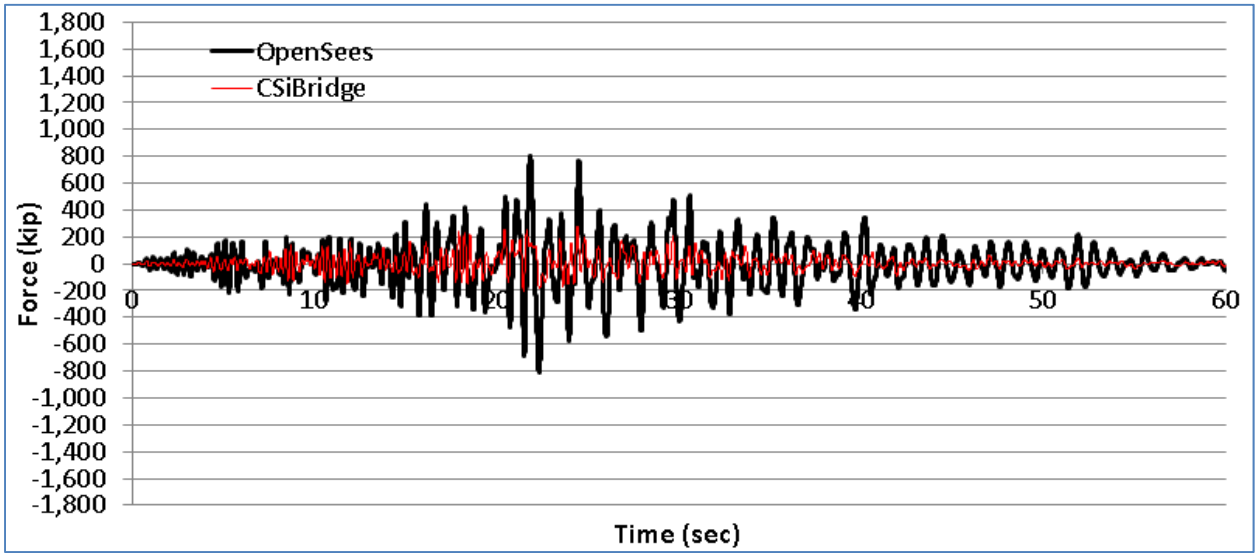

Figure I.23 Column shear force response time history

I.5.2.2 Left Abutment

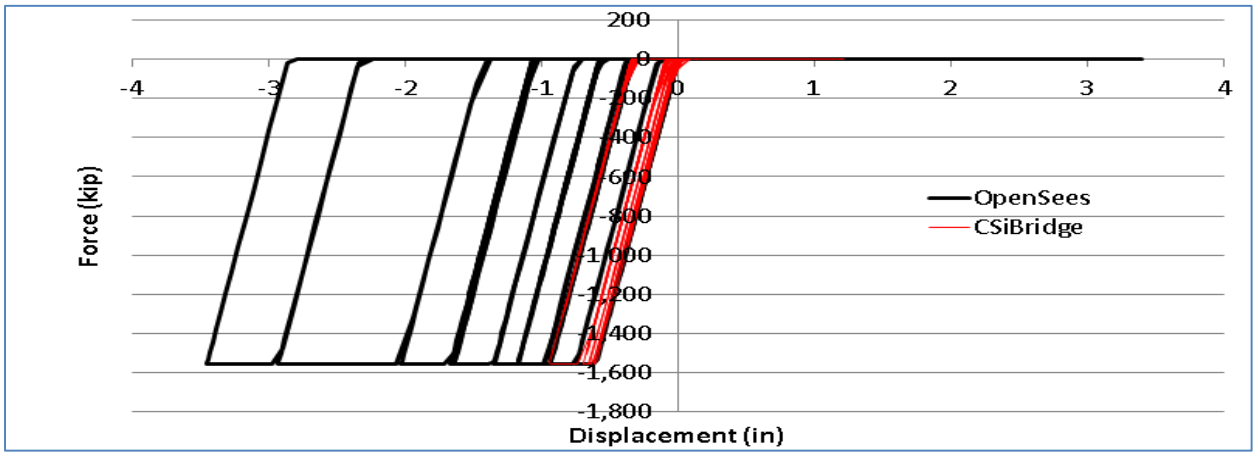

Figure I.24 Left abutment EPP-Gap model force-displacement response

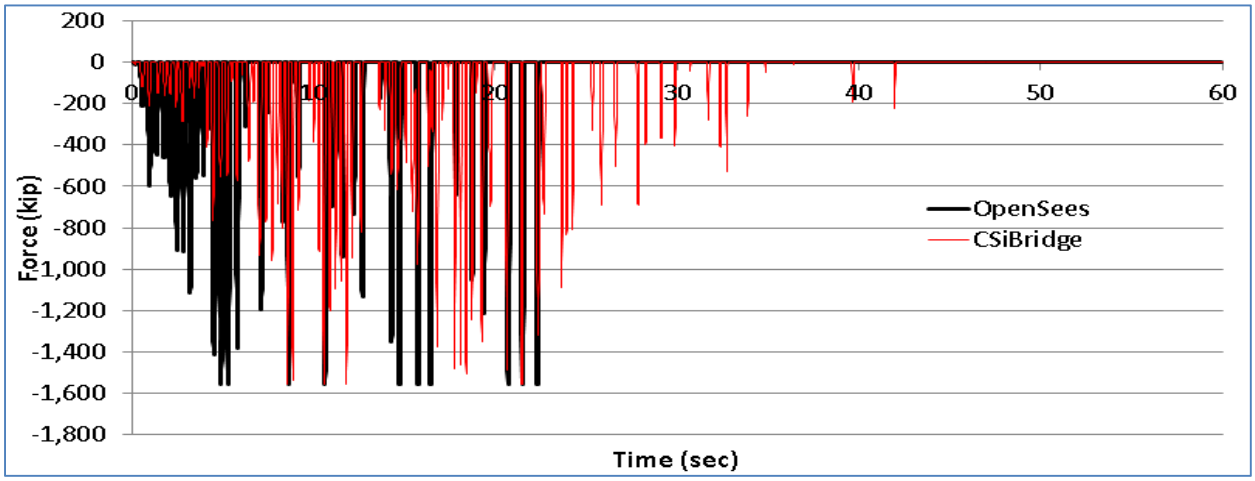

Figure I.25 Left abutment EPP-Gap model force response time history

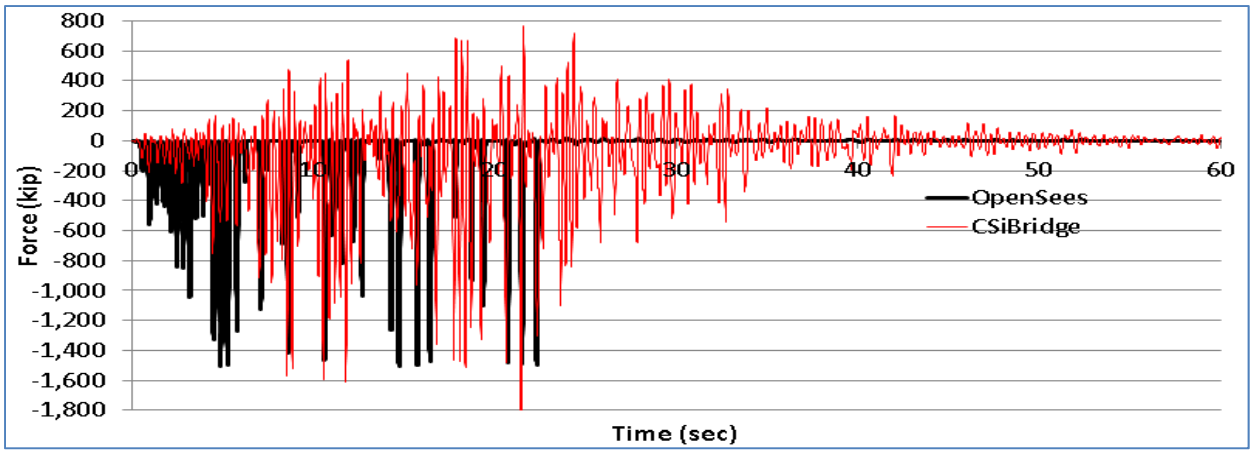

Figure I.26 Left deck-end axial force response time history

I.5.2.3 Right Abutment

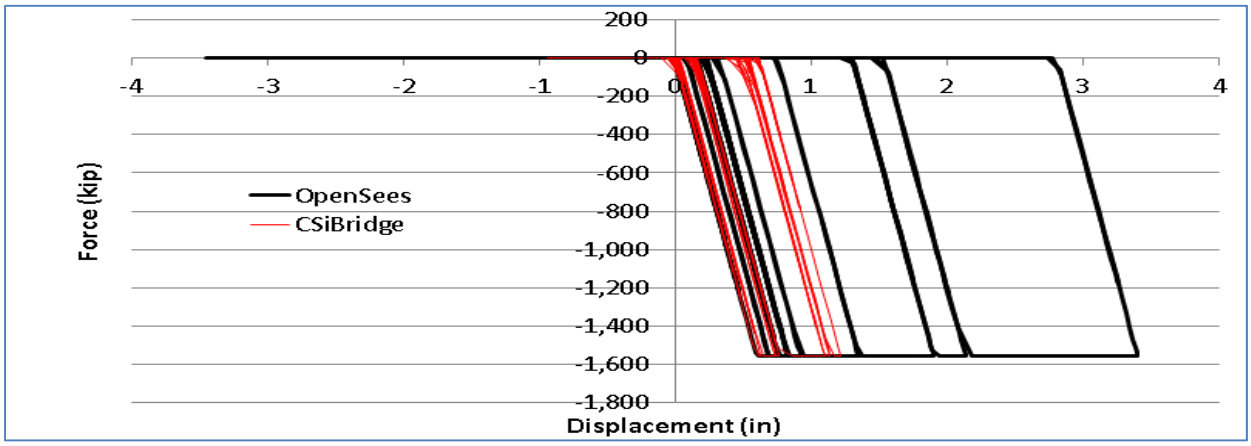

Figure I.27 Right abutment EPP-Gap model force-displacement response

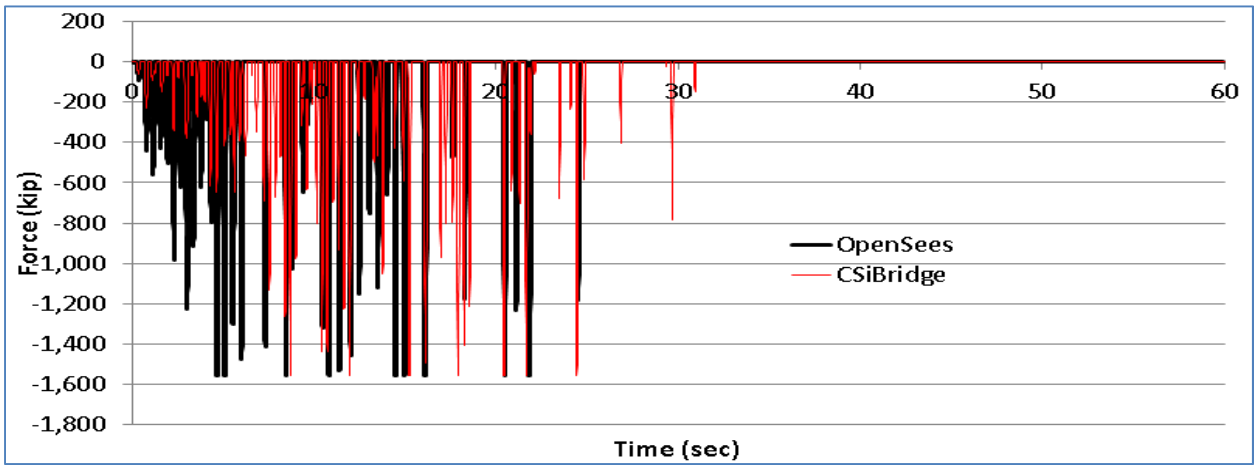

Figure I.28 Right abutment EPP-Gap model force response time history

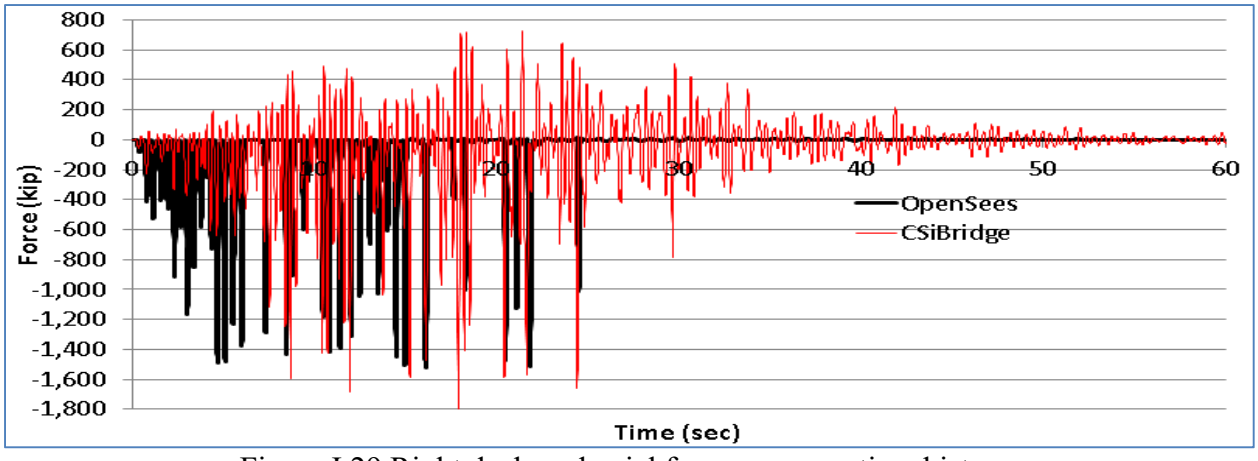

Figure I.29 Right deck-end axial force response time history

I.5.3 Mass-Proportional Damping Only

The case below was analyzed using the following Rayleigh damping coefficients (just 5% damping specified at the first frequency): Stiffness-proportional damping coefficient = 0, and Mass-proportional damping coefficient = 0.5236.

I.5.3.1 Bridge Column

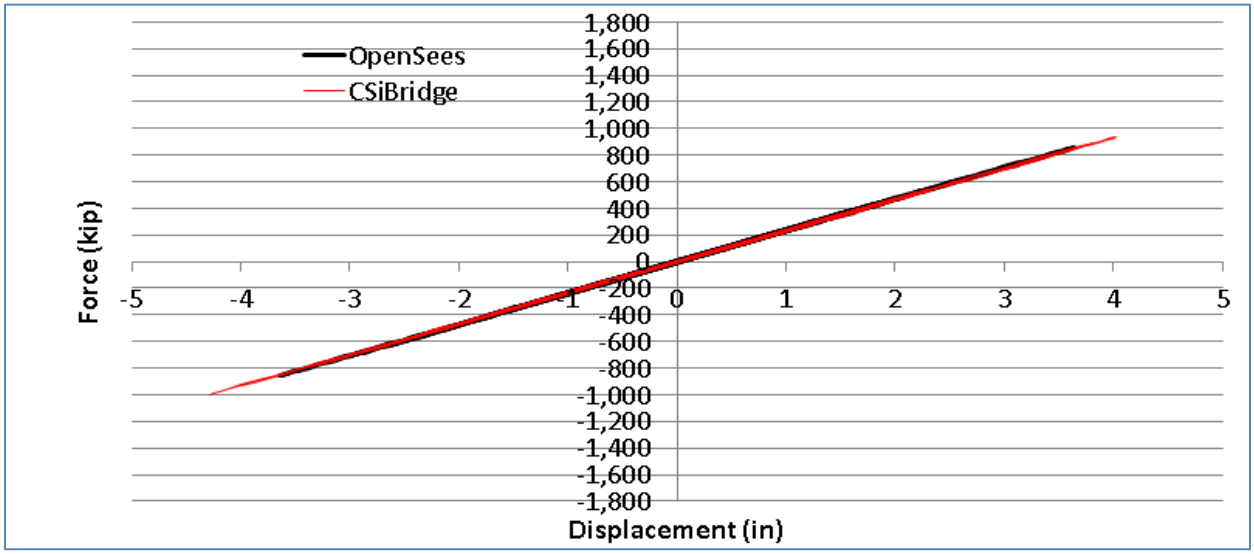

Figure I.30 Column shear force displacement response

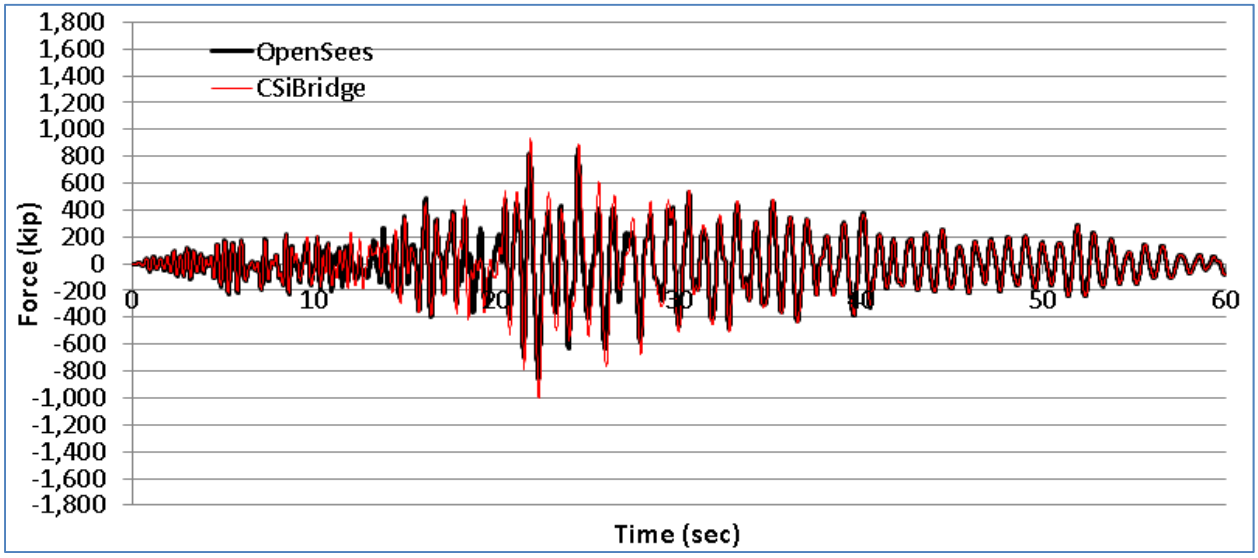

Figure I.31 Column shear force response time history

I.5.3.2 Left Abutment

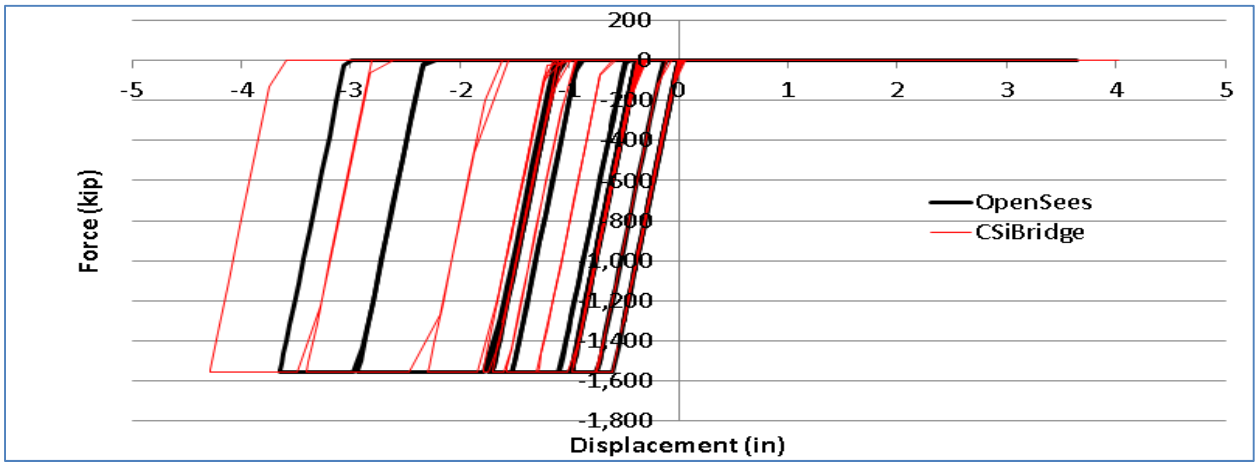

Figure I.32 Left abutment EPP-Gap model force-displacement response

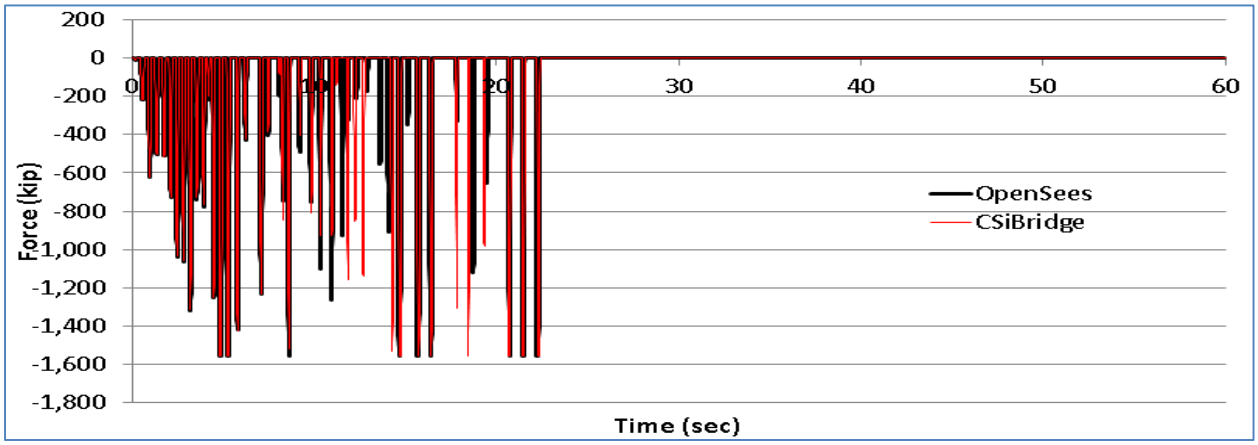

Figure I.33 Left abutment EPP-Gap model force response time history

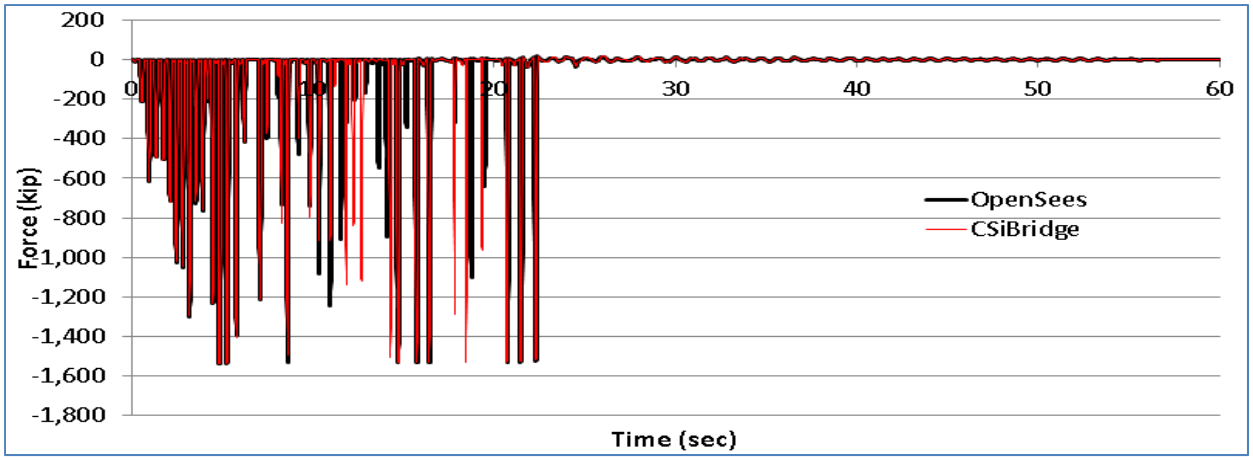

Figure I.34 Left deck-end axial force response time history

I.5.3.3 Right Abutment

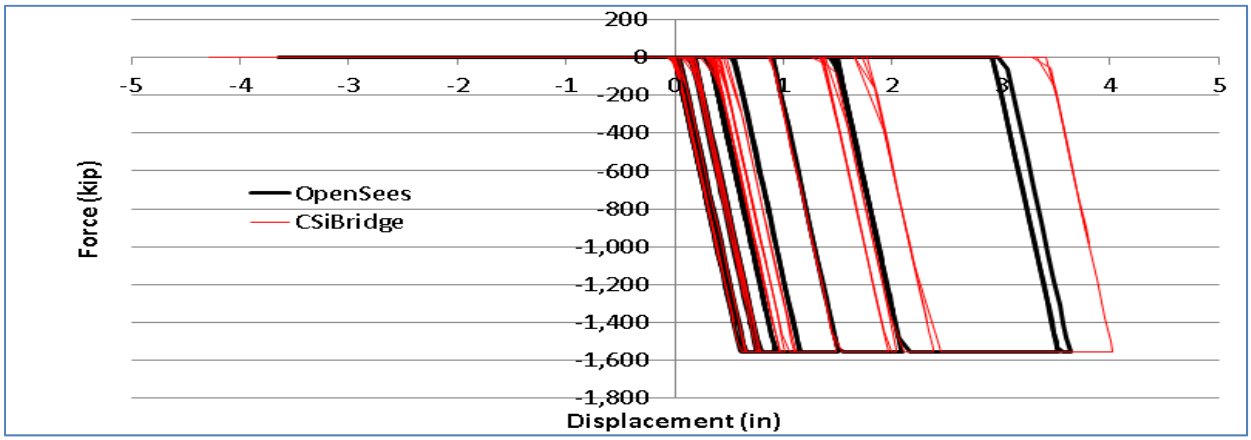

Figure I.35 Right abutment EPP-Gap model force-displacement response

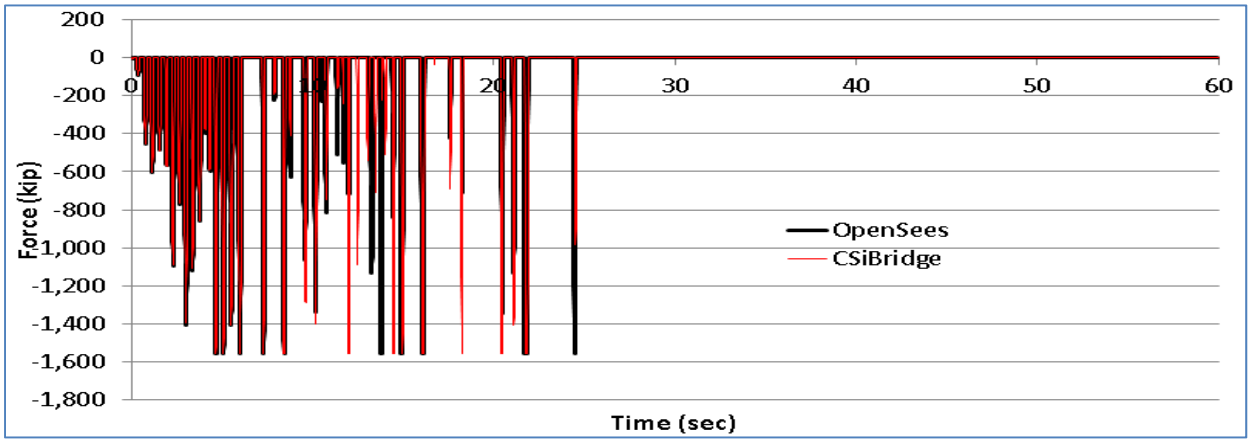

Figure I.36 Right abutment EPP-Gap model force response time history

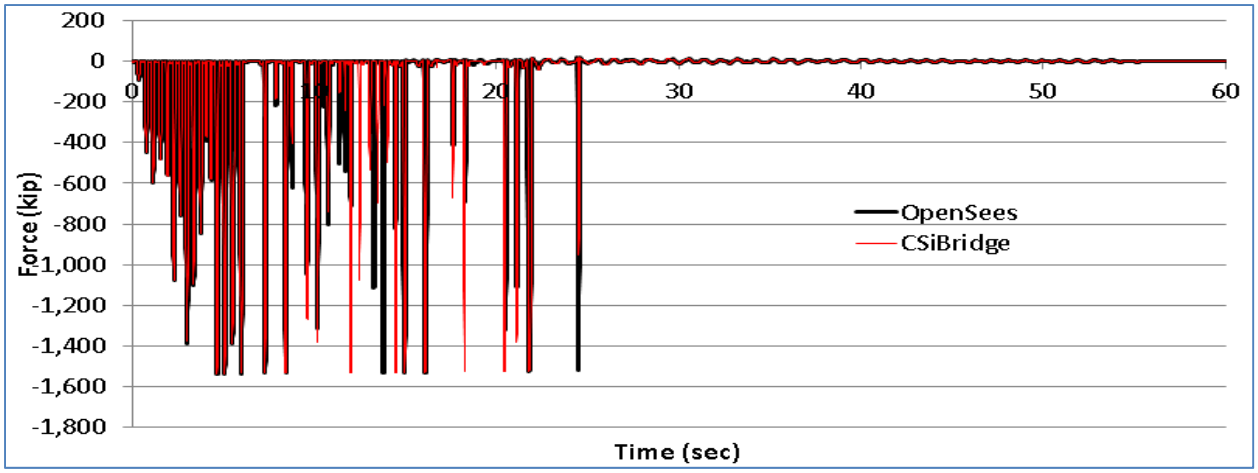

Figure I.37 Right deck-end axial force response time history

APPENDIX J: CSIBRIDGE RESULTS FOR OSB2

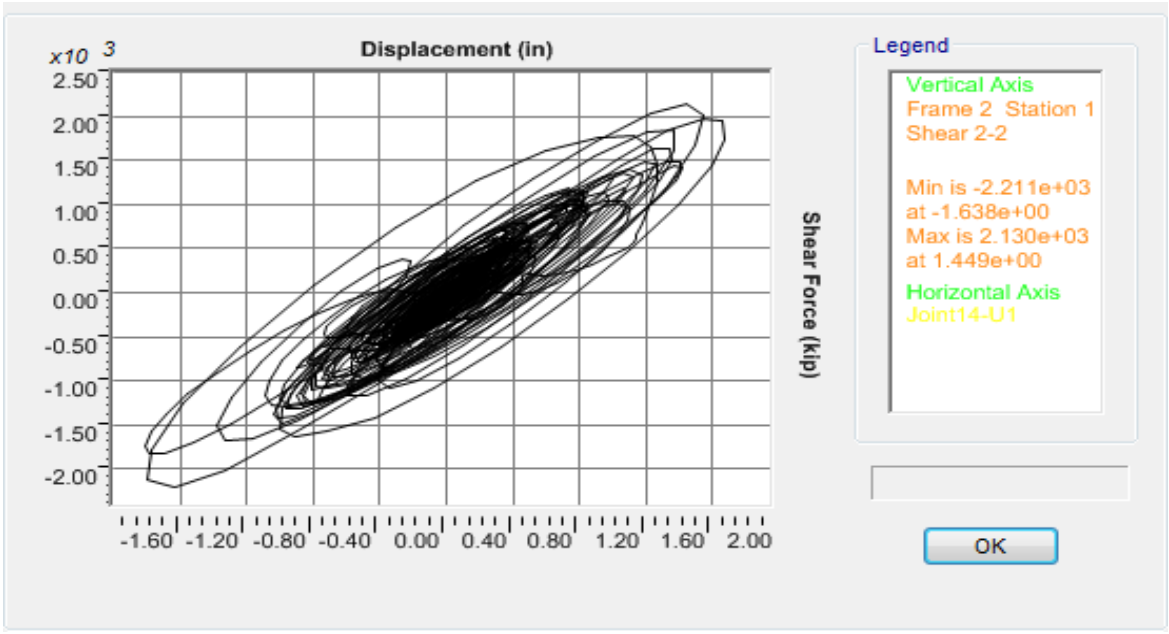

a)

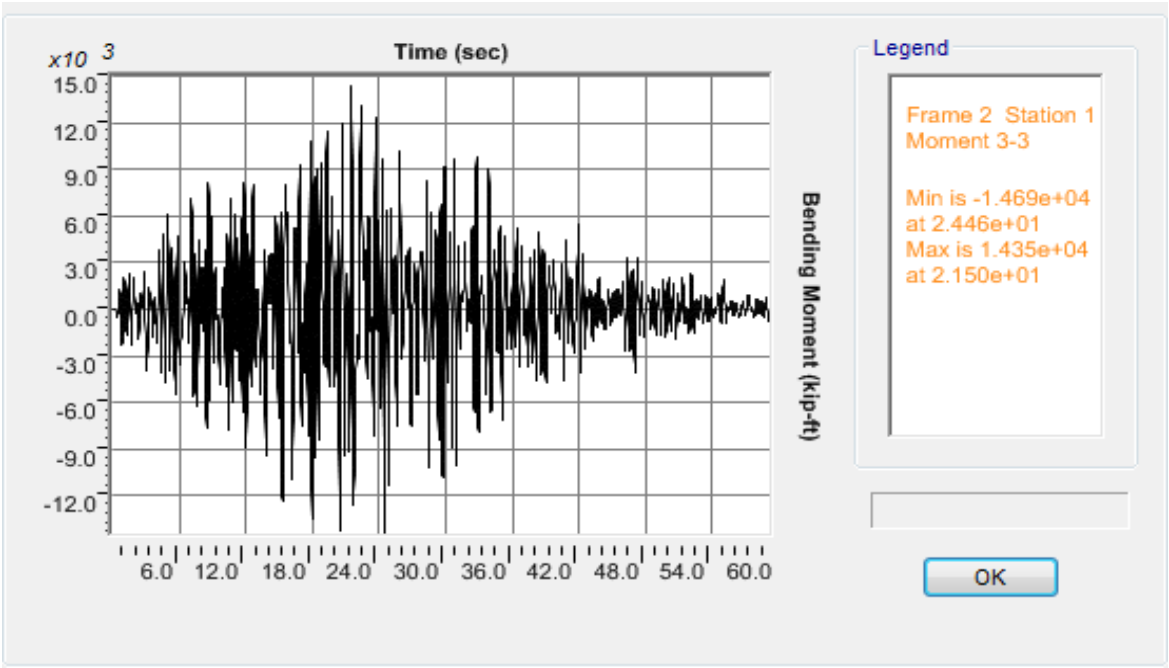

b)

Figure J.1 OSB2 column top response for Motion 1 ROCKS1N1: a) Longitudinal shear force-displacement hysteresis; b) Bending moment time history in the longitudinal direction

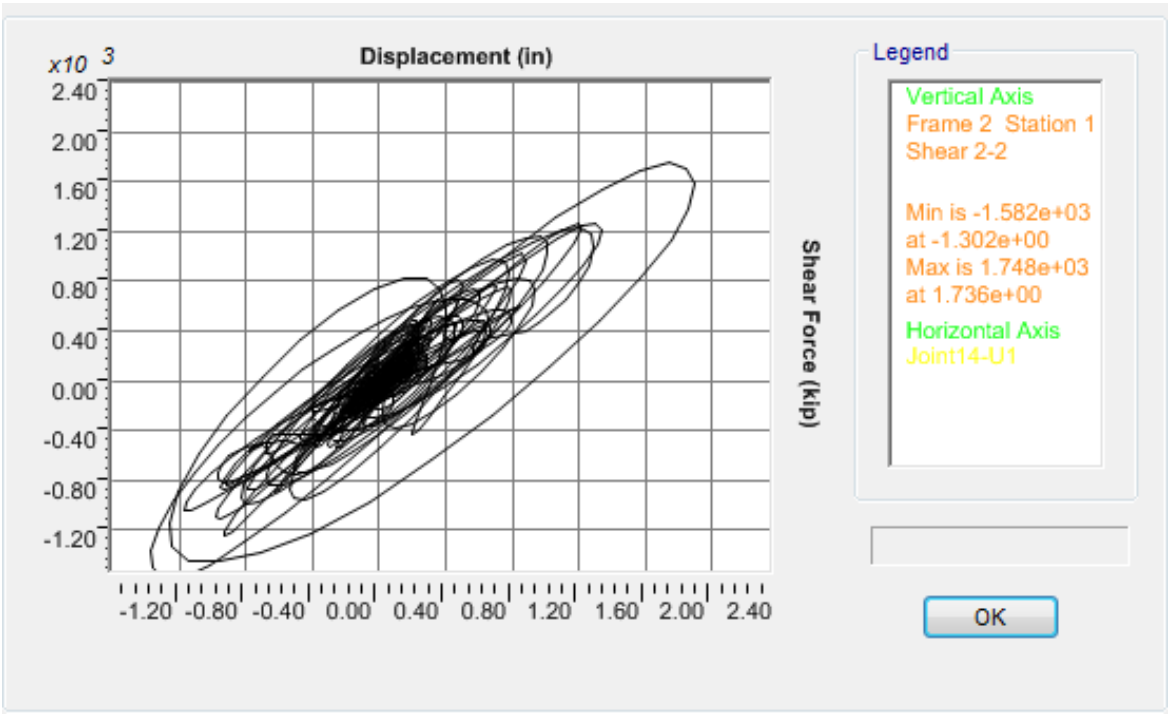

a)

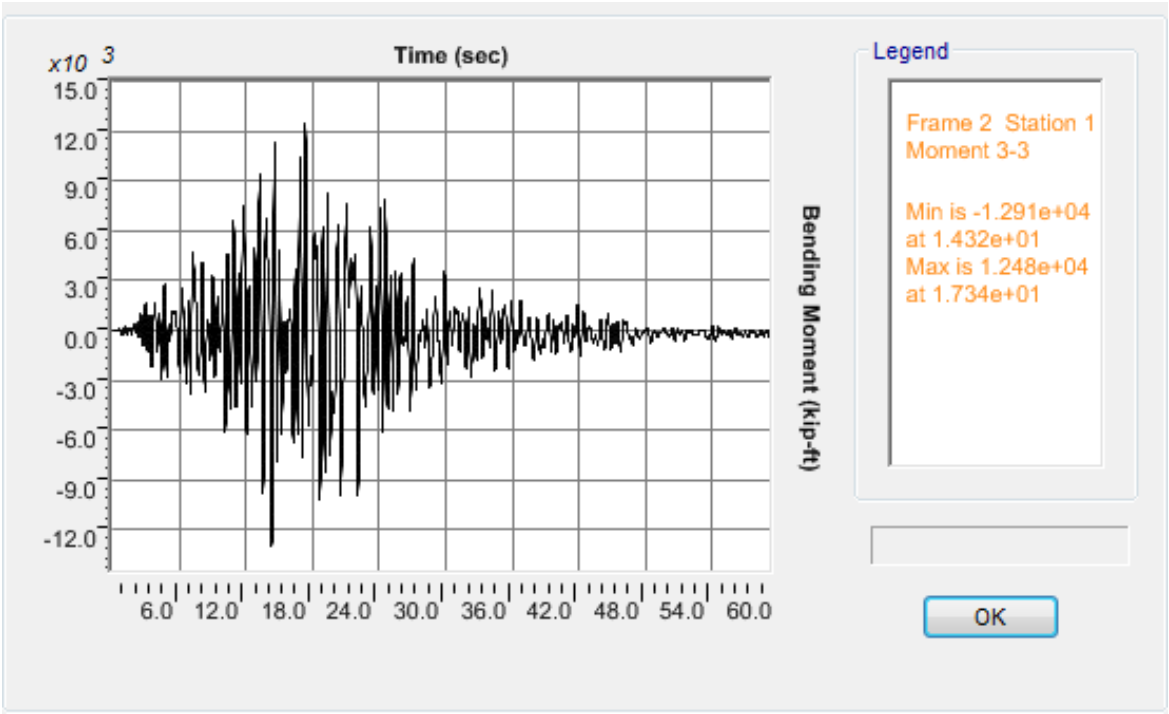

b)

Figure J.2 OSB2 column top response for Motion 2 ROCKS1N2: a) Longitudinal shear force-displacement hysteresis; b) Bending moment time history in the longitudinal direction

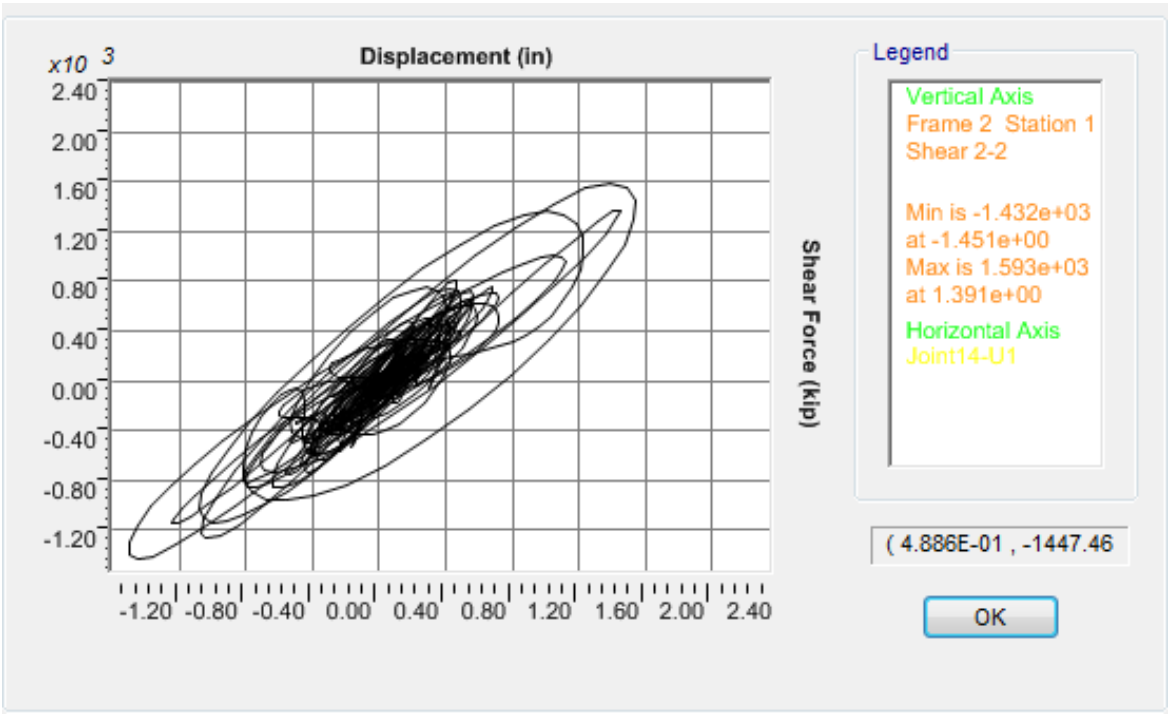

a)

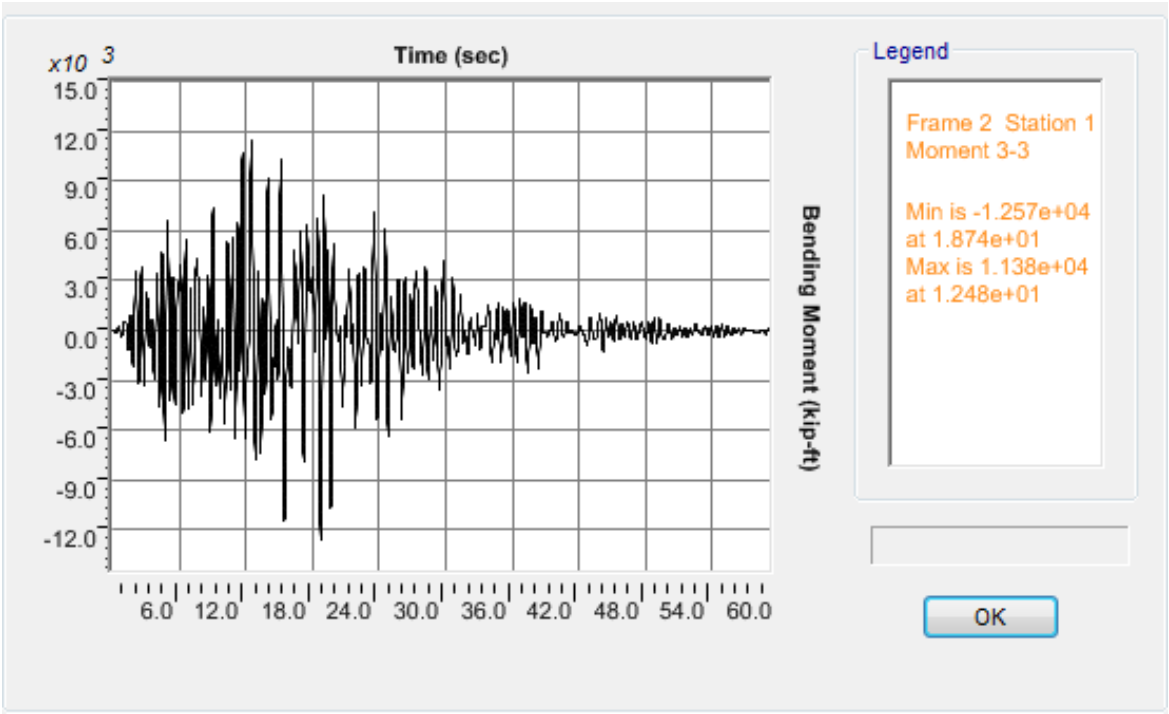

b)

Figure J.3 OSB2 column top response for Motion 3 ROCKS1N3: a) Longitudinal shear force-displacement hysteresis; b) Bending moment time history in the longitudinal direction

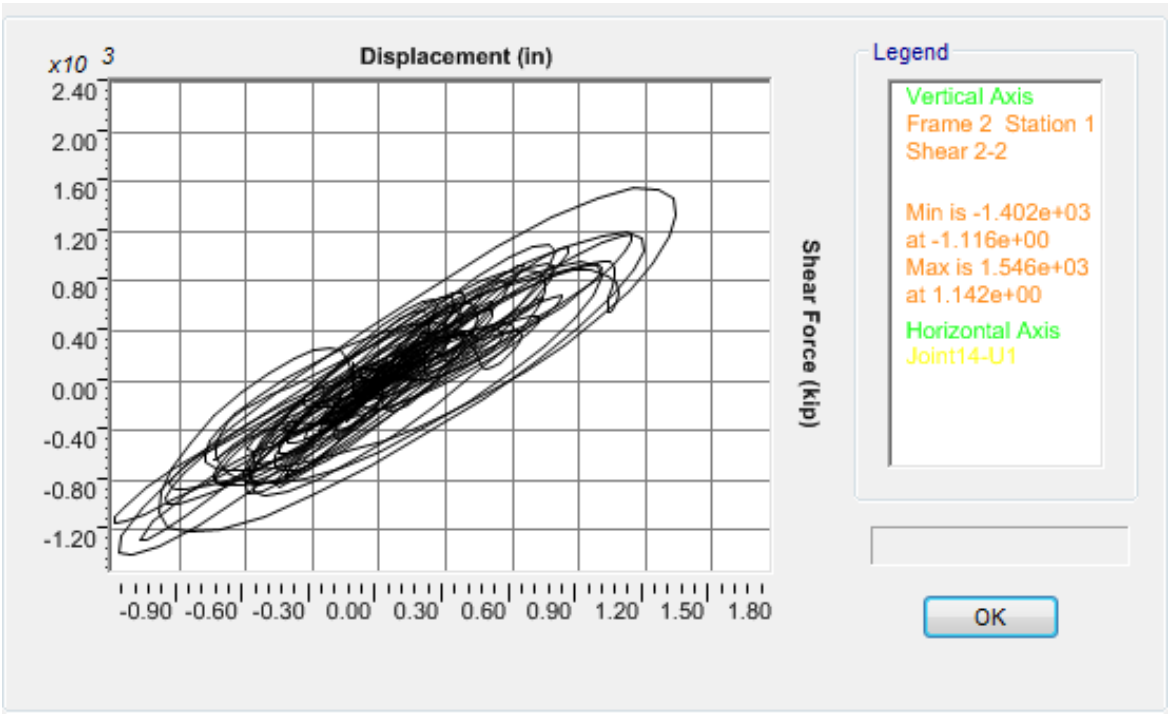

a)

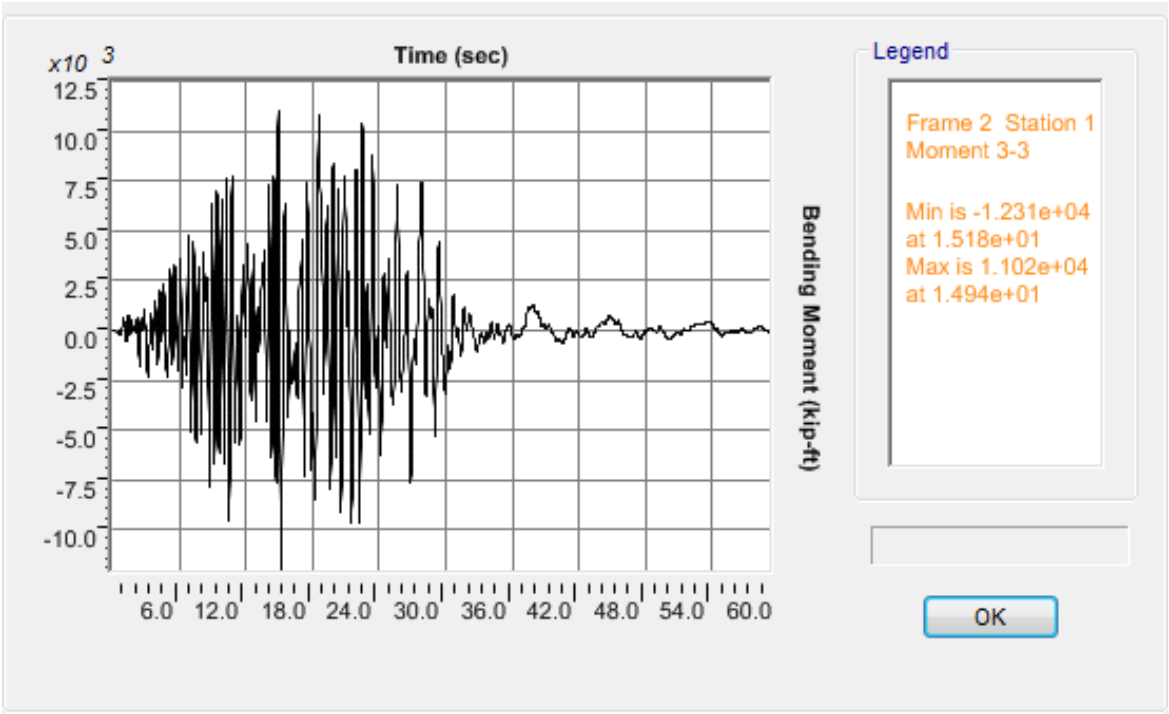

b)

Figure J.4 OSB2 column top response for Motion 4 ROCKS1N4: a) Longitudinal shear force-displacement hysteresis; b) Bending moment time history in the longitudinal direction

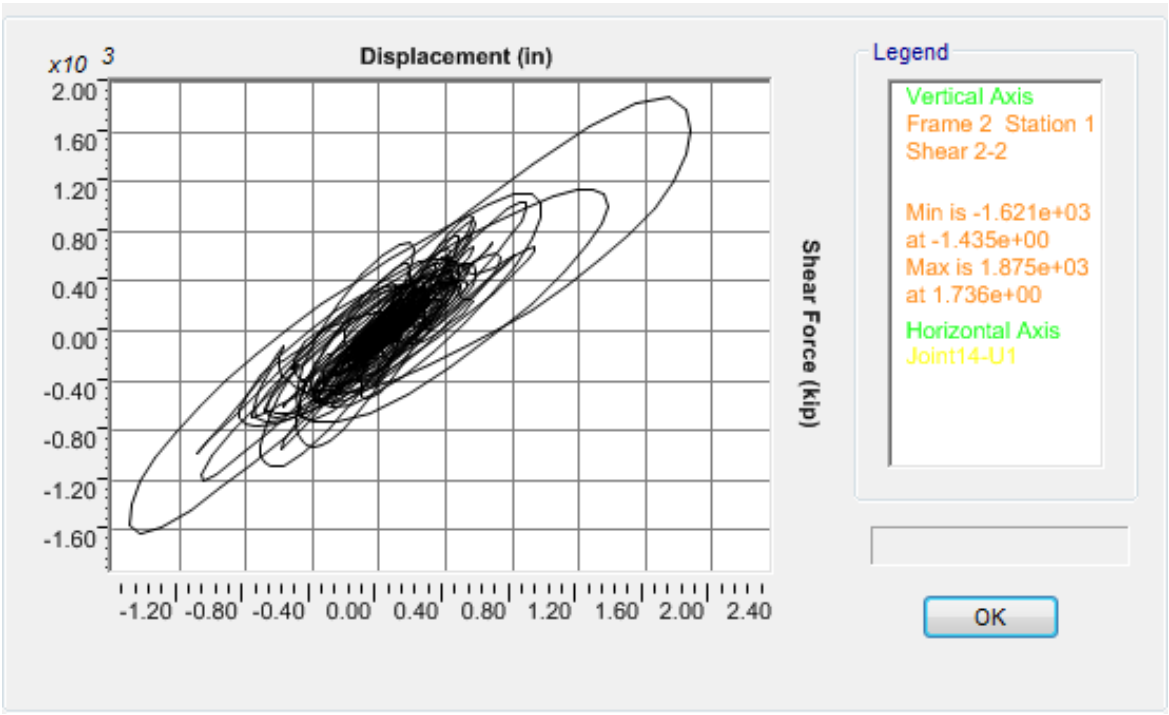

a)

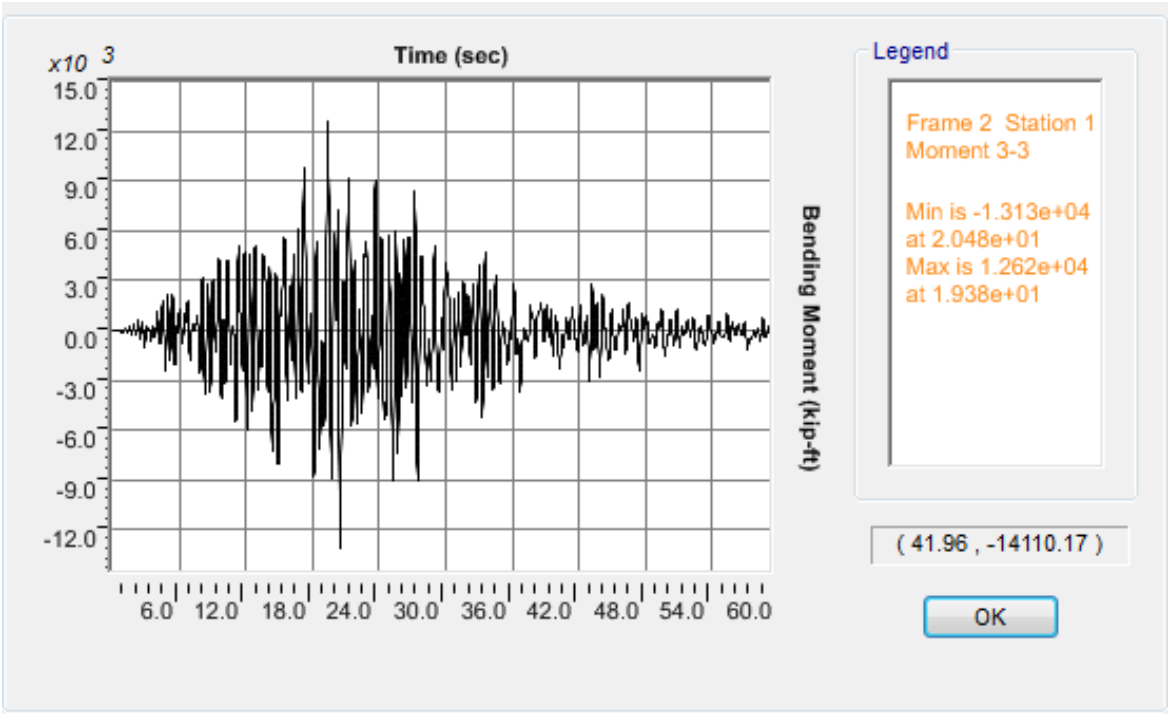

b)

Figure J.5 OSB2 column top response for Motion 5 ROCKS1N5: a) Longitudinal shear force-displacement hysteresis; b) Bending moment time history in the longitudinal direction

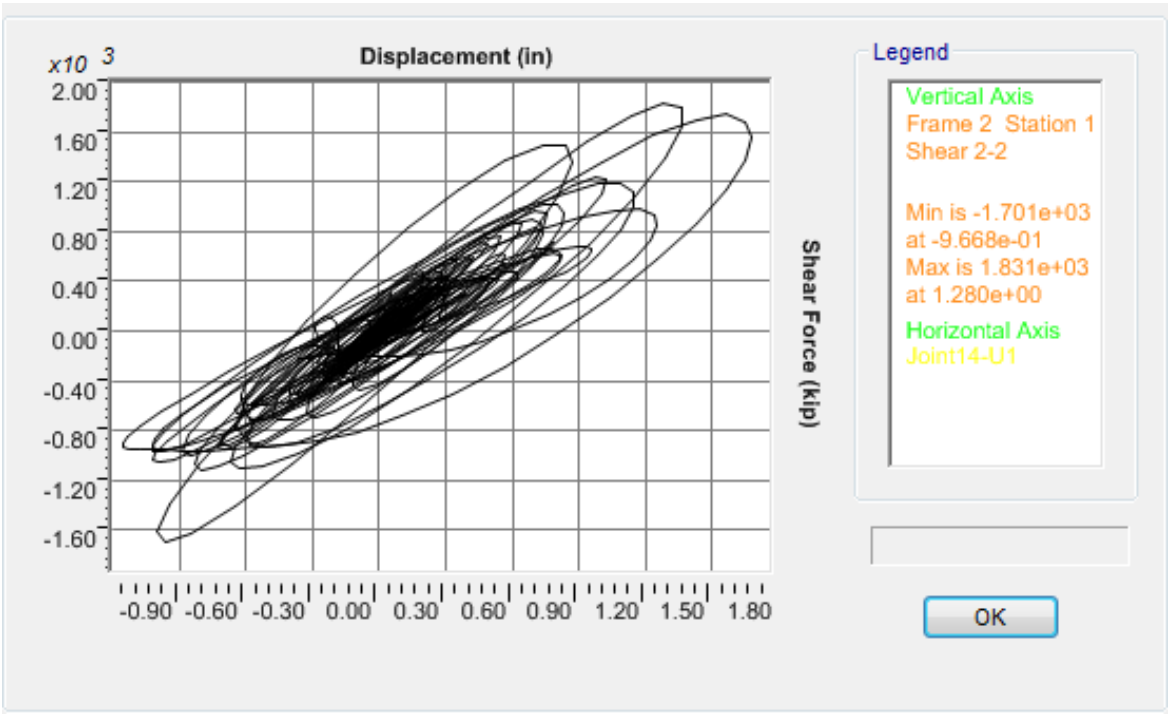

a)

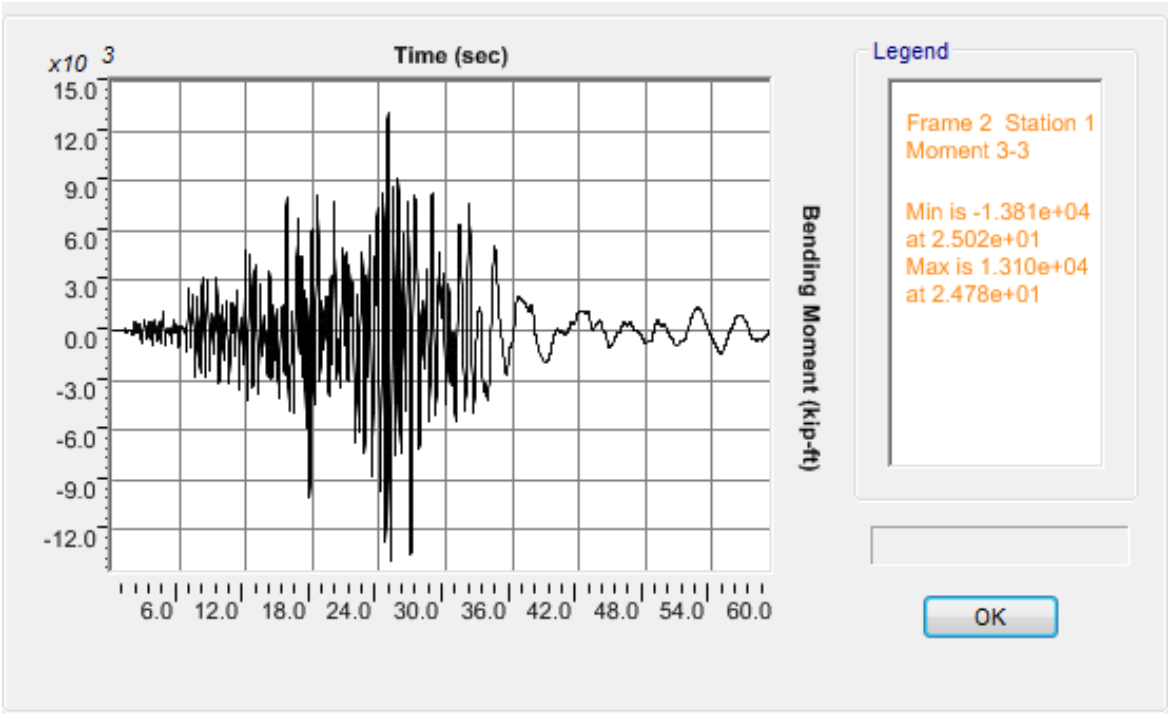

b)

Figure J.6 OSB2 column top response for Motion 6 ROCKS1N6: a) Longitudinal shear force-displacement hysteresis; b) Bending moment time history in the longitudinal direction

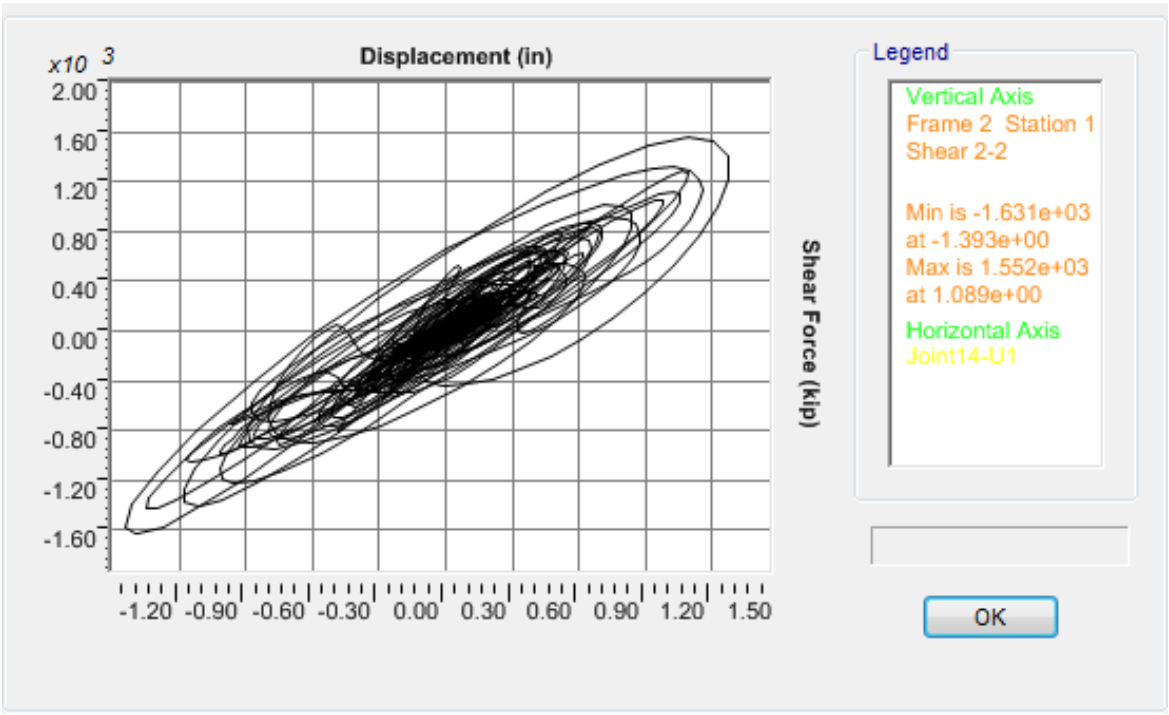

a)

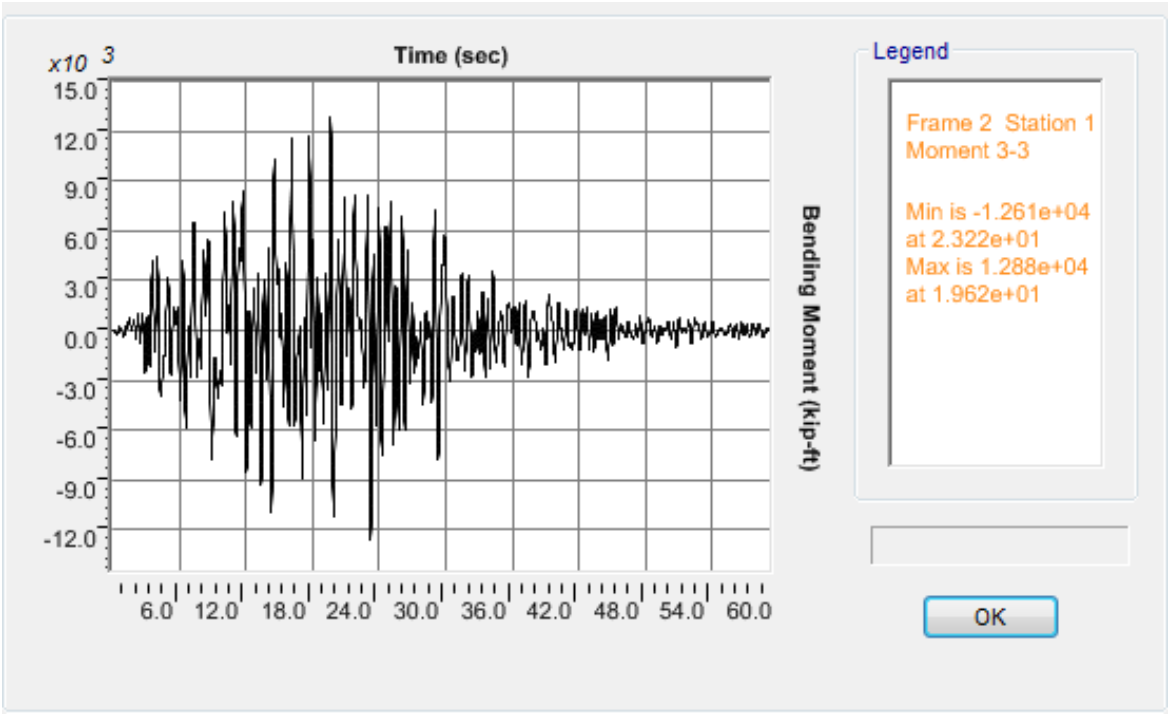

b)

Figure J.7 OSB2 column top response for Motion 7 ROCKS1N7: a) Longitudinal shear force-displacement hysteresis; b) Bending moment time history in the longitudinal direction

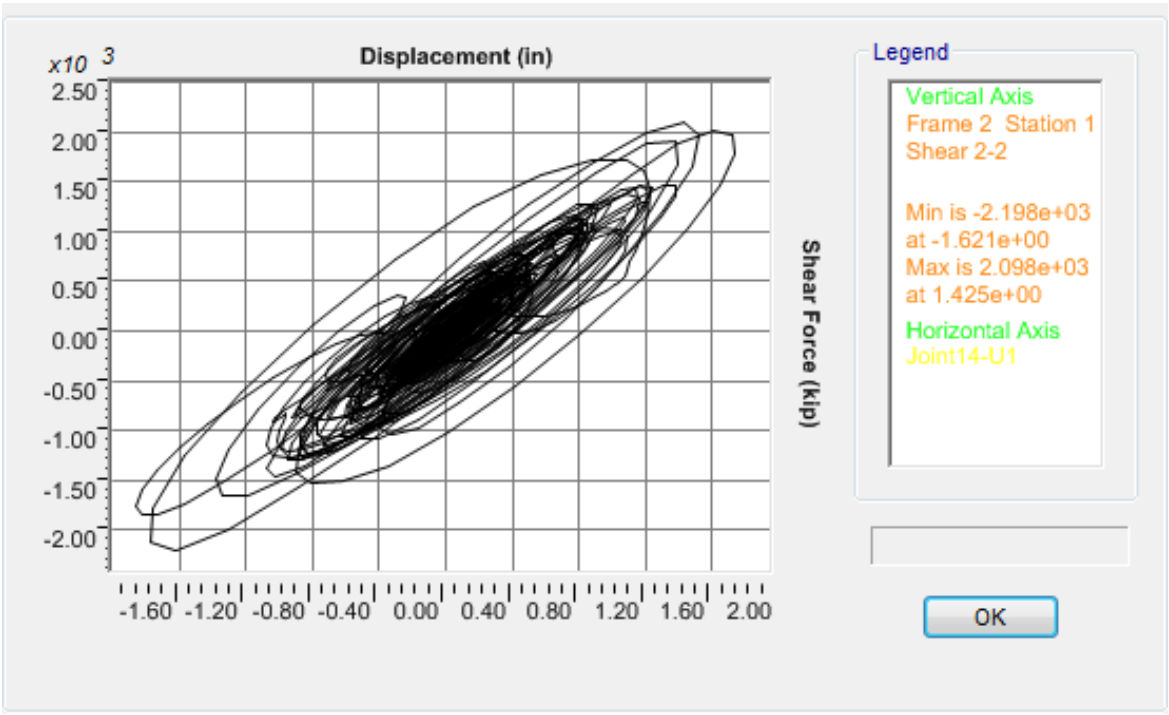

a)

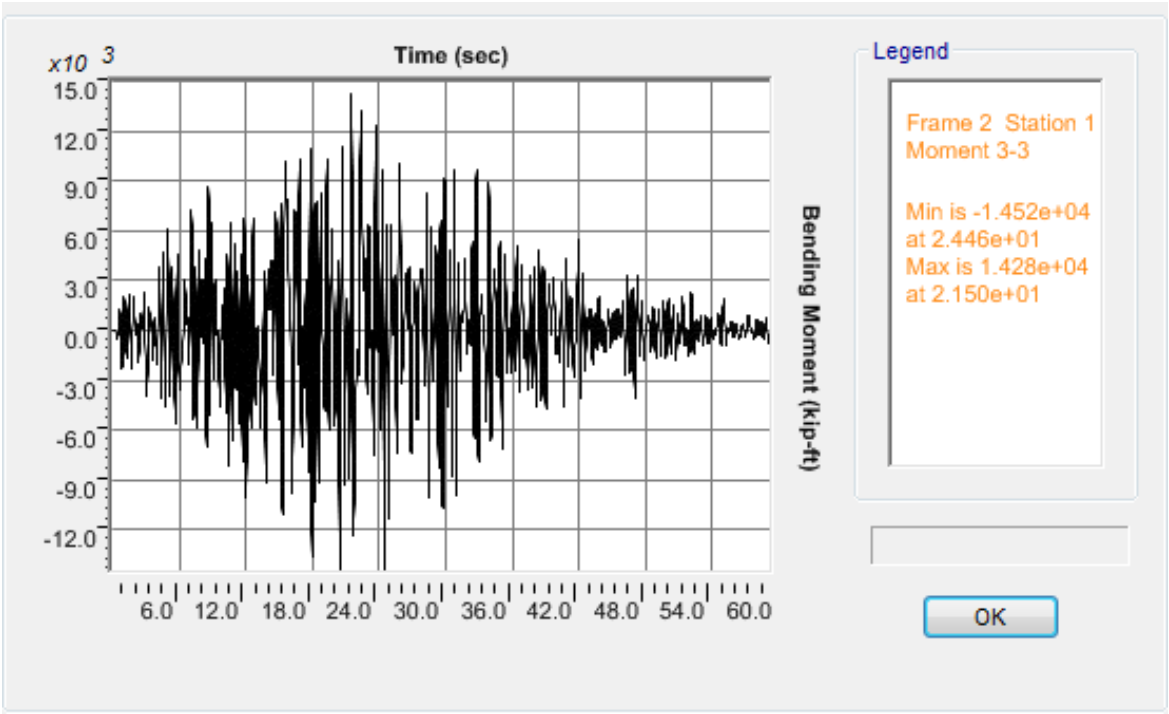

b)

Figure J.8 OSB2 column top response for Motion 8 ROCKS1P1: a) Longitudinal shear force-displacement hysteresis; b) Bending moment time history in the longitudinal direction

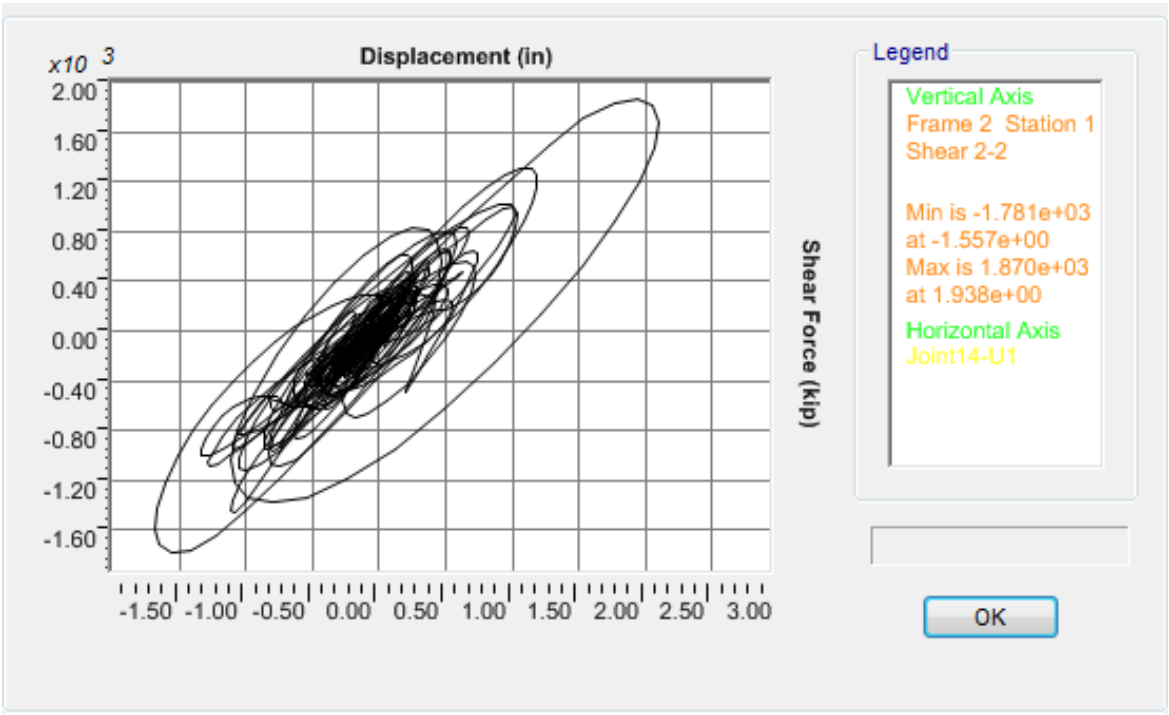

a)

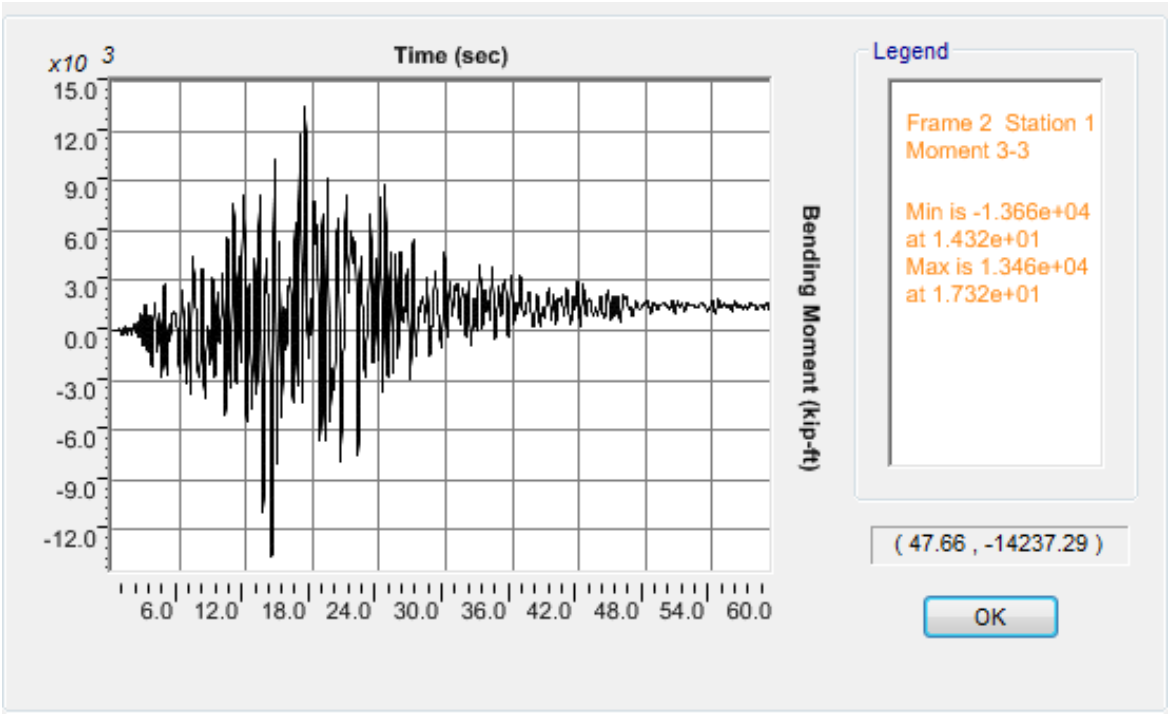

b)

Figure J.9 OSB2 column top response for Motion 9 ROCKS1P2: a) Longitudinal shear force-displacement hysteresis; b) Bending moment time history in the longitudinal direction

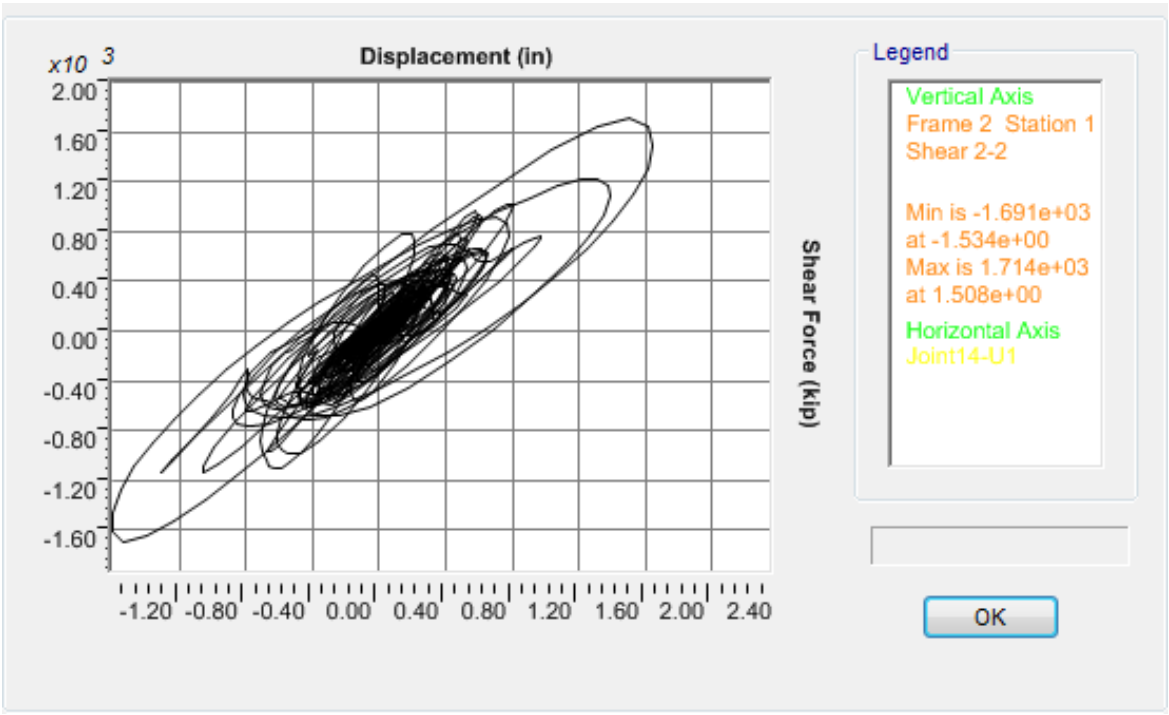

a)

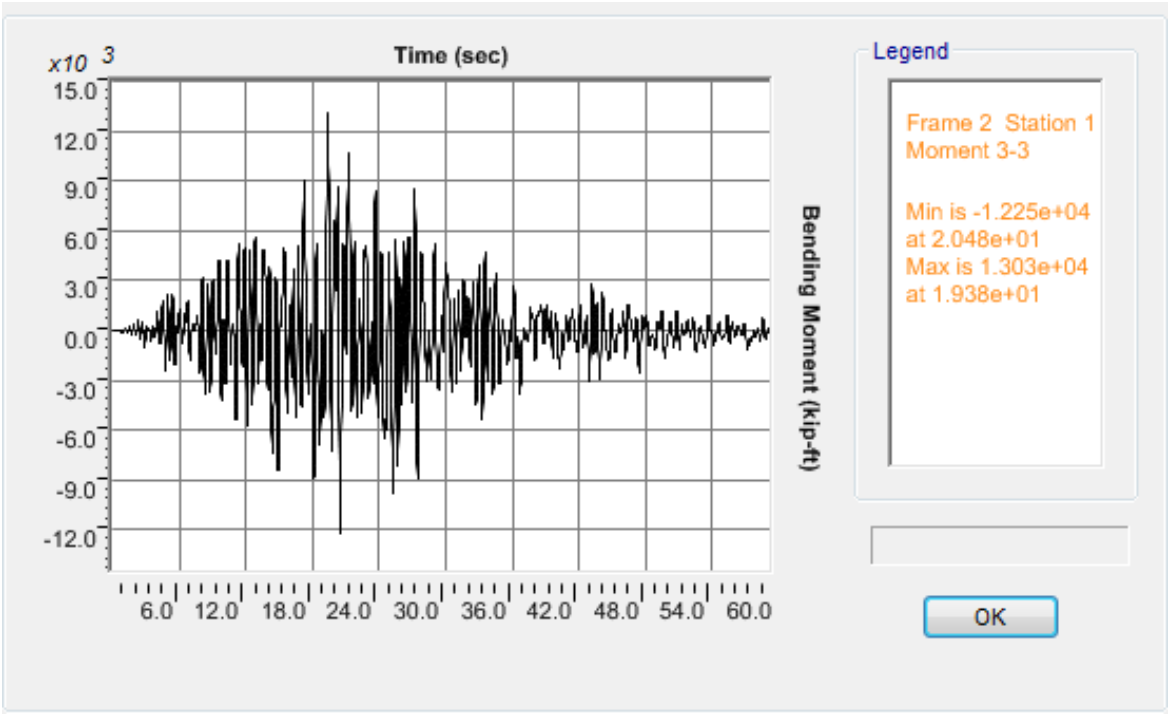

b)

Figure J.10 OSB2 column top response for Motion 10 ROCKS1P3: a) Longitudinal shear force-displacement hysteresis; b) Bending moment time history in the longitudinal direction

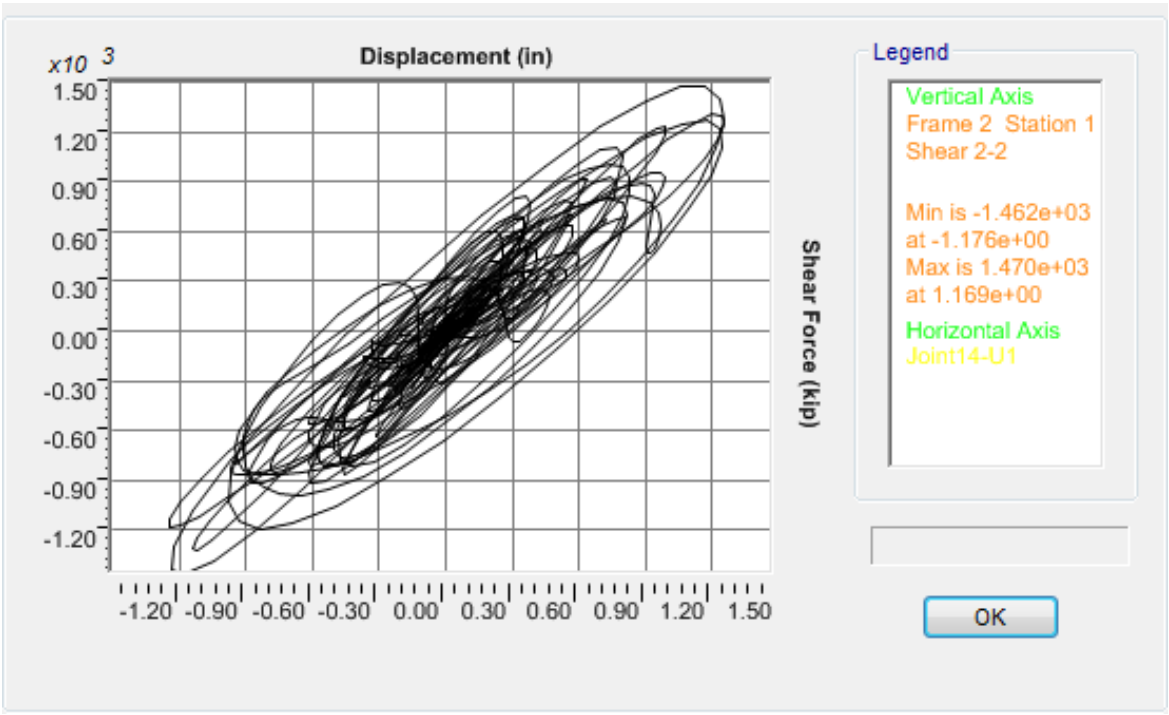

a)

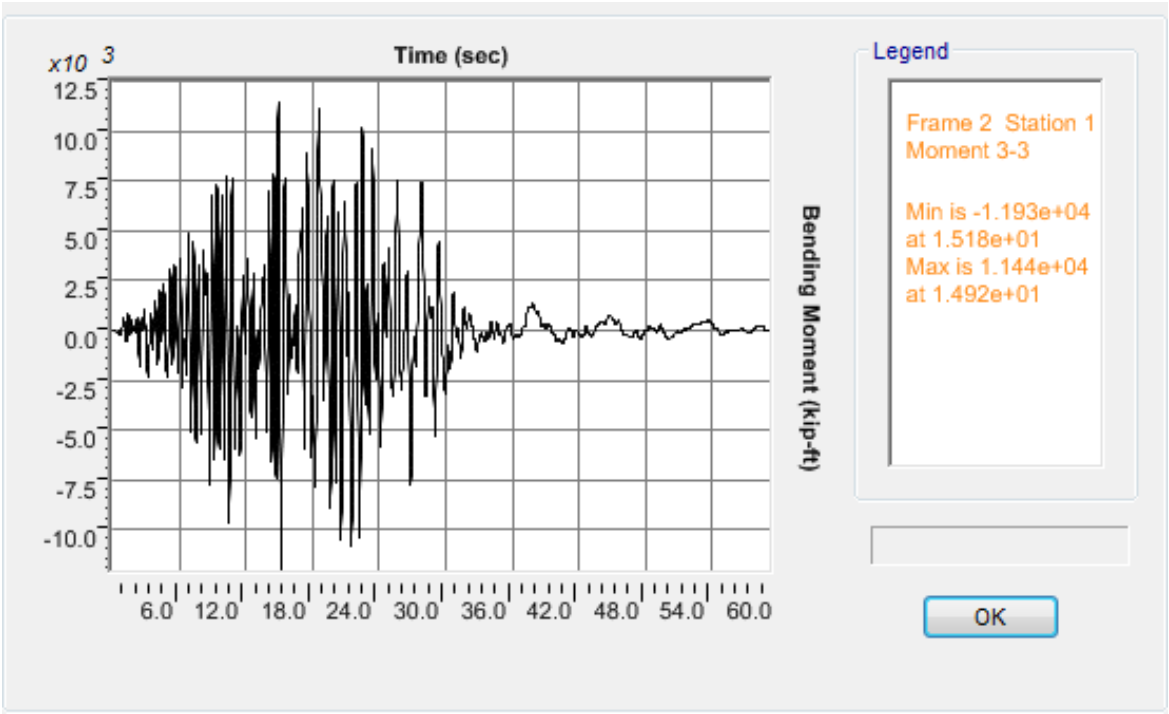

b)

Figure J.11 OSB2 column top response for Motion 11 ROCKS1P4: a) Longitudinal shear force-displacement hysteresis; b) Bending moment time history in the longitudinal direction

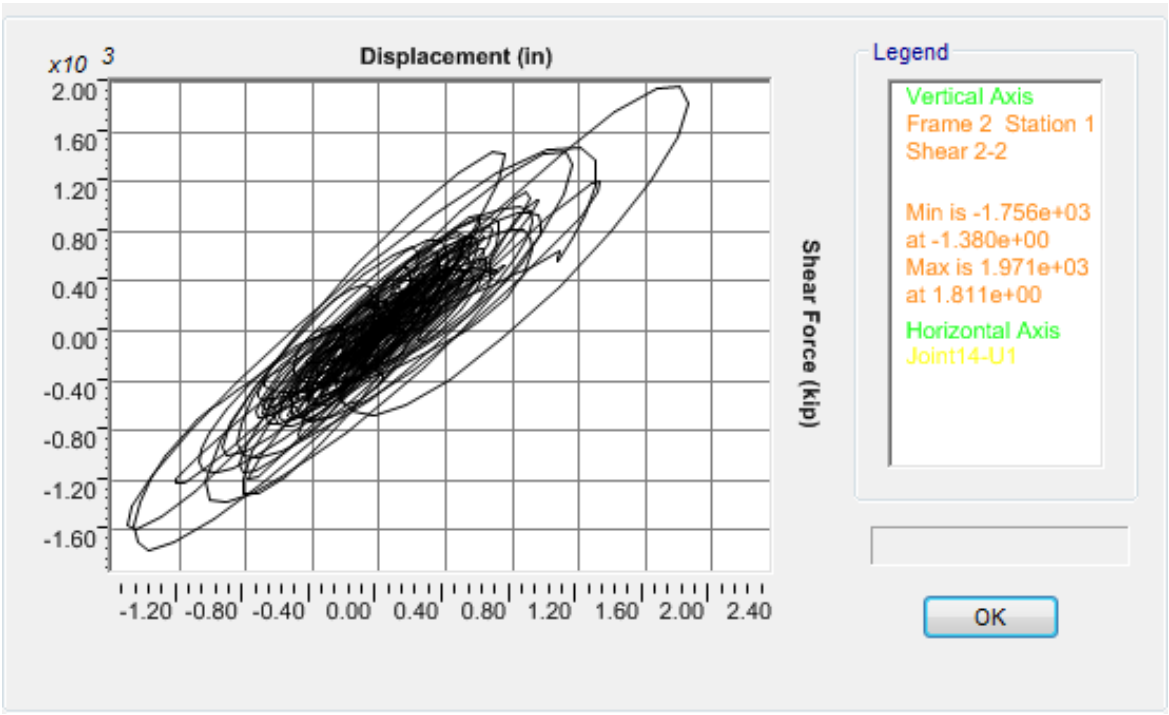

a)

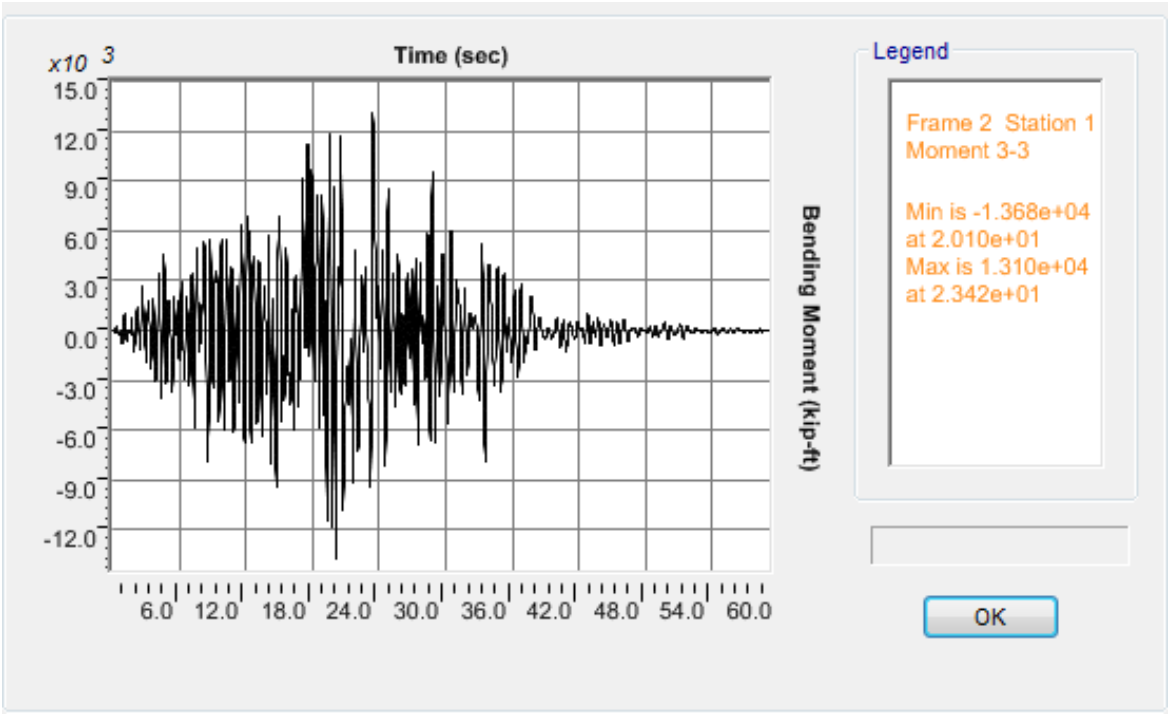

b)

Figure J.12 OSB2 column top response for Motion 12 ROCKS1P5: a) Longitudinal shear force-displacement hysteresis; b) Bending moment time history in the longitudinal direction

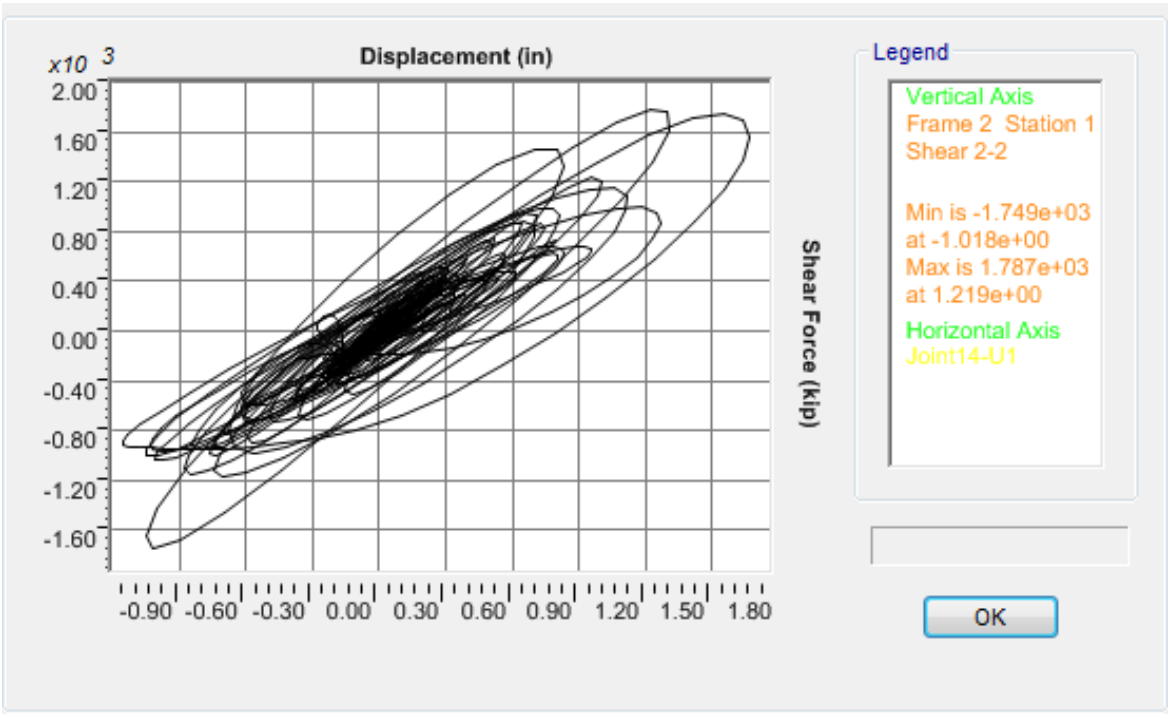

a)

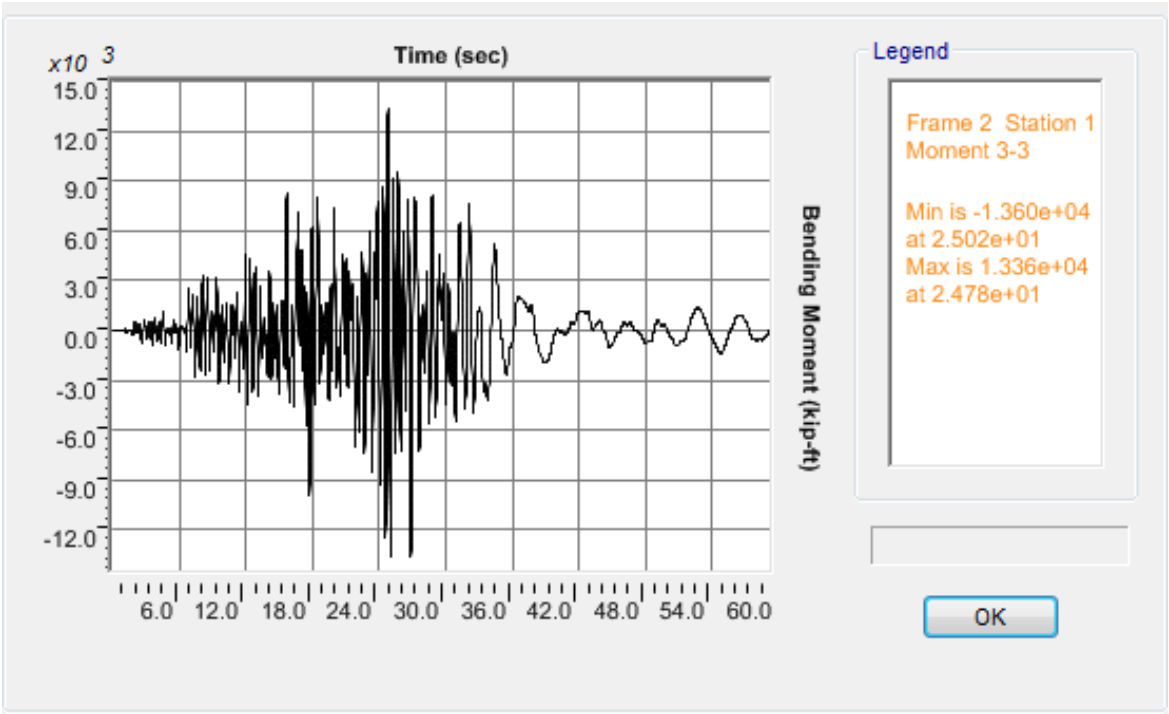

b)

Figure J.13 OSB2 column top response for Motion 13 ROCKS1P6: a) Longitudinal shear force-displacement hysteresis; b) Bending moment time history in the longitudinal direction

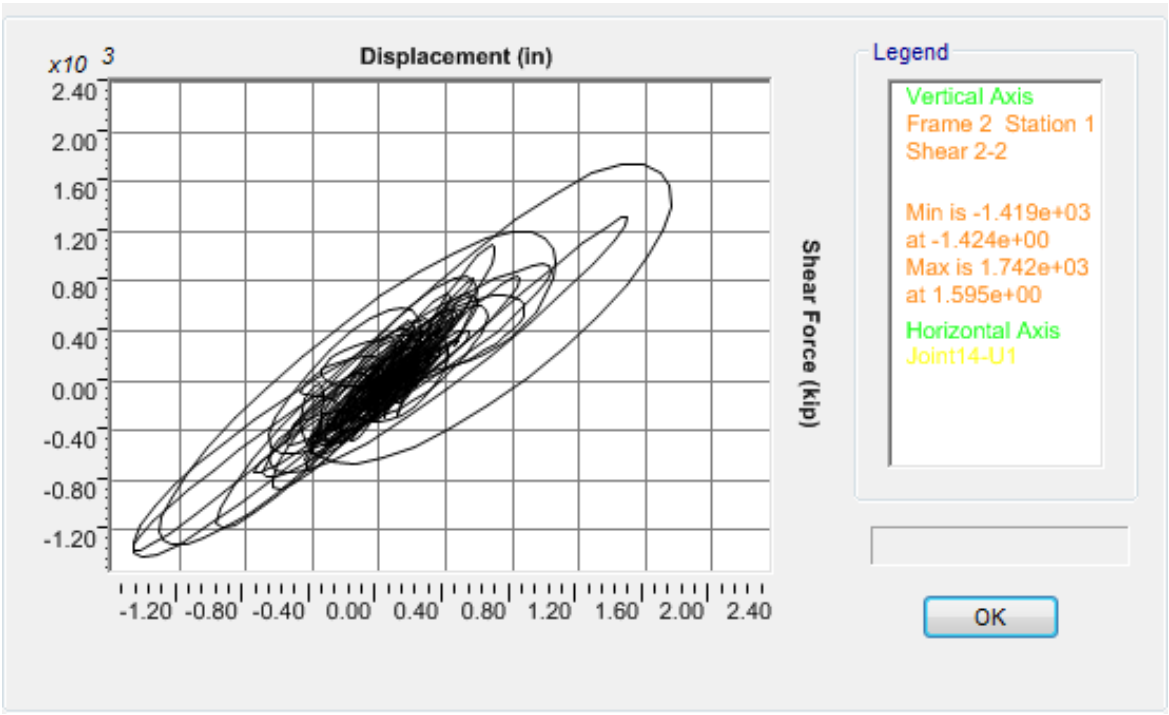

a)

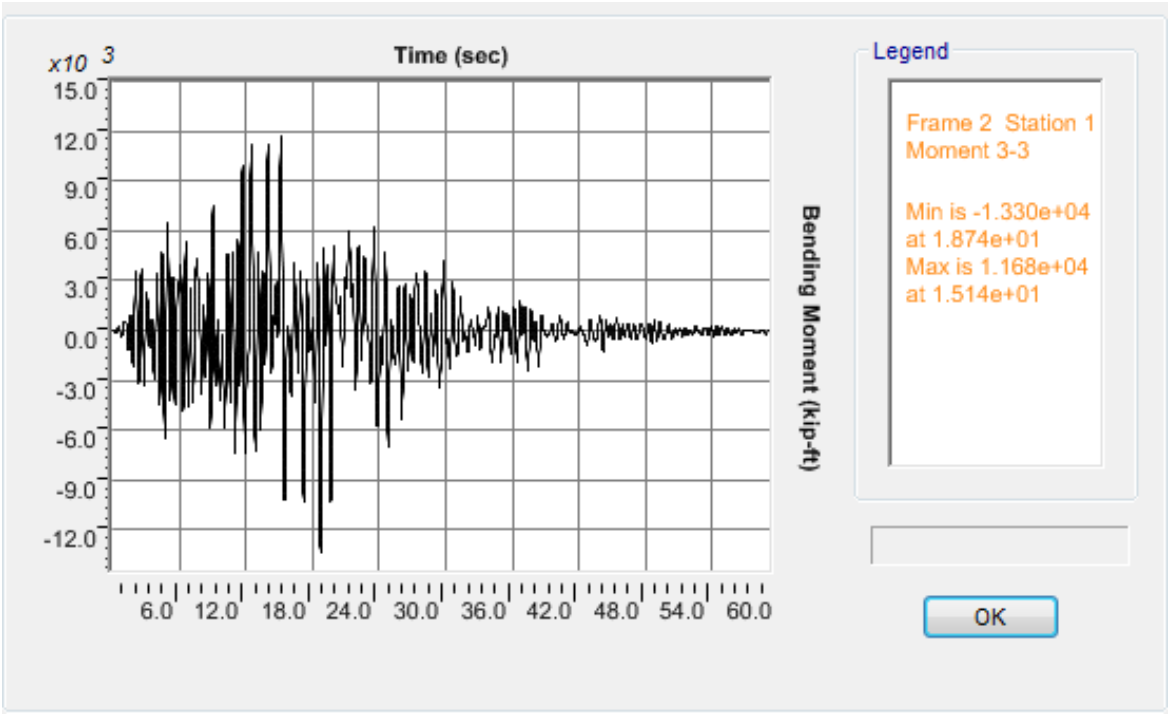

b)

Figure J.14 OSB2 column top response for Motion 14 ROCKS1P7: a) Longitudinal shear force-displacement hysteresis; b) Bending moment time history in the longitudinal direction

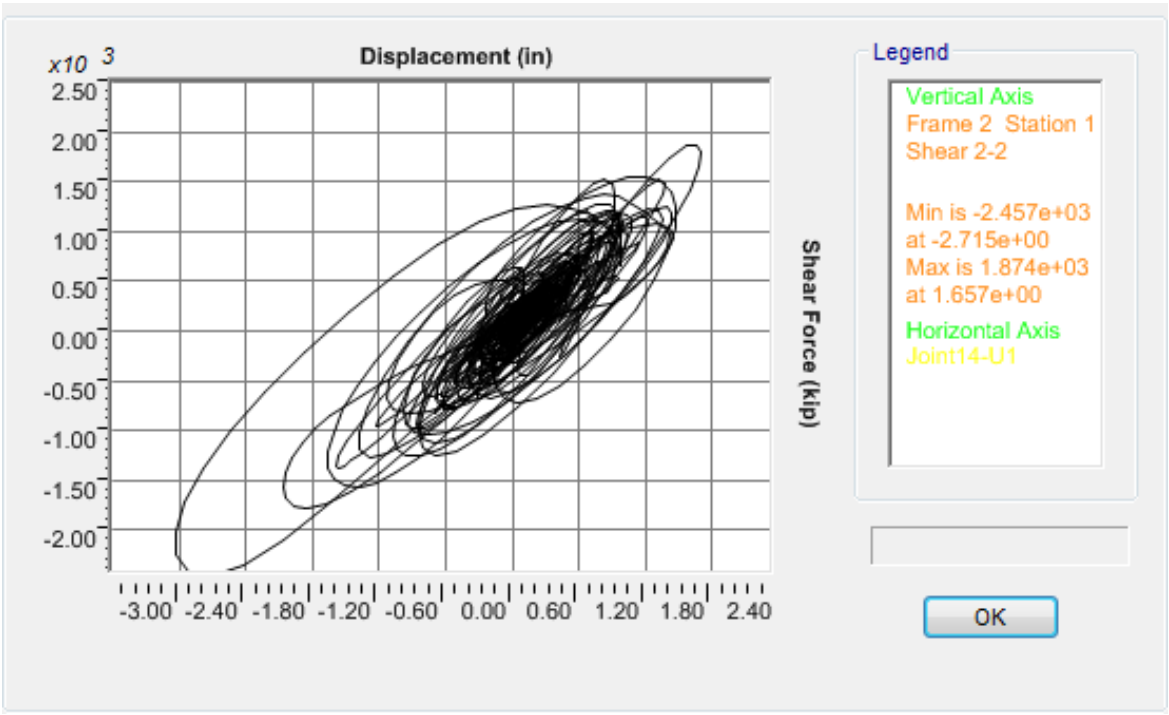

a)

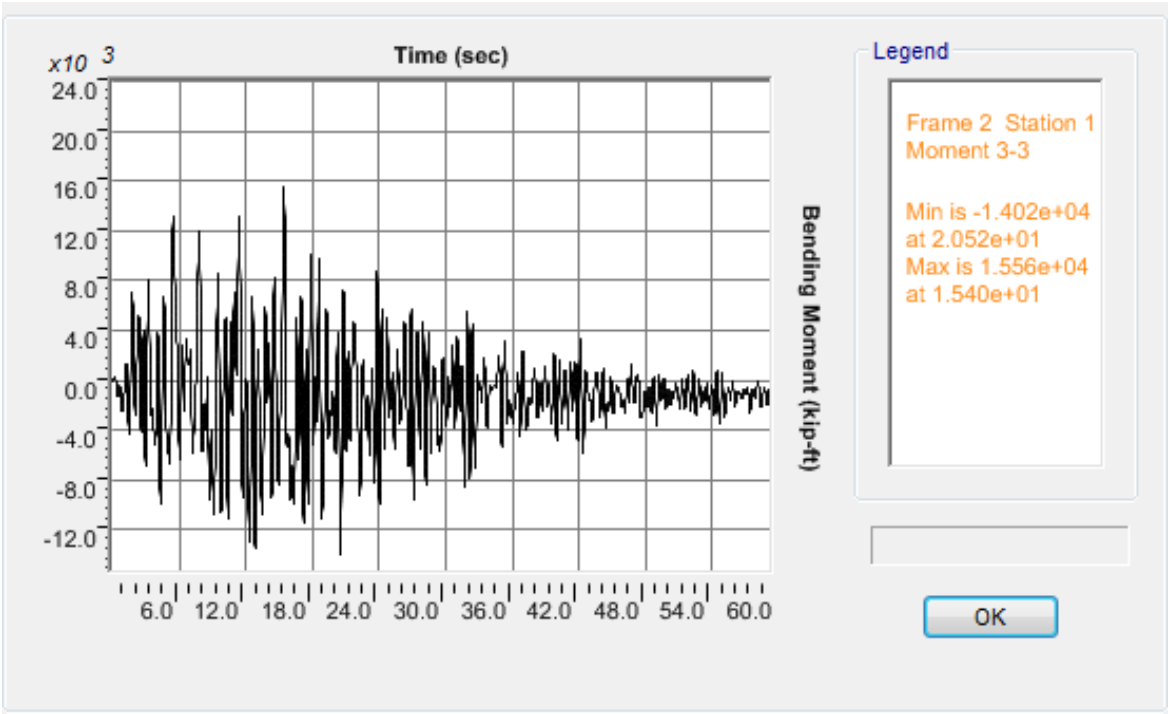

b)

Figure J.15 OSB2 column top response for Motion 15 SANDS1N1: a) Longitudinal shear force-displacement hysteresis; b) Bending moment time history in the longitudinal direction

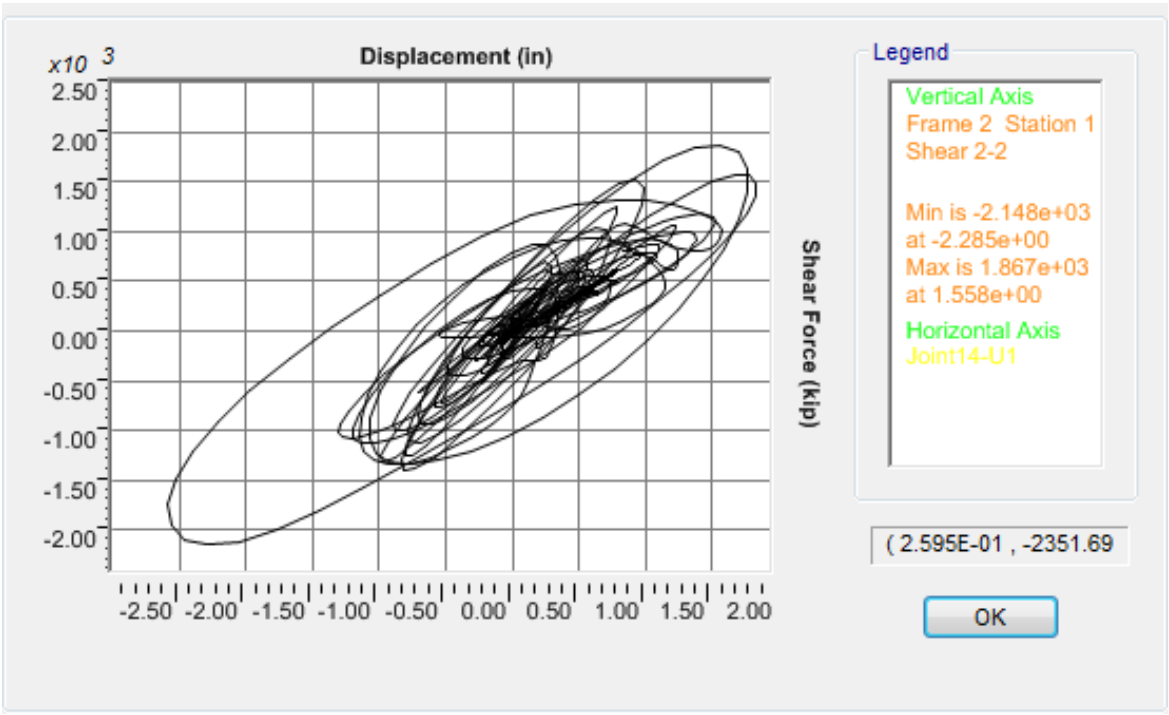

a)

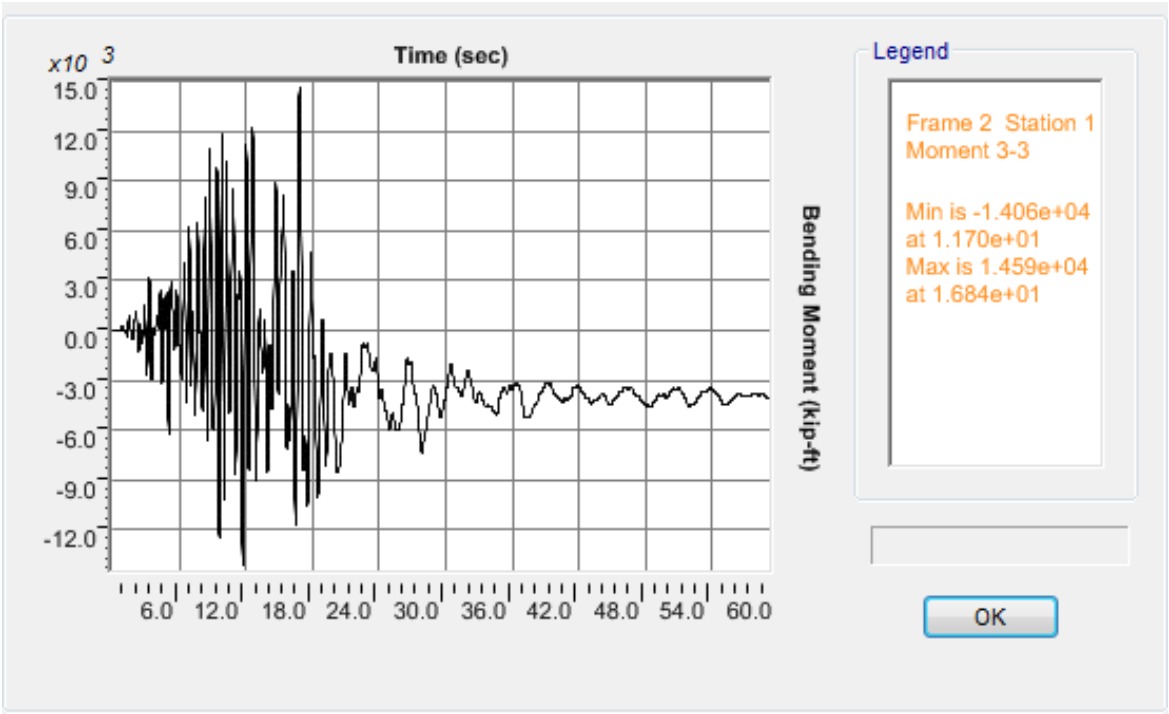

b)

Figure J.16 OSB2 column top response for Motion 16 SANDS1N2: a) Longitudinal shear force-displacement hysteresis; b) Bending moment time history in the longitudinal direction

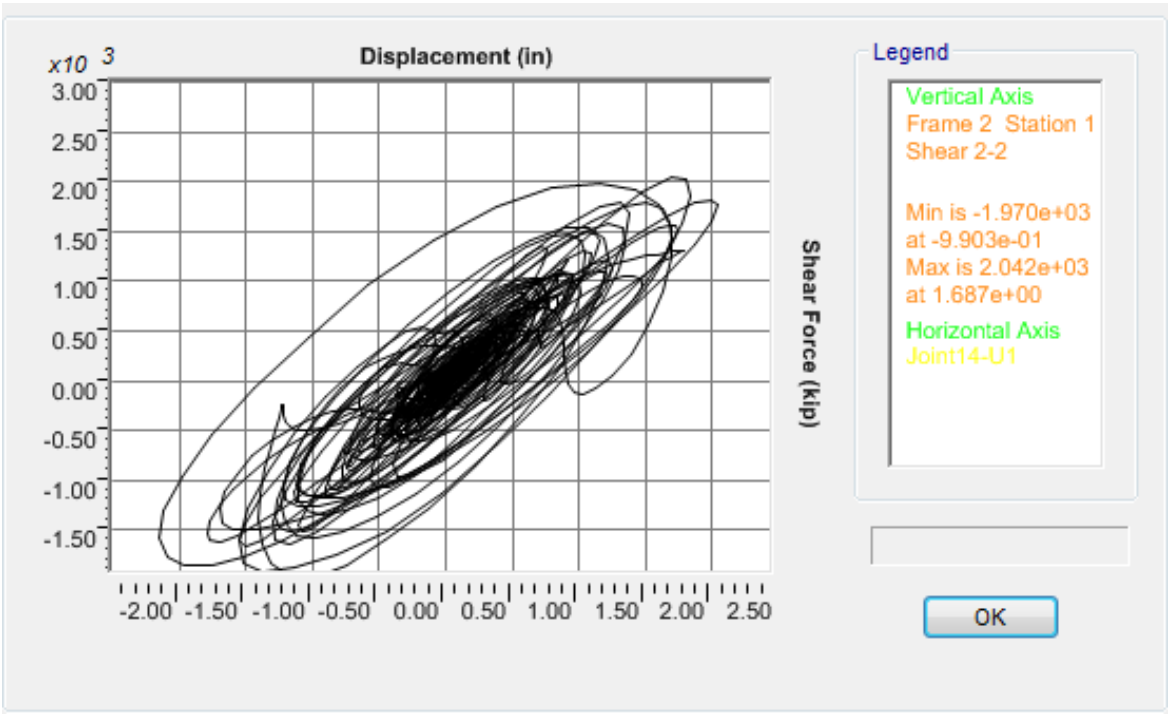

a)

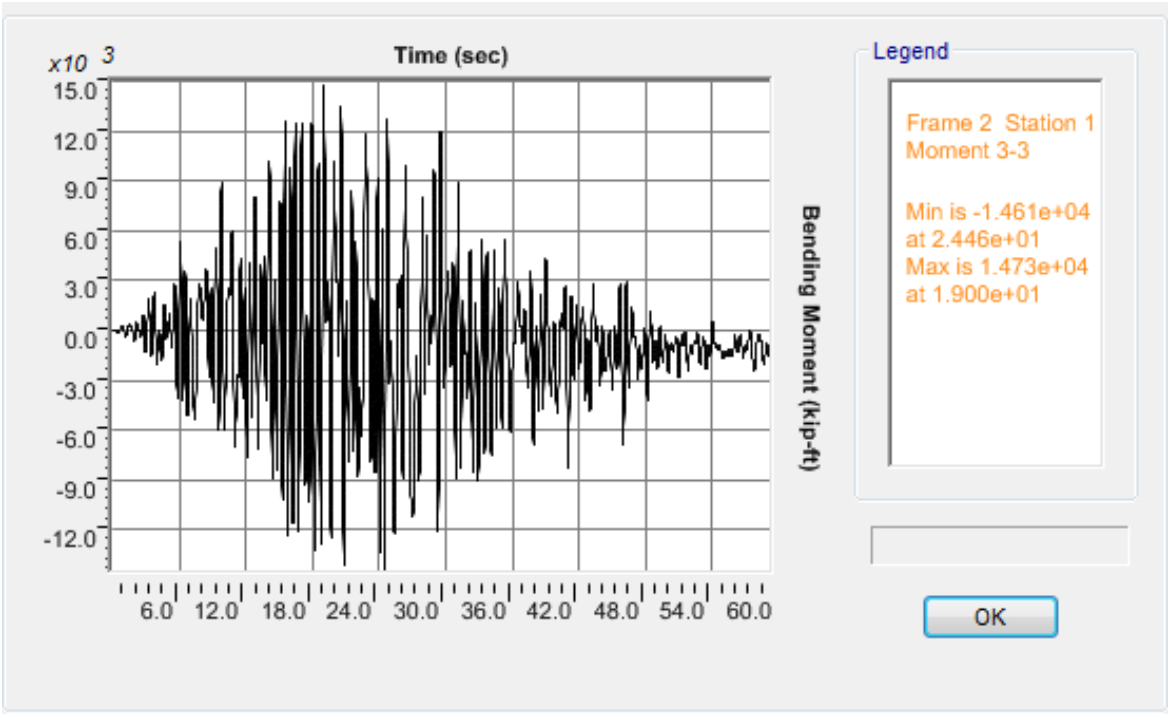

b)

Figure J.17 OSB2 column top response for Motion 17 SANDS1N3: a) Longitudinal shear force-displacement hysteresis; b) Bending moment time history in the longitudinal direction

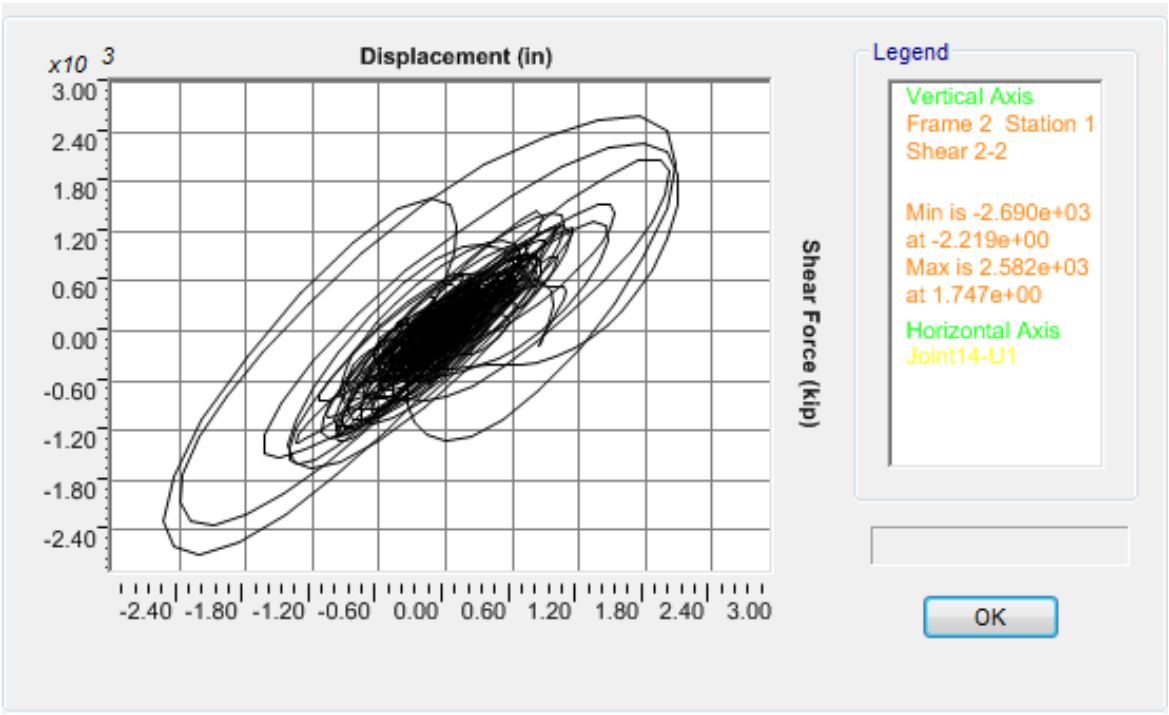

a)

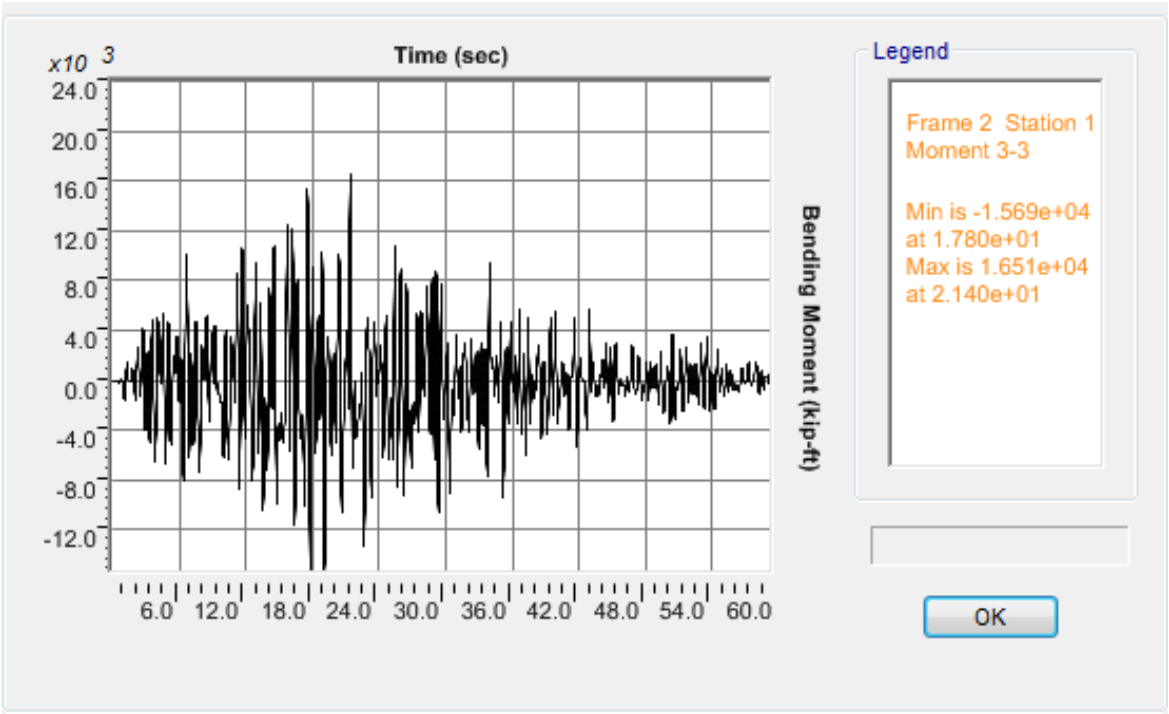

b)

Figure J.18 OSB2 column top response for Motion 18 SANDS1N4: a) Longitudinal shear force-displacement hysteresis; b) Bending moment time history in the longitudinal direction

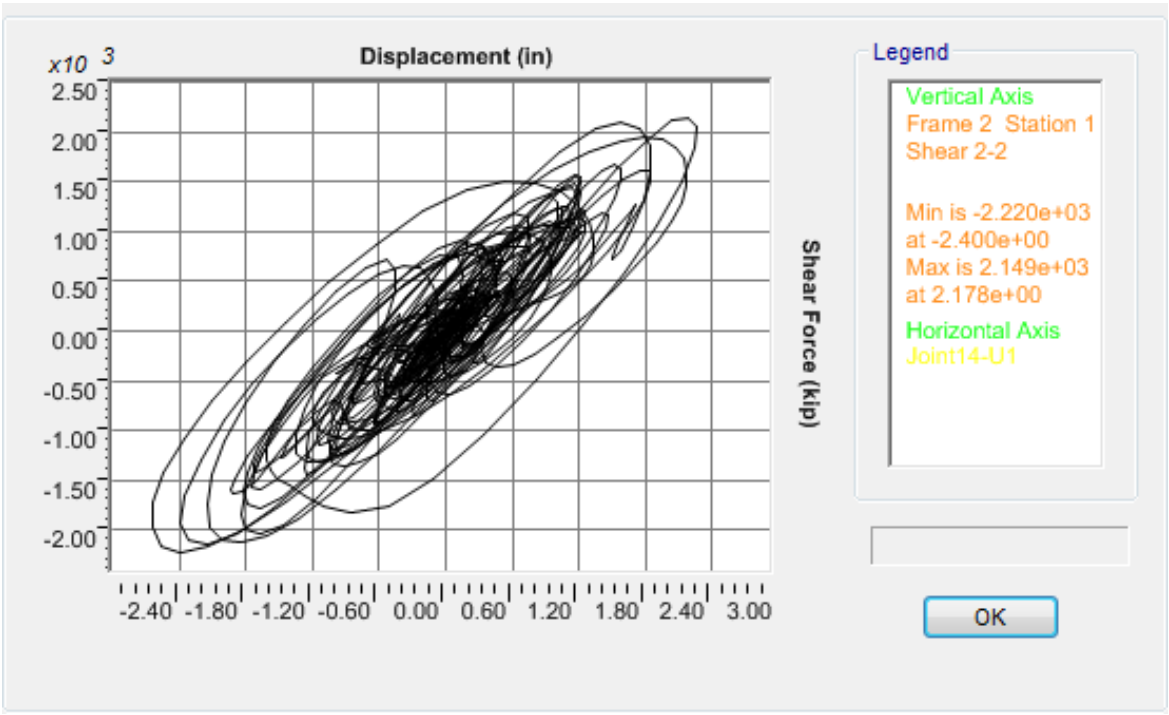

a)

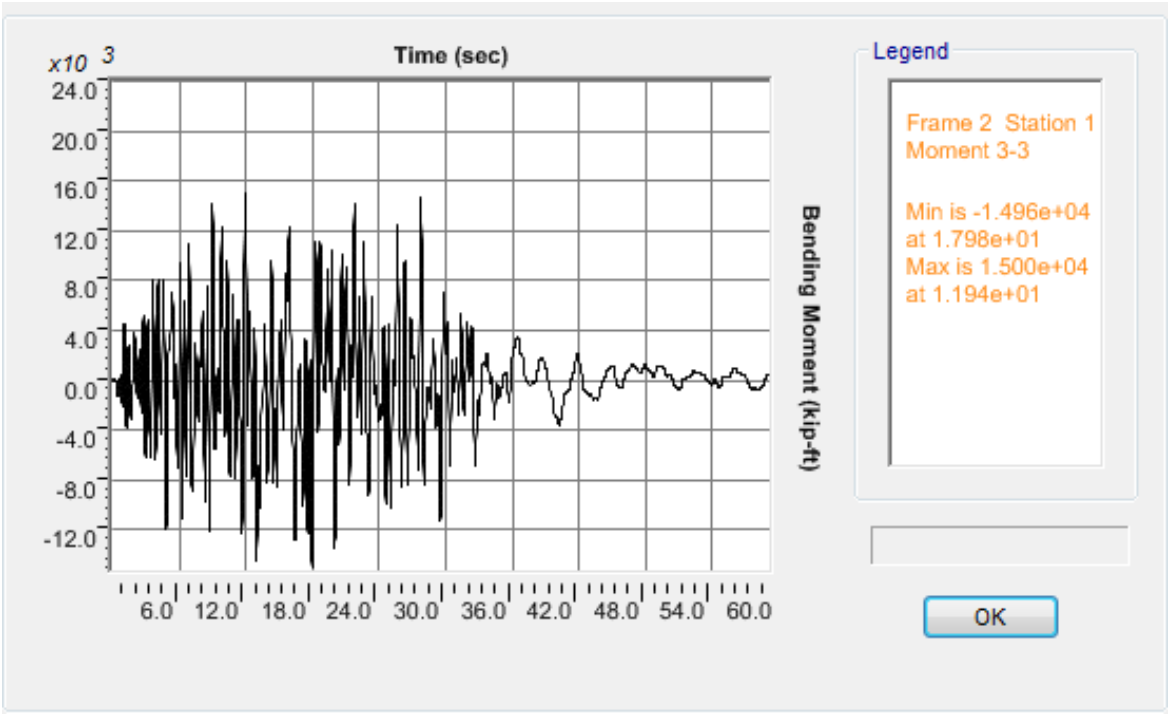

b)

Figure J.19 OSB2 column top response for Motion 19 SANDS1N5: a) Longitudinal shear force-displacement hysteresis; b) Bending moment time history in the longitudinal direction

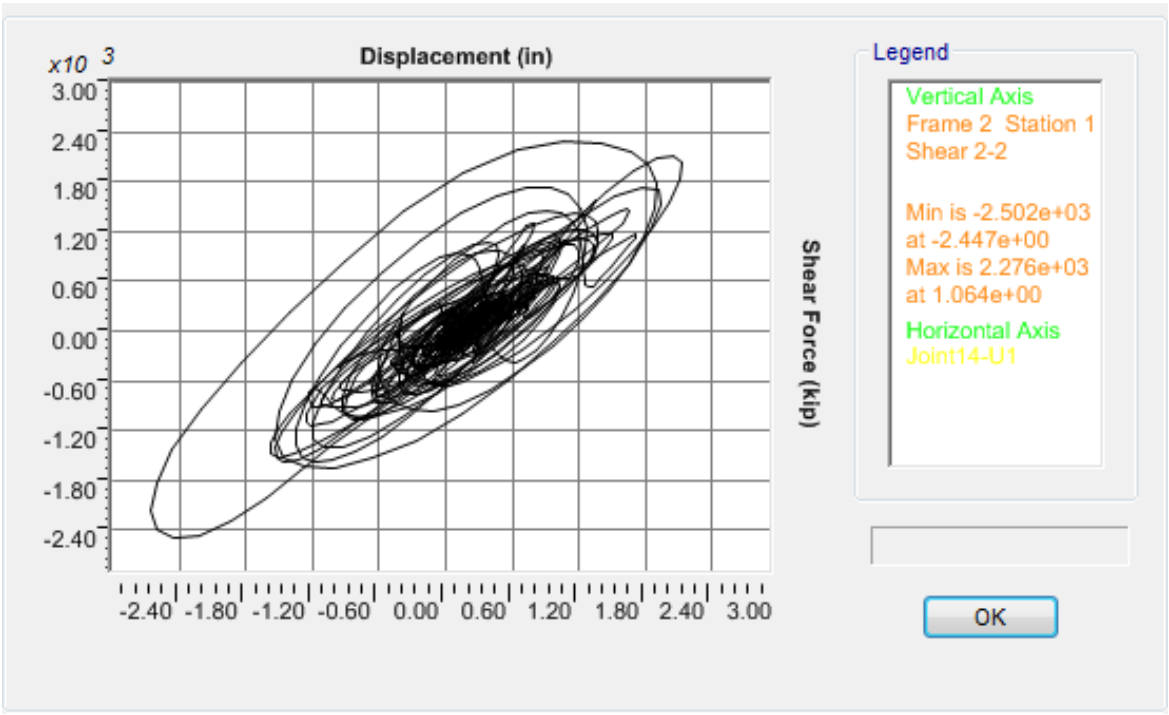

a)

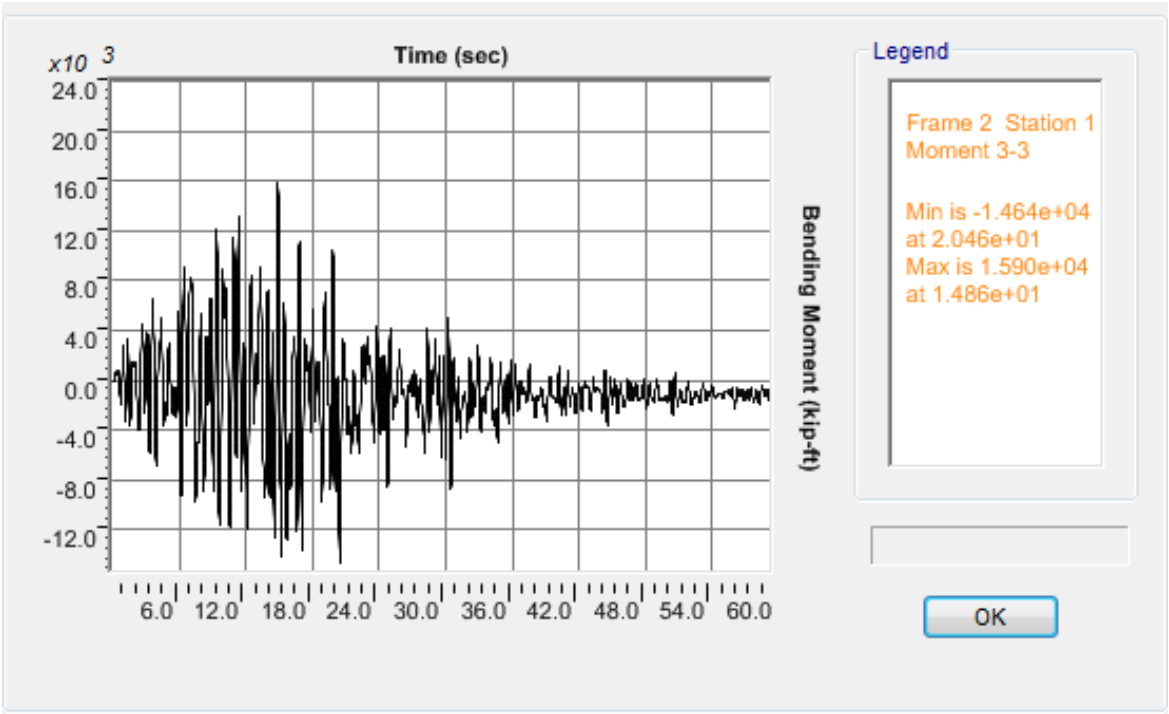

b)

Figure J.20 OSB2 column top response for Motion 20 SANDS1N6: a) Longitudinal shear force-displacement hysteresis; b) Bending moment time history in the longitudinal direction

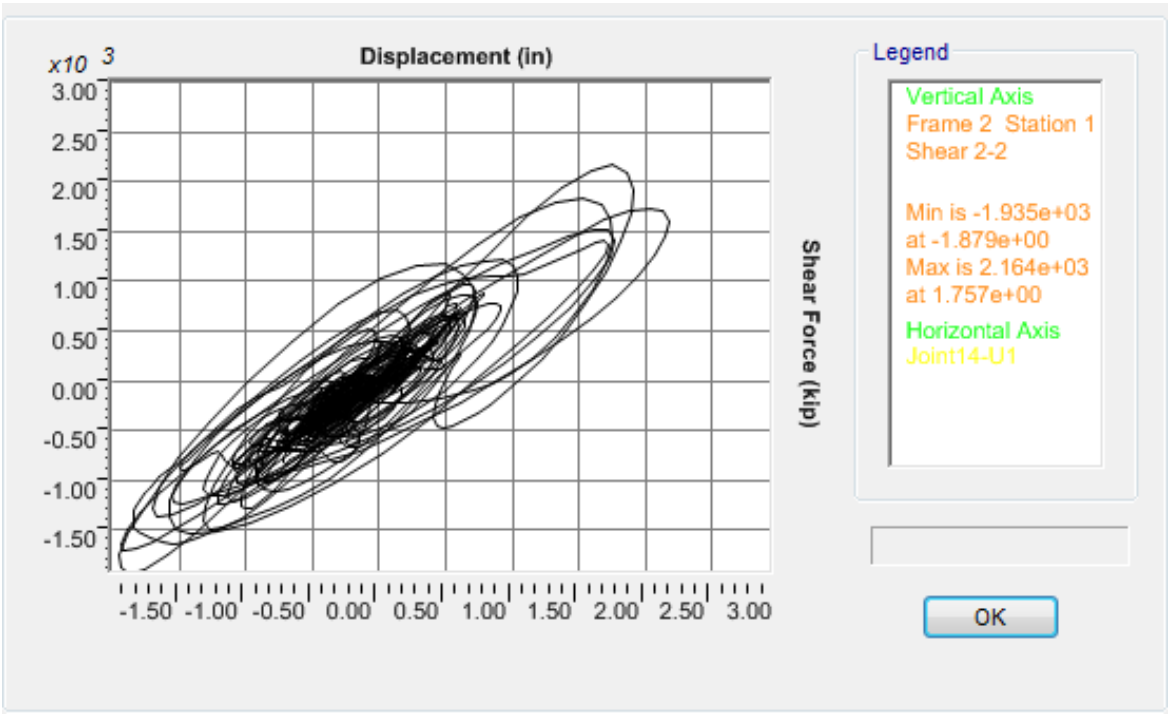

a)

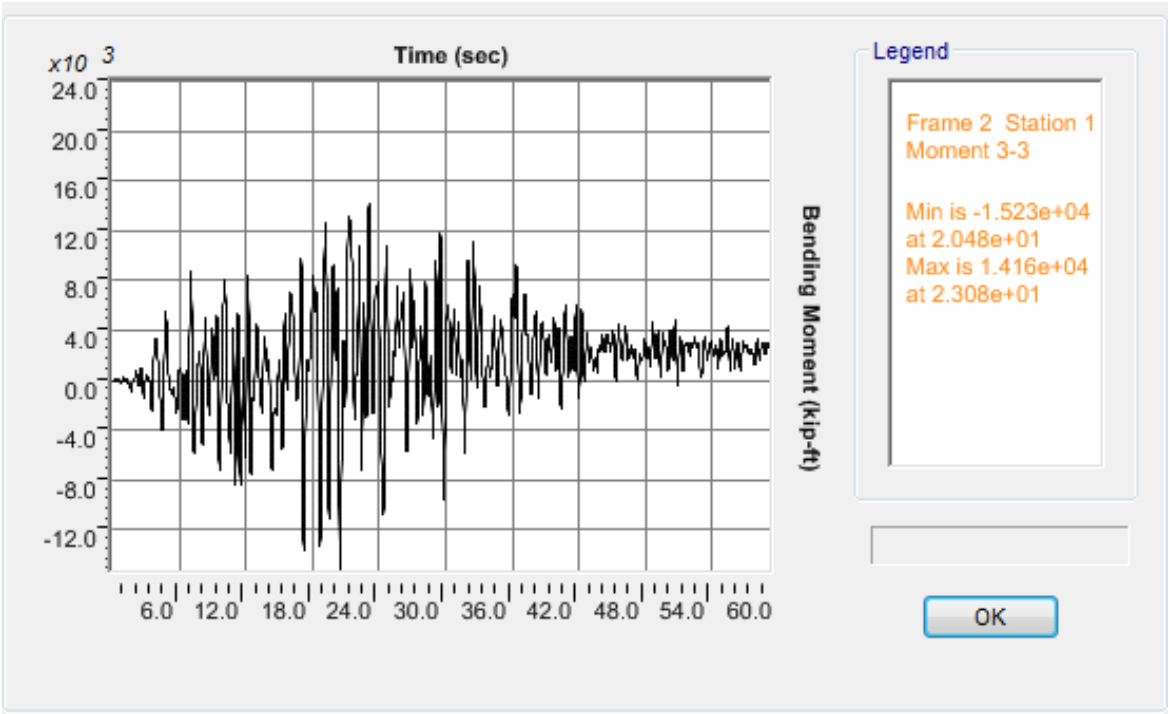

b)

Figure J.21 OSB2 column top response for Motion 21 SANDS1N7: a) Longitudinal shear force-displacement hysteresis; b) Bending moment time history in the longitudinal direction

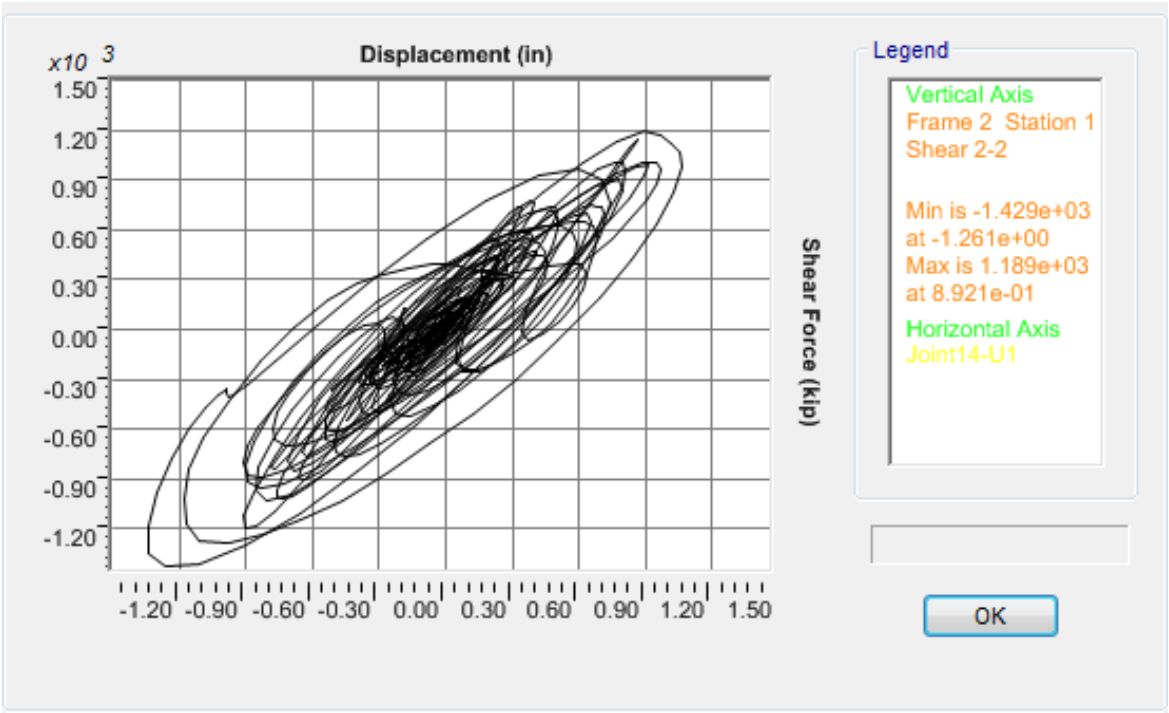
x10 3
Displacement (in)
1.50
1.20
0.90
0.60
0.30
0.00
-0.30
-0.60
-0.90
-1.20
-1.20 -0.90 -0.60 -0.30 0.00 0.30 0.60 0.90 1.20 1.50
Shear Force (kip)
Legend
Vertical Axis
Frame 2 Station 1
Shear 2-2
Min is -1.429e+03
at -1.261e+00
Max is 1.189e+03
at 8.921e-01
Horizontal Axis
Joint14-U1
OK

a)

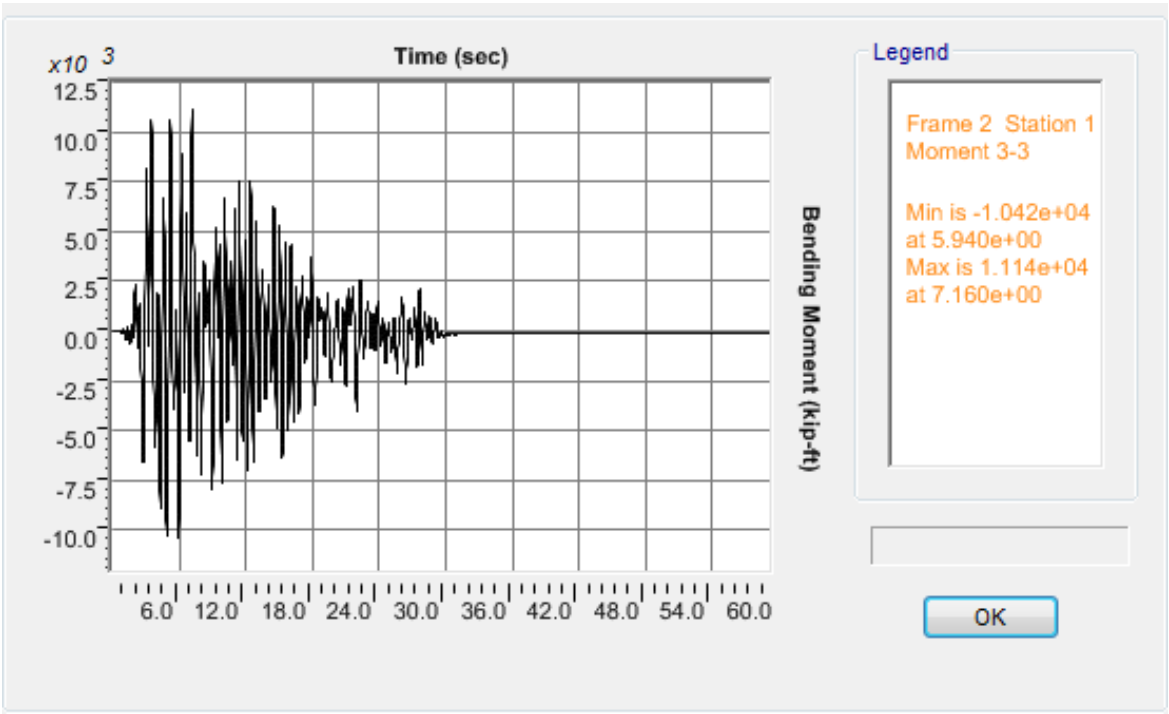
x10 3
Time (sec)
12.5
10.0
7.5
5.0
2.5
0.0
-2.5
-5.0
-7.5
-10.0
6.0 12.0 18.0 24.0 30.0 36.0 42.0 48.0 54.0 60.0
Bending Moment (kip-ft)
Legend
Frame 2 Station 1
Moment 3-3
Min is -1.042e+04
at 5.940e+00
Max is 1.114e+04
at 7.160e+00
OK

b)

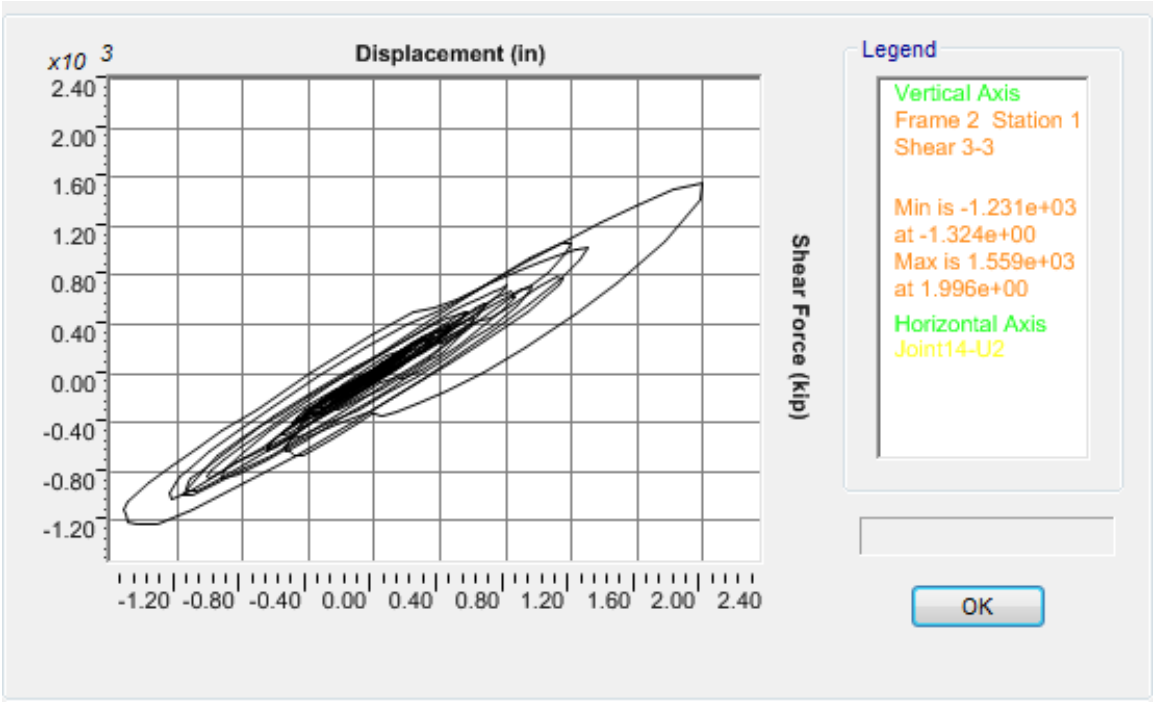

c)

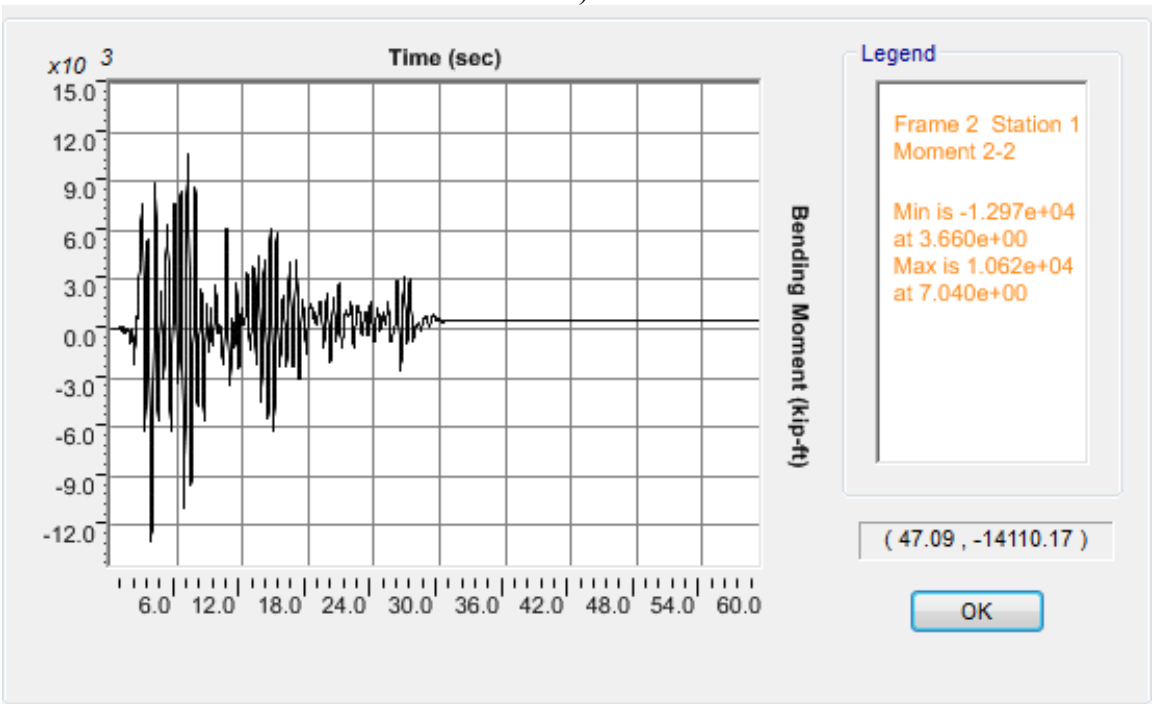

d)

Figure J.22 OSB2 column top response for Motion 22 ROCKN1N1: a) Longitudinal shear force-displacement hysteresis; b) Bending moment time history in the longitudinal direction; c) Transverse shear force-displacement hysteresis; d) Bending moment time history in the transverse direction

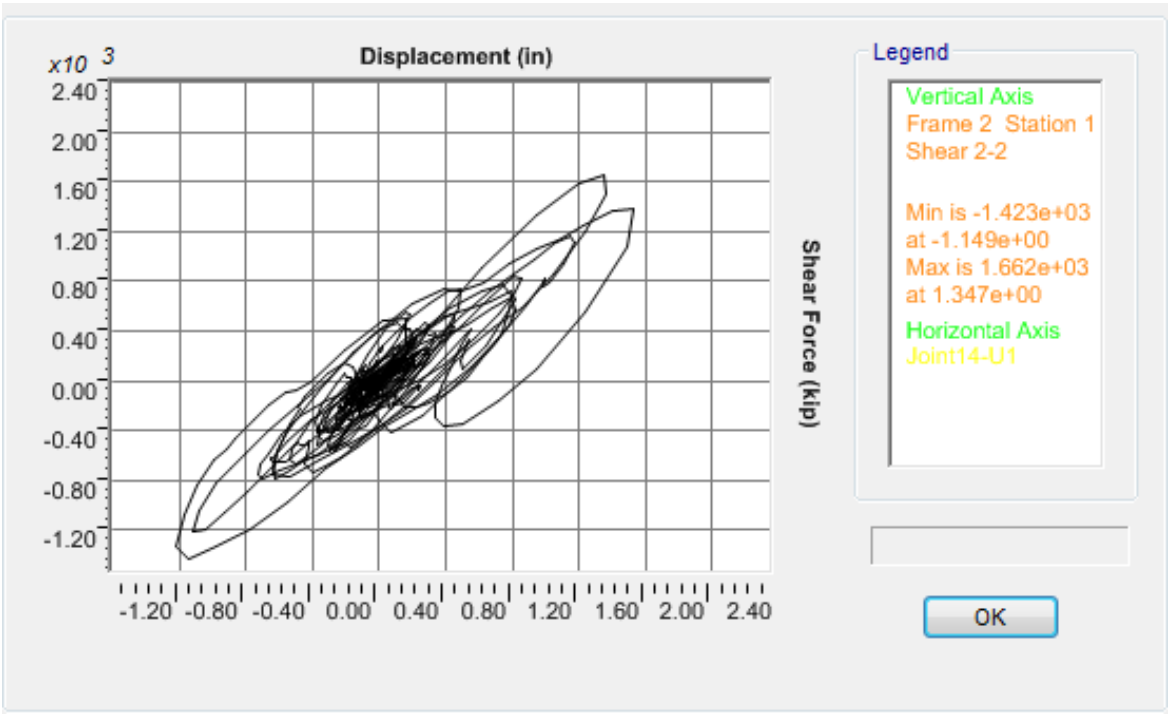
x10 3
Displacement (in)
2.40
2.00
1.60
1.20
0.80
0.40
0.00
-0.40
-0.80
-1.20
-1.20 -0.80 -0.40 0.00 0.40 0.80 1.20 1.60 2.00 2.40
Shear Force (kip)
Legend
Vertical Axis
Frame 2 Station 1
Shear 2-2
Min is -1.423e+03
at -1.149e+00
Max is 1.662e+03
at 1.347e+00
Horizontal Axis
Joint14-U1
OK

a)

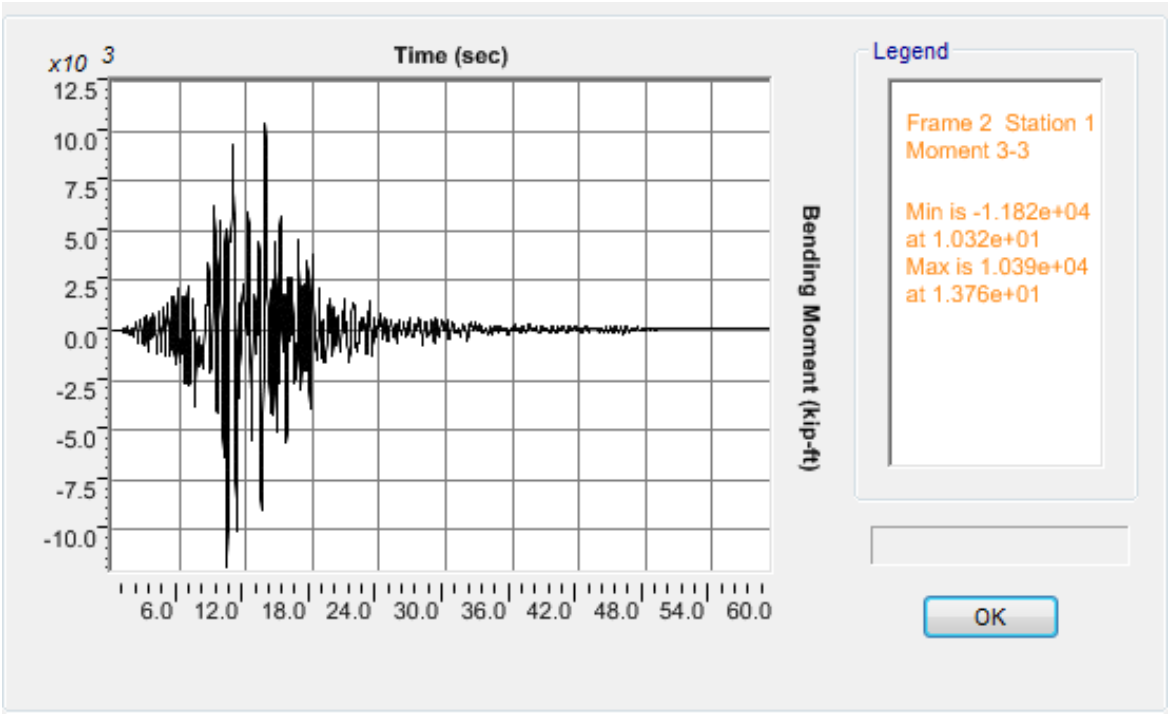
x10 3
Time (sec)
12.5
10.0
7.5
5.0
2.5
0.0
-2.5
-5.0
-7.5
-10.0
6.0 12.0 18.0 24.0 30.0 36.0 42.0 48.0 54.0 60.0
Bending Moment (kip-ft)
Legend
Frame 2 Station 1
Moment 3-3
Min is -1.182e+04
at 1.032e+01
Max is 1.039e+04
at 1.376e+01
OK

b)

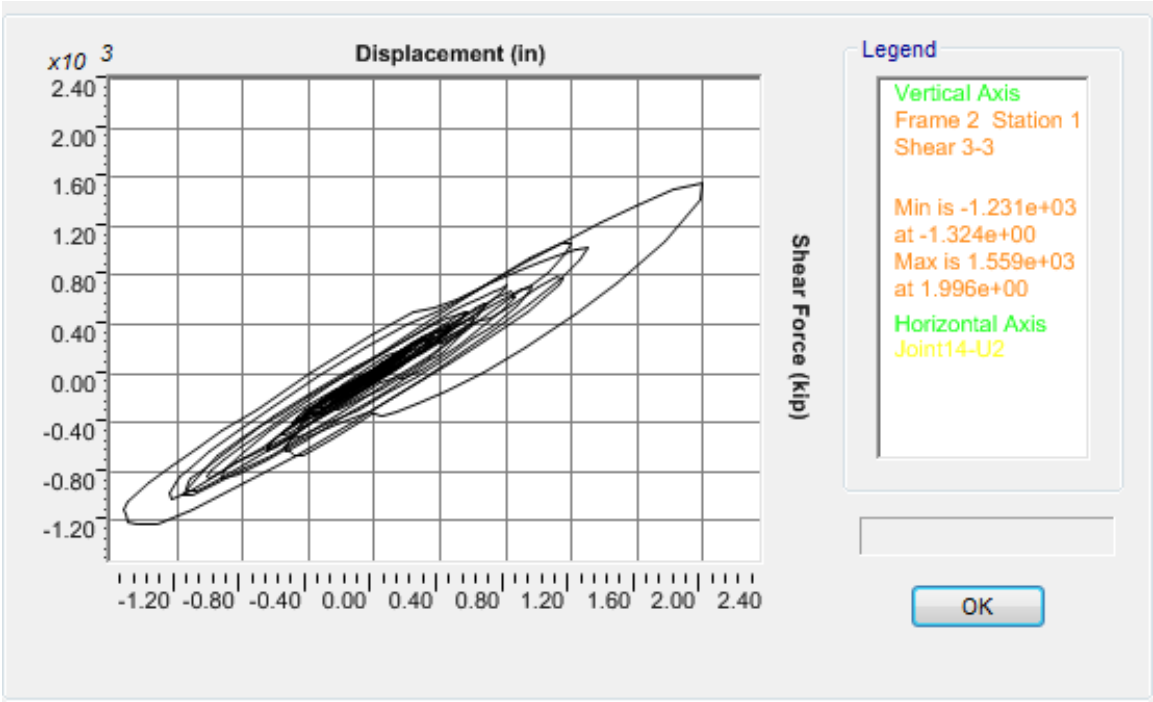

c)

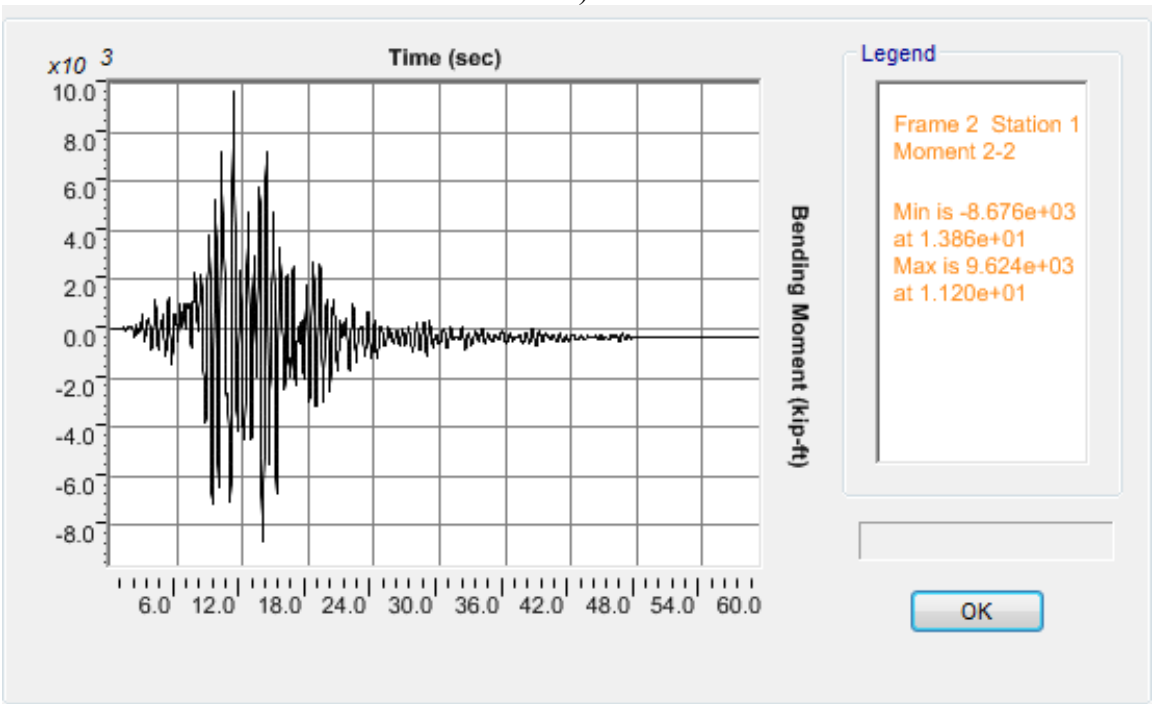

d)

Figure J.23 OSB2 column top response for Motion 23 ROCKN1P1: a) Longitudinal shear force-displacement hysteresis; b) Bending moment time history in the longitudinal direction; c) Transverse shear force-displacement hysteresis; d) Bending moment time history in the transverse direction

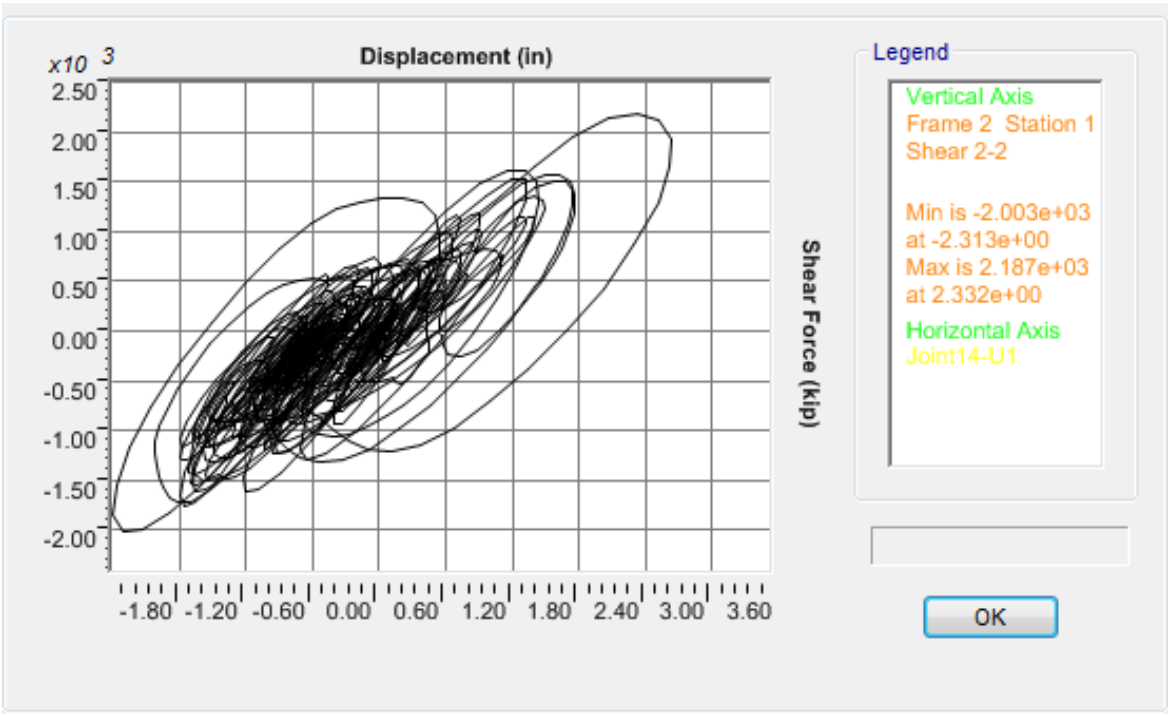
x10 3
Displacement (in)
2.50
2.00
1.50
1.00
0.50
0.00
-0.50
-1.00
-1.50
-2.00
-1.80 -1.20 -0.60 0.00 0.60 1.20 1.80 2.40 3.00 3.60
Shear Force (kip)
Legend
Vertical Axis
Frame 2 Station 1
Shear 2-2
Min is -2.003e+03
at -2.313e+00
Max is 2.187e+03
at 2.332e+00
Horizontal Axis
Joint14-U1
OK

a)

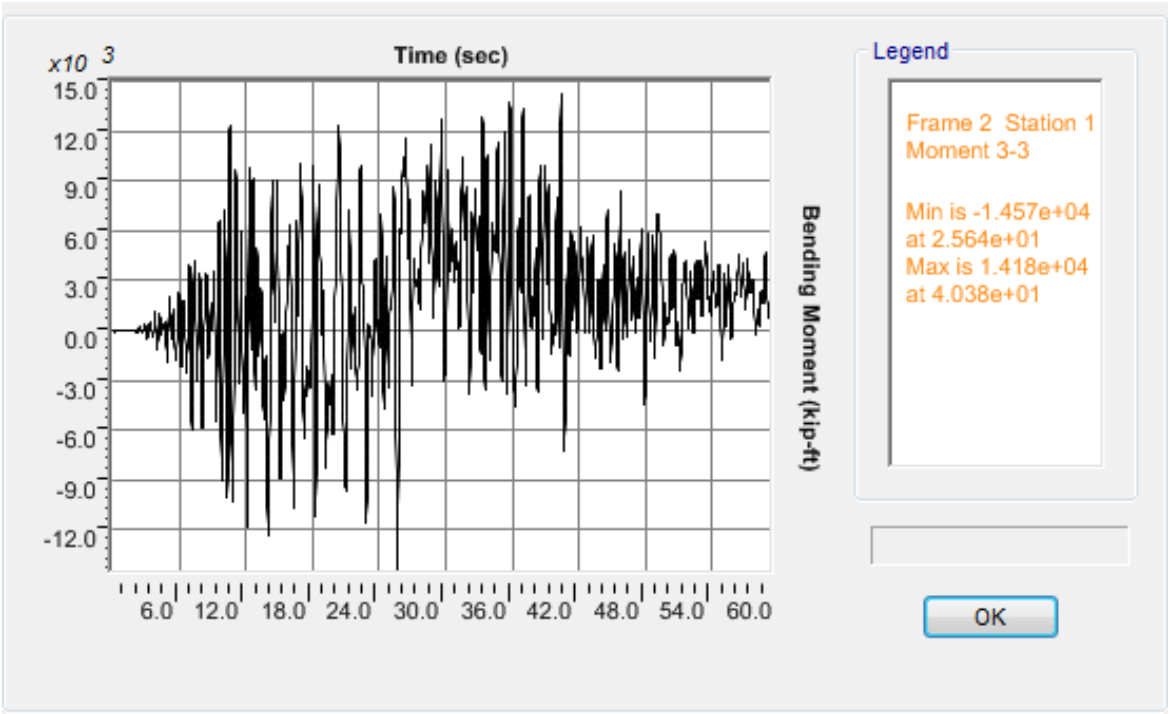
x10 3
Time (sec)
15.0
12.0
9.0
6.0
3.0
0.0
-3.0
-6.0
-9.0
-12.0
6.0 12.0 18.0 24.0 30.0 36.0 42.0 48.0 54.0 60.0
Bending Moment (kip-ft)
Legend
Frame 2 Station 1
Moment 3-3
Min is -1.457e+04
at 2.564e+01
Max is 1.418e+04
at 4.038e+01
OK

b)

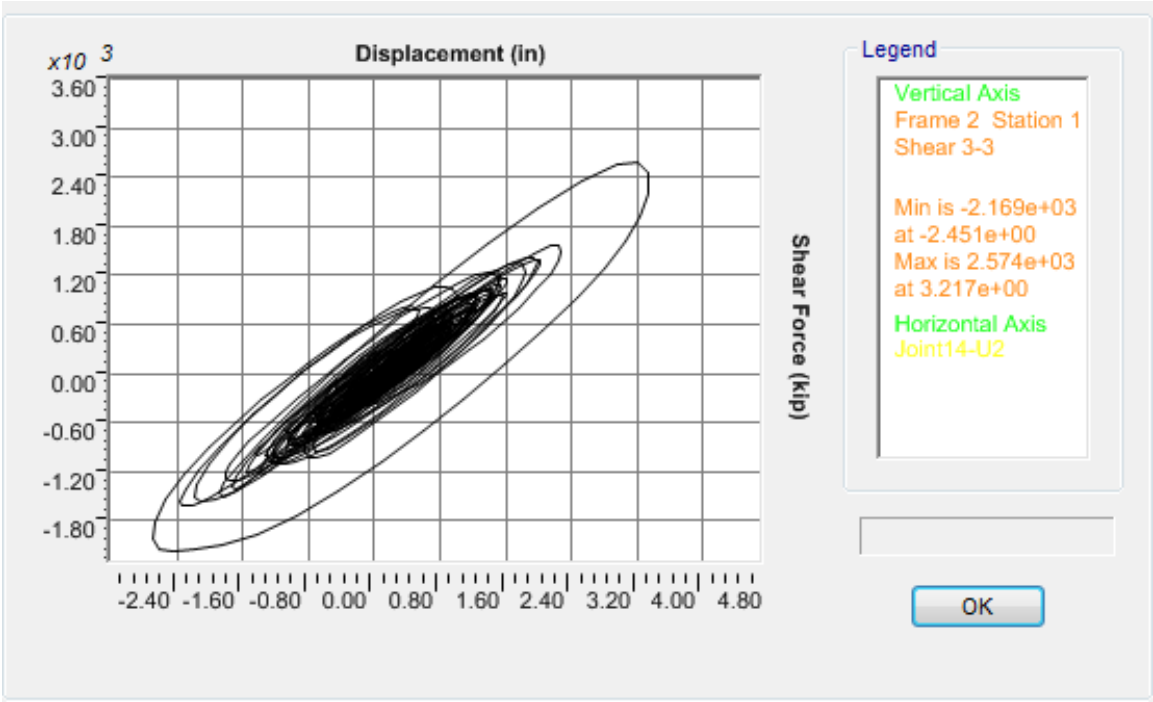

c)

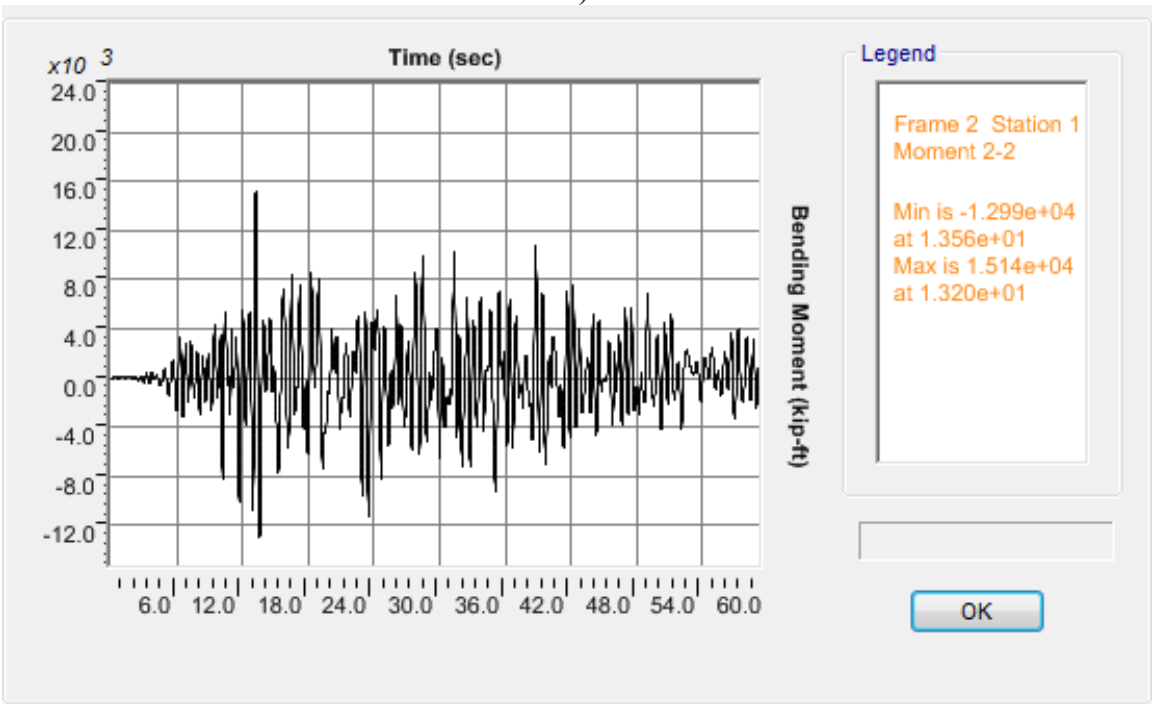

d)

Figure J.24 OSB2 column top response for Motion 24 SANDN1N1: a) Longitudinal shear force-displacement hysteresis; b) Bending moment time history in the longitudinal direction; c) Transverse shear force-displacement hysteresis; d) Bending moment time history in the transverse direction

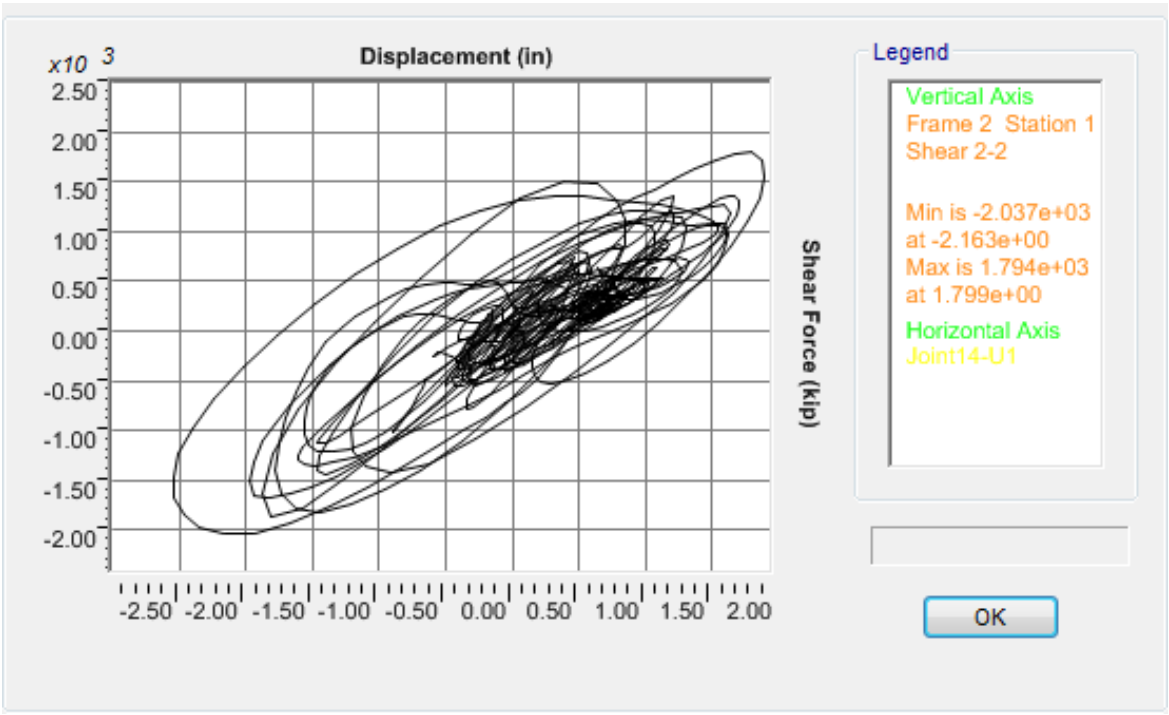
x10 3
Displacement (in)
2.50
2.00
1.50
1.00
0.50
0.00
-0.50
-1.00
-1.50
-2.00
-2.50 -2.00 -1.50 -1.00 -0.50 0.00 0.50 1.00 1.50 2.00
Shear Force (kip)
Legend
Vertical Axis
Frame 2 Station 1
Shear 2-2
Min is -2.037e+03
at -2.163e+00
Max is 1.794e+03
at 1.799e+00
Horizontal Axis
Joint14-U1
OK

a)

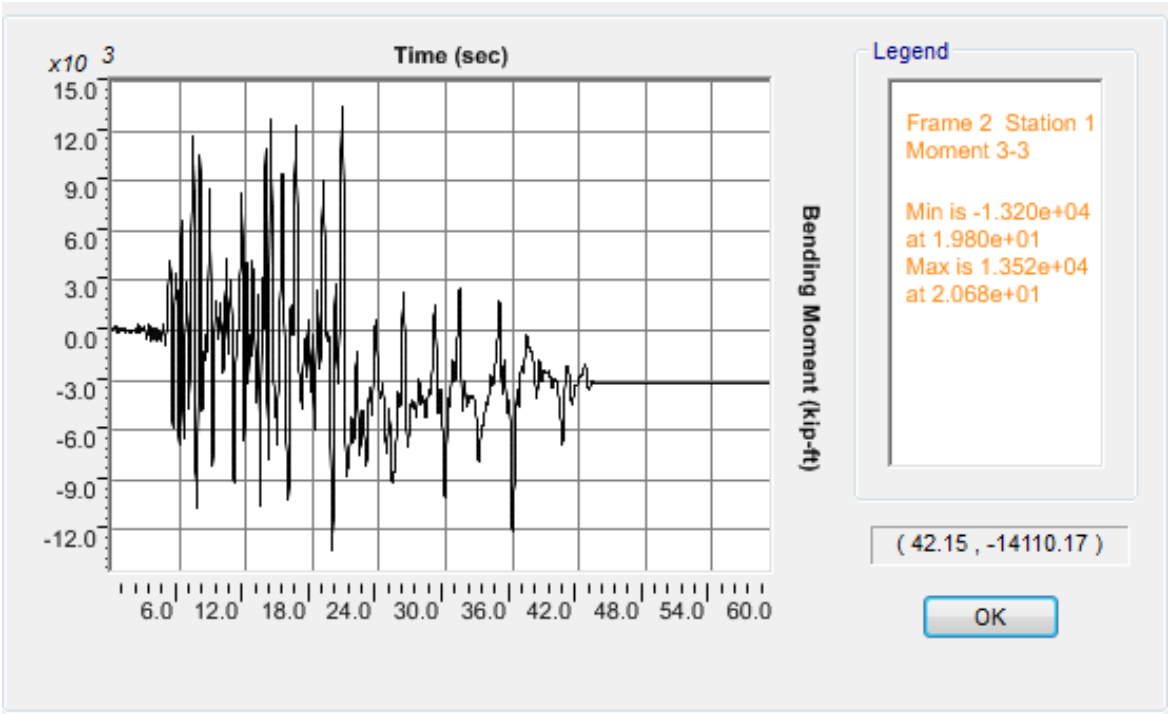
x10 3
Time (sec)
15.0
12.0
9.0
6.0
3.0
0.0
-3.0
-6.0
-9.0
-12.0
6.0 12.0 18.0 24.0 30.0 36.0 42.0 48.0 54.0 60.0
Bending Moment (kip-ft)
Legend
Frame 2 Station 1
Moment 3-3
Min is -1.320e+04
at 1.980e+01
Max is 1.352e+04
at 2.068e+01
(42.15 , -14110.17)
OK

b)

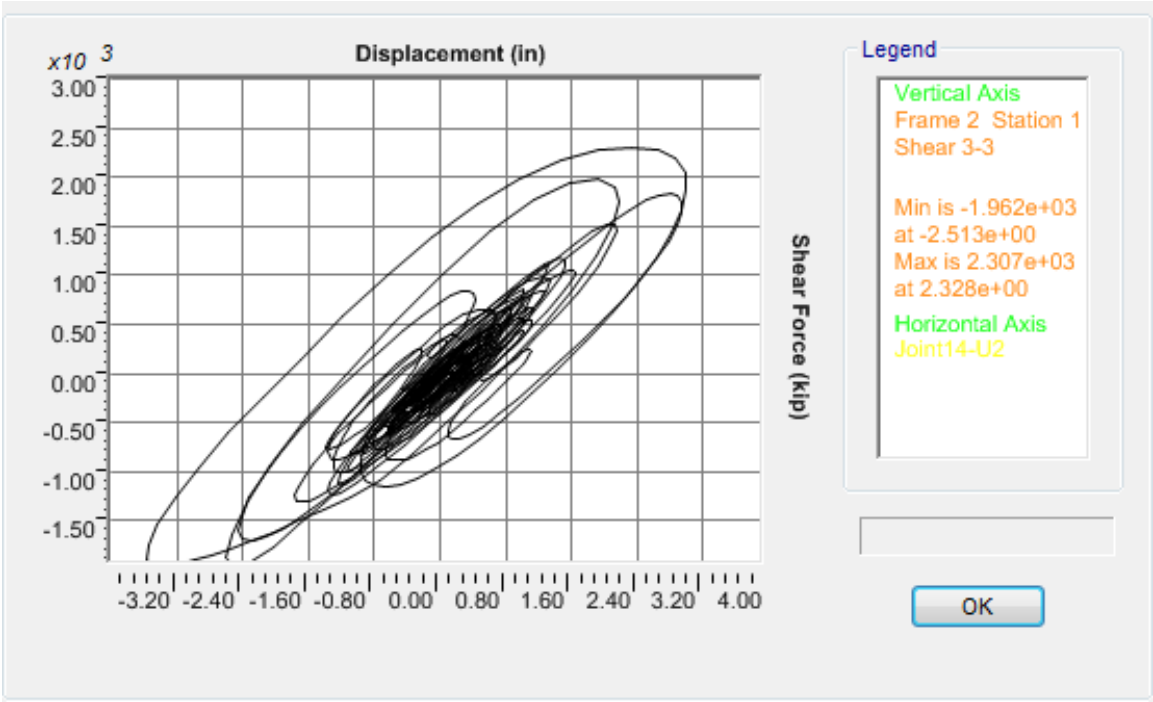

c)

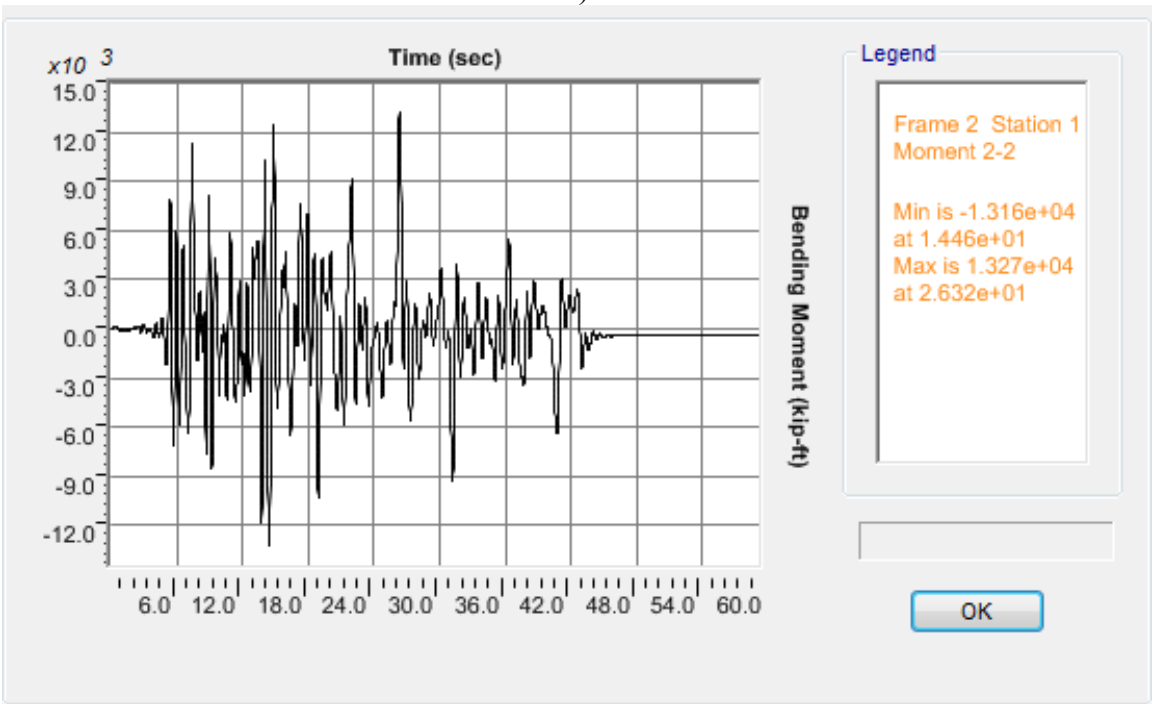

d)

Figure J.25 OSB2 column top response for Motion 25 CLAYN1N1: a) Longitudinal shear force-displacement hysteresis; b) Bending moment time history in the longitudinal direction; c) Transverse shear force-displacement hysteresis; d) Bending moment time history in the transverse direction

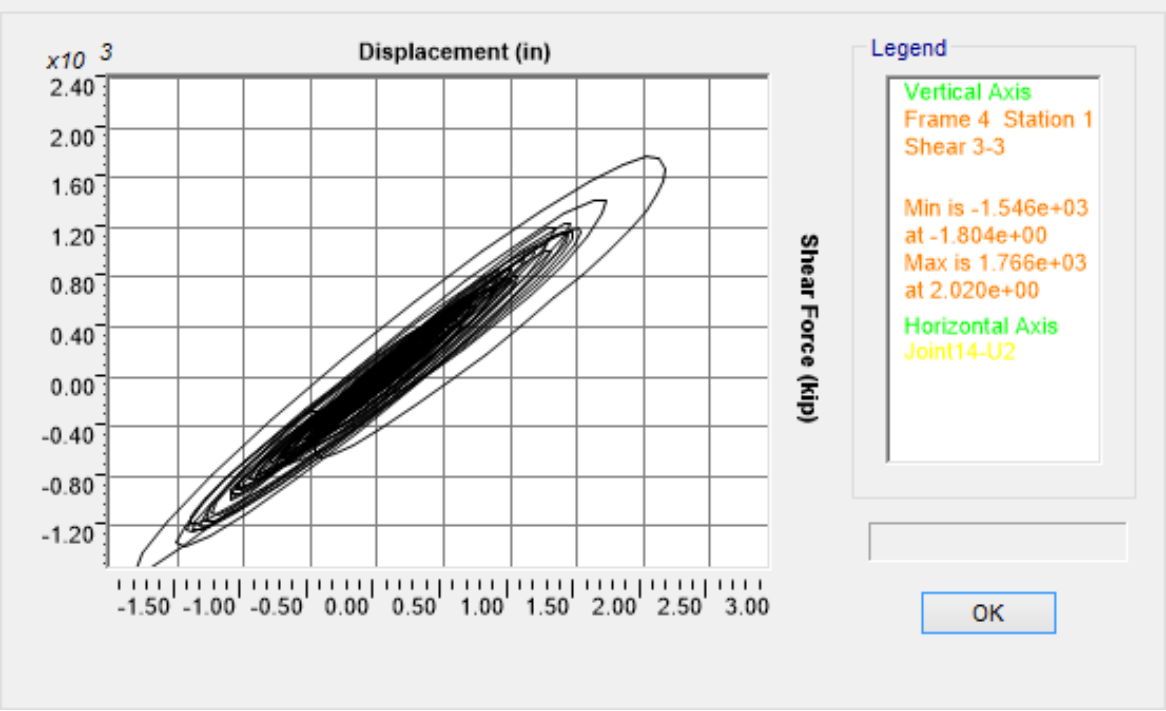

a)

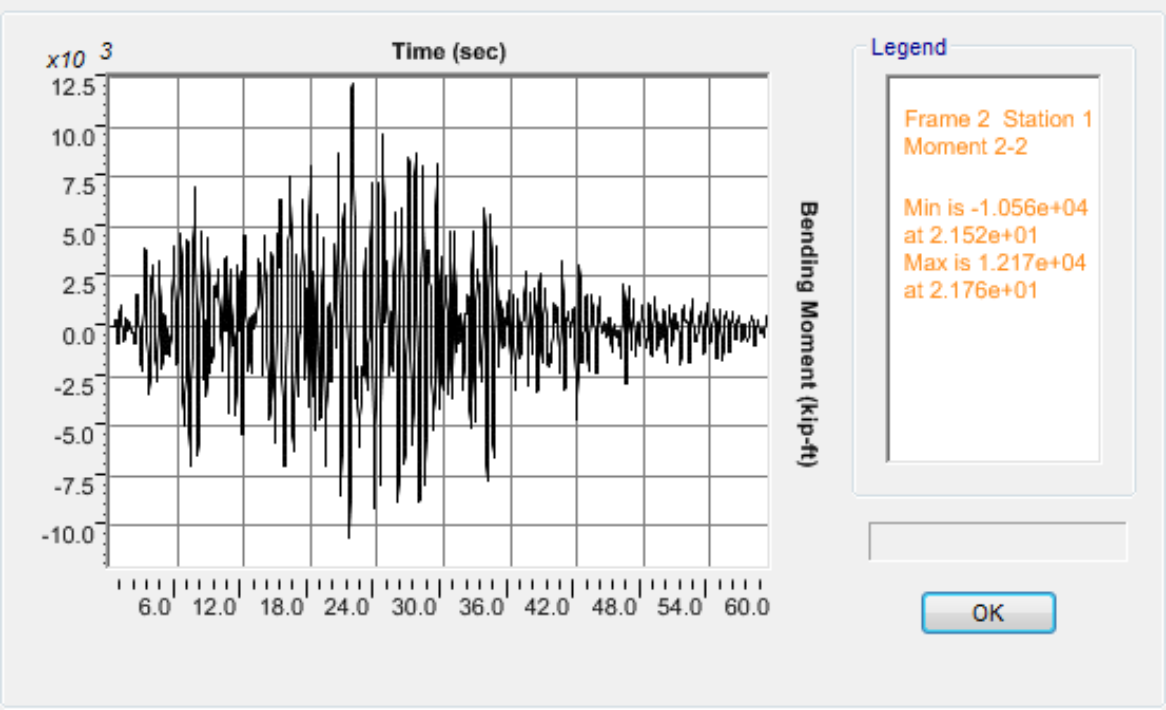

b)

Figure J.26 OSB2 column top response for Motion 26 ROCKS1N1: a) Transverse shear force-displacement hysteresis; b) Bending moment time history in the transverse direction

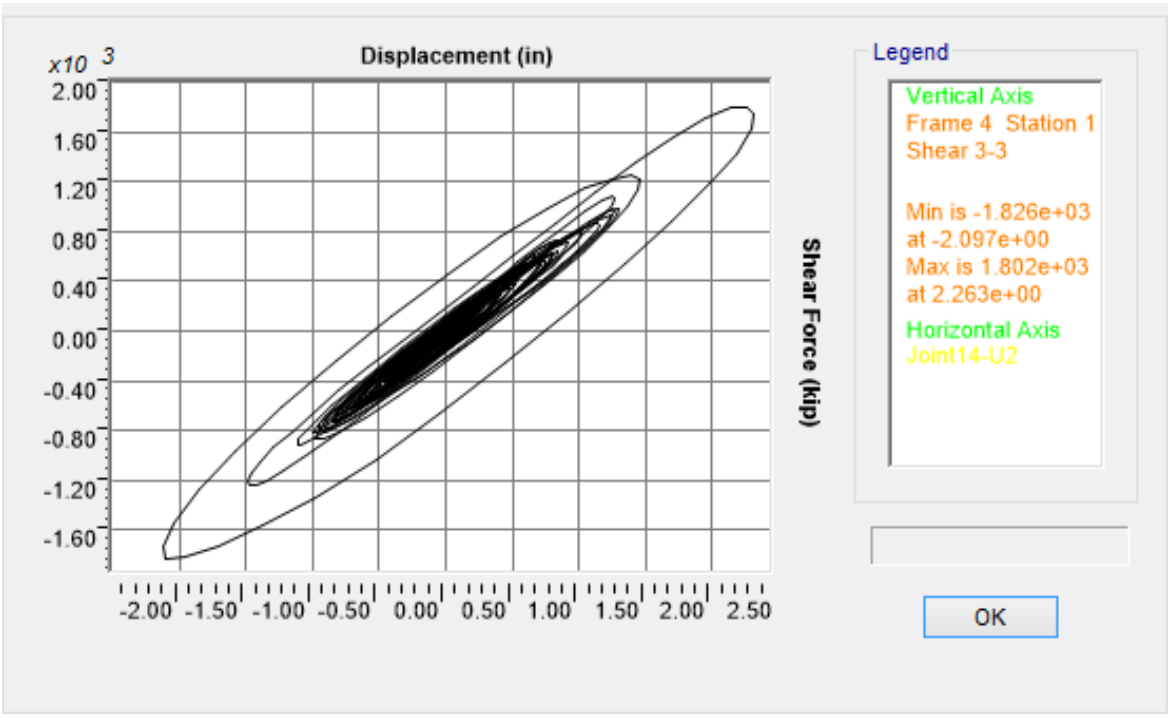

a)

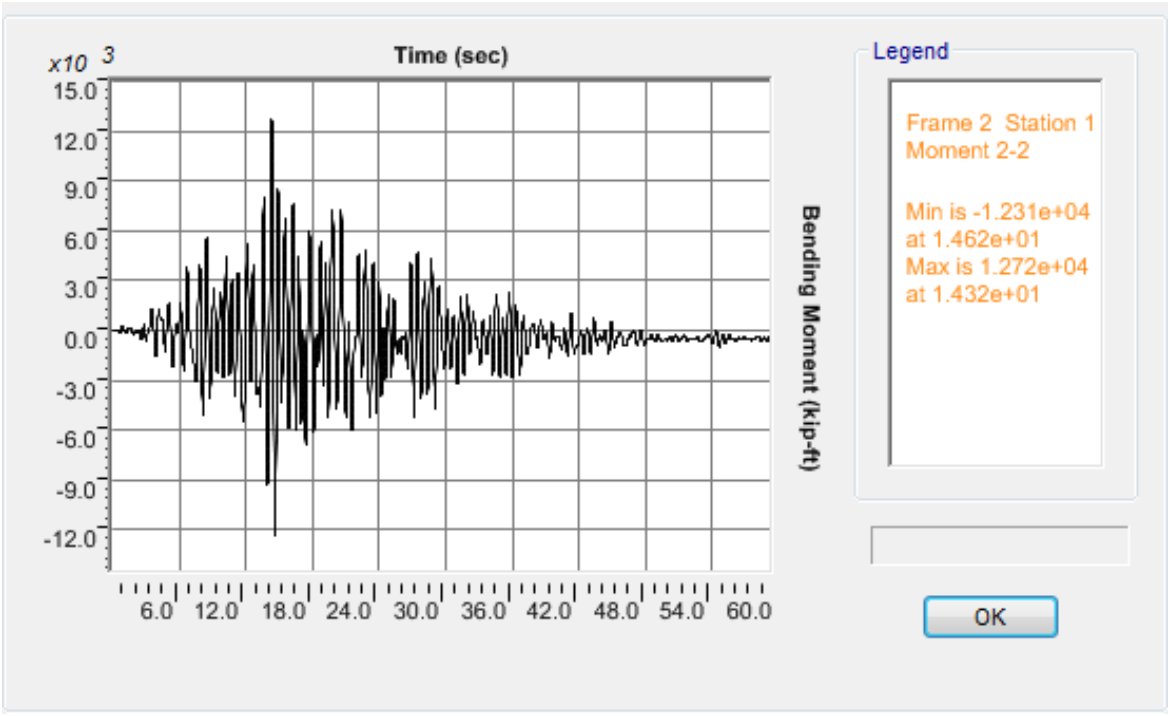

b)

Figure J.27 OSB2 column top response for Motion 27 ROCKS1N2: a) Transverse shear force-displacement hysteresis; b) Bending moment time history in the transverse direction

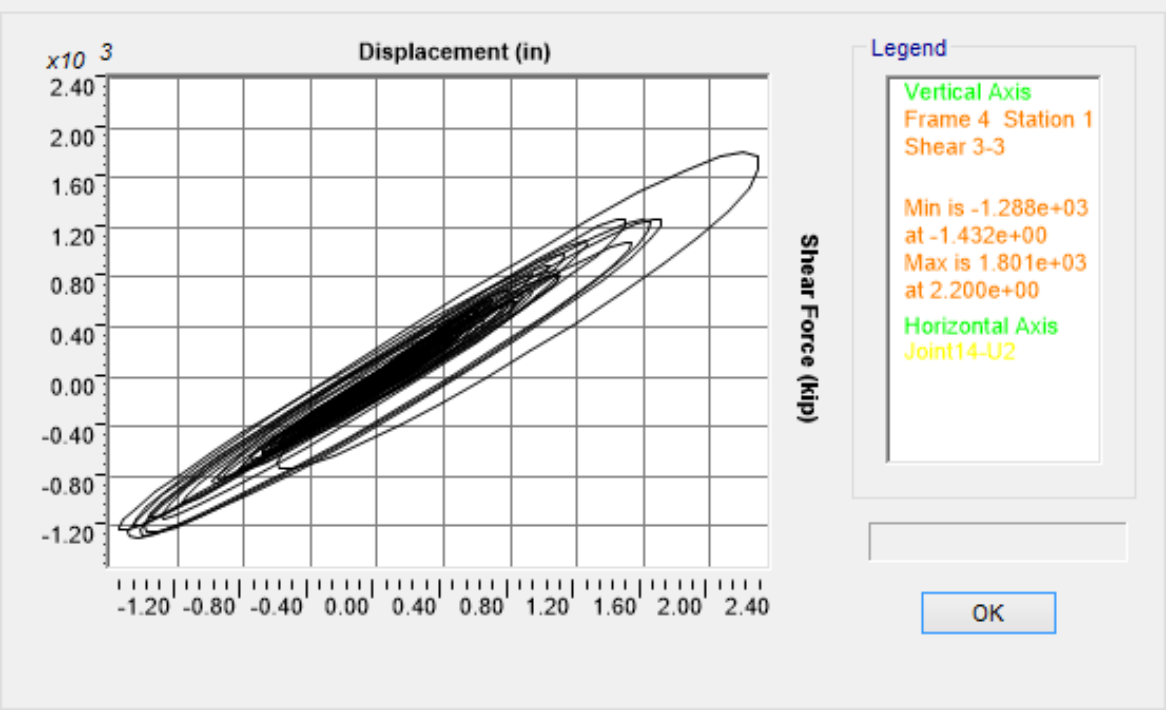

a)

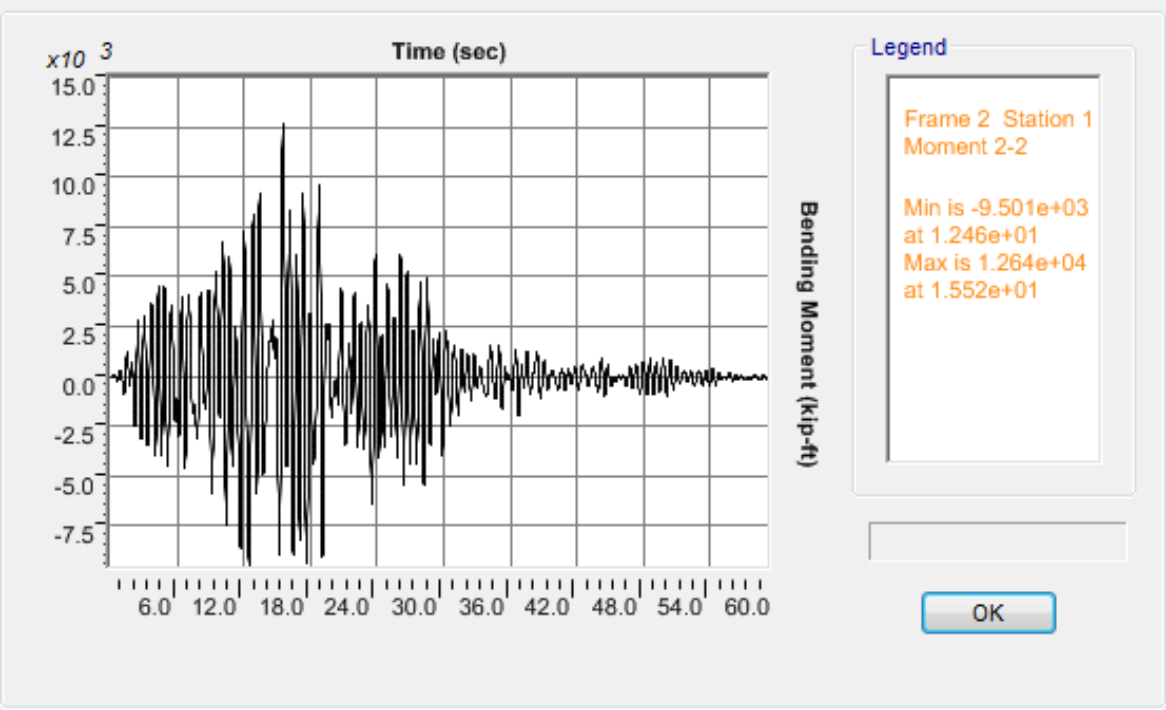

b)

Figure J.28 OSB2 column top response for Motion 28 ROCKS1N3: a) Transverse shear force-displacement hysteresis; b) Bending moment time history in the transverse direction

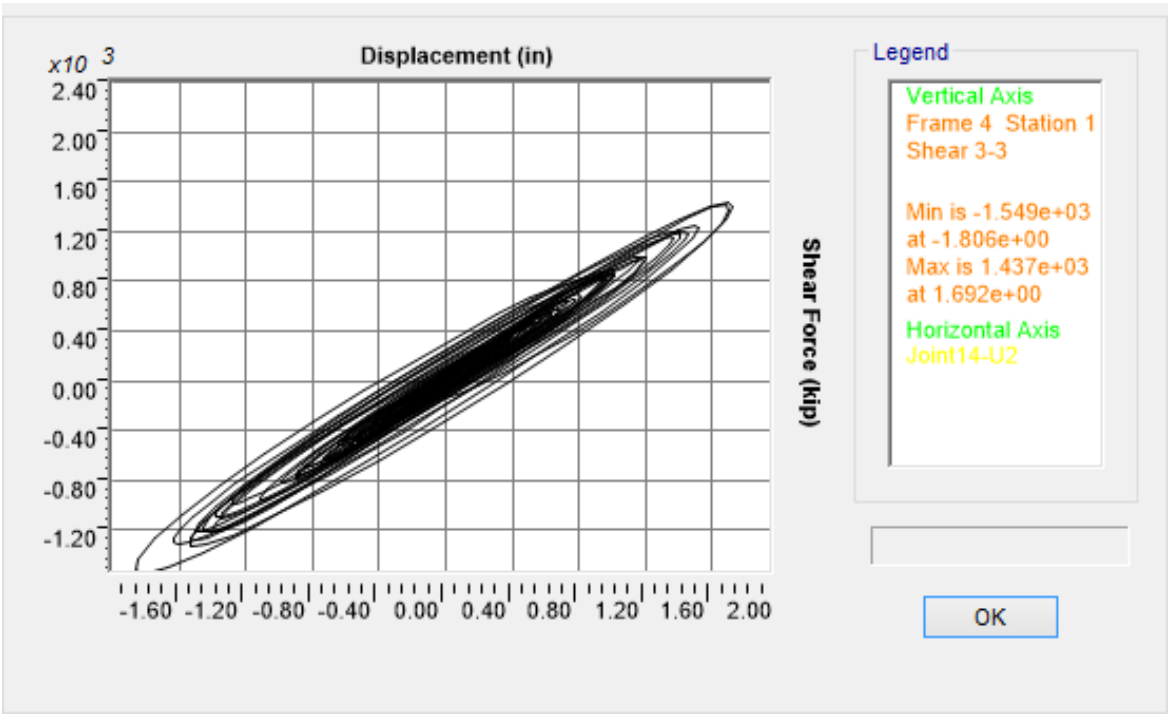

a)

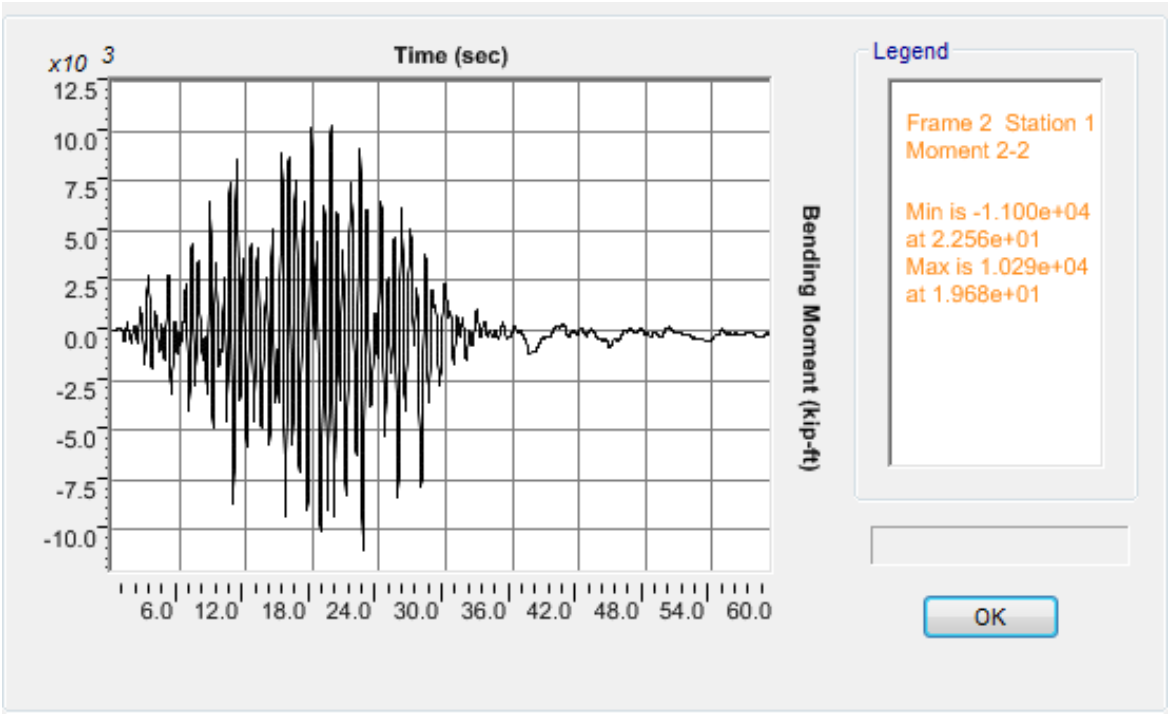

b)

Figure J.29 OSB2 column top response for Motion 29 ROCKS1N4: a) Transverse shear force-displacement hysteresis; b) Bending moment time history in the transverse direction

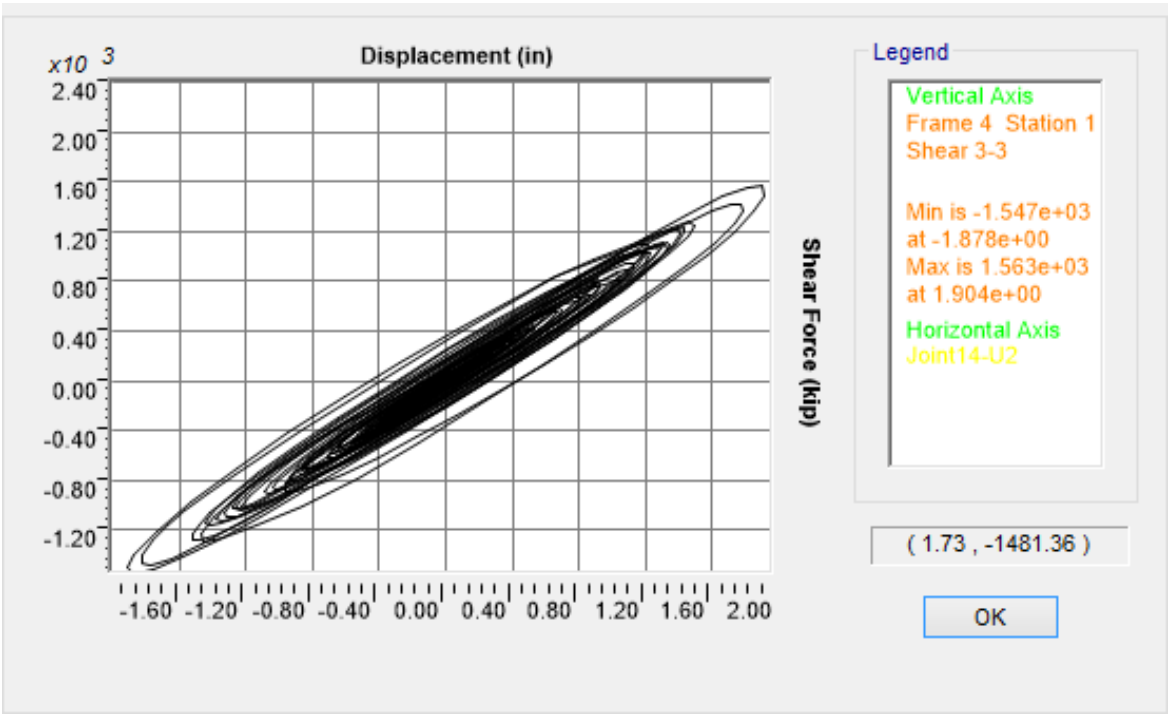

a)

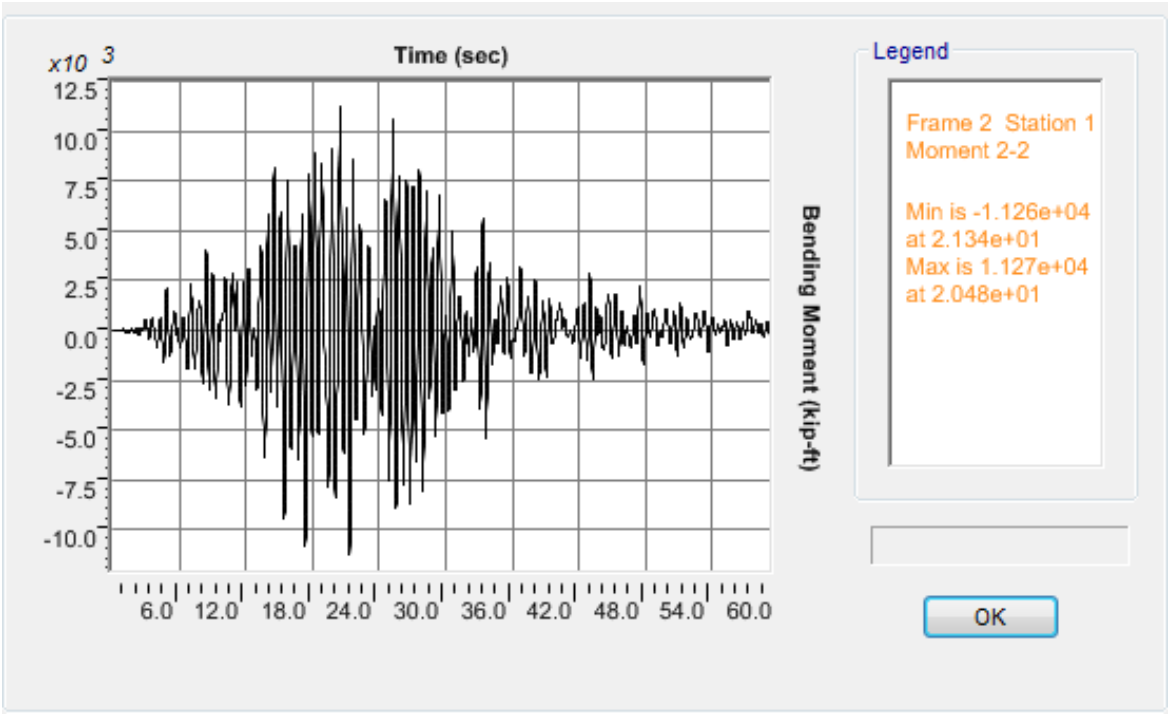

b)

Figure J.30 OSB2 column top response for Motion 30 ROCKS1N5: a) Transverse shear force-displacement hysteresis; b) Bending moment time history in the transverse direction

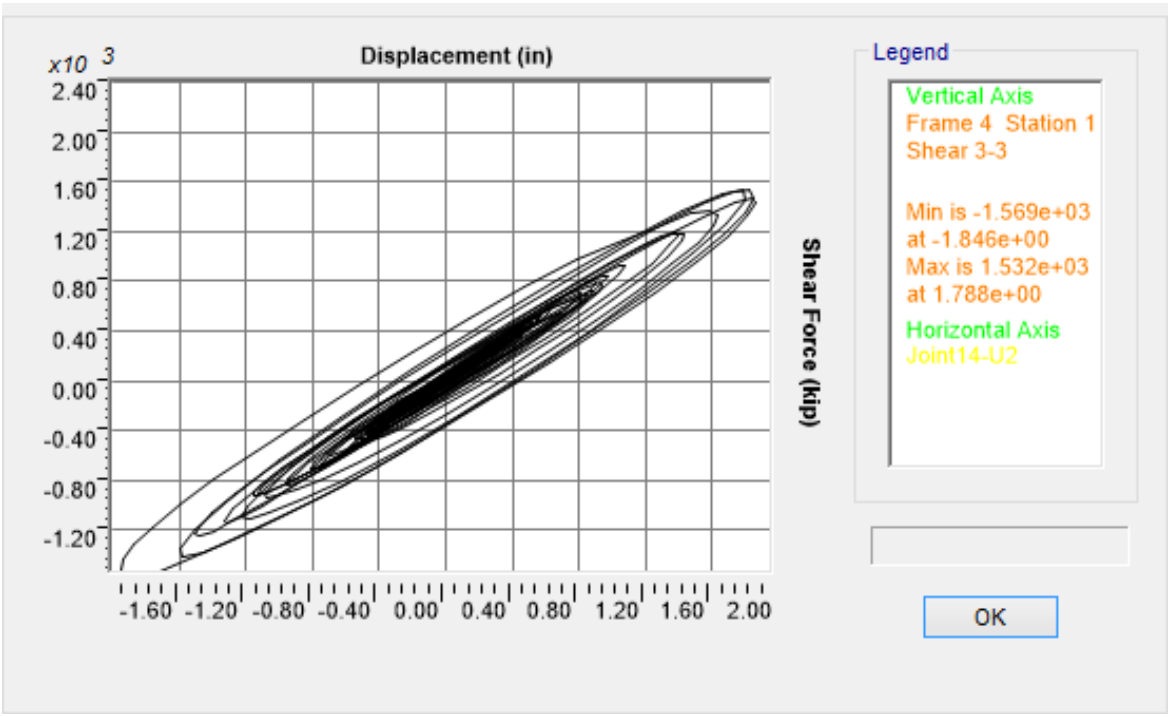

a)

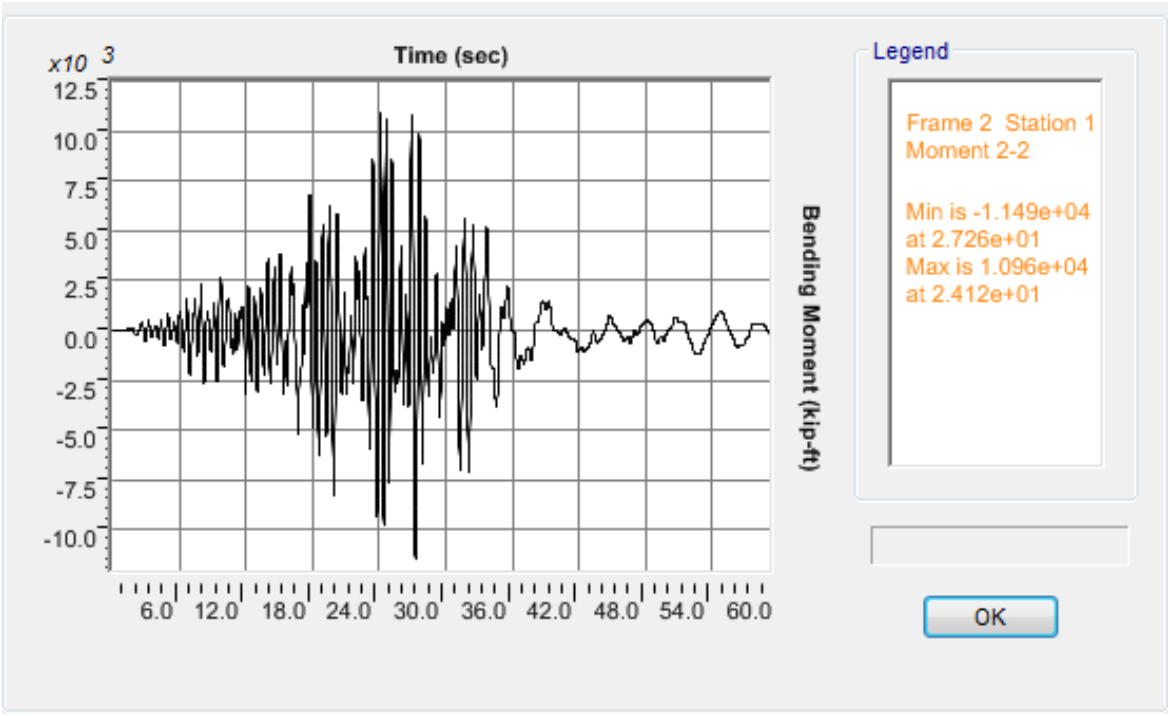

b)

Figure J.31 OSB2 column top response for Motion 31 ROCKS1N6: a) Transverse shear force-displacement hysteresis; b) Bending moment time history in the transverse direction

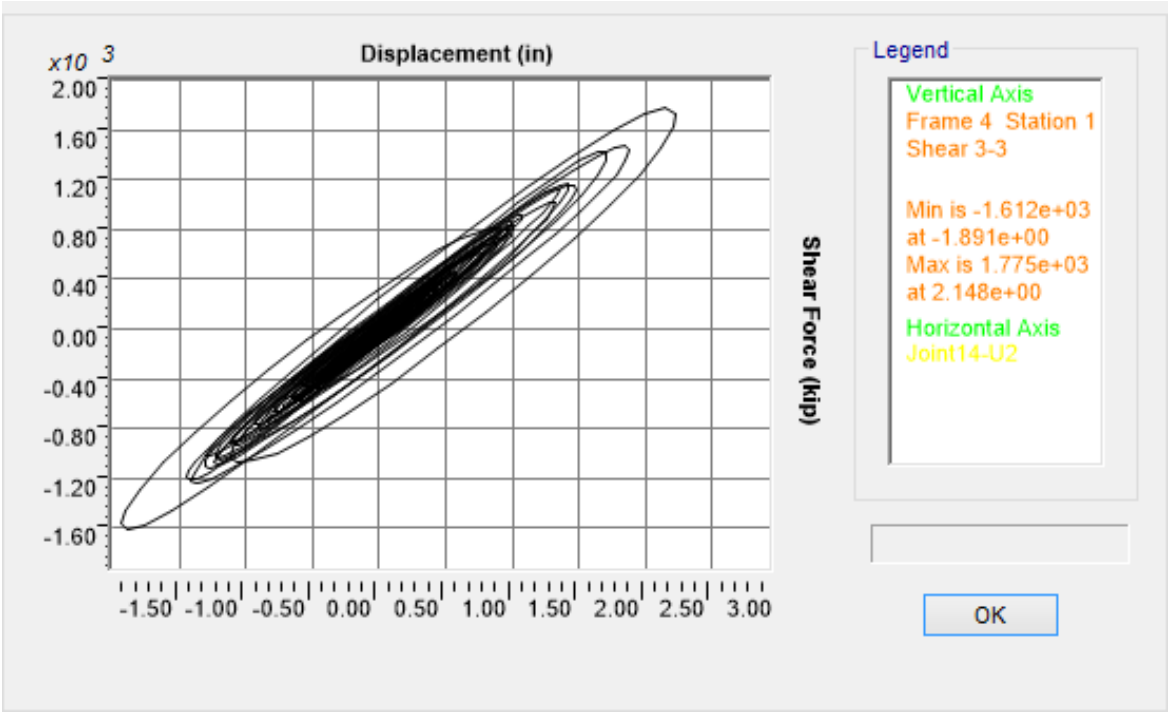

a)

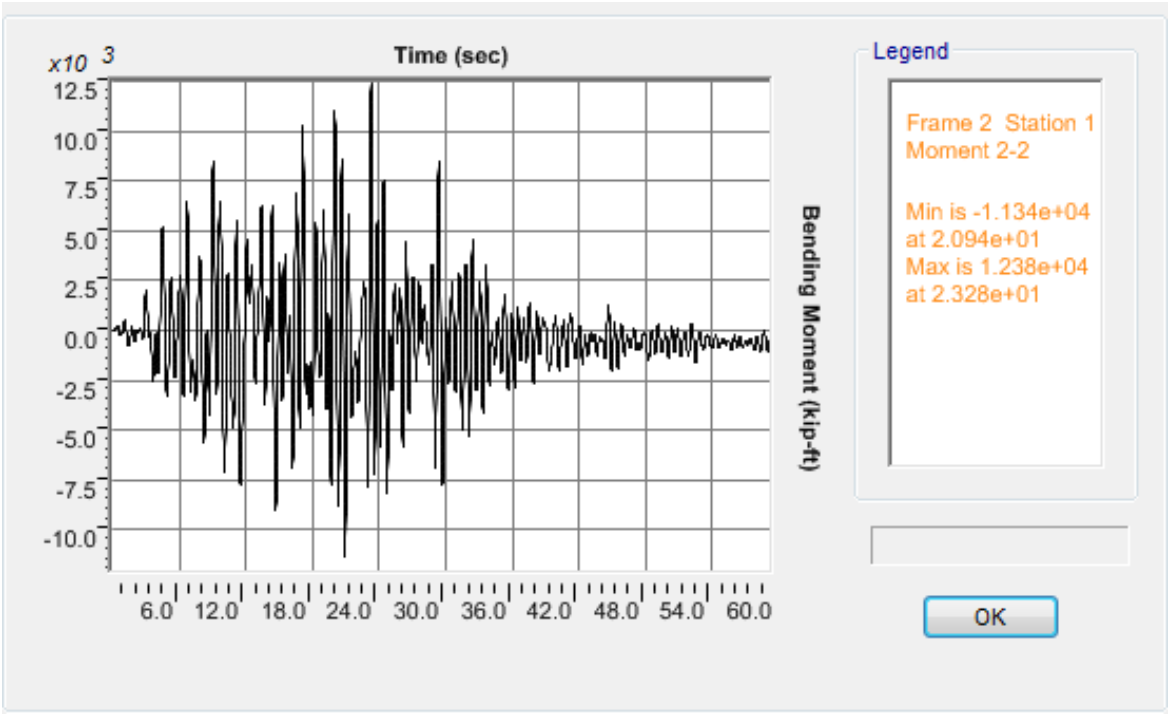

b)

Figure J.32 OSB2 column top response for Motion 32 ROCKS1N7: a) Transverse shear force-displacement hysteresis; b) Bending moment time history in the transverse direction

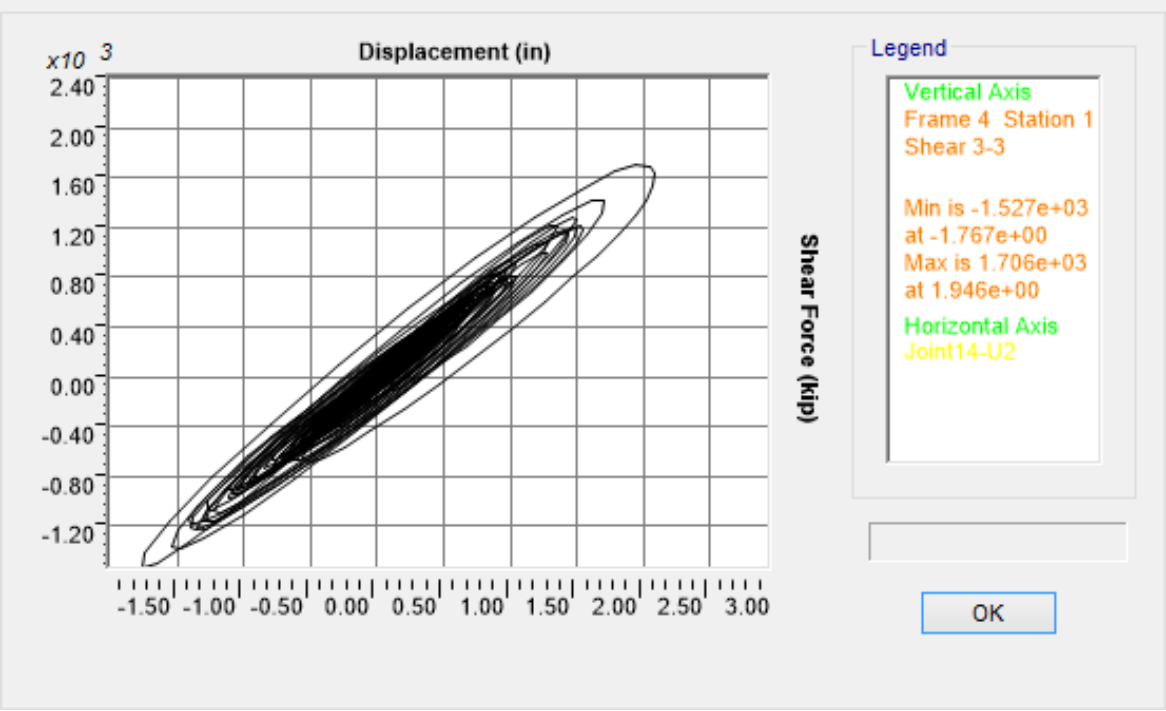

a)

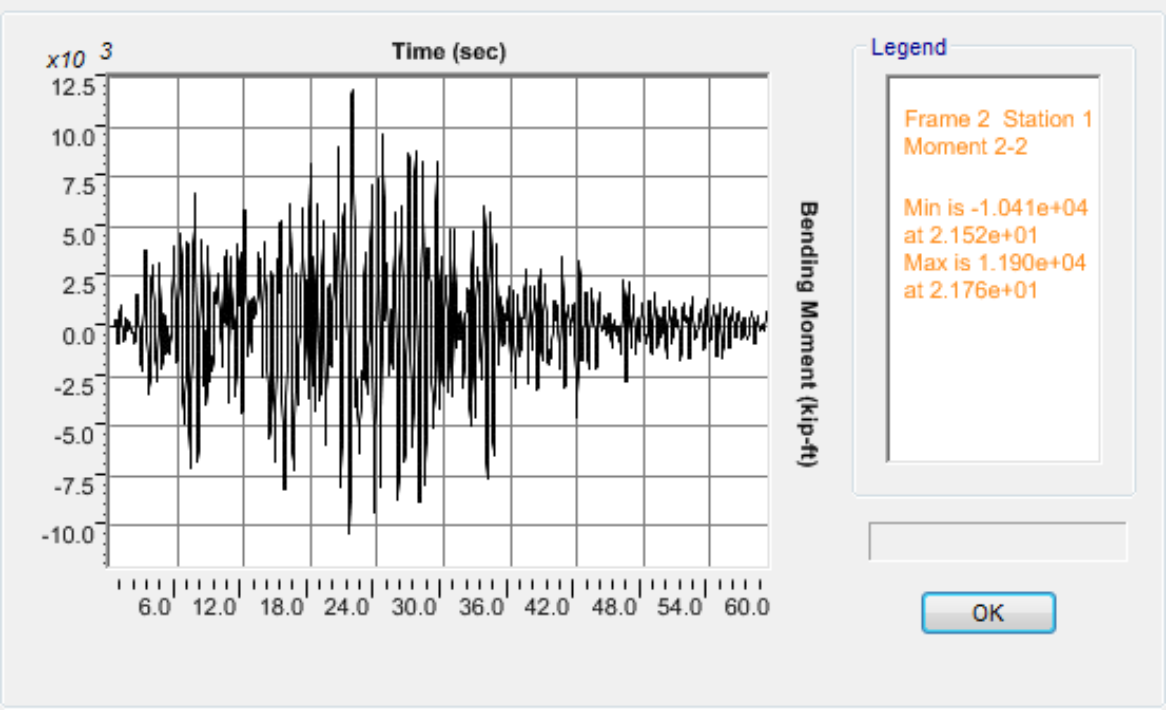

b)

Figure J.33 OSB2 column top response for Motion 33 ROCKS1P1: a) Transverse shear force-displacement hysteresis; b) Bending moment time history in the transverse direction

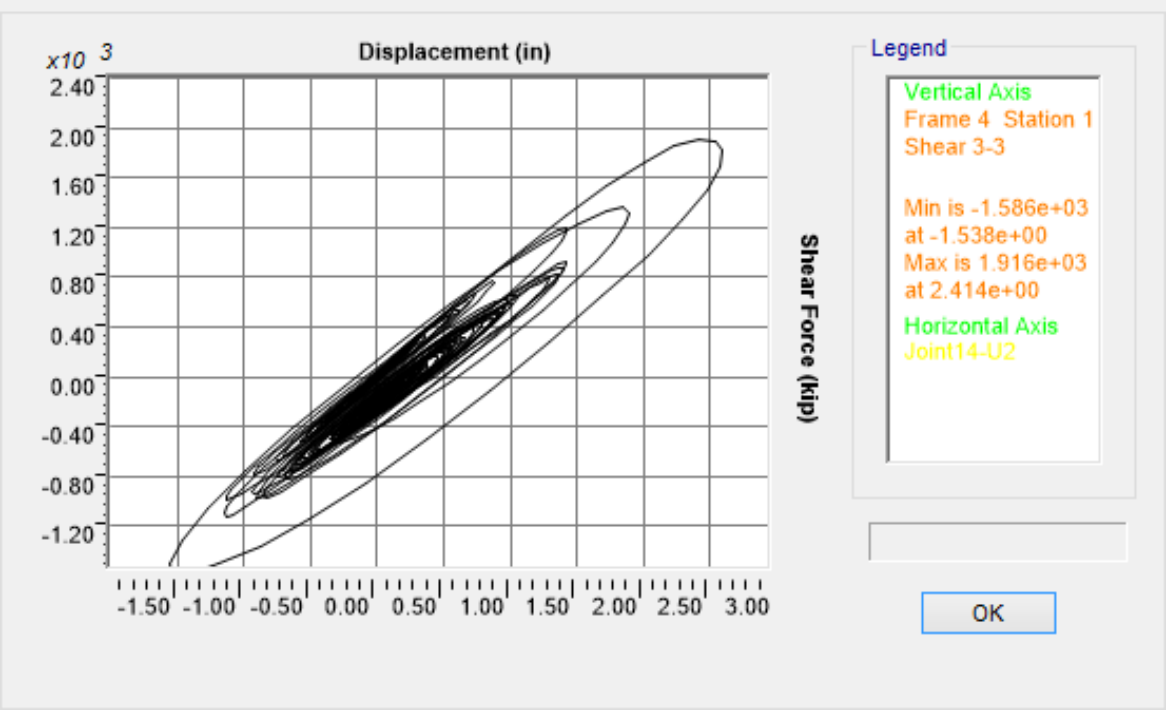

a)

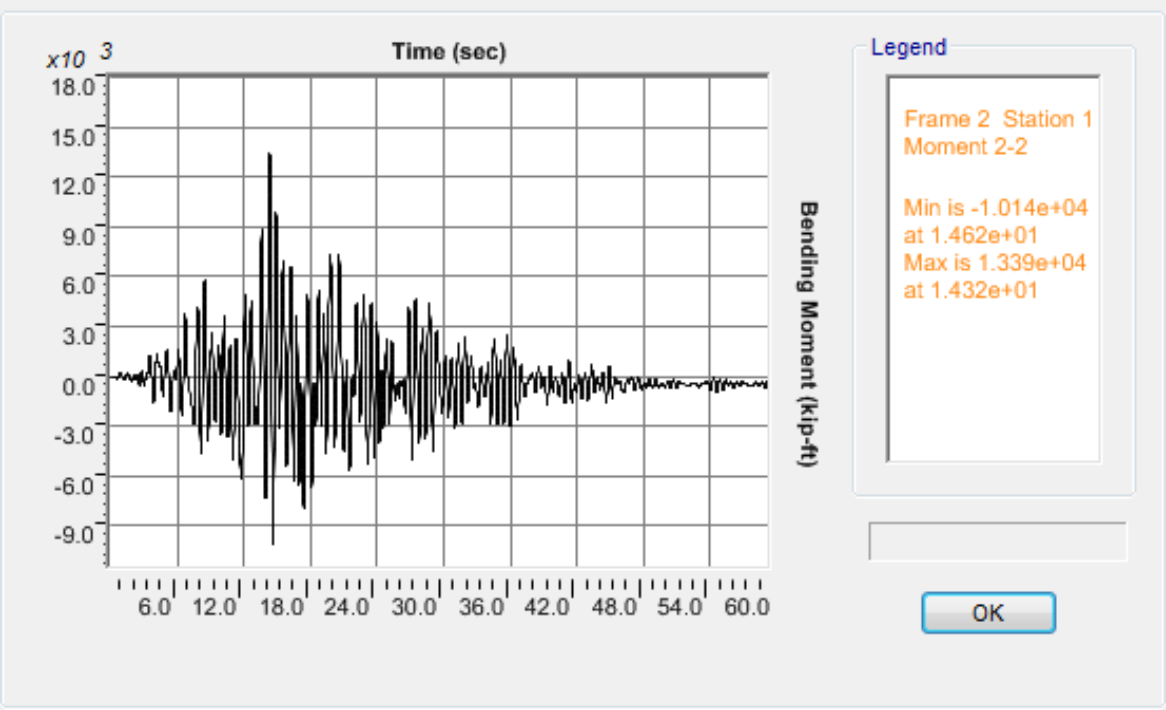

b)

Figure J.34 OSB2 column top response for Motion 34 ROCKS1P2: a) Transverse shear force-displacement hysteresis; b) Bending moment time history in the transverse direction

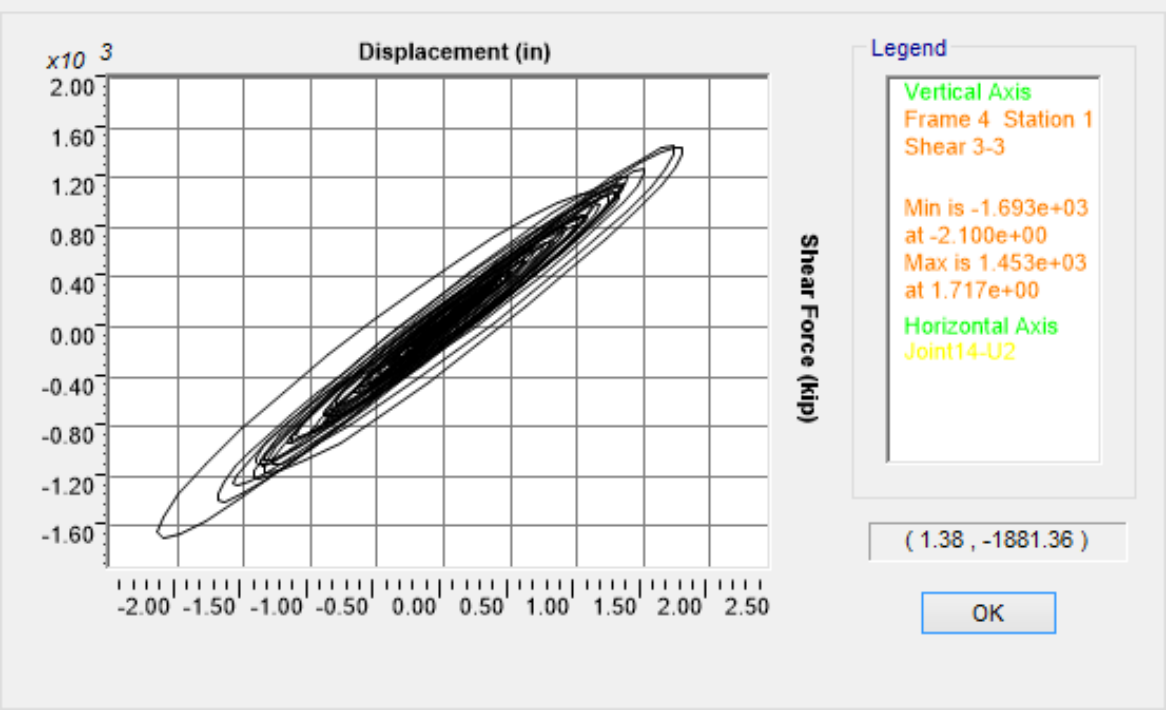

a)

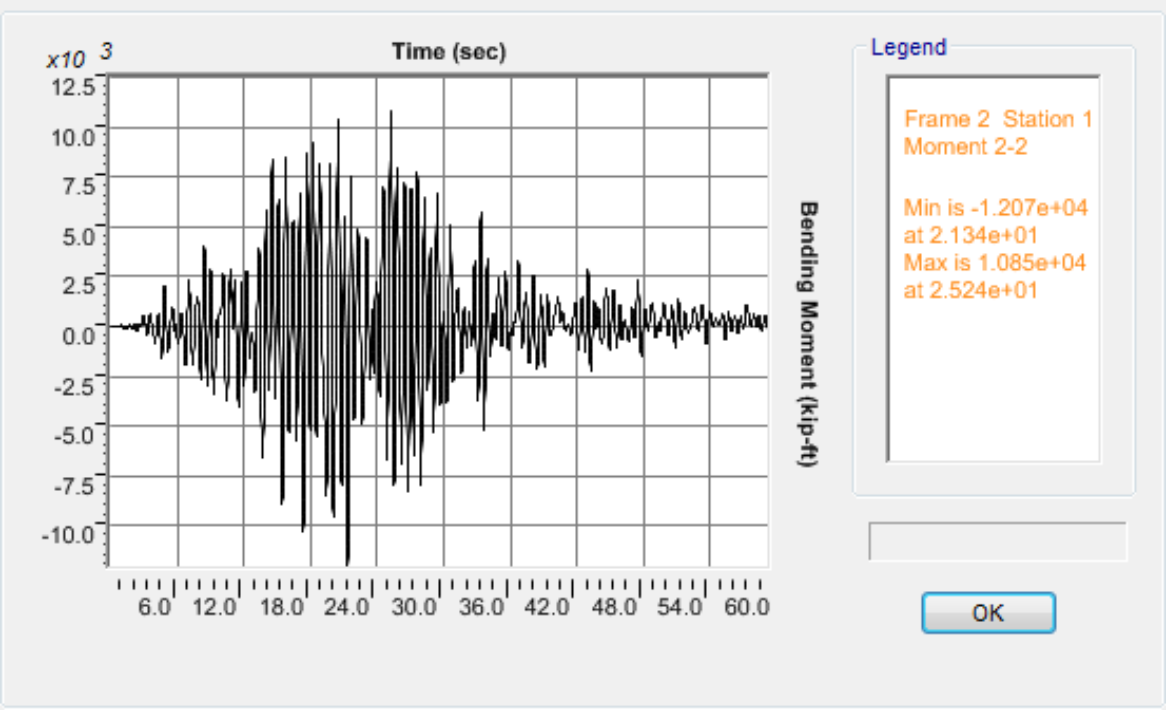

b)

Figure J.35 OSB2 column top response for Motion 35 ROCKS1P3: a) Transverse shear force-displacement hysteresis; b) Bending moment time history in the transverse direction

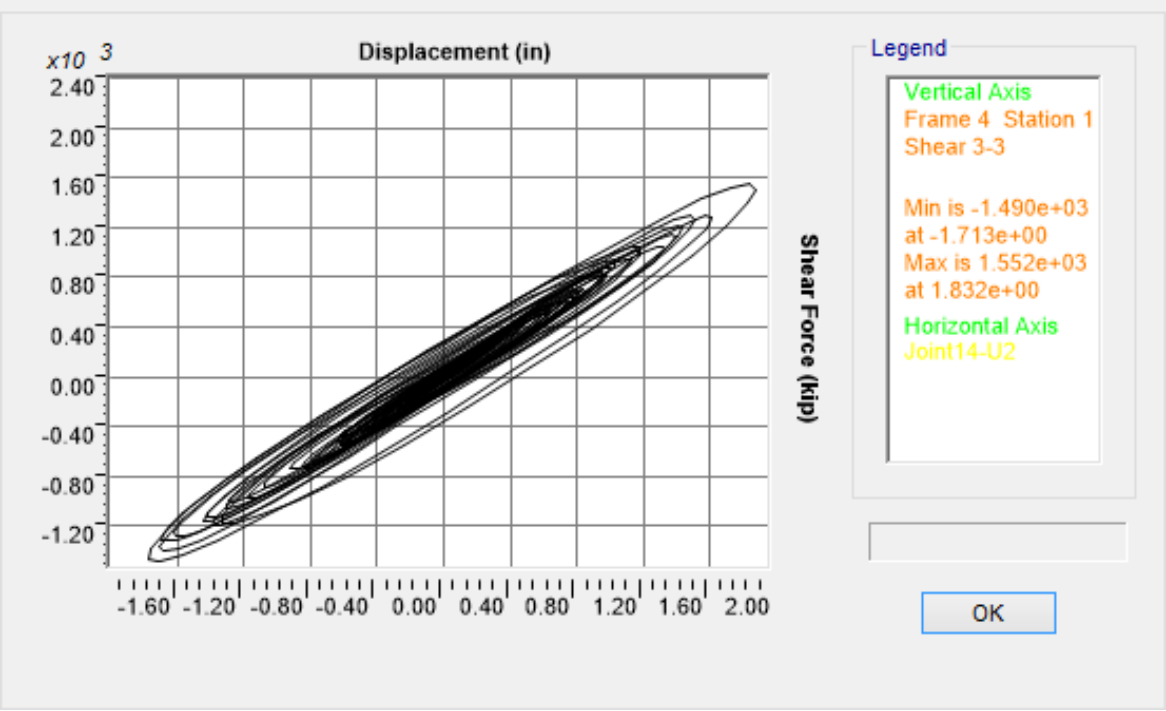

a)

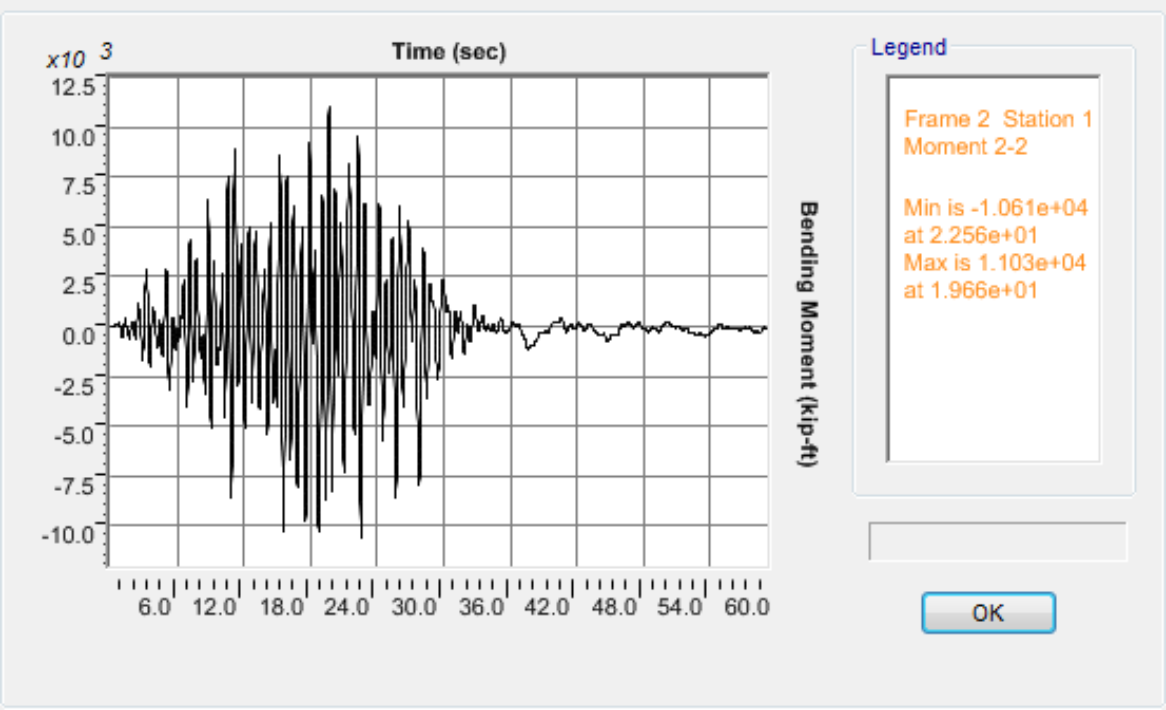

b)

Figure J.36 OSB2 column top response for Motion 36 ROCKS1P4: a) Transverse shear force-displacement hysteresis; b) Bending moment time history in the transverse direction

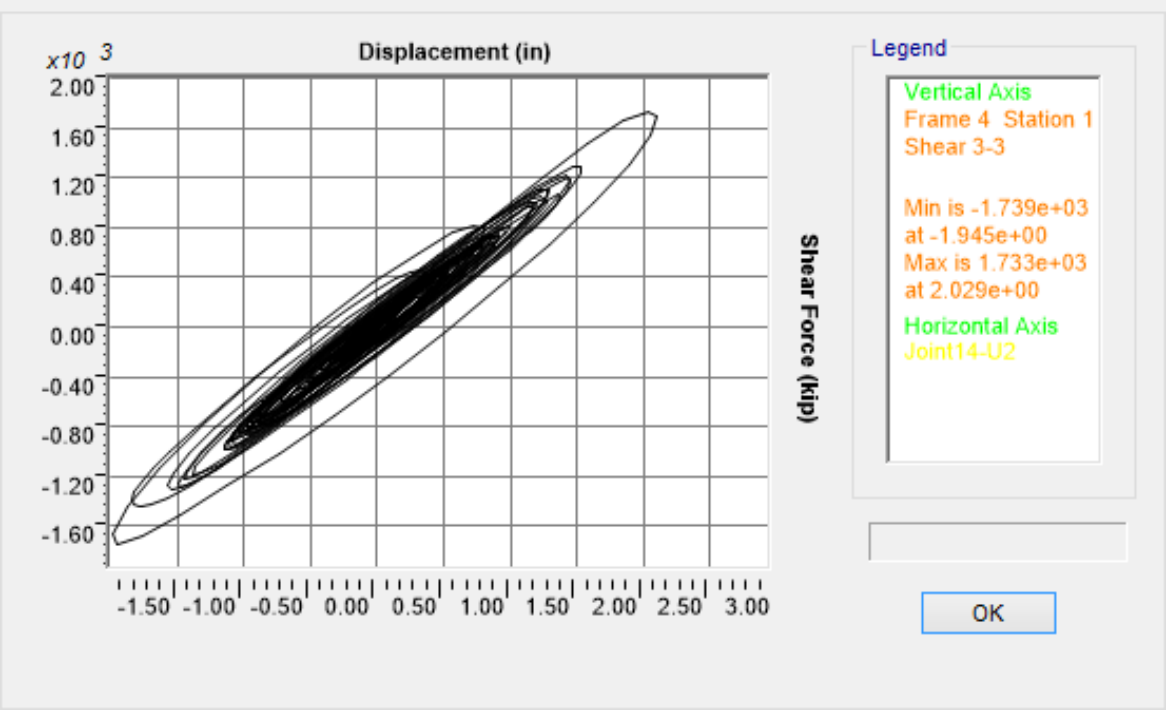

a)

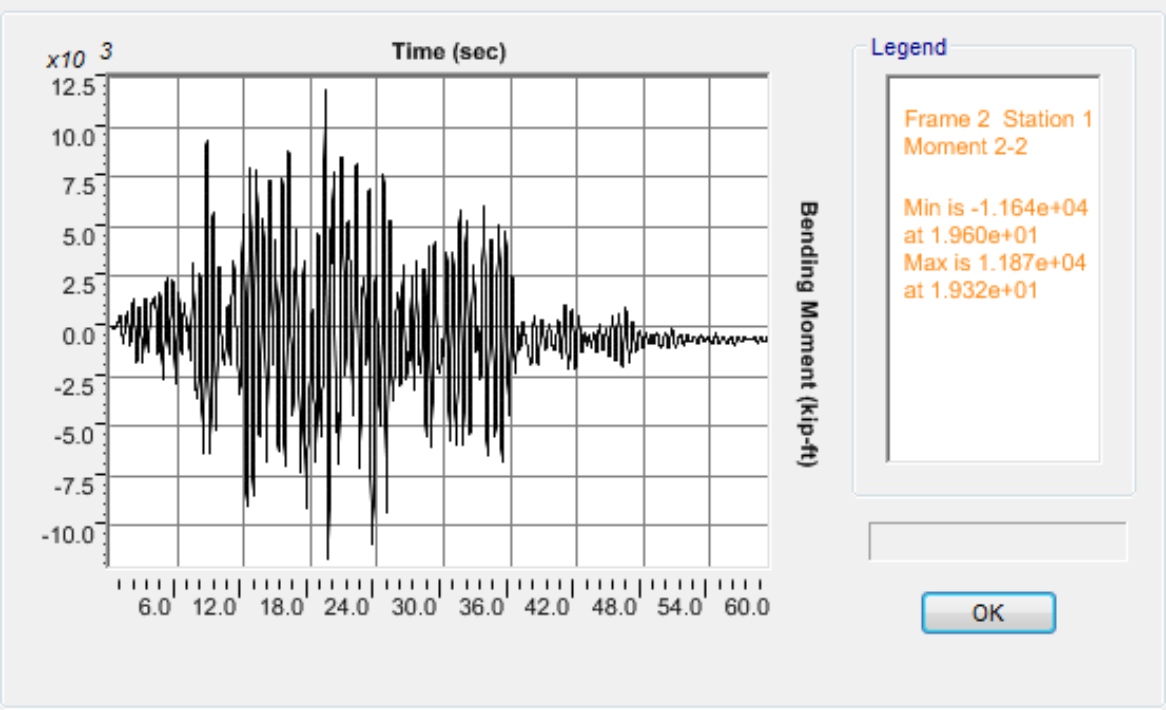

b)

Figure J.37 OSB2 column top response for Motion 37 ROCKS1P5: a) Transverse shear force-displacement hysteresis; b) Bending moment time history in the transverse direction

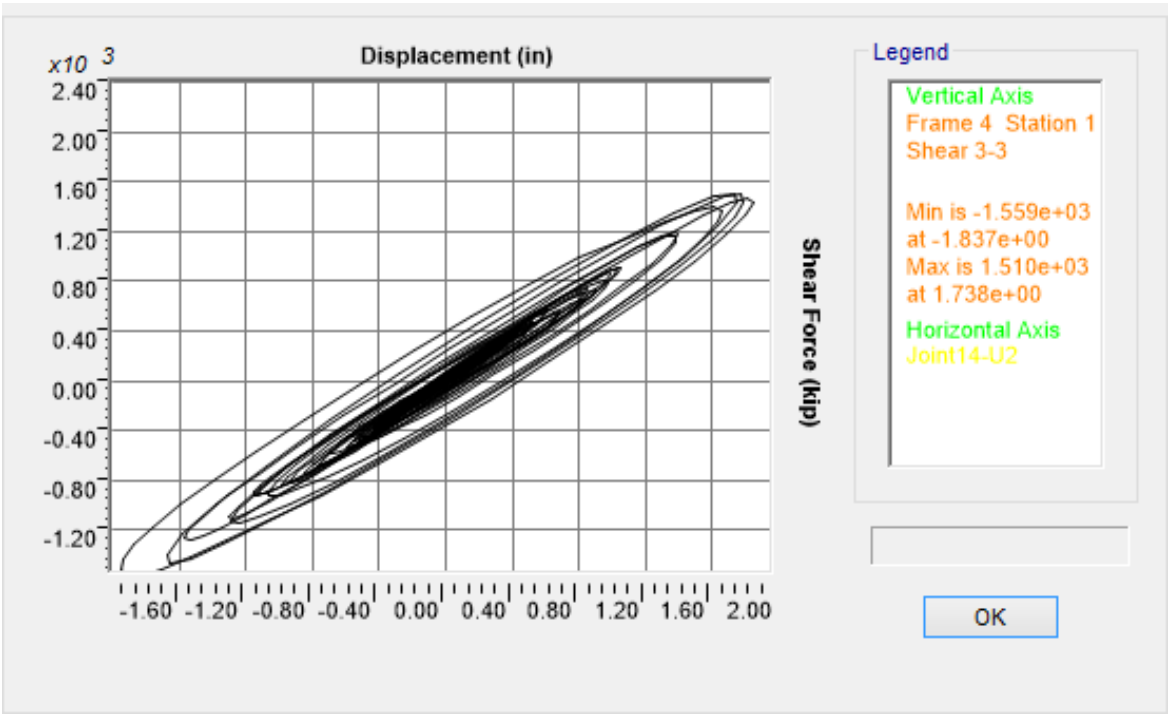

a)

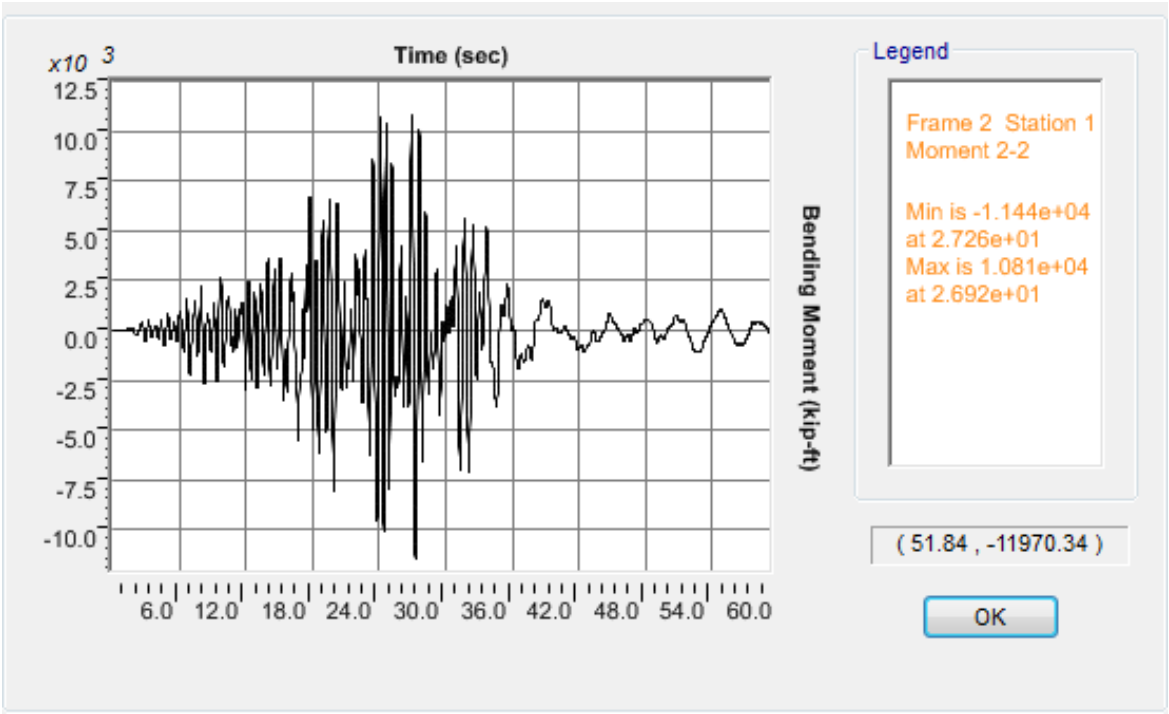

b)

Figure J.38 OSB2 column top response for Motion 38 ROCKS1P6: a) Transverse shear force-displacement hysteresis; b) Bending moment time history in the transverse direction

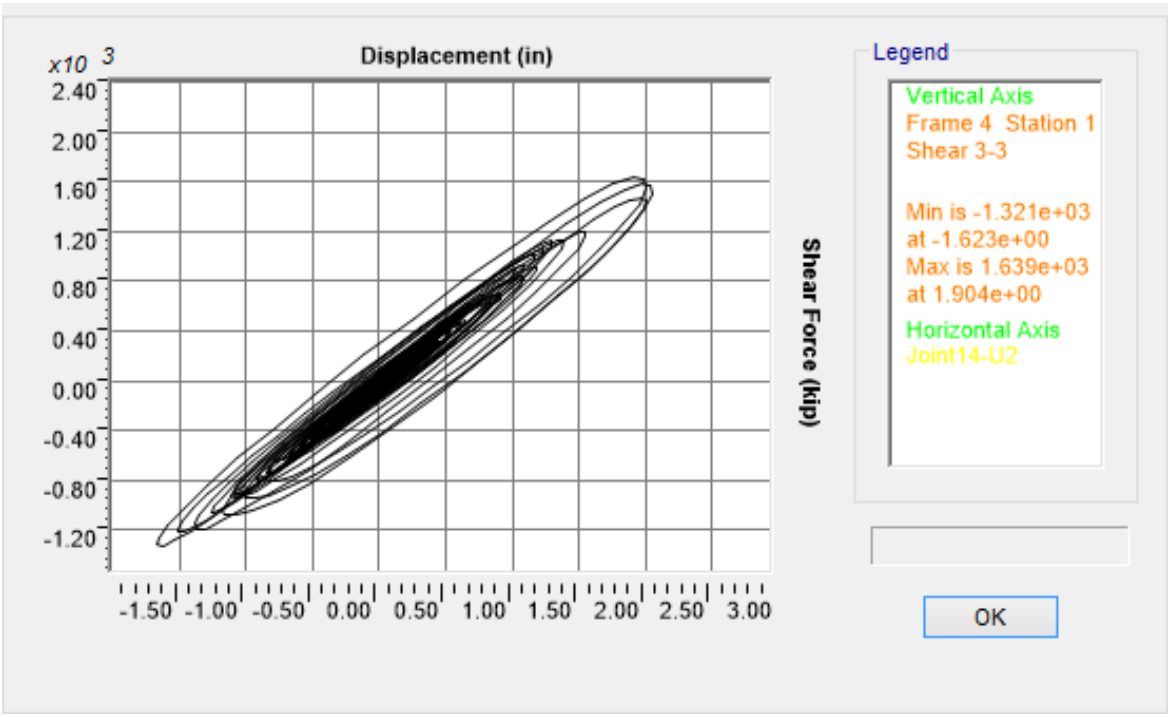

a)

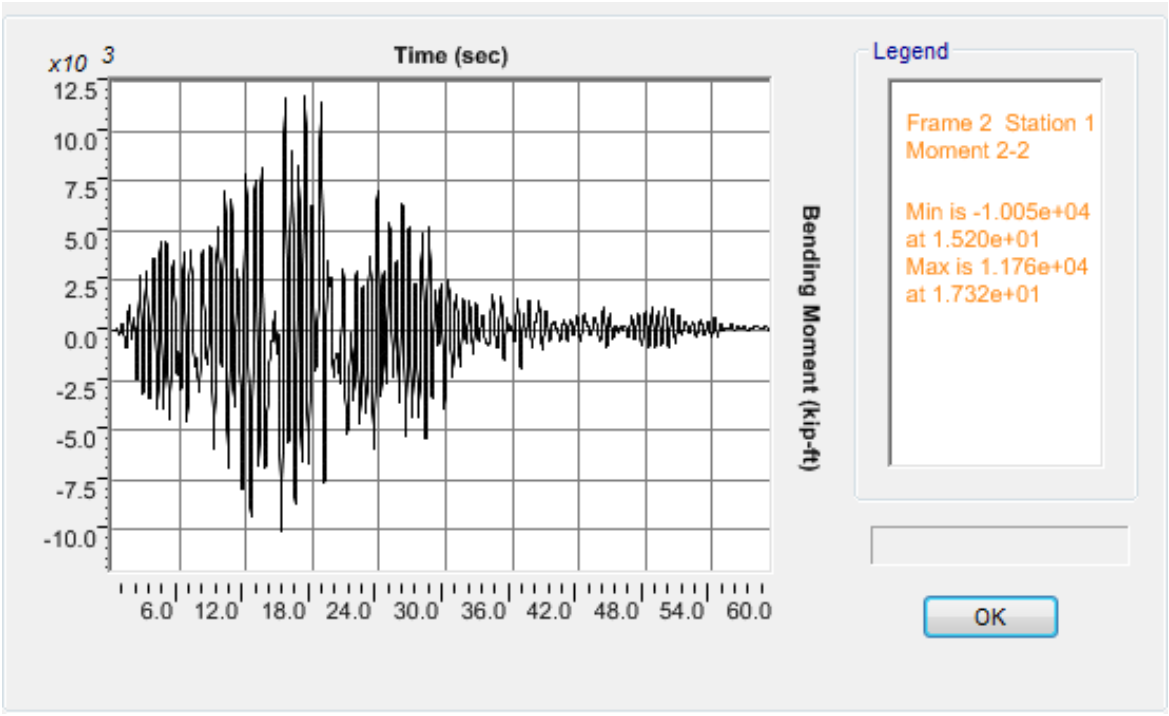

b)

Figure J.39 OSB2 column top response for Motion 39 ROCKS1P7: a) Transverse shear force-displacement hysteresis; b) Bending moment time history in the transverse direction

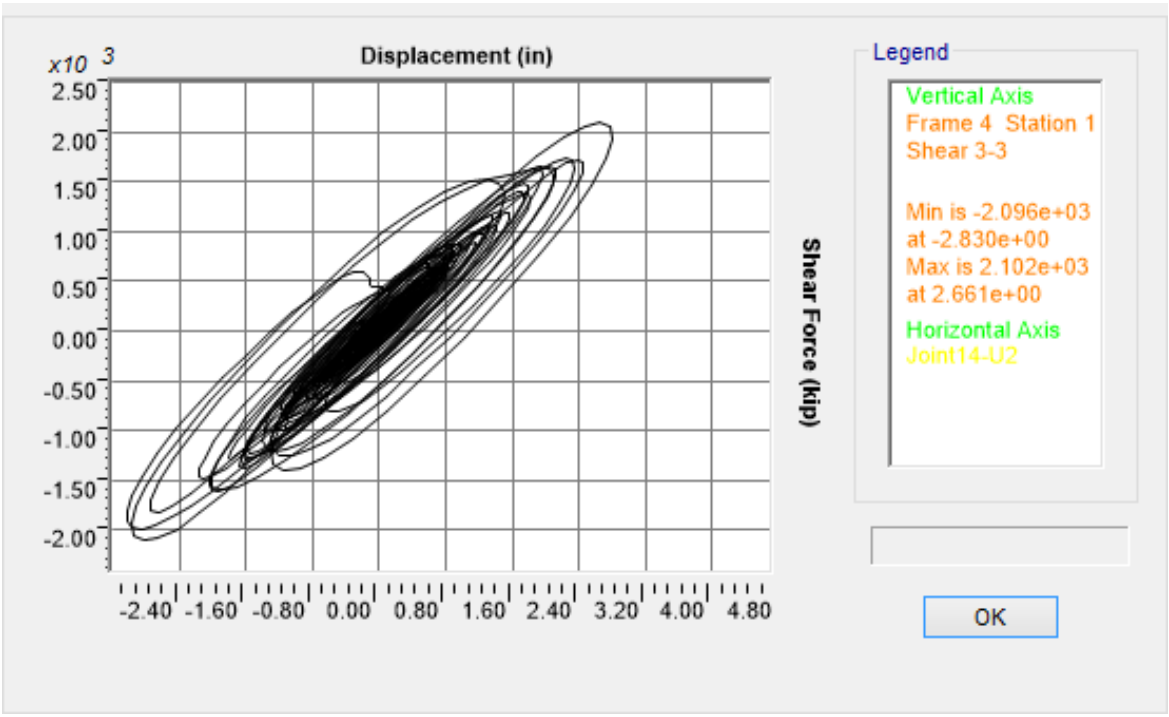

a)

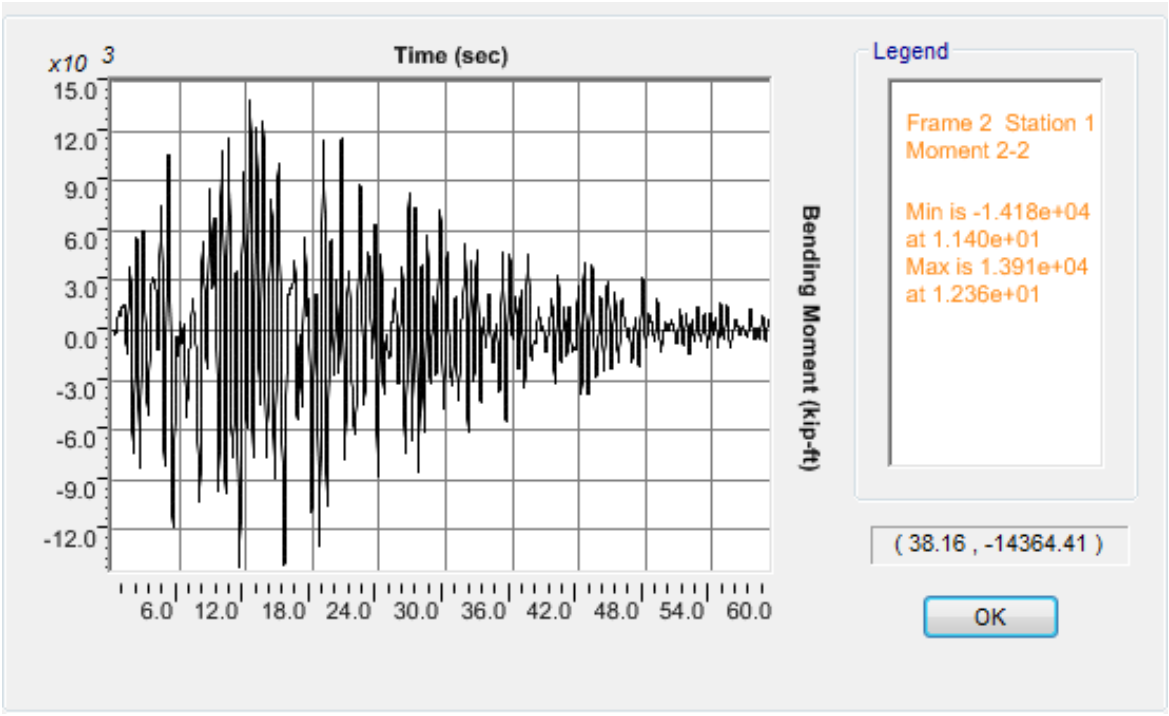

b)

Figure J.40 OSB2 column top response for Motion 40 SANDS1N1: a) Transverse shear force-displacement hysteresis; b) Bending moment time history in the transverse direction

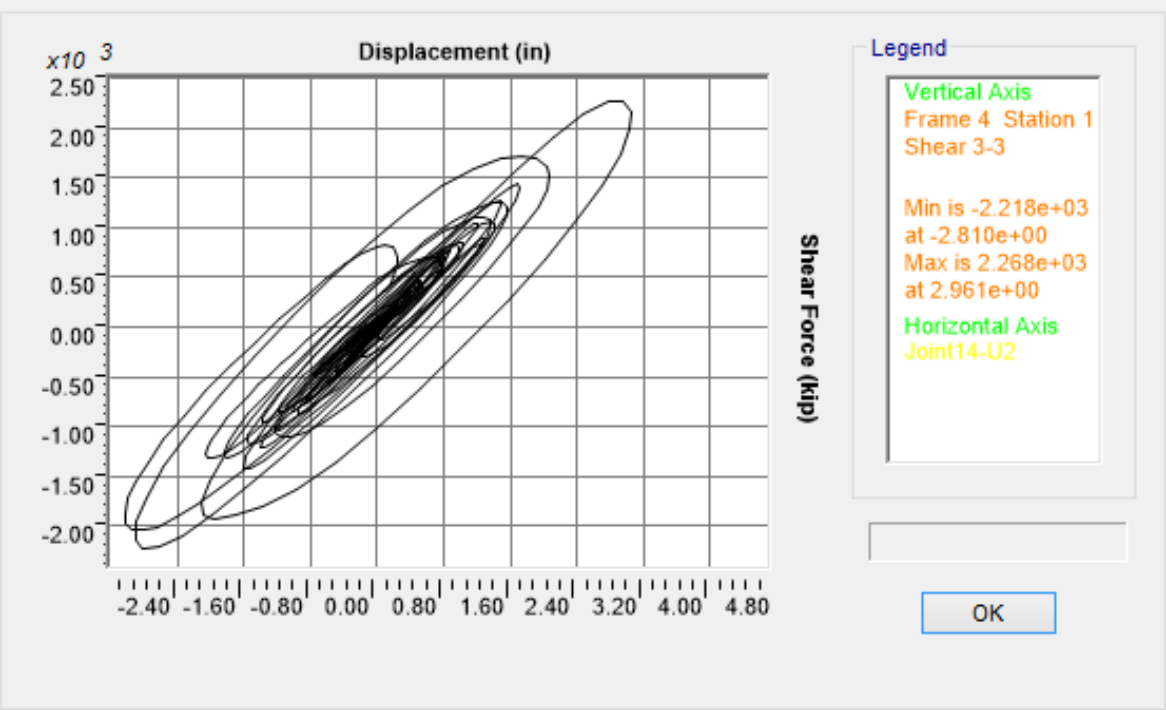

a)

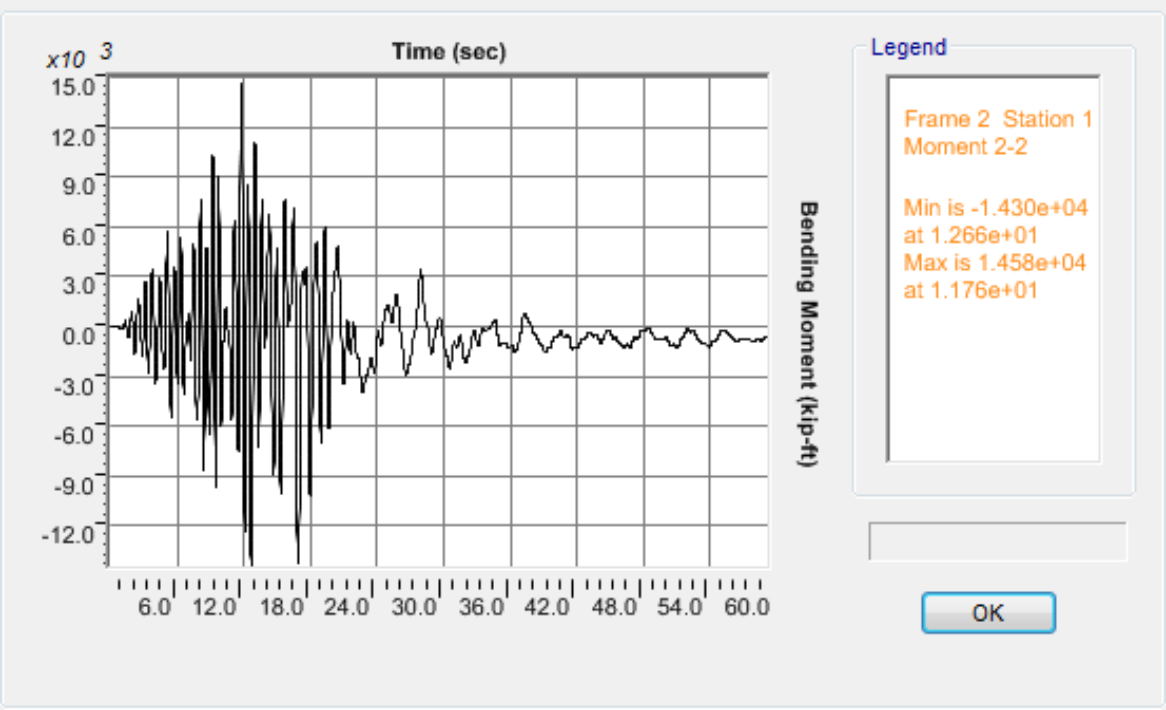

b)

Figure J.41 OSB2 column top response for Motion 41 SANDS1N2: a) Transverse shear force-displacement hysteresis; b) Bending moment time history in the transverse direction

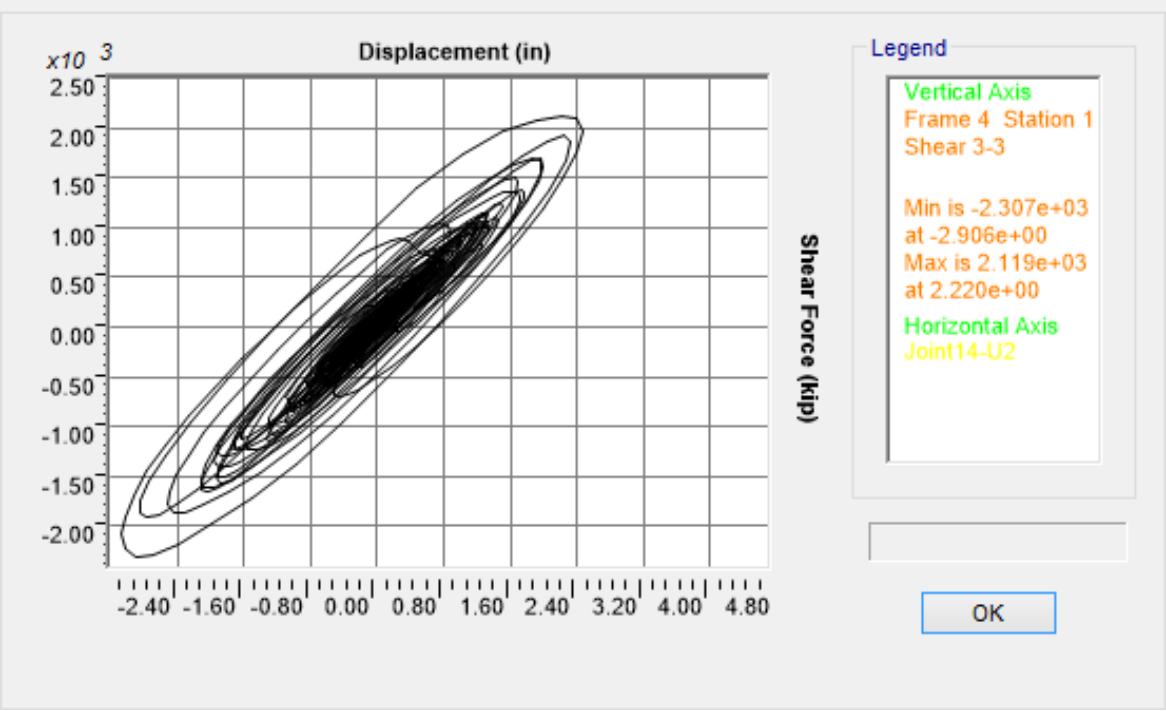

a)

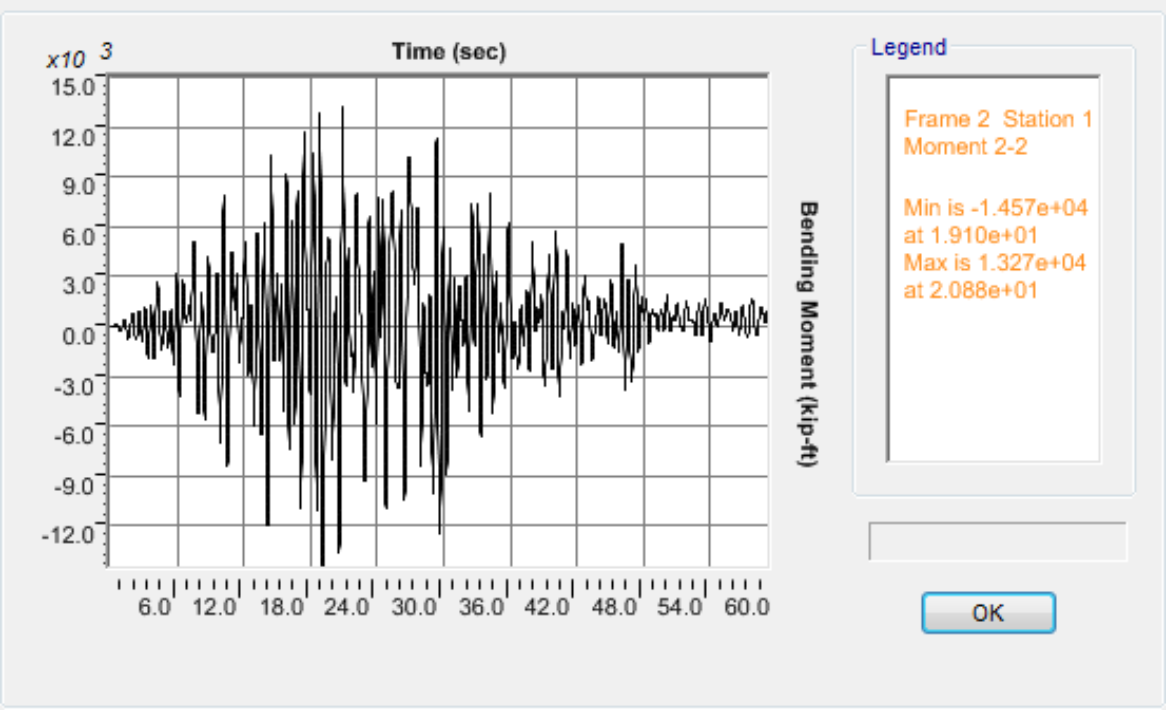

b)

Figure J.42 OSB2 column top response for Motion 42 SANDS1N3: a) Transverse shear force-displacement hysteresis; b) Bending moment time history in the transverse direction

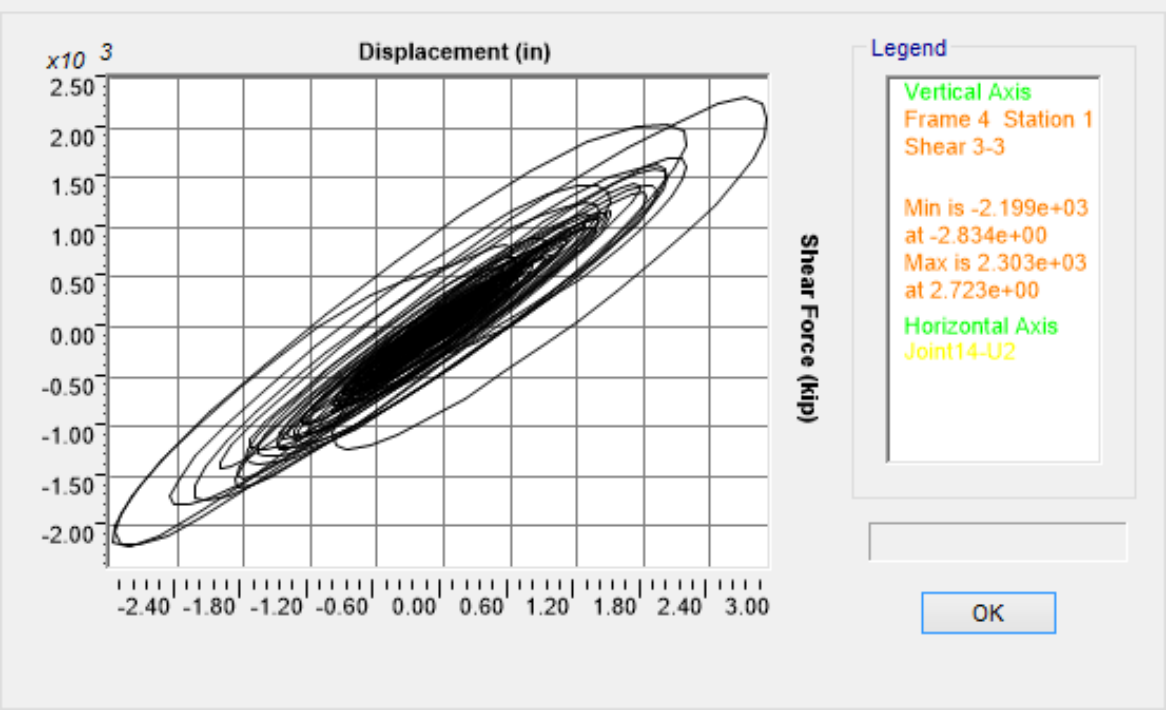

a)

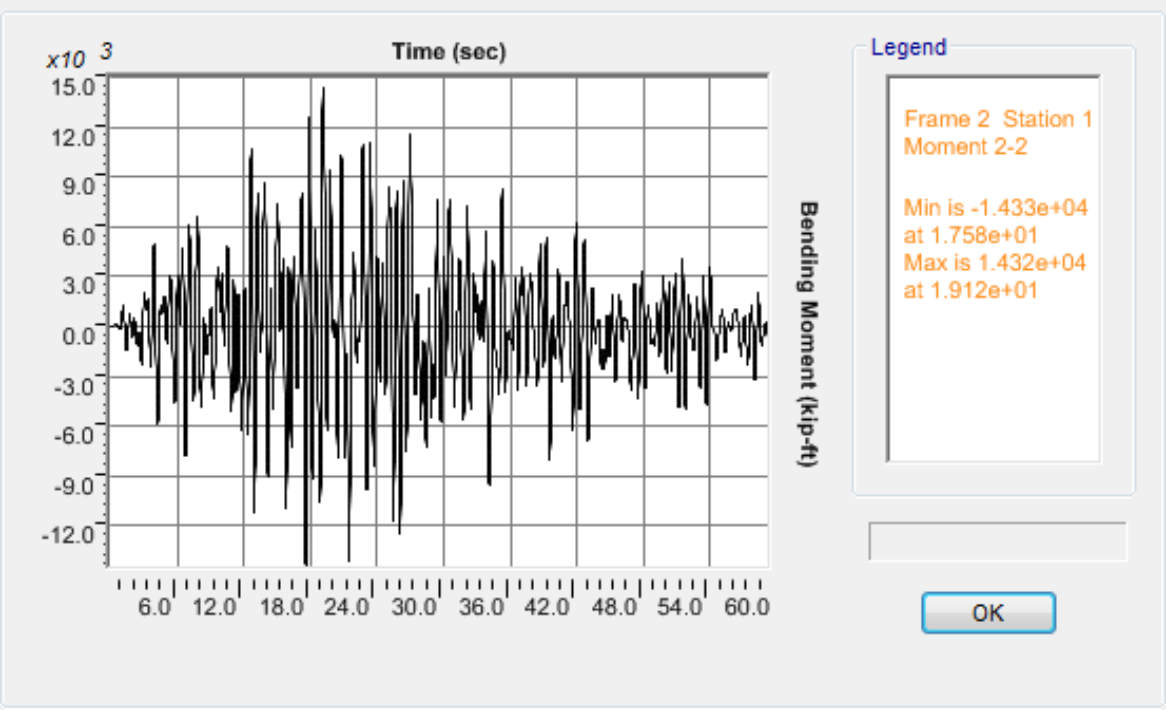

b)

Figure J.43 OSB2 column top response for Motion 43 SANDS1N4: a) Transverse shear force-displacement hysteresis; b) Bending moment time history in the transverse direction

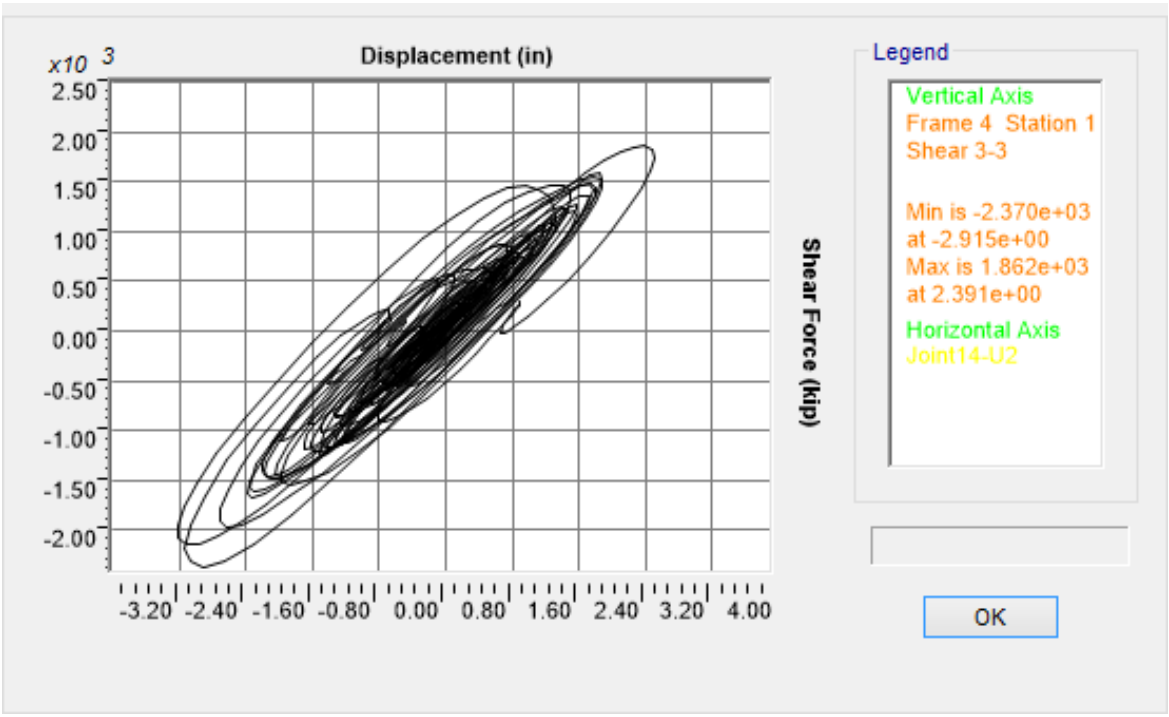

a)

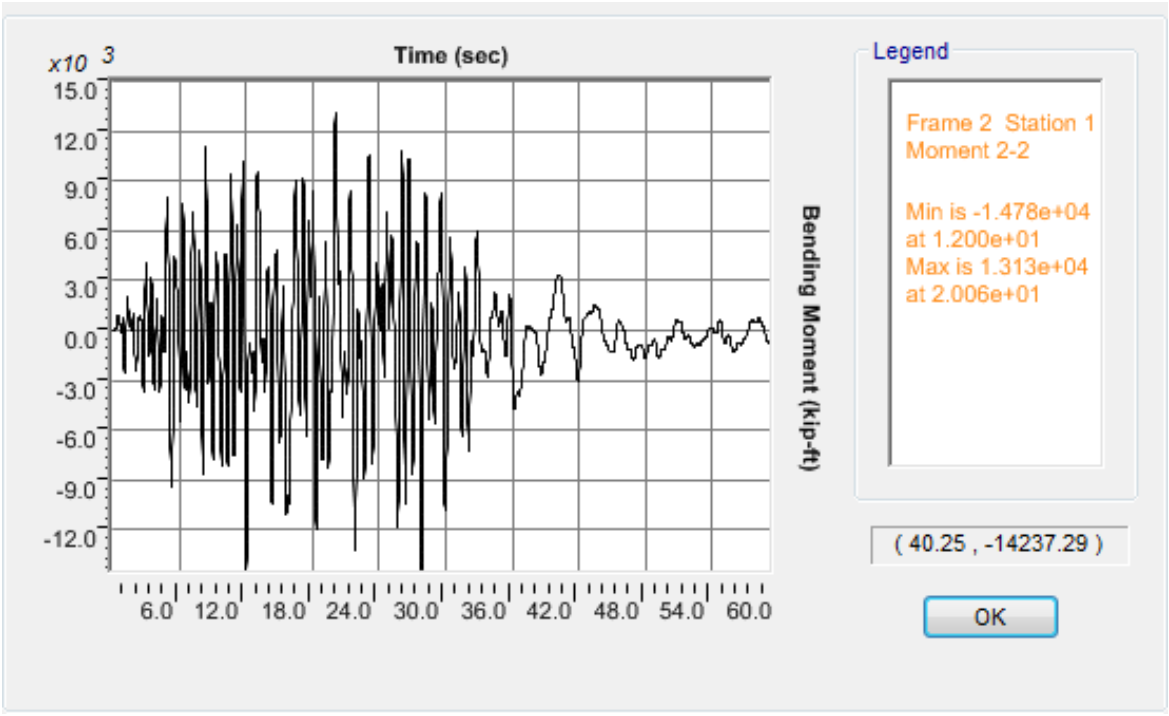

b)

Figure J.44 OSB2 column top response for Motion 44 SANDS1N5: a) Transverse shear force-displacement hysteresis; b) Bending moment time history in the transverse direction

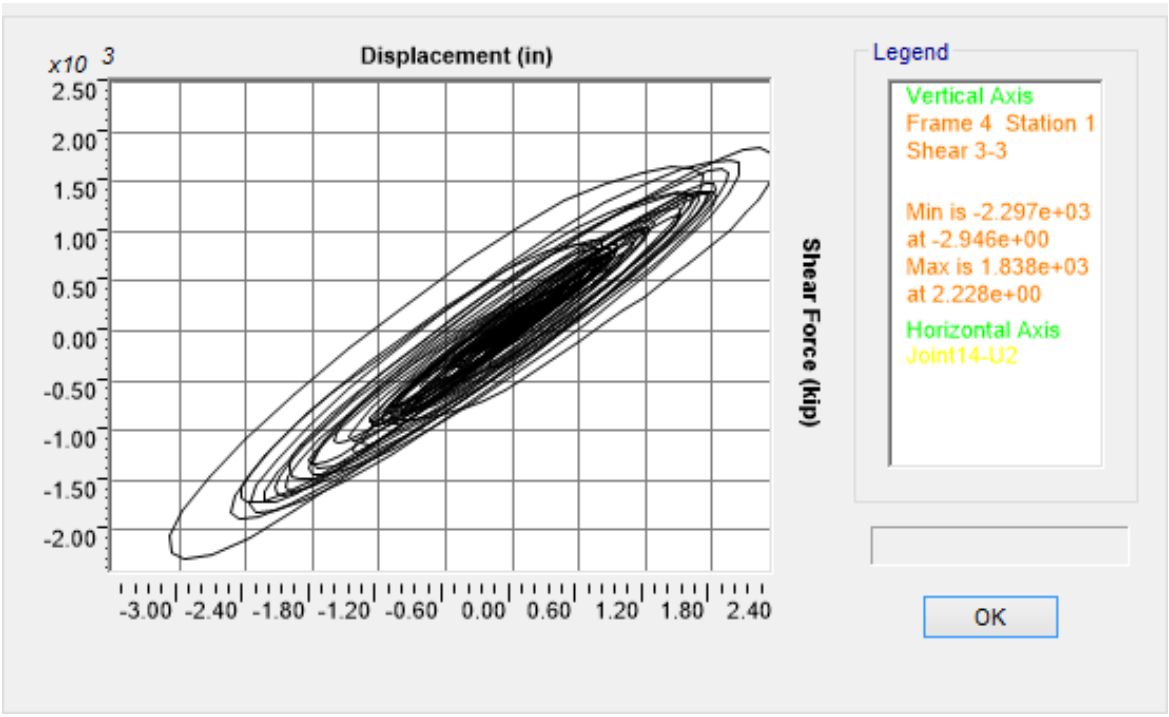

a)

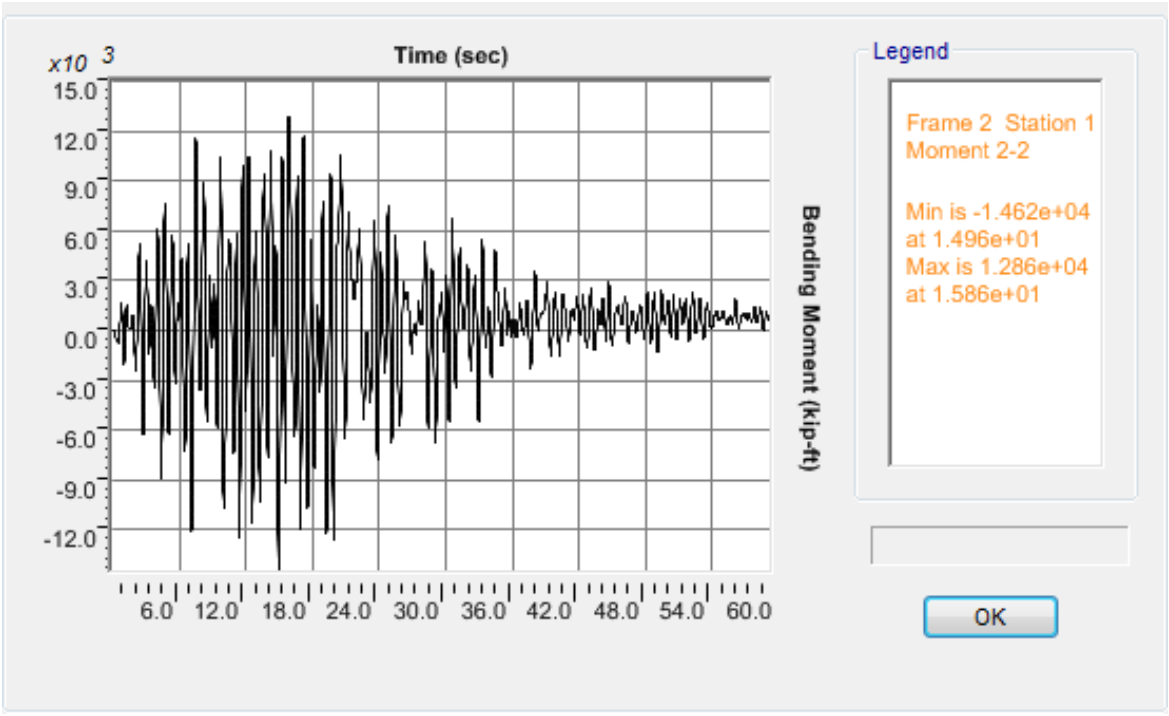

b)

Figure J.45 OSB2 column top response for Motion 45 SANDS1N6: a) Transverse shear force-displacement hysteresis; b) Bending moment time history in the transverse direction

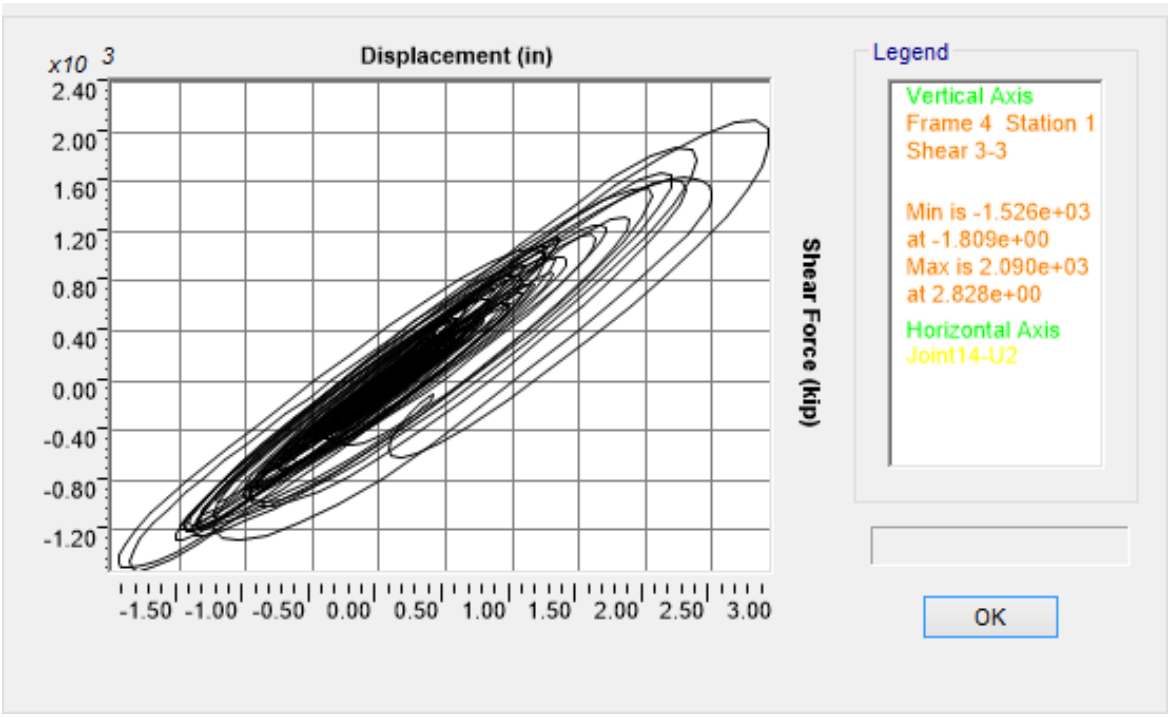

a)

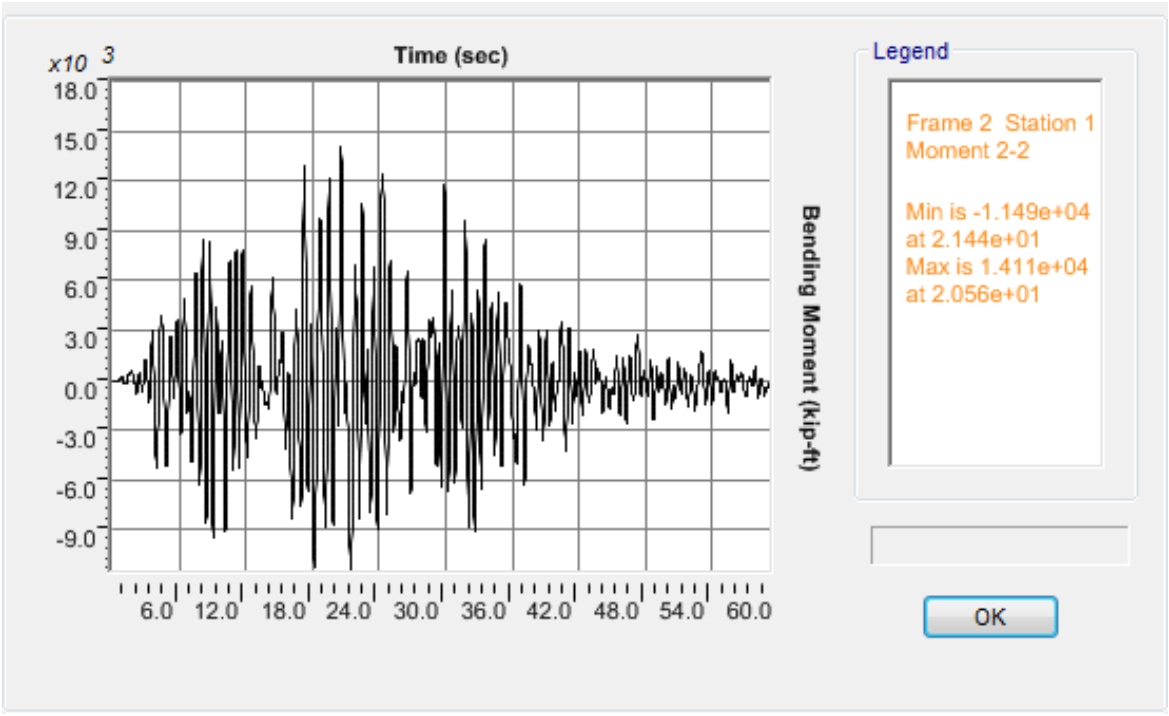

b)

Figure J.46 OSB2 column top response for Motion 46 SANDS1N7: a) Transverse shear force-displacement hysteresis; b) Bending moment time history in the transverse direction

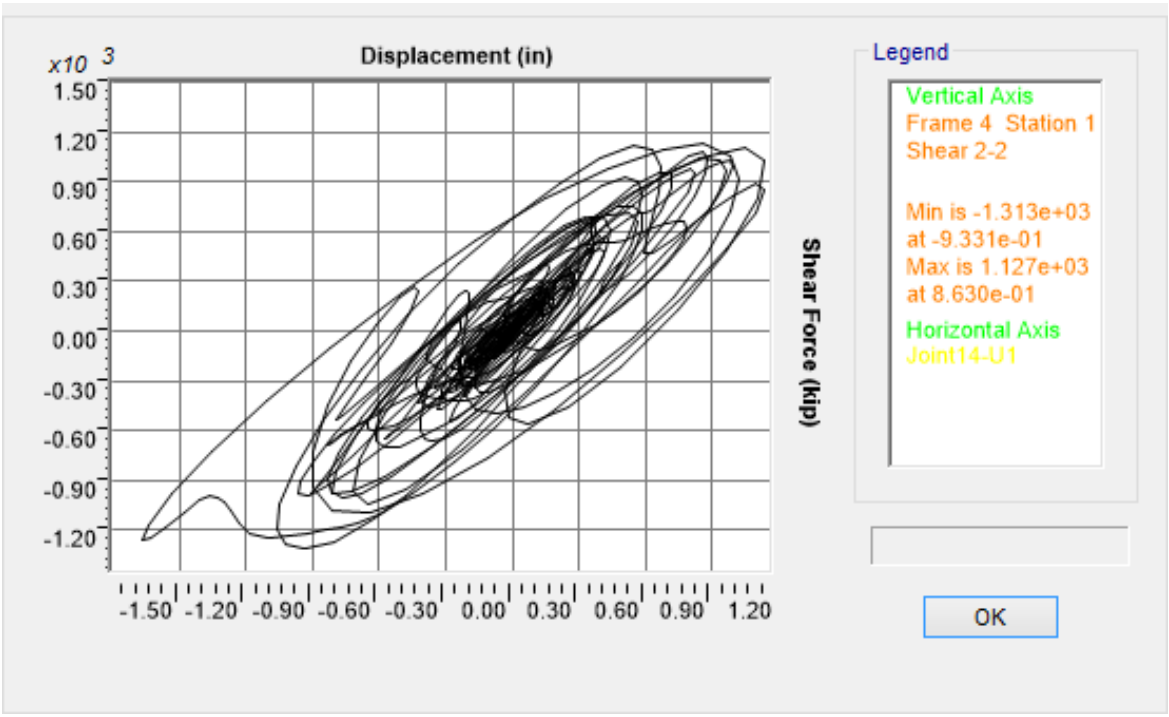
x10 3
Displacement (in)
1.50
1.20
0.90
0.60
0.30
0.00
-0.30
-0.60
-0.90
-1.20
-1.50 -1.20 -0.90 -0.60 -0.30 0.00 0.30 0.60 0.90 1.20
Shear Force (kip)
Legend
Vertical Axis
Frame 4 Station 1
Shear 2-2
Min is -1.313e+03
at -9.331e-01
Max is 1.127e+03
at 8.630e-01
Horizontal Axis
Joint14-U1
OK

a)

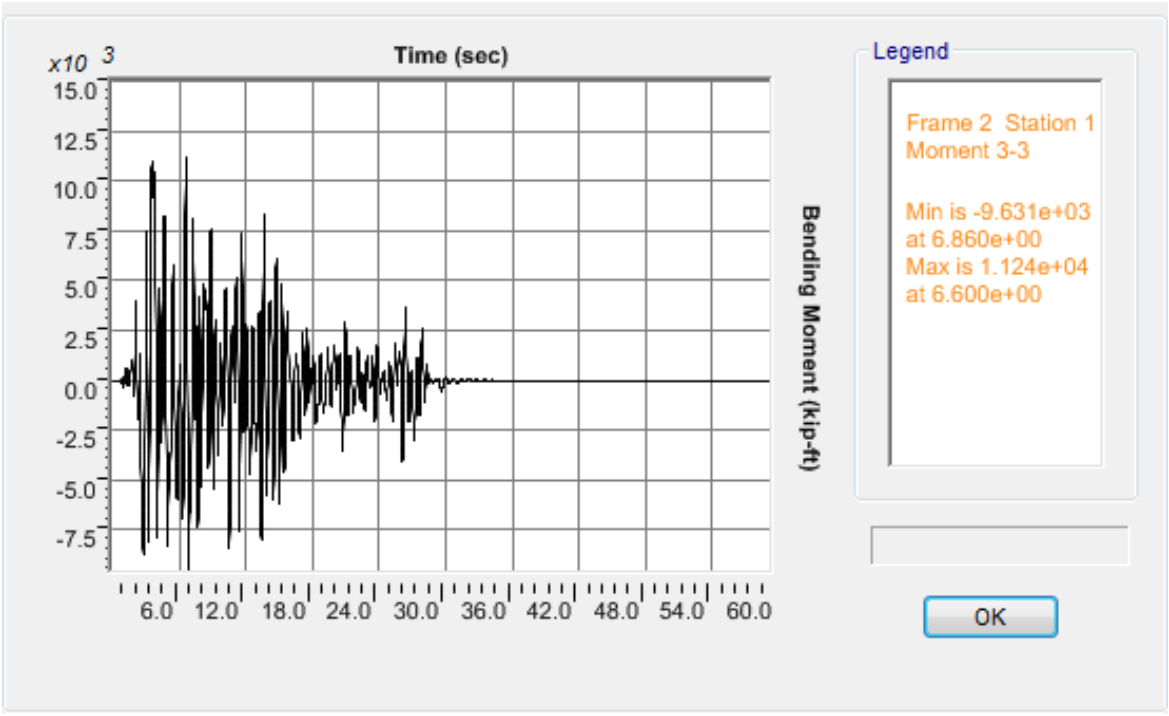
x10 3
Time (sec)
15.0
12.5
10.0
7.5
5.0
2.5
0.0
-2.5
-5.0
-7.5
6.0 12.0 18.0 24.0 30.0 36.0 42.0 48.0 54.0 60.0
Bending Moment (kip-ft)
Legend
Frame 2 Station 1
Moment 3-3
Min is -9.631e+03
at 6.860e+00
Max is 1.124e+04
at 6.600e+00
OK

b)

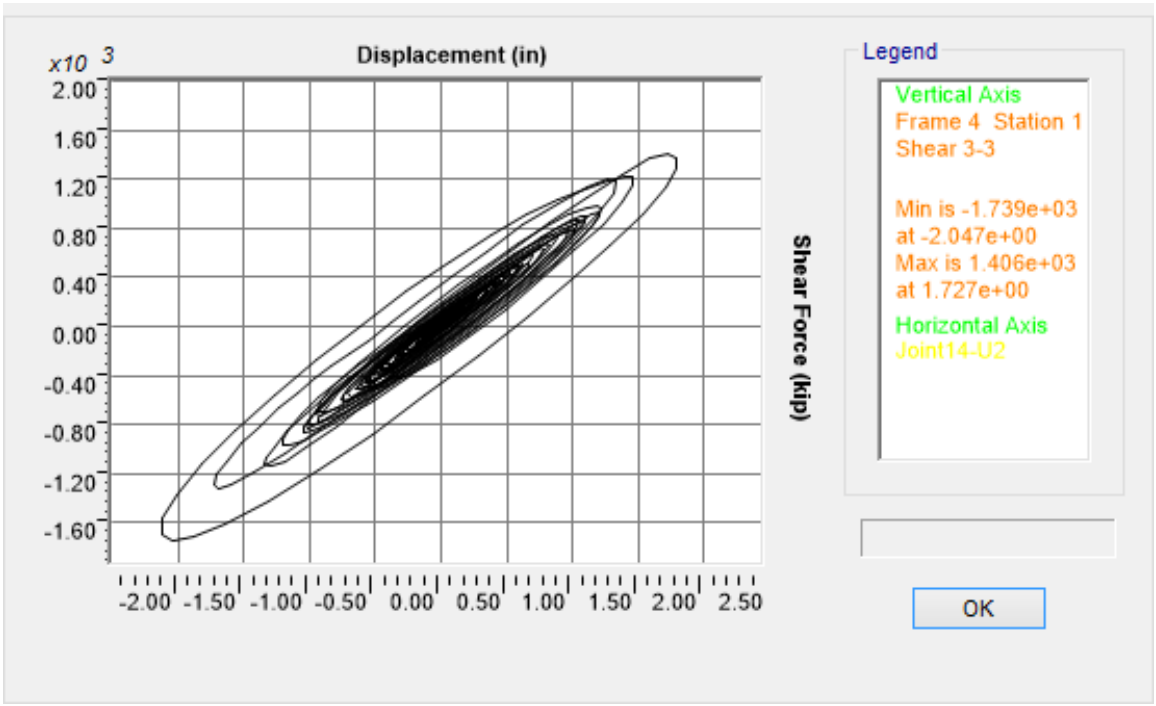

c)

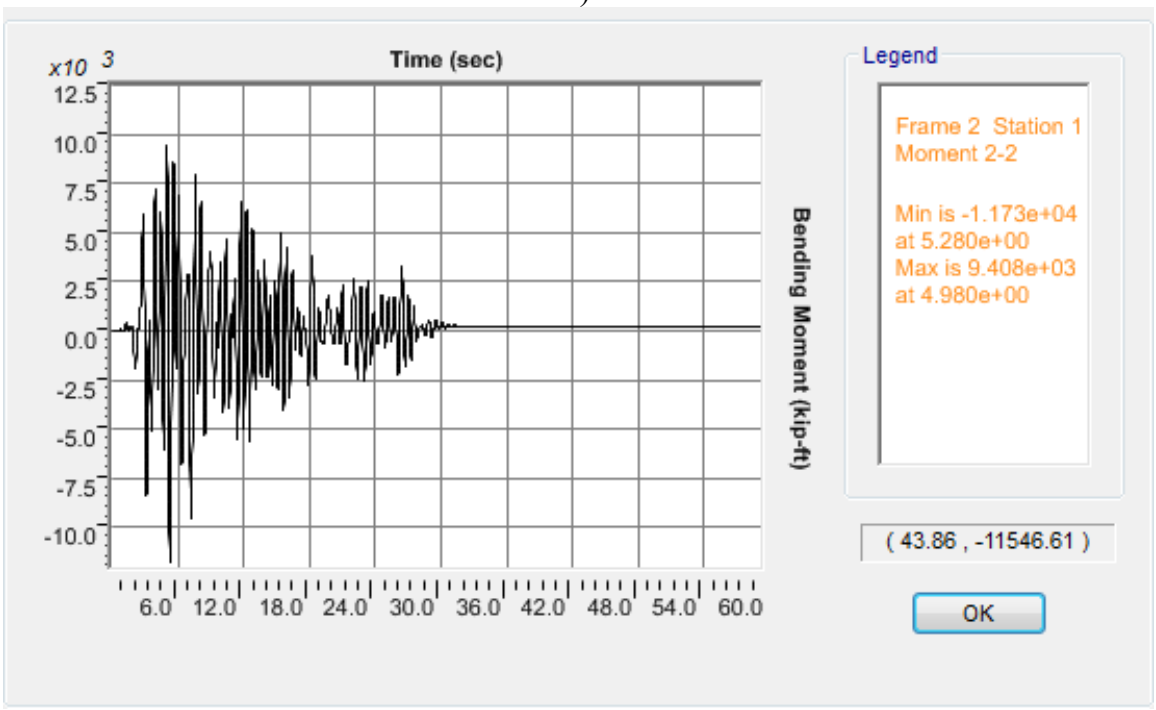

d)

Figure J.47 OSB2 column top response for Motion 47 ROCKN1N1: a) Longitudinal shear force-displacement hysteresis; b) Bending moment time history in the longitudinal direction; c) Transverse shear force-displacement hysteresis; d) Bending moment time history in the transverse direction

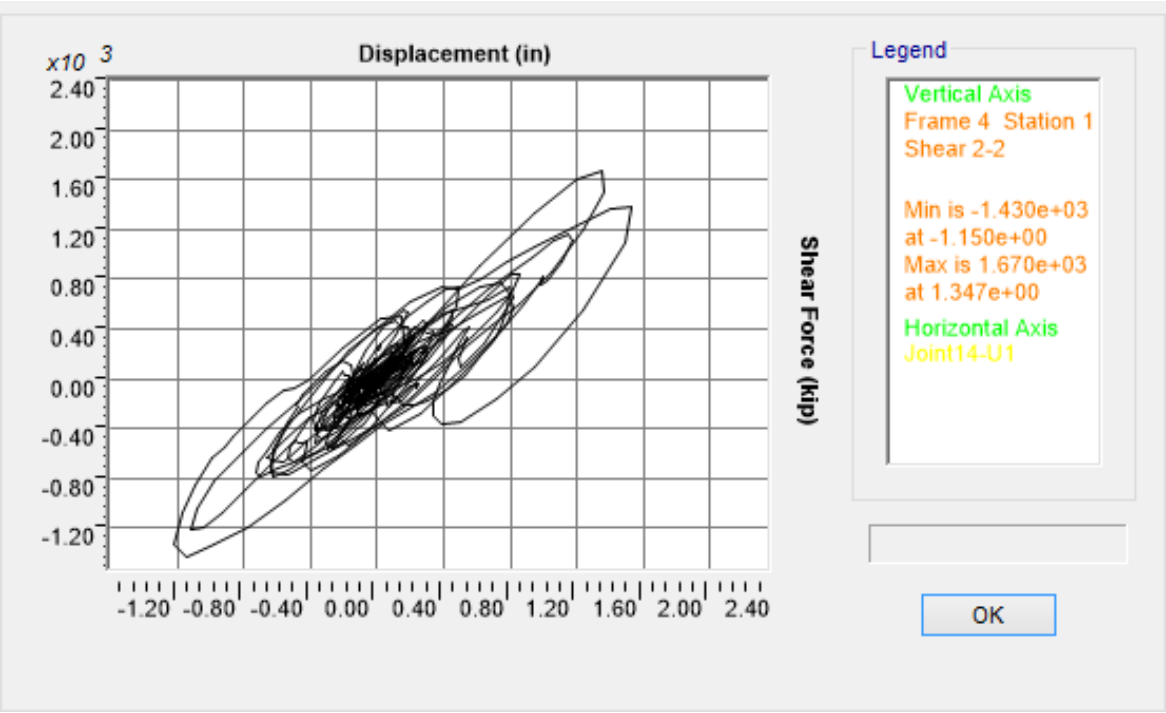
x10 3
Displacement (in)
2.40
2.00
1.60
1.20
0.80
0.40
0.00
-0.40
-0.80
-1.20
-1.20 -0.80 -0.40 0.00 0.40 0.80 1.20 1.60 2.00 2.40
Shear Force (kip)
Legend
Vertical Axis
Frame 4 Station 1
Shear 2-2
Min is -1.430e+03
at -1.150e+00
Max is 1.670e+03
at 1.347e+00
Horizontal Axis
Joint14-U1
OK

a)

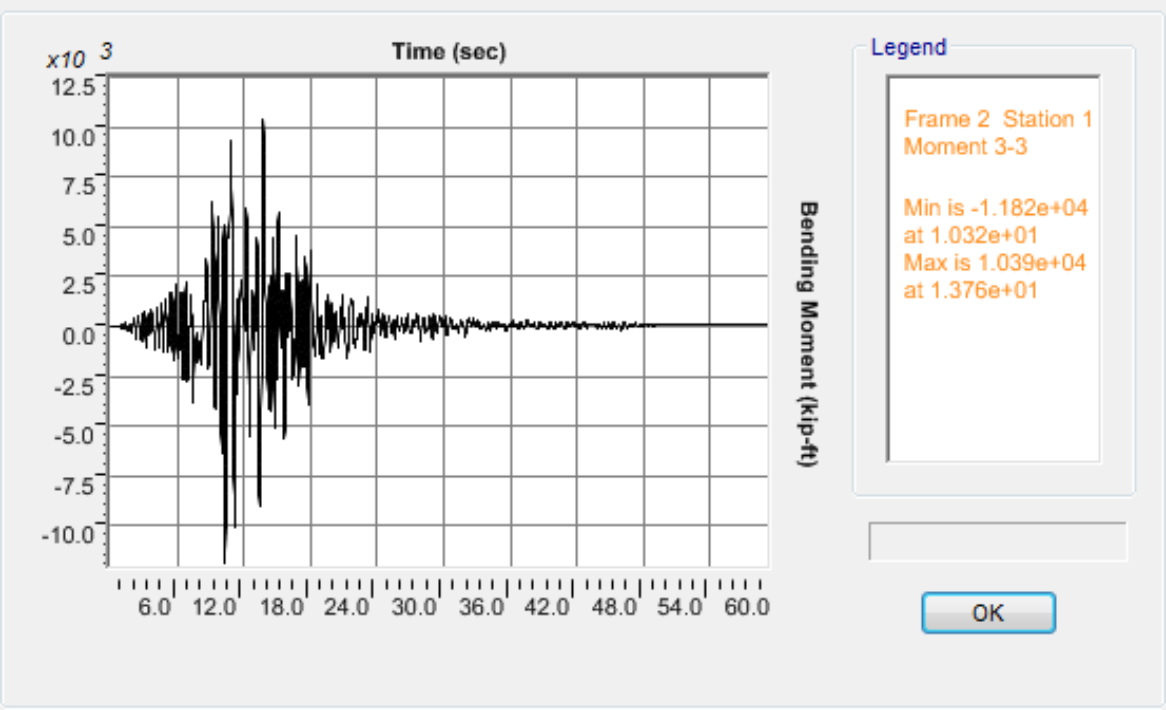
x10 3
Time (sec)
12.5
10.0
7.5
5.0
2.5
0.0
-2.5
-5.0
-7.5
-10.0
6.0 12.0 18.0 24.0 30.0 36.0 42.0 48.0 54.0 60.0
Bending Moment (kip-ft)
Legend
Frame 2 Station 1
Moment 3-3
Min is -1.182e+04
at 1.032e+01
Max is 1.039e+04
at 1.376e+01
OK

b)

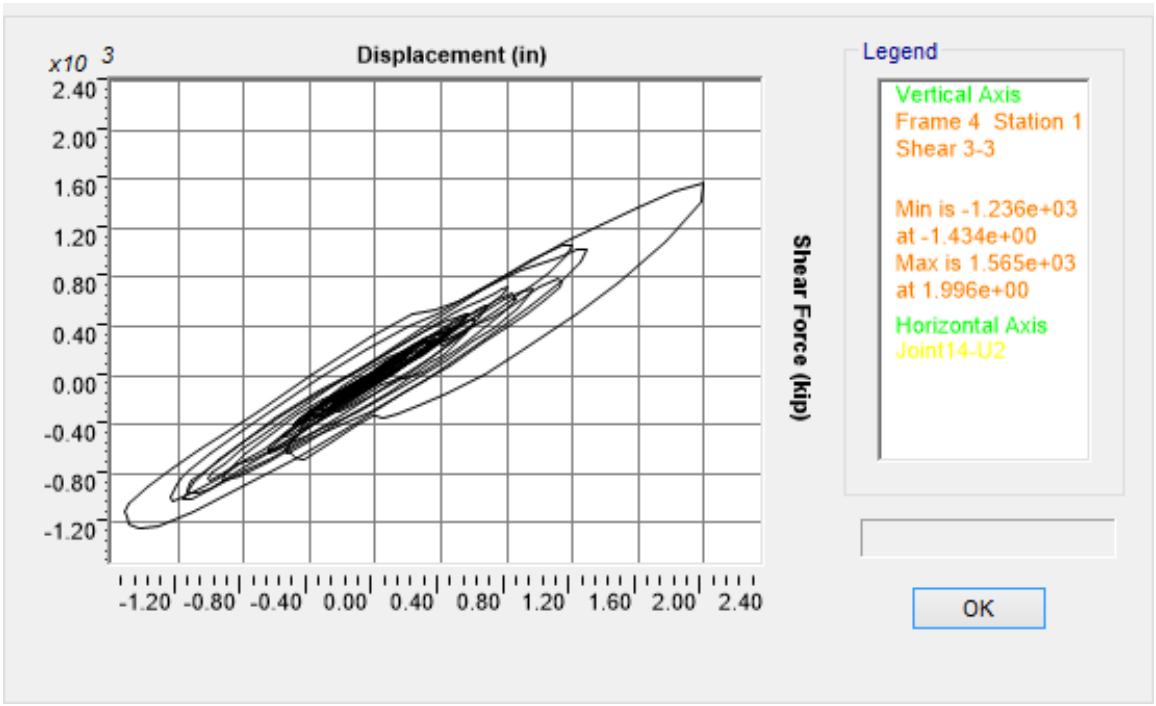

c)

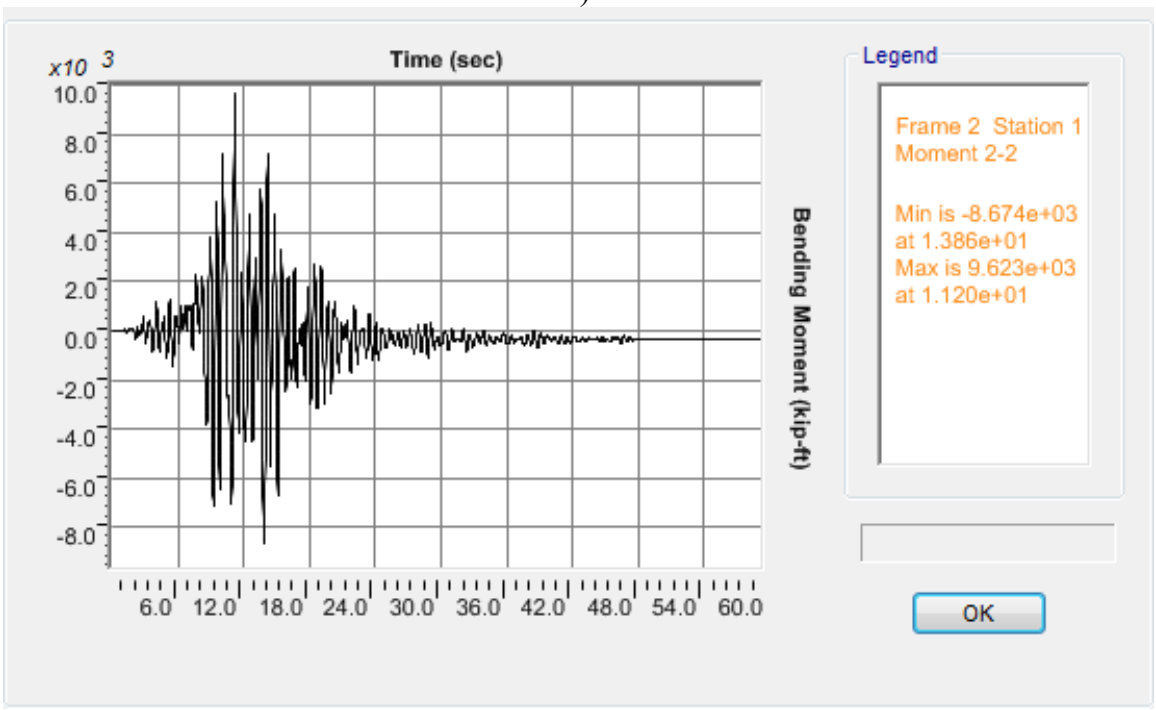

d)

Figure J.48 OSB2 column top response for Motion 48 ROCKN1P1: a) Longitudinal shear force-displacement hysteresis; b) Bending moment time history in the longitudinal direction; c) Transverse shear force-displacement hysteresis; d) Bending moment time history in the transverse direction

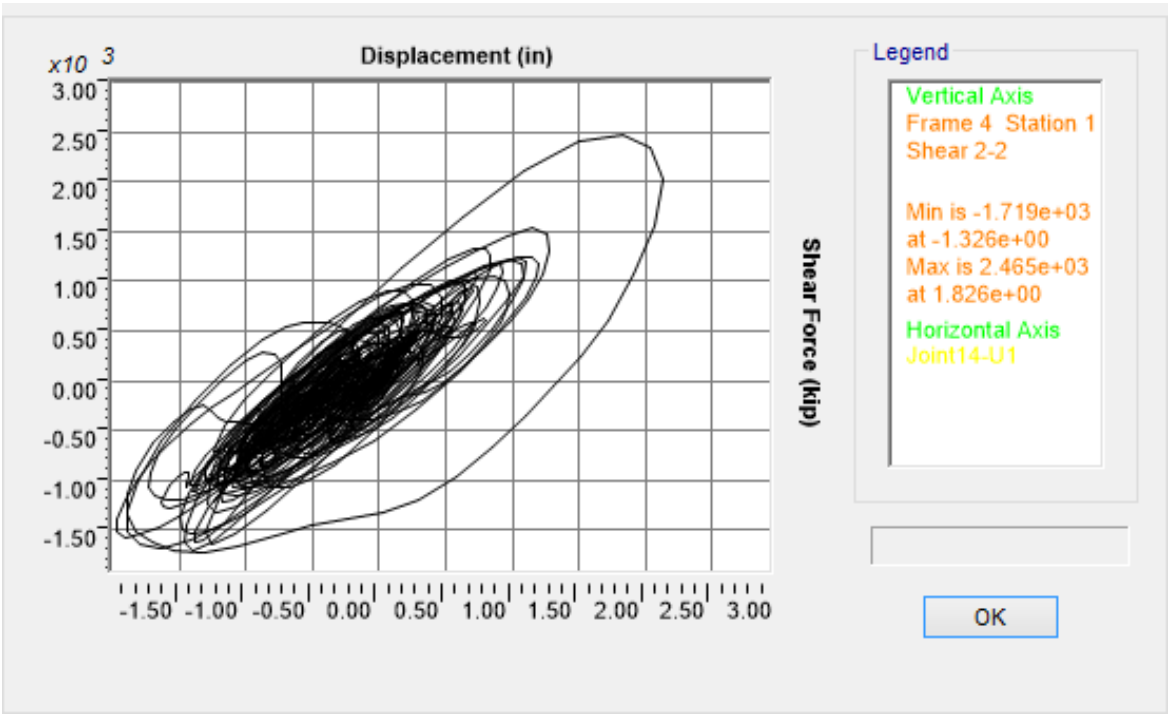
x10 3
Displacement (in)
3.00
2.50
2.00
1.50
1.00
0.50
0.00
-0.50
-1.00
-1.50
-1.50 -1.00 -0.50 0.00 0.50 1.00 1.50 2.00 2.50 3.00
Shear Force (kip)
Legend
Vertical Axis
Frame 4 Station 1
Shear 2-2
Min is -1.719e+03
at -1.326e+00
Max is 2.465e+03
at 1.826e+00
Horizontal Axis
Joint14-U1
OK

a)

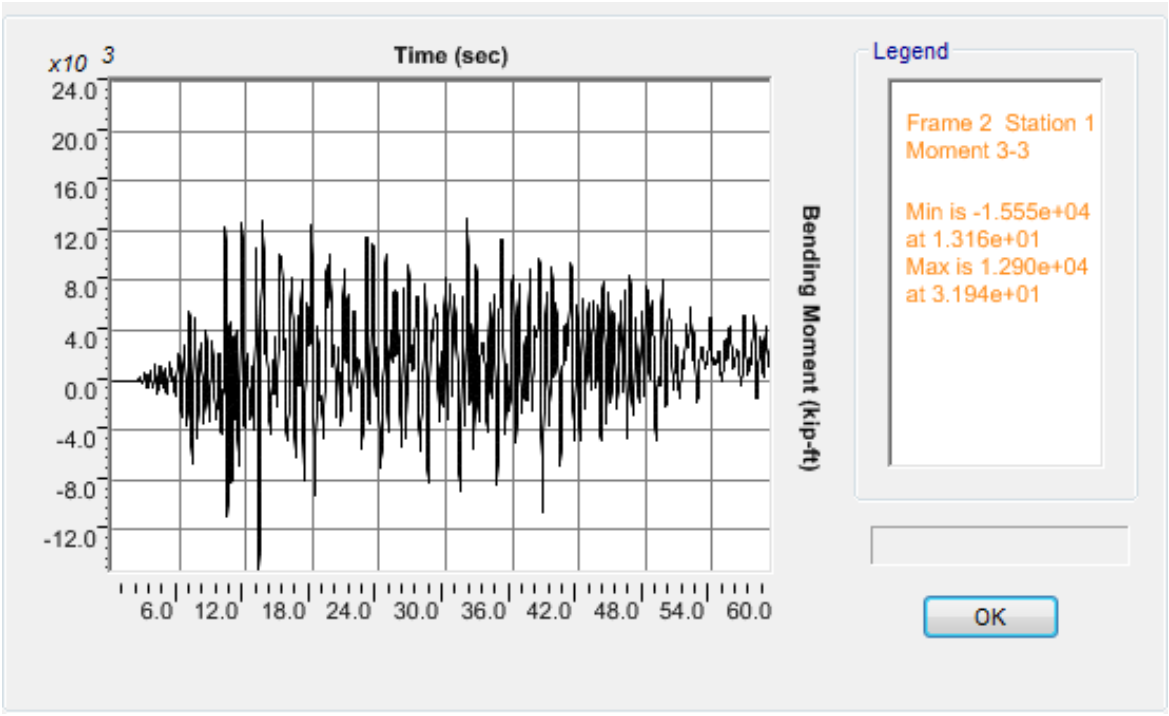
x10 3
Time (sec)
24.0
20.0
16.0
12.0
8.0
4.0
0.0
-4.0
-8.0
-12.0
6.0 12.0 18.0 24.0 30.0 36.0 42.0 48.0 54.0 60.0
Bending Moment (kip-ft)
Legend
Frame 2 Station 1
Moment 3-3
Min is -1.555e+04
at 1.316e+01
Max is 1.290e+04
at 3.194e+01
OK

b)

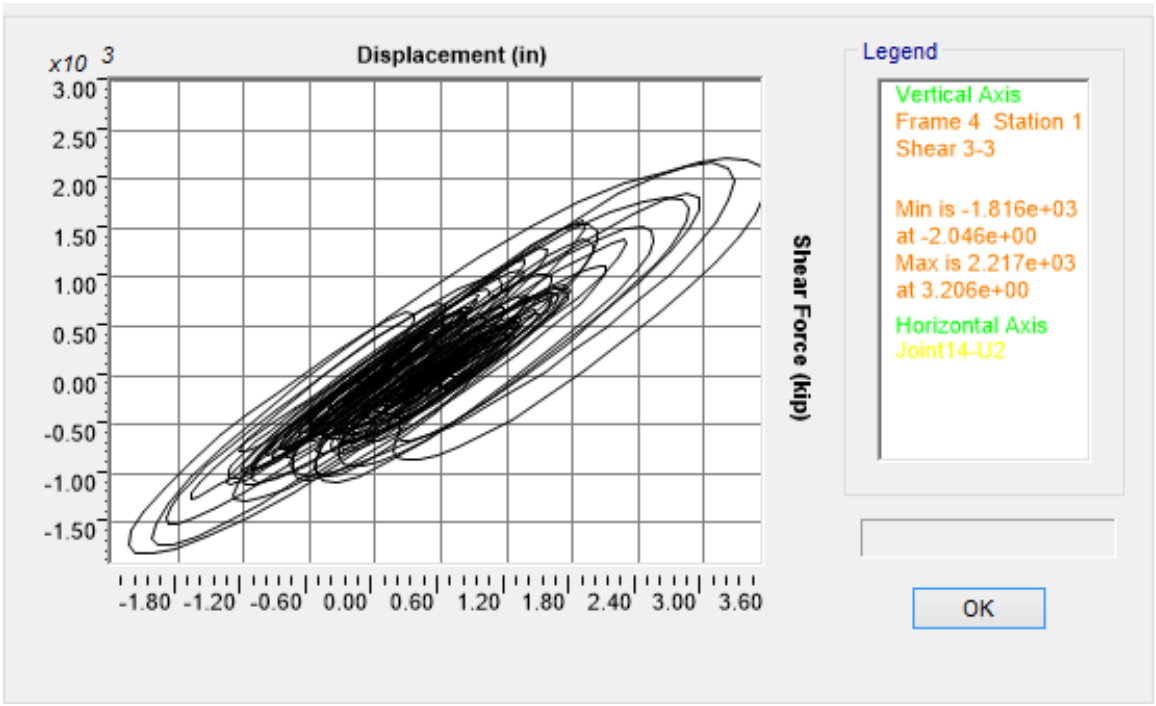

c)

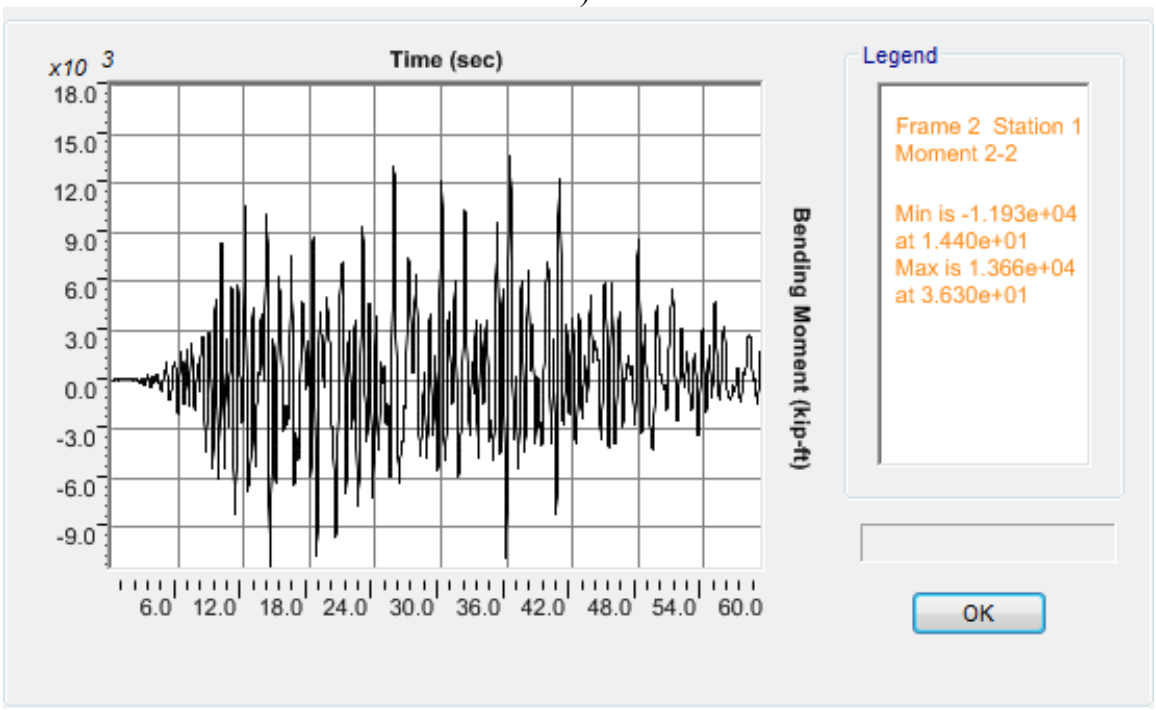

d)

Figure J.49 OSB2 column top response for Motion 49 SANDN1N1: a) Longitudinal shear force-displacement hysteresis; b) Bending moment time history in the longitudinal direction; c) Transverse shear force-displacement hysteresis; d) Bending moment time history in the transverse direction

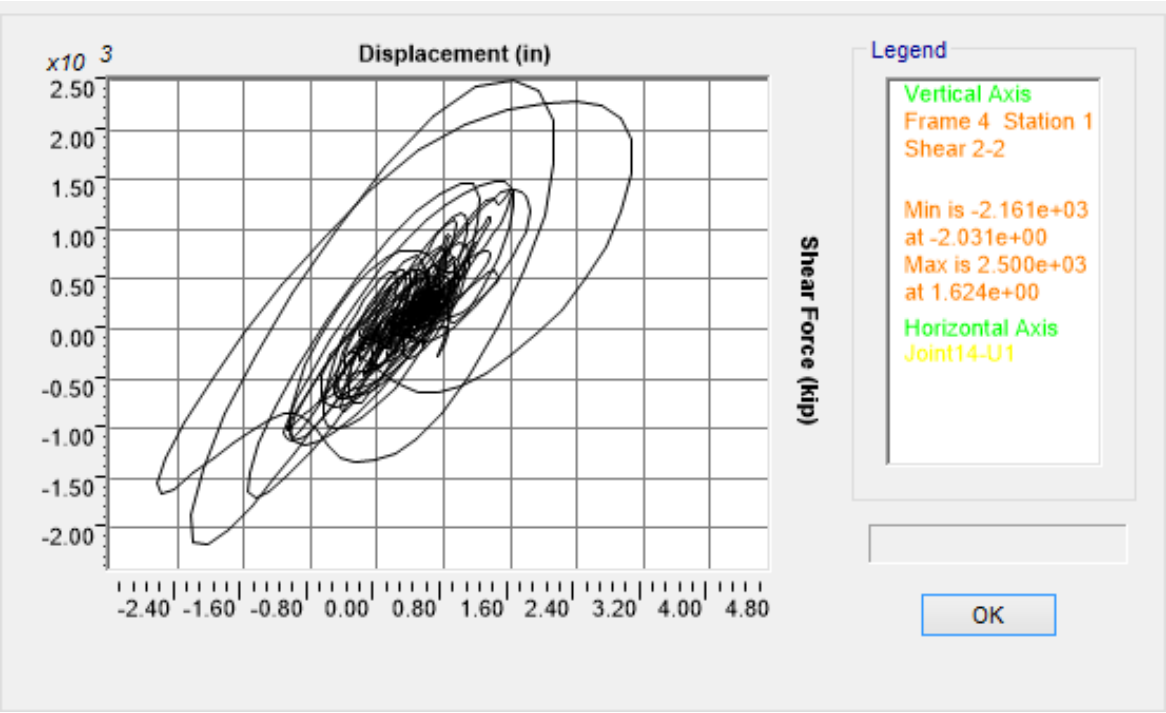
x10 3
Displacement (in)
2.50
2.00
1.50
1.00
0.50
0.00
-0.50
-1.00
-1.50
-2.00
-2.40 -1.60 -0.80 0.00 0.80 1.60 2.40 3.20 4.00 4.80
Shear Force (kip)
Legend
Vertical Axis
Frame 4 Station 1
Shear 2-2
Min is -2.161e+03
at -2.031e+00
Max is 2.500e+03
at 1.624e+00
Horizontal Axis
Joint14-U1
OK

a)

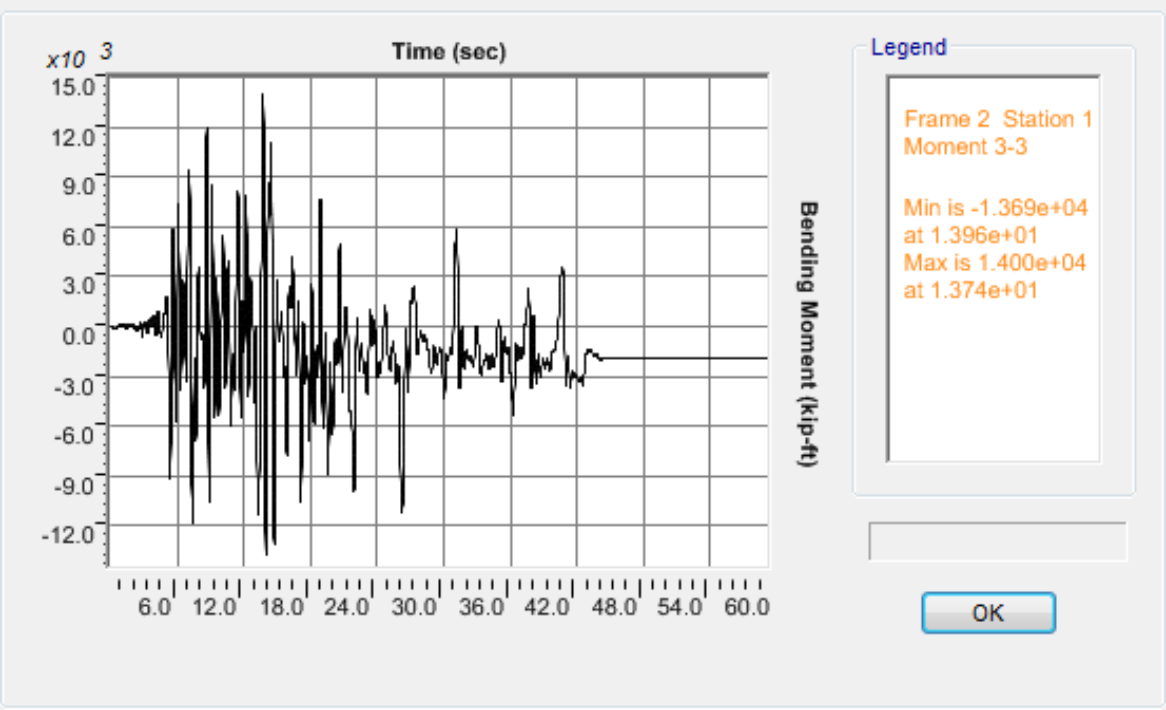
x10 3
Time (sec)
15.0
12.0
9.0
6.0
3.0
0.0
-3.0
-6.0
-9.0
-12.0
6.0 12.0 18.0 24.0 30.0 36.0 42.0 48.0 54.0 60.0
Bending Moment (kip-ft)
Legend
Frame 2 Station 1
Moment 3-3
Min is -1.369e+04
at 1.396e+01
Max is 1.400e+04
at 1.374e+01
OK

b)

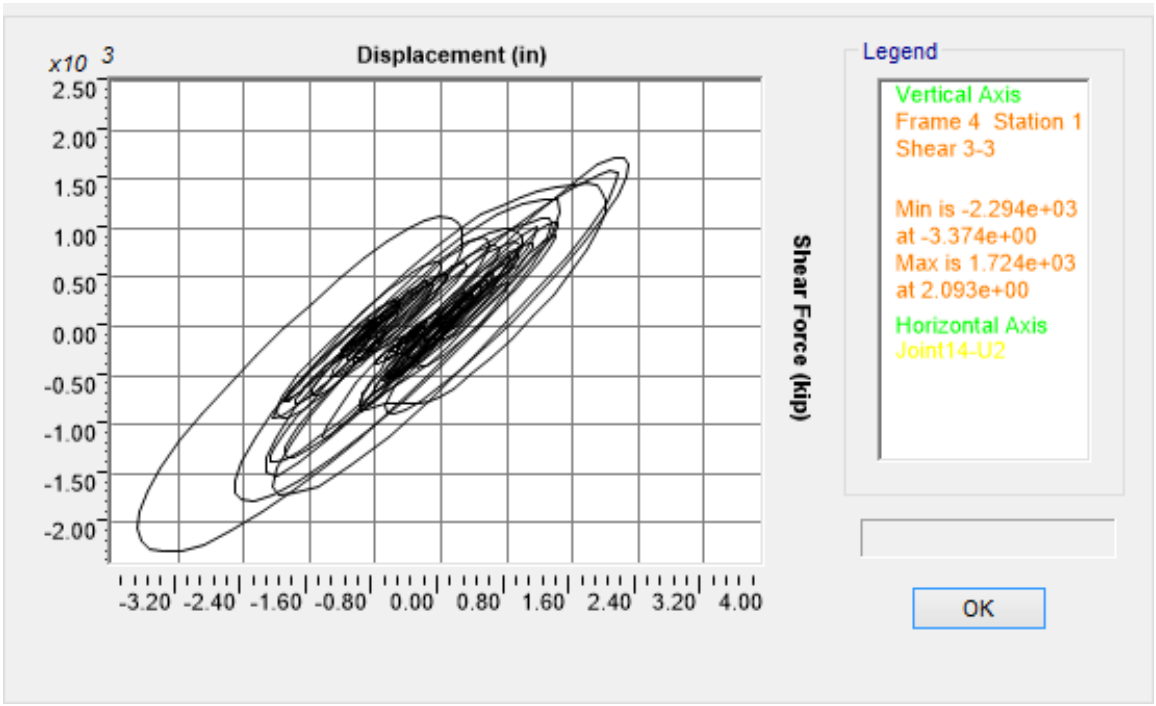

c)

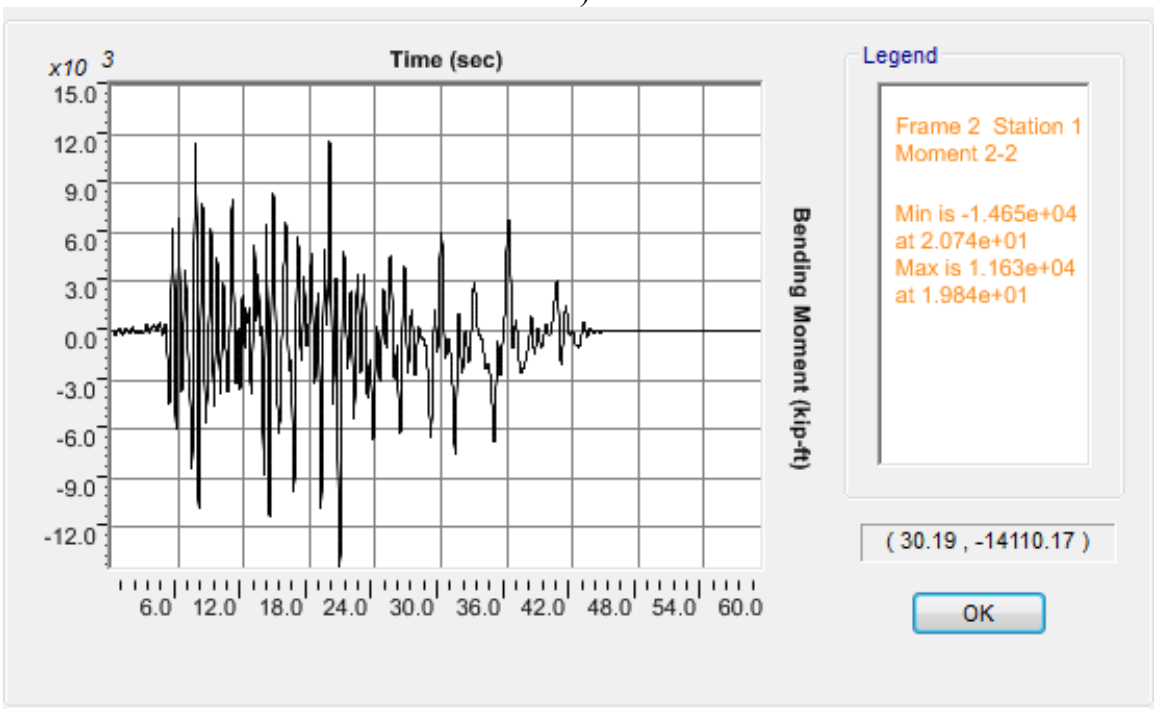

d)

Figure J.50 OSB2 column top response for Motion 50 CLAYN1N1: a) Longitudinal shear force-displacement hysteresis; b) Bending moment time history in the longitudinal direction; c) Transverse shear force-displacement hysteresis; d) Bending moment time history in the transverse direction

APPENDIX K: CSIBRIDGE RESULTS FOR OSB1

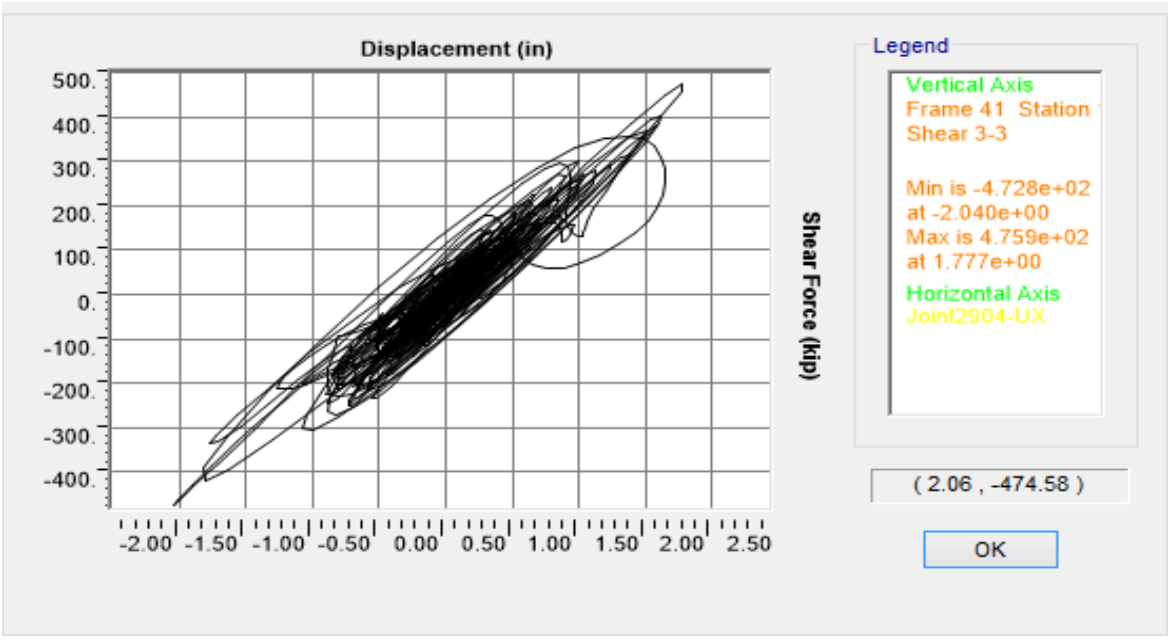

a)

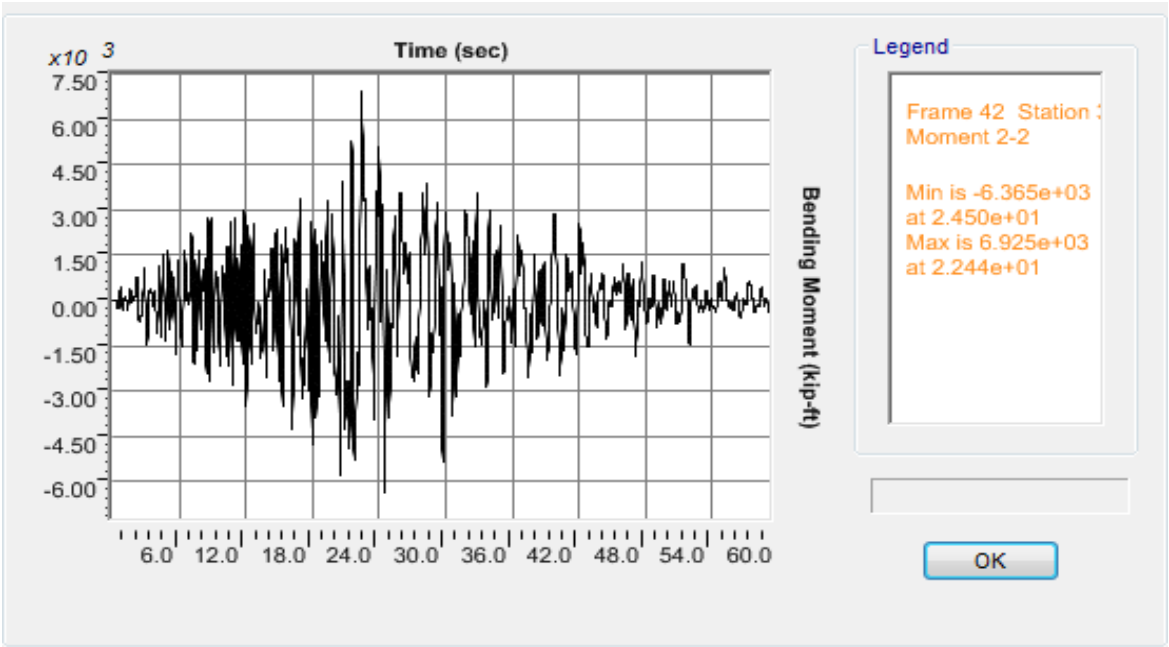

b)

Figure K.1 OSB1 column top response for Motion 1 ROCKS1N1: a) Longitudinal shear force-displacement hysteresis; b) Bending moment time history in the longitudinal direction

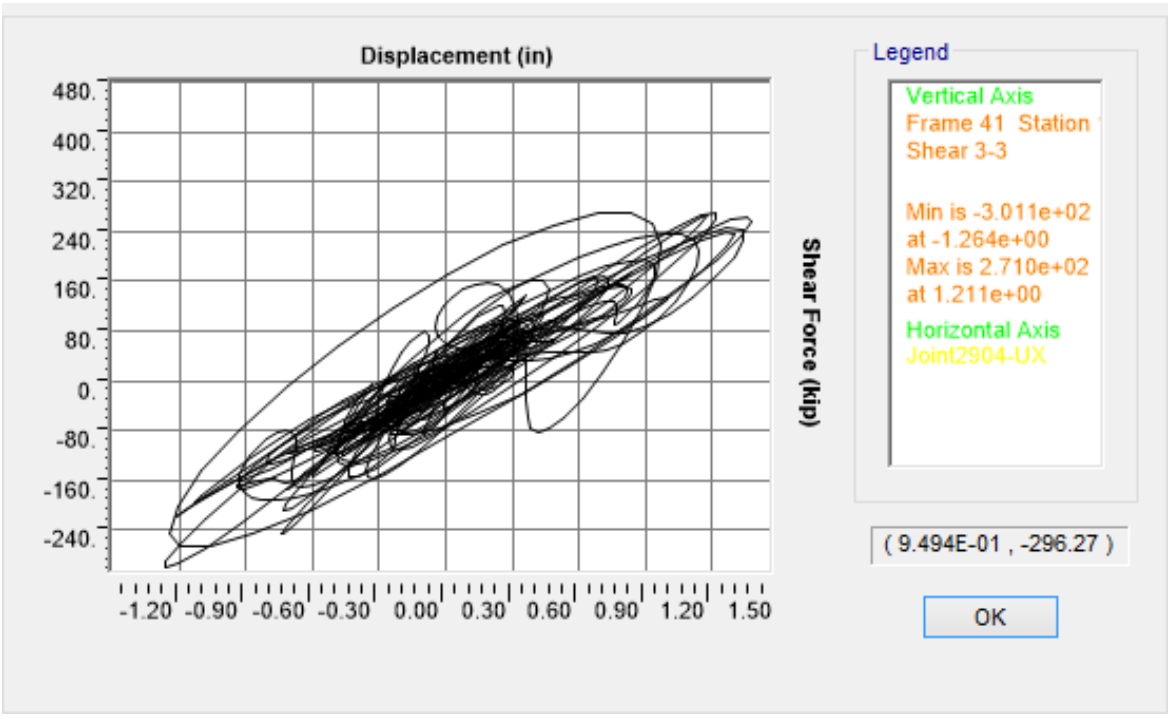

a)

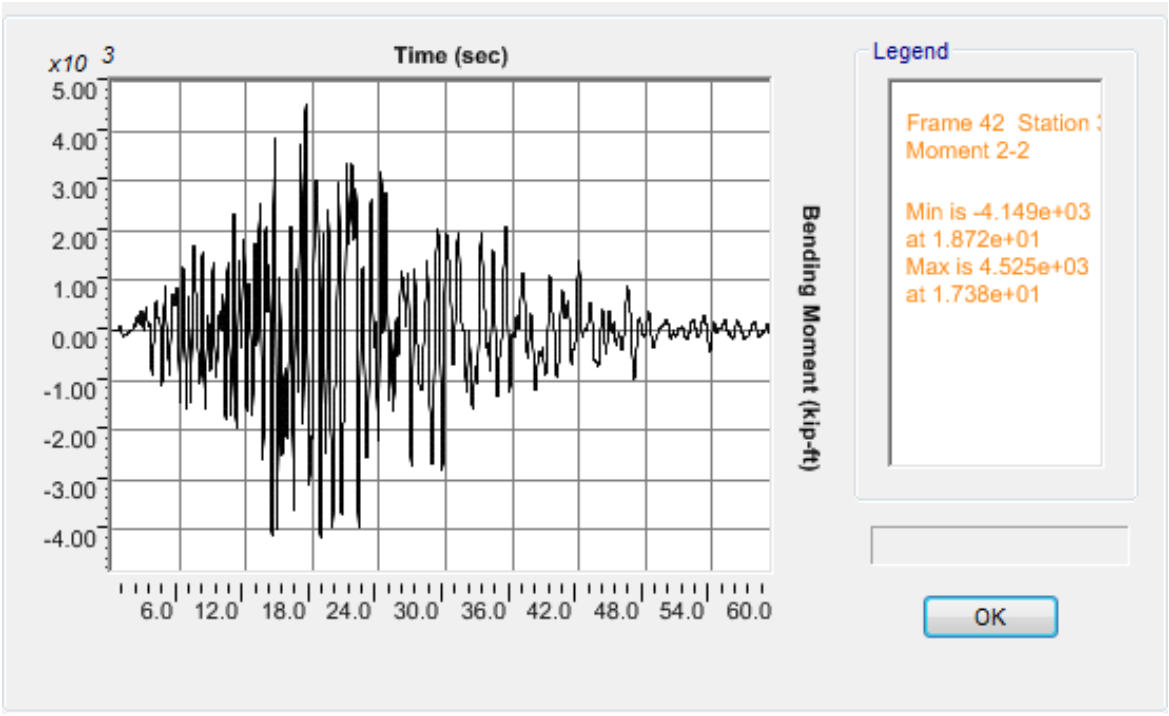

b)

Figure K.2 OSB1 column top response for Motion 2 ROCKS1N2: a) Longitudinal shear force-displacement hysteresis; b) Bending moment time history in the longitudinal direction

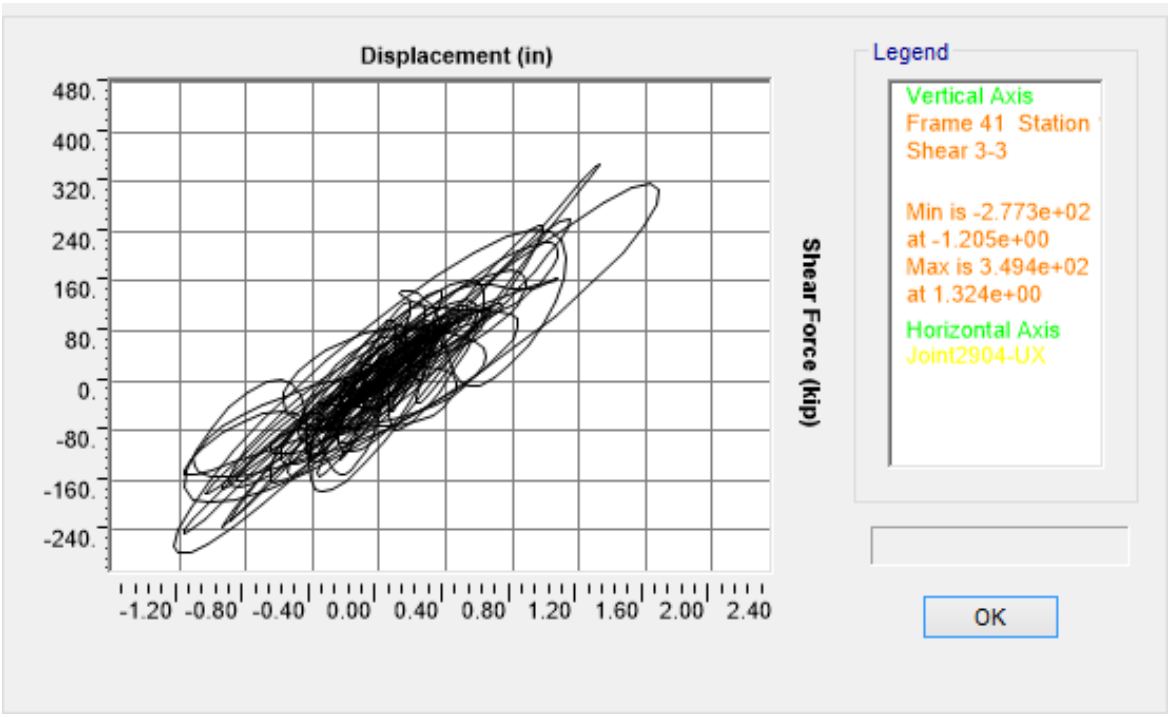

a)

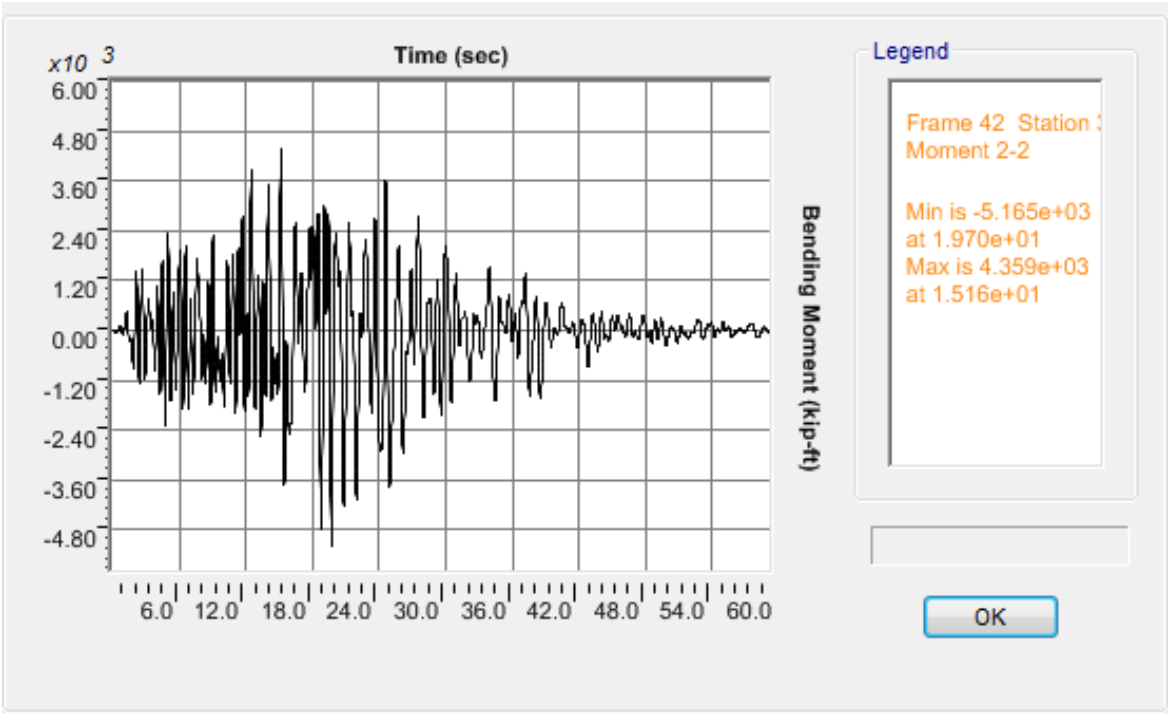

b)

Figure K.3 OSB1 column top response for Motion 3 ROCKS1N3: a) Longitudinal shear force-displacement hysteresis; b) Bending moment time history in the longitudinal direction

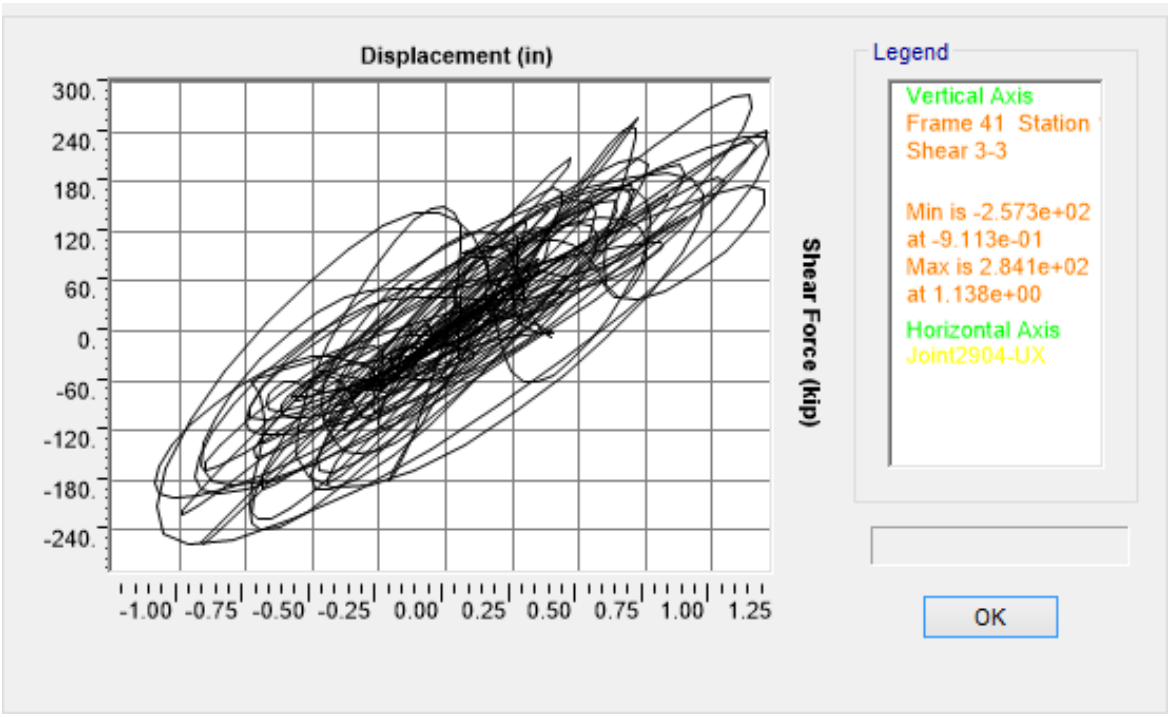

a)

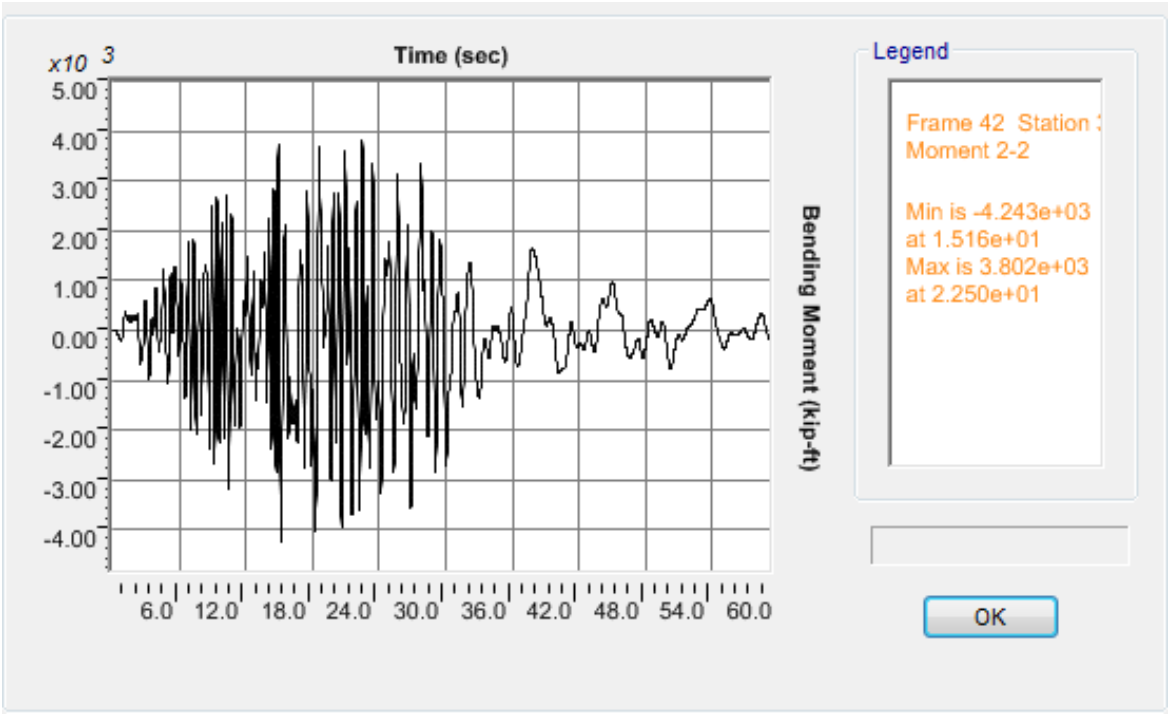

b)

Figure K.4 OSB1 column top response for Motion 4 ROCKS1N4: a) Longitudinal shear force-displacement hysteresis; b) Bending moment time history in the longitudinal direction

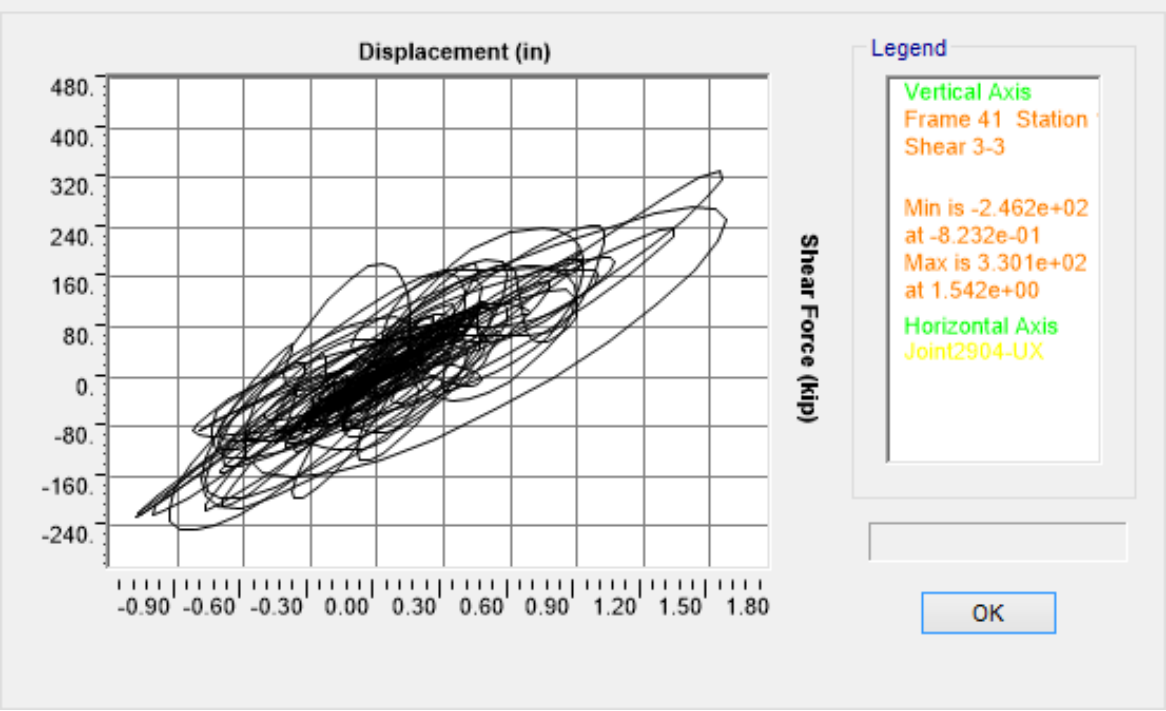

a)

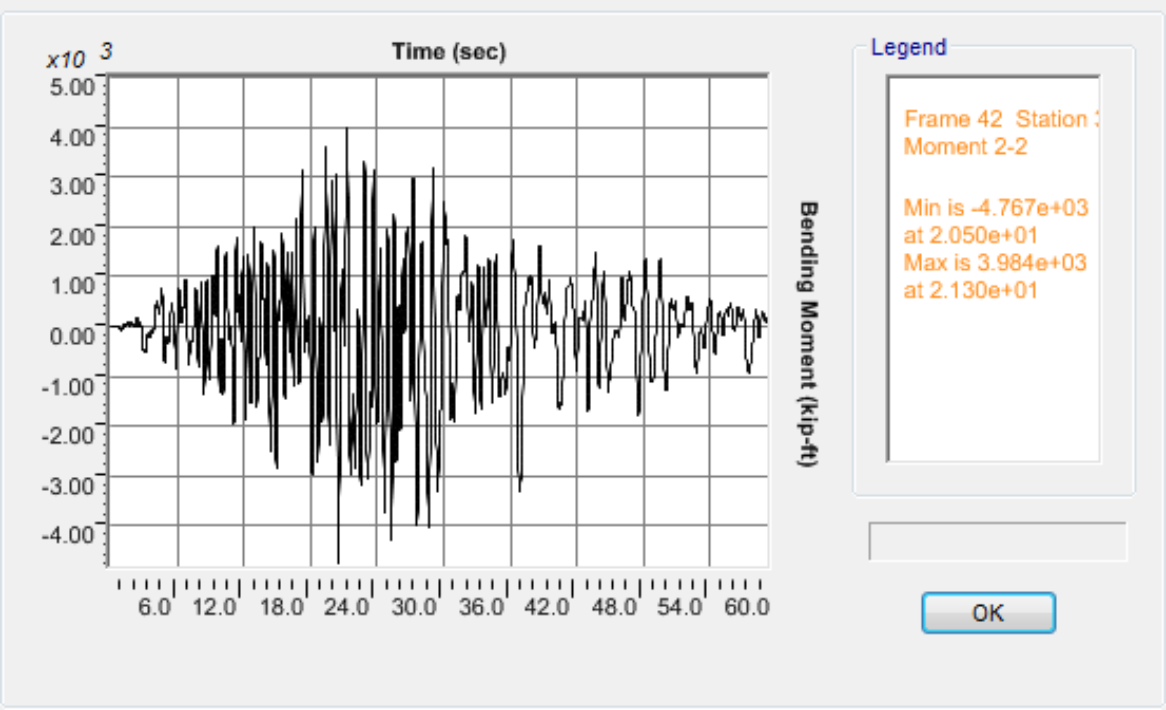

b)

Figure K.5 OSB1 column top response for Motion 5 ROCKS1N5: a) Longitudinal shear force-displacement hysteresis; b) Bending moment time history in the longitudinal direction

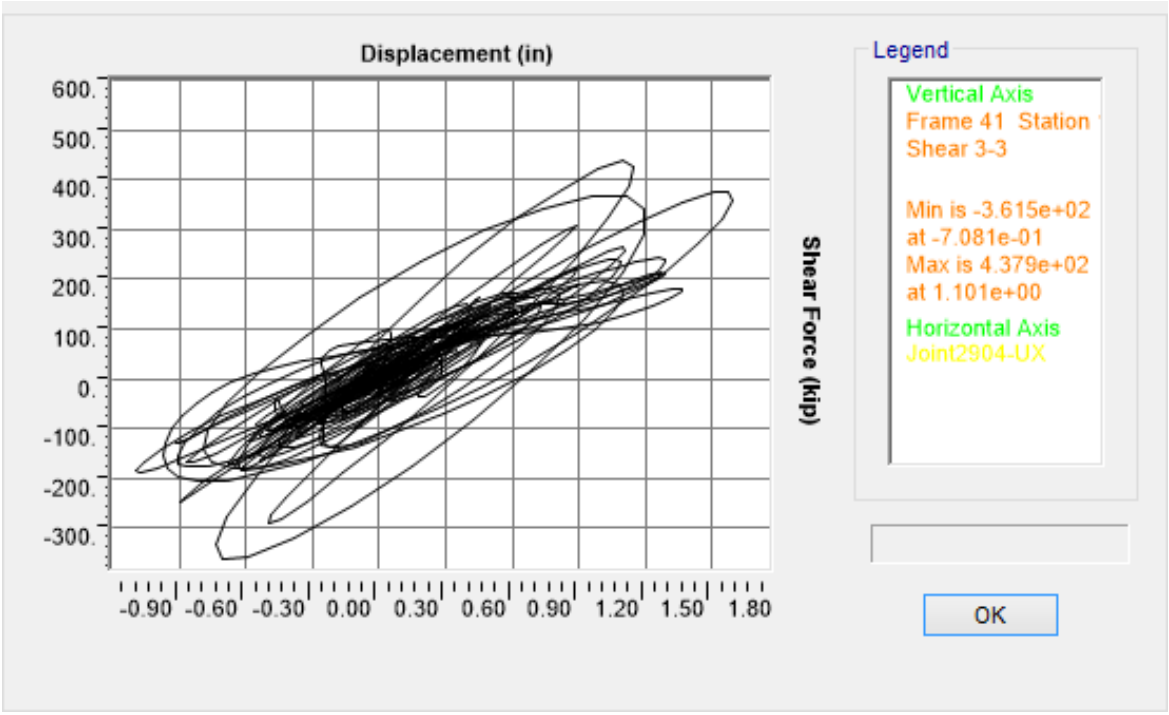

a)

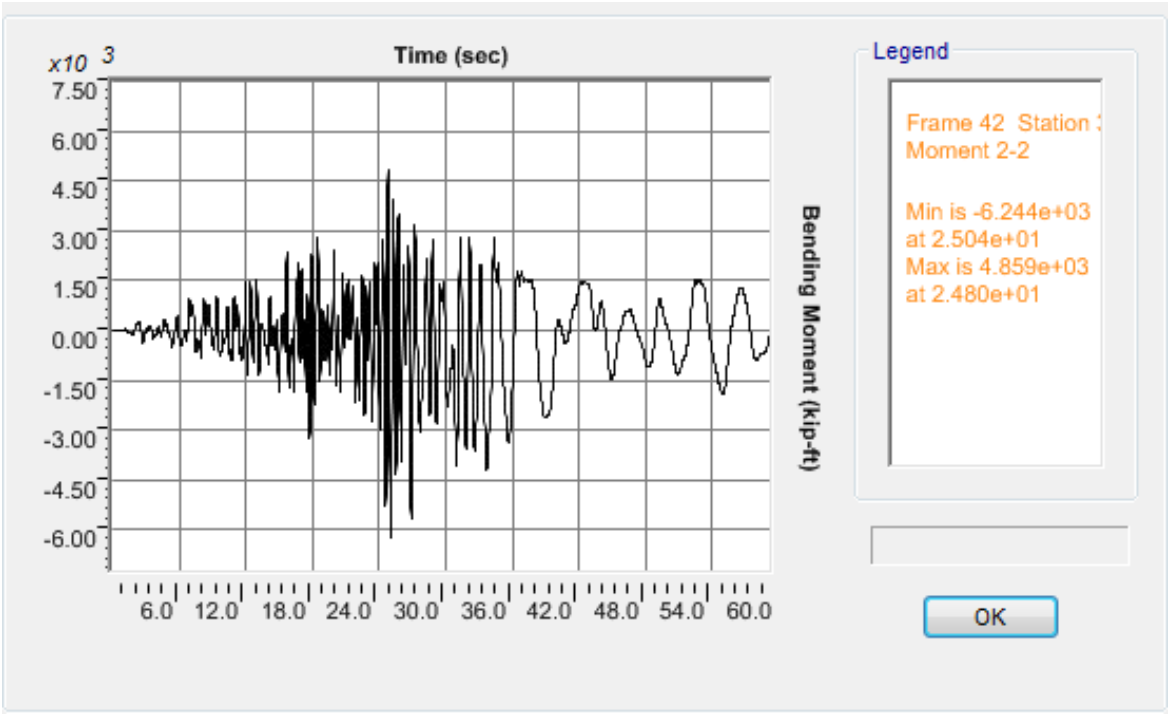

b)

Figure K.6 OSB1 column top response for Motion 6 ROCKS1N6: a) Longitudinal shear force-displacement hysteresis; b) Bending moment time history in the longitudinal direction

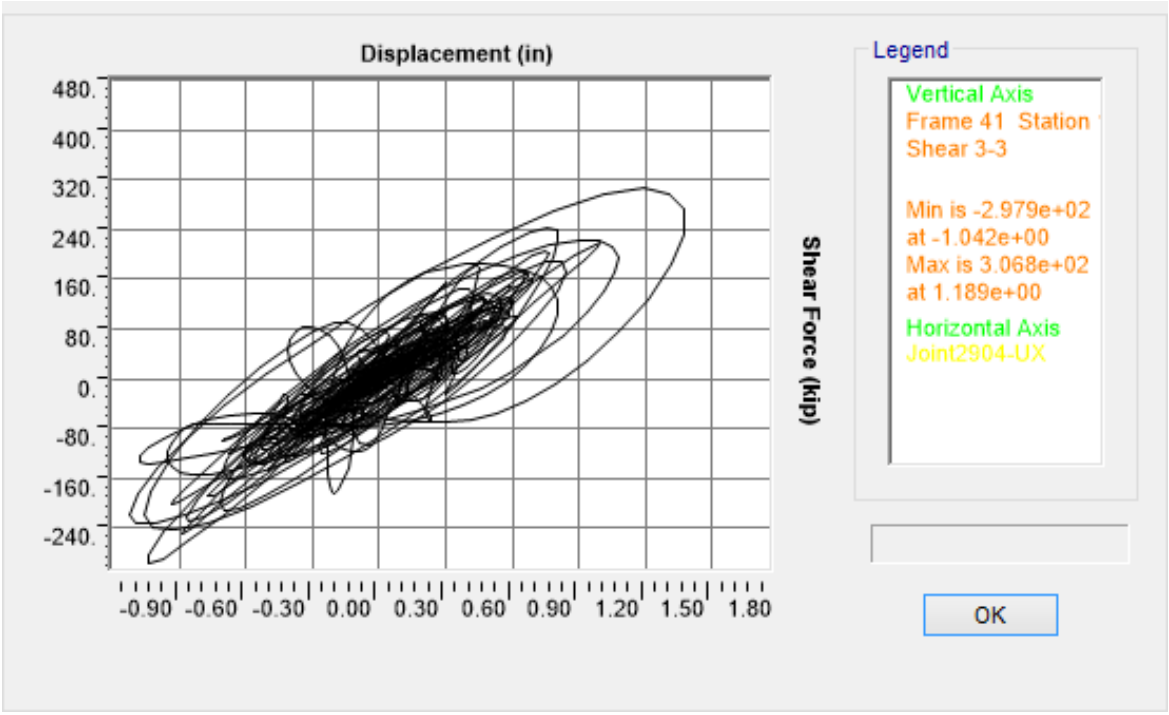

a)

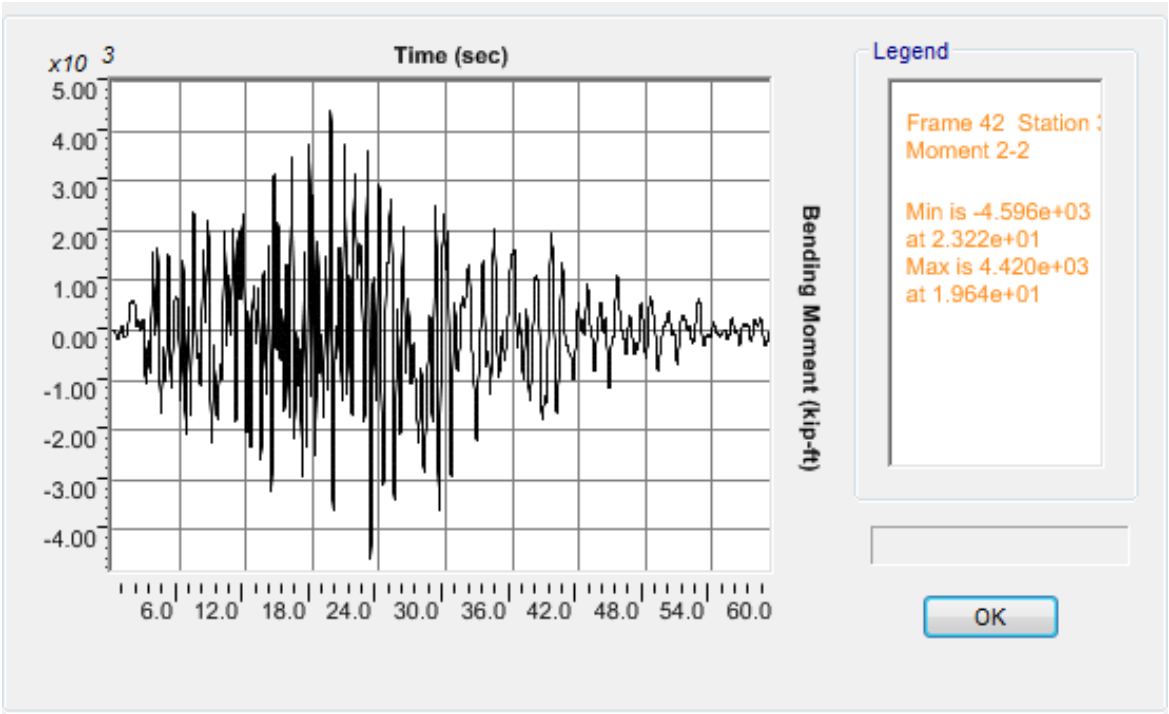

b)

Figure K.7 OSB1 column top response for Motion 7 ROCKS1N7: a) Longitudinal shear force-displacement hysteresis; b) Bending moment time history in the longitudinal direction

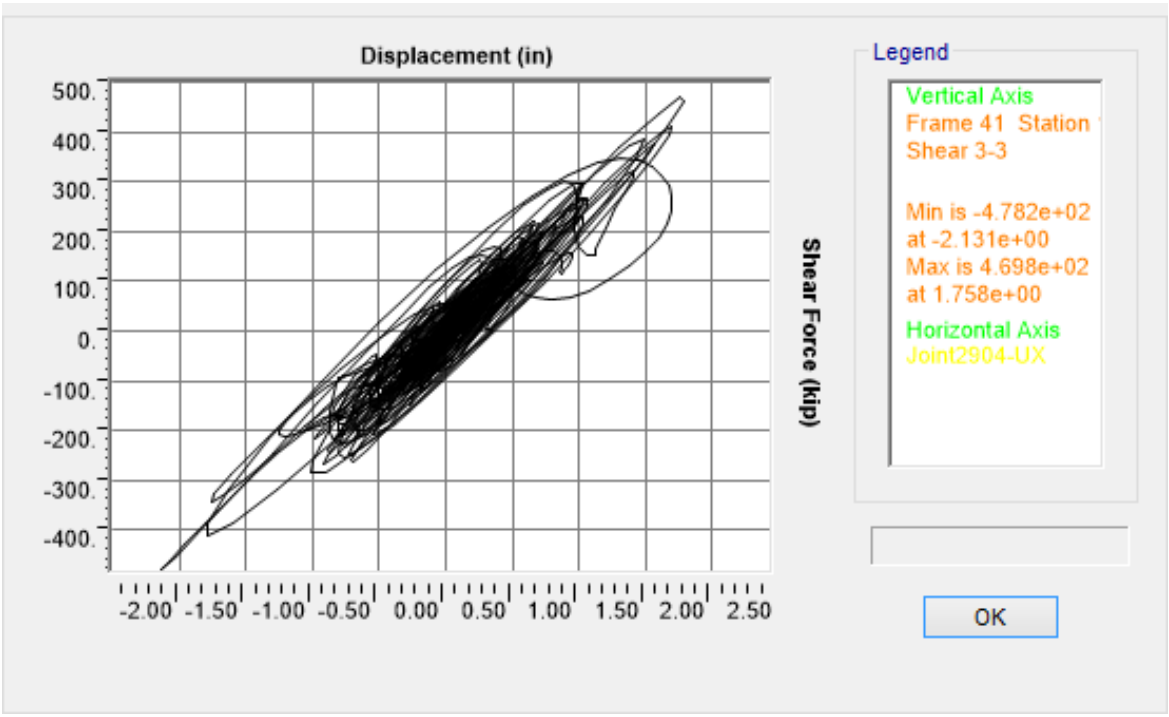

a)

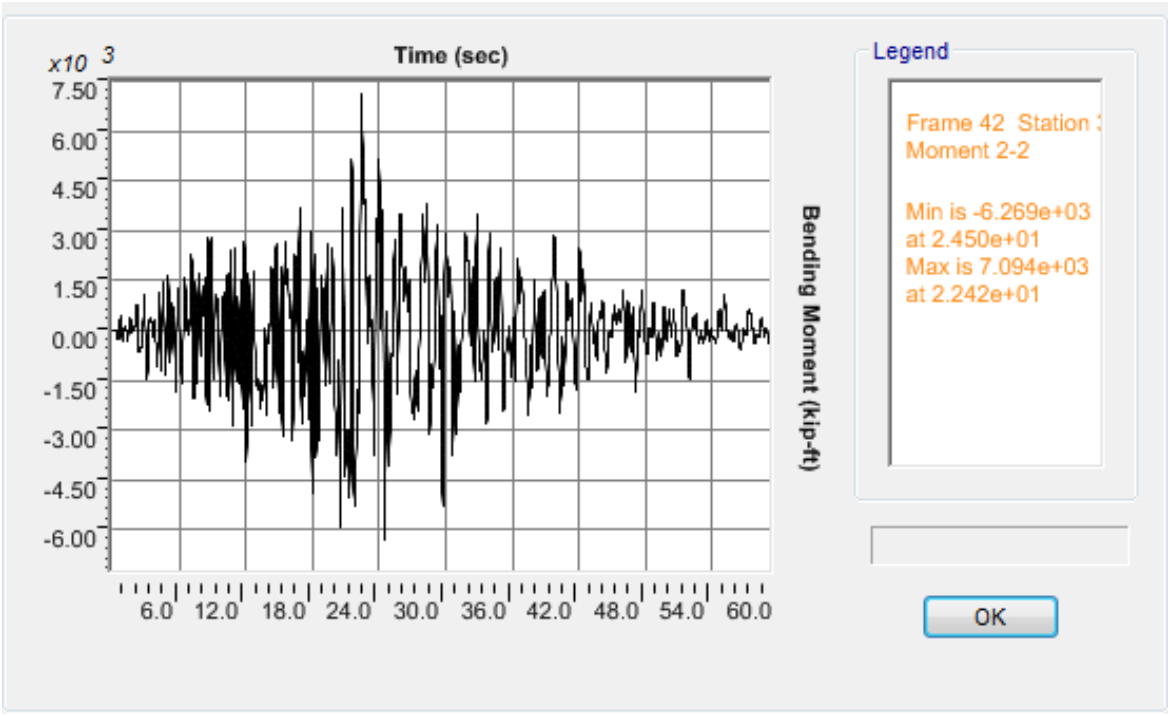

b)

Figure K.8 OSB1 column top response for Motion 8 ROCKS1P1: a) Longitudinal shear force-displacement hysteresis; b) Bending moment time history in the longitudinal direction

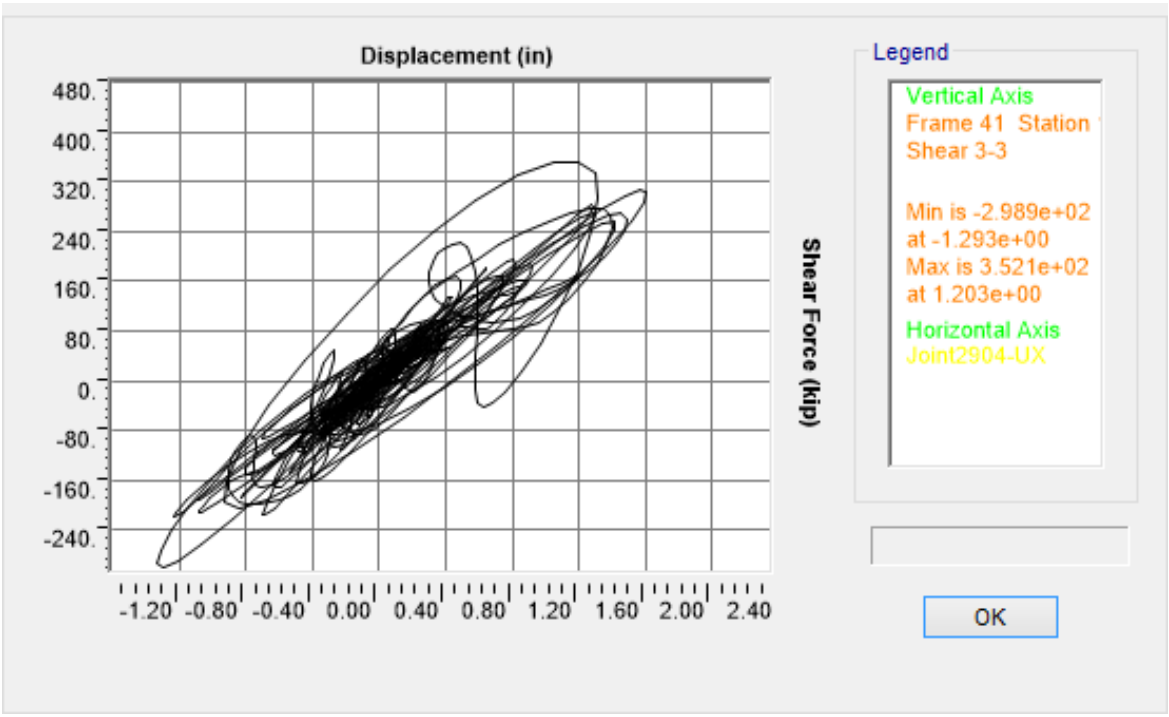

a)

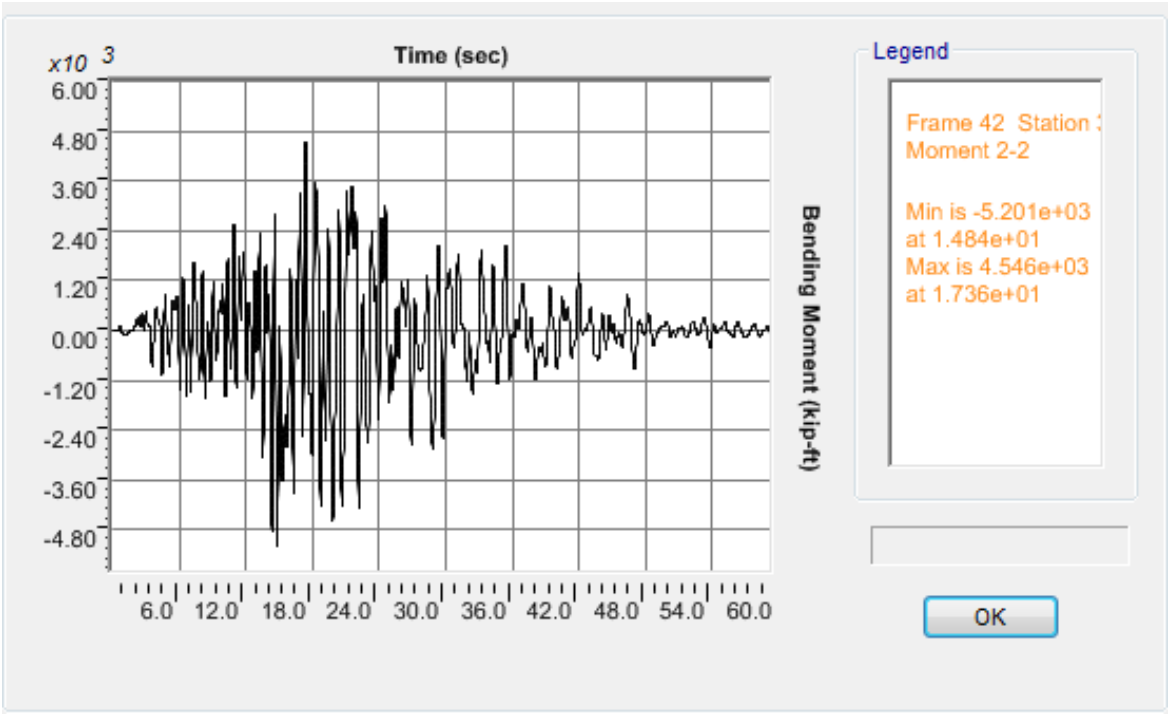

b)

Figure K.9 OSB1 column top response for Motion 9 ROCKS1P2: a) Longitudinal shear force-displacement hysteresis; b) Bending moment time history in the longitudinal direction

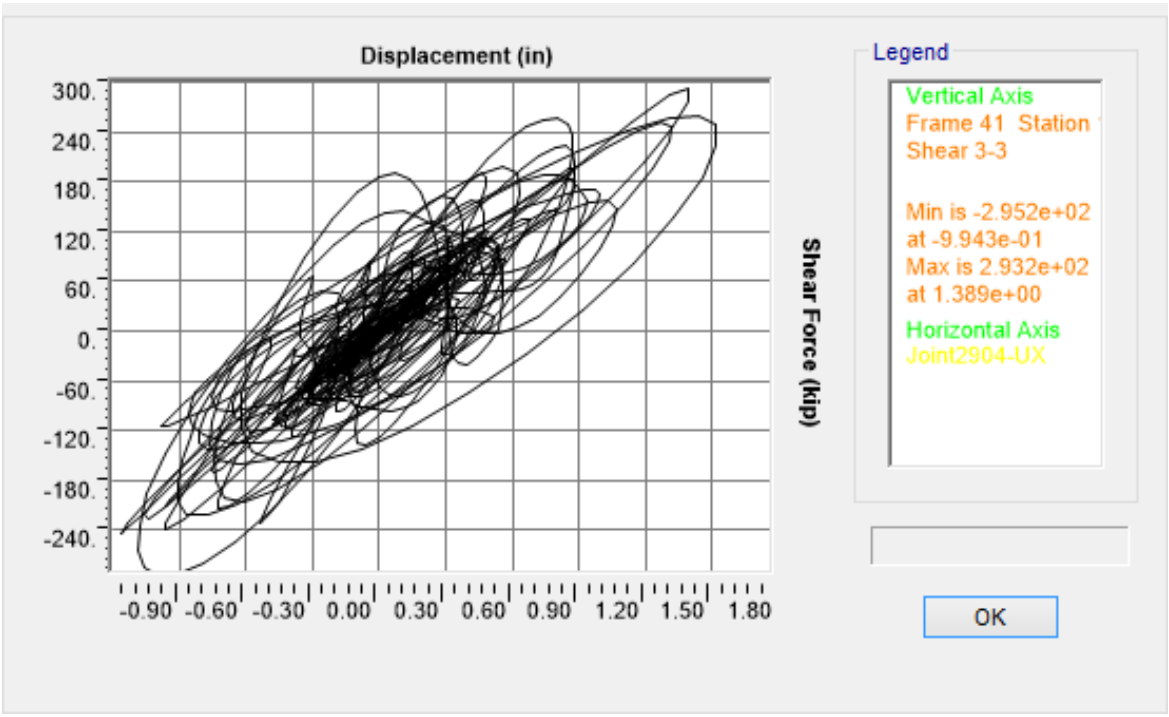

a)

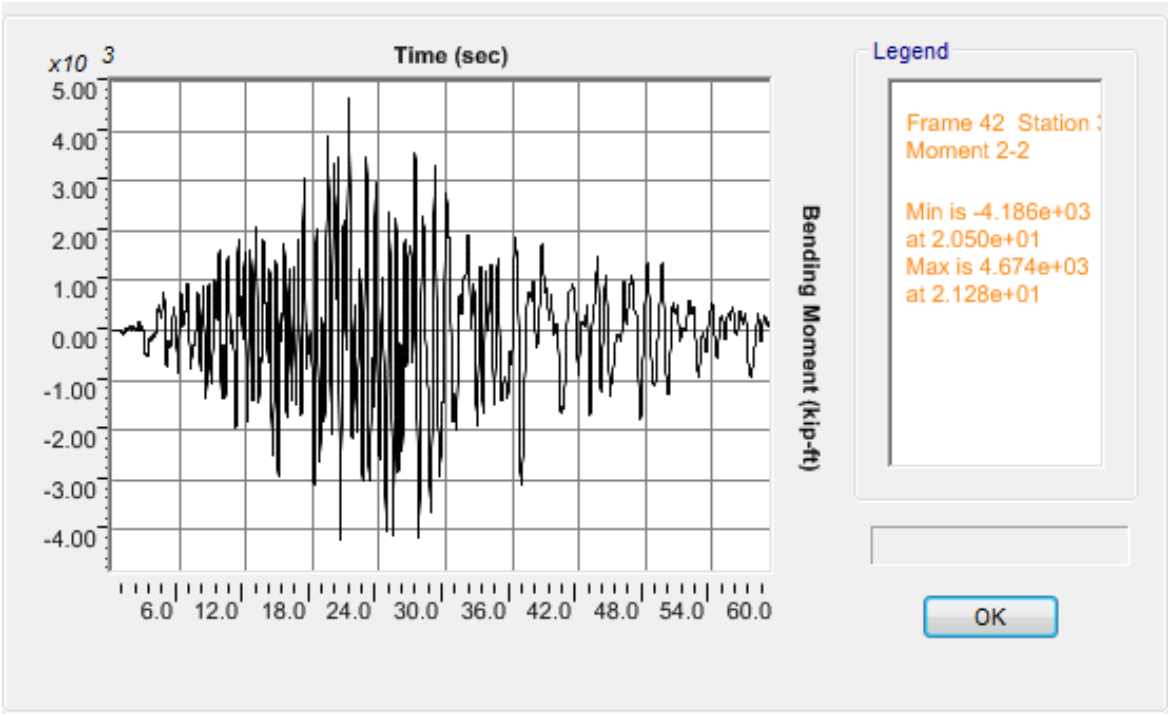

b)

Figure K.10 OSB1 column top response for Motion 10 ROCKS1P3: a) Longitudinal shear force-displacement hysteresis; b) Bending moment time history in the longitudinal direction

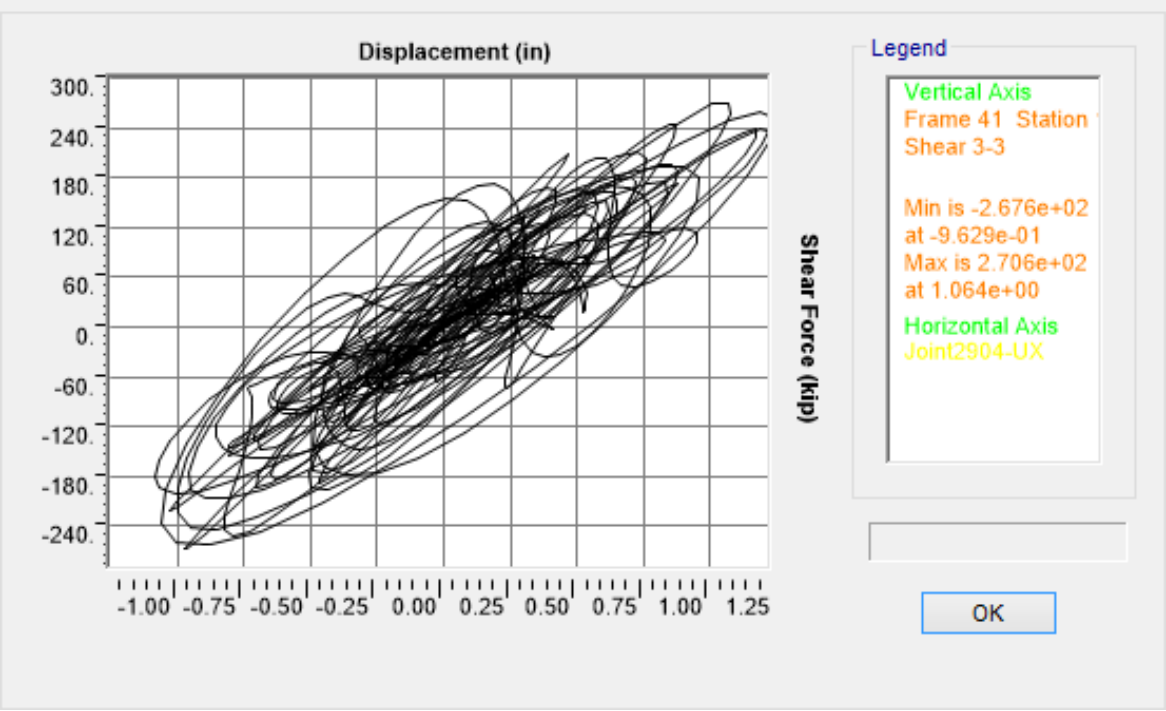

a)

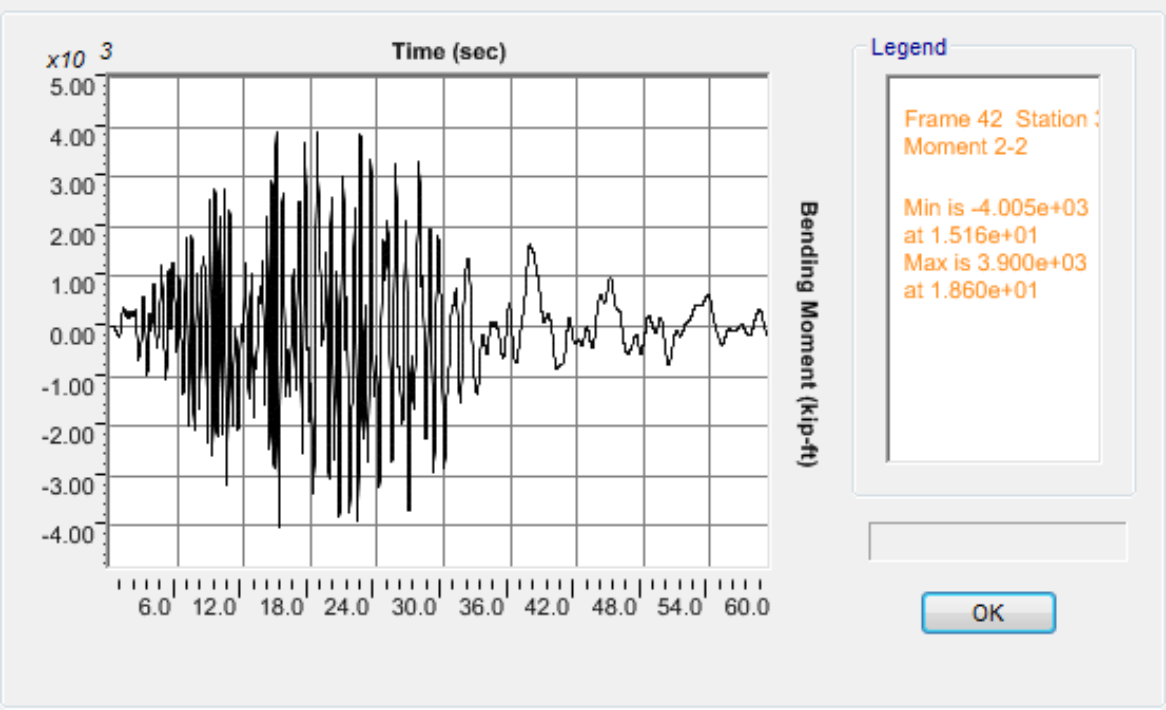

b)

Figure K.11 OSB1 column top response for Motion 11 ROCKS1P4: a) Longitudinal shear force-displacement hysteresis; b) Bending moment time history in the longitudinal direction

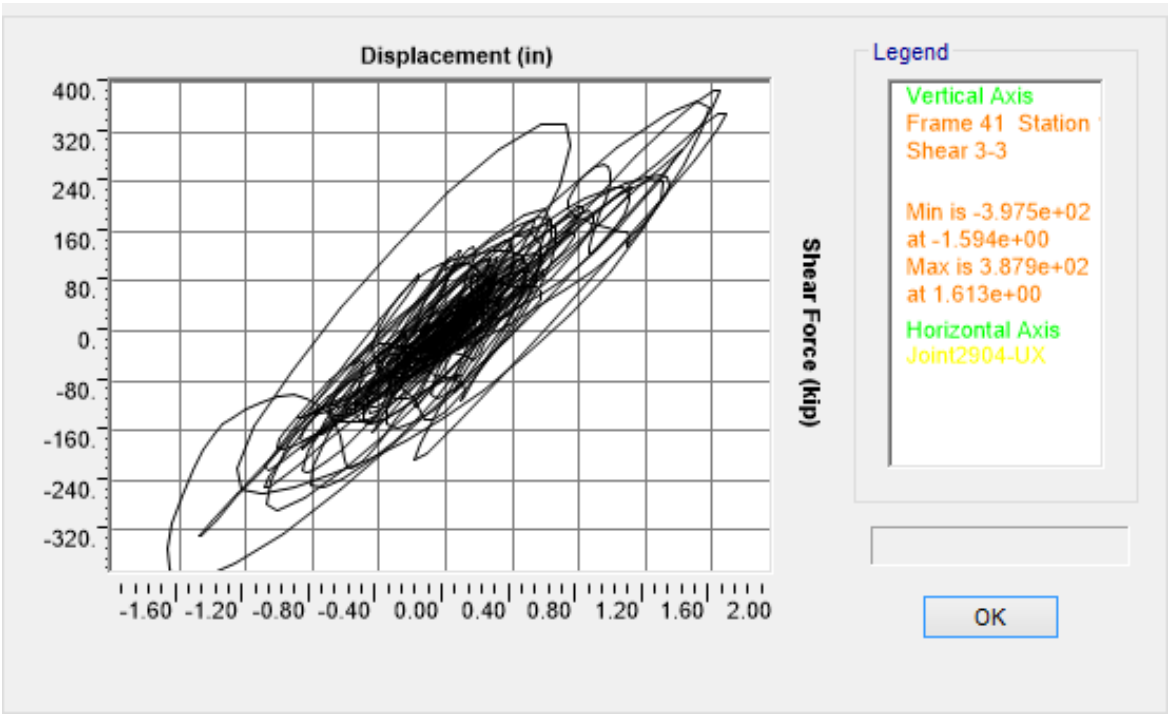

a)

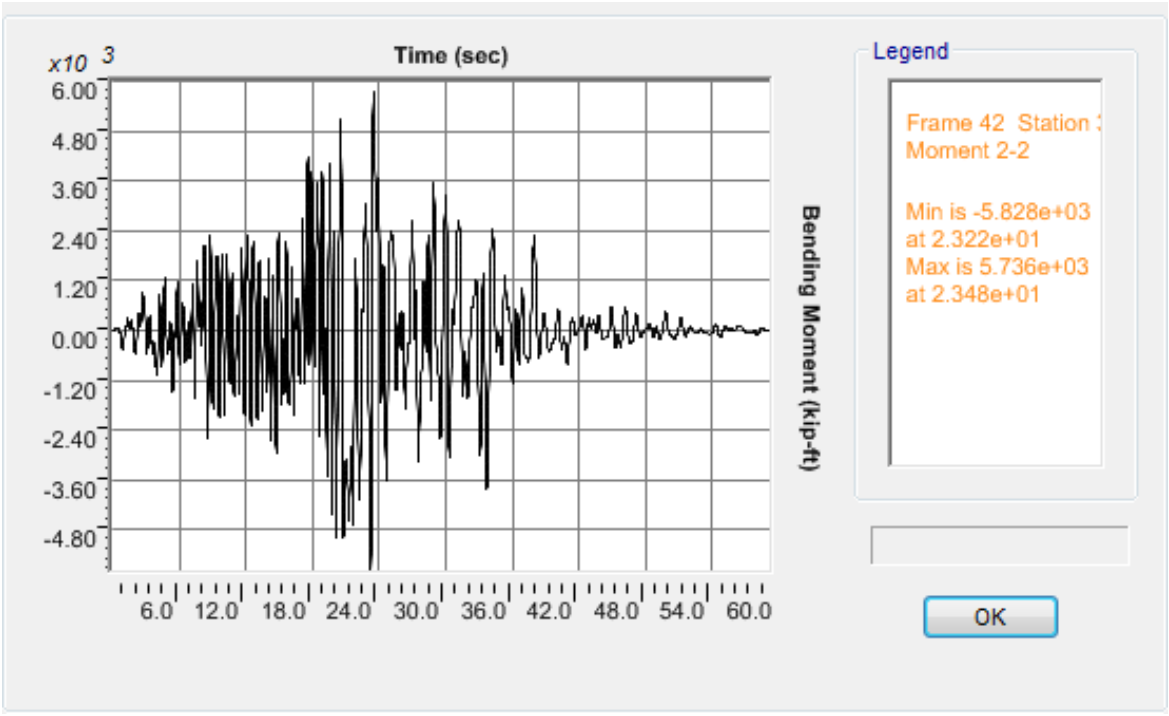

b)

Figure K.12 OSB1 column top response for Motion 12 ROCKS1P5: a) Longitudinal shear force-displacement hysteresis; b) Bending moment time history in the longitudinal direction

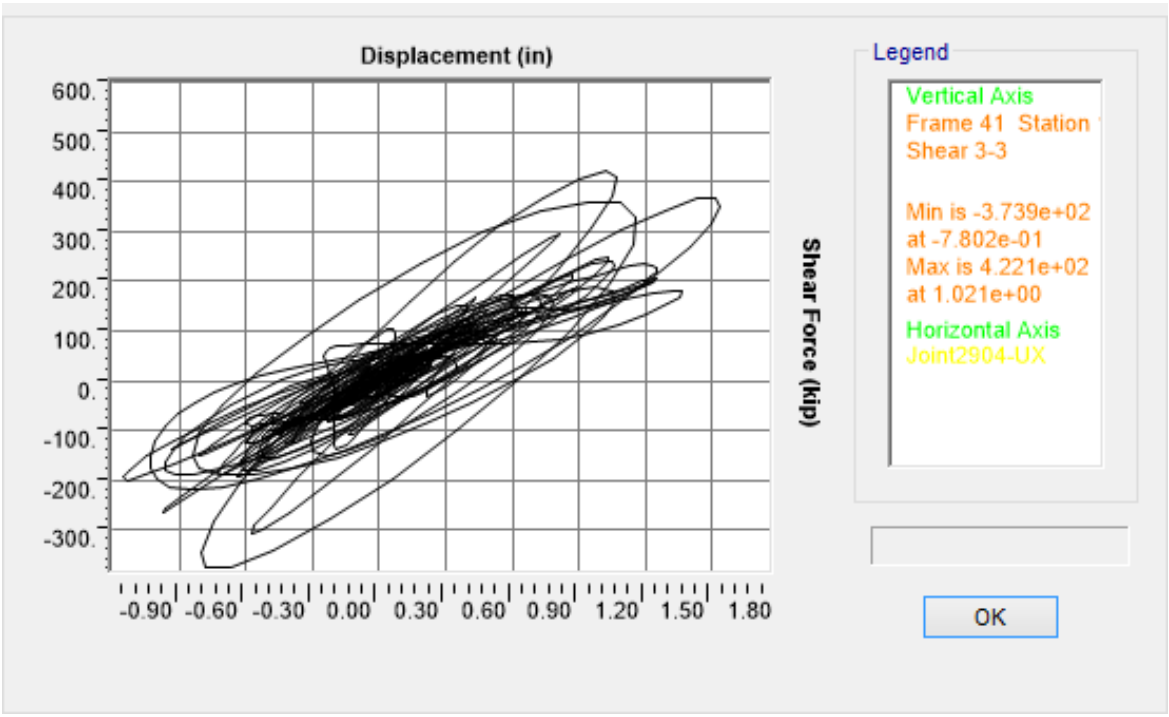

a)

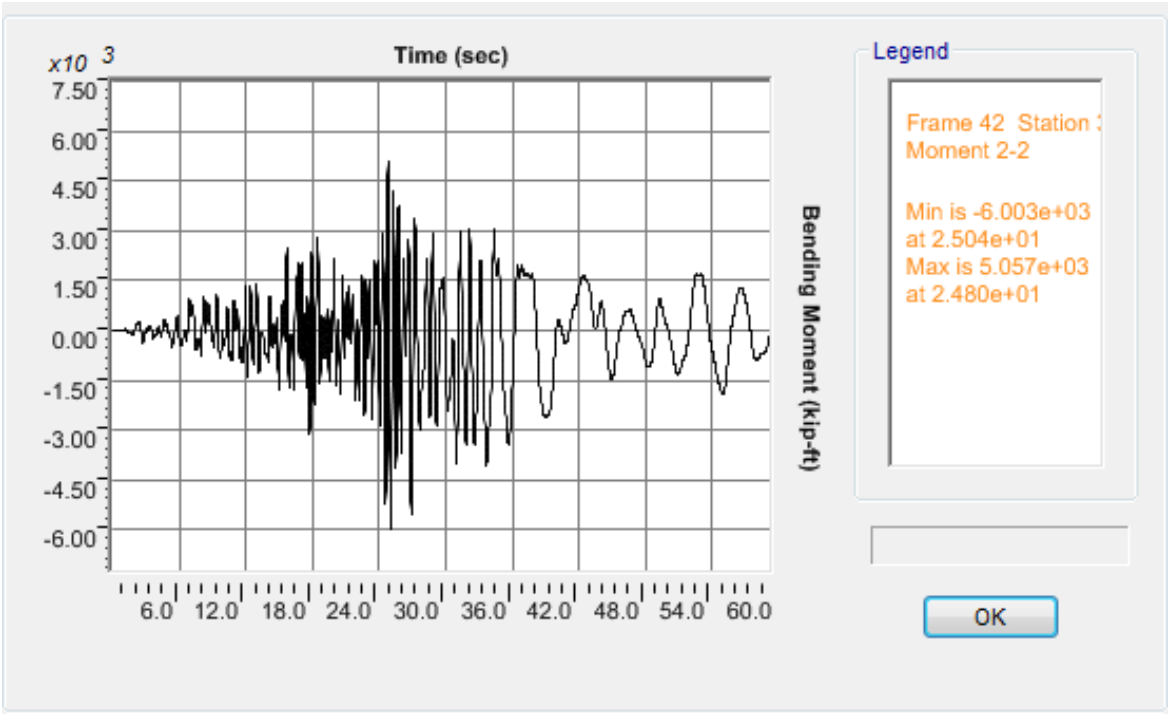

b)

Figure K.13 OSB1 column top response for Motion 13 ROCKS1P6: a) Longitudinal shear force-displacement hysteresis; b) Bending moment time history in the longitudinal direction

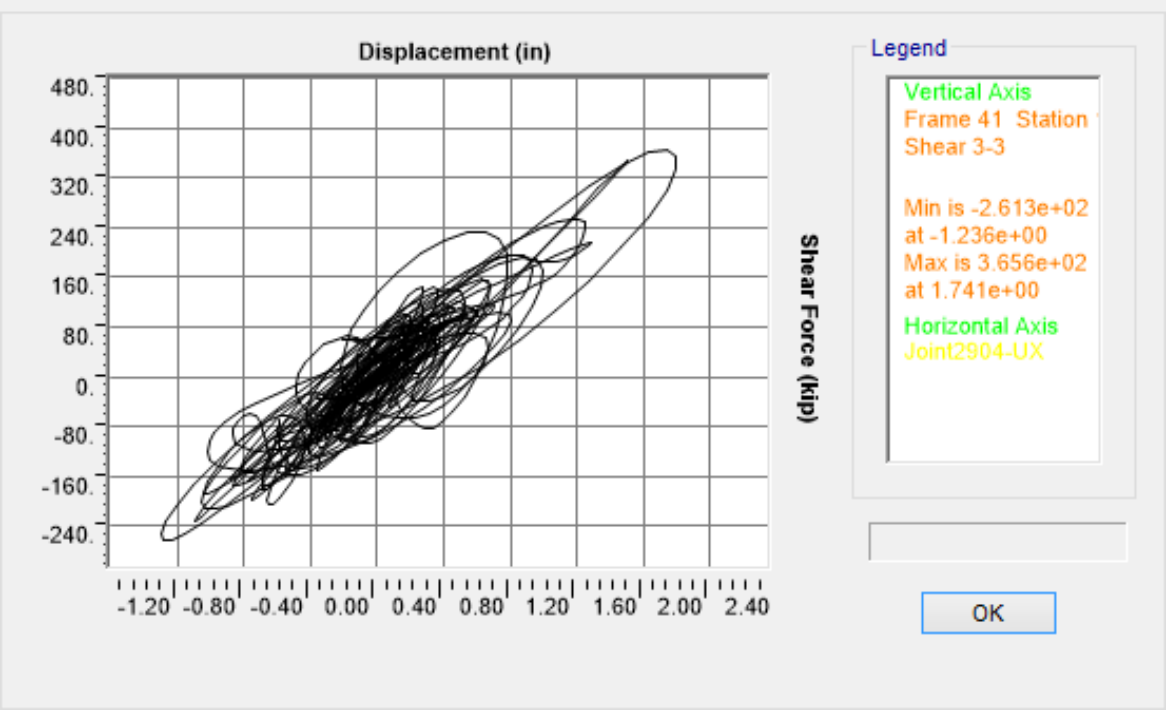

a)

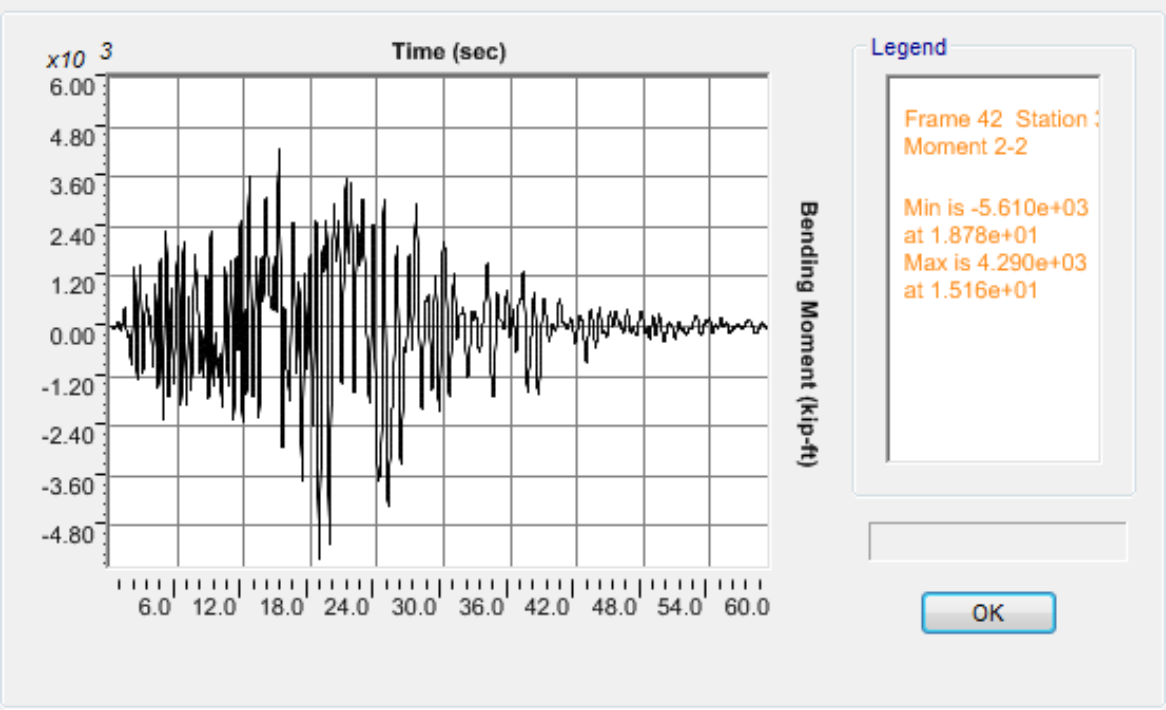

b)

Figure K.14 OSB1 column top response for Motion 14 ROCKS1P7: a) Longitudinal shear force-displacement hysteresis; b) Bending moment time history in the longitudinal direction

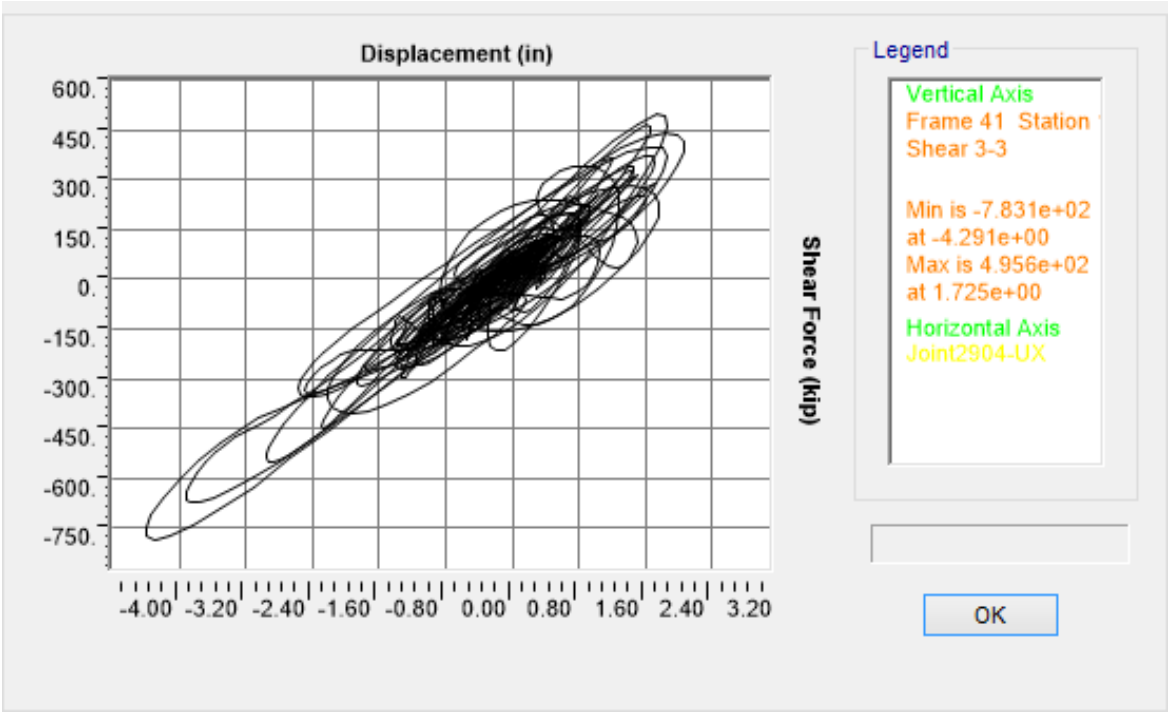

a)

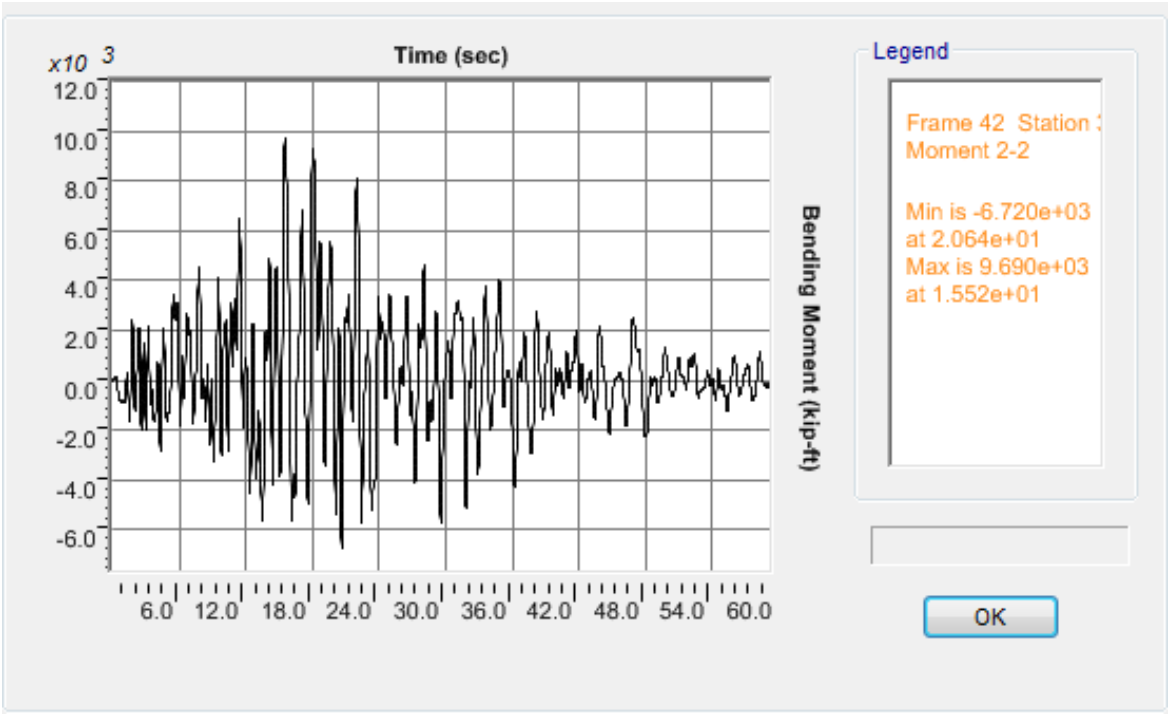

b)

Figure K.15 OSB1 column top response for Motion 15 SANDS1N1: a) Longitudinal shear force-displacement hysteresis; b) Bending moment time history in the longitudinal direction

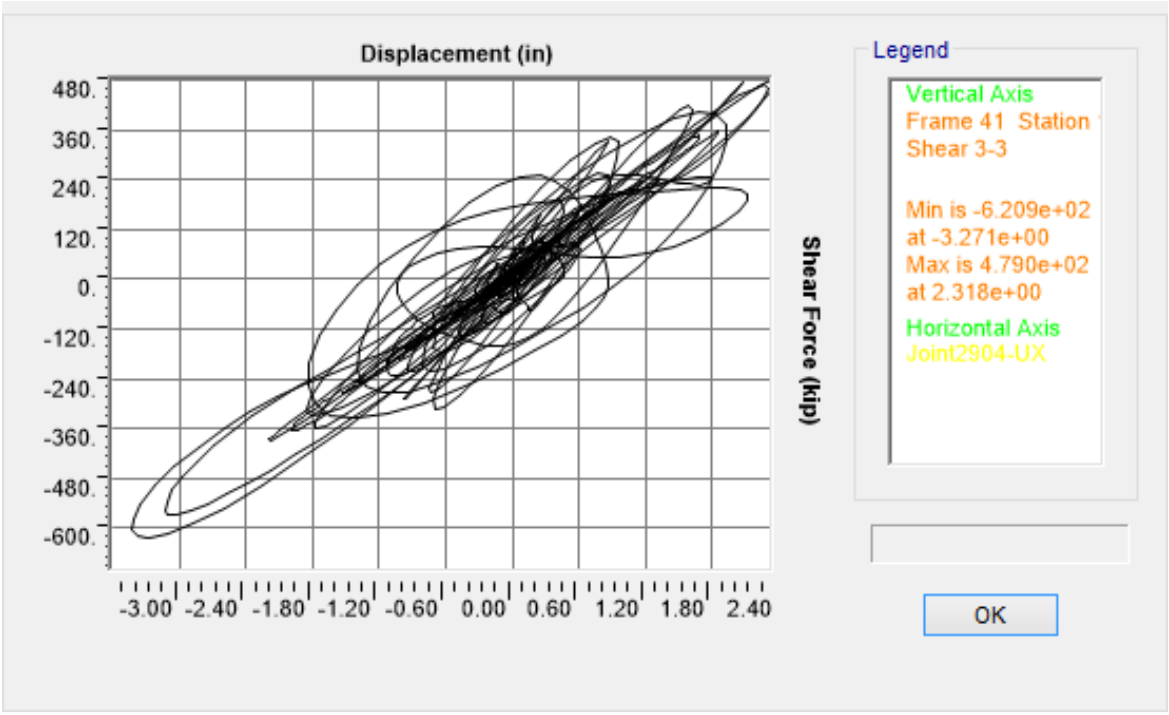

a)

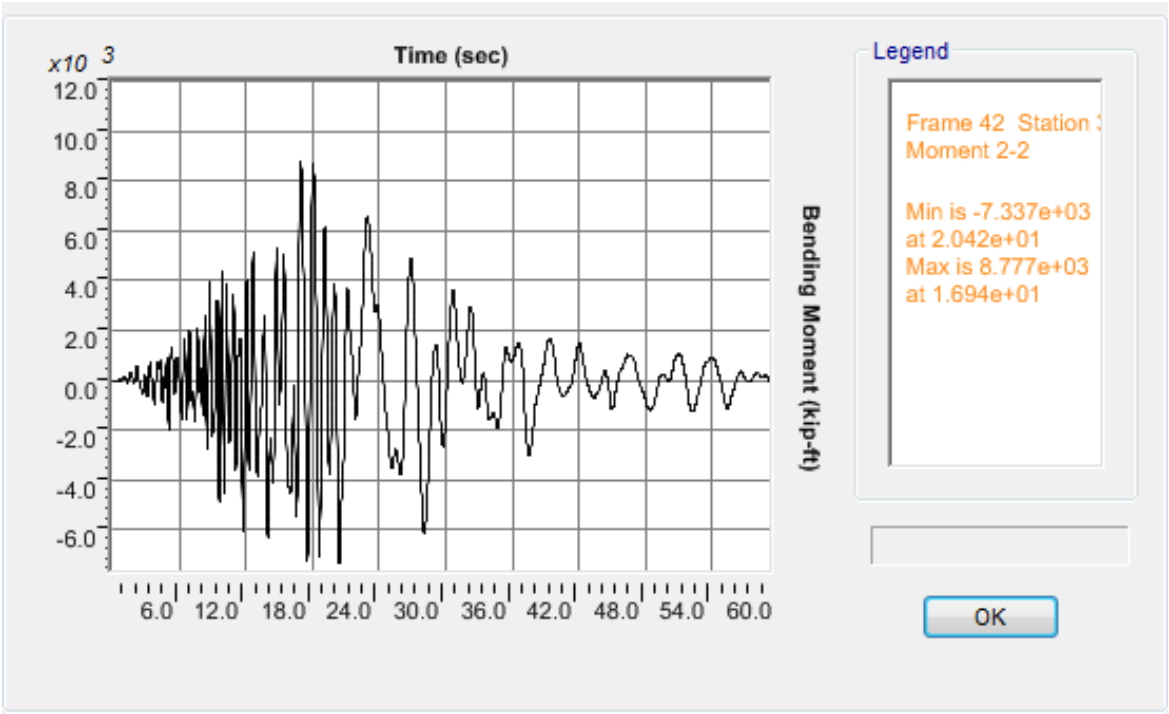

b)

Figure K.16 OSB1 column top response for Motion 16 SANDS1N2: a) Longitudinal shear force-displacement hysteresis; b) Bending moment time history in the longitudinal direction

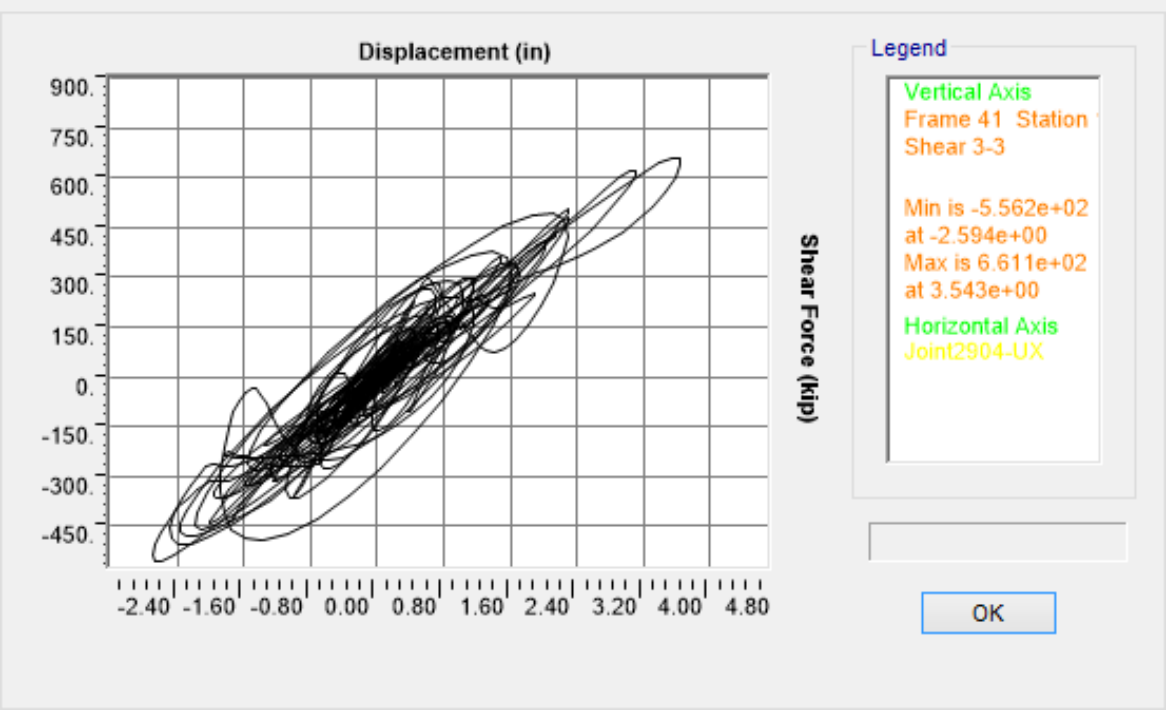

a)

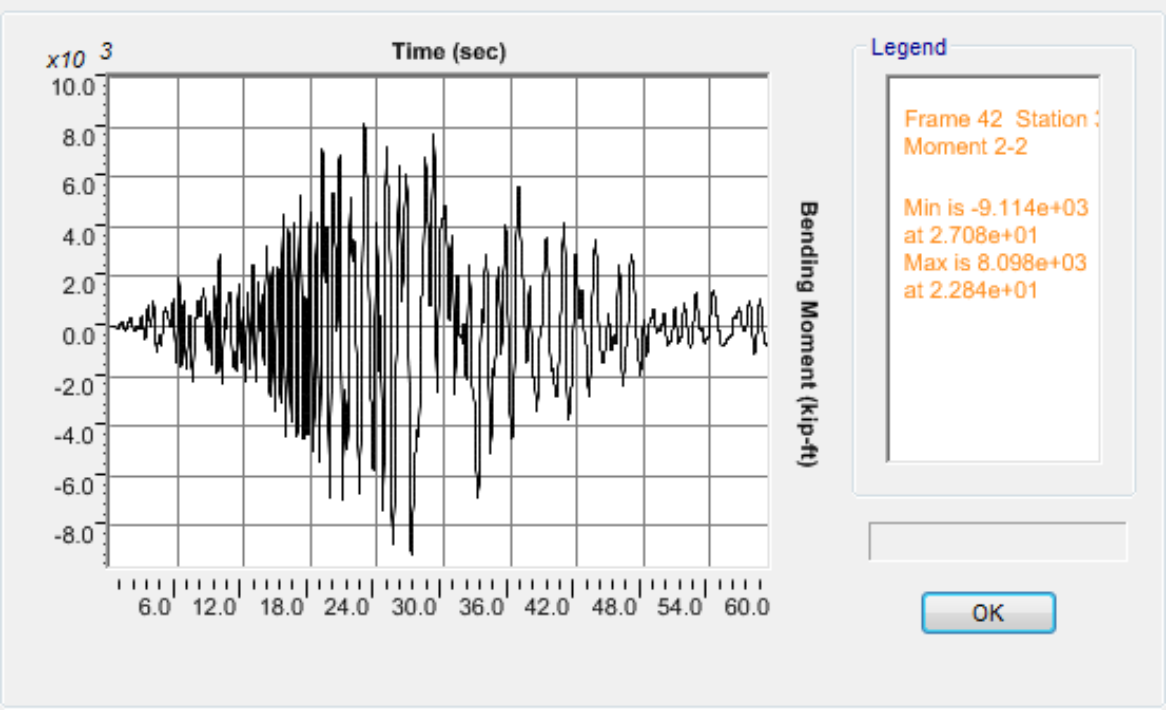

b)

Figure K.17 OSB1 column top response for Motion 17 SANDS1N3: a) Longitudinal shear force-displacement hysteresis; b) Bending moment time history in the longitudinal direction

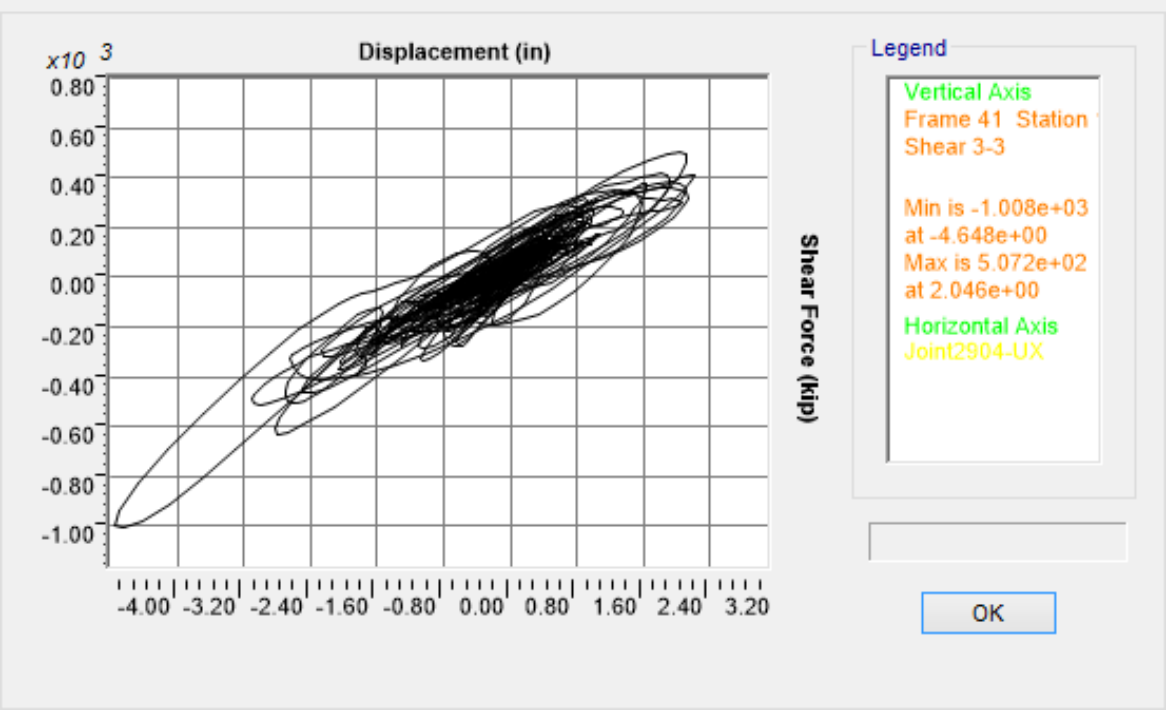

a)

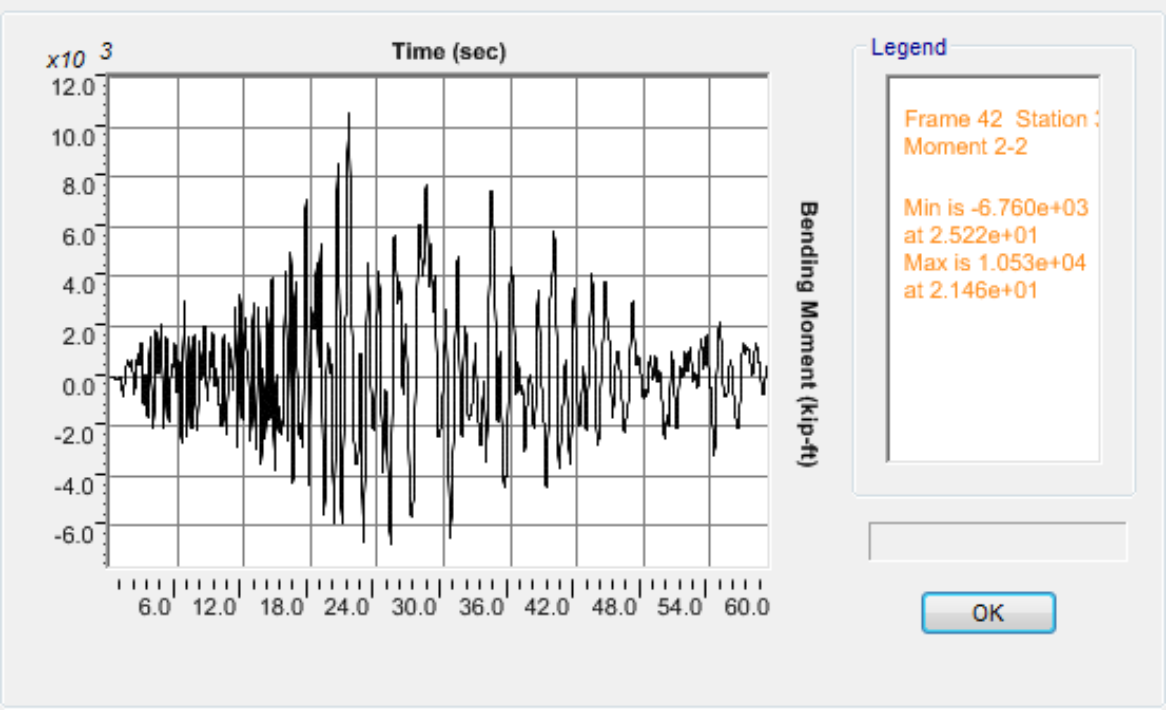

b)

Figure K.18 OSB1 column top response for Motion 18 SANDS1N4: a) Longitudinal shear force-displacement hysteresis; b) Bending moment time history in the longitudinal direction

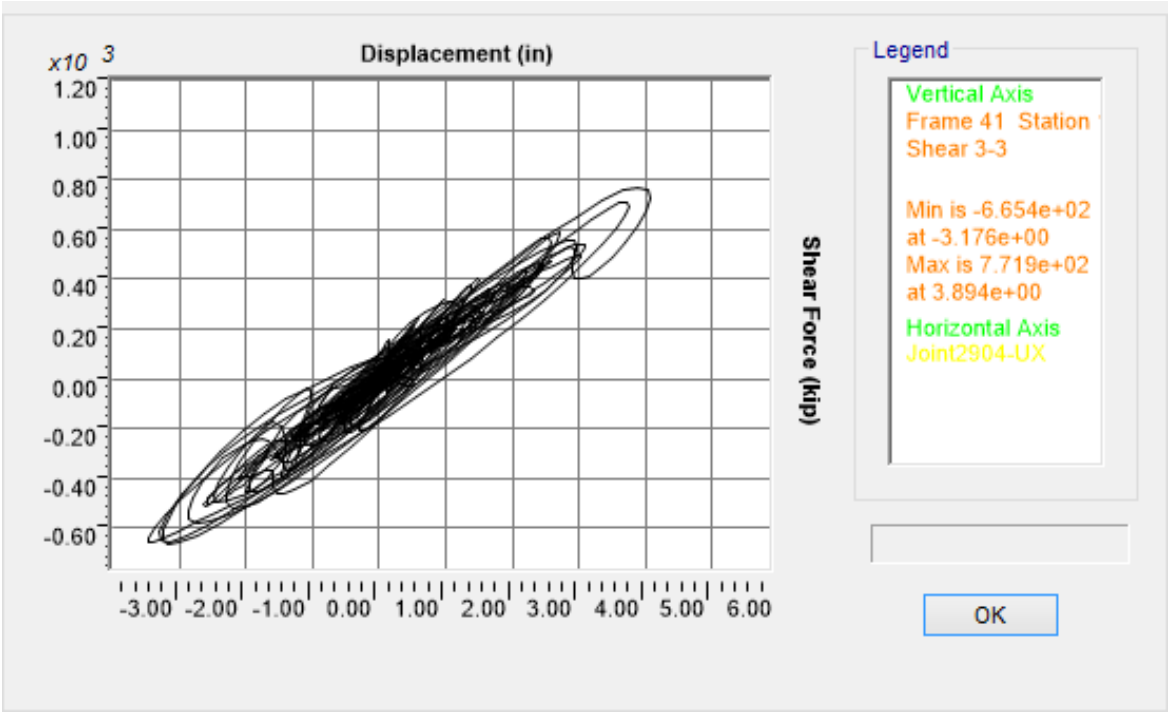

a)

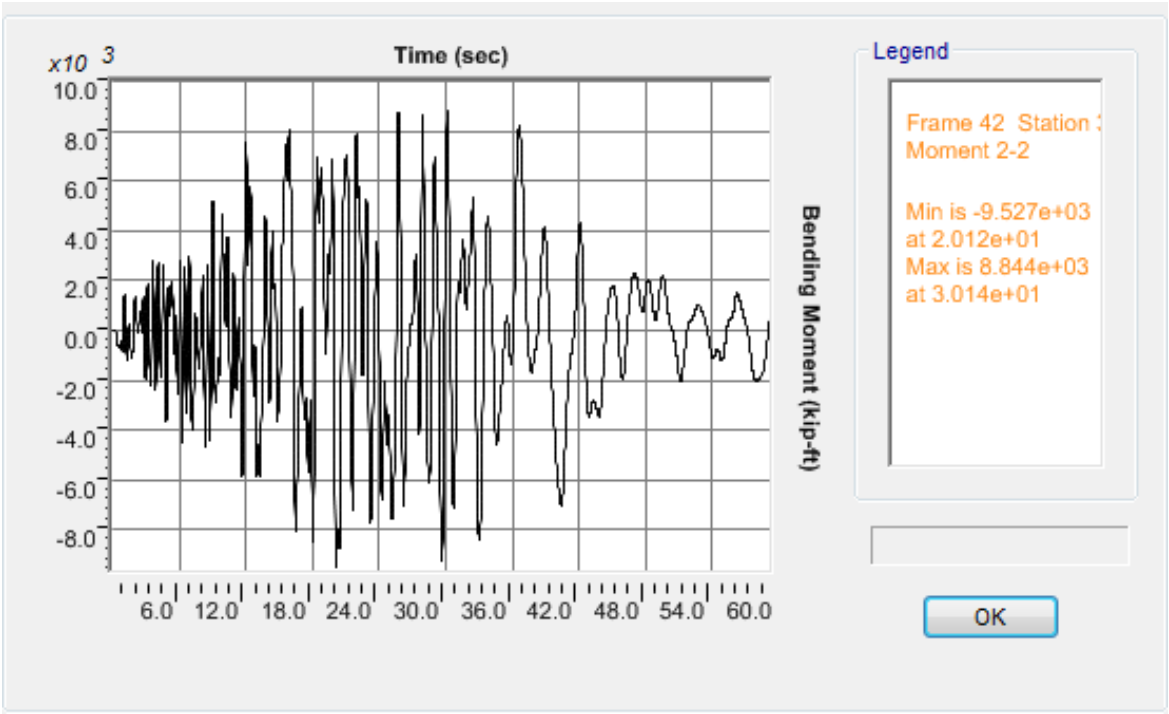

b)

Figure K.19 OSB1 column top response for Motion 19 SANDS1N5: a) Longitudinal shear force-displacement hysteresis; b) Bending moment time history in the longitudinal direction

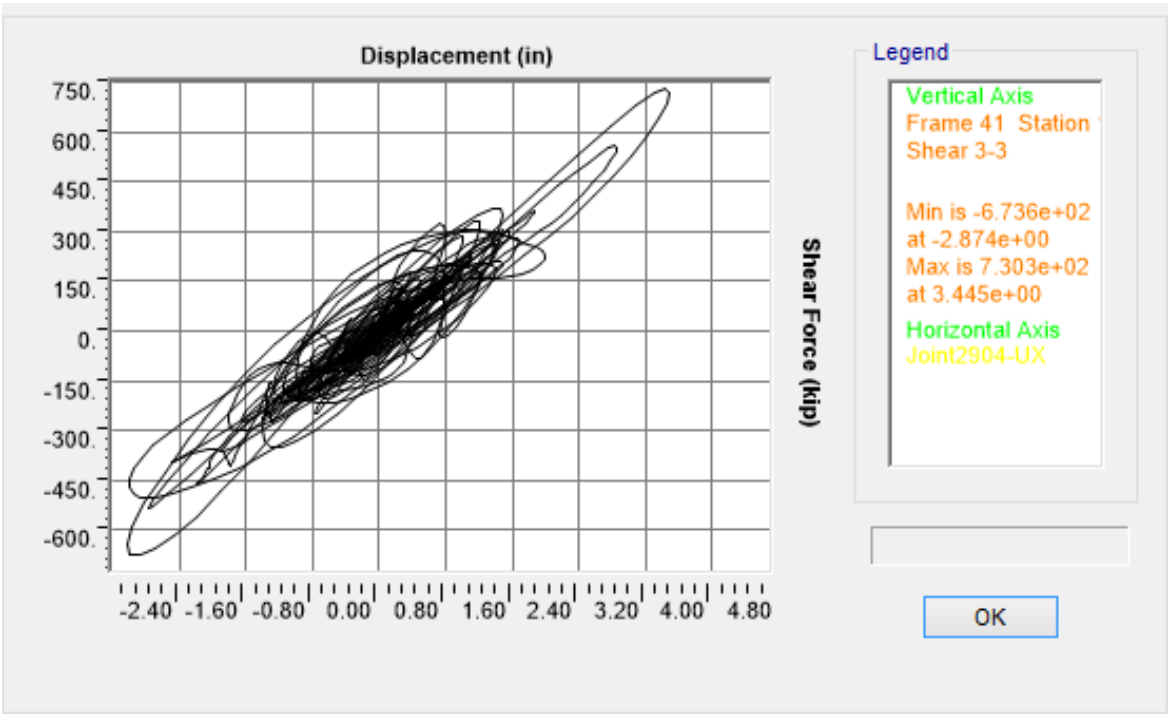

a)

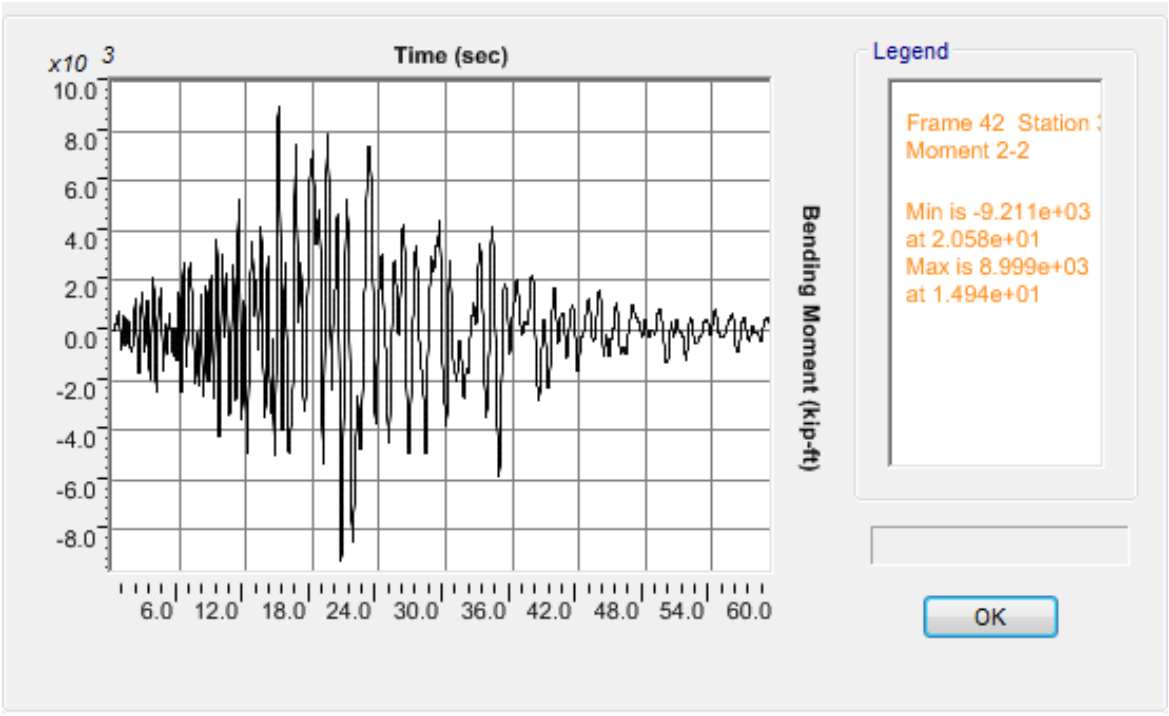

b)

Figure K.20 OSB1 column top response for Motion 20 SANDS1N6: a) Longitudinal shear force-displacement hysteresis; b) Bending moment time history in the longitudinal direction

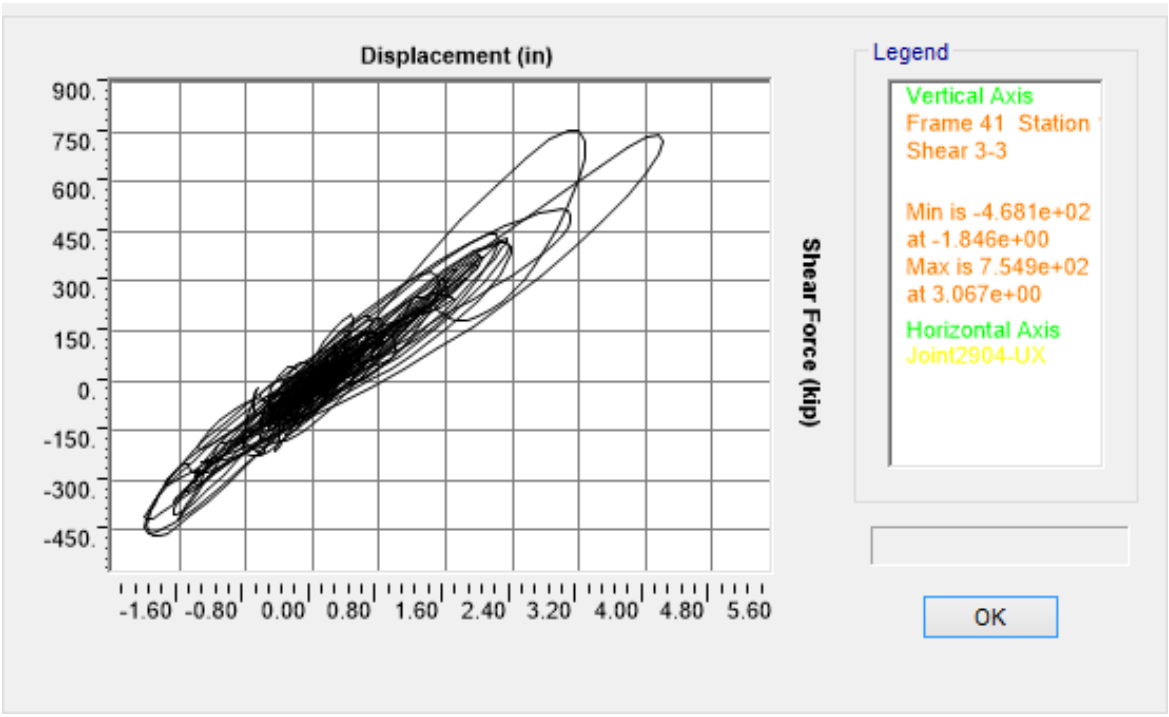

a)

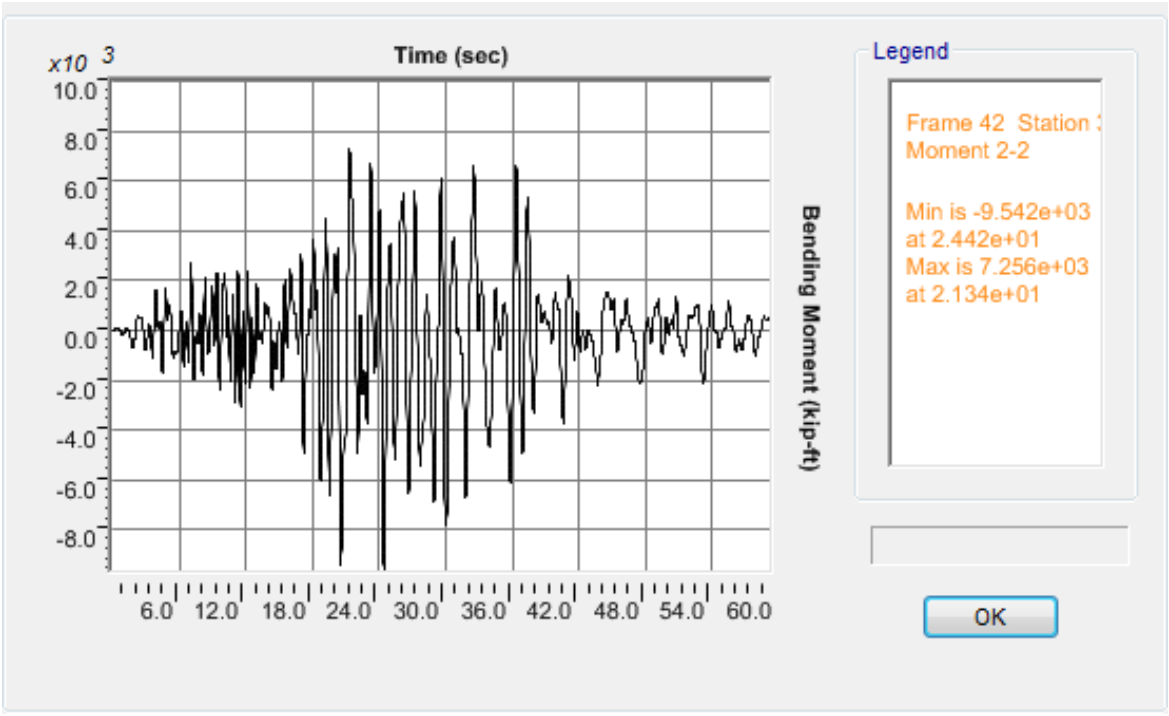

b)

Figure K.21 OSB1 column top response for Motion 21 SANDS1N7: a) Longitudinal shear force-displacement hysteresis; b) Bending moment time history in the longitudinal direction

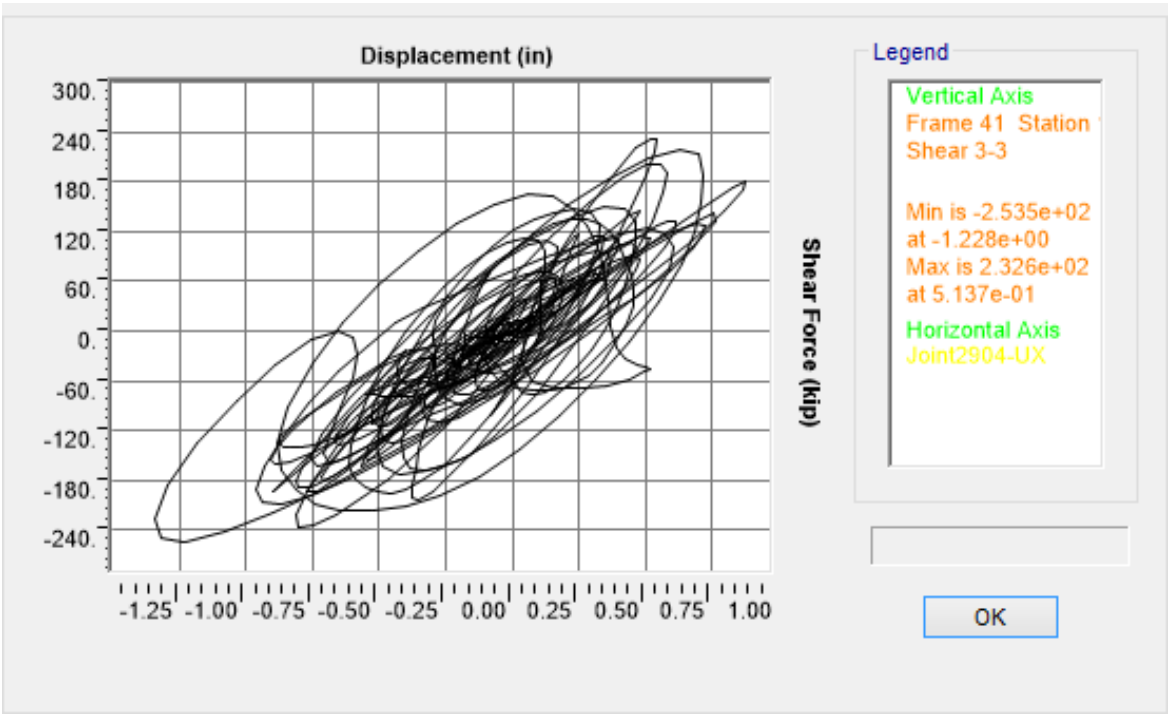
Displacement (in)
300.
240.
180.
120.
60.
0.
-60.
-120.
-180.
-240.
-1.25 -1.00 -0.75 -0.50 -0.25 0.00 0.25 0.50 0.75 1.00
Shear Force (kip)
Legend
Vertical Axis
Frame 41 Station
Shear 3-3
Min is -2.535e+02
at -1.228e+00
Max is 2.326e+02
at 5.137e-01
Horizontal Axis
Joint2904-UX
OK

a)

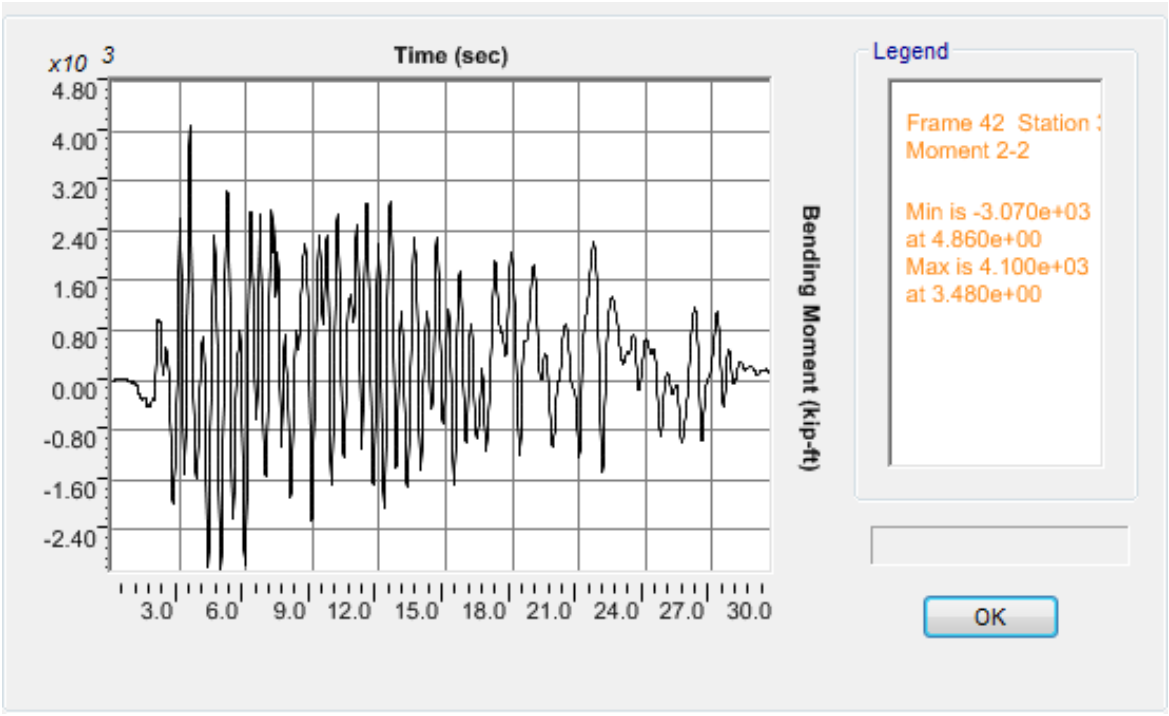
x10 3
Time (sec)
4.80
4.00
3.20
2.40
1.60
0.80
0.00
-0.80
-1.60
-2.40
3.0 6.0 9.0 12.0 15.0 18.0 21.0 24.0 27.0 30.0
Bending Moment (kip-ft)
Legend
Frame 42 Station
Moment 2-2
Min is -3.070e+03
at 4.860e+00
Max is 4.100e+03
at 3.480e+00
OK

b)

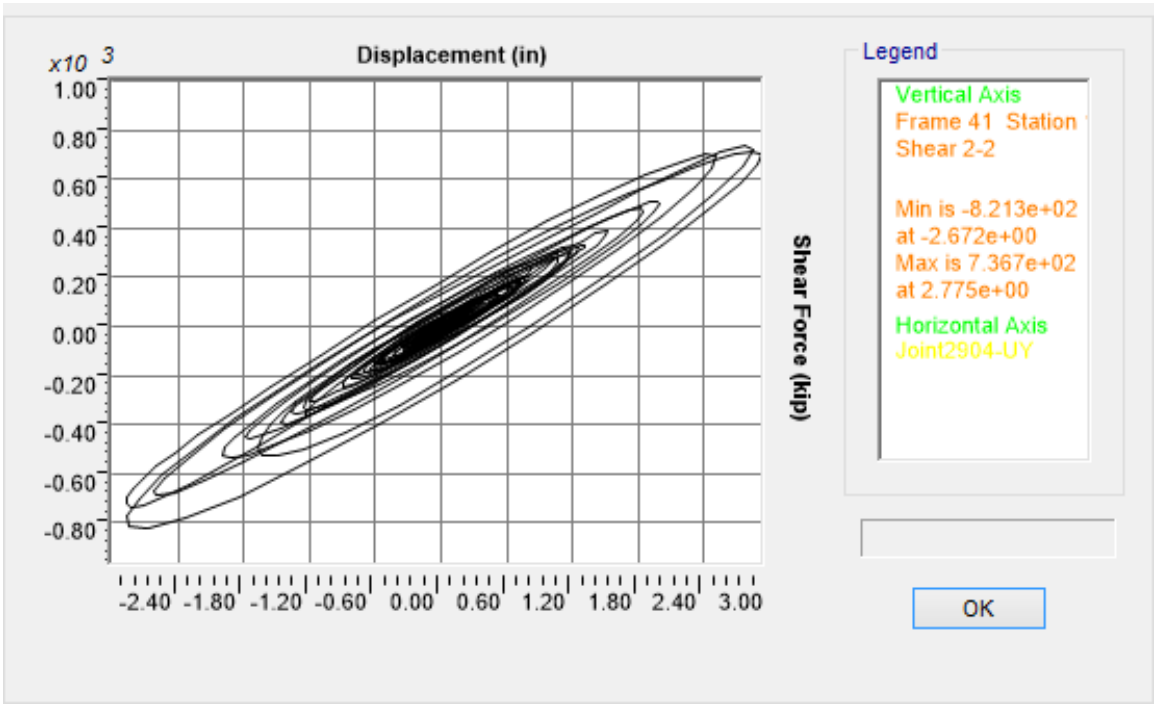

c)

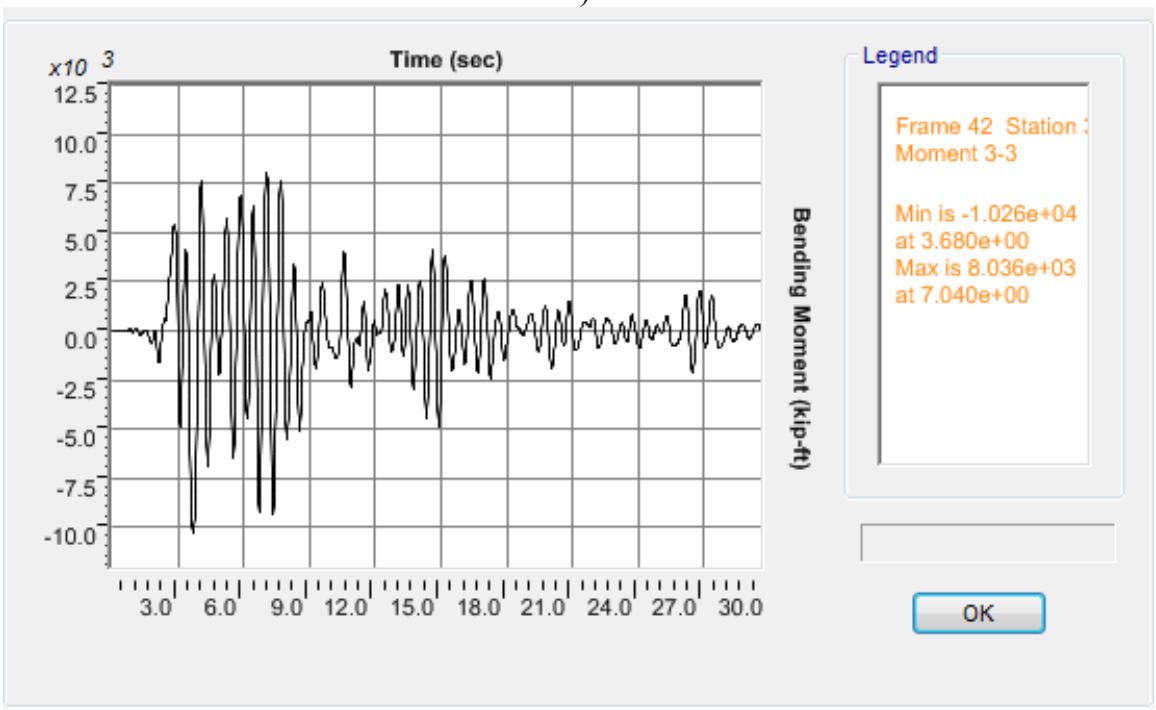

d)

Figure K.22 OSB1 column top response for Motion 22 ROCKN1N1: a) Longitudinal shear force-displacement hysteresis; b) Bending moment time history in the longitudinal direction; c) Transverse shear force-displacement hysteresis; d) Bending moment time history in the transverse direction

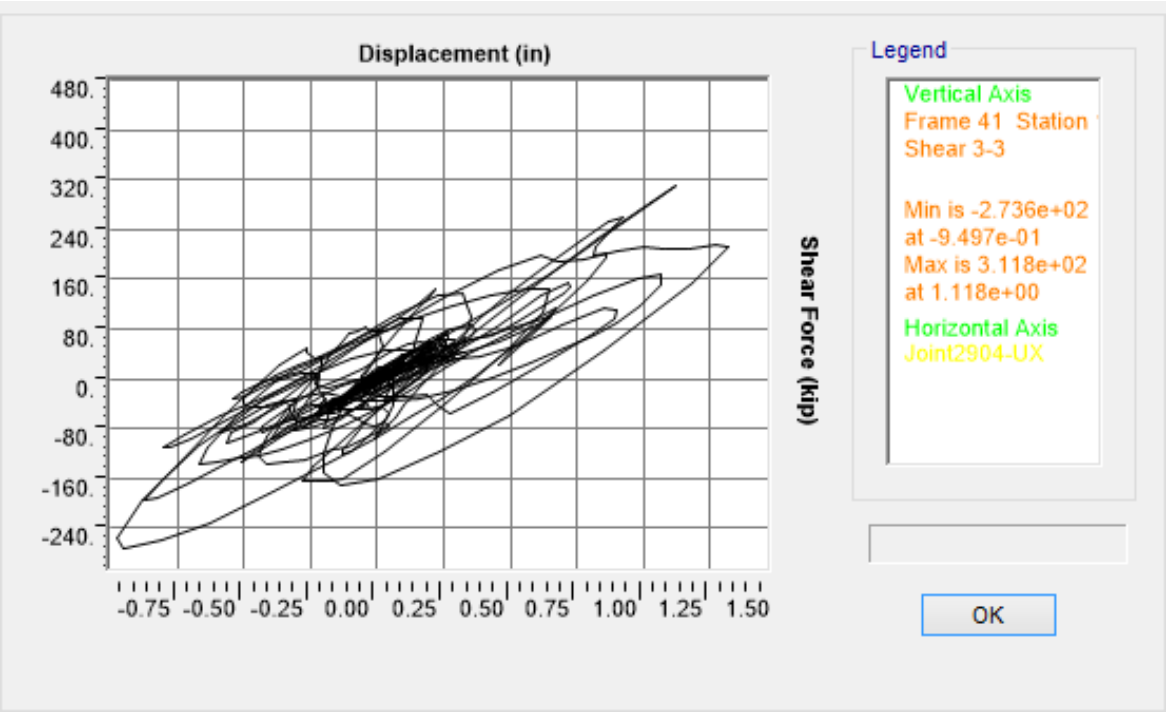
Displacement (in)
480.
400.
320.
240.
160.
80.
0.
-80.
-160.
-240.
-0.75 -0.50 -0.25 0.00 0.25 0.50 0.75 1.00 1.25 1.50
Shear Force (kip)
Legend
Vertical Axis
Frame 41 Station
Shear 3-3
Min is -2.736e+02
at -9.497e-01
Max is 3.118e+02
at 1.118e+00
Horizontal Axis
Joint2904-UX
OK

a)

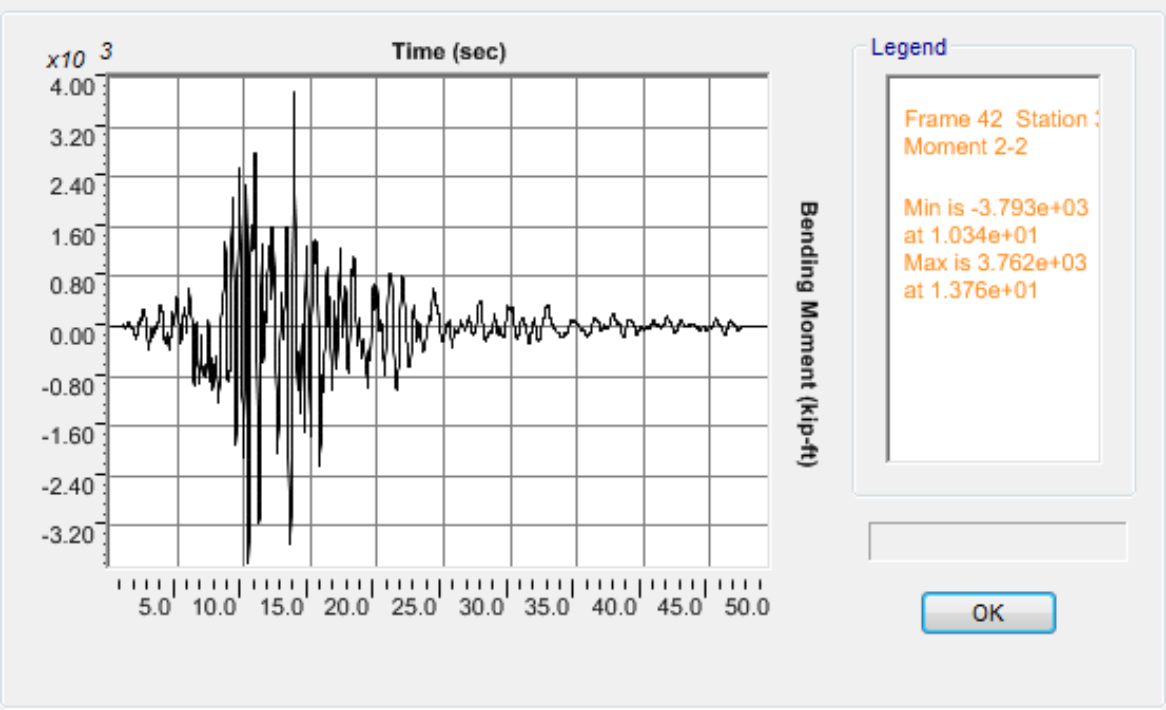
x10 3
Time (sec)
4.00
3.20
2.40
1.60
0.80
0.00
-0.80
-1.60
-2.40
-3.20
5.0 10.0 15.0 20.0 25.0 30.0 35.0 40.0 45.0 50.0
Bending Moment (kip-ft)
Legend
Frame 42 Station
Moment 2-2
Min is -3.793e+03
at 1.034e+01
Max is 3.762e+03
at 1.376e+01
OK

b)

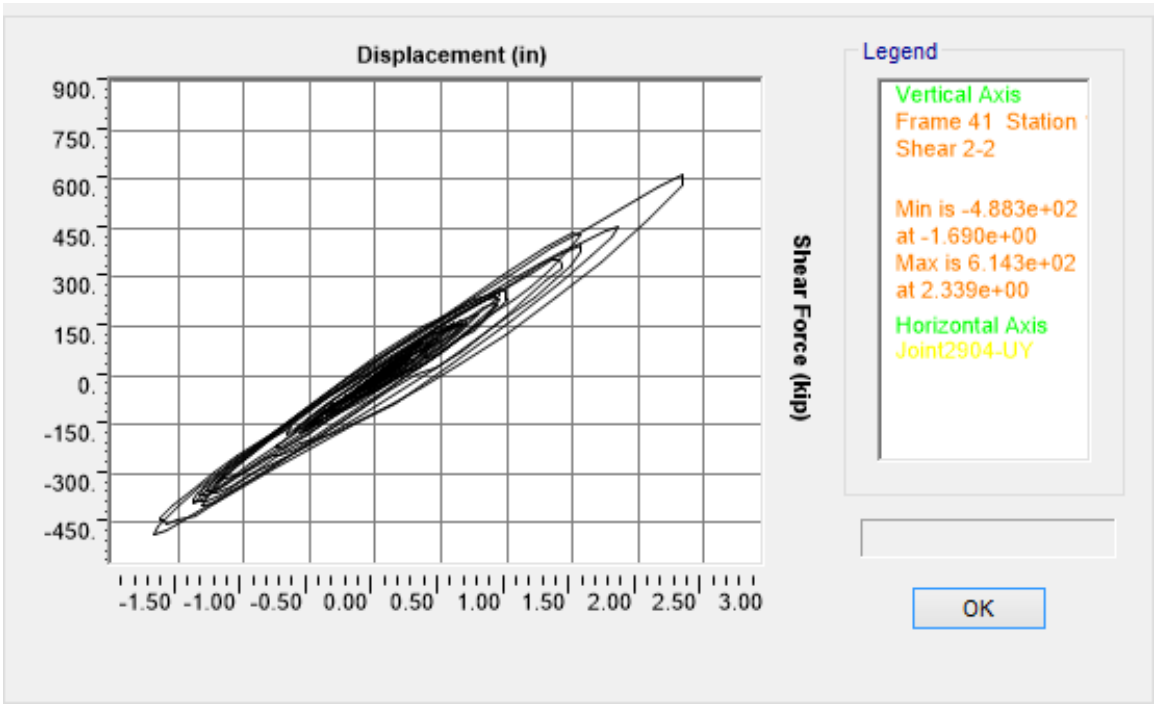

c)

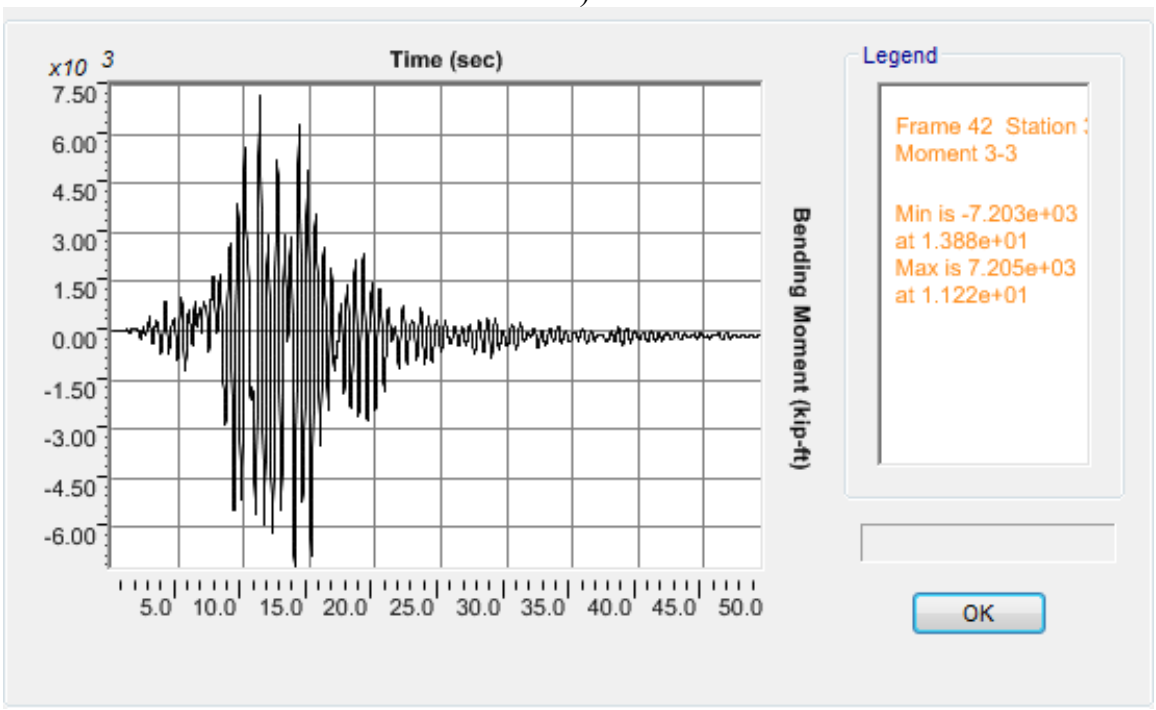

d)

Figure K.23 OSB1 column top response for Motion 23 ROCKN1P1: a) Longitudinal shear force-displacement hysteresis; b) Bending moment time history in the longitudinal direction; c) Transverse shear force-displacement hysteresis; d) Bending moment time history in the transverse direction

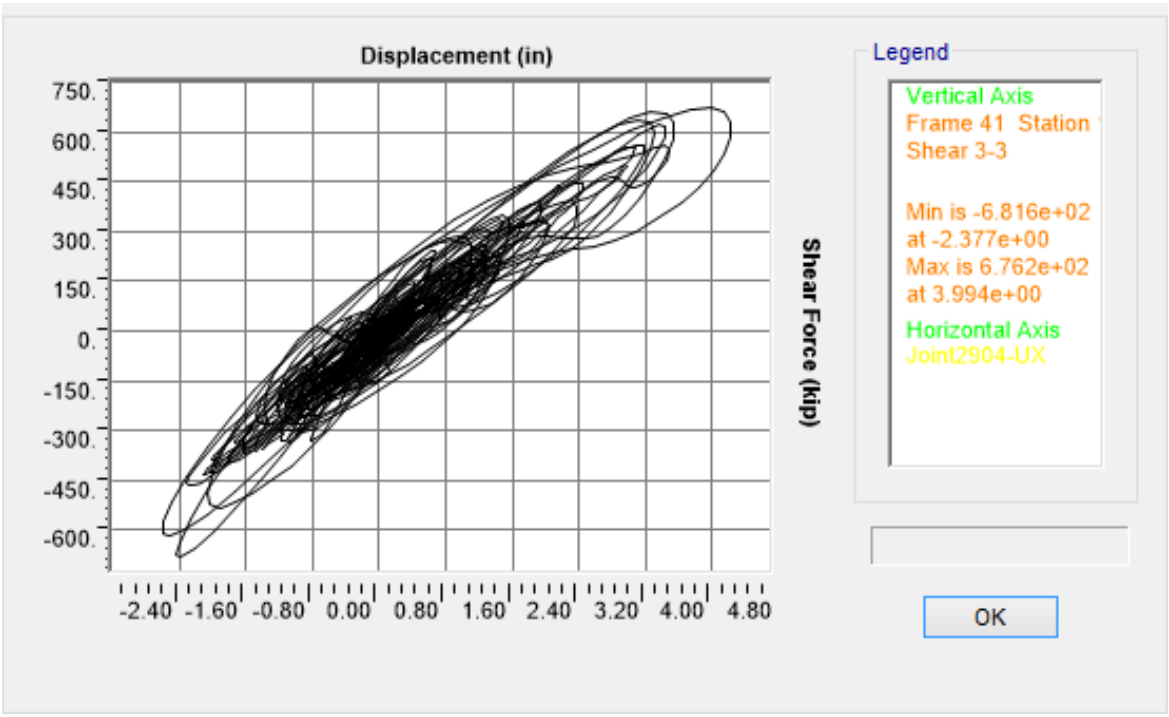
Displacement (in)
750.
600.
450.
300.
150.
0.
-150.
-300.
-450.
-600.
-2.40 -1.60 -0.80 0.00 0.80 1.60 2.40 3.20 4.00 4.80
Shear Force (kip)
Legend
Vertical Axis
Frame 41 Station
Shear 3-3
Min is -6.816e+02
at -2.377e+00
Max is 6.762e+02
at 3.994e+00
Horizontal Axis
Joint2904-UX
OK

a)

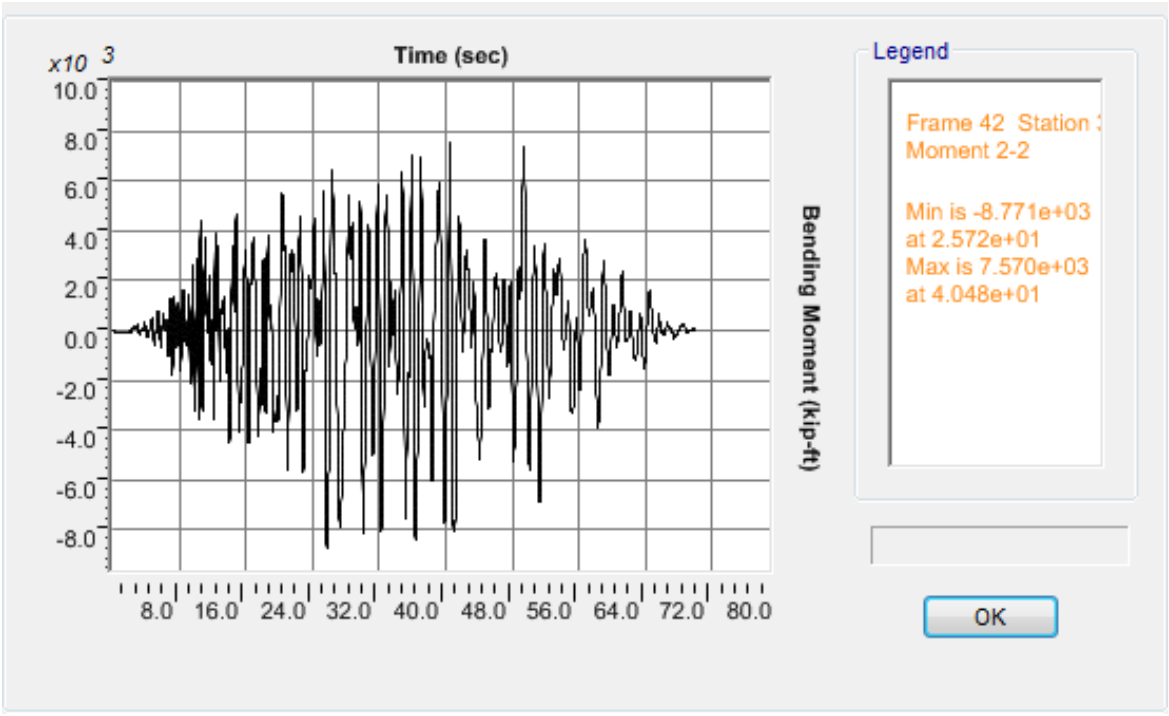
x10 3
Time (sec)
10.0
8.0
6.0
4.0
2.0
0.0
-2.0
-4.0
-6.0
-8.0
8.0 16.0 24.0 32.0 40.0 48.0 56.0 64.0 72.0 80.0
Bending Moment (kip-ft)
Legend
Frame 42 Station
Moment 2-2
Min is -8.771e+03
at 2.572e+01
Max is 7.570e+03
at 4.048e+01
OK

b)

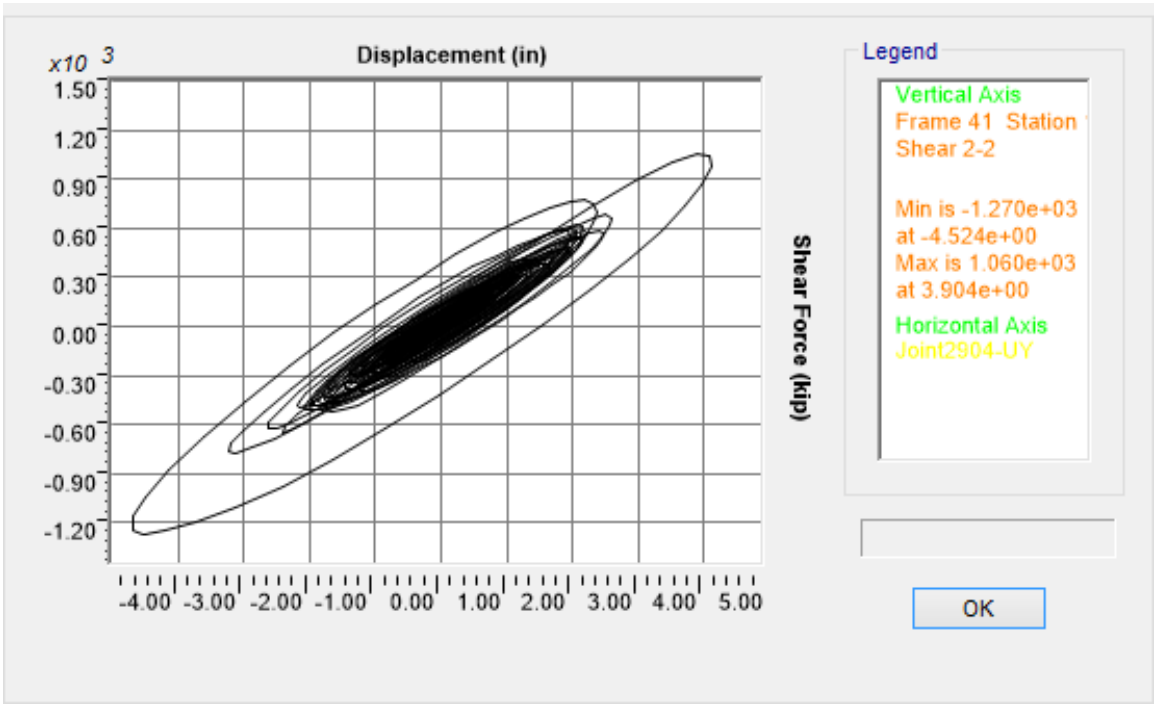

c)

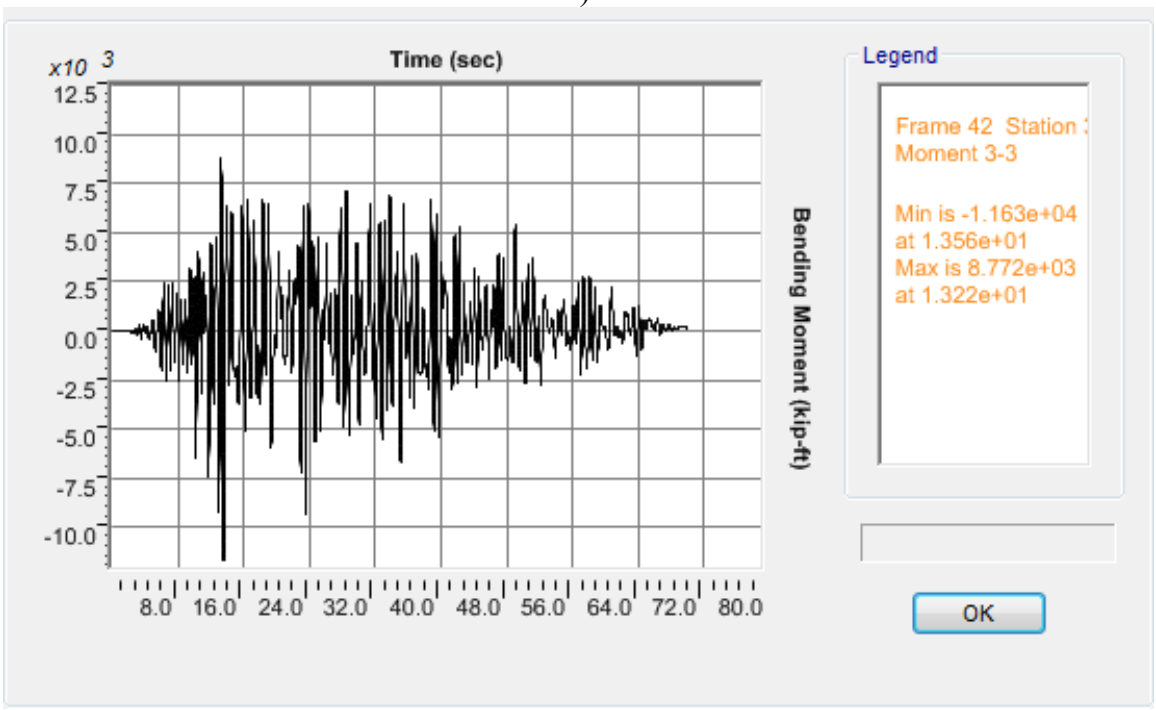

d)

Figure K.24 OSB1 column top response for Motion 24 SANDN1N1: a) Longitudinal shear force-displacement hysteresis; b) Bending moment time history in the longitudinal direction; c) Transverse shear force-displacement hysteresis; d) Bending moment time history in the transverse direction

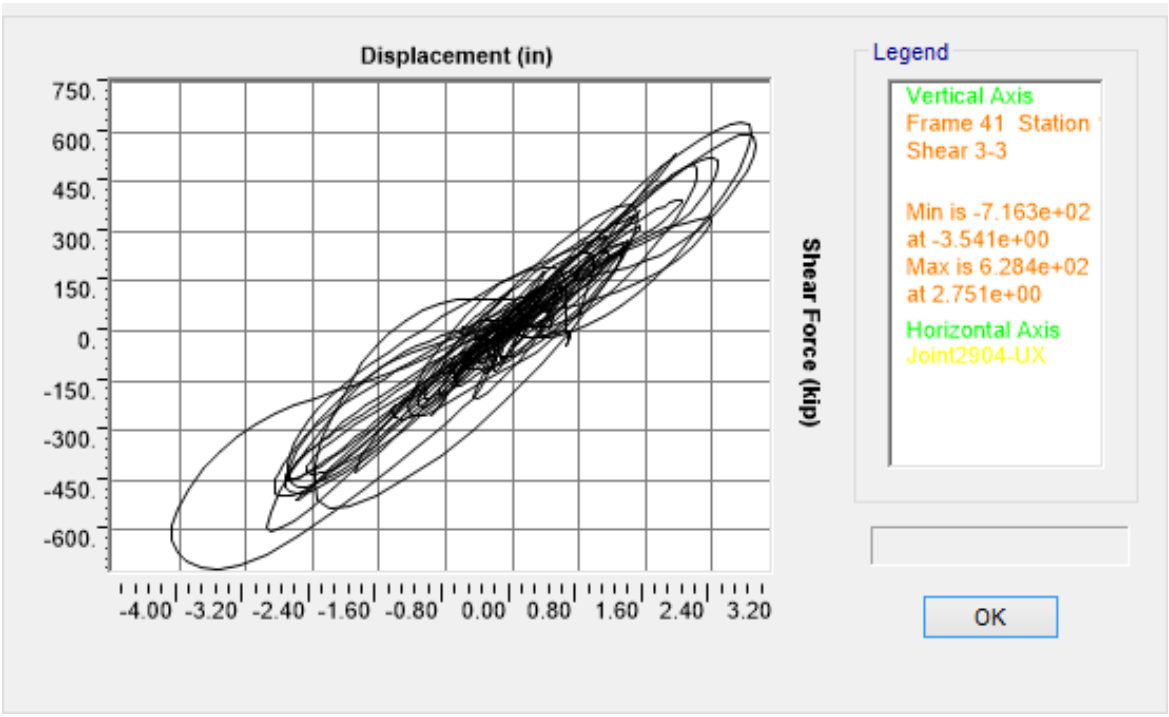
Displacement (in)
750.
600.
450.
300.
150.
0.
-150.
-300.
-450.
-600.
-4.00 -3.20 -2.40 -1.60 -0.80 0.00 0.80 1.60 2.40 3.20
Shear Force (kip)
Legend
Vertical Axis
Frame 41 Station
Shear 3-3
Min is -7.163e+02
at -3.541e+00
Max is 6.284e+02
at 2.751e+00
Horizontal Axis
Joint2904-UX
OK

a)

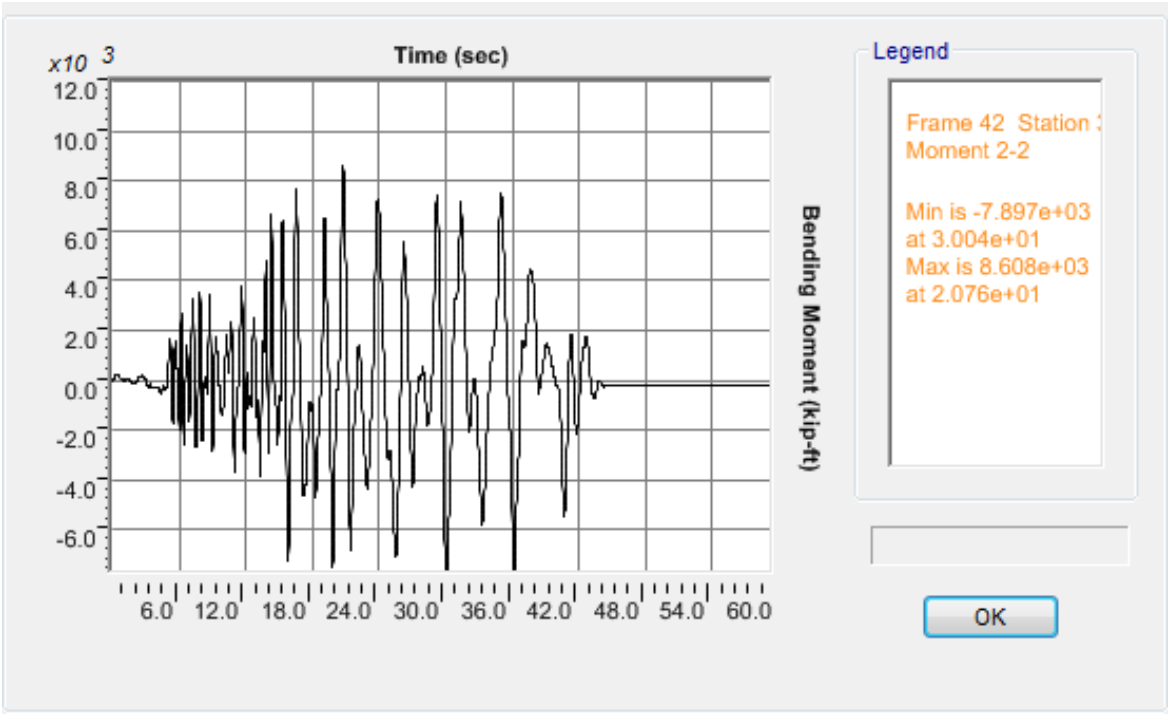
x10 3
Time (sec)
12.0
10.0
8.0
6.0
4.0
2.0
0.0
-2.0
-4.0
-6.0
6.0 12.0 18.0 24.0 30.0 36.0 42.0 48.0 54.0 60.0
Bending Moment (kip-ft)
Legend
Frame 42 Station
Moment 2-2
Min is -7.897e+03
at 3.004e+01
Max is 8.608e+03
at 2.076e+01
OK

b)

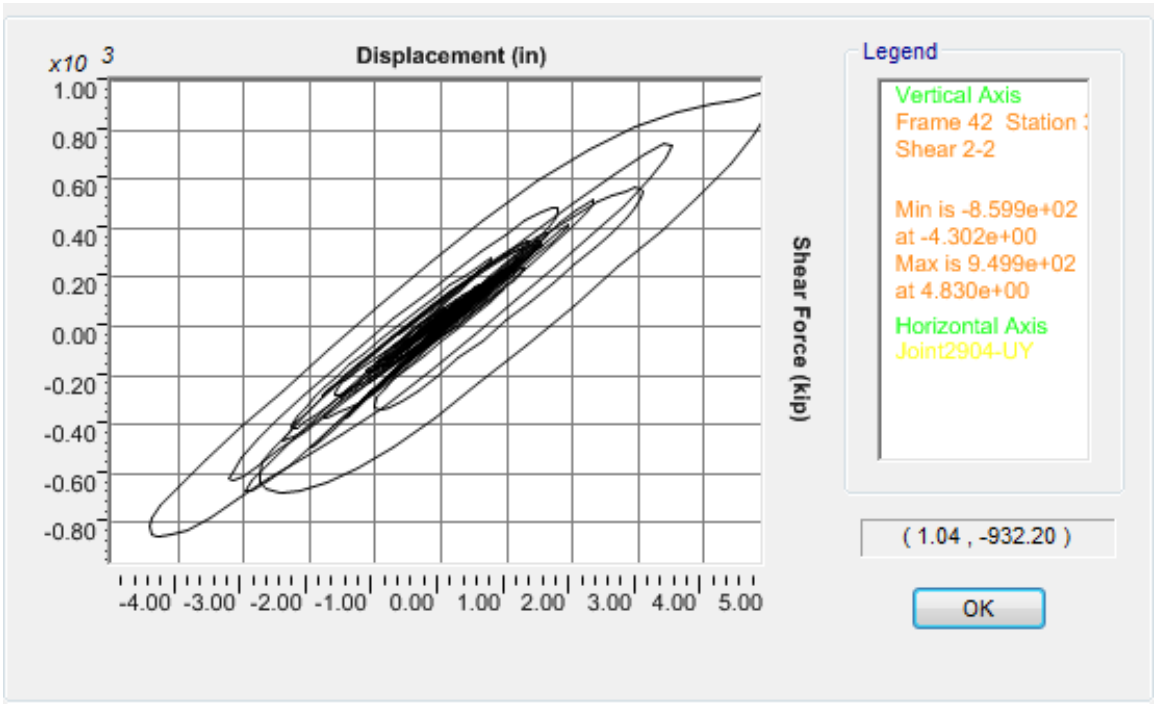

c)

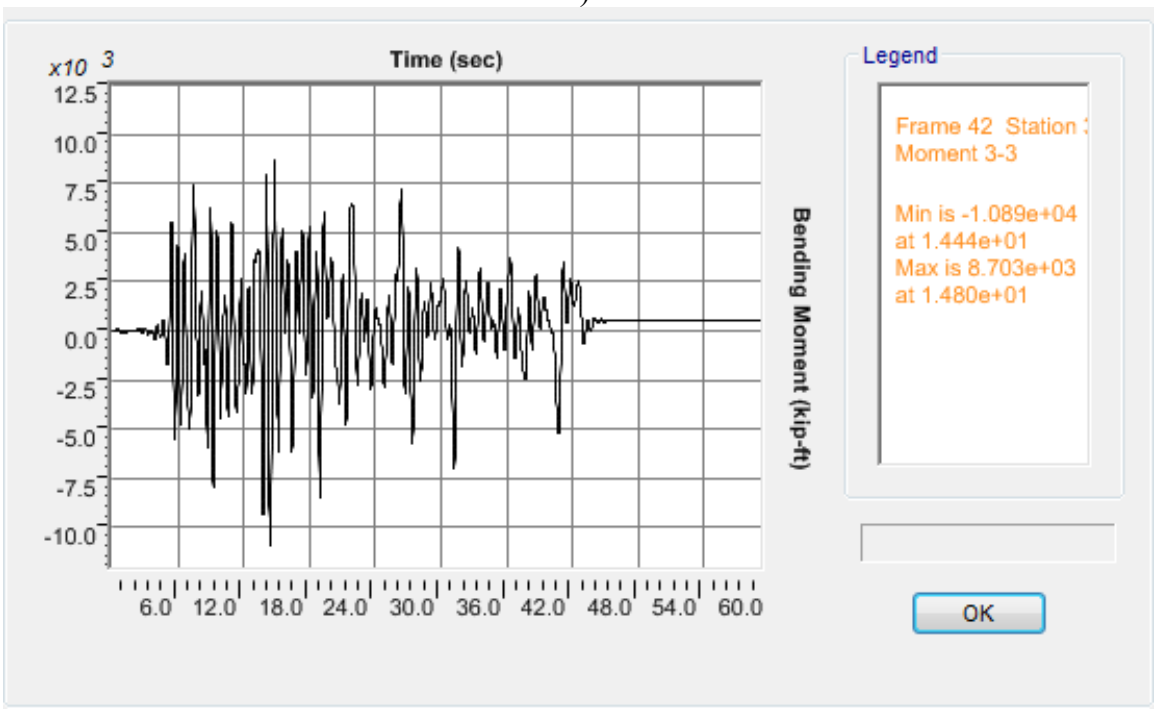

d)

Figure K.25 OSB1 column top response for Motion 25 CLAYN1N1: a) Longitudinal shear force-displacement hysteresis; b) Bending moment time history in the longitudinal direction; c) Transverse shear force-displacement hysteresis; d) Bending moment time history in the transverse direction

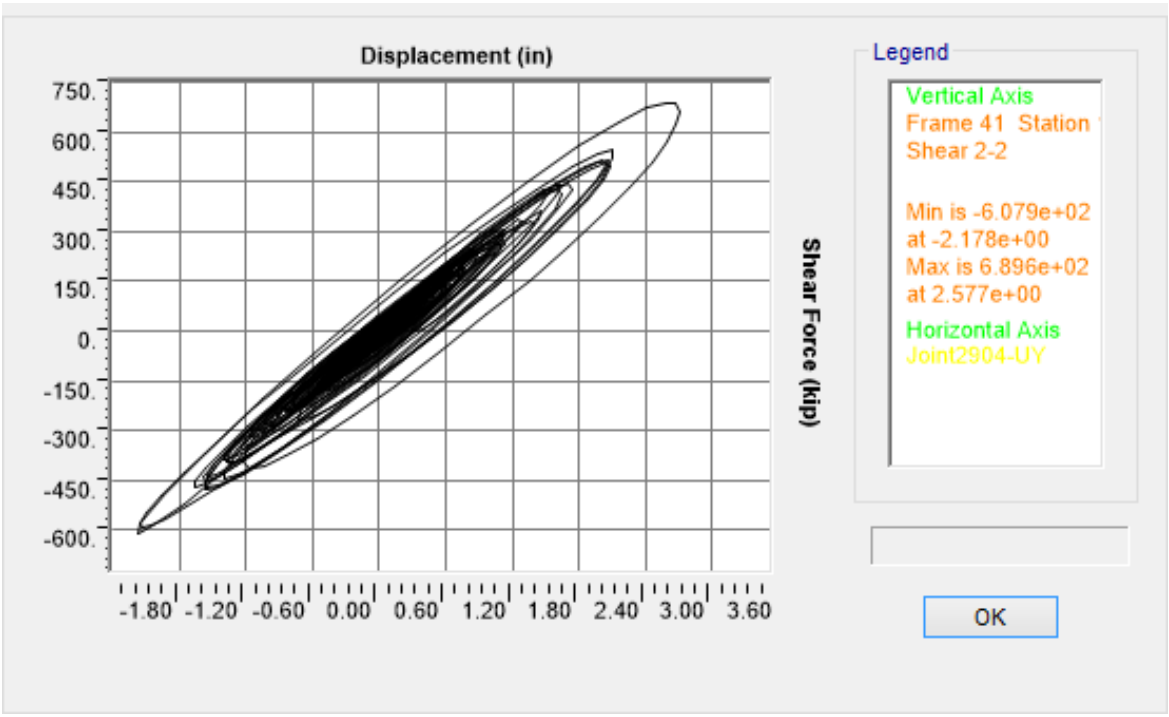

a)

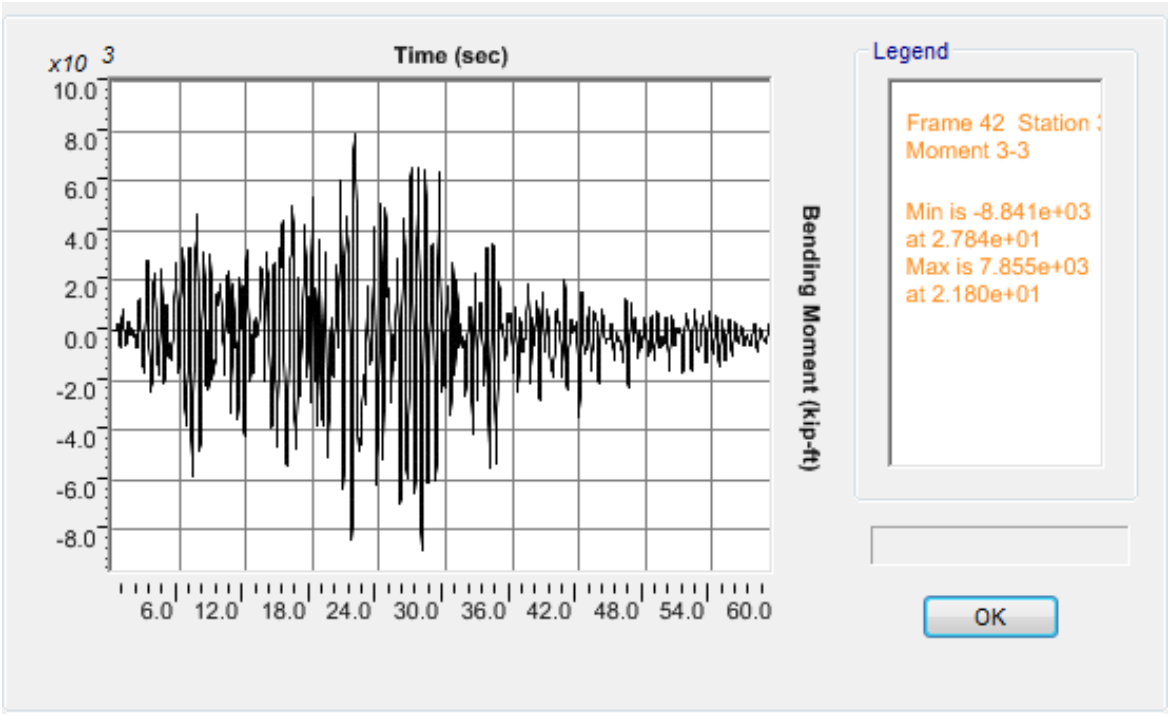

b)

Figure K.26 OSB1 column top response for Motion 26 ROCKS1N1: a) Transverse shear force-displacement hysteresis; b) Bending moment time history in the transverse direction

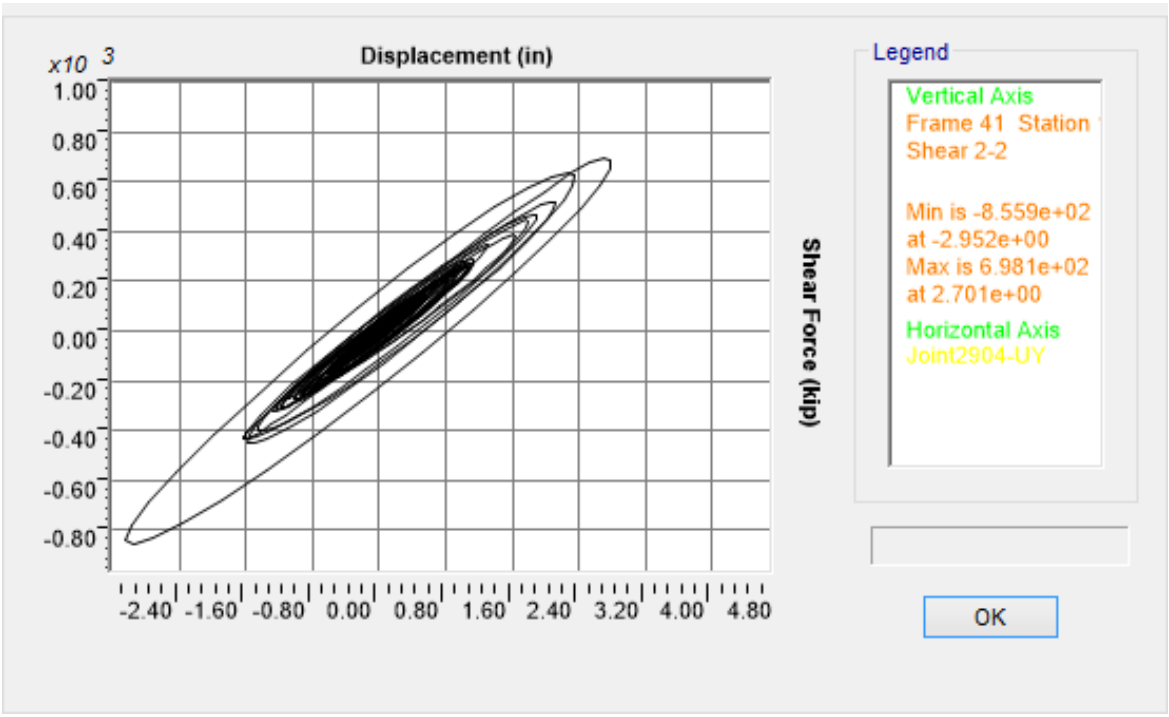

a)

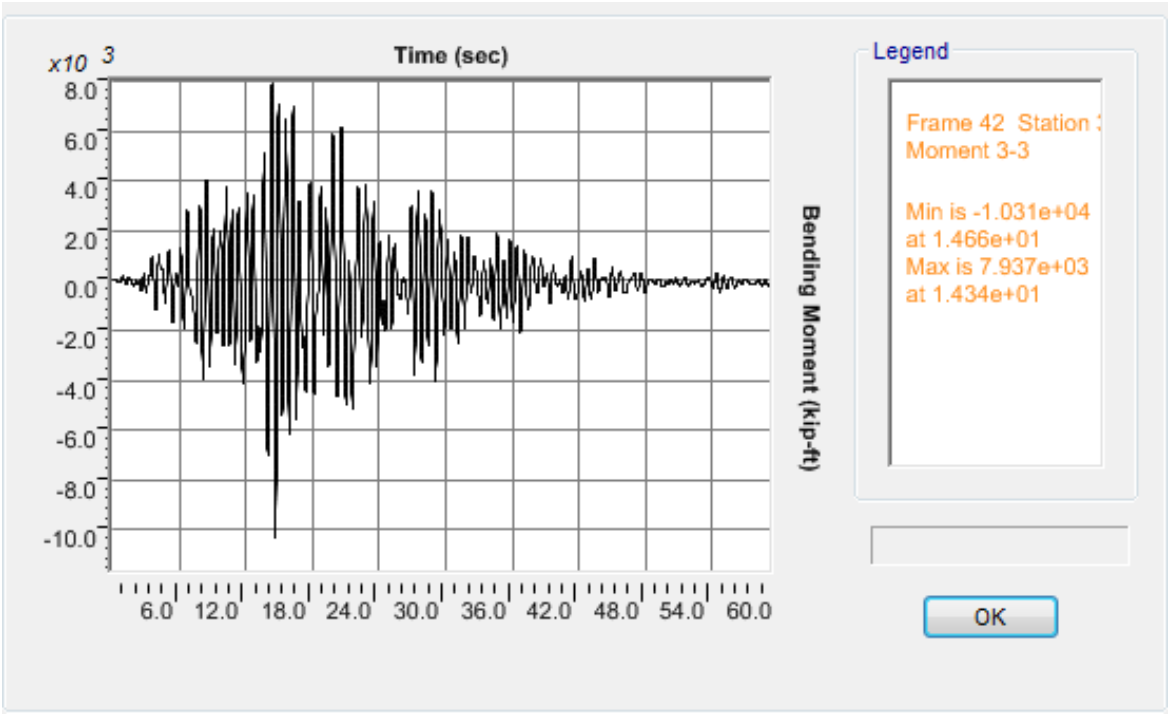

b)

Figure K.27 OSB1 column top response for Motion 27 ROCKS1N2: a) Transverse shear force-displacement hysteresis; b) Bending moment time history in the transverse direction

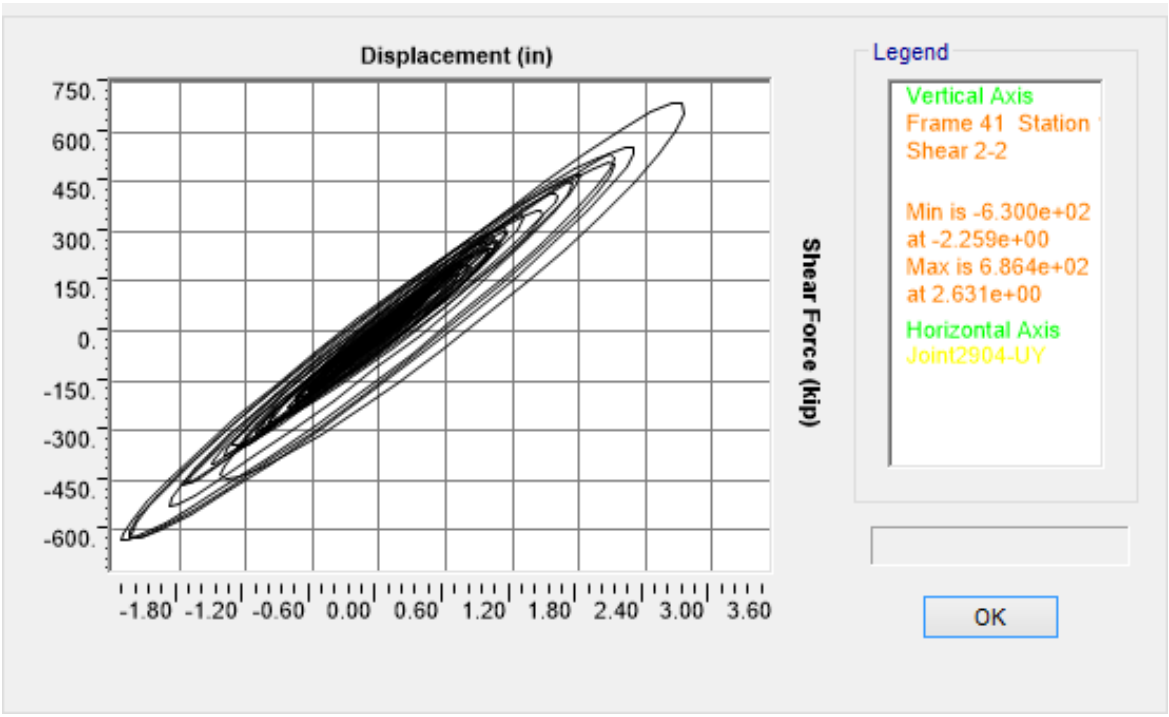

a)

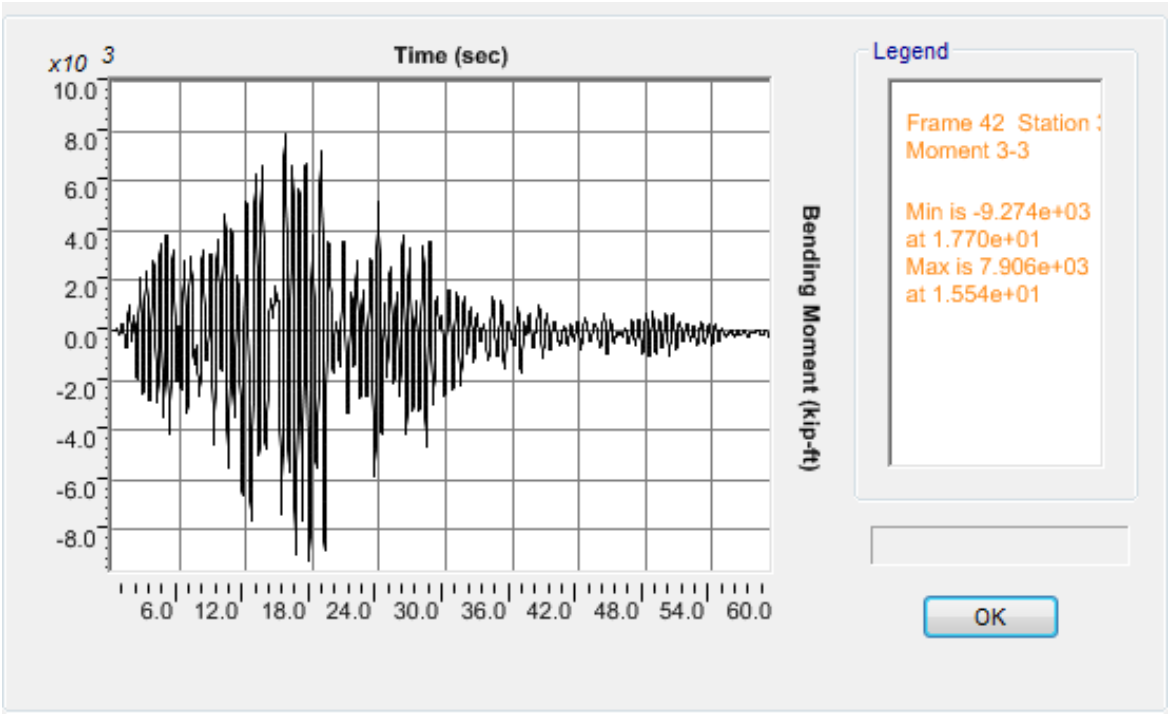

b)

Figure K.28 OSB1 column top response for Motion 28 ROCKS1N3: a) Transverse shear force-displacement hysteresis; b) Bending moment time history in the transverse direction

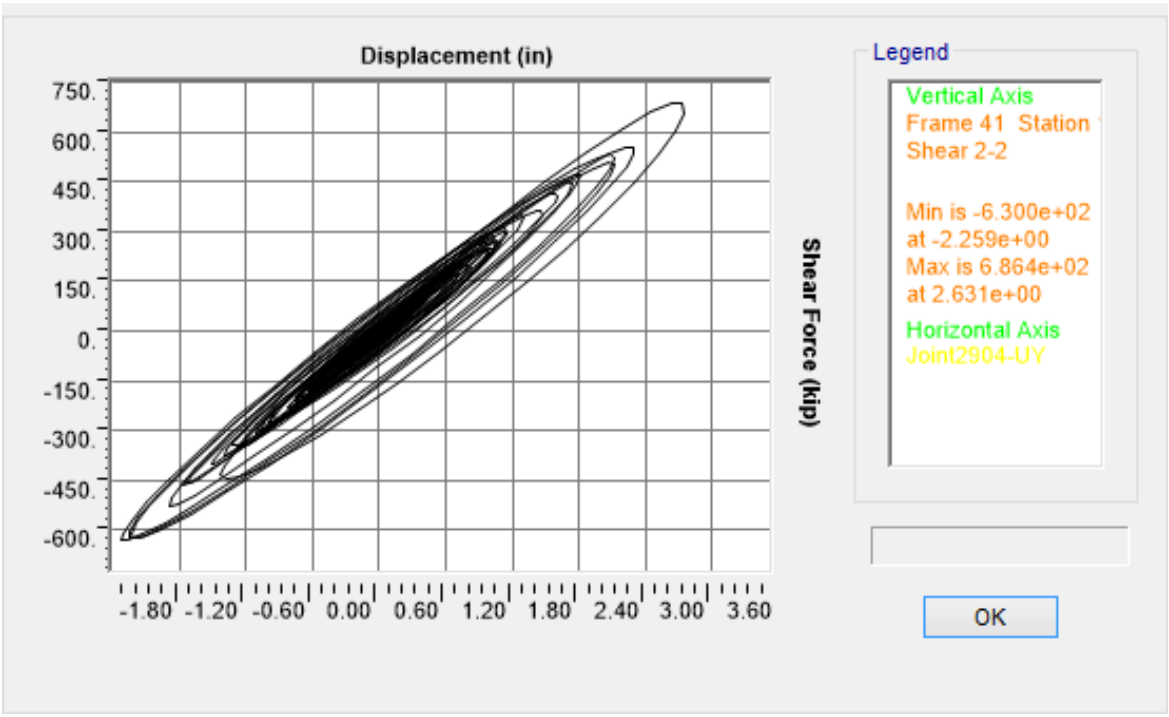

a)

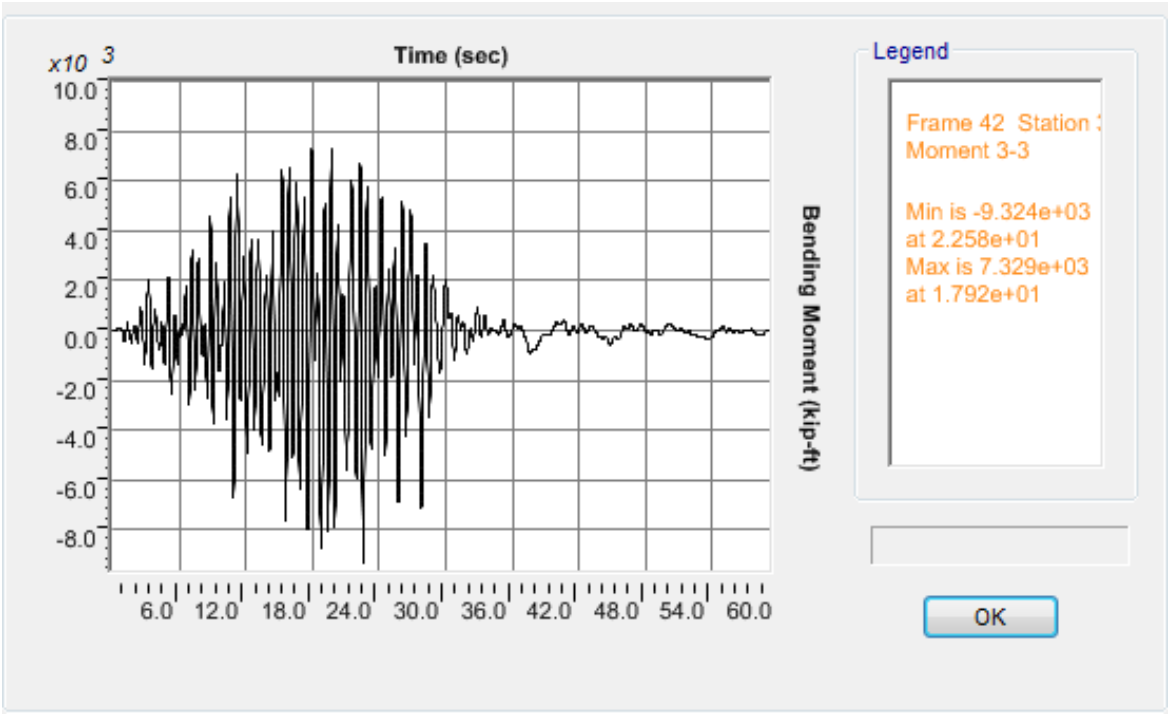

b)

Figure K.29 OSB1 column top response for Motion 29 ROCKS1N4: a) Transverse shear force-displacement hysteresis; b) Bending moment time history in the transverse direction

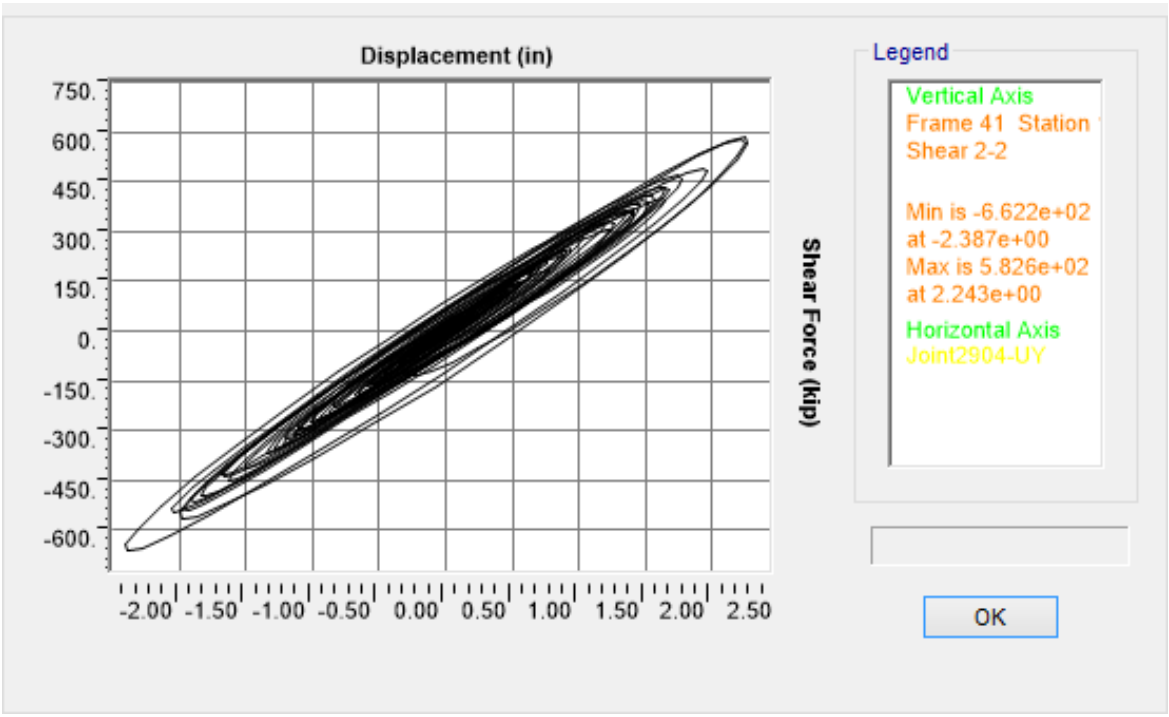

a)

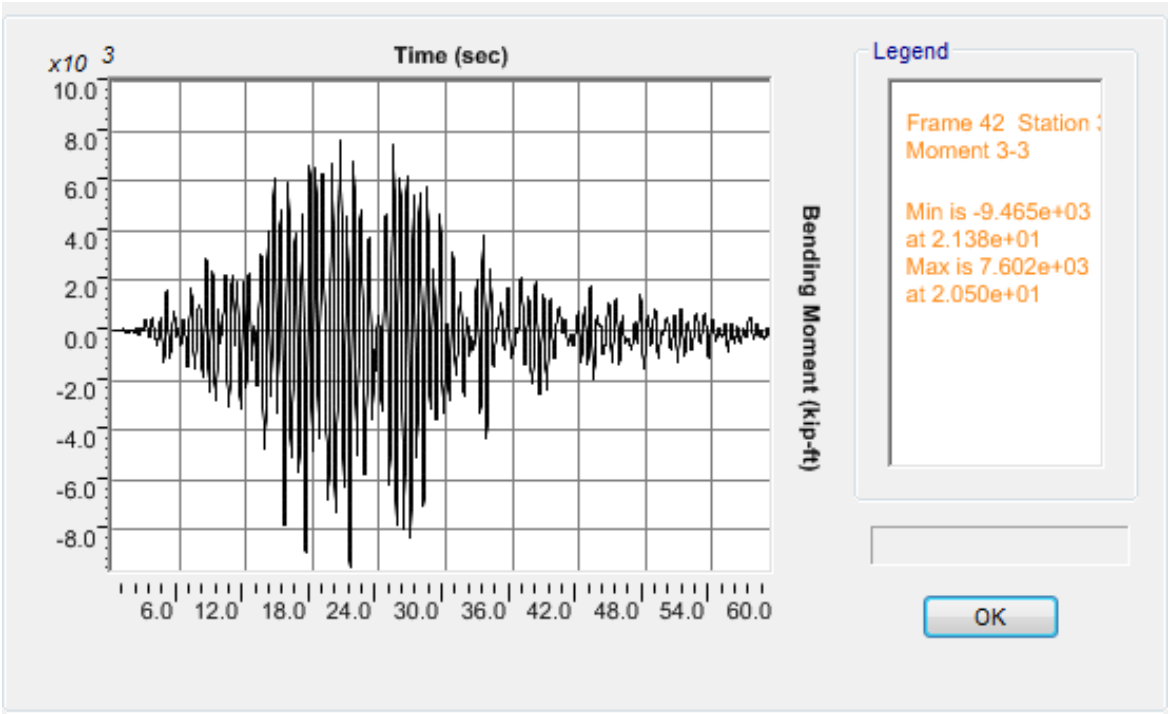

b)

Figure K.30 OSB1 column top response for Motion 30 ROCKS1N5: a) Transverse shear force-displacement hysteresis; b) Bending moment time history in the transverse direction

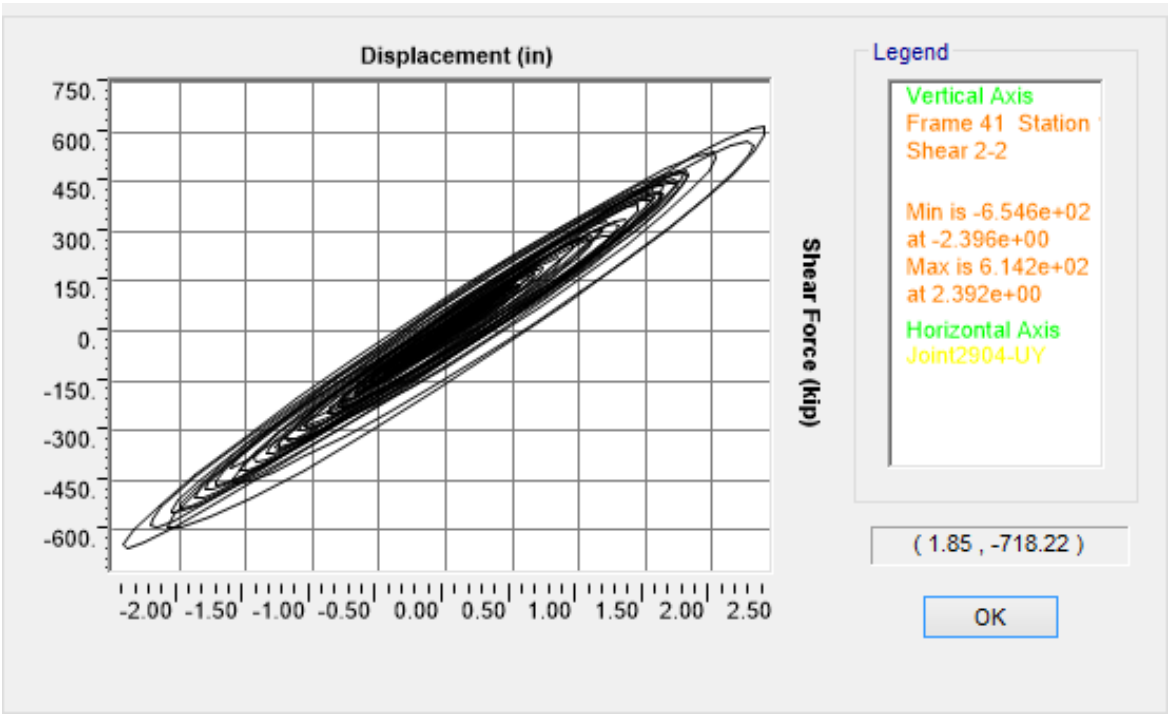

a)

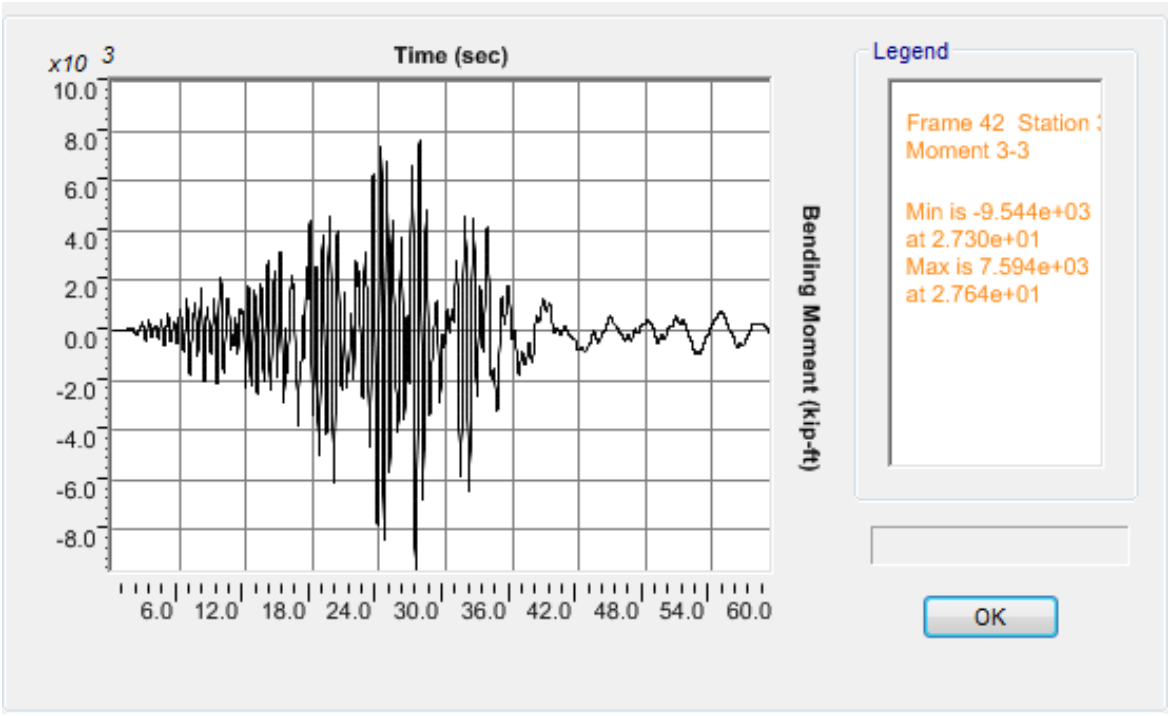

b)

Figure K.31 OSB1 column top response for Motion 31 ROCKS1N6: a) Transverse shear force-displacement hysteresis; b) Bending moment time history in the transverse direction

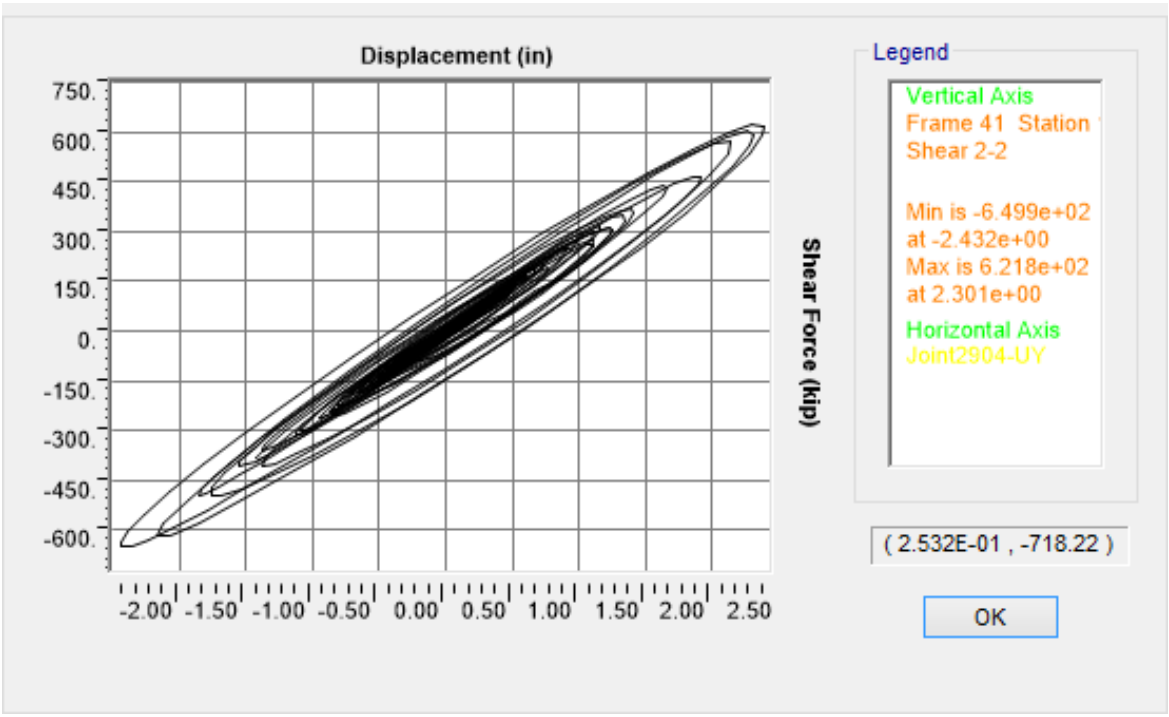

a)

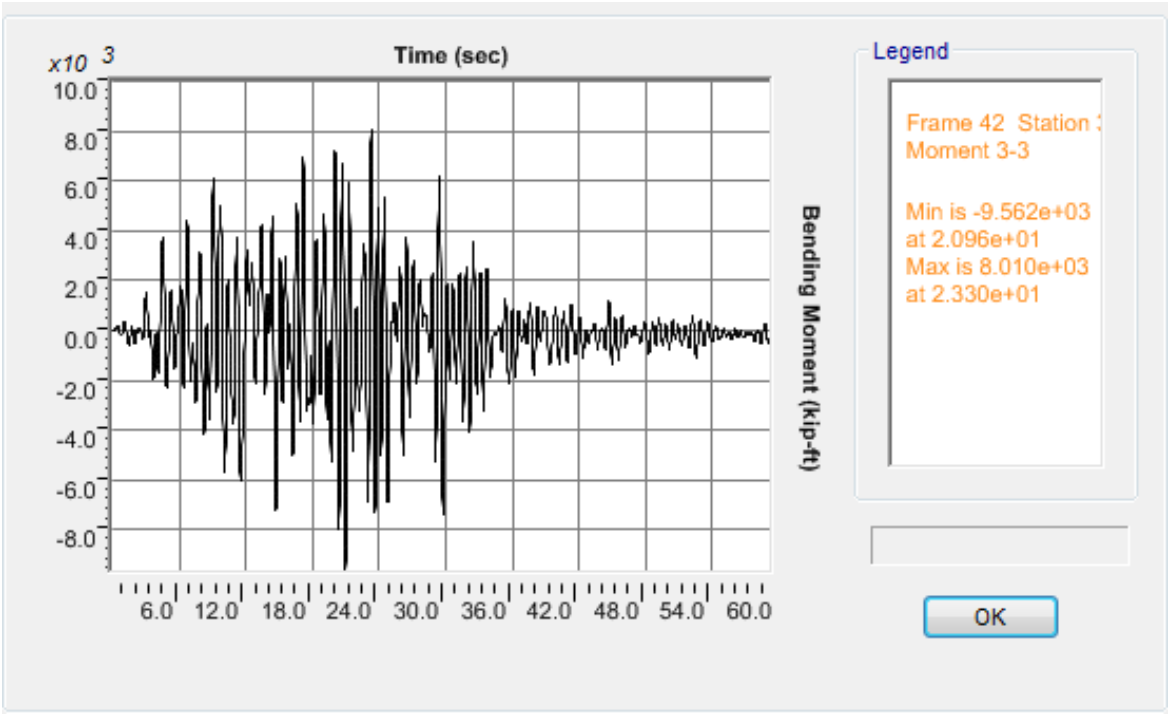

b)

Figure K.32 OSB1 column top response for Motion 32 ROCKS1N7: a) Transverse shear force-displacement hysteresis; b) Bending moment time history in the transverse direction

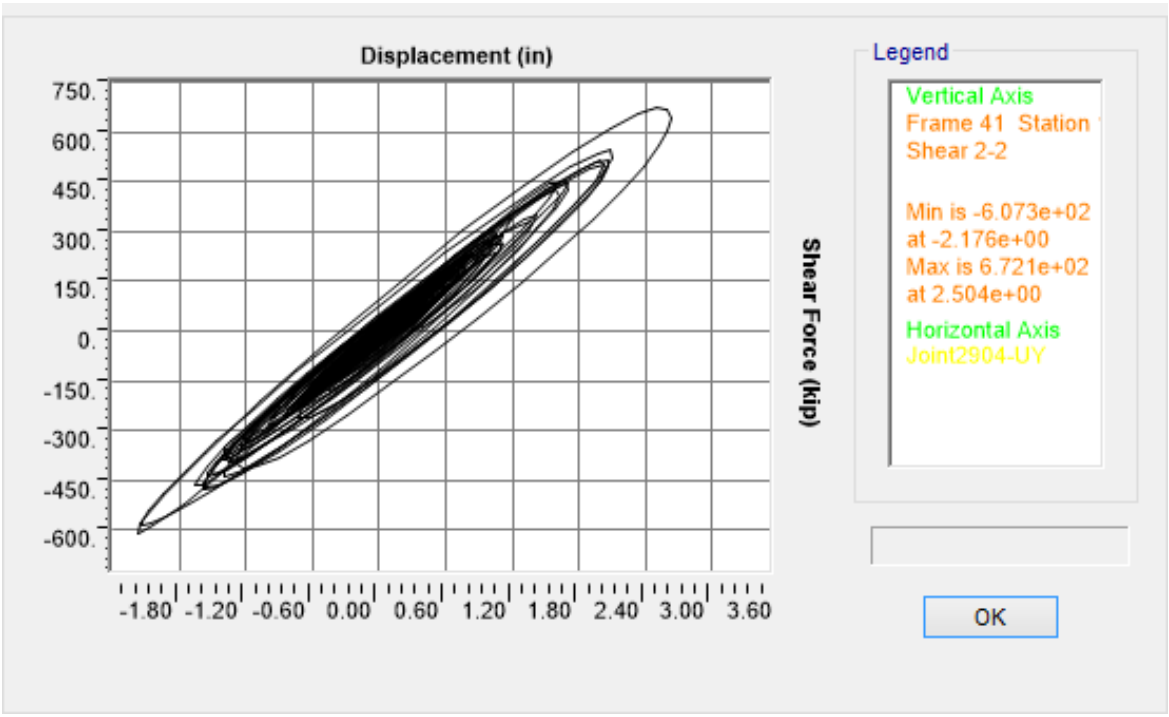

a)

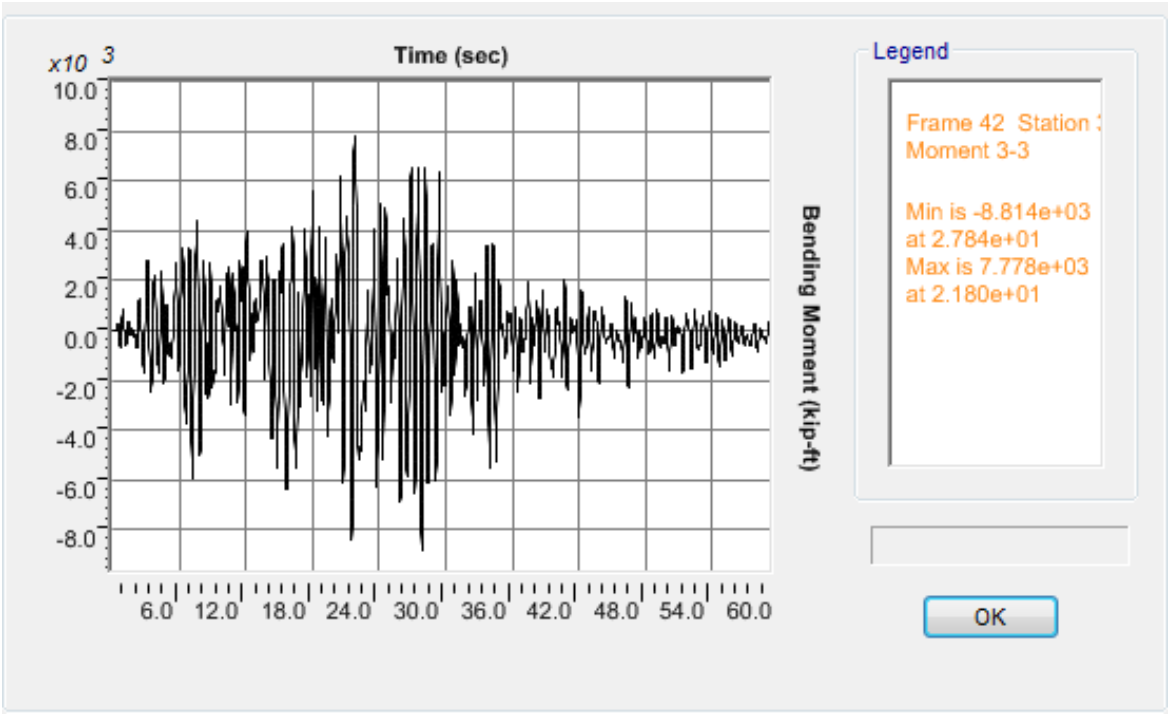

b)

Figure K.33 OSB1 column top response for Motion 33 ROCKS1P1: a) Transverse shear force-displacement hysteresis; b) Bending moment time history in the transverse direction

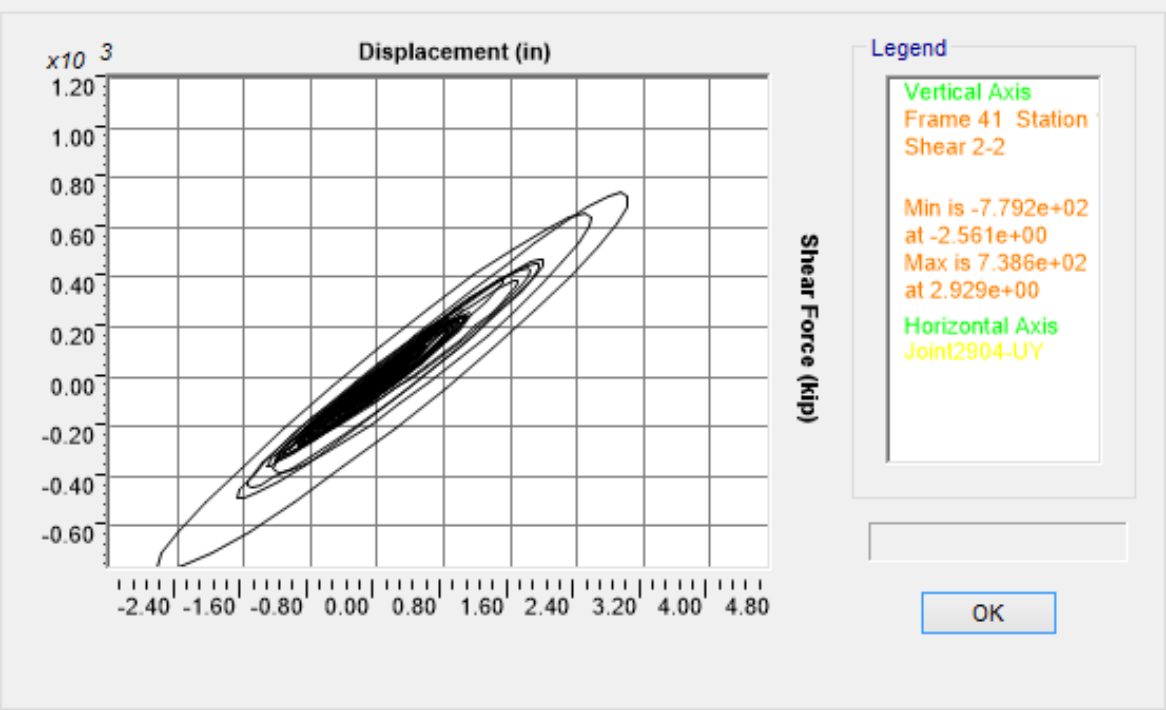

a)

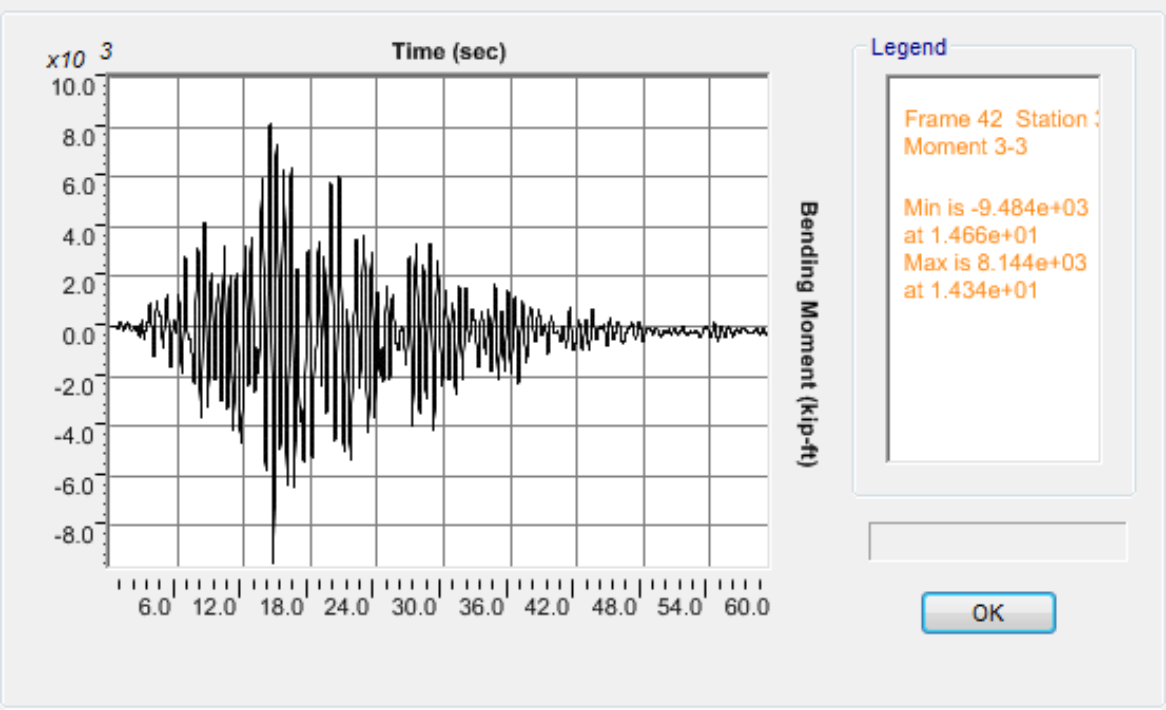

b)

Figure K.34 OSB1 column top response for Motion 34 ROCKS1P2: a) Transverse shear force-displacement hysteresis; b) Bending moment time history in the transverse direction

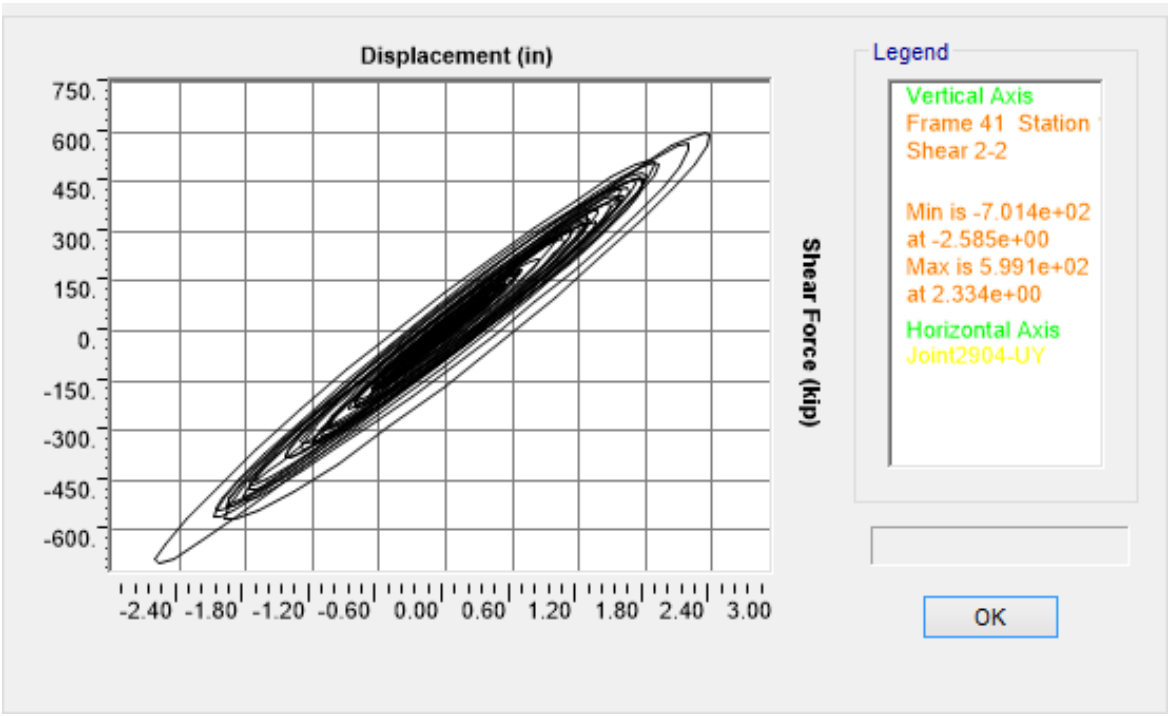

a)

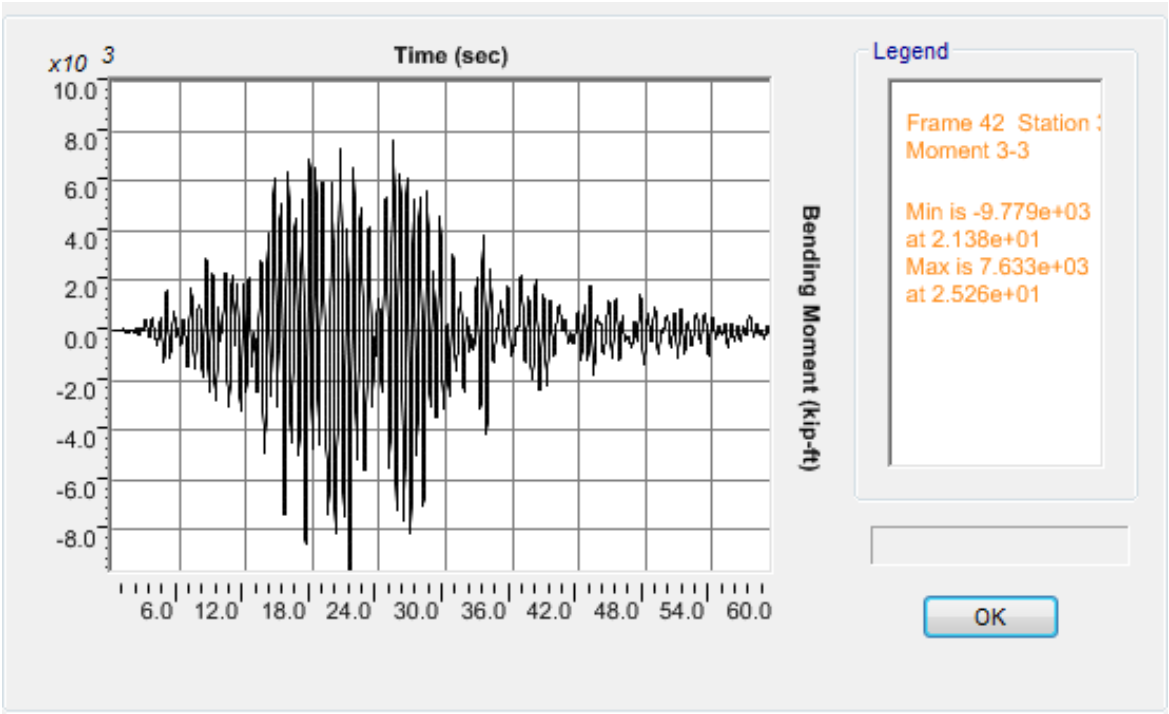

b)

Figure K.35 OSB1 column top response for Motion 35 ROCKS1P3: a) Transverse shear force-displacement hysteresis; b) Bending moment time history in the transverse direction

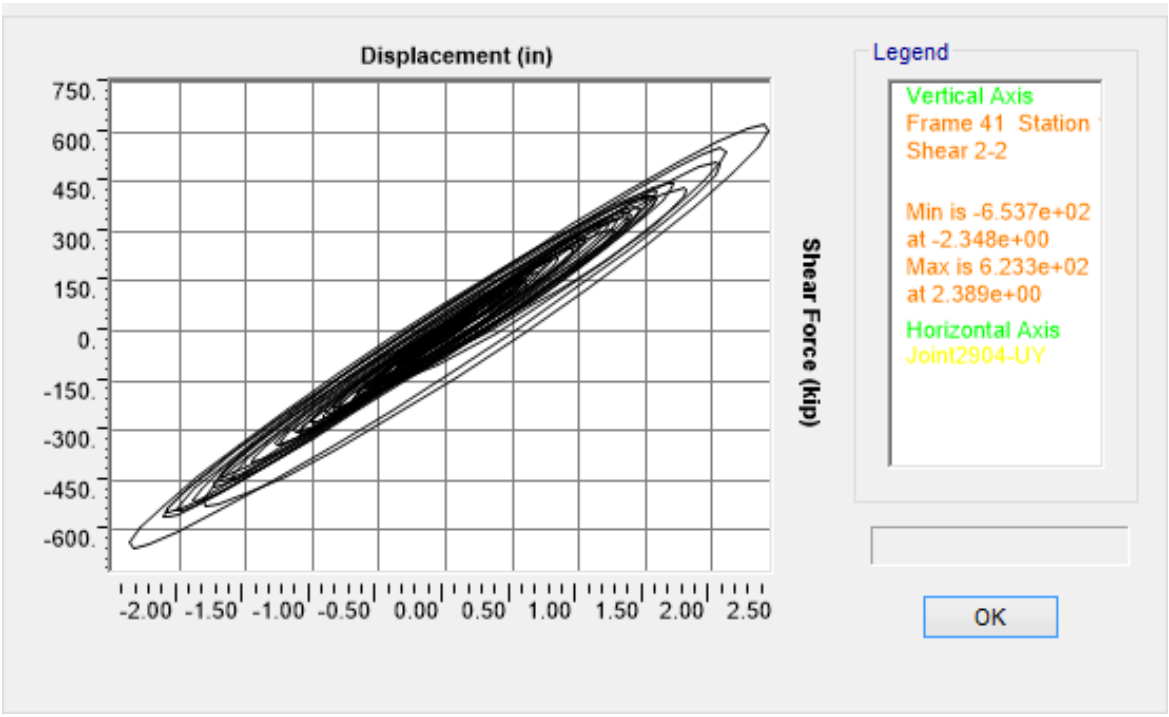

a)

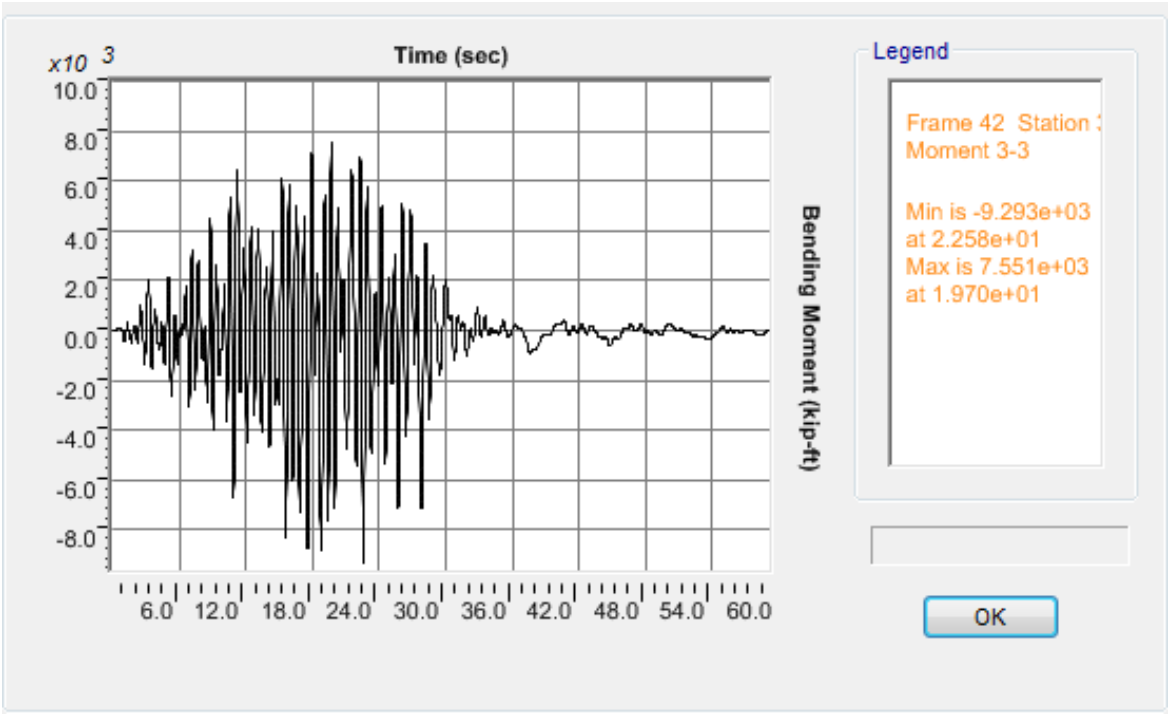

b)

Figure K.36 OSB1 column top response for Motion 36 ROCKS1P4: a) Transverse shear force-displacement hysteresis; b) Bending moment time history in the transverse direction

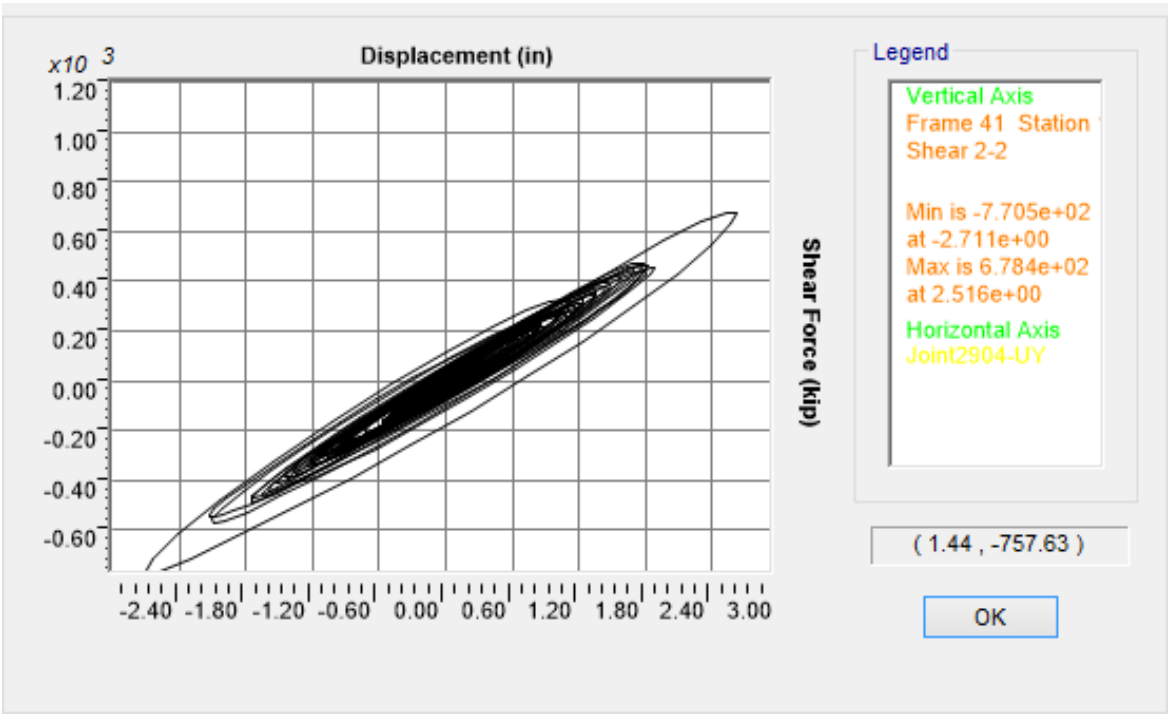

a)

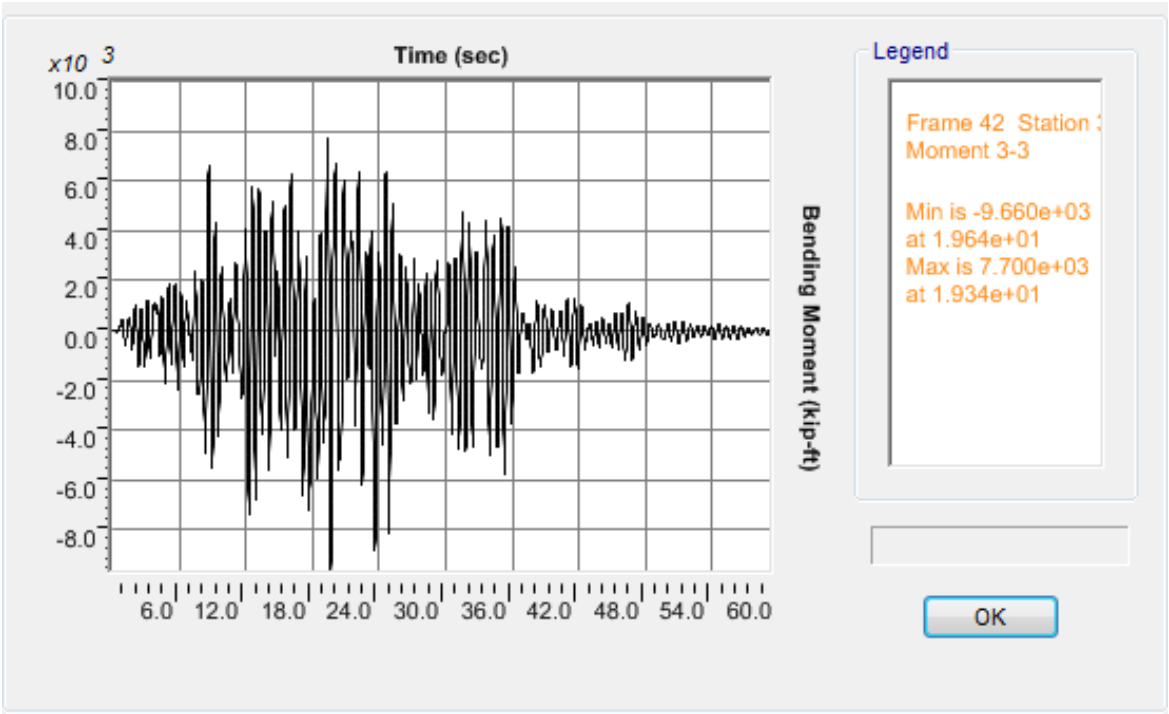

b)

Figure K.37 OSB1 column top response for Motion 37 ROCKS1P5: a) Transverse shear force-displacement hysteresis; b) Bending moment time history in the transverse direction

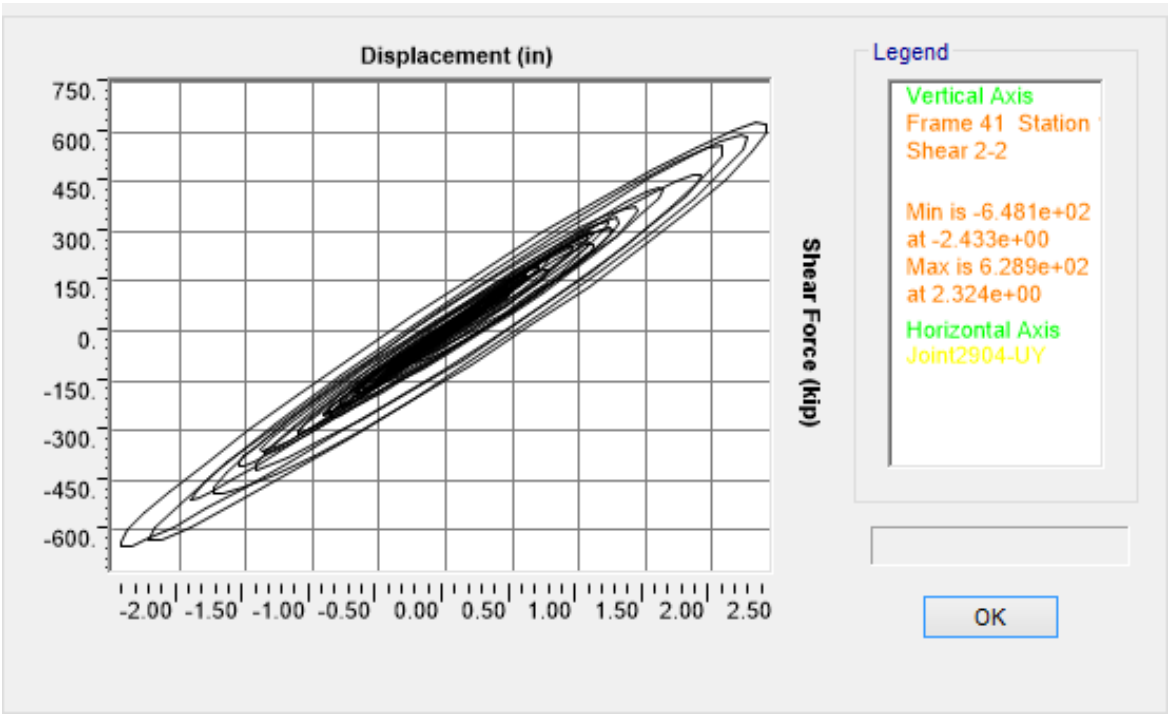

a)

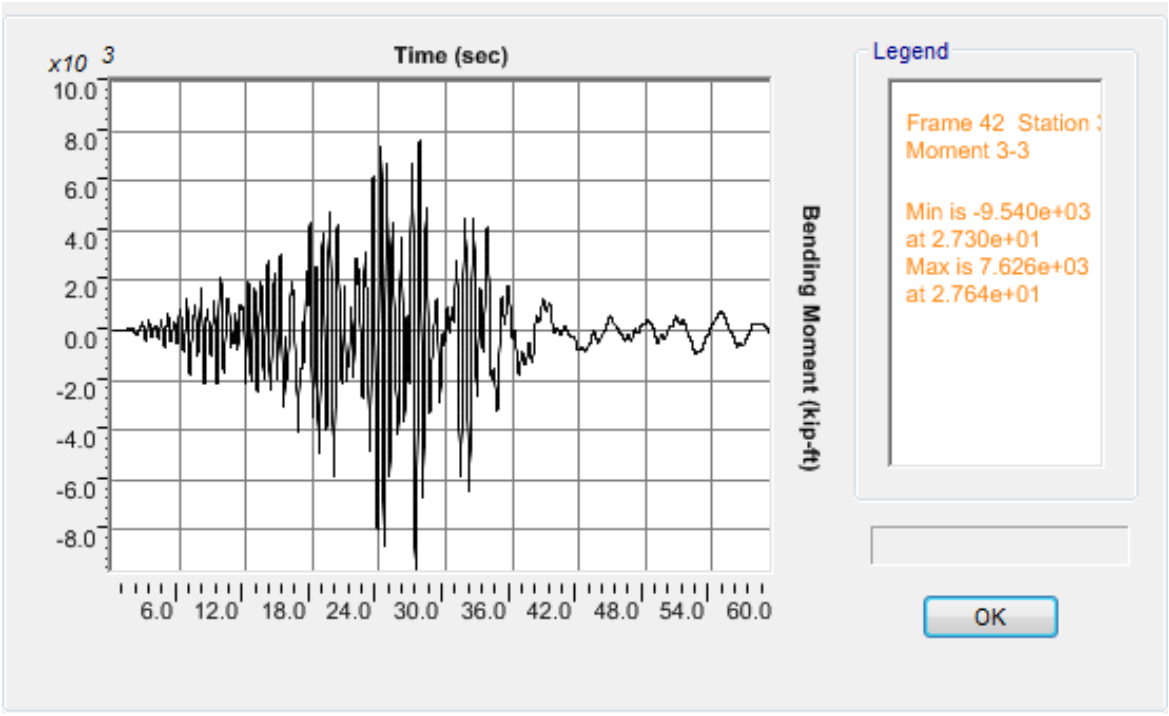

b)

Figure K.38 OSB1 column top response for Motion 38 ROCKS1P6: a) Transverse shear force-displacement hysteresis; b) Bending moment time history in the transverse direction

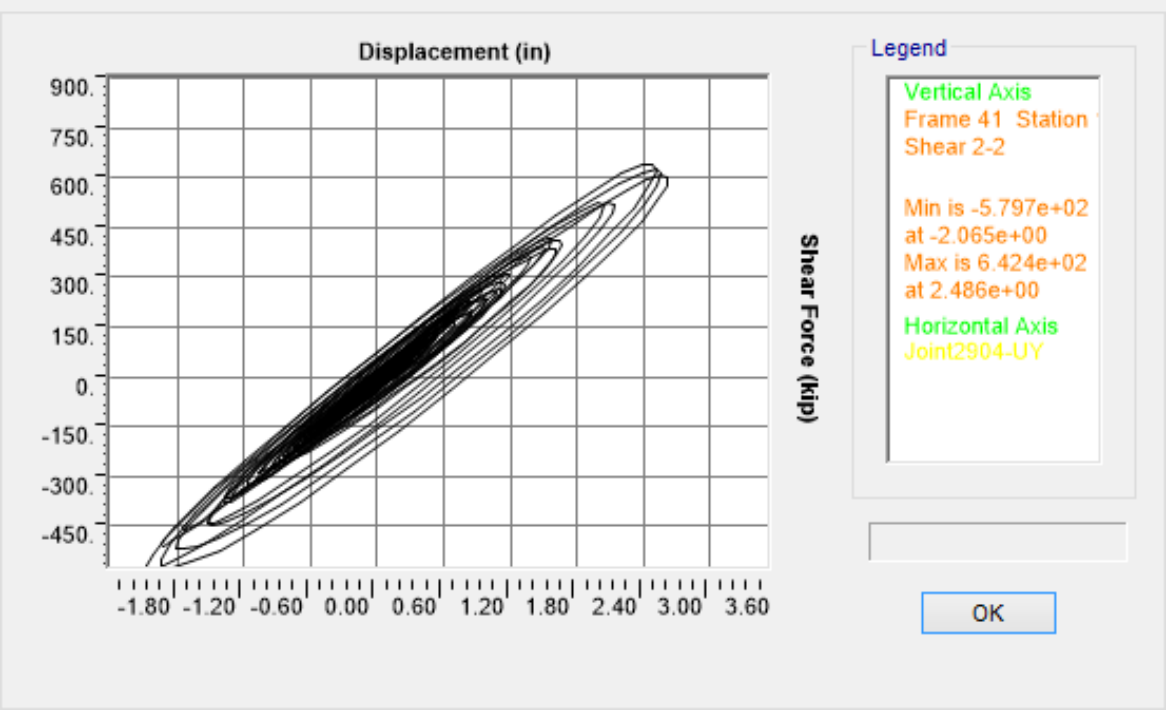

a)

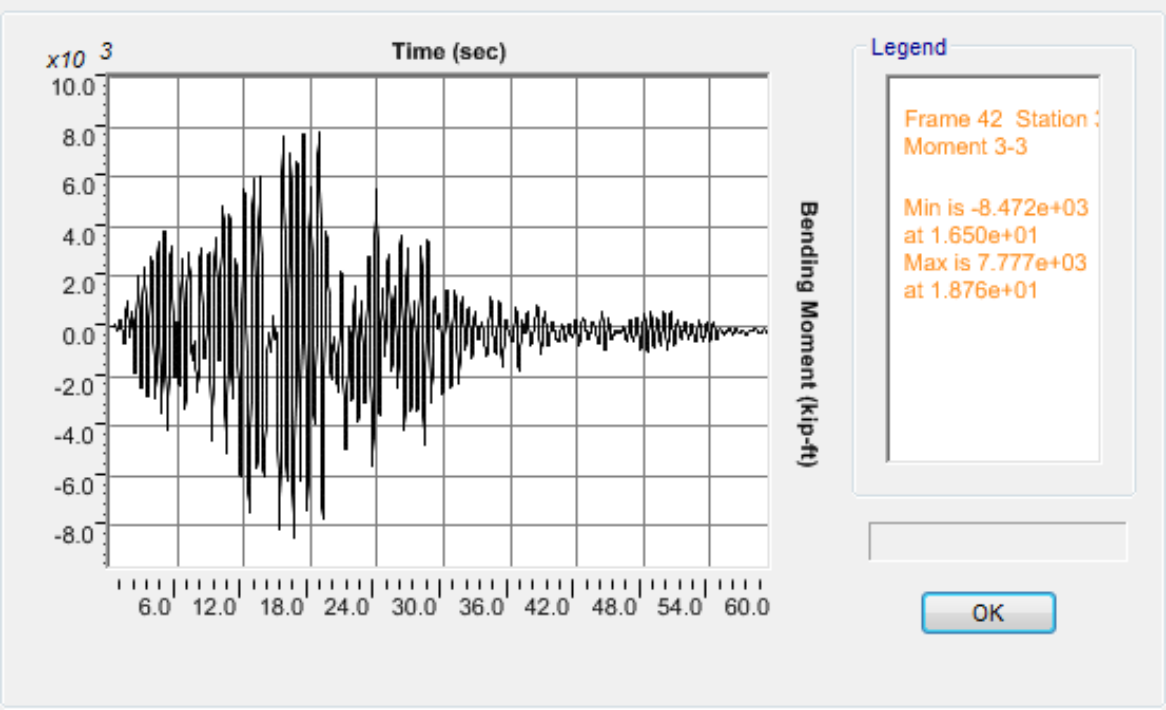

b)

Figure K.39 OSB1 column top response for Motion 39 ROCKS1P7: a) Transverse shear force-displacement hysteresis; b) Bending moment time history in the transverse direction

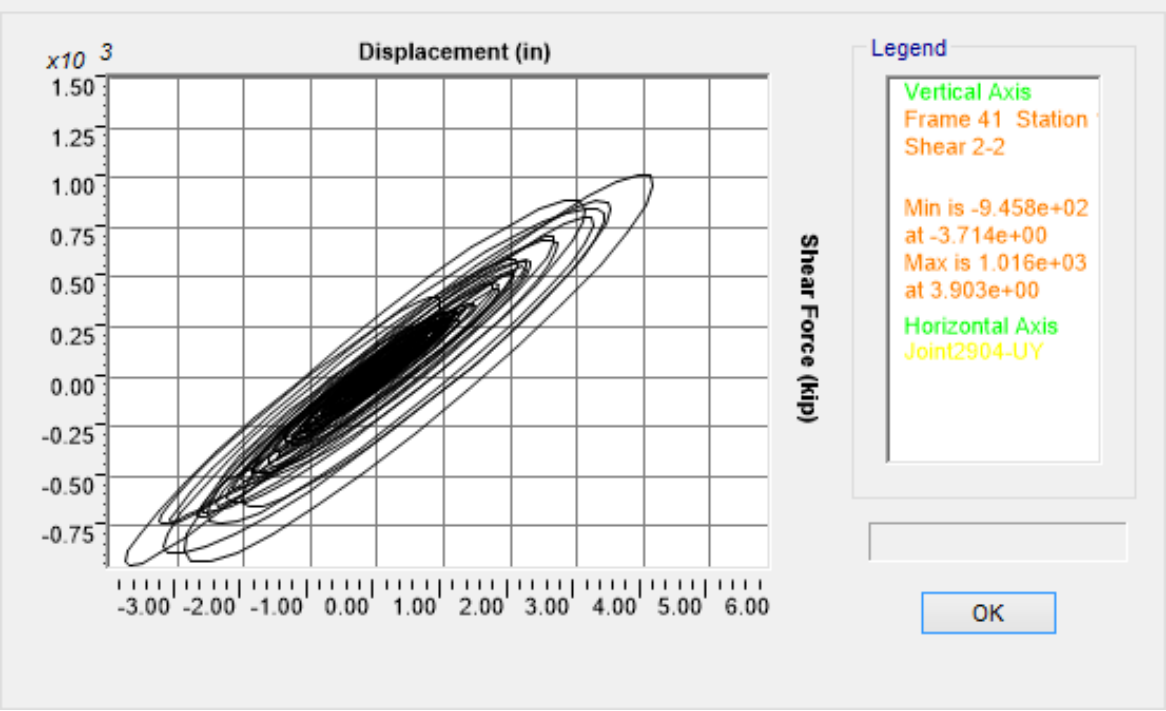

a)

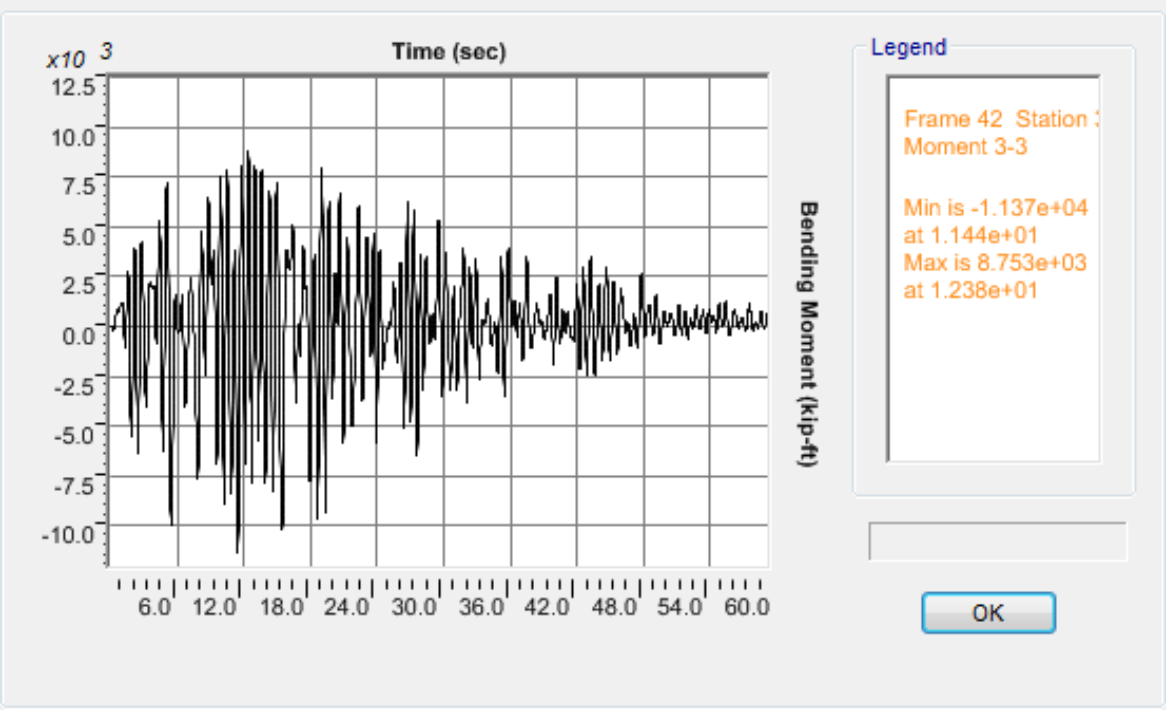

b)

Figure K.40 OSB1 column top response for Motion 40 SANDS1N1: a) Transverse shear force-displacement hysteresis; b) Bending moment time history in the transverse direction

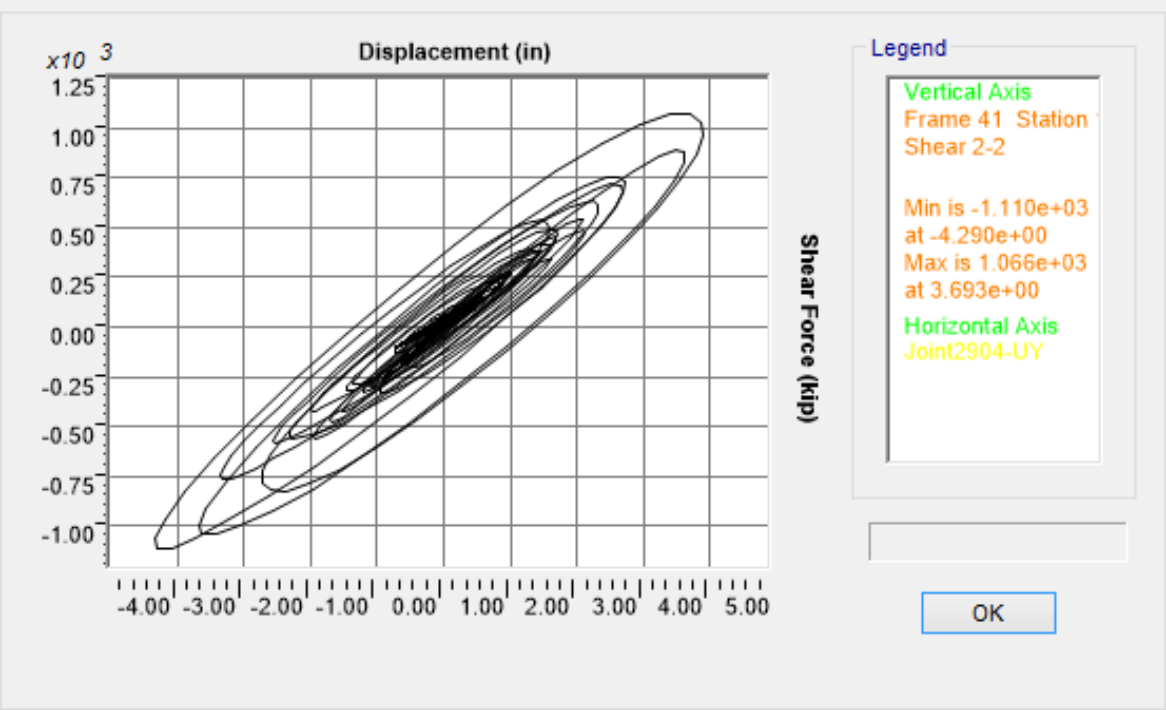

a)

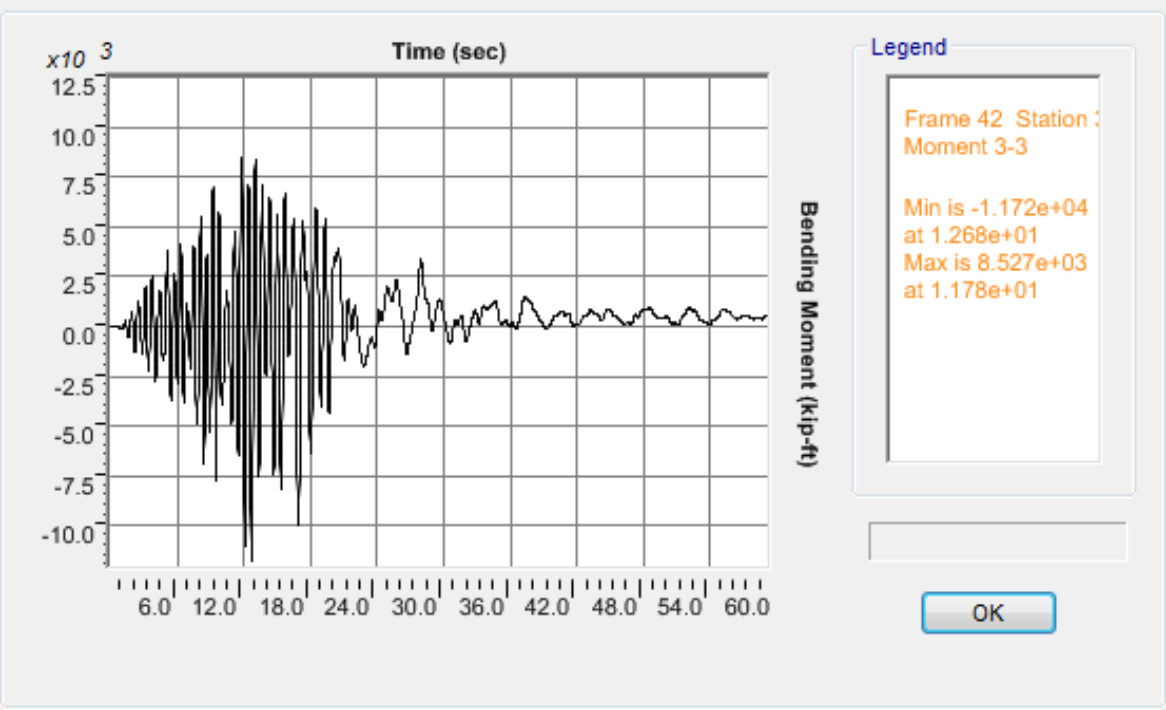

b)

Figure K.41 OSB1 column top response for Motion 41 SANDS1N2: a) Transverse shear force-displacement hysteresis; b) Bending moment time history in the transverse direction

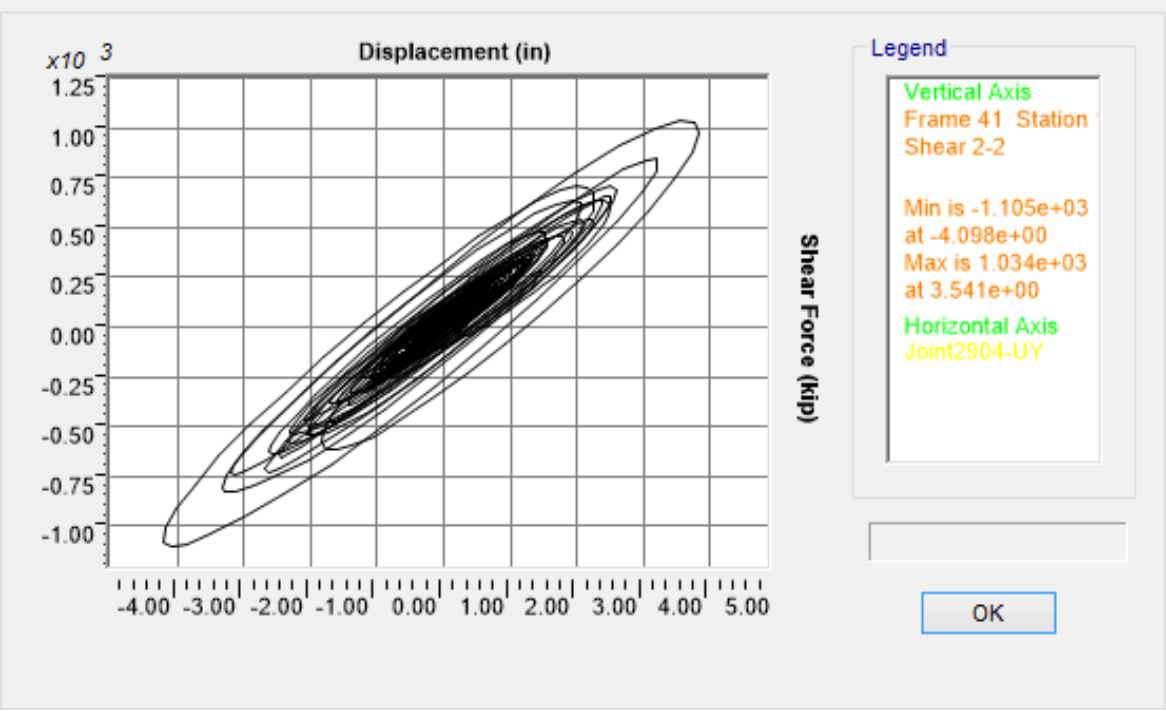

a)

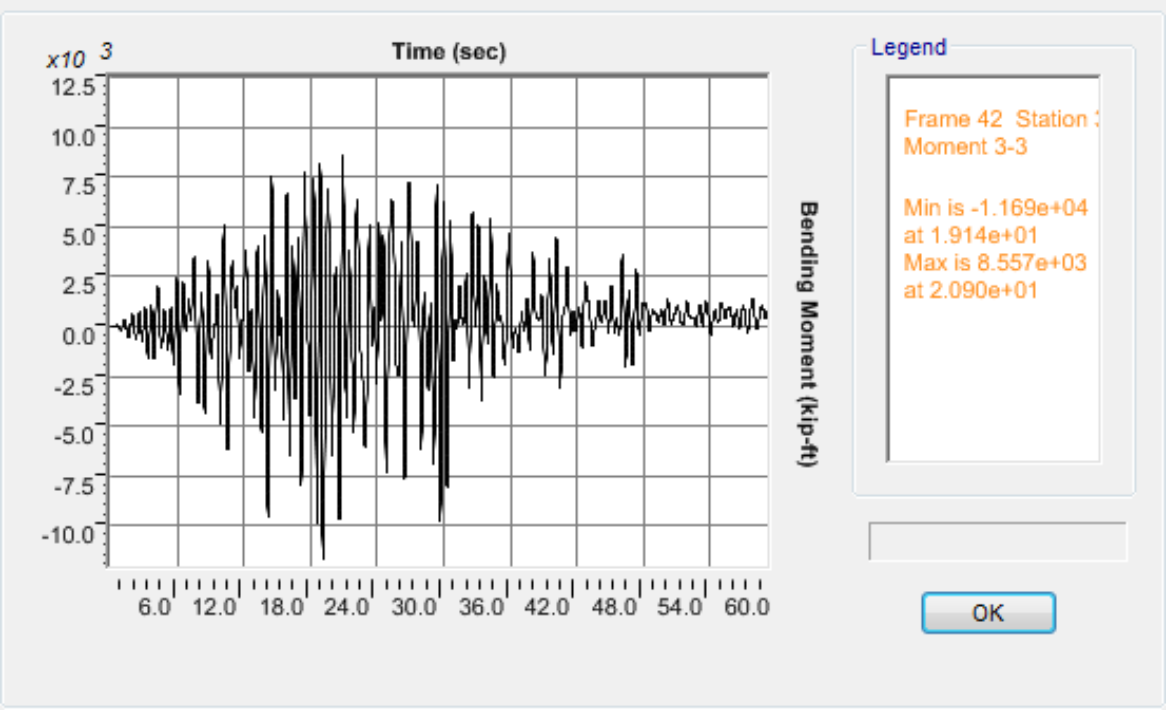

b)

Figure K.42 OSB1 column top response for Motion 42 SANDS1N3: a) Transverse shear force-displacement hysteresis; b) Bending moment time history in the transverse direction

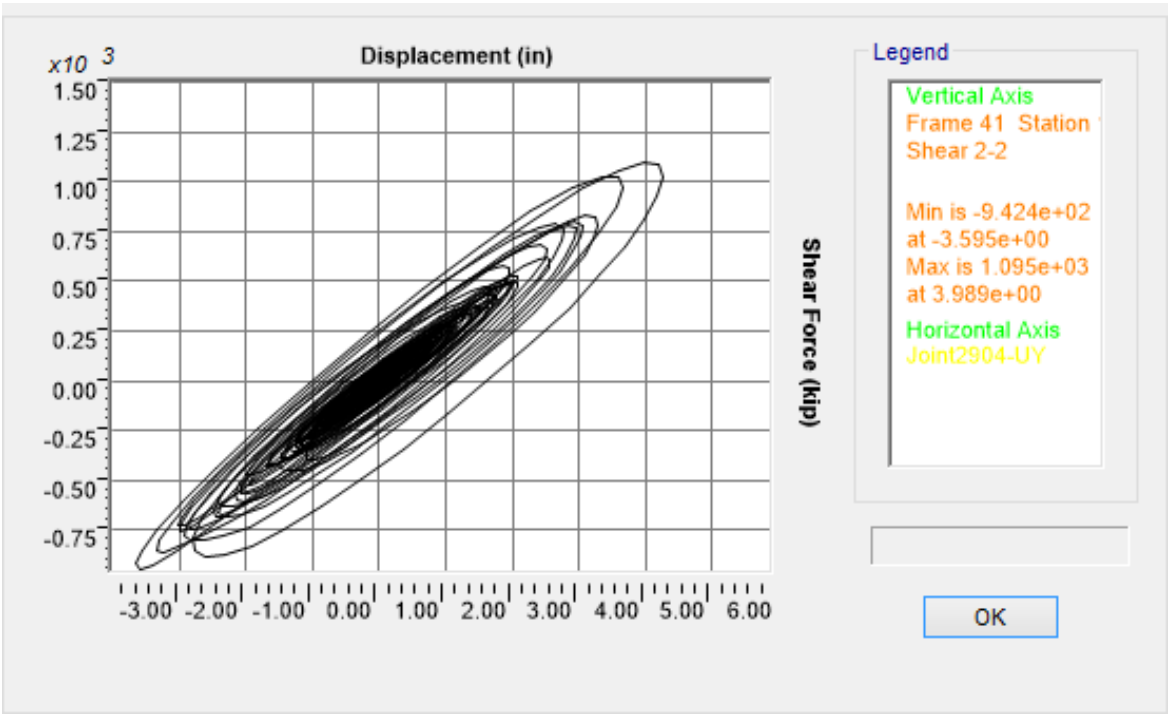

a)

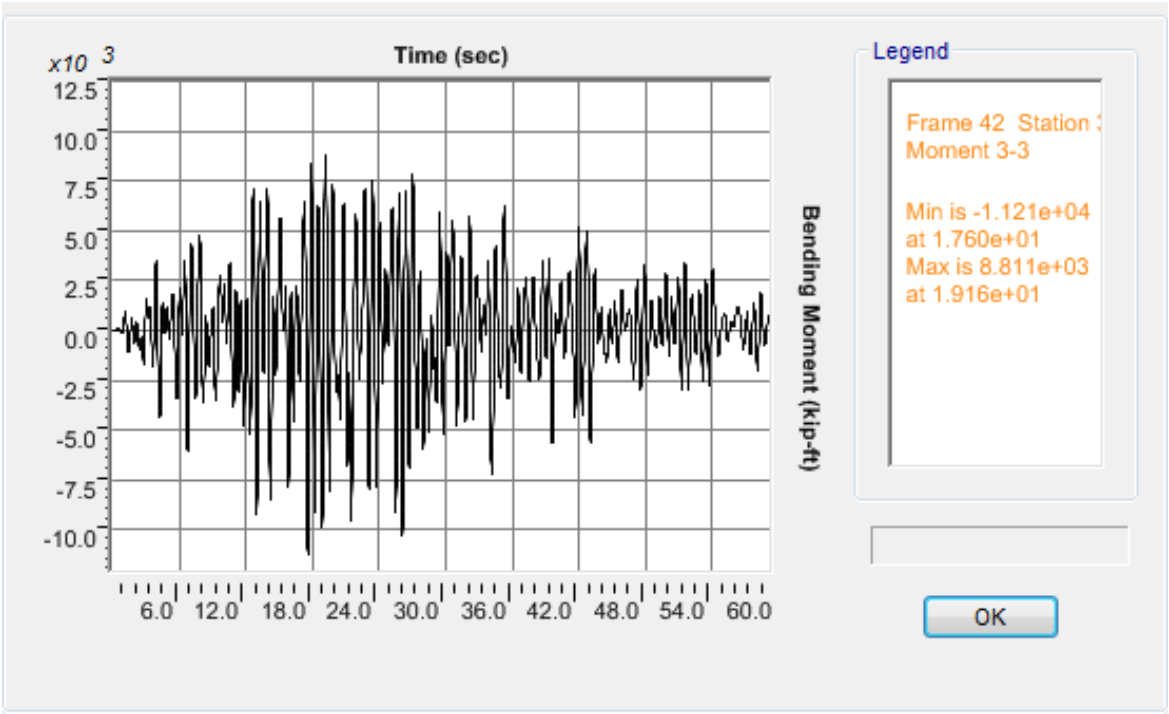

b)

Figure K.43 OSB1 column top response for Motion 43 SANDS1N4: a) Transverse shear force-displacement hysteresis; b) Bending moment time history in the transverse direction

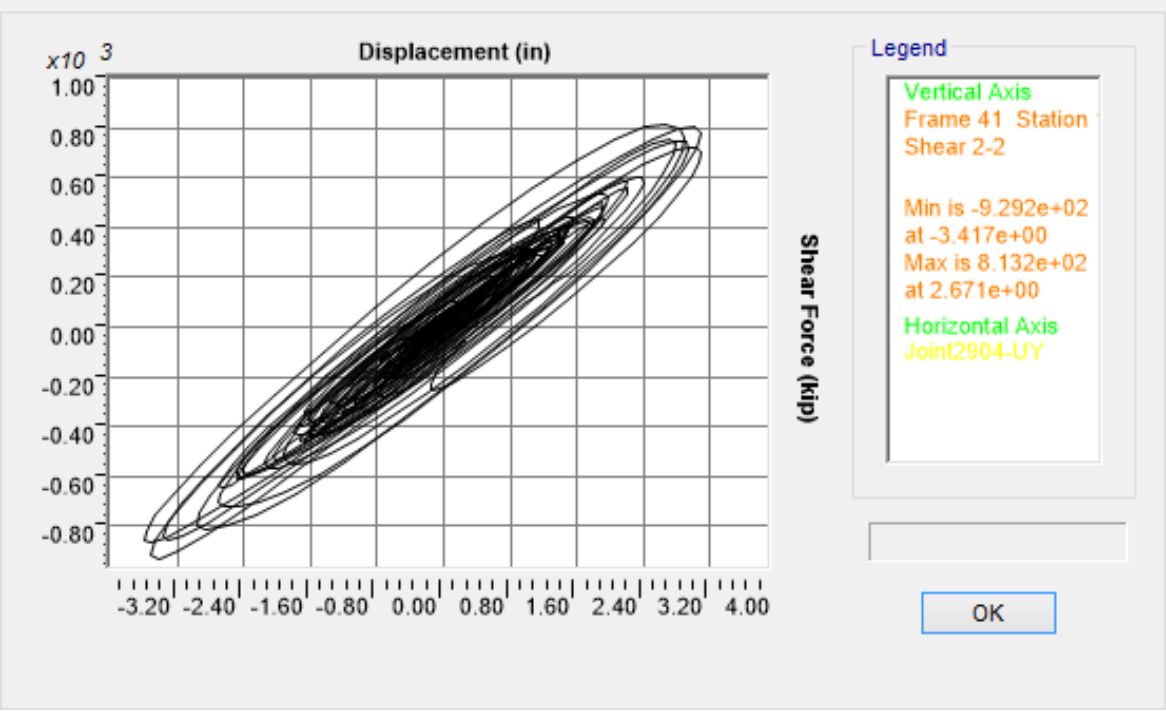

a)

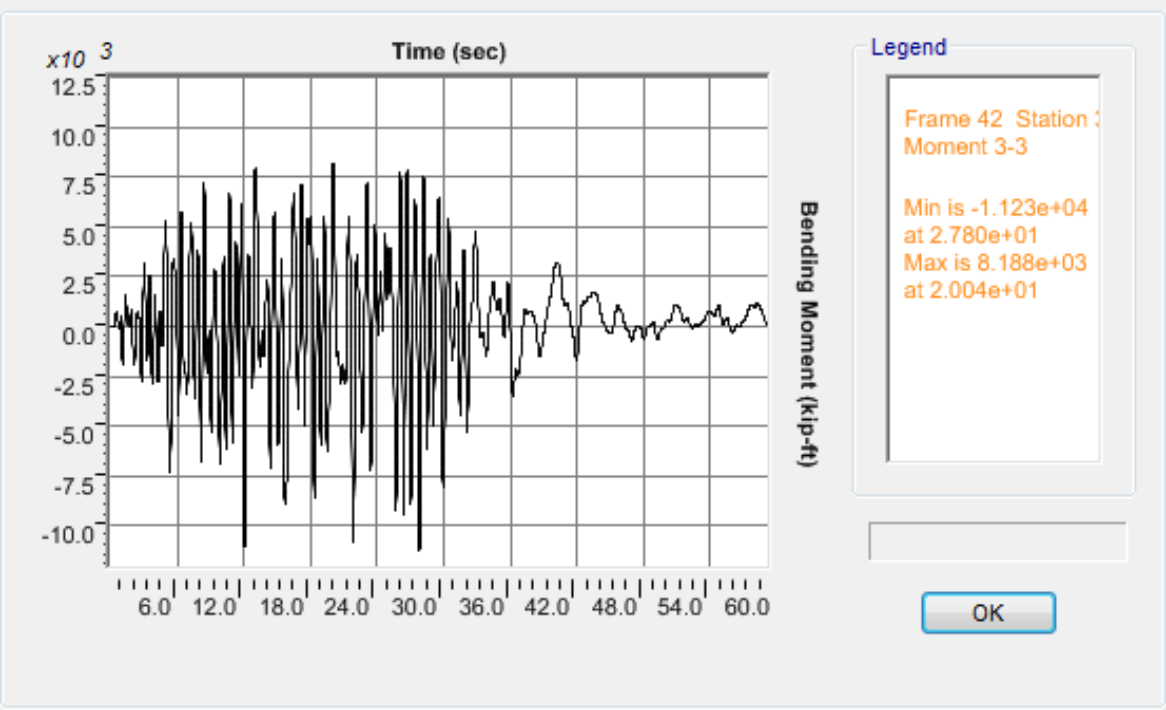

b)

Figure K.44 OSB1 column top response for Motion 44 SANDS1N5: a) Transverse shear force-displacement hysteresis; b) Bending moment time history in the transverse direction

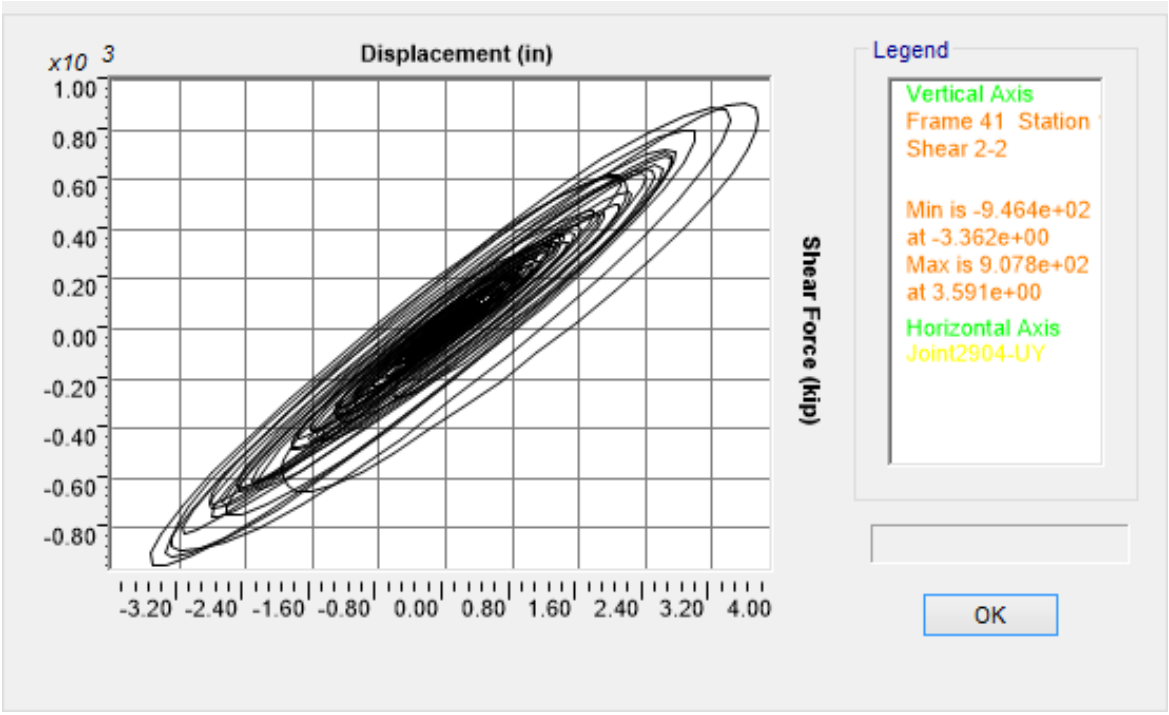

a)

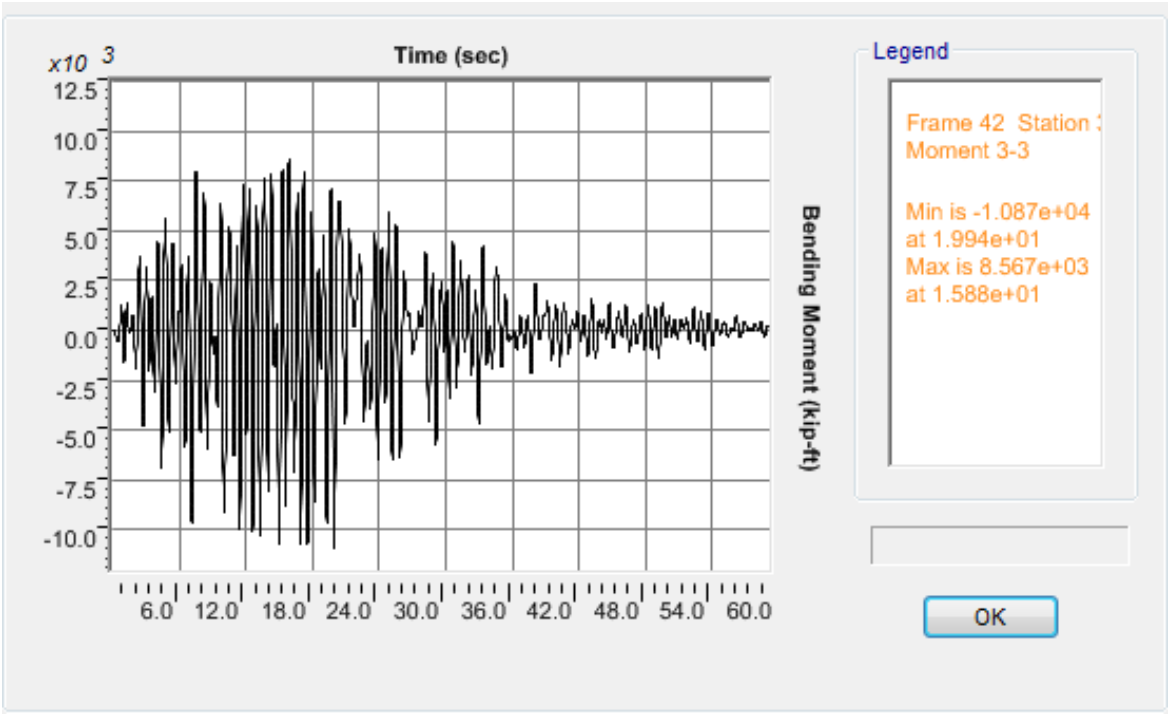

b)

Figure K.45 OSB1 column top response for Motion 45 SANDS1N6: a) Transverse shear force-displacement hysteresis; b) Bending moment time history in the transverse direction

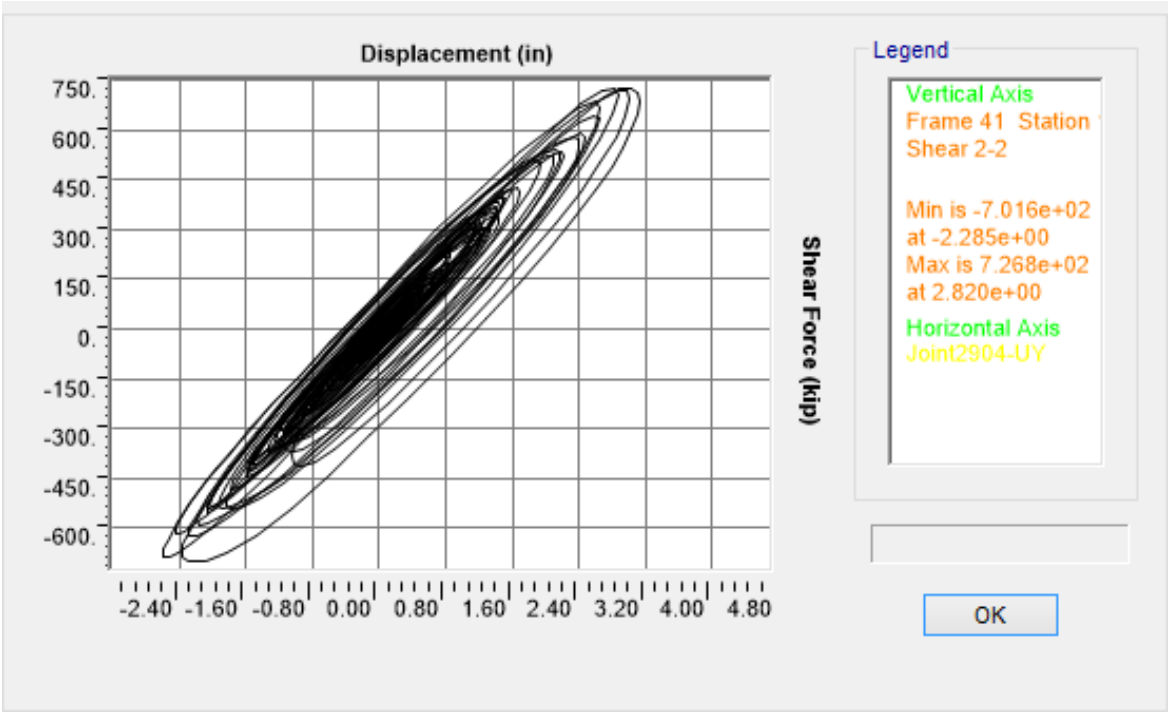

a)

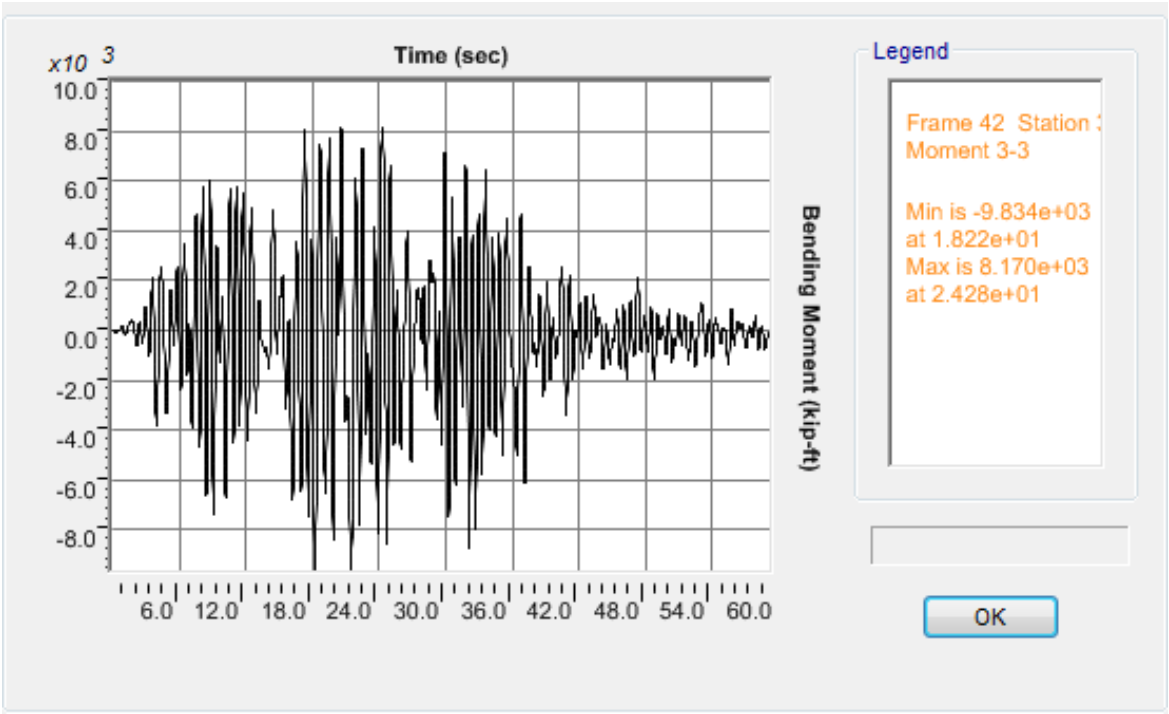

b)

Figure K.46 OSB1 column top response for Motion 46 SANDS1N7: a) Transverse shear force-displacement hysteresis; b) Bending moment time history in the transverse direction

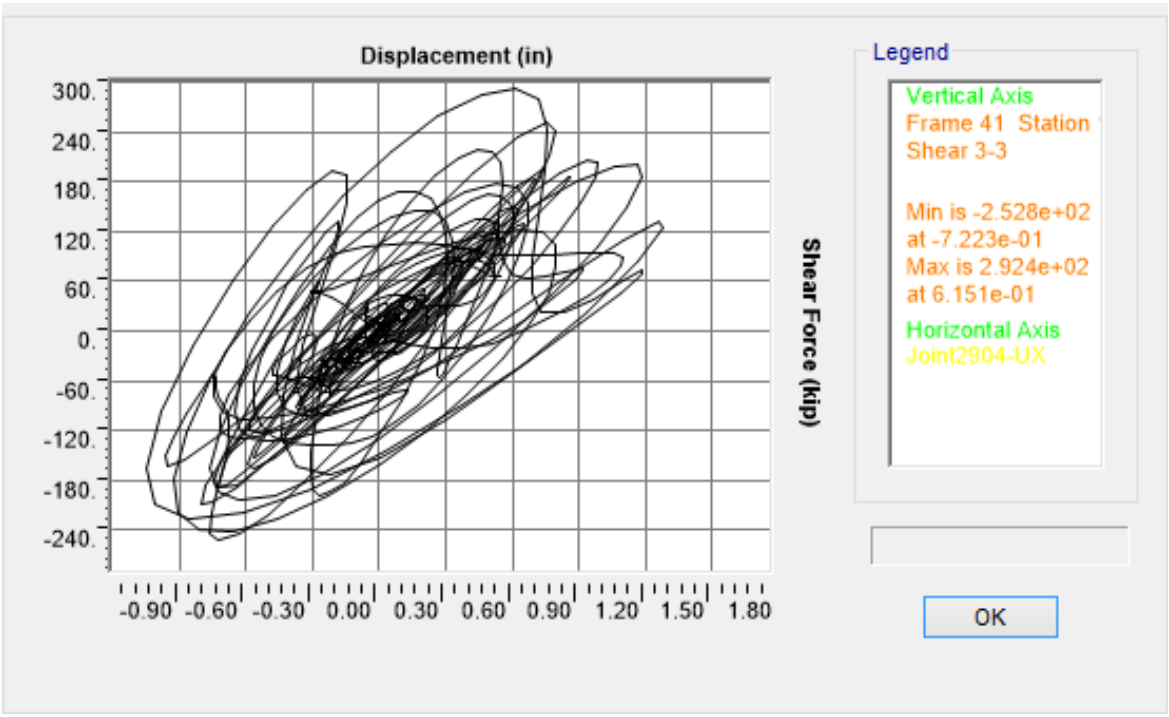
Displacement (in)
300.
240.
180.
120.
60.
0.
-60.
-120.
-180.
-240.
-0.90 -0.60 -0.30 0.00 0.30 0.60 0.90 1.20 1.50 1.80
Shear Force (kip)
Legend
Vertical Axis
Frame 41 Station
Shear 3-3
Min is -2.528e+02
at -7.223e-01
Max is 2.924e+02
at 6.151e-01
Horizontal Axis
Joint2904-UX
OK

a)

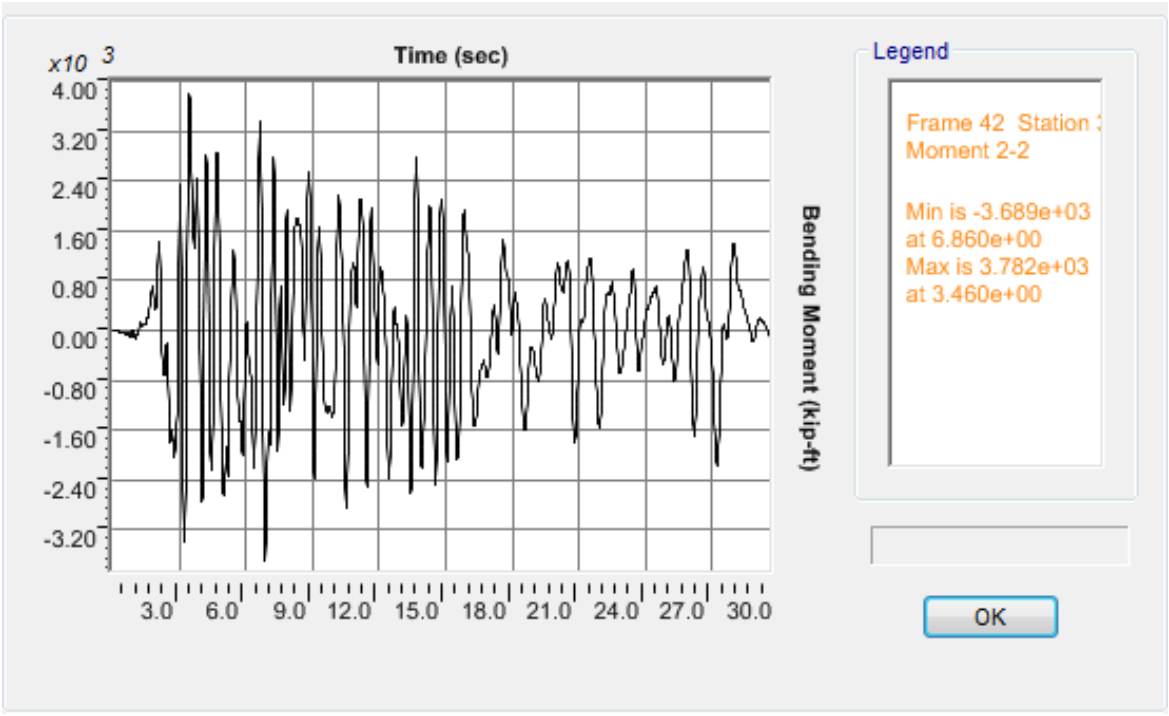
x10 3
Time (sec)
4.00
3.20
2.40
1.60
0.80
0.00
-0.80
-1.60
-2.40
-3.20
3.0 6.0 9.0 12.0 15.0 18.0 21.0 24.0 27.0 30.0
Bending Moment (kip-ft)
Legend
Frame 42 Station
Moment 2-2
Min is -3.689e+03
at 6.860e+00
Max is 3.782e+03
at 3.460e+00
OK

b)

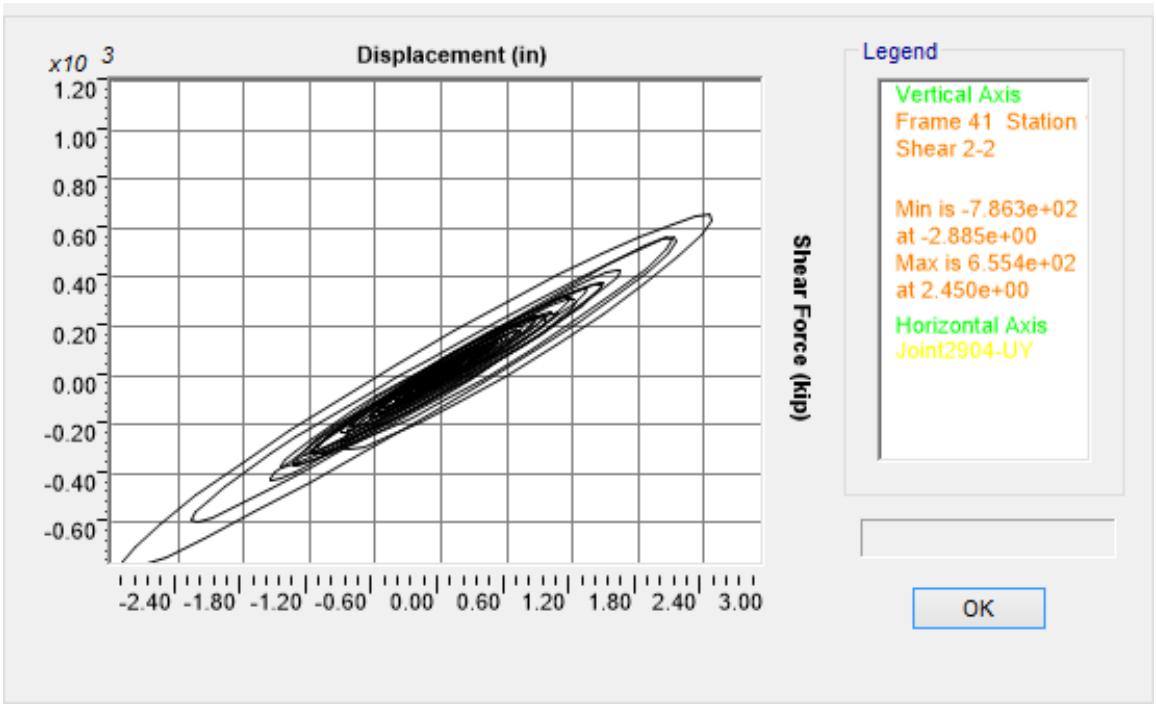

c)

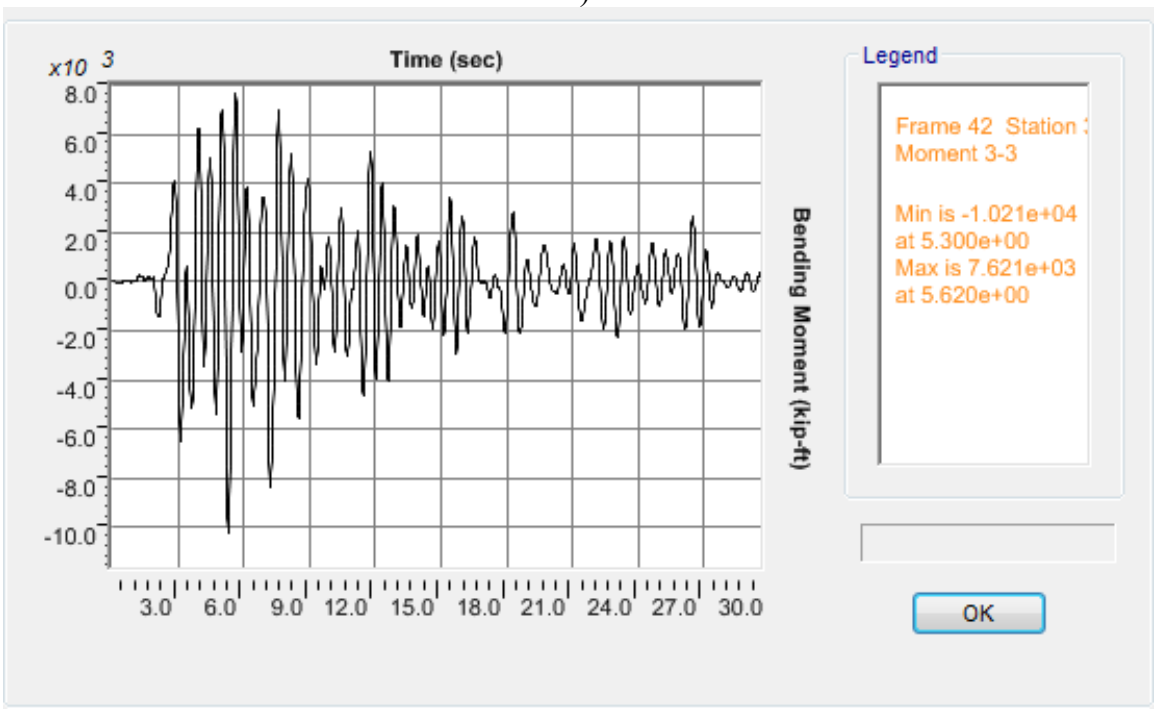

d)

Figure K.47 OSB1 column top response for Motion 47 ROCKN1N1: a) Longitudinal shear force-displacement hysteresis; b) Bending moment time history in the longitudinal direction; c) Transverse shear force-displacement hysteresis; d) Bending moment time history in the transverse direction

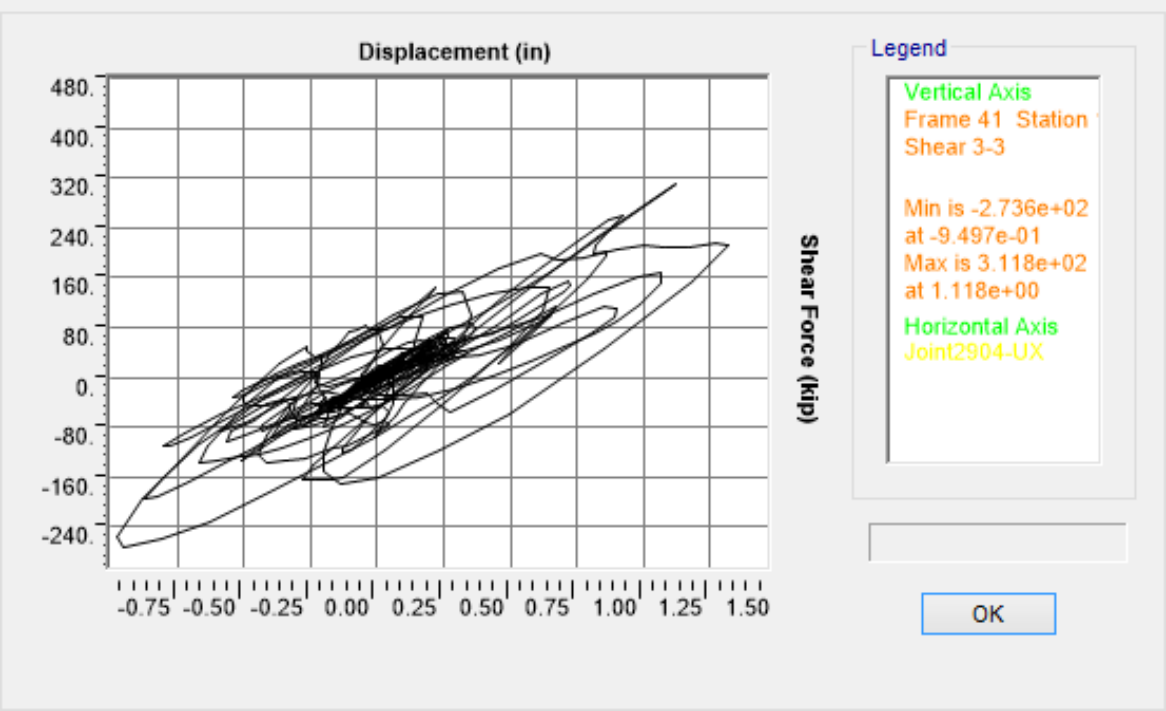
Displacement (in)
480.
400.
320.
240.
160.
80.
0.
-80.
-160.
-240.
-0.75 -0.50 -0.25 0.00 0.25 0.50 0.75 1.00 1.25 1.50
Shear Force (kip)
Legend
Vertical Axis
Frame 41 Station
Shear 3-3
Min is -2.736e+02
at -9.497e-01
Max is 3.118e+02
at 1.118e+00
Horizontal Axis
Joint2904-UX
OK

a)

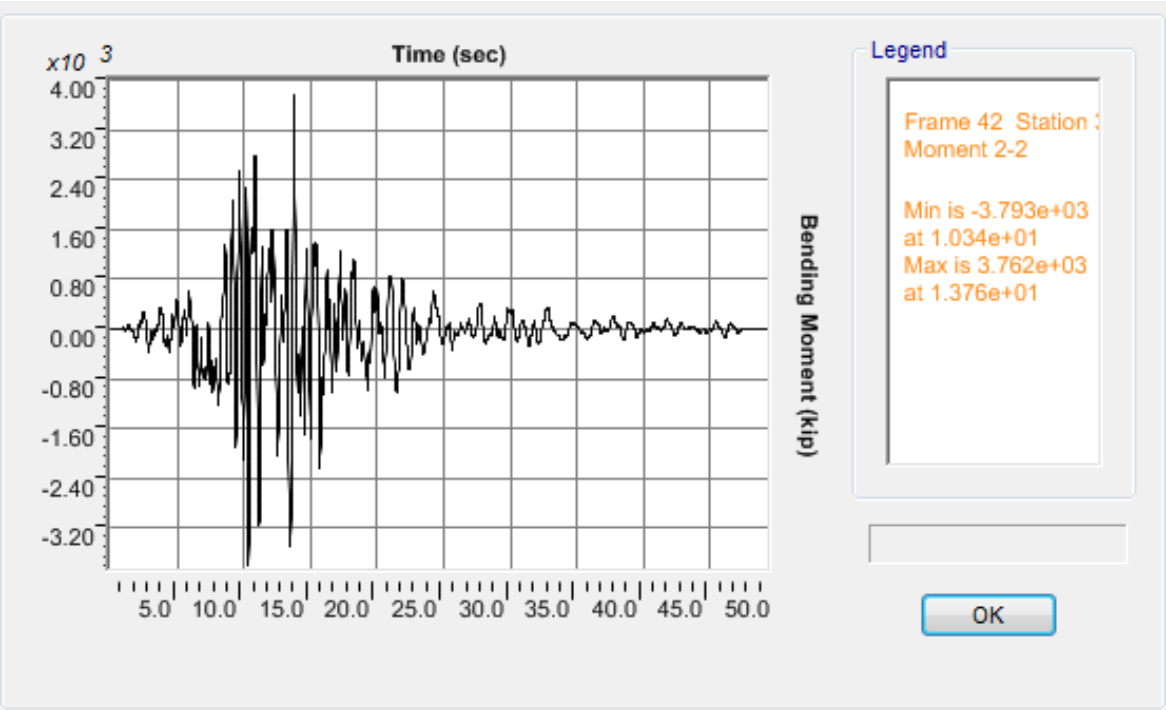
x10 3
Time (sec)
4.00
3.20
2.40
1.60
0.80
0.00
-0.80
-1.60
-2.40
-3.20
5.0 10.0 15.0 20.0 25.0 30.0 35.0 40.0 45.0 50.0
Bending Moment (kip)
Legend
Frame 42 Station
Moment 2-2
Min is -3.793e+03
at 1.034e+01
Max is 3.762e+03
at 1.376e+01
OK

b)

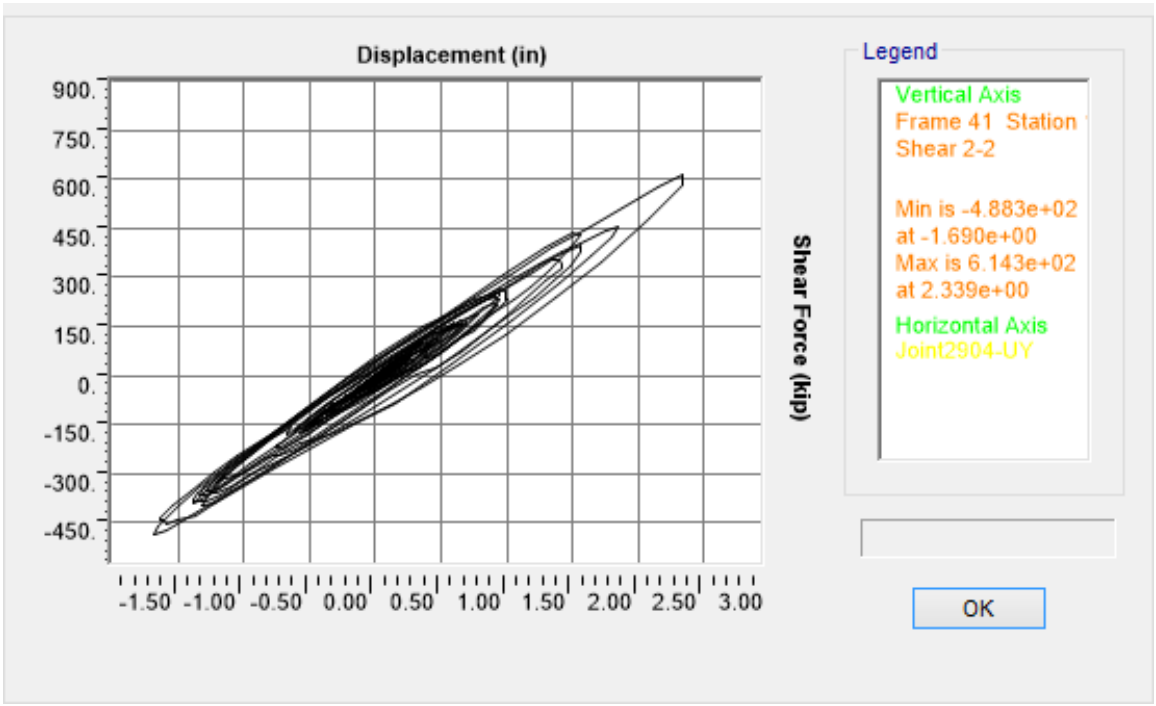

c)

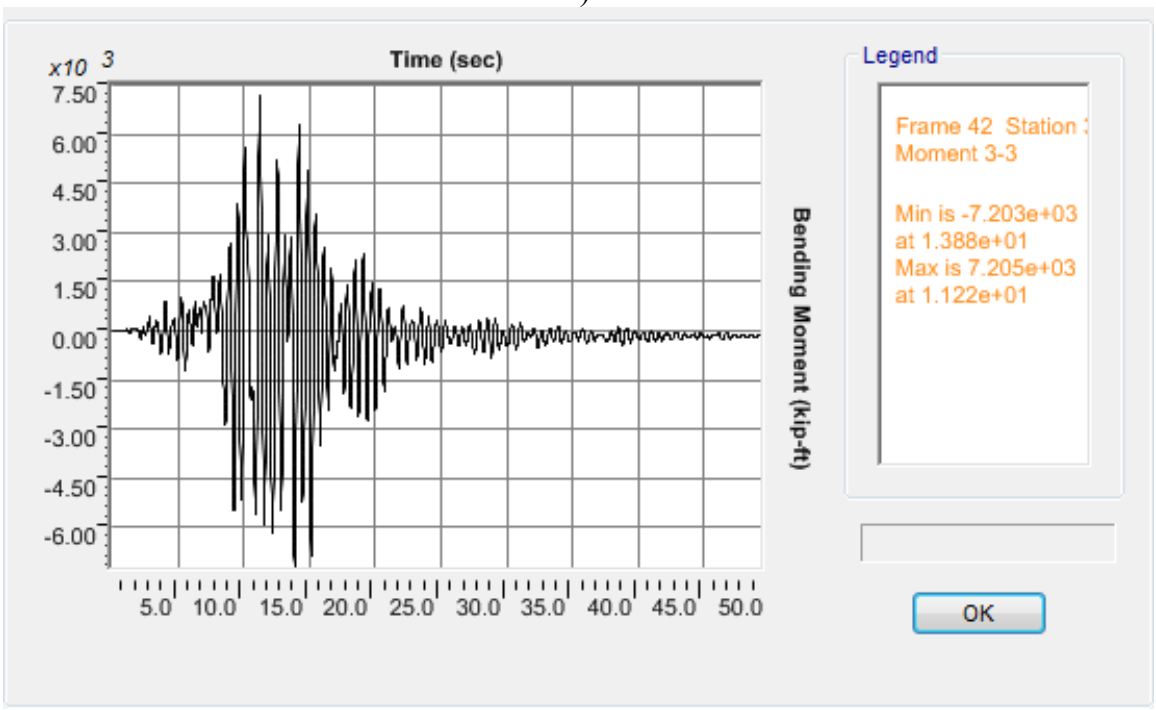

d)

Figure K.48 OSB1 column top response for Motion 48 ROCKN1P1: a) Longitudinal shear force-displacement hysteresis; b) Bending moment time history in the longitudinal direction; c) Transverse shear force-displacement hysteresis; d) Bending moment time history in the transverse direction

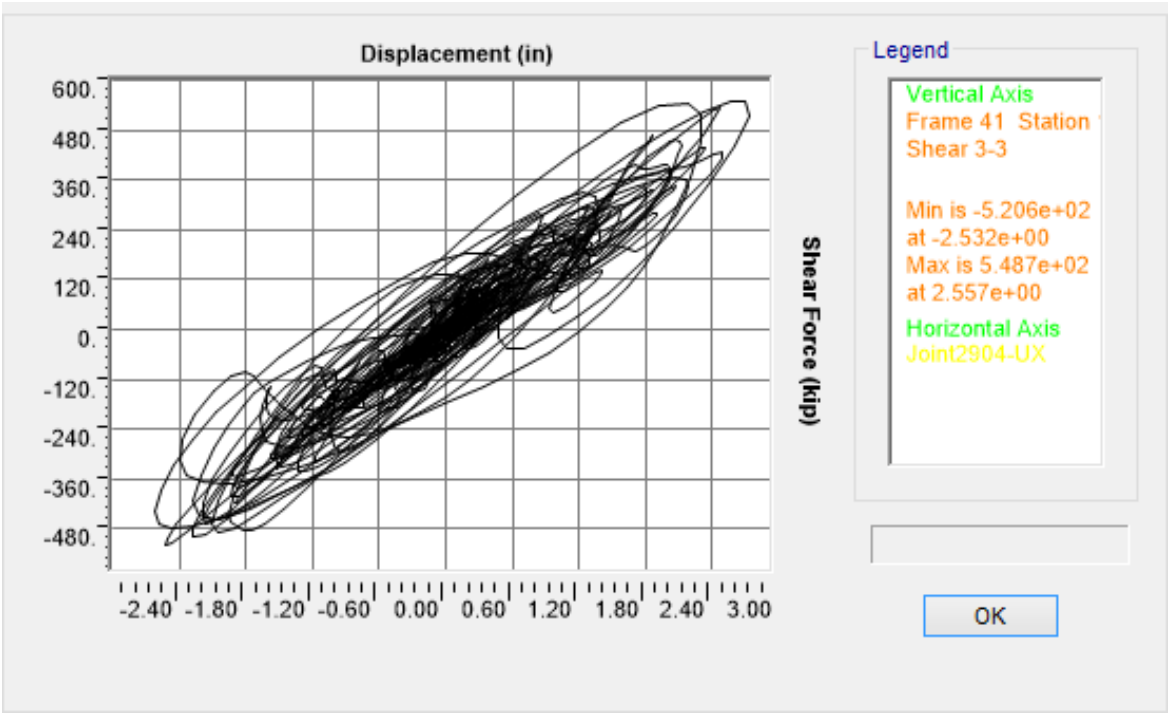
Displacement (in)
600.
480.
360.
240.
120.
0.
-120.
-240.
-360.
-480.
-2.40 -1.80 -1.20 -0.60 0.00 0.60 1.20 1.80 2.40 3.00
Shear Force (kip)
Legend
Vertical Axis
Frame 41 Station
Shear 3-3
Min is -5.206e+02
at -2.532e+00
Max is 5.487e+02
at 2.557e+00
Horizontal Axis
Joint2904-UX
OK

a)

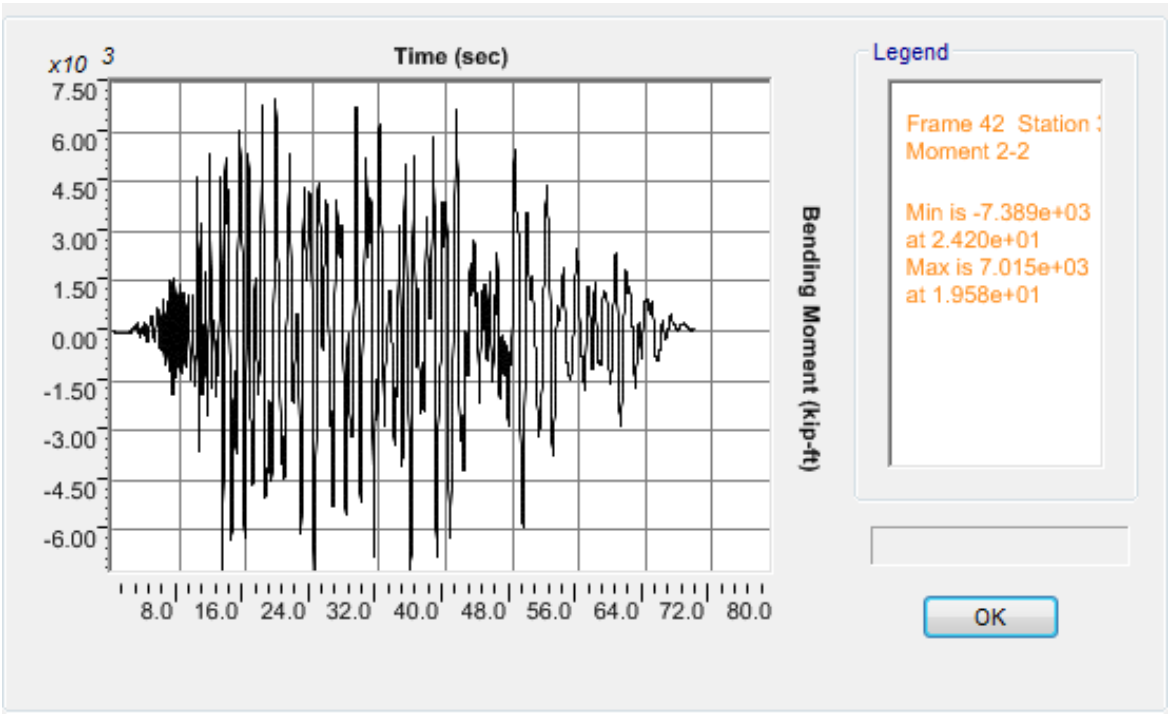
x10 3
Time (sec)
7.50
6.00
4.50
3.00
1.50
0.00
-1.50
-3.00
-4.50
-6.00
8.0 16.0 24.0 32.0 40.0 48.0 56.0 64.0 72.0 80.0
Bending Moment (kip-ft)
Legend
Frame 42 Station
Moment 2-2
Min is -7.389e+03
at 2.420e+01
Max is 7.015e+03
at 1.958e+01
OK

b)

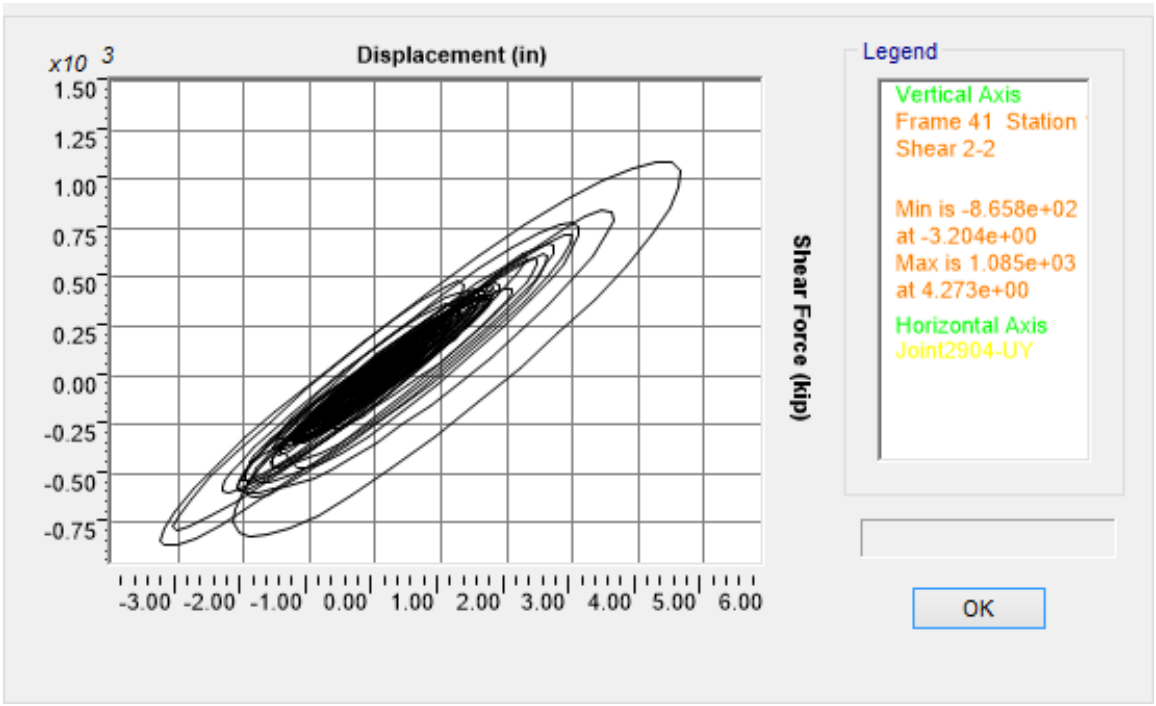

c)

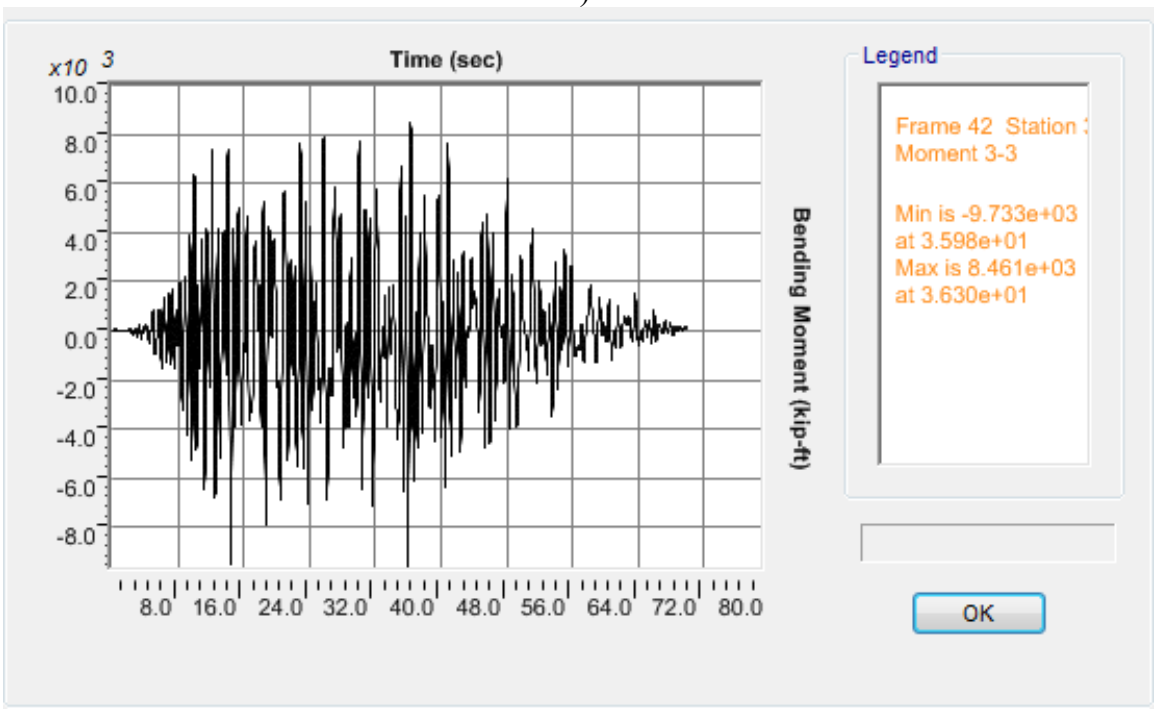

d)

Figure K.49 OSB1 column top response for Motion 49 SANDN1N1: a) Longitudinal shear force-displacement hysteresis; b) Bending moment time history in the longitudinal direction; c) Transverse shear force-displacement hysteresis; d) Bending moment time history in the transverse direction

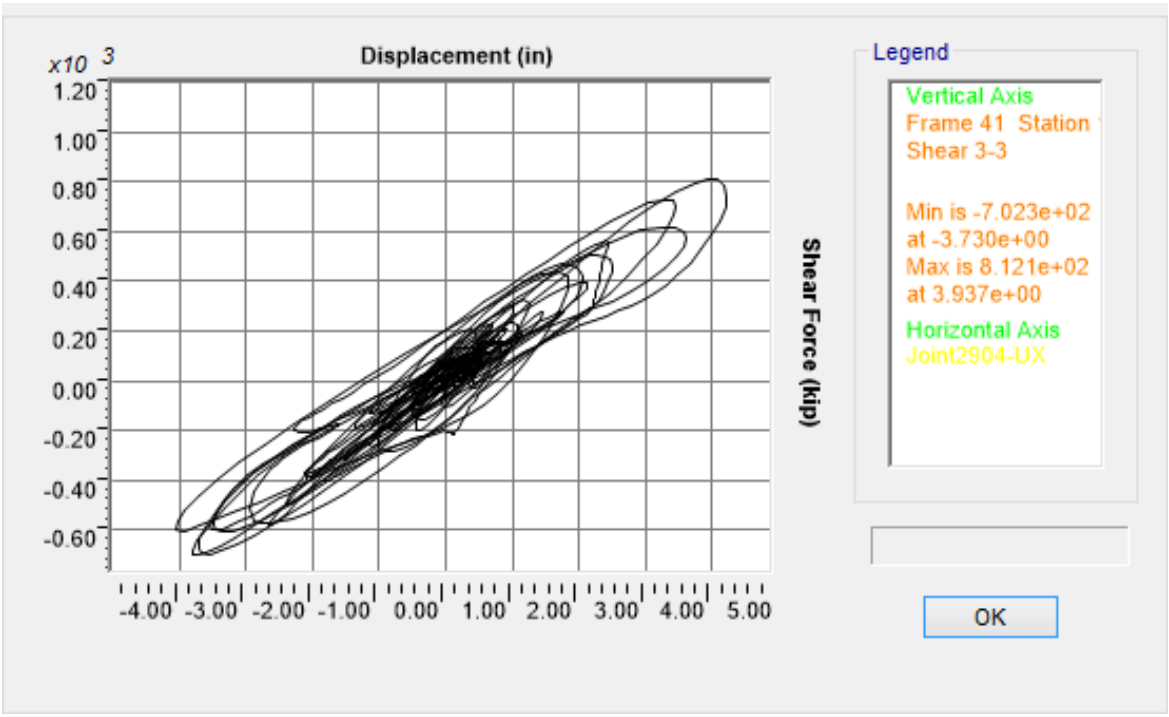
x10 3
Displacement (in)
1.20
1.00
0.80
0.60
0.40
0.20
0.00
-0.20
-0.40
-0.60
-4.00 -3.00 -2.00 -1.00 0.00 1.00 2.00 3.00 4.00 5.00
Shear Force (kip)
Legend
Vertical Axis
Frame 41 Station
Shear 3-3
Min is -7.023e+02
at -3.730e+00
Max is 8.121e+02
at 3.937e+00
Horizontal Axis
Joint2904-UX
OK

a)

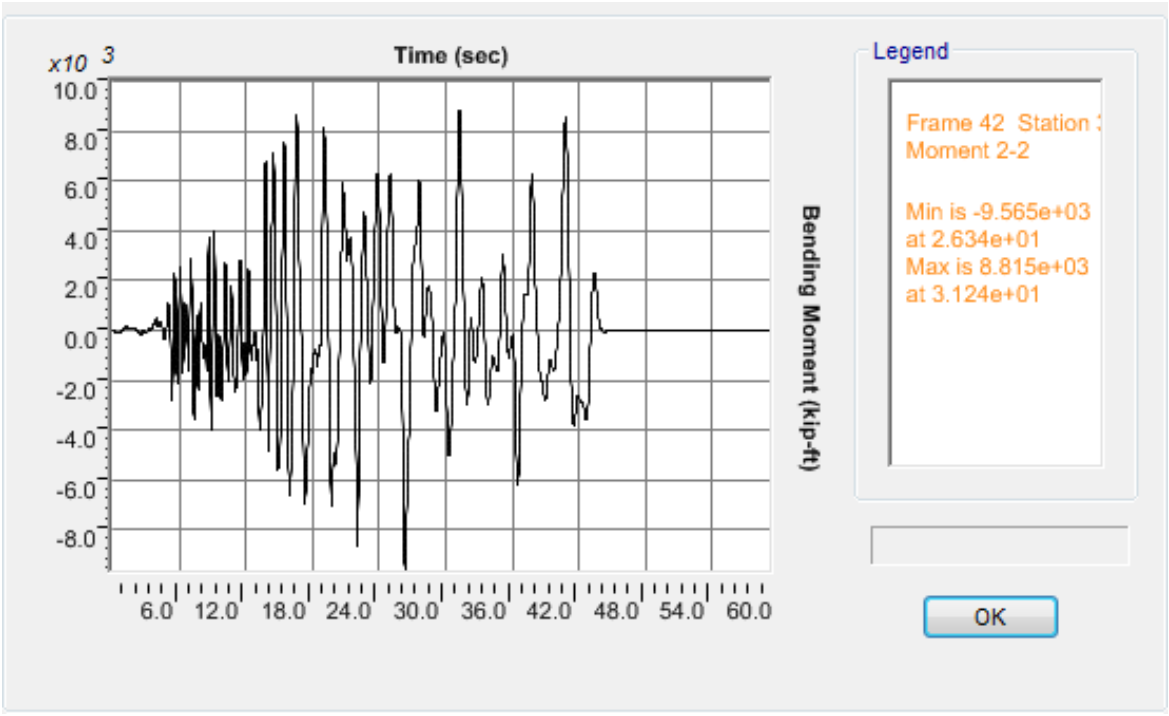
x10 3
Time (sec)
10.0
8.0
6.0
4.0
2.0
0.0
-2.0
-4.0
-6.0
-8.0
6.0 12.0 18.0 24.0 30.0 36.0 42.0 48.0 54.0 60.0
Bending Moment (kip-ft)
Legend
Frame 42 Station
Moment 2-2
Min is -9.565e+03
at 2.634e+01
Max is 8.815e+03
at 3.124e+01
OK

b)

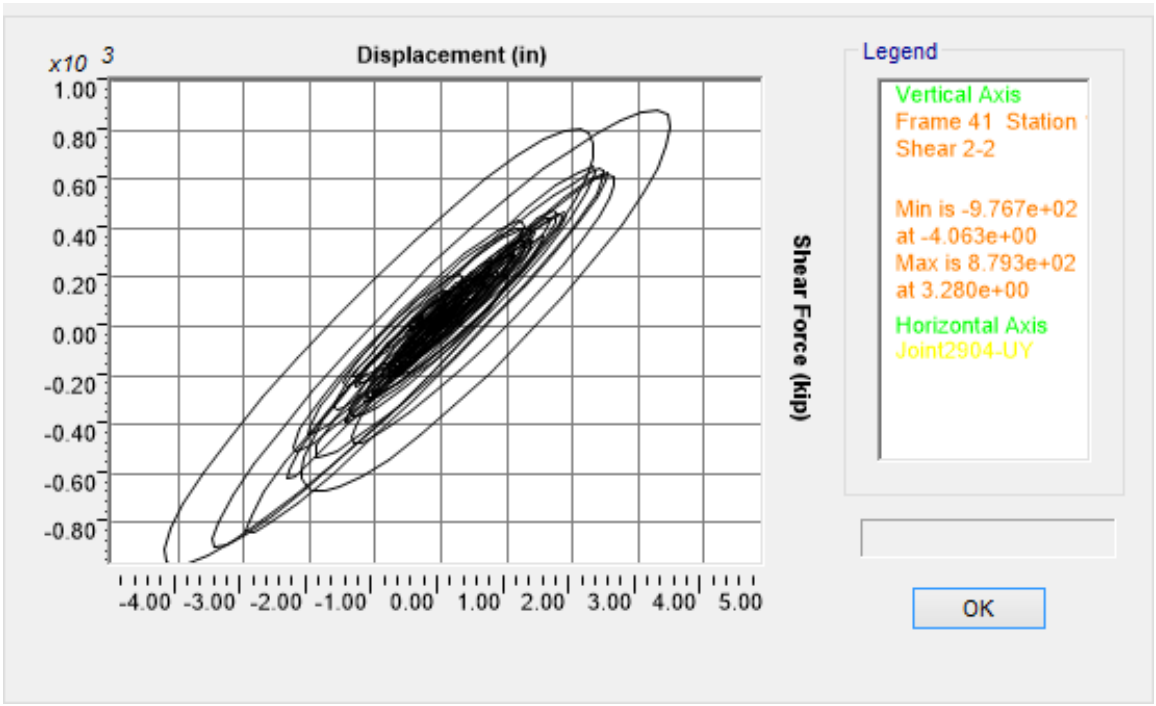

c)

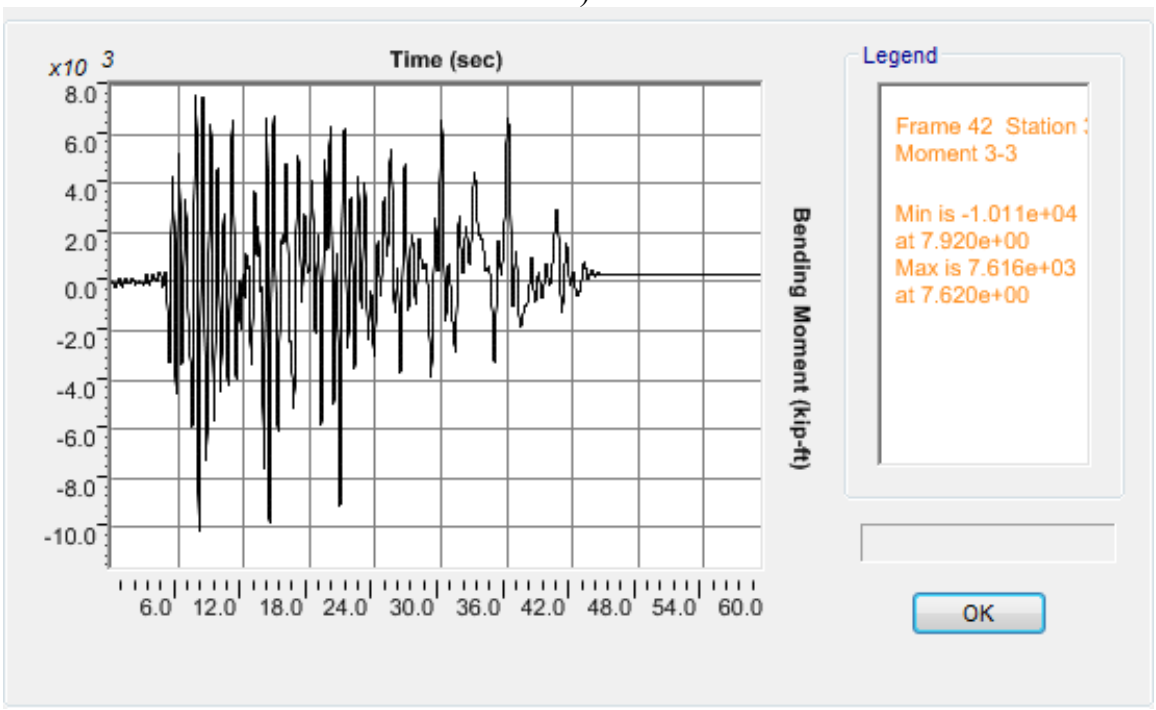

d)

Figure K.50 OSB1 column top response for Motion 50 CLAYN1N1: a) Longitudinal shear force-displacement hysteresis; b) Bending moment time history in the longitudinal direction; c) Transverse shear force-displacement hysteresis; d) Bending moment time history in the transverse direction

REFERENCES

Aviram, A., Mackie, K.R., and Stojadinovic, B. (2008a). "Effect of abutment modeling on the seismic response of bridge structures." *Earthquake Engineering and Engineering Vibration*, 7(4), 395-402.

Aviram, A., Mackie, K.R., and Stojadinovic, B. (2008b). "Guidelines for nonlinear analysis of bridge structures in California." *PEER Report No. 2008/03*, Pacific Earthquake Engineering Research Center, University of California, Berkeley.

Caltrans (1999). *xSection User Manual*, California Department of Transportation, Sacramento, California.

Caltran (2012). *OSB Study Bridges*, California Department of Transportation, Sacramento, California.

Caltrans (2013). *Caltrans Seismic Design Criteria, Version 1.7*, California Department of Transportation, Sacramento, California.

CSI (2015a). *CSI Analysis Reference Manual for SAP2000, ETABS, SAFE and CSiBridge*. Computers & Structures Inc.

CSI (2015b). *CSI Knowledge Base*, https://wiki.csiamerica.com/. Computers & Structures Inc.

Elgamal, A., Lu, J., and Mackie, K. (2014). "MSBridge: OpenSees pushover and earthquake Analysis of multi-span bridges - user manual." *Structural Systems Research Project SSRP-14/03*, University of California at San Diego, La Jolla.

Mazzoni, S., McKenna, F., Scott, M. H., Fenves, G. L., et al. (2009). *Open System for Earthquake Engineering Simulation, User Command-Language Manual*, Pacific Earthquake Engineering Research Center, University of California, Berkeley, OpenSees version 2.0, May.

McKenna, F., Scott, M., and Fenves, G. (2010). "Nonlinear Finite-Element Analysis Software Architecture Using Object Composition". *J. Comput. Civ. Eng.*, 24(1), 95–107.

Scott, M.H. and G.L. Fenves. (2006). "Plastic Hinge Integration Methods for Force-Based Beam-Column Elements*", Journal of Structural Engineering*, 132(2), 244-252.

Scott, M.H. and K.L. Ryan. (2013). "Moment-Rotation Behavior of Force-Based Plastic Hinge Elements", *Earthquake Spectra*, 29(2), 597-607.